WILEY

UNDERSTANDING MASS SPECTRA

A Basic Approach

SECOND EDITION

DropBooks

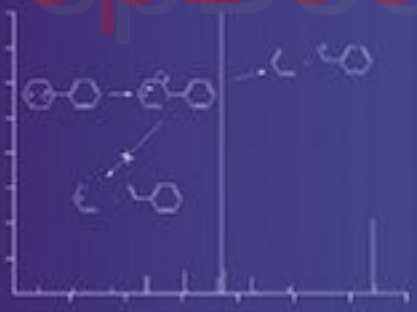

R. Martin Smith

UNDERSTANDING MASS SPECTRA

Second Edition

UNDERSTANDING MASS SPECTRA:

A Basic Approach

SECOND EDITION

R. Martin Smith

DropBooks

WILEY-INTERSCIENCE
A JOHN WILEY & SONS, INC., PUBLICATION

Copyright © 2004 by John Wiley & Sons, Inc. All rights reserved.

Published by John Wiley & Sons, Inc., Hoboken, New Jersey.
Published simultaneously in Canada.

No part of this publication may be reproduced, stored in a retrieval system, or transmitted in any form or by any means, electronic, mechanical, photocopying, recording, scanning, or otherwise, except as permitted under Section 107 or 108 of the 1976 United States Copyright Act, without either the prior written permission of the Publisher, or authorization through payment of the appropriate per-copy fee to the Copyright Clearance Center, Inc., 222 Rosewood Drive, Danvers, MA 01923, 978-750-8400, fax 978-646-8600, or on the web at www.copyright.com. Requests to the Publisher for permission should be addressed to the Permissions Department, John Wiley & Sons, Inc., 111 River Street, Hoboken, NJ 07030, (201) 748-6011, fax (201) 748-6008.

Limit of Liability/Disclaimer of Warranty: While the publisher and author have used their best efforts in preparing this book, they make no representations or warranties with respect to the accuracy or completeness of the contents of this book and specifically disclaim any implied warranties of merchantability or fitness for a particular purpose. No warranty may be created or extended by sales representatives or written sales materials. The advice and strategies contained herein may not be suitable for your situation. You should consult with a professional where appropriate. Neither the publisher nor author shall be liable for any loss of profit or any other commercial damages, including but not limited to special, incidental, consequential, or other damages.

For general information on our other products and services please contact our Customer Care Department within the U.S. at 877-762-2974, outside the U.S. at 317-572-3993 or fax 317-572-4002.

Wiley also publishes its books in a variety of electronic formats. Some content that appears in print, however, may not be available in electronic format.

Library of Congress Cataloging-in-Publication Data:

Smith, R. Martin.
Understanding mass spectra : a basic approach. – 2nd ed. / R. Martin Smith.
p. cm.
Includes bibliographical references and index.
ISBN 0-471-42949-X (acid-free paper)
1. Mass Spectrometry. I. Title.
QD96 .M3S65 2005
543′.0873–dc22 2004003683

Printed in the United States of America

10 9 8 7 6 5 4 3 2 1

CONTENTS

Preface to the Second Edition xi

Acknowledgments xv

Abbreviations and Notations Used in This Book xvii

1 Instrumentation 1

1.1. Introduction / 1
- 1.1.1. Overview / 1
- 1.1.2. Sample Introduction / 3

1.2. Ionization Source / 4
- 1.2.1. Electron Ionization Source / 5
- 1.2.2. Chemical Ionization / 8
- 1.2.3. Other Ionization Methods / 9
  - 1.2.3.1. Electrospray Ionization / 9
  - 1.2.3.2. Desorption Ionization / 12

1.3. m/z Analysis / 13
- 1.3.1. Time-of-Flight (TOF) / 13
- 1.3.2. Magnetic Sector / 15
- 1.3.3. Transmission Quadrupole / 17
  - 1.3.3.1. Selected Ion Monitoring (SIM) / 21
- 1.3.4. Quadrupole Ion Trap (QIT) / 22
- 1.3.5. Other Types of Mass Analysis / 24
  - 1.3.5.1. Mass Spectrometry/Mass Spectrometry(MS/MS) / 24
  - 1.3.5.2. Accurate m/z Analysis / 26
- 1.3.6. Spectral Skewing / 26

1.4. Ion Detection / 30
- 1.4.1. Electron Multiplier / 32
- 1.4.2. Photomultiplier Detector / 33

DropBooks

1.5. Data System / 33
1.5.1. Instrument Tuning and Calibration / 33
1.5.2. The Mass Spectrum / 37
1.5.2.1. Production of the Mass Spectrum / 37
1.5.2.2. Terminology: Ions vs. Peaks / 41
1.5.3. Library Searches / 41
1.5.4. Using the Data System to Analyze GC/MS Data / 45
1.6. Criteria for Good-Quality Spectra / 50
Additional Problems / 51
Mass Spectrometric Resources on the Internet / 52
References and Suggested Reading / 53

2 Elemental Composition from Peak Intensities 56

2.1. Natural Isotopic Abundances / 56
2.1.1. Atomic and Molecular Mass / 59
2.1.2. Calculated Exact Masses and Mass Defects / 60
2.2. Determining Elemental Composition from Isotope Peak Intensities / 64
2.2.1. One or More Atoms of a Single Element / 64
2.2.1.1. Chlorine and Bromine / 64
2.2.1.2. Ion Designation and Nomenclature / 70
2.2.1.3. Probability Considerations with Multiple Numbers of Atoms / 71
2.2.1.4. Isotope Peak Intensity Ratios for Carbon-Containing Ions—The X + 1 Peak / 74
2.2.1.5. A, A + 1, and A + 2 Elements / 77
2.2.1.6. Isotope Peak Intensity Ratios for Carbon-Containing Ions—The X + 2 Peak / 78
2.2.1.7. Overlapping Peak Clusters—Contributions from ^{13}C Only / 80
2.2.1.8. Silicon / 82
2.2.2. Complex Isotope Clusters / 83
2.2.2.1. Sulfur Dioxide / 83
2.2.2.2. Diazepam / 86
2.3. Obtaining Elemental Compositions from Isotope Peak Intensities / 89
Examples / 91
Additional Problems / 96
References / 98

3 Ionization, Fragmentation, and Electron Accounting 99

3.1. A Brief Review of Orbitals and Bonding / 99
3.2. Even- and Odd-Electron Species / 101
3.3. Site of Initial Ionization / 103
3.4. Types of Fragmentation / 107
3.5. The Nitrogen Rule / 109
3.6. Energy Considerations in Fragmentation Processes / 110
3.6.1. Fragmentation Rates / 110
3.6.2. Metastable Ions / 112
3.6.3. Energy Diagrams / 113
3.6.4. Stevenson's Rule / 116
Additional Examples / 117
Problems / 119
References / 120

4 Neutral Losses and Ion Series 121

4.1. Neutral Losses / 121
4.1.1. Losses from the Molecular Ion / 121
4.1.2. Loss of Small Molecules from Aromatic Ions / 126
4.2. Low-Mass Ion Series / 131
4.2.1. *n*-Alkane Spectra / 132
4.2.2. Effect of Chain Branching on the Spectra of Aliphatic Hydrocarbons / 134
4.2.3. Ion Series for Nonaromatic Compounds / 136
4.2.4. Aromatic Ion Series / 142
4.2.5. Use of Ion Series: Mass Chromatograms / 145
Additional Problems / 148
References / 148

5 A Rational Approach to Mass Spectral Problem Solving 150

5.1. Guidelines for Solving Mass Spectral Problems / 150
Examples / 153
Problems / 161
Reference / 163

6 α-Cleavage and Related Fragmentations 164

6.1. Introduction / 164
6.2. Benzylic Cleavage / 166

DropBooks

6.3. Cleavage Next to Aliphatic Nitrogen / 170
6.3.1. Structural Relationships: α-Cleavage in 1-Phenyl-2-aminopropanes / 171
6.3.2. Cleavage Next to Electron-Deficient Nitrogen / 176
6.3.3. α-Cleavage in Complex Nitrogenous Ring Systems / 179
6.4. Cleavages of Aliphatic Oxygenated Compounds / 180
6.4.1. α-Cleavage / 180
6.4.2. Bond Cleavage Away from the Ionization Site / 184
6.4.3. Cleavage at Carbonyl Groups / 186
6.5. Elimination Fragmentations in Oxygen and Nitrogen Compounds / 192
6.5.1. Secondary Elimination from Initial α-Cleavage Ions / 192
6.5.2. Hydride Shifts / 195
6.5.3. Elimination Fragmentations of Some Aromatic Compounds / 196
6.5.4. Water Elimination in Aliphatic Alcohols / 198
Examples / 200
Additional Problems / 202
References / 206

7 Important Mass Spectral Rearrangements / 207

7.1. Introduction / 207
7.2. γ-Hydrogen Rearrangement / 208
7.2.1. McLafferty-Type Rearrangement / 208
7.2.2. γ-Hydrogen Rearrangement in Alkylbenzenes / 213
7.2.3. γ-Hydrogen Rearrangement Initiated by a Remote Ionization Site / 217
7.3. Cyclohexanone-Type Rearrangement / 223
7.4. Retro Diels–Alder Fragmentation / 228
7.5. Double-Hydrogen (McLafferty + 1) Rearrangement / 234
Additional Problems / 236
References / 237

8 Rationalizing Mass Spectral Fragmentations 238

8.1. General Guidelines / 238
8.2. Loss of Small Molecules / 241
8.2.1. Loss of Small Molecules from Aromatic Ions Revisited / 241
8.2.2. γ-Butyrolactone / 243
8.3. Ephedrine / 246
8.4. *Ortho* Effect: The Hydroxybenzoic Acids / 251

Additional Problems / 254
References / 256

9 Structure Determination in Complex Molecules Using Mass Spectrometry 257

9.1. Introduction / 257
9.2. "Designer Drugs" Related to MDA / 258
9.3. Cocaine and Its Metabolites / 262
9.3.1. Peak Correlations / 263
9.3.2. Proposed Fragmentations / 268
9.3.3. Application / 271
9.4. Phencyclidine and Its Analogs / 274
9.4.1. Fragmentations of Phencyclidine / 274
9.4.2. Phencyclidine Analogs / 282
9.5. A Practical Problem / 284
References / 285

10 Answers to Problems 287

Index 353

DropBooks

PREFACE TO THE SECOND EDITION

Mass spectrometry (MS) has undergone a profound change over the past decade. Instrumentation and techniques related to the automated analysis of biomolecules and new drugs now account for a large percentage of the research and publications in this field. In comparison, gas chromatography/mass spectrometry (GC/MS) and electron ionization (EI) mass spectra of ''small'' molecules play a less important role than they once did. But GC/MS is far from dead, and EIMS continues to be the ionization method of choice for many laboratories that routinely analyze volatilizable low molecular mass compounds such as drugs, flavor and odor components, pesticides, and petroleum products. This situation seems unlikely to change in the near future.

The interpretation of EI mass spectra has always been a challenging subject to learn and to teach—especially to individuals who have not had the benefit of a graduate education in chemistry or who have been out of college for several years. The challenge is compounded by manufacturer-encouraged reliance on library search results for compound identification. Why learn anything about spectral interpretation when the computer can do all the work? The answer to this question is simple, as most conscientious users quickly realize. The library search often does not provide a realistic answer or (worse) may provide an answer that looks correct but is not. Even software programs that profess to ''interpret'' unknown spectra can only provide probable answers. After that, you are left to your own devices.

It was tempting to substantially increase the breadth and depth of the material that was covered in the first edition. However, my experience has been that an encyclopedic presentation of mass spectral interpretation does not give beginning mass spectrometrists what they need, which is a presentation that provides a few fundamental concepts in a logical, organized manner, without distracting and unnecessary detail. I wrote and revised this book for beginning mass spectrometrists, and I have retained the simplicity of its approach for that reason.

My own understanding of mass spectral interpretation has developed, and continues to develop, by trial and error. I am admittedly mostly self-taught. My knowledge of mass spectral literature has been limited by the nature of my career, whose primary focus was forensic science, not mass spectrometry. Some will see that as a

detriment. However, I believe that my naïveté allows me to present a different approach to this subject—one based on *learning* the subject, not on teaching it.

Although this edition has the same basic structure and content as the first, a number of significant changes have been made. In general, there are more references, especially for helping the reader gain access to in-depth information about specific subjects. Some Internet resources have also been included at the end of Chapter 1. I have tried to include examples from a broader range of chemical interests. There are still more forensic examples than other types, but I believe the molecules of forensic chemistry are not so unique that they cannot be used as a general teaching tool. Indeed, I hope that these examples are appealing because they come from a field that has captured the public interest and imagination.

Two of the more fundamental changes in content are the use of ionization energies (IEs) for determining the site of initial ionization and Stevenson's rule for determining retention of the charge in fragmentation products (Chapter 3). Fragmentation schemes for most compounds throughout the book have been altered to reflect these changes. Attention has been paid to differentiating between radical- and charge-induced fragmentations.

The material in several chapters—most notably in Chapters 2, 4, and 5—has been reorganized. The method for solving mass spectral unknowns has been placed in a separate chapter (Chapter 5), where it follows—rather than precedes—discussions of specific problem-solving tools such as neutral losses, low-mass ion series, and so forth. New problems and examples have been added to Chapters 2–4 that provide practice more specifically on the topics discussed in those chapters.

DropBooks

New material has been added to several chapters. Brief descriptions of newer techniques such as electrospray ionization (ESI) and MALDI are included in Chapter 1 simply because they are now so widespread that exposure to them is almost unavoidable. A derivation of the mass spectrometric equation for the time-of-flight (TOF) spectrometer is included for the same reason, as well as to provide a straightforward example of how m/z values are related mathematically to physical variables in the spectrometer. Discussions of orbitals and bonds, the use of ionization energies, the nitrogen rule, and Stevenson's rule have all been added to Chapter 3, and new (and I hope better) examples have replaced some of the material in the chapter on rationalizing mass spectral fragmentations (Chapter 8 in this edition). I struggled with maintaining the mathematical derivations in Chapter 2 regarding the relationship between an ion's elemental composition and the relative sizes of the isotope peaks observed in the spectrum. I decided to keep them because many texts do not show where these equations come from.

The number of chapters describing specific types of fragmentation reactions is still limited (Chapters 5–7). A ''theme and variations'' approach is used, in order to emphasize the similarities—rather than the differences—between fragmentation types. Not all reaction types are covered, because I feel it is more important for the beginning reader to fully understand a few fragmentations that have wide applicability than to try to cover every possibility. Particular emphasis is placed on single-bond cleavage, fragmentations that eliminate small unsaturated molecules, and several well-known hydrogen rearrangements. I have tried to repeat these

fragmentations in as many contexts as possible throughout Chapters 4–9 to emphasize their utility and to facilitate committing them to memory.

Each time I have taught this material, and again as I was revising this book, I reached new levels of understanding of even some of the most basic concepts that are presented here. For most readers, I doubt that the contents of this book will be thoroughly digested in one reading. Rather, I would suggest studying it slowly, even repetitively. Try to understand the answers to each of the problems, practice writing down fragmentation mechanisms, then attempt to apply each concept to the spectra encountered in your own laboratory situation. The rewards will be well worth the effort.

Madison, Wisconsin
January 2004

R.M.S.

ACKNOWLEDGMENTS

There are many people I must thank for making this book a reality. Foremost among these are members of the Wisconsin Department of Justice, Division of Law Enforcement Services, without whose backing this book would probably never have become a reality. A special thanks goes to Jerry Geurts and Mike Roberts for their support and encouragement while I was in their employ. I am also grateful for the contributions of colleagues who provided me with interesting problem samples that found their way, directly or indirectly, into this book. The recent contributions of Casey Collins, Marty Koch, Mike Larson, John Nied, Joseph Wermeling, and Guang Zhang deserve special mention.

This edition was technically edited by someone who prefers not to be named. Although I will honor that request, I cannot in good conscience fail to acknowledge the invaluable contribution this individual made to the content, style, organization, and technical detail of this edition. No matter how far this book falls short of perfection, it is immensely closer to that goal than it was when this person was first given a copy of the manuscript.

My friend Mary Upshaw has worked in a laboratory for many years, but had only a general idea of what mass spectrometry was all about until I asked her to read the entire manuscript as a ''lay person''—no small request! Our subsequent discussions and her insightful comments lent much to the final organization and readability of this edition. (Her proofreading skills are great, too.) If you find this book easy to read, it is at least partly due to her efforts.

My editor Amy Romano deserves a medal for her patience. The revision ended up taking at least a year longer than either of us suspected it would (or wanted it to). I feel strongly—and I hope she does too—that the wait was well worth it.

Finally, a special word of thanks to John Allison, who seemed to believe in what I was doing and said the right things at the right times to keep me on track.

DropBooks

ABBREVIATIONS AND NOTATIONS USED IN THIS BOOK

Atomic symbols, rather than names, of the elements are used throughout the book.

$\sim$ and $\approx$	Approximately equal to
$^{+\bullet}$	Site of unpaired electron and positive charge (odd-electron ion)
Δ	Mass defect; also, site of double bond in organic compounds
CI	Chemical ionization
EE^{+}	Even-electron ion
EI	Electron ionization
eV	Electron volt (1 eV = 23 kcal)
$\Delta G^{\ddagger}$	Energy of activation (for a chemical reaction)
GC	Gas chromatography
IE	Ionization energy
LC	Liquid chromatography
M, M + 1, M − 15, etc.	Spectral peak with *m*/*z* value at, higher than, or lower than that of the molecular ion peak by a specified number of units
$M^{+\bullet}$	Positively charged molecular ion
ΔM	Difference in mass or *m*/*z* values (mass or *m*/*z* discrimination)
MM	Molecular mass
MS	Mass spectrometry
m/*z*	Mass-to-charge ratio
$OE^{+\bullet}$	Odd-electron ion
P(X)	Probability ($\leq$1) that an event will occur
QIT	Quadrupole ion trap
RTICC	Reconstructed total ion current chromatogram
SIM	Selected ion monitoring

TOF	Time-of-flight
u	Unified atomic mass unit
X, X + 1, X − 15, etc.	Peaks with *m*/*z* values at, higher than, or lower than that of some peak in the spectrum by a specified number of units
X^+, $(X + 1)^+$, $(X - 15)^+$, etc.	Ions having masses the same as, higher than, or lower than that of some ion in the spectrum by a specified number of units
[X]	Peak intensity for an ion having an *m*/*z* value of X
$[X^+]$	Abundance of an ion having an *m*/*z* value of X

DropBooks

1

INSTRUMENTATION

1.1. INTRODUCTION

1.1.1. Overview

Mass spectrometry (MS) differs from other common forms of organic spectral analysis in that the sample does not absorb radiation such as infrared, ultraviolet, or radio waves from the electromagnetic spectrum. In contrast to infrared (IR) or nuclear magnetic resonance (NMR) spectrometry, both of which identify compounds with specificity comparable to that of mass spectrometry, MS is a destructive method of analysis—that is, the sample cannot be recovered after mass spectral analysis. On the other hand, MS is highly sensitive and requires less sample than either IR or NMR in order to provide more information about the structure of the analyte.

Mass spectrometers are typically not standalone instruments. Most often they are connected physically and electronically to a chromatograph as well as a computer. Figure 1.1 shows a typical arrangement of a chromatograph/mass spectrometer/computer system. The chromatograph separates mixtures and introduces the sample into the mass spectrometer. The mass spectrometer ionizes analyte molecules, then separates and detects the resulting ions. The computer system controls the operation of the chromatograph and the MS, and provides data manipulation and storage during and after data collection. For volatile samples, gas chromatography (GC) is

Understanding Mass Spectra: A Basic Approach, *Second Edition*. By R. Martin Smith
ISBN 0-471-42949-X © 2004 John Wiley & Sons, Inc.

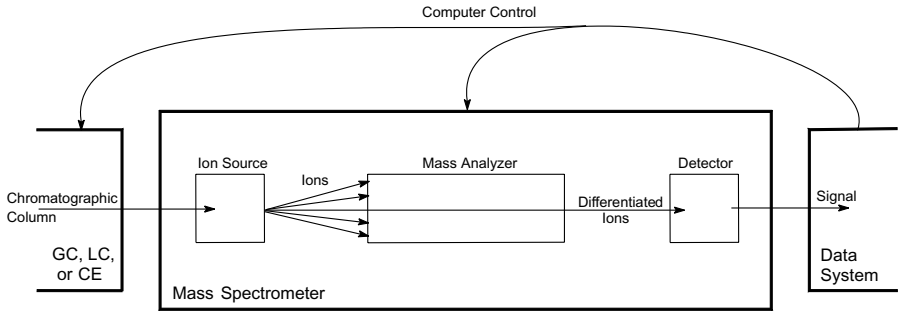

Figure 1.1. Block diagram of a chromatograph/MS/computer system.

used for mixture separation. For nonvolatile or thermally labile molecules, high pressure liquid chromatography (HPLC or just LC) is used. The abbreviated terms GC/MS and LC/MS are commonly used to describe the combination of these chromatographic techniques with MS.

In order to be analyzed by mass spectrometry, sample molecules must be ionized. In the case of electron ionization mass spectrometry (EIMS, the focus of this book), electrically neutral molecules are converted to molecular ions ($M^{+\bullet}$; see Section 3.1) by means of a beam of high-energy electrons. Ionization is followed almost immediately by fragmentation of the $M^{+\bullet}$ in which some bonds break, and in many instances new bonds form, in ways that are characteristic of the structure of the fragmenting ion. The product ions thus formed often undergo further characteristic fragmentation before leaving the ion source (Section 1.2), creating a cascade of ion-forming reactions. This is why mass spectrometry, especially when coupled with separation techniques such as GC or HPLC, is a highly specific way to identify organic compounds.

DropBooks

The components of the mass spectrometer that cause ion formation, separation, and detection are contained in an ultraclean housing usually kept at moderately high vacuum (10^{-3}–10^{-6} torr[1]; some exceptions will be mentioned later). High vacuum ensures that, once the ions formed in the ion source begin to move toward the detector, they will not collide with other molecules because this could result in further fragmentation or deflect them from their desired path. Nearly all fragmentation reactions occurring under these conditions are *intramolecular* (involving only the decomposition of individual ions) rather than *intermolecular* (involving the reaction of ions with other species that may be present). High vacuum also protects the metal and oxide surfaces of the ion source, analyzer, and detector from corrosion by air and water vapor, which could compromise the spectrometer's ability to form, separate, and detect ions.

[1] 1 torr = 1 mm Hg, which is equivalent to ~133 pascal (Pa).

1.1.2. Sample Introduction

High sample purity is critical for unambiguous identification by mass spectrometry. The simultaneous presence of several different compounds in the ion source creates a situation in which ions from all these compounds are analyzed at the same time. This results in a composite mass spectrum that may be impossible to interpret. When capillary column GC is used for sample separation prior to introduction into the mass spectrometer, sample molecules can be introduced directly into the ion source of the spectrometer through the end of the capillary column. Carrier gas flow through a capillary column is low enough that the carrier gas can be removed by the vacuum system of the mass spectrometer. Helium (He) and hydrogen (H_2) are good choices as carrier gases for GC/MS work because their extremely low atomic and molecular masses (4 u and 2 u, respectively; 1 u = 1 unified atomic mass unit[2]) fall below those of all the ions normally seen in organic mass spectrometry.

HPLC has become increasingly important as an option for sample separation prior to mass spectral analysis—especially for compounds that are nonvolatile, thermally labile, or otherwise not amenable to analysis by GC. Capillary electrophoresis (CE) has also been coupled with mass spectrometry to separate and identify inherently ionic molecules such as amino acids, proteins, and DNA fragments. Whereas separation of sample and carrier gas is relatively straightforward in GC/MS, separating sample molecules from HPLC or CE solvents is more complex, so that combinations of these techniques with mass spectrometry for routine use have occurred only recently.

Other methods of sample introduction must be mentioned briefly. Analysis of a pure volatile liquid can be accomplished by placing the liquid in a small, evacuated glass bulb that is connected to the ion source with narrow metal or glass tubing and isolated from the MS vacuum system by a valve. Opening the valve causes the sample vapor to flow directly into the ion source. This method is used for introduction of the calibration and tuning standard perfluorotri-*n*-butylamine (PFTBA; see Section 1.5.1).

Samples that have low volatility or that may decompose during their passage through the GC can be placed on the tip of a probe that is inserted directly into the ion source. The probe tip containing the sample is inserted into a chamber that is isolated from the main vacuum system by a valve. This chamber is evacuated using an auxiliary vacuum pump, after which the valve is opened and the probe tip is inserted all the way into the ion source. Gentle heating of the probe tip provides volatilization of the sample and, in ideal cases, rudimentary fractional distillation of the desired compound. Nonetheless, sample purification prior to introduction by direct insertion probe is desirable. The added expense, potential for ion source

[2] There is currently a lack of consistency regarding the terms used for the atomic mass unit. The single term *amu* was used at one time, but it had different definitions in physics and chemistry, both involving ^{16}O as a standard mass. This term was discontinued when a unified standard mass was adopted. The International Union of Pure and Applied Chemistry (IUPAC) suggests the *unified atomic mass unit* (abbreviated u), which is based on ^{12}C (Section 2.1.2). The *dalton* (abbreviated Da) is identical in size to u and is the term used in biological and biochemical applications as well as for stoichimetric calculations.

contamination by introduction of too large a sample, and the versatility of modern chromatographic techniques have made these devices increasingly rare.

1.2. IONIZATION SOURCE

Sample molecules must be ionized in order to be analyzed and detected in mass spectrometry. Until fairly recently, volatile compounds were ionized primarily in the electron ionization (EI) source, which is still the most common ion source used in GC/MS work. Since the focus of this book is the interpretation of EI mass spectra, most of this section will describe the EI source. As the number of larger and less volatile molecules requiring analysis by mass spectrometry has grown, sample introduction and ionization techniques have been developed that produce detectable numbers of ions of these compounds. Some of these ionization techniques are now used so routinely that a brief description of them is warranted. A list of ionization methods and their application to various sample types is given in Table 1.1.

Table 1.1. Molecular ionization methods in mass spectrometry

Type of Ionization	Ionizing Agent	Source Pressure	Uses
Electron ionization (EI)	50–70 eV electrons	10^{-4}–10^{-6} torr	Extensive fragmentation allows structure determination; GC/MS (Section 1.2.1)
Chemical ionization (CI)	Gaseous ions	~1 torr	Molecular mass determination; GC/MS (Section 1.2.2)
Desorption ionization (DI)		10^{-5}–10^{-6} torr	Molecular mass and structures of high mass, nonvolatile compounds in condensed phase
Fast atom bombardment (FAB)	Energetic Ar or other neutral atoms		
Laser desorption (LDI) and matrix-assisted LDI (MALDI)	Energetic photons		Section 1.2.3.2
Electrospray (ES) ionization	Electric field; ions in solution	Atmospheric or slightly reduced pressure	HPLC/MS and CE/MS (Section 1.2.3.1)
Atmospheric pressure chemical ionization (APCI)	Corona discharge; gaseous ions	Atmospheric	HPLC/MS

DropBooks

1.2.1. Electron Ionization Source

Ion sources from different instrument manufacturers (and sometimes even different models from the same manufacturer) may differ from one another both in appearance and in names assigned to the component parts. However, most have the same basic design. A typical example is shown in Figure 1.2.

The EI source is most commonly a small chamber about 1 cc in volume, in which analyte molecules interact with a beam of highly energetic electrons that have typically been accelerated through a potential difference of 50–70 volts (V) across the volume of the ion source [50–70 electron volts (eV); 1 eV = 23 kcal]. This electron beam is produced by boiling electrons off a narrow strip or coil of wire made of a tungsten-rhenium alloy. Between the filament and the center of the ion source is a metal plate with a slit called the electron aperture. This slit limits the size of the electron beam and confines ionization to a small volume within the center of the ion source. Opposite the filament is the collector, a metal plate held at a positive electrical potential ($+V$ in Figure 1.2) that attracts and intercepts the electron beam after it has passed through the source. Surrounding the entire ion source

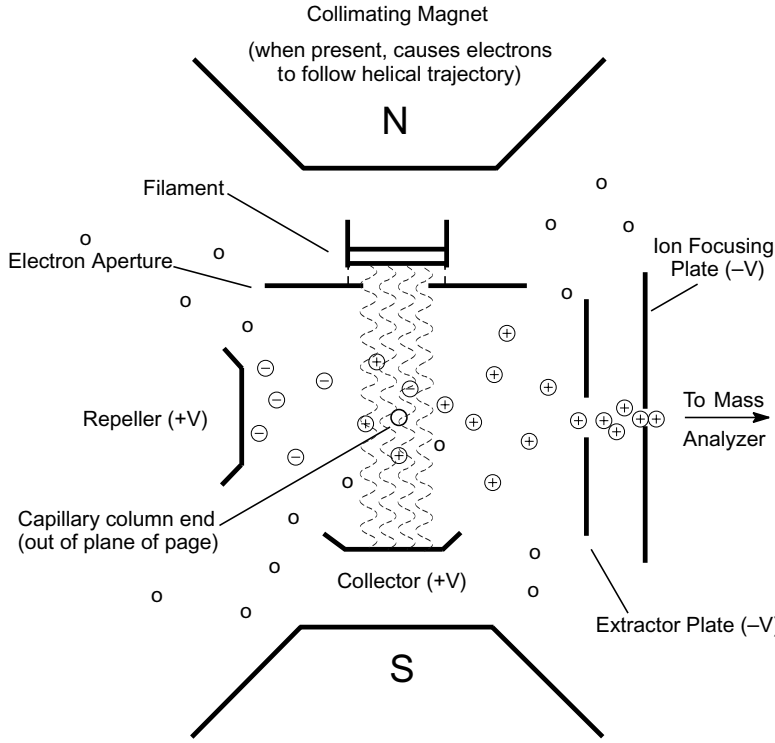

Figure 1.2. Schematic diagram of a typical electron ionization (EI) source. Samples can enter the source through a capillary GC column, a heated probe, or evacuated bulb through openings that are perpendicular to the plane of the page.

in some cases is a collimating magnet, which causes the electrons in the beam to travel in a helical path, as shown in Figure 1.2. Although this helical trajectory improves the probability that the electrons and molecules will interact, sample ionization is still very inefficient—less than one molecule in a thousand undergoes ionization.

What happens during ionization is complex. It is naïve to view electrons as literally smashing into sample molecules and knocking electrons out of orbitals. Instead, when an energetic electron approaches the electron density field of the molecule closely enough that sufficient energy is transferred quantum mechanically to overcome the ionization potential of the molecule, one electron is ejected from one of the bonding or nonbonding orbitals of the molecule (Section 3.3). Ionization energies (IE) for most organic compounds range from about 5–15 eV. Bond dissociation energies are even smaller, so this method of ionization not only causes molecules to expel one or more electrons, it also provides enough energy for substantial fragmentation of the first-formed ion (the molecular ion, $M^{+\bullet}$). Because of the excess energy present in 50–70 eV electrons, enough additional energy may be transferred to overcome the second, or even third, ionization potential of the molecule, leading to ions having +2 or +3 charges. The ionization process is discussed in more detail in Chapter 3.

Many different products form during ionization. Some of these are not positive ions. Table 1.2 lists the most important of these products. If the sample absorbs enough energy to raise an electron from the ground state to an excited state, but not enough to cause ejection of the electron, an "excited molecule" is formed (product *a* in Table 1.2). Excited molecules can return to their neutral ground state through thermal vibrations or the emission of light, and because no ions are formed in the process, they are simply pumped away from the ion source by the vacuum system.

DropBooks

Table 1.2. Types of ionization reactions

	a. Excited molecule (not detected)
	b. Negative ion formation (not detected by positive EIMS):
	$(A{-}B{-}C)^{-\bullet}$
	$(A{-}B)^{-} + C^{\bullet}$ and others
	c. Electron Ionization: $(\mathbf{A{-}B{-}C})^{+\bullet} + 2e^{-}$
	d. Dissociative ionization:
$e^{-} + (A{-}B{-}C) \rightarrow$	$A\cdot + (\mathbf{B{-}C})^{+} + 2e^{-}$
	$(\mathbf{A{-}B})^{+} + C^{\bullet} + 2e^{-}$
	$(A{-}B)^{\bullet} + \mathbf{C}^{+} + 2e^{-}$ and others
	e. Dissociative ionization with rearrangement:
	$(\mathbf{A{-}C})^{+\bullet} + B + 2e^{-}$
	$(A{-}C) + \mathbf{B}^{+\bullet} + 2e^{-}$
	f. Multiple ionization:
	$(\mathbf{A{-}B{-}C})^{2+} + 3e^{-}$
	$(\mathbf{A{-}B})^{+} + \mathbf{C}^{+} + 3e^{-}$ and others

Ions detected by positive ion EIMS are shown in boldface.

Sometimes the analyte molecule absorbs an electron and a negative ion is formed (Table 1.2, product *b*). In order to be absorbed by the molecule, the electron must be of very low energy (~0.1 eV), and there are few electrons of this energy in a standard EI source. By reversing the polarity of the repeller, ion focusing plate, and extractor plate in the ion source, and by altering the detector so that it will detect negative ions, a negative ion mass spectrum can be recorded. For most compounds negative ion MS offers few advantages over positive ion MS, and overall it tends to be less sensitive.[3] There are some specific applications, however, most notably with halogenated compounds. In this book only positive ion products and their fragmentations will be covered.

The remaining products listed in Table 1.2 are positive ions. The ion that is formed first results directly from ejection of a single electron from the neutral molecule (product *c*). This *molecular ion* ($M^{+\bullet}$) is very important because it has virtually the same mass as that of the analyte molecule (the small mass of the lost electron can be ignored). Indeed, mass spectrometry is one of the few analytical tools available for determining the molecular mass of a compound.

Ion products *d* and *e* in Table 1.2 are formed by unimolecular dissociation of $M^{+\bullet}$. In the first case a single bond is broken and a neutral group of atoms having an odd number of electrons (called a radical; see Section 3.1) is lost. The second process (dissociation with rearrangement) involves breaking some bonds while at the same time forming new ones. This results in expulsion of a fragment containing an even number of electrons, usually as a neutral molecule. The equations in Table 1.2 imply that such ions are formed in a concerted process in which ionization, bond making, and bond breaking all occur at about the same time. However, fragmentations that involve rearrangement of atoms usually occur in a stepwise fashion through one or more intermediates.

If more than one electron is ejected from the analyte molecule, ions having charges of +2, +3, or even +4 may be formed (Table 1.2, products *f*). Biopolymers such as peptides may have charge states of +10 or more from protonation of basic sites on the molecule. Since mass spectrometry actually measures the mass-to-charge ratio (*m*/*z*) of an ion, not its mass, an ion having a charge greater than +1 is found not at the *m*/*z* value corresponding to its mass (*m*), but rather at *m*/2, *m*/3, or *m*/4, depending on the number of charge states. Further, if *m* is not evenly divisible by the number of charges *z*, *m*/*z* will have a nonintegral value. For example, the double charged molecular ion (M^{2+}) of a compound having a molecular mass of 179 is found at *m*/*z* 179/2 = 89.5.

Most compounds do not produce multiple charge molecular ions in EI, but they may be formed in low abundance from small molecules that have few possible modes of fragmentation or from compounds with aromatic rings or large heteroatoms such as Cl, Br, or S. Mass spectrometers used for routine organic analysis

[3] A very sensitive and highly specific technique called resonance electron capture ionization (RECI) takes advantage of the low-energy electrons expelled during the EI of methane and results in the formation of negatively charged molecular ions ($M^{-\bullet}$).

often report m/z values only to the nearest integral mass, or they may report only one peak for each m/z value (Section 1.5.2). In such cases, detecting ions having nonintegral masses, even if they occur, is not always possible. Mass spectrometers with higher resolving power may be necessary to identify these ions with certainty.

The complex mixture of ionic and neutral products formed by any ionization method must be separated so that positive ion products travel in the direction of the m/z analyzer, and negative ions and neutral products are left behind. Neutral products are removed by the vacuum system, because the electric and magnetic fields present in the ion source have no effect on their motion. Positive and negative ions, on the other hand, can be separated by appropriately placed charged surfaces in the ion source (Figure 1.2). To accomplish this, the repeller is kept at a positive potential ($+V$) both to attract and neutralize negative ion products and to repel positive ions. Conversely, the extractor plate and ion focusing plate (the ion optics) are both kept at a negative electrical potential ($-V$) to attract and accelerate the positive ions toward the m/z analyzer. Slits in the extractor and ion focusing plates allow passage of the positive ions and help focus the ion beam as it approaches the analyzer.

When the filament is on and analyte molecules are flowing into the ion source, many reactive species are produced. Indeed, the intensity of the electron beam itself is sufficient to corrode metal surfaces in the ion source that are directly in its path—those on the electron aperture and collector. In addition, ion products may become electrically neutralized or undergo polymerization on the surfaces of the repeller, extractor plate, and ion focusing plate. Over time, the sensitivity of the instrument declines, as these surfaces are less able to maintain the potentials necessary for optimal ejection and focusing of positive ions from the source. Mechanical and chemical cleaning of the metal surfaces in the source is needed to restore sensitivity. The daily acquisition and evaluation of the spectrum of a standard compound whose ions' m/z values and abundances are known help determine when tuning and source cleaning are necessary (Section 1.5.1).

DropBooks

Keeping the filament off when high concentrations of sample are present in the ion source (especially while solvents are eluting during a GC run) allows the source to remain usable for several months without cleaning. Chemical ionization (CI) mass spectrometry (Section 1.2.2), which depends on the presence of high ion concentrations in the source, leads to the deterioration of ion source performance more rapidly than EI under normal circumstances.

1.2.2. Chemical Ionization

Unlike EIMS, in which molecules are ionized through interaction with high-energy electrons, ionization in chemical ionization mass spectrometry (CIMS) depends on collisions of ions and molecules. In positive ion CIMS the sample is ionized by reaction with ions generated within a large excess of a relatively low molecular mass reagent gas such as methane (as CH_5^+), isobutane [as $(CH_3)_3C^+$], or ammonia

(as NH_4^+), at a pressure of about 1 torr. Although some reagent gas ions are themselves formed by ion/molecule reactions

$$CH_4 + e^- \rightarrow CH_4^{+\bullet} + 2e^-$$
$$CH_4^{+\bullet} + CH_4 \rightarrow CH_5^+ + {}^\bullet CH_3$$

others are formed by unimolecular decomposition of the $M^{+\bullet}$, for example,

$$(CH_3)_3CH + e^- \rightarrow (CH_3)_3CH^{+\bullet} + 2e^- \rightarrow (CH_3)_3C^+ + H^\bullet$$

In CIMS the concentration of analyte molecules (at approximately 10^{-3} torr) is small compared to that of reagent gas molecules. Thus, the electron beam, which is more energetic than that used in EIMS (~200 eV), preferentially ionizes the reagent gas. Analyte molecules are ionized through reaction with reagent gas ions, rather than by the electron beam. Most reagent gas ions are strong proton donors and form protonated molecules (sometimes incorrectly called pseudomolecular ions) that have a mass 1 u greater than that of the molecular mass of the original compound[4]:

$$M + CH_5^+ \rightarrow MH^+ + CH_4$$

This type of ion formation (often called *soft ionization*) imparts significantly less energy to analyte molecules than do interactions with high-energy electrons, so that the resulting ions have little excess internal energy. These ions therefore fragment less than those formed by EIMS. As a result, although CIMS is useful for determining the molecular mass of compounds that do not produce a detectable $M^{+\bullet}$ by EIMS (see Figure 1.3), CI mass spectra may show an insufficient number of fragment ion peaks to yield structural information. The protonated molecules produced during CIMS can be induced to undergo fragmentation by combining CI with product-ion mass spectrometry/mass spectrometry (MS/MS; see Section 1.3.4.1). This technique yields structural information similar to that obtained by fragmentation of the $M^{+\bullet}$ in EIMS.

The interpretation of CI spectra, as well as spectra produced by electrospray and desorption ionization methods (Section 1.2.3), will not be covered in this book.

1.2.3. Other Ionization Methods

1.2.3.1. Electrospray Ionization. The conventional ion source shown in Figure 1.2 can be used for both EI and CI, provided the sample enters the ion source in the gaseous state. Although many organic compounds can be analyzed in this

[4] Some reagent gas ions may react with sample molecules by addition, rather than by proton donation. It is not unusual to observe weak intensity peaks at *m/z* values greater than that expected for the protonated molecule, corresponding to the addition of one or more reagent gas ions to the sample molecule. In some instances, CI can also result in hydride abstraction, thereby forming an $(M - H)^+$ ion, which has a mass 1 u less than the analyte molecule.

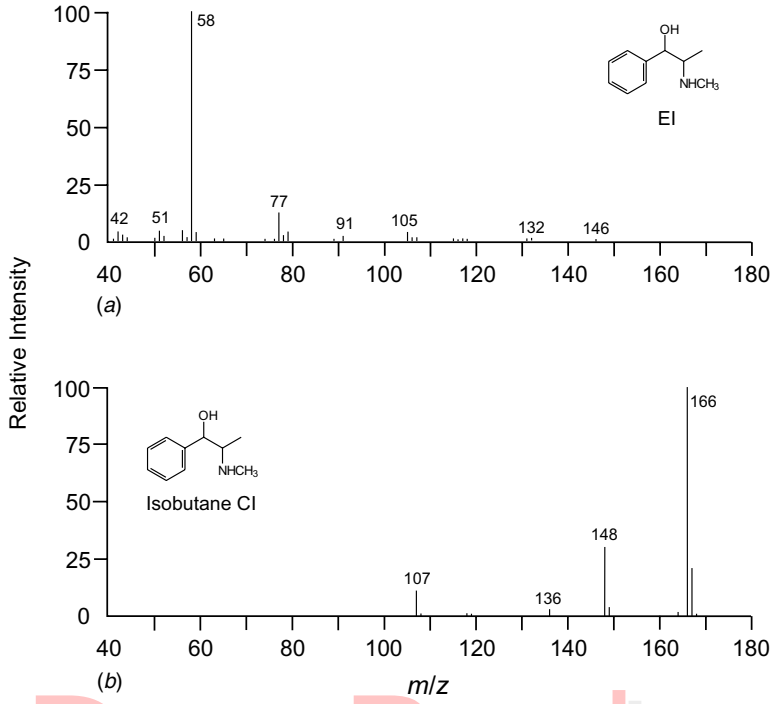

Figure 1.3. Mass spectra of ephedrine resulting from (*a*) EI and (*b*) chemical ionization (CI) using isobutane as the reagent gas (adapted with permission from Fales et al., 1975. Copyright American Chemical Society). The peak at *m/z* 166 in (*b*) corresponds to the protonated molecule.

DropBooks

manner, a large number of compounds, because of their inherent size and/or charge state, are nonvolatile or thermally labile. Many of these compounds are most easily separated by HPLC or CE, in which separation takes place in solvents that have an aqueous component. John B. Fenn and Koichi Tanaka shared the 2002 Nobel Prize in chemistry for their development of methods such as electrospray ionization (ESI) and desorption ionization in the analysis of large biological molecules.

The ESI source has allowed LC/MS and CE/MS to become routine analytical tools. Basically ESI works by converting the HPLC or CE effluent, already containing the sample in ionic form, into an aerosol and subjecting the resulting spray to high voltage in a chamber held near atmospheric pressure (Figure 1.4). This process creates a mist of charged droplets that flow toward the orifice of the capillary. In the configuration shown, the nebulizing needle, which creates the aerosol, is orthogonal (perpendicular) to the eventual direction of ion flow toward the *m/z* analyzer. Other geometric configurations are possible and have been used.

As the charged droplets travel toward the capillary opening, they are subjected to the counterflow of a drying gas, such as nitrogen (N_2), which causes evaporation of

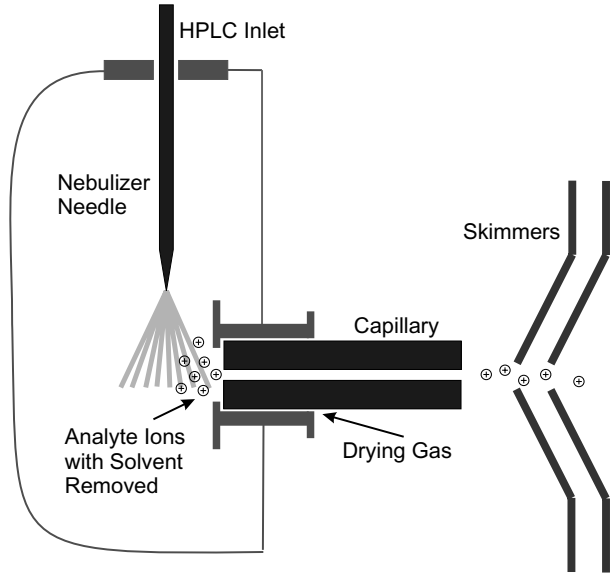

Figure 1.4. Orthogonal electrospray ionization source. Gas phase sample ions, which are desorbed from the condensed phase, exit toward the right into the *m*/*z* analyzer. (Copyright 2002 Agilent Technologies, Inc. Reproduced with permission courtesy of Agilent Technologies, Inc.)

solvent molecules from the droplets. Evaporation continues until electrostatic repulsions between the increasingly concentrated charges cause the droplet to break apart. Evaporation, charge concentration, and droplet disintegration continue until the analyte ions are finally desorbed into the vapor phase, passed into the sampling capillary, then on into the high vacuum of the *m*/*z* analyzer.

For the most part, the nature of the ions analyzed by ESI will be determined during the chromatographic run. At low pH, protonated molecules (sometimes protonated several times) will predominate. Because little additional energy is imparted to these ions in the ESI source, fragmentation is minimal (compare the EI spectrum in Figure 1.5*a* with the ESI spectrum of the same compound shown in Figure 1.5*b*). ESI thus offers an additional tool for determining the molecular mass of compounds that do not produce an $M^{+\bullet}$ by EIMS. As with CI, structural information about the analyte can be obtained by coupling ESI with MS/MS (Section 1.3.5.1).

ESI has a wide range of applications—from the analysis of low and medium molecular mass compounds (Figure 1.5) to large biomolecules such as intact proteins. High molecular mass molecules that have multiple sites for protonation will form multiple-charge ions that can be separated and detected by conventional mass spectrometers (remember that mass spectrometers measure the *m*/*z* of an ion, not its mass). Automation of HPLC equipment allows high sample throughput, which is used in the pharmaceutical industry, for example, to rapidly analyze large collections of closely related compounds that have potential as new drugs. Additional

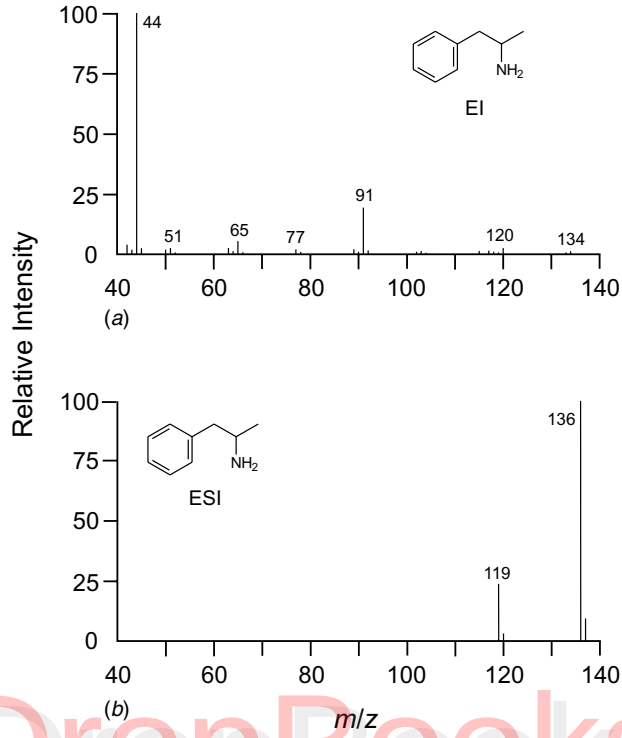

DropBooks

Figure 1.5. Mass spectra of amphetamine resulting from (*a*) EI and (*b*) electrospray ionization (ESI; figure adapted from Kataoka et al., 2000 by permission of Preston Publications, a division of Preston Industries, Inc.). The peak at *m*/*z* 136 in (*b*) corresponds to the protonated molecule.

information about ESI can be found in R. B. Cole's *Electrospray Ionization Mass Spectrometry: Fundamentals, Instrumentation and Applications* (see the References at the end of this chapter).

1.2.3.2. Desorption Ionization. Like ESI, matrix-assisted laser desorption/ionization (MALDI) has proven very effective for the analysis of some large biopolymers—especially when combined with a time-of-flight (TOF) mass spectrometer, which has an essentially limitless *m*/*z* range (Section 1.3.1). Laser desorption ionization occurs when the sample is irradiated with an intense beam of photons. Ionization and desorption are facilitated by mixing an aqueous solution of the analyte with an excess of a compound that enhances light absorption, then placing this mixture on a probe and evaporating the water. The exact mechanism by which ionization occurs is not fully understood. High sample throughput is possible by using as the "probe" a plate containing a large number of sample wells that can be sequentially irradiated and analyzed. The rapid spectral acquisition rates of TOF instruments allow analysis times of only a few seconds per sample.

Fast atom bombardment (FAB) is related to MALDI, although FAB uses a beam of energetic Ar atoms to induce ionization and desorption. MALDI has replaced FAB as a preferred ionization method for these large molecules.

1.3. m/z ANALYSIS

The mixture of molecular and fragment ions formed in the ion source contains information that would be lost were these ions not separated and identified in some meaningful way. In particular, the mass-to-charge ratio (m/z; in early literature, m/e) of each of these ions must be measured. To do this, the analyzer must be able to take advantage of some unique property of the ion that results from the imposition of an electrical or magnetic field. Although quadrupole m/z filters are commonly used in GC/MS and HPLC/MS, other types of m/z analyzers are currently used for both these and other applications. These include the time-of-flight (TOF) and magnetic sector analyzers, both of which played prominent historical roles in the development of mass spectrometry as an analytical tool, and the quadrupole ion trap (QIT). The TOF analyzer is a convenient example with which to begin because of the relative ease with which a mathematical connection can be made between physical motions of ions and their m/z values.

1.3.1. Time-of-Flight (TOF)

Ion separation in a TOF analyzer is based on the principle that ions which are given the same initial energy will have velocities that are proportional to their m/z values. In the ion source of a TOF instrument (Figure 1.6), ions of all m/z values are formed almost simultaneously using a very brief burst of energy from the filament. This method of ionization is called pulse ionization. These ions are then accelerated out of the ion source using a positive electrical potential V. From fundamental physics relationships, the potential energy given to each ion as it leaves the ion source is zV, where z is the charge on the ion ($=ne$, the number of charges times the charge on one electron). In the flight tube of the spectrometer, all of this energy is converted in the moving ion into kinetic energy ($=\frac{1}{2}mv^2$, where m is the mass of the ion and v is its velocity). The more massive the ion, the more slowly it travels.

The potential energy of each ion as it leaves the ion source must equal its kinetic energy when it reaches the detector, that is,

$$zV = \tfrac{1}{2}mv^2$$

The velocity of the ion during its journey through the flight tube is simply the length of the flight tube D divided by the time t it takes for the ion to travel this distance, so that

$$zV = \tfrac{1}{2}m(D/t)^2$$

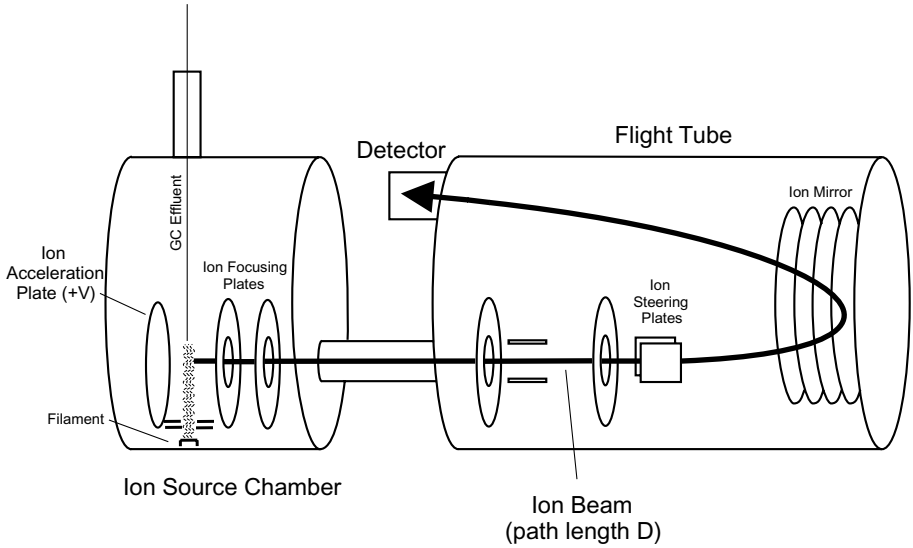

Figure 1.6. Reflectron time-of-flight (TOF) mass spectrometer. (Adapted with permission. Copyright LECO Corporation, St. Joseph, MI)

Solving for m/z leads to the mass spectrometric equation governing TOF mass spectrometry:

$$m/z = 2Vt^2/D^2 \tag{1.1}$$

In Equation 1.1, D is fixed by instrument design and V can be held constant electronically, so that m/z is proportional to the square of the travel time t. The mass spectrum is collected by plotting the signal output of the detector as a function of time, the latter of which can be converted to m/z values by the data system. Ions that differ in their flight times by as little as 1 ns can be recorded. As soon as the slowest-moving (highest m/z) ion is detected, another set of ions is formed and accelerated out of the ion source toward the detector. The range of m/z values over which the spectrum will be acquired must be selected with care, because ions having m/z values greater than the selected range will continue to drift toward the detector even though a pulse of new ions has been formed and accelerated.

TOF mass spectrometers have recently enjoyed a resurgence of popularity. Because the time between ion pulses in the source can be regulated as desired, TOF instruments can analyze ions having virtually any m/z value. Further, because the TOF mass analyzer detects essentially *all* the ions created in each ionization pulse (in contrast to many scanning analyzers; see below), it provides a very sensitive means of ion analysis and detection. When coupled with a pulsed laser ionization source such as MALDI (Section 1.2.3.2), TOF spectrometers have found widespread applications in the analysis of proteins, DNA fragments, and other

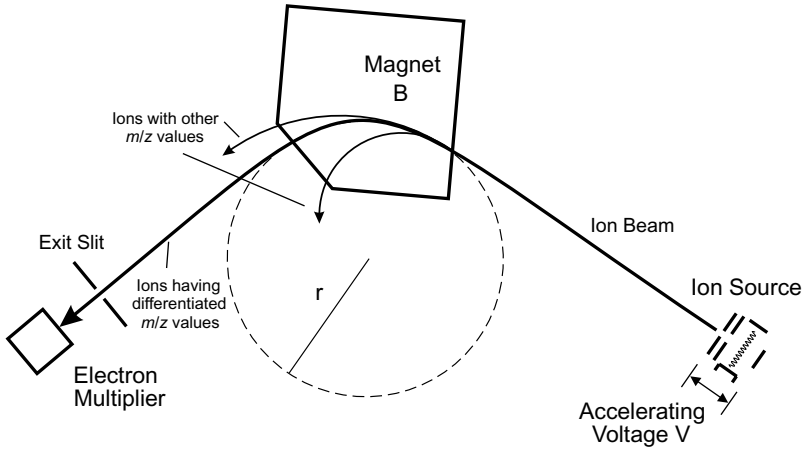

Figure 1.7. Magnetic sector mass spectrometer.

macromolecules with masses in the kilodaltons. R. J. Cotter's *Time-of-Flight Mass Spectrometry: Instrumentation and Applications in Biological Research* provides a more detailed description of TOF spectrometers.

1.3.2. Magnetic Sector

A schematic diagram of a typical magnetic sector mass spectrometer is shown in Figure 1.7. In contrast to the TOF spectrometer, ions are formed continuously in the ion source of the magnetic sector mass spectrometer and accelerated toward the detector by an electrical potential V. Once ions in a magnetic sector analyzer come under the influence of the magnetic field B, whose lines of force are perpendicular to the plane of Figure 1.7, they are constrained to travel along an arc of a circle whose radius is r. The mass spectrometric equation for this instrument can be derived from fundamental physics relationships using these variables.

In a magnetic field, an ion with mass m will experience a centripetal force (one pulling the ion toward the center of the circle) equal to Bzv, where B is a measure of the strength of the magnetic field, z is the charge on the ion, and v is the velocity of the ion. At the same time, any particle moving on a circle having a radius r experiences a centrifugal force (one pulling it away from the center of the circle) equal to mv^2/r. When these two forces are equal, the ion travels along an arc of the circle and

$$Bzv = mv^2/r \quad \text{or} \quad m/z = Br/v \tag{1.2}$$

If the velocity v were used to determine m/z, such an instrument would be essentially a TOF spectrometer, but another expression for v is available that can be substituted into Equation 1.2. Because the kinetic energy of the moving ion when it

reaches the magnet ($=\frac{1}{2}mv^2$) is equal to the potential energy ($=zV$) it had when it left the ion source (Section 1.3.1),

$$\tfrac{1}{2}mv^2 = zV \quad \text{or} \quad v^2 = 2zV/m$$

and

$$v = \sqrt{\frac{2zV}{m}}$$

When this expression for v is substituted back into Equation 1.2,

$$\frac{m}{z} = \frac{Br}{\sqrt{2zV/m}}$$

By squaring both sides and canceling like terms, the mass spectrometric equation for the magnetic sector analyzer is produced:

$$m/z = B^2r^2/2V \tag{1.3}$$

Since B, r, and V are all measurable quantities, the m/z of an ion can be determined without knowing its velocity.

In order to measure m/z and obtain a mass spectrum, two of the variables on the right-hand side of Equation 1.3 must be held constant. There are several ways of doing this in a magnetic sector instrument. In one case, both B and V are held constant. Under these conditions, ions having different m/z values pass through the magnetic field along paths with different values for r. Instead of an electron multiplier or photomultiplier detector (which only detects ions traveling along a single path of fixed radius r; see Section 1.4), a high resolution photographic plate or photodiode array is placed perpendicular to the paths of the ions after they have passed through the magnet. Under these conditions, the position at which an ion collides with the detector is related to its m/z value, and the mass spectrum is obtained by developing the photographic plate or analyzing the pattern of signals detected by the photodiode array.

A more common arrangement of the magnetic sector mass spectrometer holds V constant and requires a constant value for r by using a narrow slit and an electron multiplier or photomultiplier detector (as shown in Figure 1.7). By scanning through a range of values for B, ions of different m/z values sequentially attain the appropriate value for r, and then pass through the analyzer to the detector. At any given value of B, all other ions have different trajectories (i.e., different r) and collide with the inner surfaces of the spectrometer. This method of m/z separation, which involves continuous ion formation while scanning through a range of values for one variable, differs from the TOF. Instead of having nearly all the initially formed ions reach the detector, only a small fraction of the ions are allowed to pass through the analyzer at any given time.

DropBooks

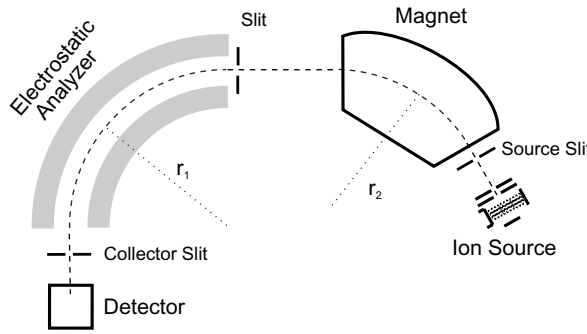

Figure 1.8. Double-focusing, high resolution mass spectrometer of the reverse Nier–Johnson geometry. The electrostatic analyzer focuses the kinetic energy of the ion beam as it emerges from the magnetic sector analyzer. This allows separation of m/z values that differ by less than 0.001. The m/z separation capability of the instrument is determined by the size of the slit openings.

Spectra can be acquired by scanning either from low to high m/z values, or vice versa. Some instruments acquire data in both directions. The rate at which a spectrum can be acquired (the scan speed) is limited by the ability of the magnet to respond to changes in field strength. Scan times of less than 0.1 s are achievable. The upper limit for the m/z range of a magnetic sector instrument is determined by the maximum field strength that can be reached.

A third way to achieve mass separation in a magnetic sector mass spectrometer is to hold B and r constant while scanning through a range of values for V. Although this type of instrument was commercially available at one time, problems with instrument stability, limited scan ranges, and arcing in the ion source prevented it from being successful. In fact, single sector magnetic sector mass spectrometers like that in Figure 1.7 are no longer commercially available. Magnetic sectors are now only found in double-focusing spectrometers such as the one in Figure 1.8. These instruments are capable of separating much smaller m/z differences than the magnetic sector instrument alone (Section 1.3.5.2).

1.3.3. Transmission Quadrupole

Quadrupole mass spectrometers, particularly when coupled with a GC, are the most widely used mass spectrometers in many types of organic analytical laboratories. As seen in Figure 1.9, the transmission quadrupole analyzer consists of four electrical poles (usually called rods) that are held in strict alignment with one another. Indeed, it is crucial that these poles remain parallel to and at a fixed distance from one another. Opposing poles are connected in pairs to both radio frequency (RF) and direct current (dc) generators, bathing ions in a combined electric and RF field during their passage through the analyzer. The output of the RF generator is energy in the radio frequency part of the electromagnetic spectrum. It can be pictured as a sinusoidal wave having a zero-to-peak amplitude U and a fixed frequency ω (the

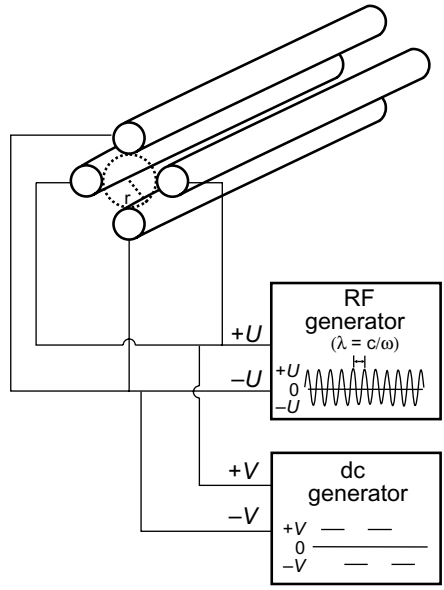

Figure 1.9. Transmission quadrupole analyzer. The RF generator produces a sinusoidal wave having a variable amplitude U and frequency ω that is held constant. The dc generator produces a voltage V that alternates in sign.

DropBooks

number of wave crests per second). The output of the dc generator is a pair of voltages, $+V$ and $-V$, the magnitude of which can be changed. The amplitude of the RF output can be changed even while the frequency is held constant.

In contrast to the mass spectrometric equations derived in previous sections for TOF and magnetic sector analyzers, those for quadrupoles are complex. Their complete derivation involves solution of the differential equations that describe the motions of ions in combined electromagnetic and electric fields. This derivation generates two combination variables a and q:

$$a = \frac{8zU}{mr^2\omega^2} \tag{1.4}$$

$$q = \frac{4zV}{mr^2\omega^2} \tag{1.5}$$

where

U = zero-to-peak voltage of the applied RF field
V = applied dc voltage
r = radius of the circle tangent to the inner surfaces of the quadrupole
ω = applied radio frequency
m/z = mass-to-charge ratio of the ion

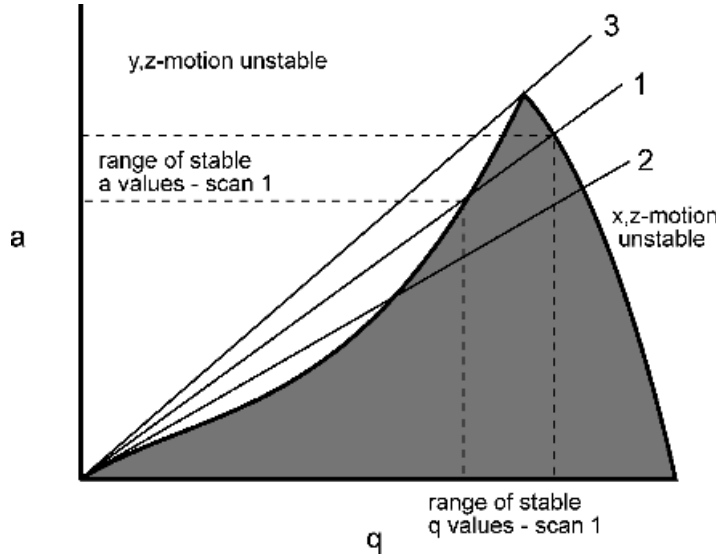

Figure 1.10. Stability diagram for quadrupole mass spectrometry. Choosing scan line 3 fixes values for *a* and *q* so that *m*/*z* varies as either of the voltages *U* or *V*.

It is important to recognize that *a* and *q* arise solely from solution of the differential equations and have no physical meaning in the instrument.

In these equations *r* and ω can be held constant (the former by physical design of the quadrupole and the latter by choice), but some further constraint must be added in order to determine *m*/*z* as a function of a single variable. To do this, *a* and *q* are chosen to be proportional to one another, so that

$$\frac{a}{q} = \frac{2U}{V} = \text{constant}$$

This is easy to accomplish instrumentally, because *U* and *V* can be controlled simultaneously through linked electronic circuitry. Once *a*, *q*, *U*, and *V* are interrelated in this manner, *m*/*z* varies with either *U* or *V*.

The relationship between all these variables and the determination of *m*/*z* can best be understood in terms of a plot of *a* vs. *q*, which is called a stability diagram (Figure 1.10). Actually, this figure shows only a small portion of the entire plot for all values of *a* and *q*; for reasons involving instrument design, only the part of the plot near the origin is normally used. The shaded area of the graph contains values for both *a* and *q* that define stable ion motion along the *z*-axis (the axis parallel to the four poles)—in other words, motion that allows ions to pass through the quadrupole to the detector. For other values of *a* and *q*, ions wander far enough from the *z*-axis that they collide with the poles and are removed from the ion beam.

The lines marked 1, 2, and 3 in Figure 1.10 are called scan lines. All scan lines in this plot are straight lines passing through the origin and having a slope *a*/*q* that is

fixed by the choice of $2U/V$ ($= a/q$) as a constant. The scan line that is used experimentally is determined by the smallest difference in m/z values (ΔM) that can be distinguished by the analyzer. For transmission quadrupoles ΔM is often set at about 1 m/z unit (referred to as *unit resolution*) over the instrument's entire range[5]. High resolution mass spectrometers that offer ΔM values of 0.001 or less are available (Section 1.3.5.2). Analyzers with $\Delta M > 1$ have only limited utility because individual masses are not distinguishable with these instruments.

Choosing scan line 1 in Figure 1.10 defines a range of values for a and q pairs (those lying along that line within the shaded area of the figure) that allows stable ion motion through the quadrupole at any instant. Because a and q are both related to m/z, all ions within the range of m/z values defined by that range of values for a and q pass through the poles at the same time. If the range of m/z values >1, m/z values for individual single-charge ions cannot be determined. If scan line 2 is chosen, the situation is worse because an even wider range of m/z values are allowed to pass at the same time.

The ideal choice, therefore, is scan line 3, which passes through the apex of the shaded area of Figure 1.10. Solving Equations 1.4 and 1.5 for m/z gives

$$\frac{m}{z} = \frac{8U}{ar^2\omega^2}$$

and

$$\frac{m}{z} = \frac{4V}{qr^2\omega^2}$$

DropBooks

By passing through a unique point of z-stable motion on this graph, scan line 3 fixes unique values for both a and q and thereby renders them constant. Because the values of r and ω were fixed during manufacture or installation, m/z then becomes dependent on only one variable—either U or V, since U and V are chosen to be dependent on one another. Thus,

$$m/z = kU \quad \text{or} \quad k'V \tag{1.6}$$

where k and k' are constants.

Equation 1.6 is convenient because m/z varies linearly with voltage, which is not only easy to control instrumentally but also can be varied rapidly over a scan with

[5] The term *resolution* is often used in MS. In general, *high resolution* spectrometers are those that can separate and detect ions having very similar m/z values. When $m/z < 500$, this usually means that ions differing by less than 0.001 unit can be distinguished. A *low resolution* spectrometer is one that can only distinguish ions differing by roughly whole m/z units. However, a *high resolution* instrument may only be able to distinguish integral m/z units when $m/z > 10{,}000$. The term $M/\Delta M$ is often defined as the resolution of the instrument, but it has also been defined as the resolving power, with the inverse term ($\Delta M/M$) defined as the resolution. In this book, the m/z separation capability of the instrument will be emphasized and the term resolution used sparingly.

little or no lag time between scans. In the Agilent Technologies Mass Selective Detector, a popular brand of benchtop quadrupole instruments designed for routine GC/MS work, the dc generator is scanned from approximately 0–200 V and the RF generator from about 0–1,200 V, producing a range of *m*/*z* values from 0 up to about 800. Like the magnetic sector analyzer, the quadrupole may be scanned from high to low values of *m*/*z*—which in fact is what happens in the Mass Selective Detector. The upper limit of the *m*/*z* range for most quadrupole GC/MS instruments is from 800–1,000, although instruments with ranges up to *m*/*z* 2,000 are used in LC/MS applications. This upper limit is determined by the RF wave, which becomes unstable after its amplitude is increased beyond a certain point.

Experimentally, the scan line that is used does not pass exactly through the apex of the stability diagram. Instead, by allowing a small range of *m*/*z* values through the analyzer at one time, the instrument is able to detect a larger number of ions and the sensitivity is improved.

Figure 1.11 illustrates how the chosen scan line applies to various *m*/*z* values during one spectral acquisition. At low values of *a* and *q* (and thus of *U* and *V*), the scan line passes through the apices of stability diagrams for low *m*/*z* ions, allowing their passage through the quadrupole. At the same values of *a* and *q*, the motions of higher *m*/*z* ions are unstable. As values for *a* and *q* increase, the scan line passes through the apices of stability diagrams for progressively higher values of *m*/*z*. These ions sequentially have stable motion through the quadrupole, and lower *m*/*z* ions do not.

A more thorough discussion of quadrupole analyzers may be found in Miller and Denton (1986), Leary and Schmidt (1996), and Henchman and Steel (1998).

1.3.3.1. Selected Ion Monitoring (SIM). One advantage of having *m*/*z* dependent on an easily controllable variable such as *U* or *V* is that the dc and RF generators

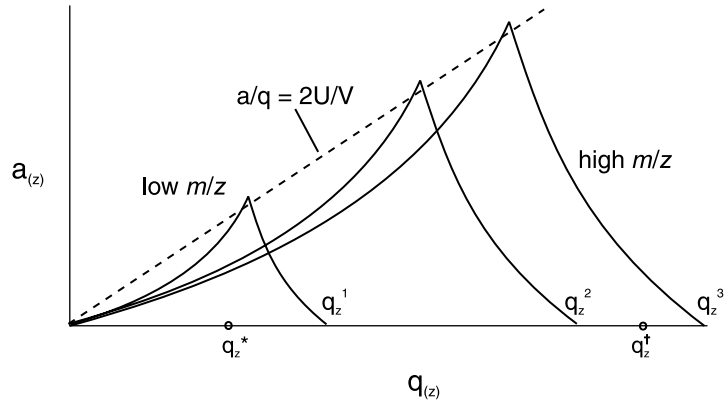

Figure 1.11. Stability diagrams for different values of *m*/*z*. The *z* subscripts are used when discussing the quadrupole ion trap (QIT; see Section 1.3.4). When the QIT is used for routine GC/MS analysis, $a_z = 0$, and only points along the q_z-axis are considered.

can be programmed to produce only discrete values for U or V. This process, called selected ion monitoring (SIM), allows ions having only specific m/z values to traverse the analyzer while all others are rejected. SIM offers enhanced sensitivity for detecting low concentrations of compounds in samples. Normally, when a transmission quadrupole repeatedly scans full spectra, most of the time is spent collecting information about m/z values for which few, if any, ions are formed by the compound in question. Thus, despite high concentrations in the ion source of fragment ions that are abundant in the spectrum, these ions pass through the analyzer for only very brief periods of time and, as a consequence, only a small fraction of them ever reach the detector. For example, if the analyzer scans from m/z 35 to 435, only 1/400th of the ions with each m/z value that were formed during the scan will be detected over this range.

In SIM the user selects a few ions (usually three) that are both abundant and characteristic of the compound's structure. By increasing the amount of time (called the *dwell time*) that the analyzer remains at a given value of U or V (and thus m/z), the fraction of these ions that reach the detector is increased. Whereas nanogram (10^{-9}) quantities of compounds normally can be detected using full-scan quadrupole mass spectra, SIM can sometimes lower the limit of detection into the picogram (10^{-12} g) range. SIM can also be performed using magnetic sector analyzers (Section 1.3.2) and quadrupole ion traps (see the next section). Instruments are now available that permit collection of both full-scan and SIM data during a single chromatographic run.

DropBooks

1.3.4. Quadrupole Ion Trap (QIT)

The quadrupole ion trap (QIT) that is shown in cross section in Figure 1.12 is related to the transmission quadrupole (March, 1997). The dome-shaped end caps and toroidal (roughly doughnut-shaped) ring electrode bathe the interior cavity with RF and/or electric fields. Although ions may be formed prior to their entering the QIT, ionization is most often provided by electrons emitted from a filament imbedded in the upper end cap and focused through an aperture in the end-cap surface. A similar opening in the lower end cap allows ions to reach the detector. As ions are formed, they do not "pass through" the analyzer as they do in the magnetic sector or quadrupole instruments, but rather are trapped in concentric, three-dimensional orbits according to their m/z values around the center of the ion trap.

The equations of motion for the QIT are almost the same as those for the transmission quadrupole, except that they relate to motion that is perpendicular to the surfaces of the end caps (here defined as the z-direction):

$$a_z = \frac{-8zV}{mr_0^2\omega^2}$$
$$q_z = \frac{4zU}{mr_0^2\omega^2} \tag{1.7}$$

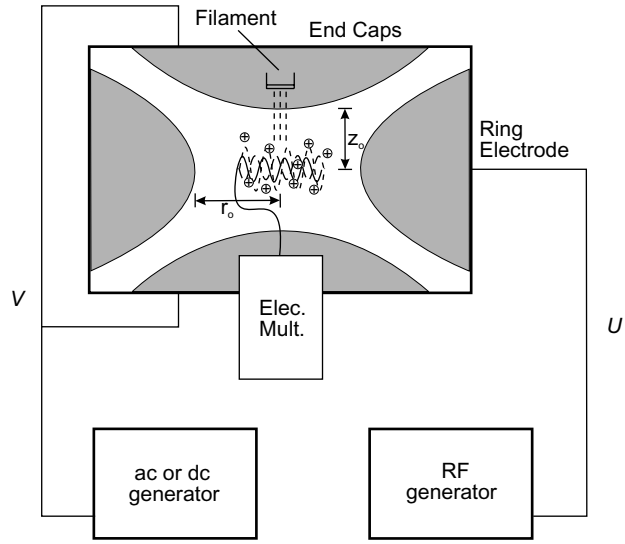

Figure 1.12. Quadrupole ion trap (QIT) mass spectrometer.

where

$V =$ dc (or ac) voltage applied to the end caps

$U =$ amplitude of the RF voltage applied to the ring electrode

$z_0 =$ distance from the closest approach of the end cap to the center of the ion trap

$r_0 = (\sqrt{2})z_0 =$ distance of closest approach of the ring electrode to the center of the ion trap

$\omega =$ applied radio frequency

As might be expected, the stability diagram for the QIT is virtually identical to that for the transmission quadrupole (Figure 1.10). For ordinary GC/MS work the dc generator in the end caps is not used, and ions are subjected only to an RF field. When $V = 0$ (i.e., the dc or ac generator is turned off), $a_z = 0$ and q_z is directly proportional to U at a given value of m/z. Because of this, only points along the q_z-axis need to be considered, and an ion having a particular m/z value will have stable motion in the QIT below some value of q_z (and thus of U) that is determined by the stability diagram for that ion (Figure 1.11). When U is set to a very low value, q_z will fall within the stable motion region for all ions except those having the smallest m/z values (q_z^* in Figure 1.11). Under these conditions most of the ions are thus ''trapped'' in complex motions in the center of the analyzer. At high values of U ($q_z^\dagger$ in Figure 1.11), only ions having large values of m/z will have stable motions.

For any given value of q_z, m/z is proportional to U:

$$\frac{m}{z} = \left(\frac{4}{r_0\omega^2 q_z}\right)U$$

As the instrument scans from low to high values of U, the motions of ions having progressively higher and higher m/z values develop larger and larger oscillations in the z-direction until they finally escape the trapped ion cloud and exit to the detector. To acquire a sequence of full-scan spectra, the QIT will:

1. Briefly turn on the filament and form ions (pulse ionization)
2. Trap most of the ions over a broad m/z range using a very low value for U
3. Sequentially destabilize ions by increasing U
4. Repeat steps (1) through (3)

A relatively high pressure of inert gas (usually 10^{-2}–10^{-3} torr of He) is used to dampen the motions of the ions so that they remain within their individual m/z orbits. This improves the ability to resolve adjacent m/z values.

Because a significant proportion of the ions formed in each pulse are available for detection over the scanned m/z range, the QIT is somewhat more sensitive in the scan mode than is the transmission quadrupole. Pulse ionization also keeps QIT spectra from exhibiting concentration-related spectral skewing while analytes are eluting from the GC (Section 1.3.6). Although its primary use has been for GC/MS, the QIT is in fact a versatile instrument. Its mass range can be extended to m/z 70,000 by a process called resonance ejection, which uses an ac, rather than a dc, generator attached to the end caps. In normal GC/MS use, the QIT provides m/z separation comparable to that of the transmission quadrupole, but it can also produce high resolution and MS/MS spectra (Section 1.3.5). A detailed discussion of these, and other, uses for the QIT is beyond the scope of this book.

DropBooks

1.1. In contrast to the transmission quadrupole and the magnetic sector analyzers, the QIT cannot be scanned from high to low m/z values. Why?

1.3.5. Other Types of Mass Analysis

1.3.5.1. Mass Spectrometry/Mass Spectrometry (MS/MS). The term MS/MS (also known as tandem mass spectrometry) refers to instruments in which two independent stages of m/z analysis are used. This type of analysis helps to establish the relationships between ions in a mass spectrum—for example, what ions are formed when the $M^{+\bullet}$ or other ions in the spectrum undergo fragmentation. This, in turn, helps to elucidate fragmentation pathways for the molecule being studied (de Hoffman, 1996) or, when used in conjunction with ionization techniques like CI and ESI that produce little fragmentation (Sections 1.2.2 and 1.2.3), to determine the structure of the analyte.

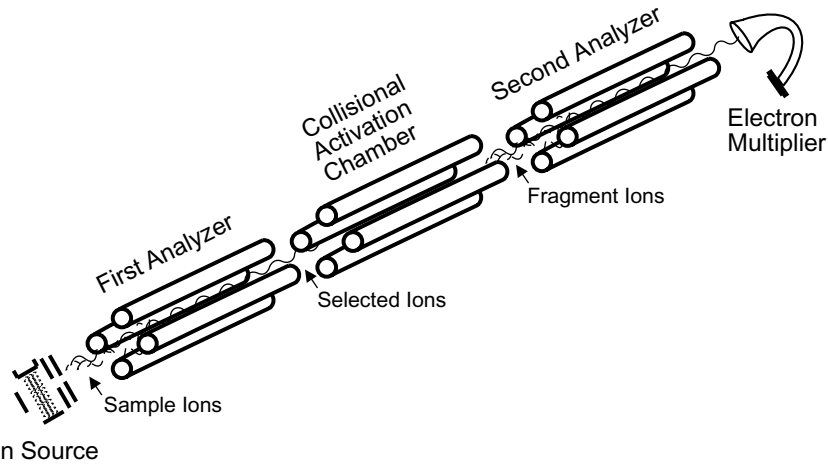

Figure 1.13. Triple-quadrupole (abbreviated QQQ) MS/MS in the mode for collecting product ion spectra. Voltages to the first analyzer are fixed to allow transmission of only a single m/z value. Collisions of these ions with an inert gas in the middle quadrupole cause fragmentation, the products of which are analyzed by scanning the second analyzer.

A typical analyzer array for doing MS/MS uses a linear arrangement of three quadrupoles between the ion source and the detector (the *triple quad*; see Figure 1.13). The first and the third quadrupoles act as independent m/z analyzers, while the second (middle) quadrupole acts as a collisional activation chamber through which ions from the first quadrupole must pass before they enter the final quadrupole. To obtain a product ion MS/MS spectrum, the first quadrupole (the ''first analyzer'' in Figure 1.13) is set to pass one or more ions of selected m/z value(s) (as in SIM, Section 1.3.3.1) into the collisional activation chamber. The ions thus selected are normally observed in the mass spectrum of the analyte and could be the $M^{+\bullet}$, a protonated molecule (MH^+), or any of the fragment ions produced by the compound. These m/z-selected ions are known as precursor ions.

The middle quadrupole is filled with an inert target gas at a pressure exceeding that normally found in either of the m/z-analyzing quadrupoles. When precursor ions pass through the middle quadrupole, collisions between these ions and gas molecules become likely. In these inelastic collisions, part of the kinetic energy of the precursor ion is converted into internal energy, which causes dissociation of the precursor ion. The middle quadrupole is also operated with only RF frequency applied to the poles, that is, $V = 0$ in Equation 1.5. As such, it acts as an ion-focusing device, conducting both precursor ions and the fragment ions formed from them into the final (third) quadrupole.

The last quadrupole (the ''second analyzer'' in Figure 1.13) is scanned over a range with its upper limit just above the m/z value of the precursor ion. The detector thus records a mass spectrum in which all the ions must have originated from the

precursor ion itself. This mass spectrum is called a product ion spectrum and provides a direct connection between a precursor ion and its fragments.

Product ion spectra have been recorded using instruments having virtually every combination of m/z analyzers, as well as with the QIT. In the case of the QIT, ion selection, collisional activation, and product ion analysis can be performed one after the other within the same chamber. Although the operational details differ from instrument to instrument, the basic description and premise of generating product ion spectra remain the same.

1.3.5.2. Accurate m/z Analysis. Mass spectrometers that measure very small differences in m/z values ($\Delta M \ll 1$) were mentioned previously. These spectrometers are often referred to as high resolution instruments. Accurate m/z measurements can be used to distinguish between ion elemental compositions that have the same nominal mass ($C_8H_5O_3^+$ vs. $C_9H_9O_2^+$ or $C_{11}H_{17}^+$, e.g., all of which have a nominal mass of 149; see Section 2.1.2). Several different types of instrumental arrangements can achieve accurate m/z analysis—a specially designed QIT (Section 1.3.4) has already been mentioned. Accurate m/z analysis is also possible with TOF and quadrupole analyzers, although in the latter case (Section 1.3.3), sensitivity may have to be sacrificed to achieve this.

More typically, accurate m/z analysis has been carried out using sector instruments such as the double-focusing instrument shown in Figure 1.8, in which the magnetic and electric sectors work in concert to correct for aberrations in ion optics. The value of ΔM achieved by the instrument is ultimately defined by the width of the slits along the ion path. Wider slits give higher ΔM values but higher ion throughput, whereas narrower slits provide lower ΔM values, but decreased ion transmission. Nonetheless, ion transmission through such double-focusing sector instruments is usually higher than through transmission quadrupole analyzers, and m/z values differing by less than 0.001 can be distinguished.

DropBooks

1.3.6. Spectral Skewing

With scanning m/z analyzers such as the magnetic sector or transmission quadrupole, the scan time may be slow enough that it affects the appearance of sequential spectra obtained during a chromatographic run. Because ions are being formed continuously in these instruments, the relative abundances of ions will not be reproducible from one scan to the next if the concentration of the analyte changes continuously during repetitive scans. This is especially a problem in capillary GC/MS, where analyte concentrations change rapidly with time over narrow GC peaks. Spectra obtained from different points on the GC peak may look quite different from one another, despite being from the same compound.

An example of this phenomenon is illustrated in Figure 1.14, which shows a narrow GC peak obtained during an analysis for Δ^9-tetrahydrocannabinol (THC) in marijuana. Notice that over 95% of the sample elutes within 0.06 min = 3.6 s. During this time the analyzer (in this case a transmission quadrupole) scanned through the range from m/z 35–400 eight times, a scan rate of 3.6/8 = 0.45 s

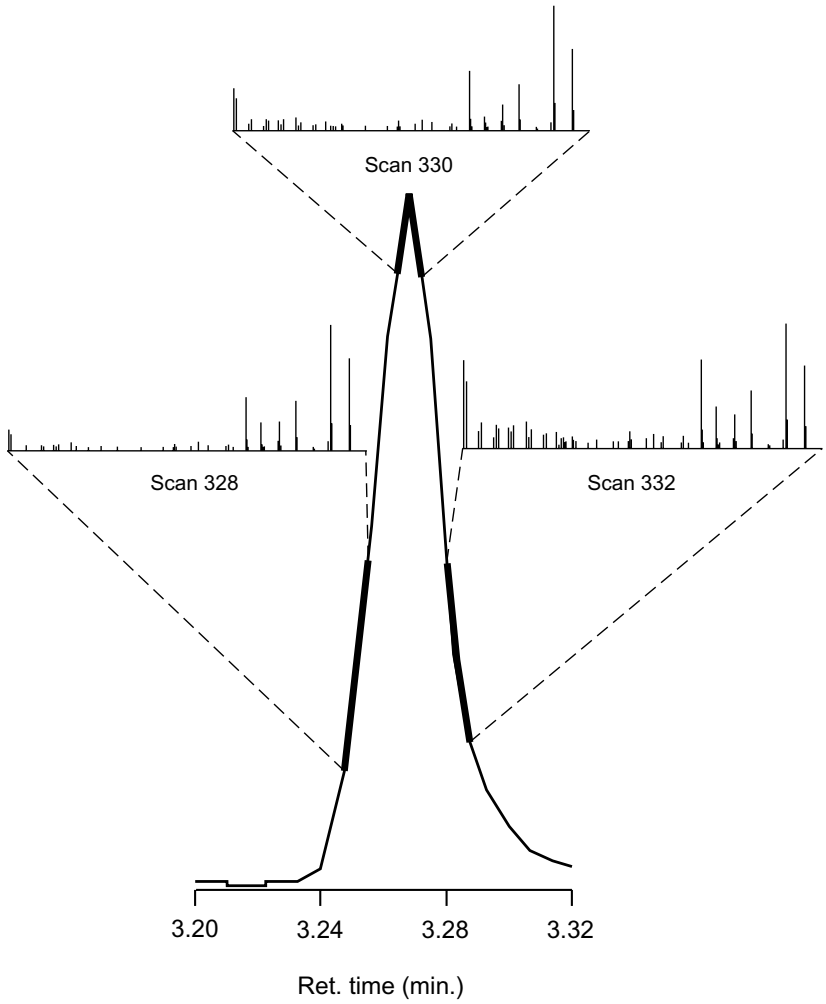

Figure 1.14. Variations in mass spectral peak intensities due to concentration differences over a narrow GC peak (spectral skewing).

scan^{-1}. As indicated by the heavy shading on the front and back sides of the peak, the concentrations of THC change by roughly a factor of 2 from the beginning to the end of the scan during scans 328 and 332. The result is that the spectra of THC obtained in scans 328 and 332 differ from one another—a phenomenon called spectral skewing. In scan 328 the high m/z peaks are intense compared to low m/z peaks, because the concentration of the analyte at the end of the scan is nearly twice what it was at the beginning of the scan. In scan 332 the low m/z peaks are more prominent because the analyte concentration was greater when those ions were detected. Scan 330, obtained at the top of the chromatographic peak, shows an intermediate situation.

The spectra shown in Figure 1.14 are obtained if the spectrometer is scanned from low to high *m*/*z* values. Under these conditions the low *m*/*z* ions in scan 328 reach the detector when the concentration of THC is relatively low, whereas the high *m*/*z* ions are detected when sample concentration is higher. In scan 332 the reverse is true. Since magnetic sector and quadrupole analyzers can also be scanned from high to low *m*/*z* values, you can convince yourself that the spectra obtained from scans 328 and 332 under these circumstances will be interchanged.

For GC peaks resulting from only a single component, the fact that the spectra change over the course of the peak is not a significant problem because the single scan over the crest of the peak, or a composite spectrum derived from averaging the spectra over the entire peak, will represent a "normal" spectrum for that compound. When two or more compounds coelute, however, the ability to obtain "clean" spectra of each of the compounds present (i.e., spectra lacking peaks due to the other coeluting substances) may be compromised unless spectra from the sides of the individual chromatographic peaks are used.

In theory, the data system should be able to eliminate contributions from unwanted background spectra, but selecting a good "background" spectrum for subtraction when chromatographic peaks overlap can prove problematic. For example, if the desired component elutes first, the concentration of the second component will still be increasing when that of the first has reached its maximum (Figure 1.15). The logical choice for a background spectrum, then, is the point

DropBooks

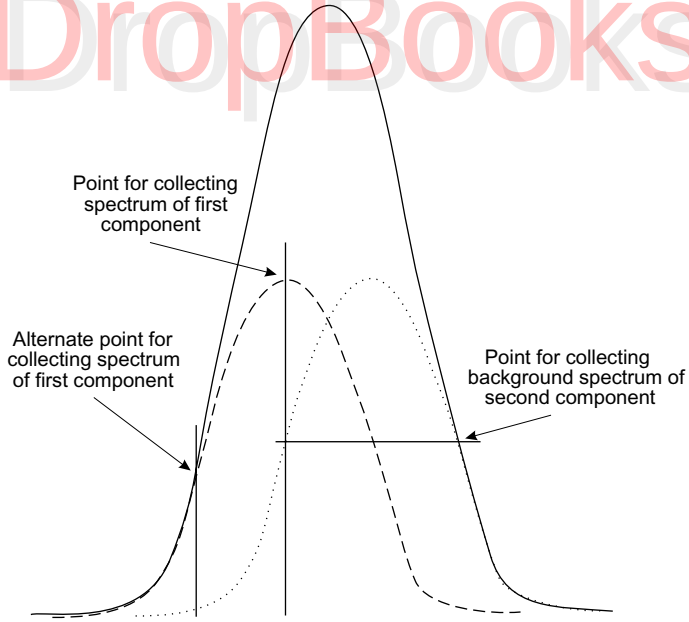
Point for collecting spectrum of first component
Alternate point for collecting spectrum of first component
Point for collecting background spectrum of second component

Figure 1.15. Coeluting GC peaks present a special problem for obtaining acceptable spectra of the individual components. Obtaining a "clean" spectrum may be limited to points on the back or front sides of the peak.

on the backside of the chromatographic peak for the second component where its concentration is approximately equal to that at the point where the spectrum of the first component was taken. However, the two spectra of the second component that are to be subtracted from one another *are not the same*, because the concentration of this compound is changing in opposite directions during the two scans. Thus, some residual peaks from the spectrum of the second component will remain in the spectrum of the first, despite background subtraction. The only way to eliminate peaks due to the second component may be to choose a spectrum of the first component on the front side on the first chromatographic peak—but in that case the relative intensities over the entire spectrum may not be representative of ''standard'' spectra for that compound.

Spectral skewing does not occur with spectrometers like TOF (Section 1.3.1) or QIT (Section 1.3.4) that use pulse ionization to produce ions, because pulse ionization forms ions in discrete packets that are subsequently analyzed for their *m*/*z* values. In the case of TOF, time intervals between spectra are also very short ($<$500 μs) when compounds of low molecular mass are analyzed. When ions are not formed continuously during each spectral acquisition, or when spectra can be collected in rapid succession, the changing concentration of the analyte will not significantly alter the relative intensities of the peaks observed in the acquired spectra. As a result, background subtraction with these instruments should produce spectra that are devoid of peaks from coeluting compounds.[6]

The reproducibility of rapidly acquired GC/TOF mass spectra is good enough that chromatographic resolution can be severely reduced without sacrificing mass spectral quality. This technique, known as fast GC, allows complex mixtures to be analyzed in a fraction of the time needed on slower scanning instruments.

Figure 1.16 shows part of the chromatogram from a 4-min GC/TOFMS analysis of naphtha—an analysis that may take up to an hour or more on a more traditional GC/transmission quadrupole MS. Mass chromatographic plots for characteristic ions (see Section 1.5.4) showed that at least four components elute under this single chromatographic envelope. After data acquisition the software sequentially compared adjacent pairs of spectra to see which peaks were increasing, and which were decreasing, in intensity. The retention time for each component was identified as the time when a whole set of peak intensities uniformly reached a maximum. All peaks not at maximum intensity at that instant were assumed to be those of other components and were subtracted from the spectrum. The resulting spectra of the four components are shown in Figure 1.17.

[6] The National Institute for Standards and Technology (NIST) offers a free computer program called AMDIS (Automated Mass Spectral Deconvolution and Identification System) that examines multiple component GC/MS chromatographic peaks from most commercial instruments and provides the spectra of the individual components. AMDIS can be downloaded from http://chemdata.nist.gov/mass-spc/amdis.

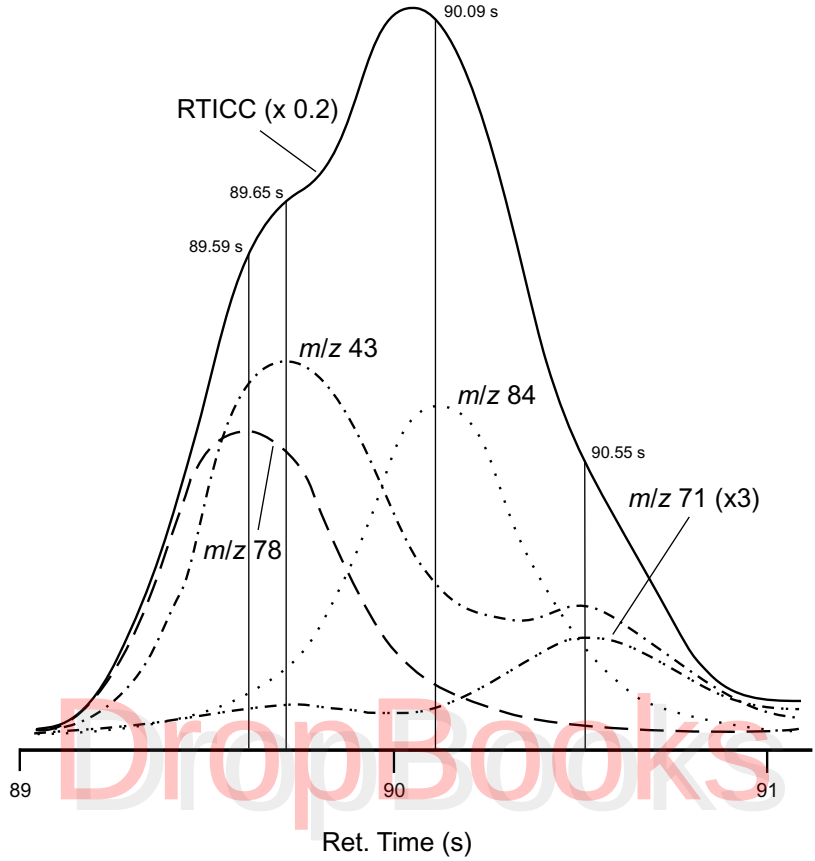

DropBooks

Figure 1.16. Complex chromatographic peak obtained from a 4-min fast GC analysis of naphtha. Individual ion chromatograms (mass chromatograms) indicate where four major components elute. Data were generated using Automated Unique Peak Find and Deconvolution software from a LECO Pegasus® II TOF mass spectrometer. (Data courtesy of LECO Corporation, St. Joseph, MI; adapted with permission)

1.4. ION DETECTION

Because the EI process is inefficient (Section 1.2), the number of positive ions that actually reach the detector is very small. Consider the capillary GC/MS analysis of a 100-ng sample of a compound having a molecular mass of 200 using a transmission quadrupole spectrometer. This sample, which is large for GC/MS work, contains approximately 3×10^{14} molecules. A spectrum acquired at the top of the GC peak may represent only 10–20% of the eluting material, lowering by a factor of 5–10 the amount available for ionization. Even if one molecule in 10^3 becomes ionized, only 10^{10}–10^{11} ions are produced at maximum sample concentration.

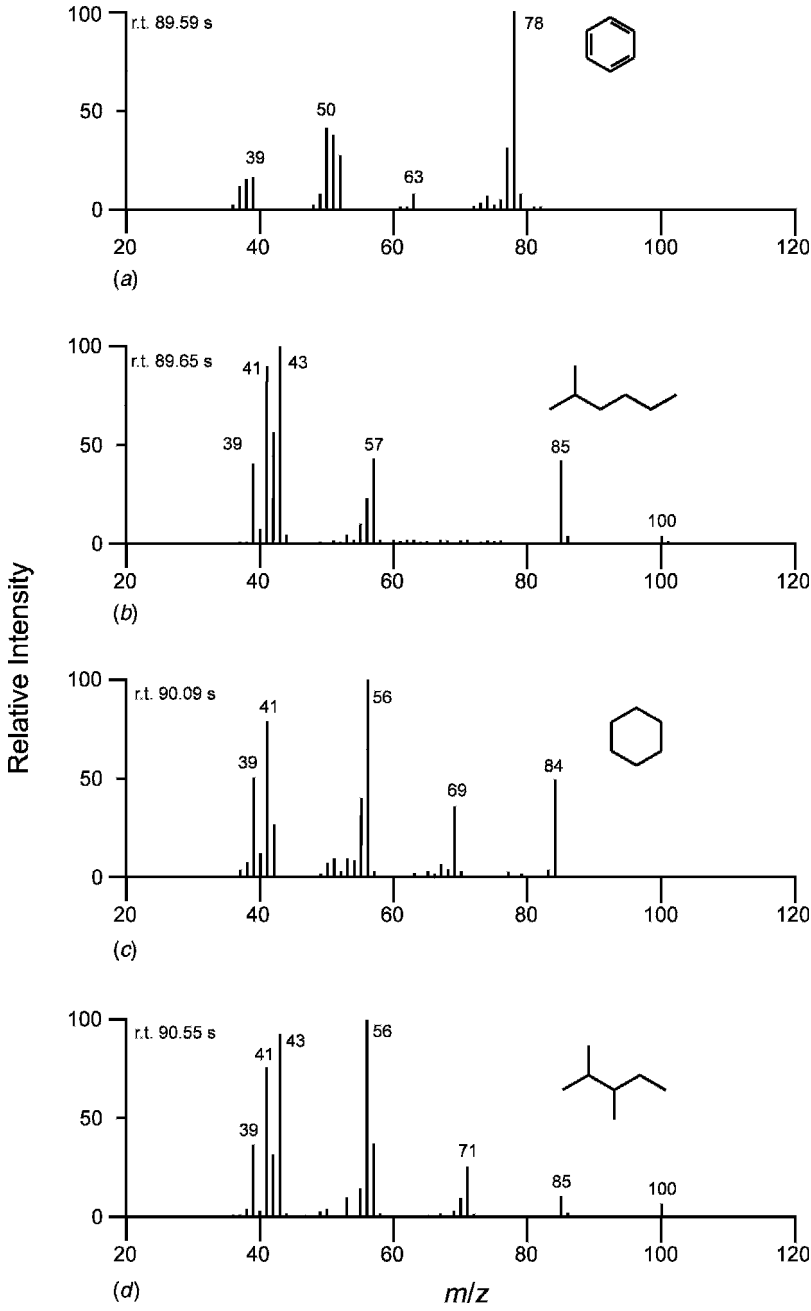

Figure 1.17. Mass spectra of four compounds eluting under the chromatographic peak shown in Figure 1.16. (*a*) Benzene, (*b*) 2-methylhexane, (*c*) cyclohexane, and (*d*) 2,3-dimethylpentane. (Data courtesy of LECO Corporation, St. Joseph, MI)

Further, in a scanning spectrometer most of these ions never make it to the detector, because the analyzer allows passage of only one m/z value at a time. If the instrument scans over a range of 300 m/z units, ions having any given m/z value pass through the analyzer only 1/300th of the time. This leaves a maximum concentration of $10^{14} \times 1/10 \times 1/10^3 \times 1/300 \approx 10^7$–$10^8$ of the most abundant ions (10^{-15}–10^{-16} moles) striking the detector during that scan. For a 100-pg sample, only about 10^4–10^5 ions will be observed. Because each ion carries a charge of only 1.6×10^{-19} coulomb (C), the current generated even under the best conditions will be very weak. Some means of amplifying the signal is clearly needed.

1.4.1. Electron Multiplier

An electron multiplier detector restores this lost sensitivity by exploiting the ability of surfaces that contain glass doped with about 10–20% lead oxide to expel more than one electron when a charged particle collides with it. Figure 1.18 shows a diagram of a continuous dynode electron multiplier, in which the entire surface of the multiplier is physically and electrically continuous. Other types of electron multipliers may have discrete dynodes or stages that are physically distinct but electrically connected to one another. Until recently, electron multiplier surfaces have been sensitive to air and especially sensitive to high concentrations of ions, so that venting the vacuum system when the multiplier is on, or leaving the filament on while the solvent is eluting during a GC run, could seriously damage the multiplier. With GC/MS, it is desirable not to measure ion current below m/z 10 because of the high concentration of He (m/z 4) or H_2 (m/z 2) in the ion source. Many users routinely do not acquire spectra below m/z 35 to avoid ions due to air and water background. Electron multipliers having less sensitive surfaces, as well as

DropeBooks

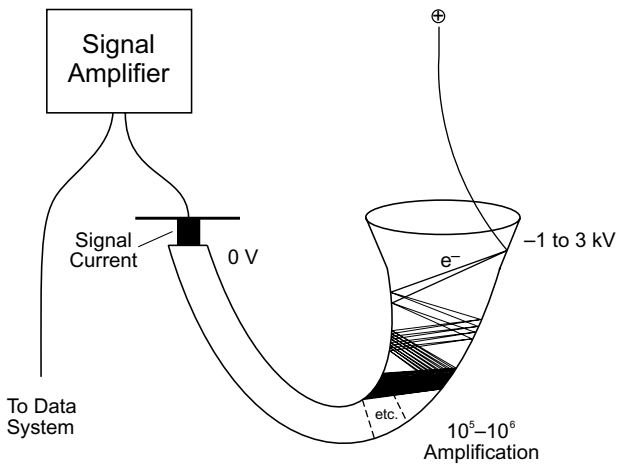

Figure 1.18. Continuous dynode electron multiplier detector.

photomultipliers (Section 1.4.2), are becoming more popular as detectors in MS because of their decreased sensitivity to such degradation.

The interior surface of the electron multiplier that is located near the entrance is held at a highly negative potential (usually -1.2 to -3 kV); the exit end is referenced to ground (0 V). As each incoming ion collides with the multiplier surface, approximately two electrons are ejected from the surface. To the ejected electrons the remaining interior of the multiplier appears more positive than the entrance does, so that they are attracted further into the multiplier where they collide with the interior surface. Each electron ejected by the second collision also results in the ejection of two electrons, and this process continues down to the exit or last dynode of the multiplier.

The total number of electrons ejected depends on the gain of the multiplier, which is roughly a function of the total potential difference between the entrance and exit to the multiplier surface. The gain can be adjusted daily during instrument tune-up so that a standard quantity of a reference sample such as PFTBA (Section 1.5.1) will produce approximately the same signal intensity. The total signal amplification is approximately 2^n, where n is the total number of collisions with the multiplier surface. Most multipliers provide about a 10^5- to 10^6-fold increase in signal—about 18–20 collisions. Electrons generated in the last collision with the multiplier surface constitute the signal current output of the multiplier. This current is sent to an external electronic signal amplification circuit and finally to the data system.

1.4.2. Photomultiplier Detector

Photomultipliers have been in use for a long time as detectors in radiation-based spectrometry such as IR and UV. Magnification of the signal in a photomultiplier is based on the same principle as that governing the electron multiplier, except that the inner surface of the photomultiplier is sensitive to photons rather than to charged particles. In order to use a photomultiplier as a detector in EIMS, the positive ions must cause the generation of photons that can be detected by the photomultiplier. This is accomplished by means of a fluorescent screen placed across the entrance to photomultiplier. As positive ions collide with the fluorescent screen, photons are produced in proportion to the number of ions present.

1.5. DATA SYSTEM

1.5.1. Instrument Tuning and Calibration

A mass spectrometer will produce no meaningful information if the analyzer does not satisfy the mass spectrometric equations given in Section 1.3. Once these equations are satisfied and a reasonable degree of m/z separation and sensitivity is achieved, each instrument also must be fine-tuned to adjust for the slight variations

that exist from unit to unit, as well as for changes in the ion source, analyzer, and electron multiplier surfaces that occur during routine use. Mass spectrometers should be tuned regularly if their performance is to remain optimal and reliable. Indeed, standards for good laboratory practice require that the instrument's tune be evaluated daily.

Tuning is accomplished by introducing a standard calibration compound into the instrument, and then adjusting variables until both the sensitivity and *m*/*z* separation are within acceptable limits. In many units this can be accomplished automatically by the data system with almost no user input. The most commonly used calibration standard for routine GC/MS work is perfluorotri-*n*-butylamine [$(CF_3CF_2CF_2\text{-}CF_2)_3N$; PFTBA], which gives fragment ions over the range from *m*/*z* 30 – 600 (see Problem 1.2). Prominent peaks at *m*/*z* 69, 219, and 502 in the spectrum of this compound can be used to adjust settings for instrument variables. Some laboratories prefer to tune manually using a compound that is frequently encountered during their analyses so that its mass spectrum is reproduced as closely as possible each day.

Usable sensitivity is achieved by adjusting both the voltage gain applied to the detector, which directly affects the intensity of the signal output, and voltages to various components in the ion source. The latter adjustments must be made because the metal surfaces inside the source change somewhat each time a sample is run. As more and more ions are formed, collisions with the source surfaces cause polymeric organic deposits to build up, leading to local variations in the electric fields present in the source. This interferes with both ionization and the movement of ions out of the source and into the analyzer. Tuning helps counteract the effects of these deposits.

DropBooks

After long-term use, ion source surfaces become so dirty that even tuning does not provide the necessary remedy. At this point the source has to be removed from the instrument, disassembled, and cleaned. Ironically, clean sources may need to be tuned more often than dirty ones since the amount of effective deposit on the surfaces increases dramatically at first, then tapers off after several samples have been run.

Achieving good *m*/*z* separation and peak shape is complex and cannot be done without some loss of sensitivity—the more restrictive the conditions for allowing ions through the analyzer, the fewer the number of ions that will be allowed through (Section 1.3.3). Peak shape and *m*/*z* separation are affected by variables in both the ion source and analyzer, and these must be adjusted against each other in order to obtain both acceptable *m*/*z* separation and sensitivity.

Once peaks of reasonable intensity having an acceptable degree of *m*/*z* separation are obtained, the *m*/*z* value of each peak must be determined. It is easy to forget that the MS/computer combination really is not very "intelligent"—that is, the MS can only provide information as either voltages or electric currents that must be interpreted by the computer through its software. Conversely, the MS will produce no meaningful results without intelligent direction. The interactions between the MS and computer during one mass spectral acquisition in a transmission quadrupole are shown in Figure 1.19.

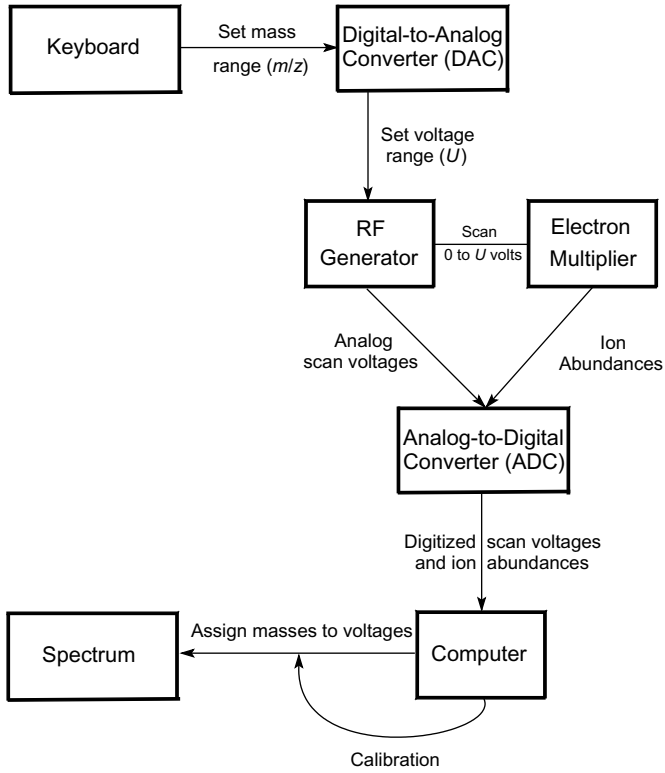

Figure 1.19. Interactions between the MS and computer during a scan.

The operator, through the computer keyboard or other input device, tells the MS the *m*/*z* range over which data are to be acquired and rate at which spectra are to be collected. This information is stored in digital form (i.e., having only distinct values) by the computer, but it must be converted to analog (continuously variable) form if it is to be used by the electronic circuits in the MS. This conversion is accomplished by means of a digital-to-analog converter (DAC)—an electronic circuit that takes the digital values provided by the computer and approximates the analog condition by causing small incremental ''steps'' to occur in the voltage circuitry.

During a typical GC/MS run, the computer, at a time determined by the operator, turns on the ion source and causes current to flow through the filament. The ions thus formed are separated repetitively by the analyzer over the assigned *m*/*z* range. Throughout this time the detector produces a variable signal current, the magnitude of which depends on how many ions of each *m*/*z* value there are at the time that ions having those *m*/*z* values are allowed to reach the detector. To be understood by the computer, the analog signal produced by the detector must first be converted to digital form by passage through an analog-to-digital converter (ADC).

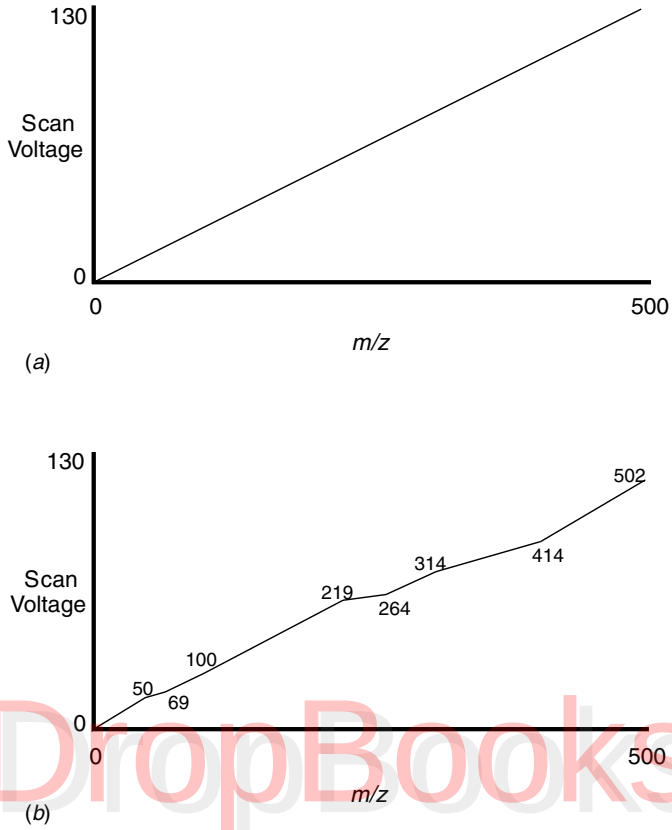

DropBooks

Figure 1.20. Mass spectrometers must be calibrated by direct assignment of analyzer variables to known *m*/*z* values. The situation for the quadrupole analyzer is shown here. (*a*) Theoretical scan of voltage vs. *m*/*z*. (*b*) Actual scan, in which the computer matches known *m*/*z* values for the calibration standard with observed voltages and interpolates between them.

The variable(s) used by the analyzer (time, magnetic field strength, RF voltage, etc.) to separate ions must be correlated to the output of the detector in order to produce the mass spectrum. If the *m*/*z* values of interest were related to analyzer variables in a completely reproducible manner (as they should be in theory; see Figure 1.20*a*, e.g.), the computer would have little difficulty assigning *m*/*z* values to each value for the analyzer variable and could produce the mass spectrum from those values and detector signal output alone. However, the relationship between these variables and *m*/*z* values is usually not ideal (see Figure 1.20*b*; the deviations in this figure are purposely exaggerated), so that the analyzer variables must be calibrated to correspond to known *m*/*z* values if the computer is to assign them correctly. With magnetic sector instruments, the relationship between *m*/*z* and the scanned variable is not linear (Section 1.3.2) and requires more closely chosen points in order to calibrate the *m*/*z* scale. Because time is the ''analyzer variable'' in TOFMS, these instruments can be calibrated using a single point.

Calibration is accomplished by obtaining the spectrum of a known standard. The calibration standard most commonly used for the analysis of compounds having molecular masses in the 10–700 range is PFTBA, the same compound used for tuning (see above). Other calibration standards include perfluorokerosene and homologs of PFTBA (with mass ranges up to about 900). The compound whose structure is shown below can be used up to *m/z* 3,000 (Fishman et al., 2001). Highly

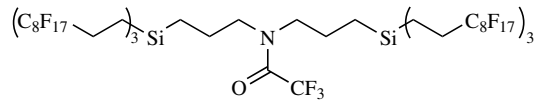

MM 2933

fluorinated compounds tend to make good calibration standards because they are more volatile than H-containing compounds in the same molecular mass range and produce ions having almost no mass defect (Section 2.1.2).

The known *m/z* values of the fragment ions of calibration standards can be preprogrammed into the computer, along with a range of probable analyzer variables that will produce these values. The computer then compares the observed values with those expected for the calibration standard and assigns the corresponding values for analyzer variables to the correct *m/z* values. Between these values for the observed fragment ions of the standard, the computer must interpolate. Although instruments should have their calibration evaluated on a daily basis to ensure correct *m/z* assignments, transmission quadrupole mass spectrometers tend to be very stable and may hold nearly the same calibration for weeks or months at a time.

1.5.2. The Mass Spectrum

1.5.2.1. Production of the Mass Spectrum. The output of the detector varies with time as ions of different *m/z* values are detected. The *m/z* values reaching the detector at any given time are related to the value of some instrument variable (e.g., magnetic field strength or voltage) at that moment. But what does a mass spectral ''peak'' really look like to the detector? Consider, as an example, an ion having an *m/z* value of 200.

It may seem at first as if all the *m/z* 200 ions strike the multiplier surface at the precise instant when the instrument variable allows passage of ions having *m/z* 200. However, when $\Delta M \sim 1$, there are several reasons why this does not happen. First, ions having the same *m/z* value have a small range of initial energies as they leave the ion source and thus are not expected to reach the analyzer and detector at exactly the same time. Second, at these values of ΔM, a small range of *m/z* values is permitted through the analyzer at any given time (Section 1.3.3), so that a few *m/z* 200 ions will begin to ''leak'' through the analyzer when the value of the appropriate variable corresponds to approximately *m/z* 199.5. As the value of this variable approaches that corresponding to *m/z* 200.0, the number of ions will increase, then taper off again as it approaches the value corresponding to *m/z* 200.5. If many *m/z* 200 ions pass through the analyzer at lower or higher values, they will overlap with the passage of *m/z* 199 or 201 ions, resulting in lower *m/z* separation.

In some cases, ions that have the same nominal *m*/*z* value, but differ in elemental composition, may be present at the same time. These ions will have slightly different exact *m*/*z* values (Section 2.1.2) and thus are not expected to pass through the analyzer at the same instant. For example, $C_{13}H_{27}OH$ has an exact mass of 200.2133, whereas $C_{15}H_{30}$ has an exact mass of 200.2340. This will lead to a small degree of peak broadening if $\Delta M \sim 1$. To detect both of these ions separately, ΔM must be decreased at least to 0.02 (Section 1.3.5.2). In that case, ions will not arrive at the detector until analyzer values correspond more closely to that of the exact *m*/*z* value of the ion. However, in no case will all identical ions reach the detector at precisely the same instant.

The mass spectral peak for the ion under discussion is a curve similar to a typical GC peak, having a maximum value at approximately *m*/*z* 200.0 (Figure 1.21) and a peak width that is determined by the *m*/*z* discrimination ability of the instrument. The actual *m*/*z* value of the maximum will usually differ somewhat from *m*/*z* 200.0 for reasons discussed in Section 2.1.2 (note the exact masses of the examples in the previous paragraph), but will usually not be lower than approximately 199.8 or greater than approximately 200.3 for most organic compounds.

In order for the data system to recognize this peak, it must identify a maximum signal coming from the detector during the time window when analyzer variables allow the detection of ions having *m*/*z* values from 199.5–200.5. In practice, this window of permissible *m*/*z* values is programmed to be from about 199.7–200.7 because, on average, the actual current maximum will occur at values slightly greater than *m*/*z* 200.0 (Section 2.1.2). The data system then assigns two values

DropBooks

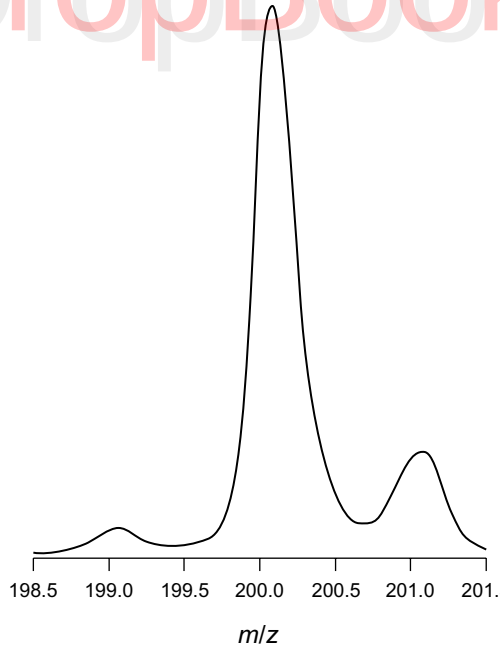

Figure 1.21. Mass spectral "peak."

to these data—one identifying the *m/z* value, the other quantifying the amplitude of the maximum signal produced by the detector during that window. Some data systems assign only the nearest integral *m/z* value to the maximum, so that any peak in the *m/z* 199.7–200.7 window would be labeled *m/z* 200. Others report the maximum more accurately, sometimes to the nearest 0.05 *m/z* value.

Most data systems used with spectrometers having $\Delta M \sim 1$ do not assign more than one signal maximum per window. In these cases, multiple charged or metastable ions (Section 3.6.2) that occur at fractional *m/z* values will not be identified separately if they are located between two more intense single charged fragment ions at sequential *m/z* values.

The mass spectrum, then, consists of the collection of *m/z* values and the corresponding values for detector signal maxima that are obtained during the windows for the analyzer variable that define those *m/z* values, over the entire range of *m/z* values for which data are acquired. It is customary to assign the value of 100% to the largest of all the ion current maxima obtained during the acquisition of an individual spectrum and to report the remaining values relative to this figure. The largest peak in the mass spectrum (100% relative intensity) is called the *base peak*. Although it is easy to think of the base peak as fixed for the mass spectrum of any given compound, it is, in fact, dependent on the displayed *m/z* range. For example, if the spectrum of an intermediate molecular mass, primary aliphatic amine is acquired (and displayed) from *m/z* 10–300, the base peak in the spectrum will nearly always occur at *m/z* 30 (Section 6.3). If the spectrum is only acquired (or displayed) from *m/z* 35–300, however, the peak at *m/z* 30 will not be reported, and some other peak in the spectrum, depending on the structure of the compound, will appear as the base peak.

Graphically, *m/z* values are plotted along the horizontal axis and relative peak intensities along the vertical axis. The mass spectra shown in the illustrations in this book are in this form. The same data may be presented in tabular form, such as that in Table 1.3 (compare this with the graphical presentation in Figure 1.22). Although the graphical presentation is more visually instructive, the tabular

Figure 1.22. Graphic presentation of the mass spectrum of Δ^9-tetrahydrocannabinol that is given in tabular form in Table 1.3.

Table 1.3. Tabulated mass spectrum of Δ^9-THC

m/z	Rel. Int.	*m/z*	Rel. Int.	*m/z*	Rel. Int.	*m/z*	Rel. Int.
36.85	0.19	64.05	0.67	86.15	0.39	108.10	6.31
39.05	7.57	65.05	4.25	88.15	0.25	109.10	2.75
41.05	33.58	66.05	1.30	89.05	1.31	110.00	0.32
42.15	2.39	67.05	9.27	91.05	11.27	111.10	0.39
43.05	26.97	69.05	8.03	92.05	1.92	112.00	0.25
44.05	1.11	70.15	0.66	93.05	4.96	113.10	0.58
44.95	0.17	71.05	1.73	94.05	1.11	115.00	6.72
50.05	0.35	72.05	0.19	95.05	6.88	116.10	1.68
51.05	2.01	75.05	0.36	96.05	0.84	117.10	2.46
52.05	1.09	77.05	8.67	97.05	0.57	118.10	0.69
53.05	5.51	78.05	2.54	98.05	0.32	119.10	4.39
54.15	0.89	79.05	6.30	99.15	0.35	120.10	1.48
55.05	9.98	80.15	1.42	100.75	1.25	121.10	4.44
56.05	1.51	81.05	9.77	102.15	0.82	122.10	2.77
57.05	1.81	82.05	1.19	103.00	2.33	123.10	3.40
58.05	0.27	83.05	1.37	104.10	0.89	124.10	1.32
59.05	0.67	84.15	0.49	105.00	5.65	125.00	0.26
62.05	0.23	85.15	0.29	106.10	1.61	126.10	0.40
63.05	1.03	86.15	0.25	107.10	6.31	127.10	2.24
128.10	5.62	148.10	1.03	167.10	0.95	186.05	1.16
129.00	3.63	149.10	1.82	168.10	0.98	187.05	5.57
130.00	1.00	150.00	0.81	169.10	1.54	188.05	2.34
131.10	2.73	151.10	0.92	170.10	0.75	189.15	1.65
132.10	0.91	152.10	2.92	171.05	1.91	190.15	1.21
133.10	2.09	153.10	2.44	172.05	1.02	191.15	1.35
134.00	1.43	154.10	1.12	173.05	3.62	193.05	8.60
135.10	1.97	155.10	1.47	174.05	8.21	194.15	1.40
136.10	1.22	156.10	0.83	175.05	4.60	195.05	1.33
137.00	1.40	157.10	2.23	176.05	1.89	196.15	0.73
138.10	0.43	158.10	1.36	177.05	1.07	197.05	1.90
139.00	0.57	159.10	2.27	178.05	1.29	198.05	1.09
141.10	3.38	160.10	2.36	179.05	0.76	199.05	3.23
142.10	1.47	161.10	3.51	180.05	0.53	200.05	2.08
143.10	1.51	162.10	0.90	181.05	1.88	201.05	6.42
144.00	1.41	163.10	1.56	182.05	1.09	202.15	2.19
145.10	2.76	164.10	0.63	183.05	1.78	203.15	1.07
146.10	0.82	165.10	3.60	184.05	0.79	204.15	0.30
147.10	4.39	166.10	1.29	185.05	1.95	205.05	0.55
206.25	0.32	224.15	0.45	246.10	3.41	274.20	0.21
207.15	1.70	225.15	1.03	247.10	0.67	281.20	0.52
208.05	0.43	226.15	0.59	253.10	0.31	282.20	0.20
209.05	0.55	227.15	1.57	254.20	0.23	283.20	0.72
210.15	0.54	228.15	1.34	255.10	1.09	284.20	0.43
211.05	1.42	229.15	2.59	256.20	1.08	285.20	3.03

DropBooks

Table 1.3 (*Continued*)

m/z	Rel. Int.	*m/z*	Rel. Int.	*m/z*	Rel. Int.	*m/z*	Rel. Int.
212.15	0.95	231.15	46.22	257.20	7.02	286.20	2.16
213.05	2.78	232.15	10.54	258.20	21.89	287.20	0.49
214.15	1.93	233.15	4.27	259.10	4.62	295.20	0.30
215.15	3.88	234.15	0.55	260.10	0.71	297.20	5.96
216.15	1.15	239.15	0.36	267.10	0.25	299.20	100.00
217.15	6.79	240.10	0.50	268.20	0.19	300.20	22.01
218.15	1.47	241.10	1.16	269.10	0.96	301.20	2.46
219.15	0.88	243.10	27.41	271.20	38.45	314.15	70.52
221.15	3.39	244.10	6.00	272.20	9.38	315.25	16.83
222.15	0.69	245.10	3.21	273.20	1.52	316.15	2.46
223.25	0.30						

presentation often contains additional information that is not readily apparent from the graphic display.

Not every *m/z* value is represented in Table 1.3 or in any other mass spectrum. In fact, no organic compound can produce fragment ions at every *m/z* value. In addition, to minimize the number of spurious "noise" peaks that occur in all spectra, the data system often applies a threshold value for detector output below which peaks will not be reported. In Table 1.3 the threshold appears to be approximately 0.1% of the size of the most intense peak.

1.5.2.2. Terminology: Ions vs. Peaks. It is important to distinguish between the terms *ions* and *peaks* in mass spectrometry. Ions are particles that have both mass and charge, and they can fragment to form other ions. There can be large or small numbers of ions, so that it is appropriate to speak of their relative *abundance*. On the other hand, peaks in a mass spectrum correspond to localized maximum signals produced by the detector and have only *m/z* values associated with them. These signals are either weak or strong (depending on the numbers of ions produced) and therefore are best described as having *intensity*. The abundance of peaks implies that there are many peaks, not that a given peak is big or little.

The previous section described how the ions that are produced inside the spectrometer are recorded as spectral peaks. In that sense, the peaks in the spectrum represent the ions formed by the compound in question. However, the correspondence of ions to peaks is often not one to one. When $\Delta M \sim 1$, two or more ions that have nearly the same *m/z* ratios cannot be distinguished by the detector and thereby give rise to a single peak that represents all these ions. Throughout this book an attempt will be made to distinguish between the peaks that are observed in the mass spectra and the ions that those peaks represent.

1.5.3. Library Searches

Although the computer can perform many data reduction and manipulation routines, the identification of an unknown mass spectrum by comparison against

a collection of spectra stored in the computer is one of the most useful. This library search is a very powerful tool because it accomplishes in a few seconds what might take the operator many hours or more to perform manually. It is important to remember, however, that library searches are not foolproof.

Computer libraries may contain either full or condensed spectra—the latter being spectra that contain only the most meaningful (characteristic) peaks for each compound. The number of peaks retained in condensed spectra can vary from 10–50, depending on the search program. In practice, very little is sacrificed by using condensed spectra (McLafferty et al., 1999).

Spectra used in library searches may be weighted in order to give increased importance to peaks at higher m/z values. These peaks are usually more characteristic of the compound in question than those at lower values. A common weighting factor is the square root of the m/z value, so that

$$\text{Weighted intensity} = \text{observed intensity} \times \sqrt{(m/z)}$$

In the probability-based matching (PBM) algorithm, developed by Fred McLafferty of Cornell University, individual uniqueness and abundance factors are assigned to various peaks in each spectrum (McLafferty et al., 1974). Like the weighting factor above, the uniqueness of the peak increases logarithmically with its m/z value.

The library search can be performed either as a forward search or as a reverse search. The forward search algorithm compares the weighted unknown spectrum with similarly weighted library spectra. This comparison is often made by treating each m/z value/weighted intensity pair as a vector originating at the origin. The vectors for all the peaks in the unknown spectrum are added, and the result is compared with a similarly summed vector generated from the peaks in each library spectrum. The relative degree of ''match'' between these vectors reflects the relative similarity between the spectra (Stein and Scott, 1994). In a reverse search, each spectrum in the library is compared with the unknown spectrum to allow for the possibility that the unknown mass spectrum might actually be a mixture of spectra. If the data system has access to more than one spectral library, the algorithm may be set up to search all the libraries sequentially and provide a composite list of search results.

DropBooks

Library search programs have obvious strengths: rapid comparison of an unknown spectrum with up to several hundred thousand standards; the possibility of compound identification even when the spectrum is not that of a pure compound; and relative insensitivity to the types of instruments (but *not* to the type of ionization) on which the spectra were obtained.[7]

However, a high correlation (high *match index* or *probability of match*) between an unknown spectrum and a library spectrum does not necessarily mean that the unknown has been identified unequivocally. This point cannot be overstated. *The*

[7] Although most search algorithms will correctly identify spectra from different instruments or obtained under different conditions, the best matches will be obtained from spectra run on your instrument under your conditions.

criteria needed to identify an unknown by mass spectrometry must include a visual comparison of the unknown and library spectra by the analyst and may also demand additional information such as a comparison of GC retention times.

There are several reasons why this is so. First, similar structures often give spectra that are not easily distinguished by library search (or even visually, for that matter). Optical isomers cannot be distinguished at all, and other stereoisomers may be distinguishable only if enough spectra are acquired to determine that minor differences are repeatable. Even positional isomers (see Figure 1.23, e.g.) may not be identifiable with complete certainty by mass spectrometry alone.

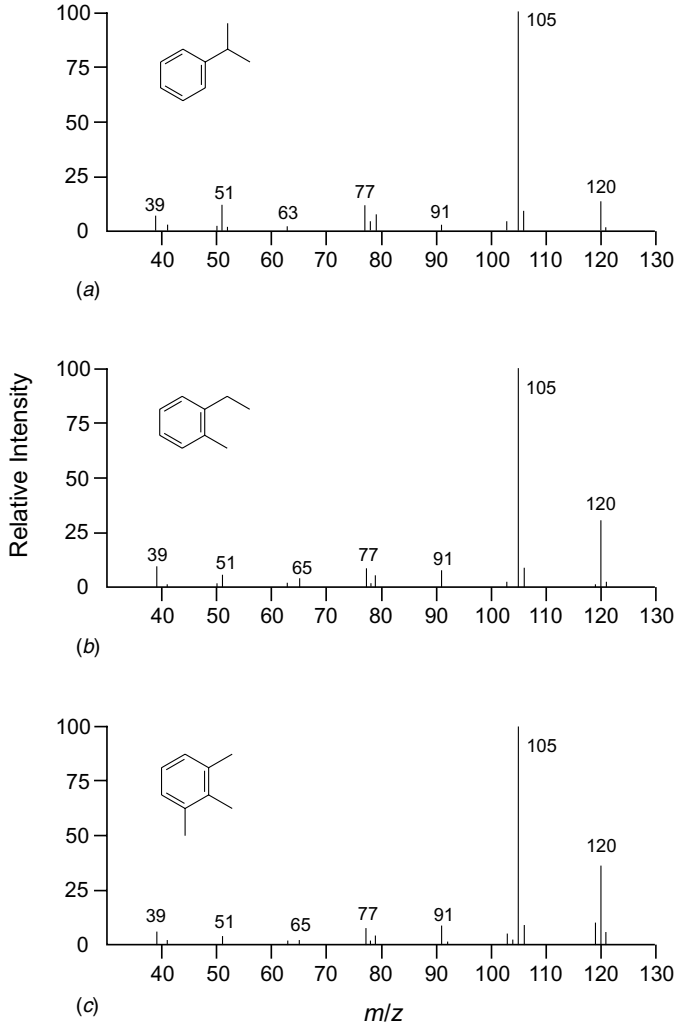

Figure 1.23. Mass spectra of these positional isomers are so similar that they may not be distinguishable at all. (*a*) Isopropylbenzene, (*b*) 2-methylethylbenzene, and (*c*) 1,2,3-trimethylbenzene.

```
PBM Search of library C:\DATABASE\DRUGS.L

    Name                                    MolWt  Formula    Qual
1.  Phenol, 4-[2-(methylamino)propyl-         165  C10H15NO    40
2.  Ephedrone (Methcathinone)                 163  C10H13NO     9
3.  N-Methyl-3,4-Methylenedioxyamphetamine    193  C11H15NO2    9
4.  1-Phenyl-2-butanamine                     149  C10H15N      9
5.  Butanedioic acid, salt with N,N-dimeth    388  C21H28N2O5   4
```

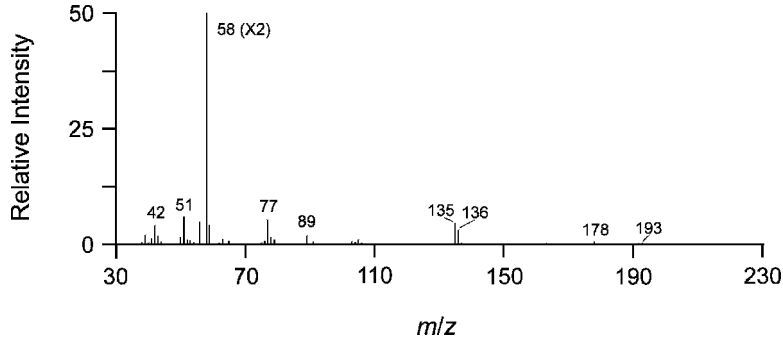

Figure 1.24. Mass spectrum of *N*-methyl-3,4-methylenedioxyamphetamine (MDMA) obtained during analysis of an illicit drug sample. The correct match is not listed first in the search results, in spite of the fact that the spectrum matches well with the standard (Figure 9.2*b*). All the compounds listed in the search results produce intense *m*/*z* 58 peaks.

DropBooks

Second, some search algorithms are more discriminating among certain types of compounds than others. The PBM algorithm, in fact, has such difficulty discriminating among certain aliphatic amines that the "correct match" may not appear at the top of match list, if it appears at all (Figure 1.24). Even with spectra containing several characteristic high *m*/*z* peaks, this search may fail to produce a viable match candidate under some circumstances (Figures 1.25*a* and *b*).

Third, search algorithms may fail to match spectra that are run on different types of instruments, particularly if ionization of the compound is achieved in different ways. Spectra that are produced by "soft" ionization methods such as CI (Section 1.2.2) or ESI (Section 1.2.3.1) cannot be compared directly with EI spectra.

Even though the search algorithm may show strong correlations between the unknown and one or more library spectra, the library may not contain the correct match for the unknown spectrum. Further, if the spectrum is not "clean" (i.e., numerous peaks due to extraneous materials are present), search results may identify the impurities rather than the unknown. Finally, although editors of mass spectral databases have become more and more critical of the spectra that are included in their libraries (Ausloos et.al., 1999), errors occur just often enough that it should give any user pause. *Never just assume that the library spectrum is correct!* Indeed, one of the purposes of this book is to give you tools that will

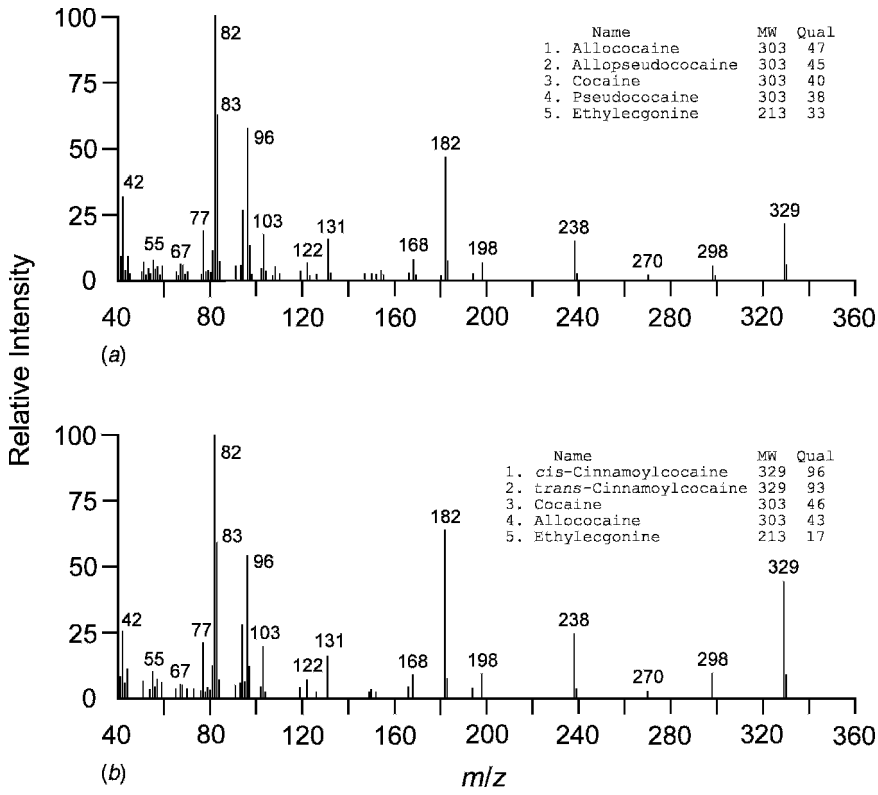

Figure 1.25. Mass spectra of *cis*-cinnamoylcocaine obtained from two different, but otherwise similar, samples. The correct match does not even appear in the search results for the upper spectrum (*a*), while the lower spectrum (*b*) is correctly identified using the same search algorithm.

help you evaluate whether a given spectrum reflects the assigned chemical structure or not.

If the library search fails to identify an unknown spectrum by direct match, software is available to help the user develop structural characteristics about the compound. Probably the best known of these programs is the Self-Training Interpretive and Retrieval System (STIRS) developed by McLafferty et al. (Kwok et al., 1973; McLafferty and Stauffer, 1985). This interactive program compares spectral features of the unknown, such as losses from the $M^{+\bullet}$, characteristic peaks, and series of peaks at low *m*/*z* values (Section 4.2), to those of compounds contained in a large library. If the unknown spectrum shares several features in common with a class of compounds in the library, the program indicates that the unknown probably contains a certain structural feature which is found in this class of compounds. If

STIRS identifies several probable structural features in the unknown, the analyst may be able to determine its overall structure.

More widely available is MS interpretation software from the National Institute of Standards and Technology (NIST) in association with the NIST/EPA/NIH Mass Spectral Library. This program identifies peaks that may result from simple cleavage of the $M^{+\bullet}$ and generates isotopic intensity patterns for ions whose elemental compositions are consistent with the proposed structure. A demonstration of this software is available at http://www.nist.gov/srd/nist1a.htm.

1.5.4. Using the Data System to Analyze GC/MS Data

Even before sophisticated data collection and manipulation software began to appear commercially, the combination of GC and MS revolutionized the analysis of complex mixtures. Because many of the readers of this book will (or already do) work in laboratories where GC/MS is an important method of sample analysis, it is worthwhile to explore how the data system can be used in the analysis of sample mixtures. Alternate data handling methods for other highly complex mixtures are given in Sections 1.3.6 and 4.2.5.

As an example, consider an unknown solid brought to a forensic laboratory for illicit drug analysis. To minimize sample workup, a small portion of the solid was dissolved directly in methanol, and 1 μL of this solution was injected onto a 10-m phenylmethylsilicone (HP-1) capillary column. The GC oven was programmed (via the data system) to begin the analysis at 160°C, increase the temperature from 160–280°C over a 6-min period, and then remain at 280°C for an additional minute. During the same time interval, the MS was programmed to (1) keep the filament and electron multiplier *off* for 1 min while the methanol was passing through the GC column (Sections 1.2 and 1.4); (2) acquire spectra repeatedly from *m*/*z* 35–350 at a rate of about 0.5 s $scan^{-1}$ for the next 3 min; and (3) scan repeatedly from *m*/*z* 35–400 for the remainder of the analysis.

DropBooks

By acquiring data continuously in this way, the MS acts as an elaborate GC detector. In fact, one way to report GC/MS data is as a reconstructed total ion current chromatogram or RTICC, which is a plot of the total ion current output of the detector for each mass spectral acquisition over the time required by the analysis. These plots are sometimes also referred to simply as total ion current chromatograms (TICC) or just total ion chromatograms (TIC). In the RTICC for this sample (Figure 1.26), the ion current intensity reflects the total number of ions produced in each spectrum (Section 1.4). The RTICC looks like chromatograms produced by other GC detectors, but because MS measures a different property of the analytes than other detectors do, the same sample mixture can produce somewhat different chromatograms by MS and by other common detectors such as flame ionization (FID).

The advantage of using MS as a GC detector is that the computer stores the data from the analysis not as total ion current, but rather as a collection of sequentially acquired mass spectra. Therefore, these spectra can be retrieved one at a time, and the makeup of the GC effluent at any given time during the run can be identified.

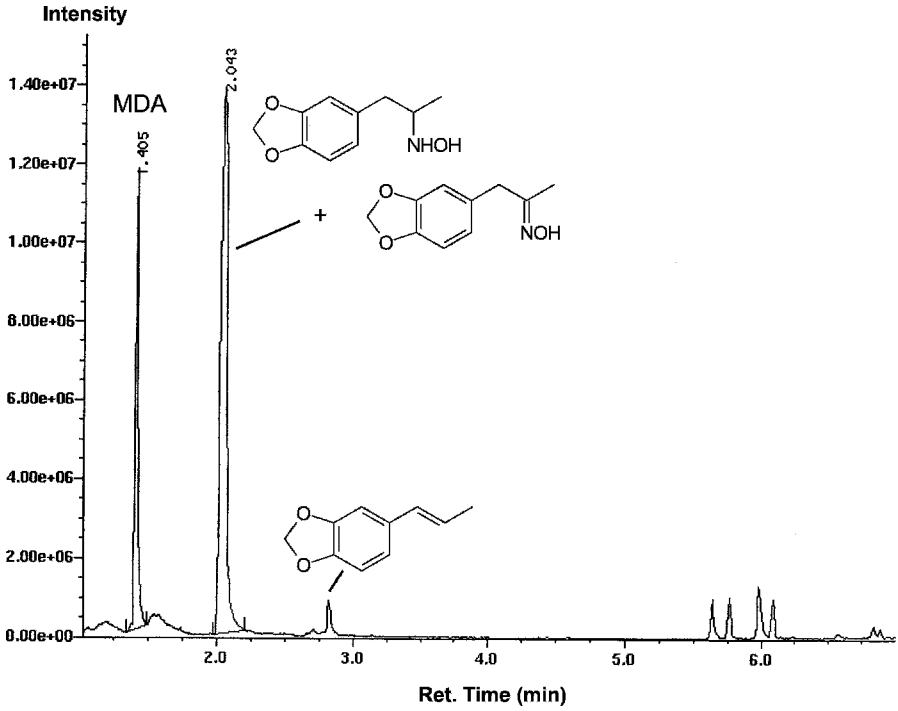

Figure 1.26. Reconstructed total ion current chromatogram (RTICC) generated from mass spectral data collected during analysis of an illicit drug sample.

Using the software available with most GC/MS units, spectra can be retrieved simply by having the operator move the cursor on the monitor to the point on the RTICC that requires investigation, then press "Enter" on the keyboard, or click a mouse button. For single-component GC peaks, an acceptable spectrum can be obtained either by placing the cursor at the top of the chromatographic peak or by asking the data system to average several spectra from the top of the peak (Section 1.3.6). The data system can subtract from this spectrum background that is reasonably constant over the peak by choosing a point near the front (or back) base of the chromatographic peak or by averaging background spectra from the same area(s). Background subtraction may not be necessary if the GC peak is intense and background from substances bleeding off the GC column or septum (commonly called *column bleed*) is minimal.

Such a process produced the spectra in Figures 1.27*a* and *d*, which were identified by library search and visual confirmation by the analyst as 3,4-methylenedioxyamphetamine [with a retention time (r.t.) of 1.405 min] and 1-(3,4-methylenedioxyphenyl)propene (with a r.t. of 2.8 min). 3,4-Methylenedioxyamphetamine (MDA) is a hallucinogenic drug (Section 9.2) and 1-(3,4-methylenedioxyphenyl)

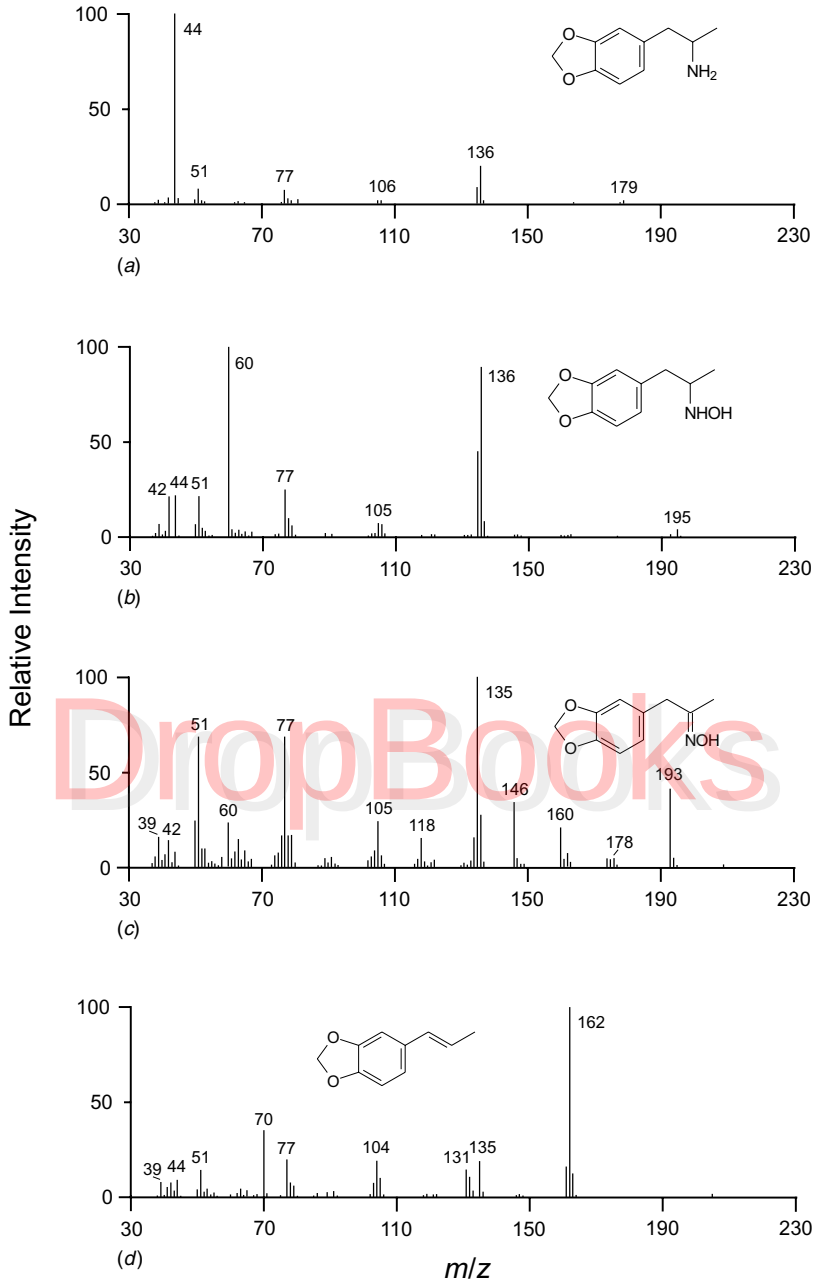

DropBooks

Figure 1.27. Mass spectra of four components found in the illicit drug sample whose RTICC is shown in Figure 1.26. (*a*) 3,4-Methylenedioxyamphetamine (MDA; r.t. 1.40 min), (*b*) *N*-hydroxy-MDA (r.t. 2.02 min), (*c*) 1-(3,4-methylenedioxyphenyl)-2-propanone oxime (r.t. 2.05 min), and (*d*) 1-(3,4-methylenedioxyphenyl)propene (r.t. 2.81 min).

propene is an intermediate produced during one of the common syntheses of MDA and its analogs.

Similar treatment of the large, broad chromatographic peak at r.t. 2.04 min led to a spectrum that was much like the one shown in Figure 1.27*c*, except for the addition of a few small peaks—most notably that at *m*/*z* 195. This component was identified by library search as 1-(3,4-methylenedioxyphenyl)-2-propanone oxime, which was an unexpected result because IR analysis of the solid identified only the presence of *N*-hydroxy-MDA. Further examinations of individual spectra indicated that two different compounds were coeluting under this chromatographic peak.

In order to produce an acceptable spectrum for each of these compounds (one not contaminated by peaks from the other), the elution time of each component had to be determined (see Section 1.3.6 and Figures 1.15 and 1.16). Although mathematical deconvolution can be done even in the absence of MS data (Stein, 1999), the data already collected in this case contained enough information to generate the desired result. The mass spectra of the two coeluting compounds (Figures 1.27*b* and *c*) each contained intense, characteristic peaks not present in the other—in particular, the base peak (*m*/*z* 60) in the spectrum of the first-eluting compound and the relatively intense $M^{+\bullet}$ peak (*m*/*z* 193) in the spectrum of the second.

Plots of the intensities of only these two characteristic peaks—a process known by a variety of names including mass chromatography and reconstructed ion chromatography (RIC)—are shown in Figure 1.28 for the small window of time between r.t. 1.75 and 2.27 min. Mass chromatography differs from selected ion monitoring (SIM; see Section 1.3.3.1) in that the mass chromatogram is generated *after collecting continuously scanned mass spectral data* for the entire chromatogram. In SIM, ions must be selected prior to sample injection. A mass chromatogram can be generated for any *m*/*z* value in the acquired range, but no data are available in SIM for any *m*/*z* values other than those monitored during the analysis.

Figure 1.28 makes clear that, although the two compounds elute less than 2 s apart and with a considerable amount of overlap, it is possible to obtain spectra of both compounds that have little contamination due to peaks from the other. The spectrum of *N*-hydroxy-3,4-methylenedioxyamphetamine (*N*-hydroxy-MDA; see Figure 1.27*b*) was obtained from the upper front side of the peak in the *m*/*z* 60 mass chromatogram, at a point corresponding to the base of the peak in the *m*/*z* 193 chromatogram. The spectrum of the oxime (Figure 1.27*c*) was obtained at a point just beyond the top of the *m*/*z* 193 mass chromatogram where the first compound had stopped eluting (Figure 1.28).

These results indicate that *N*-hydroxy-MDA had undergone partial disproportionation to MDA and the oxime in the injection port of the GC. This is an important point to consider: Even when the mass spectra obtained from the sample are of high quality, there is no guarantee that they represent the actual composition of the original sample. Instead, they may arise as an artifact of some aspect of the analysis.

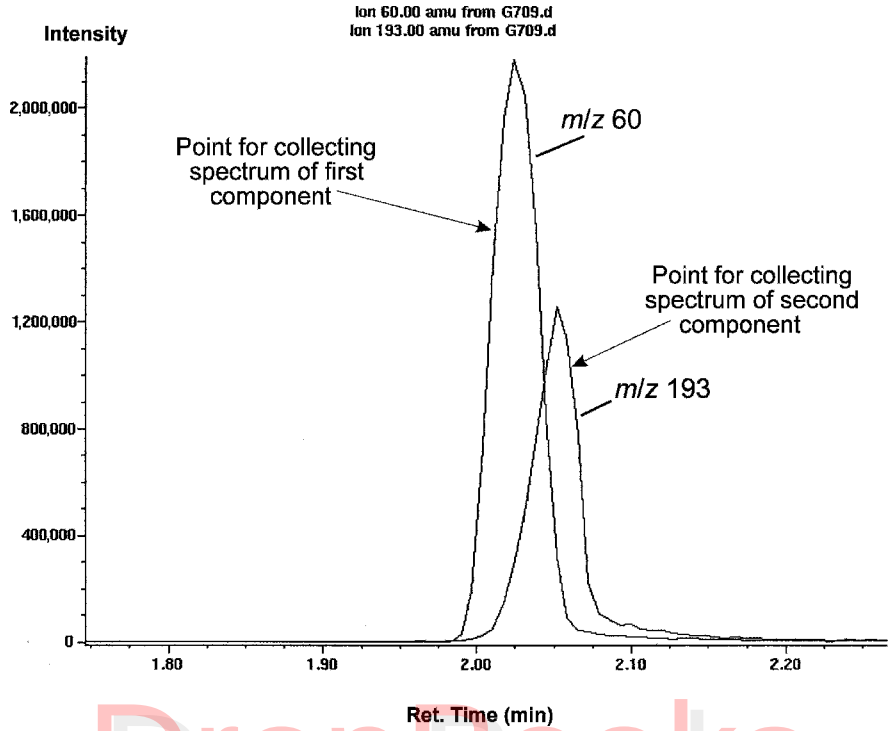

Figure 1.28. Mass chromatograms for *m/z* 60 and 193 generated from the data collected during the run shown in Figure 1.26. These chromatograms were used to generate acceptable spectra for each of the coeluting components (shown in Figures 1.27*b* and *c*).

DropBooks

1.6. CRITERIA FOR GOOD-QUALITY SPECTRA

Mass spectra cannot be interpreted if they contain misinformation. Unfortunately, even refered journals and carefully edited collections of standard spectra sometimes contain spectra that fail to meet this criterion. Judging whether or not a mass spectrum is credible is sometimes the most critical step in its interpretation.

Several criteria are useful for evaluating the quality of spectra. These apply not only to spectra generated in your own laboratory but also to those in the literature or under consideration for placement in user-generated libraries or for publication. Good-quality spectra:

1. Should show appropriate isotope peaks (e.g., should not be missing expected peaks due to ^{13}C), especially at high *m/z* values (see Chapter 2);
2. Should not exhibit excessive background noise (e.g., spurious peaks of instrument origin throughout the mass range) or the obvious presence of extraneous materials (column bleed, coeluting GC peaks, contaminants in the ion source); and

3. Must be consistent with the known or proposed structure—that is,
   a. all *m/z* values must be correct;
   b. the $M^{+\bullet}$ peak, if present, must correspond to the molecular mass;
   c. important peaks at high *m/z* values that reflect the loss of neutral fragments must correspond to functional groups or structural arrangements present in the molecule (Chapter 4); and
   d. the base peak must be consistent with the structure (Chapters 6–8).

After reading the next several chapters of this book, it should become evident why these criteria are important. You may want to review this section after solving some mass spectral unknowns and studying the material contained in later chapters.

ADDITIONAL PROBLEMS

Although answers to all the problems are given in the final chapter of this book, you are strongly encouraged to try to solve each problem before proceeding further. Experience has shown that there is no substitute for solving unknowns if you want to become proficient at interpreting mass spectra. Because most of the topics in this book build on preceding material, beginning students who do not spend time working problems soon get lost. Very few readers, unless they are already adept at mass spectral interpretation, will be able to absorb the concepts illustrated in the problems if they depend entirely on the explanations provided.

1.2. The compound commonly used for tuning and calibration of mass spectrometers is PFTBA, a trade name for perfluorotri-*n*-butylamine, $(CF_3CF_2CF_2CF_2)_3N$. This compound exhibits peaks of at least moderate intensity over the entire mass range normally used in GC/MS work (Figure 1.29). The most prominent

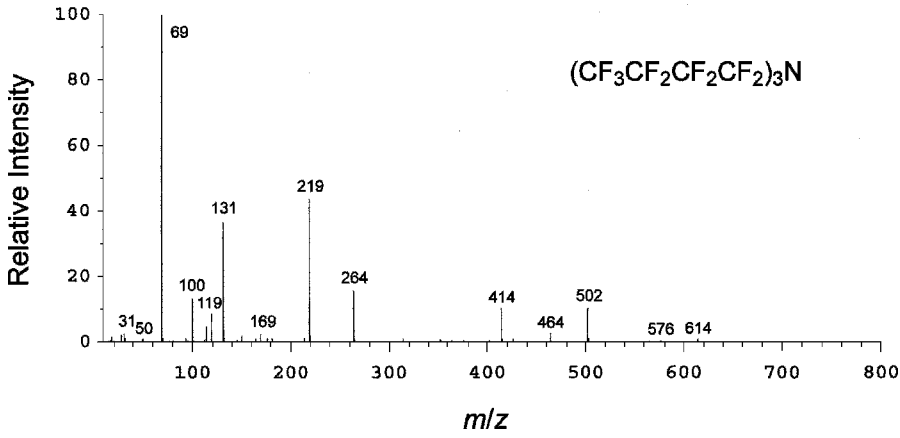

Figure 1.29. Mass spectrum of perfluorotributylamine (PFTBA; Problem 1.2).

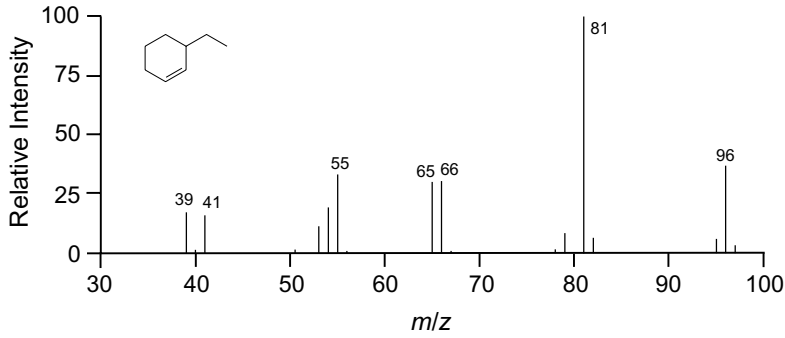

Figure 1.30. Library spectrum for 3-ethylcyclohexene (Problem 1.3).

peaks in the spectrum of PFTBA occur at *m/z* 31, 69, 100, 114, 119, 131, 219, 264, 414, 464, 502, 576, and 614. Devise elemental compositions (and, if possible, hypothesize structures) for the ions that correspond to each of these peaks.

1.3. The spectrum for 3-ethylcyclohexene shown in Figure 1.30 is from a published mass spectral library collection. This spectrum exhibits a $M^{+\bullet}$ peak at *m/z* 96 and a base peak at *m/z* 81. What is wrong with this spectrum? (*Hint*: Organic compounds do not lose fragments of 14 u from the $M^{+\bullet}$—see Section 4.1.1.)

DropBooks

MASS SPECTROMETRIC RESOURCES ON THE INTERNET

Anyone interested in mass spectrometry will find a number of resources available on the Internet. These include access to publications, professional societies, instrument vendors, employment, mass calculators, and tutorials—even tips on troubleshooting instruments. A list of websites for specific information can be found by using your Internet provider's search engine. The following websites provide examples of the types of information that are available.

General

- *http://base-peak.wiley.com* Part of a European-based website that includes all areas of spectroscopy. It contains links to articles, groups, books, conferences, employment, and MS software.
- *http://www.i-mass.com* Also a European-based site similar to base-peak. The isotope pattern calculator (see Chapter 2) is versatile and easy to use.
- *http://www.sisweb.com/mslinks.htm* A U.S.-based site sponsored by Scientific Instrument Services, Inc. It includes links to spectra for MS calibration compounds, as well as a table of exact masses and isotopic abundances for all the elements.

- *http://jeol.com/ms/ms.html* Sponsored by one of the manufacturers of mass spectrometers. The link to ''Essays and Tutorials'' contains brief descriptions and diagrams of instruments and other aspects of MS theory. The site also includes a discussion of elemental composition calculations.

Calculators

- *http://www.cem.msu.edu/~reusch/OrgPage/mass.htm* (*Note*: The URL is case-sensitive.) Calculators for exact masses and isotopic peak intensity ratios (see Chapter 2). Maintained by Michigan State University.
- *http://www.shef.ac.uk/~chem/chemputer/isotopes.html* Isotope peak intensity ratio calculator (see Chapter 2). Maintained by the University of Sheffield.
- *http://www.chem.uni-potsdam.de/tools/index.html* Calculator for losses from the $M^{+\bullet}$ (see Chapter 4). Maintained by the University of Potsdam.
- *http://www.nist.gov/srd/nist1a.htm*. This website, maintained by the National Institute for Standards and Technology (NIST), contains an aid to mass spectral interpretation, as well as isotope and formula calculators associated with a demonstration version of NIST's MS Search program. This version also contains about 1,000 EI spectra.

Standard Spectra

The following two sites provide free access to a reasonable, but not extensive, number of standard spectra that can be searched by molecular mass, name, or empirical formula. The spectra can be printed.

- *http://webbook.nist.gov/chemistry* Maintained by NIST.
- *http://www.aist.go.jp/RIODB/SDBS/menu-e.html* Maintained by the Japanese National Institute of Advanced Industrial Science and Technology.

REFERENCES AND SUGGESTED READING

The field of mass spectrometry is very large and growing at a rapid pace in different directions. Even the interpretation of mass spectra is a broad topic. Thus, any list of suggested sources for additional information must necessarily be incomplete. Rather than duplicate here lists that have already been compiled by others, the reader is referred to other books that provide additional references and resources that are not found in this book.

F. W. McLafferty and F. Tureček's *Interpretation of Mass Spectra*, 4th edition (University Science Books, Mill Valley, CA, 1993) presents a more detailed approach to spectral interpretation than is offered in this book. The appendices contain an extensive collection of useful data. McLafferty's texts remain classics in the field.

O. D. Sparkman's *Mass Spec Desk Reference* (Global View Publishing, Pittsburgh, PA, 2000) could serve as a large appendix to any book about mass spectral theory and interpretation. Two important assets of this book are the carefully constructed glossary of MS terms, with discussions of which terms are currently in use and why, and a list of original references that should suffice to introduce the beginning student to the most important mass spectral literature up to 2000. Both of these books are relatively inexpensive.

Two other books that serve as general references are J. Throck Watson's *Introduction to Mass Spectrometry*, 3rd edition (Lippincott Raven, Philadelphia-New York, 1997) and W. L. Budde's *Analytical Mass Spectrometry: Strategies for Environmental and Related Applications* (Oxford University Press for the American Chemical Society, New York, 2001). Watson's book expands on most of the topics covered in this chapter, whereas Budde's book deals primarily with GC/MS applications.

The books and articles listed below are references to specific topics:

P. Ausloos, C. L. Clifton, S. G. Lias, A. I. Mikaya, S. E. Stein, D. V. Tchekhovskoi, O. D. Sparkman, V. Zaikin, and D. Zhu, "The Critical Evaluation of a Comprehensive Mass Spectral Library," *J. Amer. Soc. Mass Spectrom.*, **10**, 287–299 (1999).

R. B. Cole, *Electrospray Ionization Mass Spectrometry: Fundamentals, Instrumentation and Applications* (John Wiley and Sons, New York, 1997).

R. J. Cotter, *Time-of-Flight Mass Spectrometry: Instrumentation and Applications in Biological Research* (American Chemical Society, Washington, DC, 1997).

E. de Hoffman, "Tandem Mass Spectrometry: A Primer," *J. Mass Spectrom.*, **31**, 129–137 (1996).

H. M. Fales, G. W. A. Milne, H. U. Winkler, H. D. Beckey, J. N. Damico, and R. Barron, "Comparison of Mass Spectra of Some Biologically Important Compounds as Obtained by Various Ionization Techniques," *Anal. Chem.*, **47**, 207–218 (1975).

V. N. Fishman, B. Linclau, D. P. Curran, and K. V. Somayajula, "Tris(Perfluoroalkylethyl)silyl Alkyl Amines as Calibration Standards for Electron Ionization in the Mass Range of 100–3,000 Da," *J. Amer. Soc. Mass Spectrom.*, **12**, 1050–1054 (2001).

A. G. Harrison, *Chemical Ionization Mass Spectrometry*, 2nd edition (CRC Press, Boca Raton, FL, 1992).

M. Henchman and C. Steele, "Understanding the Quadrupole Mass Filter Through Computer Simulation," *J. Chem. Ed.*, **75**, 1049–1054 (1998).

H. Kataoka, H. L. Lord, and J. Pawliszyn, "Simple and Rapid Determination of Amphetamine, Methamphetamine, and Their Methylenedioxy Derivatives in Urine by Automated In-Tube Solid-Phase Microextraction Coupled with Liquid Chromatography–Electrospray Ionization Mass Spectrometry," *J. Analyt. Toxicol.*, **24**, 259 (2000).

K.-S. Kwok, R. Venkataraghavan, and F. W. McLafferty, "Computer-Aided Interpretation of Mass Spectra. III. A Self-Training Interpretive and Retrieval System," *J. Am. Chem. Soc.*, **95**, 4185–4194 (1973).

G. Lawson and J. F. J. Todd, "Radiofrequency Quadrupole Mass Spectrometers," *Chem. Britain*, **8**, 373–380 (1972).

J. J. Leary and R. L. Schmidt, "Quadrupole Mass Spectrometry: An Intuitive Look at the Math," *J. Chem. Ed.*, **73**, 1142–1144 (1996).

DropBooks

R. E. March, ''An Introduction to Quadrupole Ion Trap Mass Spectrometry,'' *J. Mass Spectrom.*, **32**, 351–369 (1997).

F. W. McLafferty, R. H. Hertel, and R. D. Villwock, ''Probability Based Matching of Mass Spectra,'' *Organic Mass Spectrom.*, **9**, 690–702 (1974).

F. W. McLafferty and D. A. Stauffer, ''Retrieval and Interpretative Computer Programs for Mass Spectrometry,'' *J. Chem. Inf. Comp. Sci.*, **25**, 245–252 (1985).

F. W. McLafferty, D. A. Stauffer, S. Y. Loh, and C. Wesdemiotis, ''Unknown Identification Using Reference Mass Spectra. Quality Evaluation of Databases,'' *J. Amer. Soc. Mass Spectrom.*, **10**, 1229–1240 (1999).

P. E. Miller and M. B. Denton, ''The Quadrupole Mass Filter: Basic Operating Concepts,'' *J. Chem. Ed.*, **63**, 617–622 (1986).

J. Roboz, *Mass Spectrometry: Instrumentation and Techniques* (John Wiley and Sons, New York, 1968), pp. 26–105 (on magnetic sector mass spectrometry).

S. E. Stein, ''An Integrated Method for Spectrum Extraction and Compound Identification from Gas Chromatography/Mass Spectrometry Data,'' *J. Amer. Soc. Mass Spectrom.*, **10**, 770–781 (1999).

S. E. Stein and D. R. Scott, ''Optimization and Testing of Mass Spectral Library Search Algorithms for Compound Identification,'' *J. Amer. Soc. Mass Spectrom.*, **5**, 859–866 (1994).

2

ELEMENTAL COMPOSITION FROM PEAK INTENSITIES

2.1. NATURAL ISOTOPIC ABUNDANCES

DropBooks

The EI mass spectrum of methane is shown in Figure 2.1. Interpretation of this spectrum seems straightforward, even for the novice. The molecular ion ($CH_4^{+\bullet}$)[1] produces the base peak in the spectrum at *m/z* 16, corresponding to the molecular mass (MM) of methane (16 u). The $M^{+\bullet}$ shows consecutive losses of hydrogen radicals ($H^\bullet$) and/or molecules of hydrogen (H_2) to give ions with *m/z* 15 (CH_3^+), 14 ($CH_2^{+\bullet}$), 13 (CH^+), and 12 ($C^{+\bullet}$). The relative abundances of these ions, as measured in the intensities of the peaks in the spectrum, show that, after loss of the first $H^\bullet$, further fragmentation becomes increasingly difficult.

It is easy to overlook the small peak at *m/z* 17 in this spectrum. Although it might be tempting to disregard this peak as just background "noise," repeated scanning under ideal conditions shows this is not the case. If the spectrometer is working properly, the peak at *m/z* 17 is always there and has an intensity of about 1.1% relative to that of the peak at *m/z* 16. The presence and size of this peak are generally independent of the type of mass spectrometer used.

More careful reasoning might suggest that this peak is due to a small amount of CH_5^+ formed by ion-molecule reactions between the $M^{+\bullet}$ and neutral molecules of

[1] The $^{+\bullet}$, $^+$, and $^\bullet$ conventions for denoting the electronic state of ions and radicals will be discussed in Section 3.2.

Understanding Mass Spectra: A Basic Approach, *Second Edition*. By R. Martin Smith
ISBN 0-471-42949-X © 2004 John Wiley & Sons, Inc.

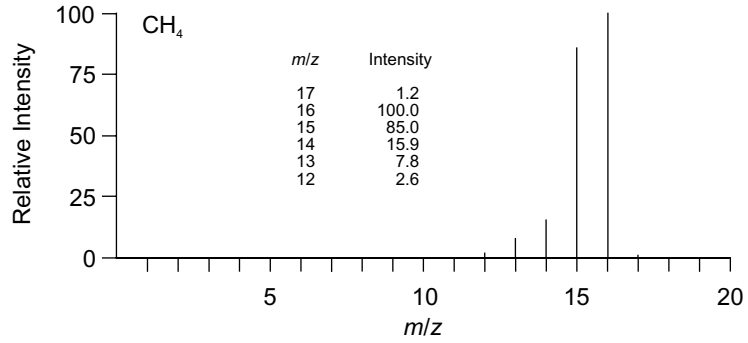

Figure 2.1. EI mass spectrum of methane.

methane. Indeed, if this spectrum were acquired using about 1 torr of methane in the ion source (as occurs when methane is used as a reagent gas in CIMS; see Section 1.2.2), this explanation would be correct. Under such conditions, in fact, *m/z* 17 would undoubtedly become the base peak in the spectrum. However, at the source pressures normally used for EIMS, the intensity of the peak at *m/z* 17 is independent of concentration over a fairly wide range, indicating that this ion is not formed via an ion-molecule reaction.

Where does this peak come from? A clue about its origin comes from the peak at *m/z* 45 in the spectrum of the C-containing compound shown in Figure 2.2.

2.1. Identify what compound produced the spectrum in Figure 2.2 before reading any further.

Like methane, the unknown compound in Problem 2.1 contains one C atom and, in addition, its mass spectrum exhibits a peak 1 *m/z* unit higher than the $M^{+\bullet}$ peak. The intensity of this peak is also slightly more than 1% that of the $M^{+\bullet}$ peak. Since

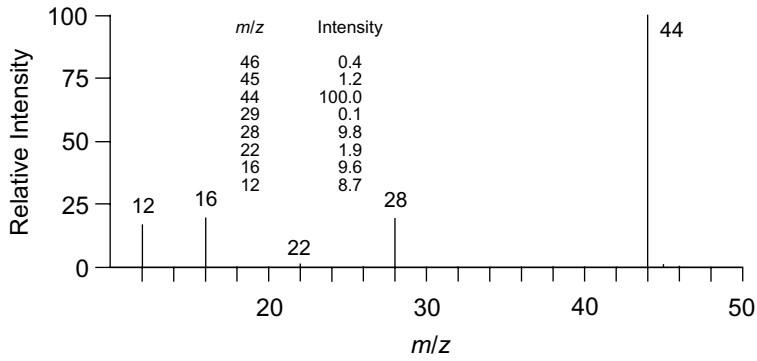

Figure 2.2. Mass spectrum for Problem 2.1.

Table 2.1. Natural isotopic abundances of some common elements

Isotope	Mass	% Abund.	Rel. Pk. Ht.	Isotope	Mass	% Abund.	Rel. Pk. Ht.
^{1}H	1.0078	99.99	100	^{28}Si	27.9769	92.23	100
^{2}H	2.0141	0.015	0.015[a]	^{29}Si	28.9765	4.67	5.1[a]
^{12}C	12.0000	98.89	100	^{30}Si	29.974	3.10	3.4[a]
^{13}C	13.0034	1.11	1.1[a]	^{31}P	30.9738	100.00	100
^{14}N	14.003	99.63	100	^{32}S	31.9721	95.02	100
^{15}N	15.000	0.37	0.37[a]	^{33}S	32.9715	0.75	0.8[a]
^{16}O	15.9949	99.76	100	^{34}S	33.9678	4.21	4.4[a]
^{17}O	16.9991	0.04	0.04[a]	^{35}Cl	34.9689	75.77	100
^{18}O	17.9992	0.20	0.2[a]	^{37}Cl	36.9659	24.23	32.0[a]
^{19}F	18.9984	100.00	100	^{79}Br	78.9183	50.69	100
				^{81}Br	80.9163	49.31	97.3[a]
				^{127}I	126.9045	100.00	100

[a] Contribution to the intensity of the X + 1 or X + 2 peak for each atom of that type present.

these two molecules have nothing in common other than a single atom of C, it appears that these small peaks originate from the presence of C in the molecule. This hypothesis turns out to be correct. But why are both peaks about 1% in intensity?

DropBooks

Most elements occur naturally as mixtures of various isotopes—atoms of the same element that differ in mass because, although they contain the same number of protons and electrons, they differ in the number of neutrons. A list of some common elements and their naturally occurring isotopes is given in Table 2.1, which is also found inside the front cover of this book.

The abundances of the isotopes listed in Table 2.1 are those found in nature; they are not the result of laboratory or commercial manufacture. As an example, diamonds recently mined from Earth would contain 98.9% C atoms that were ^{12}C and 1.1% that were ^{13}C. Elsewhere in the universe these values appear to vary widely. In fact, measuring relative abundances for the isotopes of various elements can be used to determine whether material is of extraterrestrial origin or not. Even on Earth the relative proportions of ^{12}C and ^{13}C show small variations, especially in living systems from different geographical areas (Ehleringer et al., 2000; Rubenstein et al., 2002).

It may seem surprising that ^{14}C is missing from this list, because it is undoubtedly familiar to many readers as the basis for radioactive C dating in archaeology. Although ^{14}C is indeed a naturally occurring isotope of C, it undergoes continual radioactive decay, which makes it unsuitable for determining elemental compositions in MS.

If this information is applied to methane, the MM of $^{12}CH_4$ is calculated to be 16 u (12 u for the C and 1 u for each H), whereas that of $^{13}CH_4$ is 17 u (13 u for the C and 1 u for each H). Because ions are separated in mass spectrometry according

to their m/z values, the mass spectrum exhibits a peak for each of these ions. Indeed, mass spectrometry offers one of the best ways to identify and quantify the presence of different isotopes in a sample. The ratio of the intensities of the peaks at m/z 17 and 16 are directly related to the natural abundances of the two C isotopes (1.1% for ^{13}C / 98.9% for $^{12}C = 1.1\%$). The same logic applies to the intensity of the m/z 45 peak in the spectrum of the unknown in Problem 2.1.

2.1.1. Atomic and Molecular Mass

Mass spectrometry measures mass only as the m/z value. There are a number of terms regarding atomic and molecular mass that sound as though they refer to the same thing, but do not. For example, Table 2.1 lists the atomic masses of designated isotopes of several elements. However, the so-called atomic mass or atomic weight of C that appears in most literature sources (including the periodic table) is 12.01, which is different from the mass of either ^{12}C or ^{13}C.

The *average atomic mass* (also called the *average atomic weight* or just *atomic weight*) of an element is defined as the weighted average of the masses of all its naturally occurring stable isotopes. Similar definitions distinguish between the MM of a compound that contains specified isotopes of all the constituent elements (the monoisotopic mass) vs. the average MM (or *molecular weight*) of a compound derived from the average atomic weights of all the constituent elements.

For C, the atomic mass of ^{12}C is 12.0000 u and that of ^{13}C is 13.003 u. The average atomic mass (atomic weight) of C is calculated by taking into account the natural abundances of ^{12}C and ^{13}C:

$$\begin{aligned}\text{Atomic weight} &= [(\text{nat. abund. of } ^{12}\text{C})(12.000) \\ &\quad + (\text{nat. abund. of } ^{13}\text{C})(13.003)]/100\% \\ &= [(98.9\%)\,(12.000) + (1.1\%)\,(13.003)]/100\% \\ &= 12.011\end{aligned}$$

In the spectra of low MM compounds acquired with $\Delta M \sim 1$, this difference is not large enough to be of particular concern, because the average MM of a compound having even 25 C atoms will only be 0.27 u higher than that of the same compound containing all ^{12}C. The same is not true for some of the other elements, however. Consider Cl, whose two naturally occurring stable isotopes differ by not 1 u, but 2. In addition, ^{35}Cl accounts for only about 75% of all natural Cl; ^{37}Cl accounts for the rest. By using the natural abundances and atomic masses for ^{35}Cl and ^{37}Cl from Table 2.1, the atomic weight of Cl is calculated in the same manner as that of C:

$$\begin{aligned}\text{Atomic weight} &= [(\text{nat. abund. of } ^{35}\text{Cl})\,(34.969) \\ &\quad + (\text{nat. abund. of } ^{37}\text{Cl})\,(36.966)]/100\% \\ &= [(75.77\%)\,(34.969) + (24.23\%)\,(36.966)]/100\% \\ &= 35.453\end{aligned}$$

If the atomic weight of Cl is used to calculate the MM of the chlorine molecule (Cl_2), a value of 70.91, or 71 to the nearest integral mass, is obtained. This number, which is found in references that list "molecular weights" (and most references do!), has no meaning in MS. Since MS responds to the masses of individual isotopes, *no peak is observed at m/z 71 in the spectrum of* Cl_2. Instead, $^{35}Cl_2$ has a mass of 70, $^{35}Cl^{37}Cl$ has a mass of 72, and $^{37}Cl_2$ has a mass of 74. Peaks resulting from each of these isotopic combinations will be observed in the mass spectrum of Cl_2, with the entire cluster of peaks at all these *m/z* values representing the $M^{+\bullet}$ of Cl_2.

2.2. Using Table 2.1, calculate the atomic weight of Br and the molecular weight of Br_2. What peaks would you expect to see in the $M^{+\bullet}$ region of the mass spectrum of Br_2? What isotopic composition does each of these peaks represent?

2.1.2. Calculated Exact Masses and Mass Defects

The standard unit of mass, the *unified atomic mass unit*, is defined as 1/12 of the mass of ^{12}C and is denoted by the symbol u. Conversely, the atomic mass of ^{12}C is defined as 12.0000 u. The atomic masses of the isotopes of all the other elements are determined as ratios against this standard, leading to nonintegral values for essentially all of them (see Table 2.1). It is important not to confuse these nonintegral atomic masses for individual isotopes with the atomic weights of elements discussed in the previous section. The difference between the actual atomic mass of an isotope (relative to ^{12}C) and the nearest integral mass is called the *mass defect*, which is denoted by the capital Greek letter Δ.[2] Variation in the size of mass defects over the Periodic Table is shown in Figure 2.3. The mass defects for the lightest elements (most notably ^{1}H, ^{2}H, ^{13}C, ^{14}N, and ^{15}N) are small and slightly positive, but they are negative for the vast majority of elements.

DropBooks

The atomic masses listed in Table 2.1 for individual isotopes are used to calculate exact masses for ions having specific isotopic compositions. This calculated exact mass is called the *monoisotopic mass* for the ion, because only one isotope of each element is present. For example, the monoisotopic mass of $^{12}C_{21}{}^{1}H_{30}{}^{16}O_2$ is $(21 \times 12.0000) + (30 \times 1.0078) + (2 \times 15.9949) = 314.2238$. The monoisotopic mass can also be calculated using mass defects. In this case,

$$\begin{aligned}\Delta &= (12.0000 - 12.0000)\,(21\text{ C atoms}) + (1.0078 - 1.0000)\,(30\text{ H atoms}) \\ &\quad + (15.9949 - 16.0000)\,(2\text{ O atoms}) \\ &= (0.0000)\,(21) + (0.0078)\,(30) + (-0.0051)\,(2) \\ &= 0.0000 + 0.2340 - 0.0102 \\ &= 0.2238\end{aligned}$$

[2] This is the same symbol used in the naming of THC, where it denotes the position of an isolated double bond.

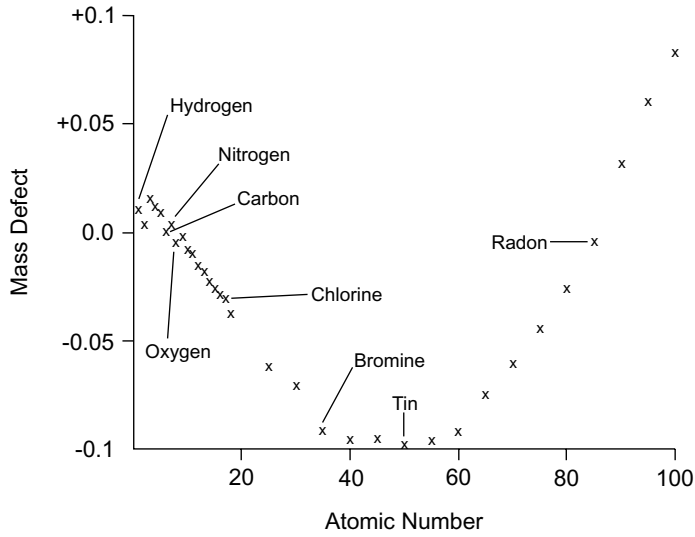

Figure 2.3. Mass defects for the elements.

The calculated exact mass for this ion is not 314.0000, but rather 314.2238 because of the mass defects for ^{1}H, which is positive, and ^{16}O, which is negative. Once again, the accurate MM for this combination of isotopes must not be confused with the average MM or molecular weight (based on atomic weights of the elements) discussed in the previous section. (In this case, the average MM of $^{12}C_{21}{}^{1}H_{30}{}^{16}O_2$ is about 314.45, because the atomic weights of C, H, and O are approximately 12.01, 1.008, and 16.00, respectively.)

The calculated exact mass of $^{12}C_{21}{}^{1}H_{30}{}^{16}O_2$ (Δ^9-tetrahydrocannabinol) is reflected to some degree in the *m*/*z* value for the $M^{+\bullet}$ peak shown in Table 1.3 (314.15), where *m*/*z* values are reported with an accuracy of about ± 0.1. A closer examination of the *m*/*z* values reported for all the peaks in Table 1.3 reveals that ions having *m*/*z* values below about 140 have little or no mass defect, those from about *m*/*z* 140–250 show an average mass defect of about 0.1, and those above *m*/*z* 250 exhibit a mass defect of about 0.2. These numbers reflect in a general way the number of H atoms in the ions since the mass defect of H makes the largest contribution to the overall mass defect in the mass of this ion, or any ion that contains a large number of H atoms.

The exact masses of ions cannot be determined from spectra that are generated on instruments having $\Delta M \sim 1$, where *m*/*z* values are often given only to the nearest integer. It is convenient to calculate the mass of an ion using only integral values for the atomic masses of the constituent elements. The *nominal mass* of an element is defined as the mass of the most abundant natural isotope of that element expressed as the nearest integer. Thus, the nominal mass of H is 1, the nominal mass of C is 12, that of S is 32, etc. For all the elements listed in Table 2.1, the most abundant isotope also occurs at the lowest mass.

The nominal mass of an ion is calculated by adding the nominal masses of each of the constituent atoms. For example, the monoisotopic mass of $C_{17}H_{20}NO_4Cl$ is $(12.0000 \times 17) + (1.0078 \times 20) + (14.003 \times 1) + (15.9949 \times 4) + (34.9689 \times 1) = 337.1075$, and its nominal mass is $(12 \times 17) + (1 \times 20) + (14 \times 1) + (16 \times 4) + (35 \times 1) = 337$. For ions containing the elements listed in Table 2.1 and having a mass <500, the nominal mass will be the same as the monoisotopic mass expressed as the nearest integer. For ions having $M > 500$, however, rounding off to the nearest integer may result in a number higher than the nominal mass. Even the monoisotopic mass of $C_{35}H_{72}$ is 492.56, which, if rounded up to the nearest integer, gives an incorrect "nominal mass" of 493. For biomolecules, the situation is worse. A single-charged polypeptide ion having an elemental composition of $C_{109}H_{171}N_{30}O_{33}S$ has a monoisotopic mass of 2460.2276, but its nominal mass is 2459.

Calculated exact masses and mass defects are usually not considered if *m/z* values are reported only to the nearest integer. However, instruments that have *m/z* discrimination of <0.001 (Section 1.3.5.2) provide important information that is not available at lower resolution. The elemental compositions of most organic compounds have calculated exact masses that differ from one another in the third or fourth decimal place, even if the compounds have the same nominal mass. Therefore, accurate *m/z* measurement can usually determine a unique elemental composition for an ion. This provides either the elemental composition for the compound (if the ion is the $M^{+\bullet}$) or the composition of a fragment that has been lost from the $M^{+\bullet}$ to produce the observed fragment ion. Such information helps determine fragmentation pathways and can lead to an understanding of why ions fragment the way they do.

DropBooks

For example, the mass spectrum of the drug clonazepam, whose structure is shown below, exhibits a peak at *m/z* 287 that could arise either from loss of a molecule of N_2 or by successive losses of $H^{\bullet}$ and a molecule of HCN. The resulting

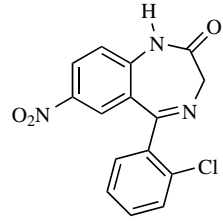

ions have the same nominal mass of 287 but different elemental compositions: $^{12}C_{15}{}^{1}H_{10}{}^{14}N^{16}O_3{}^{35}Cl$ vs. $^{12}C_{14}{}^{1}H_8{}^{14}N_2{}^{16}O_3{}^{35}Cl$. Using the values from Table 2.1, the calculated exact mass for the first ion is

$$12.0000\,(15C) + 1.0078\,(10H) + 14.0031\,(1N) + 15.9949\,(3O) + 34.9689\,(1Cl)$$
$$= 180.0000 + 10.0780 + 14.0031 + 47.9847 + 34.9689 = 287.0347$$

whereas that of the second is

$$= 12.0000\,(14C) + 1.0078\,(8H) + 14.0031\,(2N) + 15.9949\,(3O) + 34.9689\,(1Cl)$$
$$= 168.0000 + 8.0604 + 28.0062 + 47.9847 + 34.9689 = 287.0202$$

It is easy to see that these two ions, which differ in their elemental compositions, can be distinguished from one another by accurate mass measurement. As a result, the loss from the $M^{+\bullet}$ of clonazepam that produces the *m*/*z* 287 peak can be known with certainty, rather than by conjecture. Another example of the use of accurate mass measurements to elucidate fragmentation pathways is given in Section 9.3.

Optimization of sensitivity in SIM (Section 1.3.3.1) requires knowing the monoisotopic mass for each ion selected. For example, the presence of Δ^9-tetrahydrocannabinol can be determined at very low concentrations in biological samples by analysis of the trimethylsilyl derivative $C_{21}H_{29}O_2$-Si$(CH_3)_3$. An intense fragment ion peak for this compound, due to the loss of a methyl radical ($^{\bullet}CH_3$) from the $M^{+\bullet}$, occurs at *m*/*z* 371. The corresponding ion, which has an elemental composition of $(C_{23}H_{35}O_2Si)^+$, is well suited for SIM. If $\Delta M \sim 1$, the intensity of the detector current as the *m*/*z* analyzer scans over this *m*/*z* value is a curve having a maximum value at about *m*/*z* 371.25 (Figure 2.4; see Section 1.5.2), with the peak width determined by the *m*/*z* discrimination ability of the instrument. Setting the instrument to monitor *m*/*z* 371.0 will result in lower sensitivity than if it is set to

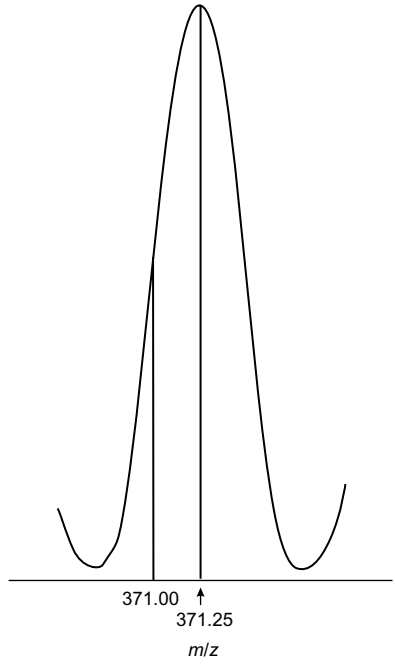

Figure 2.4. Mass spectral peak for $(C_{23}H_{35}O_2Si)^+$ at $\Delta M \sim 1$, showing the effect of the mass $(C_{23}H_{35}O_2Si)$ defect on maximum intensity.

monitor *m/z* 371.25, simply because *m/z* 371.0 is not located at the top of the peak. The amount of sensitivity lost will depend on the *m/z* discrimination ability of the instrument—the greater the *m/z* discrimination ability, the narrower the peak and the greater the loss in sensitivity.

2.2. DETERMINING ELEMENTAL COMPOSITION FROM ISOTOPE PEAK INTENSITIES

Most EI mass spectrometers in use today lack sufficient resolving power to provide accurate mass measurement for the determination of elemental compositions. However, the elemental composition of an ion can sometimes be determined from the ratios of peak intensities of the isotope peaks for that ion to the intensity of the nominal mass peak.

Three of the elements listed in Table 2.1 (F, P, and I) occur without natural stable isotopes. This means that these elements will contribute only one peak at a single *m/z* value for each ion in which they occur. The small amount of deuterium (^{2}H) that occurs naturally (0.015%) is usually ignored in the MS analysis of compounds having $M < 500$ u because its contribution falls at or below the normal limits of detection, which are often 0.1–0.5% of the base peak. This is not true for very large molecules, however, because the ^{2}H contribution for an ion containing even 100 H atoms is $100 \times 0.015\% = 1.5\%$ (see Section 2.2.1.4 for an explanation of this calculation). For the compounds discussed in this book, the contributions of naturally occurring ^{2}H to isotope peaks will not be considered.

DropBooks

For compounds containing only H, F, P, and I, or only one atom of an element that has a naturally occurring isotope, isotopic abundance considerations are fairly trivial. Unfortunately, only a few compounds of interest to analytical organic chemists fall into this category, so that understanding the effects of isotopic abundances on peak intensities is important.

2.2.1. One or More Atoms of a Single Element

2.2.1.1. Chlorine and Bromine. Figure 2.5 shows the spectra of three simple compounds containing Cl or Br. The most striking aspects of these spectra are the clusters of intense peaks that are each separated by 2 *m/z* units. In the case of methyl bromide (CH_3Br), the pattern is particularly striking because both of the intense peak clusters at high *m/z* values have two peaks of approximately equal intensity. On the other hand, the peaks at *m/z* 36 and 38 in the spectrum of HCl and those at *m/z* 61 and 63 in the spectrum of 1,2-dichloroethylene have patterns that are similar to one another; in each case, the lower *m/z* peak of each pair is approximately three times more intense than the higher *m/z* peak.

The data in Table 2.1 explain why the peaks in the HCl and CH_3Br spectra have the intensities they do. In the case of HCl, the $M^{+\bullet}$ consists of two entities: $^1H^{35}Cl^{+\bullet}$ produces the peak at *m/z* 36 and $^1H^{37}Cl^{+\bullet}$ the one at *m/z* 38. The ratio of these two peaks is approximately 75% to 25% (3:1), reflecting the relative natural abundances of ^{35}Cl and ^{37}Cl. Similarly, the $M^{+\bullet}$ of CH_3Br consists of

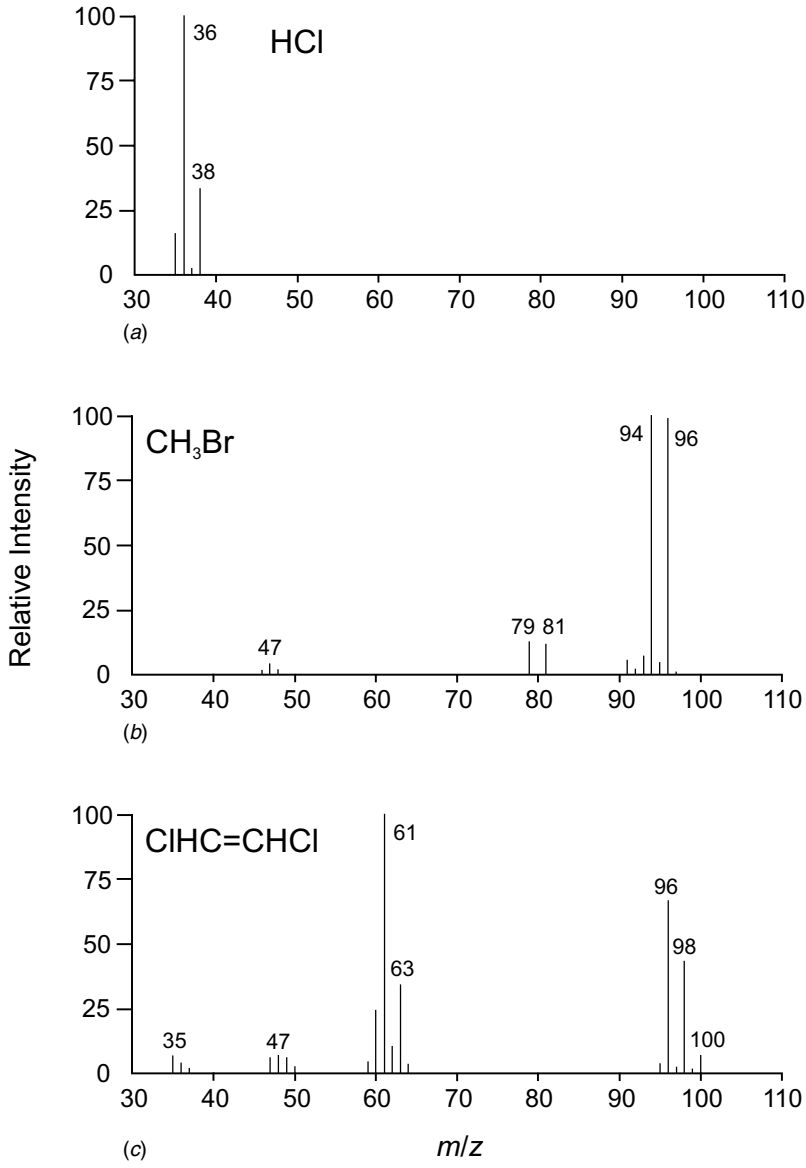

Figure 2.5. Mass spectra of three halogen-containing compounds: (*a*) hydrogen chloride, (*b*) methyl bromide, and (*c*) 1,2-dichloroethylene.

$^{12}C^{1}H_3{}^{79}Br^{+\bullet}$ (*m*/*z* 94) and $^{12}C^{1}H_3{}^{81}Br^{+\bullet}$ (*m*/*z* 96) in an approximate ratio of 50% to 50% (1:1). The peaks at *m*/*z* 35 and 37 in the HCl spectrum have an intensity ratio of 3:1, reflecting the presence of Cl^+, and the peaks of nearly equal intensity at *m*/*z* 79 and 81 in the spectrum of CH_3Br are caused by the presence of Br^+.

The peaks at *m/z* 61 and 63 in Figure 2.5*c*, in an approximate ratio of 3:1, also indicate that one Cl atom is present in this ion. Coupling this with the observation that 61 is exactly 35 u (the mass of ^{35}Cl) less than the apparent MM of 96, one can infer that the peak at *m/z* 96 must be due to $^{12}C_2{}^1H_2{}^{35}Cl_2{}^{+\bullet}$, which also has ^{37}Cl components at *m/z* 98 and 100. The relative sizes of the peaks at *m/z* 96, 98, and 100 in the 1,2-dichloroethylene spectrum are not intuitive, however.

If the notation *P*(X) is used to denote the probability that a given isotope or set of isotopes will occur, the presence of one Cl atom in an ion can be written as the probabilities of finding each of the individual isotopes, that is,

$$P(^{35}\text{Cl}) = 0.75 \qquad \text{and} \qquad P(^{37}\text{Cl}) = 0.25$$

where the numerical probabilities are the *approximate* natural isotopic abundances of ^{35}Cl and ^{37}Cl, adjusted so that their sum is 1.0, rather than 100%. (Throughout the following discussion, the approximate abundances for the naturally occurring isotopes of Cl and Br will be used in order to emphasize relationships between the probabilities. The values in Table 2.1 must be used for more accurate calculations.) The ratio of intensities of the two peaks that result because of the presence of this Cl atom is given by the equation

$$[\text{X}]/[\text{X}+2] = [\text{X}^+]/[(\text{X}+2)^+] = P(^{35}\text{Cl})/P(^{37}\text{Cl}) = 0.75/0.25 = 3/1 = 100/33.3$$

where [X] is the intensity of the peak corresponding to the ion having the lower *m/z* value (X^+) and [X + 2] is the intensity of the peak 2 *m/z* units higher. These intensities are directly proportional to the relative abundances of the corresponding ions, which are denoted by the terms $[X^+]$ and $[(X+2)^+]$.

DropBooks

The situation is similar if there is one Br atom in an ion:

$$P(^{79}\text{Br}) = 0.5, \qquad P(^{81}\text{Br}) = 0.5$$

and

$$[\text{X}]/[\text{X}+1] = P(^{79}\text{Br})/P(^{81}\text{Br}) = 0.5/0.5 = 1/1 = 100/100$$

When two Br atoms occur in the same ion, three combinations of isotopes are possible, all of which have approximately the same probability of occurrence because the relative abundances of ^{79}Br and ^{81}Br are nearly the same:

$$P(2\,^{79}\text{Br}) = P(^{79}\text{Br})P(^{79}\text{Br}) = (0.5)\,(0.5) = 0.25$$
$$P(^{79}\text{Br}\,^{81}\text{Br}) = P(^{79}\text{Br})P(^{81}\text{Br}) = (0.5)(0.5) = 0.25$$
$$P(2\,^{81}\text{Br}) = P(^{81}\text{Br})P(^{81}\text{Br}) = (0.5)(0.5) = 0.25$$

Note that the probability for each combination is calculated by taking the product of the individual probabilities, because the probability of the second isotope being

^{79}Br or ^{81}Br is completely independent of the nature of the first. A more familiar example should make this clearer. The probability of rolling "snake eyes" (two 1's) using two dice is calculated by multiplying the probability of rolling one 1 (which is 1/6, assuming that each side of the die may be rolled with equal facility) by the probability of obtaining a second 1—that is, $1/6 \times 1/6 = 1/36$.

For ions that contain exactly one atom of each isotope, there are two different orientations that are not distinguishable by MS: $^{79}Br^{81}Br$ and $^{81}Br^{79}Br$. The probability that *either one or the other* orientation will occur is equal to the sum of the individual probabilities for the two orientations. Looking again at the example of rolling two dice, consider the probability of rolling a 3 and 4. The probability of rolling first a 3, then a 4, is $1/6 \times 1/6 = 1/36$ because the two events are independent of one another. However, rolling first a 4, then a 3, also accomplishes the desired result. The probability of this occurrence is also 1/36, so that the overall probability is the sum of the two: $1/36 + 1/36 = 2/36 = 1/18$.

The relative intensities for the three peaks due to the presence of two Br atoms are therefore

$$\begin{aligned}[\mathrm{X}]/[\mathrm{X}+2]/[\mathrm{X}+4] &= P(2\,{}^{79}\mathrm{Br})/[P({}^{79}\mathrm{Br}{}^{81}\mathrm{Br}) + P({}^{81}\mathrm{Br}{}^{79}\mathrm{Br})]/P(2\,{}^{81}\mathrm{Br}) \\ &= (0.25)/[(0.25) + (0.25)]/(0.25) \\ &= (0.25)/(0.5)/(0.25) \\ &= 50/100/50 \\ &= 1/2/1\end{aligned}$$

Without taking the separate orientations into account, the sum of the probabilities for all isotopic occurrences would only be $0.25 + 0.25 + 0.25 = 0.75$. When all orientations are considered, the total of all the probabilities becomes 1.0.

When two Cl atoms are present in a molecule, a similar situation occurs, although in this case the two isotopes of Cl do not occur with equal probability:

$$P(2\,{}^{35}\mathrm{Cl}) = (0.75)^2 = 0.563, \qquad P({}^{35}\mathrm{Cl}{}^{37}\mathrm{Cl}) = (0.75)\,(0.25) = 0.188$$
$$P(2\,{}^{37}\mathrm{Cl}) = (0.25)^2 = 0.063$$

Again, MS cannot distinguish between $^{35}Cl^{37}Cl$ and $^{37}Cl^{35}Cl$, so that

$$\begin{aligned}[\mathrm{X}]/[\mathrm{X}+2]/[\mathrm{X}+4] &= P(2\,{}^{35}\mathrm{Cl})/[P({}^{35}\mathrm{Cl}{}^{37}\mathrm{Cl}) + P({}^{37}\mathrm{Cl}{}^{35}\mathrm{Cl})]/P(2\,{}^{37}\mathrm{Cl}) \\ &= (0.563)/[(0.188) + (0.188)]/0.063 \\ &= (0.563)/(0.375)/(0.063) \\ &= 100/66/11\end{aligned}$$

Careful examination of Figure 2.5*c* shows that the peaks at *m/z* 96, 98, and 100 in the 1,2-dichloroethylene spectrum have these approximate intensities relative to one another, which confirms the presence of two Cl atoms in the $M^{+\bullet}$ of this compound.

Determining relative intensities when three Br atoms are present in an ion is approachable by extending the concepts developed so far:

$$P(3\,^{79}\mathrm{Br}) = (0.5)^3 = 0.125, \qquad P(2\,^{79}\mathrm{Br})(^{81}\mathrm{Br}) = (0.5)^2\,(0.5) = 0.125$$
$$P(^{79}\mathrm{Br})(2\,^{81}\mathrm{Br}) = (0.5)\,(0.5)^2 = 0.125, \qquad P(3\,^{81}\mathrm{Br}) = (0.5)^3 = 0.125$$

(It should be emphasized again that the relative probabilities for these four isotopic combinations are approximately equal only because the relative natural abundances of ^{79}Br and ^{81}Br are so similar.) For ions containing two atoms of ^{79}Br and one of ^{81}Br, three different orientations are not distinguishable by mass spectrometry: ^{79}Br^{79}Br^{81}Br, ^{79}Br^{81}Br^{79}Br, and ^{81}Br^{79}Br^{79}Br. For ions having a single ^{79}Br and two atoms of ^{81}Br, three analogous orientations are possible. Therefore,

$$\begin{aligned}
&[\mathrm{X}]/[\mathrm{X}+2]/[\mathrm{X}+4]/[\mathrm{X}+6] \\
&\quad = P(3\,^{79}\mathrm{Br})/[3 \times P(2\,^{79}\mathrm{Br})(^{81}\mathrm{Br})]/[3 \times P(^{79}\mathrm{Br})(2\,^{81}\mathrm{Br})]/P(3\,^{81}\mathrm{Br}) \\
&\quad = (0.125)/3 \times (0.125)/3 \times (0.125)/(0.125) \\
&\quad = 1/3/3/1
\end{aligned}$$

When one Cl atom and one Br atom occur together in an ion,

$$P(^{35}\mathrm{Cl}^{79}\mathrm{Br}) = (0.75)\,(0.5) = 0.375, \qquad P(^{37}\mathrm{Cl}^{79}\mathrm{Br}) = (0.25)\,(0.5) = 0.125$$
$$P(^{35}\mathrm{Cl}^{81}\mathrm{Br}) = (0.75)\,(0.5) = 0.375, \qquad P(^{37}\mathrm{Cl}^{81}\mathrm{Br}) = (0.25)\,(0.5) = 0.125$$

DropBooks

In this case, however, not only are the two middle orientations not identical, but whether or not they are distinguished by MS depends on the *m/z* resolving ability of the analyzer. The four isotopes have different mass defects so that the ^{35}Cl^{81}Br combination has a slightly different absolute mass (115.885) than that of ^{37}Cl^{79}Br (115.884). Under low *m/z* discriminating conditions, the two will not be distinguishable, and

$$\begin{aligned}
[\mathrm{X}]/[\mathrm{X}+2]/[\mathrm{X}+4] &= P(^{35}\mathrm{Cl}^{79}\mathrm{Br})/[P(^{37}\mathrm{Cl}^{79}\mathrm{Br}) + P(^{35}\mathrm{Cl}^{81}\mathrm{Br})]/P(^{37}\mathrm{Cl}^{81}\mathrm{Br}) \\
&= (0.375)/[(0.125) + (0.375)]/(0.125) \\
&= (0.375)/(0.5)/(0.125) \\
&= 75/100/25 \\
&= 3/4/1
\end{aligned}$$

At high resolution, however, four peaks will be discernible: the middle two (at X + 2) separated by 0.001 *m/z* unit, in a ratio of (0.375):(0.125):(0.375):(0.125) or 3:1:3:1.

These intensity ratios need not be calculated each time Cl and/or Br are encountered in an ion. Instead, the results of calculations like these are readily available, either in tabular or graphic form in many MS reference books (e.g., McLafferty and

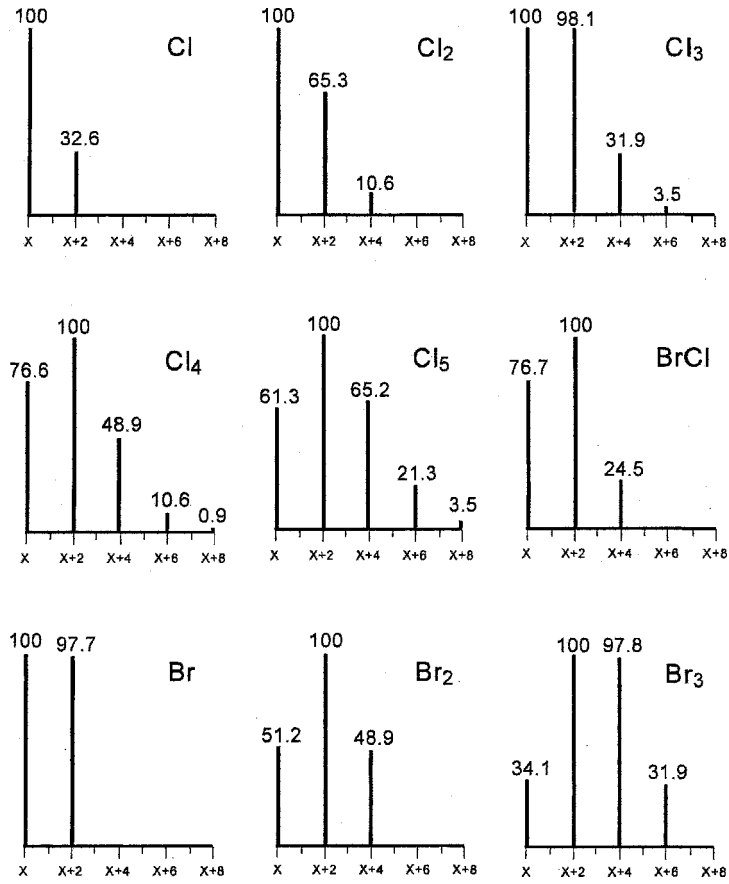

Figure 2.6. Peak intensities for some isotope clusters containing Br and Cl.

Tureček, 1993; Sparkman, 2000) or through some of the Internet websites listed at the end of Chapter 1. Figure 2.6 shows graphically the results calculated in this section, as well as those for three, four, and five Cl atoms.

The visual patterns in Figure 2.6 have an impact that will become apparent as more and more mass spectra are encountered. Each pattern is characteristic of a specific Cl/Br content in the ion, and with experience you can learn to identify the presence of various combinations almost immediately upon glancing at a spectrum (look, e.g., at the spectra in Figure 2.7). Examining a spectrum for the presence of Cl and Br is one of the first steps in mass spectral interpretation, simply because the evidence is almost always so easy to find.

2.3. Following the same logic used in Section 2.2.1.1 for three Br atoms, calculate the relative intensities of the four peaks you would expect to see from the presence of three Cl atoms in an ion. Remember to use the isotopic abundances for Cl, not Br.

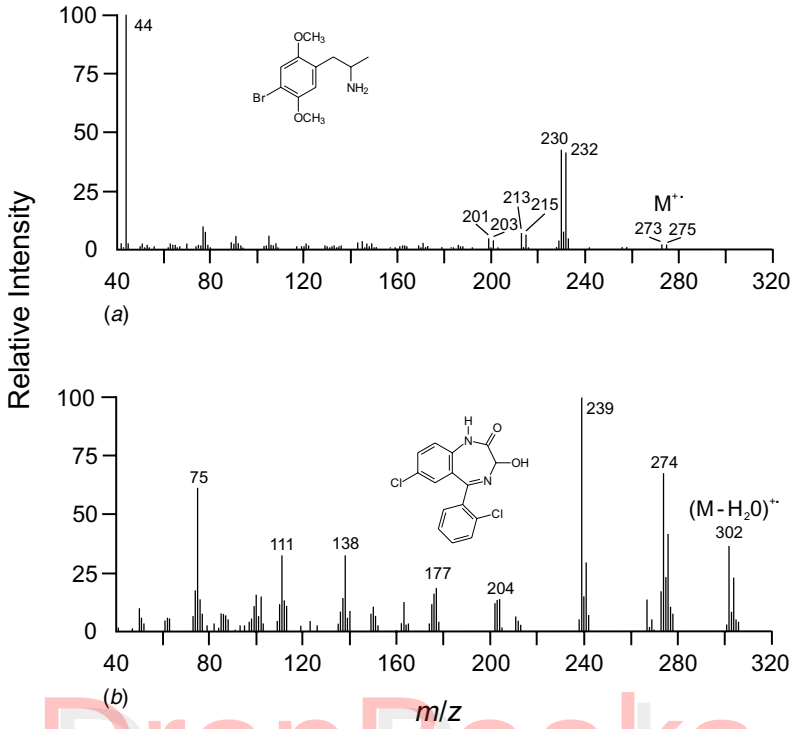

DropBooks

Figure 2.7. Mass spectra of (*a*) 4-bromo-2,5-dimethoxyamphetamine and (*b*) lorazepam showing the presence of Cl and Br in the clusters at high *m*/*z* values.

2.2.1.2. Ion Designation and Nomenclature. One consequence of the unusually high natural abundances of ^{37}Cl and ^{81}Br is that, with ions containing more than three Cl atoms or one Br atom, the peak at the lowest *m*/*z* value in the isotope cluster is no longer the most intense peak. In fact, for highly chlorinated and brominated compounds, the intensity of the lowest *m*/*z* peak in the cluster may be rather small. But the problem is not limited to Cl and Br. For example, a compound containing more than about 90 C atoms and an average number of attached H atoms will produce an M + 1 peak that is slightly more intense than the $M^{+\bullet}$ peak (Section 2.2.1.4). Compounds larger than this are routinely analyzed in many biochemical applications.

This creates a problem regarding how to refer to the ion, because ions are not normally referred to as having a specific isotopic content. For all the elements listed in Table 2.1, the most abundant isotope is also the lowest in mass. For this reason an ion is usually designated by the peak having the lowest *m*/*z* value in the isotope cluster *regardless of whether it is the most intense peak in the cluster or not*. This designation may not be appropriate for some of the elements not discussed in this book, however.

The presence of two or more intense peaks in a cluster means that care must be exercised when calculating losses from one cluster to another. For example, in the spectrum of CH_3Br (Figure 2.5*b*), the $M^{+\bullet}$ peak, from the definition above, is *m/z* 94 ($^{12}CH_3{}^{79}Br$), even though the peak at *m/z* 96 is almost equally as intense. The spectrum also contains two peaks of nearly equal intensity at *m/z* 79 and 81, which correspond to $^{79}Br^+$ and $^{81}Br^+$, respectively. Knowing this, it makes no sense to talk about a loss from *m/z* 94 to 81 (a loss of 13) because the two ions that are responsible for these peaks contain different isotopes of Br. A nuclear transformation would have to occur for this loss to take place! Instead, loss of a methyl radical ($^{12}C^{\bullet}H_3$) from the *m/z* 94 ion accounts for the peak at *m/z* 79, just as loss of $^{12}C^{\bullet}H_3$ from the ion having *m/z* 96 accounts for the peak at *m/z* 81. Both the precursor and product ions must contain the same isotope of Br.

2.4. Using the data in Figure 2.6, identify how many Cl and/or Br atoms there are in each of the indicated clusters in the spectra shown in Figure 2.8. The intensities of these peaks, relative to the base peak in each spectrum, are tabulated below:

(*a*)		(*b*)		(*c*)	
m/z	Rel. Int.	*m/z*	Rel. Int.	*m/z*	Rel. Int.
239	3.3	278	1.0	132	21.2
238	47.3	276	3.5	131	1.0
237	6.5	274	10.3	130	89.4
236	100.0	272	12.4	129	0.7
235	3.5	270	6.0	128	69.0
234	50.9	243	$\ll 1$	95	17.7
158	2.4	241	21.2	93	23.0
157	34.8	240	4.0	91	5.3
156	2.6	239	63.7	81	7.1
155	35.7	238	5.3	79	7.1
		237	100.0	51	31.9
		236	4.0	50	1.3
		235	61.1	49	100.0
		206	1.0		
		204	3.1		
		202	7.1		
		200	5.5		
		169	4.1		
		167	14.1		
		165	14.1		

2.2.1.3. Probability Considerations with Multiple Numbers of Atoms. For ions containing more than one atom of an element, the calculations in Section 2.2.1.1 were seen to depend on not only the natural abundances of the individual

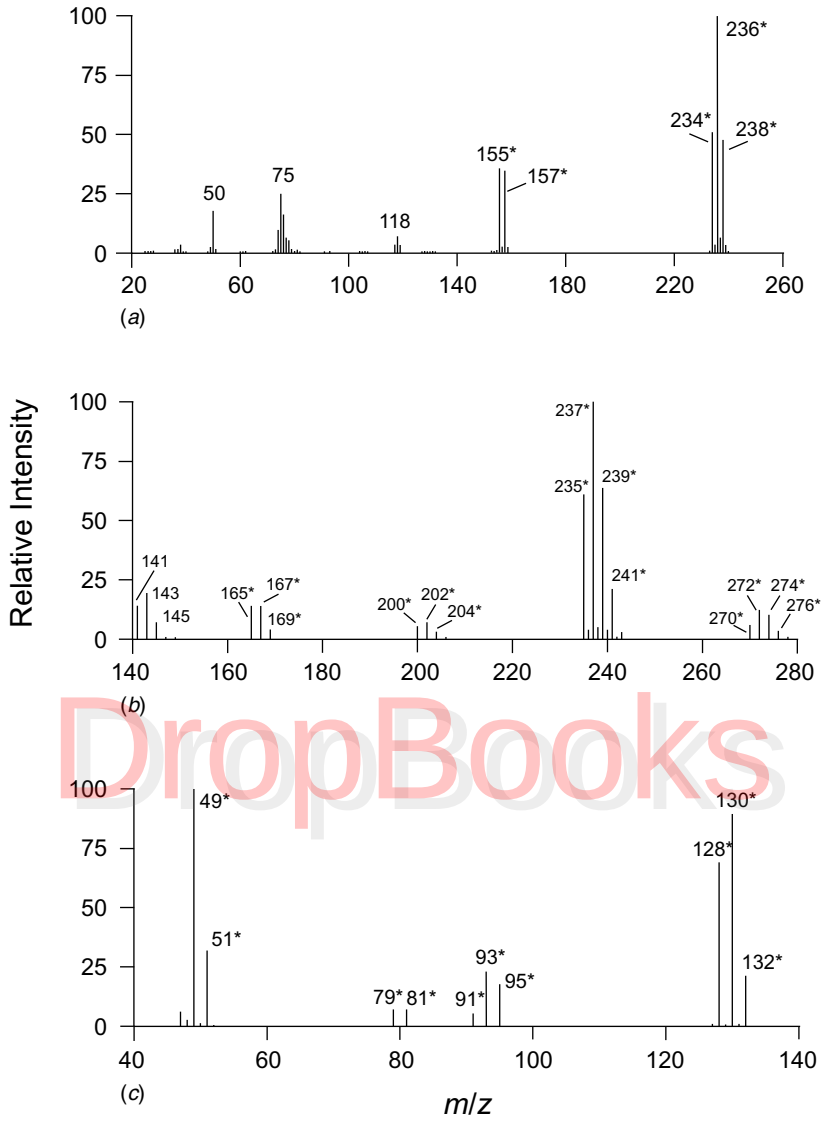

DropBooks

Figure 2.8. Mass spectra for Problem 2.4. Intensities for peaks marked with asterisks (*) are given in the text.

isotopes, but also the number of indistinguishable orientations of the isotopes. Values for these ''probability factors'' are seen most clearly in intensities for ion clusters containing several atoms of Br (Figure 2.6): When one Br atom is present, the values are 1:1 (i.e., there is only one possible orientation for the isotopes in each of the two ions); when there are two Br atoms, the values are 1:2:1 (one orientation

for the lowest and highest mass ions and two for the ion containing one atom of each isotope); for three Br atoms, they are 1:3:3:1.

These numbers are also the coefficients obtained in the binomial expansion of the expression $(a+b)^n$, where n is an integer. When $n=1$, the expression is written as $(1)a+(1)b$; when $n=2$, $(1)a^2+2ab+(1)b^2$; when $n=3$, $(1)a^3+3a^2b+3ab^2+(1)b^3$, and so forth. These expressions are useful because they provide a means of calculating peak intensities in isotope clusters. If n is the total number of atoms of a given element in an ion and a and b are numbers representing the abundances of two naturally occurring stable isotopes of that element, then the relative intensities of the peaks in the isotope cluster that are due to those two isotopes can be calculated using the terms in the expression for that value of n. Using the example of three Br atoms in an ion, if a is the relative natural abundance of ^{79}Br (0.5069 from Table 2.1) and b is the relative natural abundance of ^{81}Br (0.4931), the relative ratios of the four observed peaks are calculated as follows:

$$
\begin{aligned}
&[\mathrm{X}]/[\mathrm{X}+2]/[\mathrm{X}+4]/[\mathrm{X}+6]\\
&\quad = (1)a^3/3a^2b/3ab^2/(1)b^3\\
&\quad = (1)[P(^{79}\mathrm{Br})]^3/3[P(^{79}\mathrm{Br})]^2[P(^{81}\mathrm{Br})]/3[P(^{79}\mathrm{Br})][P(^{81}\mathrm{Br})]^2/(1)[P(^{81}\mathrm{Br})]^3\\
&\quad = (0.5069)^3/3(0.5069)^2(0.4931)/3(0.5069)(0.4931)^2/(0.4931)^3\\
&\quad = 0.1302/0.3800/0.3698/0.1199\\
&\quad = 34.3/100/97.3/31.6
\end{aligned}
$$

The coefficients in these expressions, which represent the number of different ways two isotopes may be arranged while keeping the sum of their masses the same, can be calculated for any value of n. In general, this is the number of ways in which n objects can be arranged when m of them differ from the remaining $n-m$. In mathematical terms, this is called the combination of n things taken m at a time. The formula for calculating the combination of n things taken m at a time, where m is an integer less than n, is

$$C(n,m)=\frac{n(n-1)\cdots(n-m+1)}{m!} \tag{2.1}$$

where $C(n,m)$ denotes the combination of n things taken m at a time, the numerator on the right side of the equation is the product of all the integers from n down to $(n-m+1)$, and the denominator $m!$ (m factorial) is the product of all integers from 1 through m.

When $m=0$, $C(n,0)=1$ by definition, because neither the numerator nor denominator of Equation 2.1 has meaning under those circumstances. This definition reflects the fact that when all the isotopes of the element under consideration are the same, there is only one way to arrange them.

When $m=1$, $C(n,1)=n/1!=n/1=n$. This coefficient is used to determine the relative intensity of the peak that is next highest in m/z value above the peak that

corresponds to the nominal mass of the ion (the ion in which all the isotopes of the element have the lowest mass). For Cl, Br, and the two most abundant isotopes of O and S (Table 2.1), this corresponds to a peak 2 *m/z* units higher than the lowest *m/z* peak (denoted as X + 2, or M + 2 in the case of the $M^{+\bullet}$ peak). For C and N, this peak is only 1 *m/z* unit higher (denoted as X + 1, or M + 1 for the $M^{+\bullet}$ peak). The value for this coefficient is always the number of atoms of the element under consideration. If there are five Cl atoms in an ion, there are five different ways of writing this combination that cannot be distinguished by MS: $^{35}Cl^{35}Cl^{35}Cl^{35}Cl^{37}Cl$, $^{35}Cl^{35}Cl^{35}Cl^{37}Cl^{35}Cl$, $^{35}Cl^{35}Cl^{37}Cl^{35}Cl^{35}Cl$, $^{35}Cl^{37}Cl^{35}Cl^{35}Cl^{35}Cl$, and $^{37}Cl^{35}Cl^{35}Cl^{35}Cl^{35}Cl$. Therefore, the value of the coefficient is 5.

When *n* things are taken 2 at a time, Equation 2.1 becomes

$$C(n, 2) = \frac{n(n-1)}{2!} = \frac{n(n-1)}{(2)(1)} = \frac{(n)(n-1)}{(2)}$$

This expression is used to determine the relative intensity of the peak that is second highest in *m/z* value above the peak corresponding to the nominal mass of the ion. This will be the X + 4 peak for Br, Cl, O, and S and the X + 2 peak for C and N. If this equation is applied to the X + 4 peak for four Br atoms, the coefficient can be calculated by the expression

$$C(4, 2) = \frac{(4)(3)}{2!} = \frac{(4)(3)}{(1)(2)} = 6$$

DropBooks

This is the number of indistinguishable, but not identical, arrangements that can be written for the Br isotopes in this ion: $^{79}Br^{79}Br^{81}Br^{81}Br$, $^{81}Br^{81}Br^{79}Br^{79}Br$, $^{79}Br^{81}Br^{79}Br^{81}Br$, $^{81}Br^{79}Br^{81}Br^{79}Br$, $^{79}Br^{81}Br^{81}Br^{79}Br$, and $^{81}Br^{79}Br^{79}Br^{81}Br$.

When $m = 3$,

$$C(n, 3) = \frac{n(n-1)(n-2)}{3!} = \frac{n(n-1)(n-2)}{(3)(2)(1)} = \frac{(n)(n-1)(n-2)}{6}$$

The relationships between these coefficients are seen in an array that is called Pascal's triangle (Figure 2.9) in honor of the seventeenth-century French mathematician Blaise Pascal. In this array, the values of the binomial expansion coefficients are given horizontally in the same row as the value of *n* shown in the left-hand column. Every number in the array is equal to the sum of the two numbers that flank it in the row immediately above. Thus, the third coefficient in the row where $n = 6$ (which has the value 15) is obtained by adding the two numbers immediately above it in the triangle, namely 10 and 5. Similarly, the next coefficient (20) is the sum of the two 10's that appear just above it in the array. On the basis of this one relationship, the entire array can be derived.

2.2.1.4. Isotope Peak Intensity Ratios for Carbon-Containing Ions—the X + 1 Peak. Calculating peak intensities for Br- and/or Cl-containing compounds

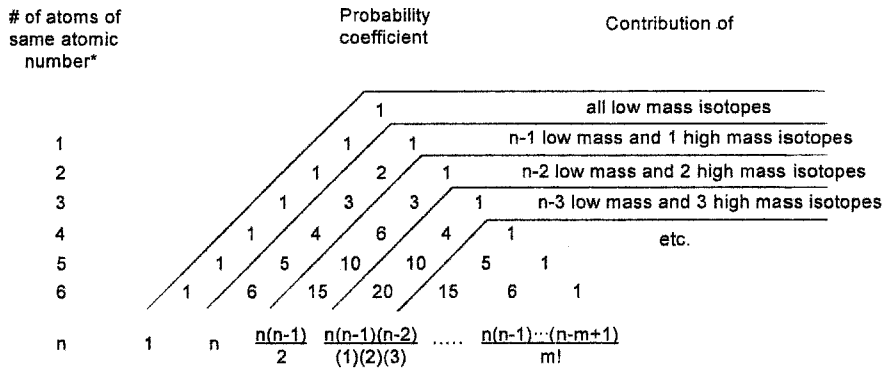
# of atoms of same atomic number*
Probability coefficient
Contribution of
all low mass isotopes
n-1 low mass and 1 high mass isotopes
n-2 low mass and 2 high mass isotopes
n-3 low mass and 3 high mass isotopes
etc.
1 1
1 1 1
2 1 2 1
3 1 3 3 1
4 1 4 6 4 1
5 1 5 10 10 5 1
6 1 6 15 20 15 6 1
n 1 n n(n-1)/2 n(n-1)(n-2)/(1)(2)(3) ..... n(n-1)···(n-m+1)/m!

*Assuming the element has only two isotopes contributing to isotope peak ratios.

Figure 2.9. Binomial expansion (Pascal's) triangle.

was pursued in some detail in order to develop a feeling for how peak intensities in isotope clusters depend on both the natural abundances of the isotopes and the probability factors related to the number of atoms of the element present in the ion. This same logic can now be applied to calculating the relative intensities of the X + 1 and X peaks for an ion containing n C atoms. For the time being, assume that no atoms other than C contribute to the size of the X + 1 peak.

Following the symbols and logic developed in the previous sections, the intensity of a peak X that represents an ion containing n ^{12}C atoms is

$$[\mathrm{X}] = 1 \times P(n\,^{12}\mathrm{C}) = 1 \times [P(^{12}\mathrm{C})]^n = (0.989)^n$$

where 1 is the coefficient identifying the number of indistinguishable ways in which the isotopes can be arranged and $[P(^{12}\mathrm{C})]^n$ is the probability of finding one ^{12}C (0.989, its natural abundance from Table 2.1) multiplied by itself n times. The X + 1 peak represents an ion containing exactly $(n-1)$ ^{12}C atoms and one ^{13}C. The intensity of this peak is expressed by

$$\begin{aligned}[\mathrm{X}+1] &= P[(n-1)^{12}\mathrm{C} + 1^{13}\mathrm{C}] = n\{P[(n-1)^{12}\mathrm{C})] \times P(^{13}\mathrm{C})\} \\ &= n(0.989)^{n-1}(0.011)\end{aligned}$$

where the coefficient n appears because there are n different positions for the ^{13}C atom that are indistinguishable by MS (Section 2.2.1.3). The 0.011 term comes from the natural abundance of ^{13}C.

The ratio of intensities of the X and X + 1 peaks is therefore

$$\begin{aligned}[\mathrm{X}+1]/[\mathrm{X}] &= n(0.989)^{n-1}(0.011)/(0.989)^n \\ &= n(0.011)/(0.989) \\ &= n(0.0111)\end{aligned}$$

To convert this equation to percentages, both numerator and denominator are multiplied by 100, giving

$$\begin{aligned} n(0.011)\,(100)/(100) &= n \times 1.1/100 \\ &= n \times 1.1\% \end{aligned} \tag{2.2}$$

Equation 2.2 has consequences that may not be apparent at first glance. First, if the number of C atoms in an ion is known, their contribution to the size of the X + 1 peak can be calculated. For example, the molecular formula for Δ^9-tetrahydrocannabinol (THC) is $C_{21}H_{30}O_2$, and because neither H nor O have isotopes that contribute significantly to the X + 1 peak, the intensity of the M + 1 peak at *m/z* 315 can be calculated directly from the number of C atoms. This intensity should be $n \times 1.1\% = 21 \times 1.1\% = 23.1\%$ that of the $M^{+\bullet}$ peak at *m/z* 314 in the spectrum of THC. When this value is compared with the value actually measured for this peak in Table 1.3 (where the ratio is 16.8/70.5 = 23.8%), the observed intensity is seen to be close, but not identical, to the calculated value. This reflects an experimental error inherent in MS, which is that the relative intensities of peaks in the spectrum are reproducible under normal circumstances only to about ±10%. For peaks under about 5% relative intensity, the relative error is often higher. Using these criteria, you can see that the agreement here is actually quite good.[3]

If peak intensities are reasonably accurate, the intensity of the X + 1 peak can be used to calculate the number of C atoms in the ion. Consider, for instance, the spectrum of a compound that shows an $M^{+\bullet}$ peak at *m/z* 118 and a peak at *m/z* 119 having an intensity approximately 9% that of the *m/z* 118 peak. If the compound contains no heteroatoms other than O, the number of C atoms in this compound can be determined as follows:

$$9.0\% = n \times 1.1\% \qquad \text{or} \qquad n = 9.0\%/1.1\% = 8.2 \approx 8\text{C atoms}$$

In everyday applications this formula often yields less information than one would like. Most importantly, it works *only* if there are no interferences from other ions. This means that its use for fragment ion peaks is always risky, because the ''isotope peaks'' may represent fragment ions in their own right. In addition, the 10% experimental error inherent in measuring relative peak intensities becomes limiting for higher numbers of C atoms. For example, an X + 1 peak having a relative intensity of 22.5% has an experimentally usable relative intensity of 22.5 ± 2.3%, which covers the range from 20.2–24.8%. If the relative intensity were exactly 22.5%, the number of C atoms in the ion would be 20 (~22.5%/1.1%). Instead, with experimental error this number becomes 20 ± 2 C atoms, which is not very helpful for determining the elemental composition of an unknown. Nonetheless, for smaller molecules Equation 2.2 can prove useful, as will become apparent as some of the problems in this book are solved.

[3] The contribution of 30 deuterium atoms (^{2}H) to the size of the M + 1 peak is 30 × 0.015 = 0.45%, and that from two ^{17}O atoms is 2 × 0.04 = 0.08% (Section 2.2.1.5). This increases the expected intensity of this ion to 23.1 + 0.45 + 0.08 = 23.63%, which is even closer to the observed intensity.

DropBooks

2.2.1.5. A, A + 1, and A + 2 Elements. The derivation of Equation 2.2 became unique for C only when the actual isotopic abundances for ^{12}C and ^{13}C were substituted into more general expressions. The same logic can be used for calculating the relative contribution to the X + 1 and X + 2 peaks for other elements as well. The common elements are divided into three primary categories. Those that have no naturally occurring isotopes are called *A elements*. The A elements are H, F, P, and I, although the contribution of ^{2}H can be ignored only when the number of H atoms is not large. The *A + 1 elements* (C and N) are those that have only one naturally occurring isotope which differs from the nominal mass of the element by 1 u. The *A + 2 elements* (O, Si, S, Cl, and Br) have an isotope that has a mass 2 u higher than the nominal mass. As seen in Table 2.1, O, Si, and S each have two naturally occurring stable isotopes, all separated by 1 u.

The results of the calculations for each of the isotopes not discussed so far are as follows:

A + 1

For ^{2}H, when n is large:

$$[X+1]/[X] = n(0.00015)/(0.9998) = n \times 0.00015 \rightarrow n \times 0.015\%$$

For ^{15}N: $$[X+1]/[X] = n(0.0037)/(0.9963) = n \times 0.0037 \rightarrow n \times 0.37\%$$

For ^{17}O, when n is large:

$$[X+1]/[X] = n(0.0004)/(0.9996) = n \times 0.0004 \rightarrow n \times 0.04\%$$

For ^{29}Si: $$[X+1]/[X] = n(0.0467)/(0.9223) = n \times 0.0506 \rightarrow n \times 5.1\%$$

For ^{33}S: $$[X+1]/[X] = n(0.0075)/(0.9502) = n \times 0.0079 \rightarrow n \times 0.79\%$$

A + 2

For ^{18}O: $$[X+2]/[X] = n(0.0020)/(0.9976) = n \times 0.0020 \rightarrow n \times 0.20\%$$

For ^{30}Si: $$[X+2]/[X] = n(0.0310)/(0.9223) = n \times 0.0336 \rightarrow n \times 3.4\%$$

For ^{34}S : $$[X+2]/[X] = n(0.0421)/(0.9502) = n \times 0.0443 \rightarrow n \times 4.4\%$$

These are the values given in Table 2.1. Because the abundances of ^{28}Si and ^{32}S are somewhat different from 100%, the percentages by which n must be multiplied for the higher isotopes of both these elements differ from the actual natural abundances for these isotopes.

When more than one contributing isotope is present in the $(X+1)^+$ ion, the effect on the size of the X + 1 peak is additive because all of them cannot contribute to this peak at the same time (in that case, the mass of the ion would be X + 2 or greater). That this should be so can be seen from the fact that an ion containing a certain number of ^{12}C's and ^{14}N's, and one ^{13}C will possess a different calculated exact mass from an ion having ^{12}C's, ^{14}N's, and one ^{15}N, and thus will be distinguishable at high *m/z* discrimination. For an ion containing both C and N, the relative intensity of the X + 1 peak at low *m/z* discrimination is given by

$$[X+1]/[X] = (\text{no. of C atoms} \times 1.1\%) + (\text{no. of N atoms} \times 0.37\%)$$

Table 2.2. Relative intensities of X + 1 and X + 2 peaks at low *m*/*z* discrimination

For compounds containing only C, H, N, O, F, Si, P, and S:

A + 1 Isotopes

$$[X+1]/[X] = (\text{no. of C} \times 1.1\%) + (\text{no. of N} \times 0.37\%) + (\text{no. of Si} \times 5.1\%) + (\text{no. of S} \times 0.8\%)[+(\text{no. of H} \times 0.015\%, \text{ if no. of H is large})] [+(\text{no. of O} \times 0.04\%, \text{ if no. of O is large})]$$

A + 2 Isotopes

$$[X+2]/[X] = (\text{no. of C} \times 1.1)^2\%/200 + (\text{no. of O} \times 0.20\%) + (\text{no. of Si} \times 3.4\%) + (\text{no. of S} \times 4.4\%)$$

For compounds containing Cl and Br, see Figure 2.6.

If Si and/or S were also present, the contributions from ^{29}Si and ^{33}S would have to be added as well. More generalized forms of these equations for all the common elements are given in Table 2.2, which is also found inside the front cover of this book.

2.2.1.6. Isotope Peak Intensity Ratios for Carbon-Containing Ions—the X + 2 Peak. When several C atoms are present in an ion, the contribution from two ^{13}C's also produces a detectable effect on the size of the X + 2 peak. The magnitude of this effect for n C atoms is seen to be

$$[X+2] = P[(n-2)^{12}C + 2^{13}C] = \frac{(n)\,(n-1)}{2}[P(^{12}C)]^{n-2}[P(^{13}C)]^2$$
$$= \frac{(n)\,(n-1)}{2}(0.989)^{n-2}(0.011)^2$$

where the coefficient $[(n)\,(n-1)/2)]$ is the one calculated previously in Section 2.2.1.3. The intensity of this peak relative to that of the X peak (Section 2.2.1.4) is

$$\frac{[X+2]}{[X]} = \frac{(n)\,(n-1)}{2}\frac{(0.989)^{n-2}(0.011)^2}{(0.989)^n}$$
$$= \frac{n(n-1)\,(0.011)^2}{2(0.989)^2} = \frac{n^2(0.011)^2}{2(0.989)^2} - \frac{n(0.011)^2}{2(0.989)^2}$$

This equation is inconvenient for routine use so, as a rough approximation, the assumption is made that $(0.989)^2 \sim 1$ and $n^2 \gg n$ if n is relatively large (and if n is not large, the size of this peak is going to be very small anyway). These approximations are made so that the second term of the equation above can be ignored because it is small compared to the first term. The denominator of the remaining

DropBooks

term becomes $2 \times 1 = 2$, and

$$\frac{[X+2]}{[X]} = \frac{n^2(0.011)^2}{2}$$

To translate this into percentage terms, the numerator and denominator are multiplied by $(100)^2$, and

$$\frac{[X+2]}{[X]} = \frac{n^2(0.011)^2(100)^2}{2(100)\,(100)} = \frac{n^2(1.1)^2}{(200)\,(100)} = \frac{(n \times 1.1)^2\%}{200} = 0.006n^2\% \quad (2.3)$$

This is the form in which this equation is usually found in the mass spectral literature.

The ^{13}C contribution to the size of the $X+2$ peak for compounds containing few C atoms is small—even the presence of 10 C atoms leads to a peak of only about 0.6% relative to the intensity of the X peak and may be visible only if the X peak itself is at least moderately intense. For greater numbers of C atoms, contributions increase rapidly. For Δ^9-THC, which has 21 C atoms, the contribution of two ^{13}C's to the $X+2$ peak is seen to be $(21 \times 1.1)^2/200 = (23.1)^2/200 = 533.6/200 = 2.67\%$, a peak that cannot be ignored. If the number of C atoms is very large, the contributions of three or more ^{13}C's to the peaks at $X+3$, $X+4$, and so forth are significant. Calculating the intensities of these peaks follows the same logic as was just used for the $X+2$ peak.

^{13}C is not the only contributor to the $X+2$ peak. In addition to the large contributions from ^{37}Cl and ^{81}Br, those of ^{30}Si and ^{34}S are smaller but still significant, and ^{18}O makes a small, but detectable contribution, especially if more than one O atom is present. If any of these elements are present together with C in the same molecule, the effects are additive and independent of one other, for reasons discussed in the previous sections. For organic compounds having no heteroatoms other than N and O, the relative size of the $X+2$ peak is commonly given by the following equation:

$$[X+2]/[X] = (\text{no. of C atoms} \times 1.1)^2\%/200 + (\text{no. of O atoms} \times 0.20\%) \quad (2.4)$$

A more generalized form for all $A+2$ isotopes is given in Table 2.2. If all contributors are taken into account, the calculated size of the $X+2$ peak for Δ^9-THC ($C_{21}H_{30}O_2$) is

$$[X+2]/[X] = (21 \times 1.1)^2\%/200 + (2 \times 0.2\%) = 2.67 + 0.4 = 3.1\%$$

which compares fairly well with the observed value of 3.5% (Table 1.3).

2.5. Buckminsterfullerene is a form of C having the shape of a soccer ball. This compound was named in honor of Buckminster Fuller, the inventor of the

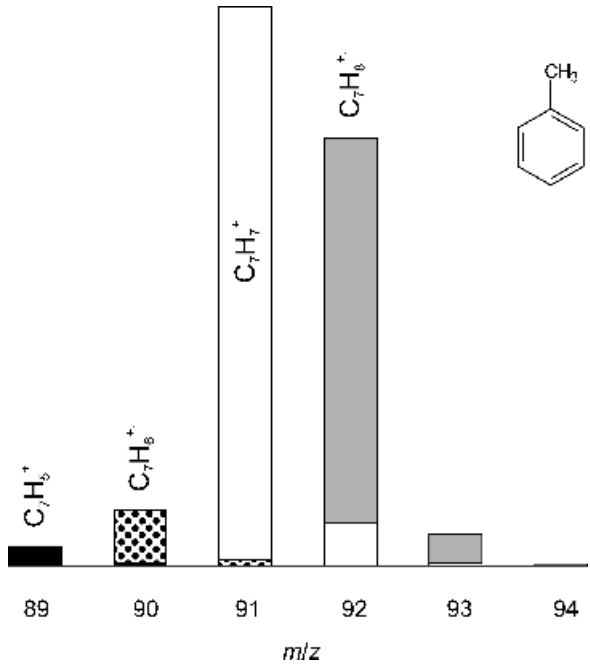

Figure 2.10. Overlapping peak clusters with contributions from ^{13}C only; the $M^{+\bullet}$ region from the mass spectrum of toluene.

DropBooks

geodesic dome, which has a similar shape. The elemental composition of buckminsterfullerene is C_{60} (there are no H atoms), and the base peak in its mass spectrum is due to the $M^{+\bullet}$. Calculate the intensities of the X + 1, X + 2, X + 3, and X + 4 peaks for this ion.

2.6. In Problem 2.4 you determined from peak intensities the number of Cl and/or Br atoms that were present in several ions in the mass spectra in Figure 2.8. Now determine the number of C atoms in those ions, using the data given for some of the X + 1 peaks in the text of Problem 2.4. Using logic and a little arithmetic (X + 1 intensity data is not given, but is not necessary, for the $M^{+\bullet}$ peak in spectrum *b*), determine elemental compositions for the three compounds that produced these spectra.

2.2.1.7. Overlapping Peak Clusters—Contributions from ^{13}C Only. Mass spectra often contain peaks at adjacent *m/z* values that result from the overlap of isotope clusters due to two or more ions. For example, the $M^{+\bullet}$ region in the mass spectrum of the aromatic hydrocarbon toluene (C_7H_8) is illustrated in expanded form in Figure 2.10 (the full spectrum of toluene is shown in Figure 4.15*b*). The observed intensities for these peaks are given on the right side of Table 2.3. The isotopic contribution from each ion in the cluster affects the intensities of subsequent peaks.

Table 2.3. Overlapping peak clusters from toluene (contributions from ^{13}C only)

m/z	$C_7H_5^+$		$C_7H_6^{+\bullet}$		$C_7H_7^+$		$C_7H_8^{+\bullet}$	Observed Intensity
89	3.8^o							$= 3.8^o$
90	0.3^c	+	9.6^o					$= 9.9^o$
91			0.7^c	+	99.3^o			$= 100.0^o$
92			$(0.02)^c$	+	7.6^c	+	68.7^o	$= 76.3^o$
93					0.3^c	+	5.2^c	$= (6.1)^o$
94							0.2^c	$= (<0.5)^o$

^{o} = observed intensity.
^{c} = calculated intensity.

The cluster begins at *m/z* 89 with a peak for $(^{12}C_7H_5)^+$ having an observed intensity of 3.8% relative to that of the base peak at *m/z* 91. The size of this peak is determined by energy distribution between the various fragmentation pathways open to the $M^{+\bullet}$ (Section 3.6) and is completely independent of isotope effects. The next lower peak occurs at *m/z* 78. Because there is a peak at *m/z* 89 for $(^{12}C_7H_5)^+$, there *must* be a corresponding peak at *m/z* 90 for $(^{13}C^{12}C_6H_5)^+$, and the intensity of this peak must be 7.7% (= 7 C atoms × 1.1%) of the size of the peak at *m/z* 89. Because the *m/z* 89 peak has an intensity of 3.8%, the peak at *m/z* 90 for $(^{13}C^{12}C_6H_5)^+$ must have an intensity of 3.8% × 7.7% = 0.3%, which is small, but measurable.

In this spectrum the observed intensity of the *m/z* 90 peak is 9.9% relative to that of the base peak and 260% that of the peak at *m/z* 89—far greater than that predicted for $(^{13}C^{12}C_6H_5)^+$. Indeed, it should not be surprising that there is a fragment ion peak corresponding to $(^{12}C_7H_6)^{+\bullet}$ at *m/z* 90. On the other hand, $(^{12}C_7H_6)^{+\bullet}$ does not account for all the observed intensity of 9.9%—only this value *minus* the 0.3% contribution from $(^{13}C^{12}C_6H_5)^+$. It is worth repeating that the two peaks seen at *m/z* 90 are indistinguishable only at low resolution. A mass spectrometer that has better *m/z* discrimination capability would show them as separate peaks because the ions have different absolute masses due to the mass defect of ^{13}C. This also means that the contributions of these two ions to *m/z* 90 are additive at low *m/z* discrimination.

Because the observed intensity for $(^{12}C_7H_6)^{+\bullet}$ at *m/z* 90 has been shown to be $9.9 - 0.3 = 9.6\%$, there must be a corresponding peak at *m/z* 91 due to $(^{13}C^{12}C_6H_6)^{+\bullet}$. The intensity of that peak is 7.7% of the intensity of the peak for $(^{12}C_7H_6)^{+\bullet}$ at *m/z* 90 (there are still seven C atoms in this ion); this is $9.6\% \times 7.7\% = 0.7\%$. In addition, because the peak for $(^{12}C_7H_6)^{+\bullet}$ at *m/z* 90 is of moderate intensity, the possible contribution of $(^{13}C_2{}^{12}C_5H_6)^{+\bullet}$ to the intensity of the *m/z* 92 peak must be considered. This contribution, which is calculated using Equation 2.3, is $(0.006 \times 7^2)\%$ of the size of the $(^{12}C_7H_6)^{+\bullet}$ peak at *m/z* 90, or $0.30\% \times 9.6\% = 0.03\%$. Peaks of this size are ignored under normal conditions because they usually are at or below the level of background from the instrument.

Given a contribution of 0.7% to the peak at *m/z* 91 by $(^{13}C^{12}C_6H_6)^{+\bullet}$, the remaining 99.3% of this peak must be due to $(^{12}C_7H_7)^+$. As with the other ions just considered, the presence of a peak having an intensity of 99.3% at *m/z* 91 due to $(^{12}C_7H_7)^+$ dictates that there must be a peak at *m/z* 92 corresponding to $(^{13}C^{12}C_6H_7)^+$ with an intensity of $7.7\% \times 99.3\% = 7.6\%$. Also, because the peak due to $(^{12}C_7H_7)^+$ is so intense, a contribution to the *m/z* 93 peak from $(^{13}C_2{}^{12}C_5H_7)^+$ is now expected. This contribution turns out to be $(7.7)^2\%/200 \times 99.3\% = 0.3\%$, just above the limit of significance.

The peak at *m/z* 92 already has a 7.6% contribution from $(^{13}C^{12}C_6H_7)^+$ and an ignorable contribution from $(^{13}C_2{}^{12}C_5H_6)^{+\bullet}$. Because the observed intensity of the *m/z* 92 peak is 76.3%, the contribution from $(^{12}C_7H_8)^{+\bullet}$ (the $M^{+\bullet}$ peak) must be $76.3\% - 7.6\% = 68.7\%$. The contribution of $(^{13}C^{12}C_6H_8)^{+\bullet}$ to the *m/z* 93 peak is calculated to be 7.7% of 68.7%, or 5.2%.

The total *calculated* contributions to the peak at *m/z* 93 are therefore 0.3% from $^{13}C_2{}^{12}C_5H_7^+$ and 5.2% from $^{13}C^{12}C_6H_8^{+\bullet}$—a total of 5.5%. The *observed* intensity of *m/z* 93 in this spectrum is 6.1%, and there are no other ions that can reasonably account for the size of this peak. The difference between 5.5 and 6.1% is right at the 10% cutoff for experimental error in intensity measurement, so it appears that the observed and calculated intensities do, in fact, agree.

Finally, there should be a contribution of $68.7\% \times (0.006 \times 7^2)\% = 0.2\%$ from $(^{13}C_2{}^{12}C_5H_8)^{+\bullet}$ to the ion at *m/z* 94. The observed intensity of this peak is not recorded but is less than 0.5%, consistent with the calculated value.

DropBooks

2.2.1.8. Silicon. As shown previously, Br and Cl produce striking isotope patterns that usually give immediate visual clues in the mass spectrum about their presence in an ion (Section 2.2.1.1). Silicon, having three naturally occurring stable isotopes with detectable abundances (Table 2.1), produces isotopic patterns that are more subtle but nonetheless distinctive. Figure 2.11 shows the mass spectrum of background taken from a GC/MS run with the GC oven at about 260°C. Except for the peaks between *m/z* 40 and 44, nearly every peak in the spectrum is due to low levels of Si-containing ions that come from compounds that have bled off the GC column or septum into the ion source of the mass spectrometer (column bleed). The peak clusters beginning at *m/z* 73, 207, and 281 are expanded above the main spectrum.

A peak at *m/z* 73 is often encountered in the spectra of trimethylsilyl derivatives of compounds containing —OH, $—NH_2$, or other derivatizable groups. Although the intensity of the *m/z* 74 peak is not particularly striking for a peak of that *m/z* value (a compound containing four or five C atoms would produce a peak of similar intensity), the peak at *m/z* 75 is too intense to be due to contributions from ^{13}C alone.

The isotope clusters beginning at *m/z* 207 and 281 more readily catch the eye. Although the X + 1 peak has an intensity that is slightly higher than that expected for ions containing only C and H at this *m/z* value, the sizes of X + 2 and X + 3 peaks are inconsistent with the presence of C alone. Learning the pattern for these Si-containing ions helps identify their presence as background peaks in the mass spectra of other compounds.

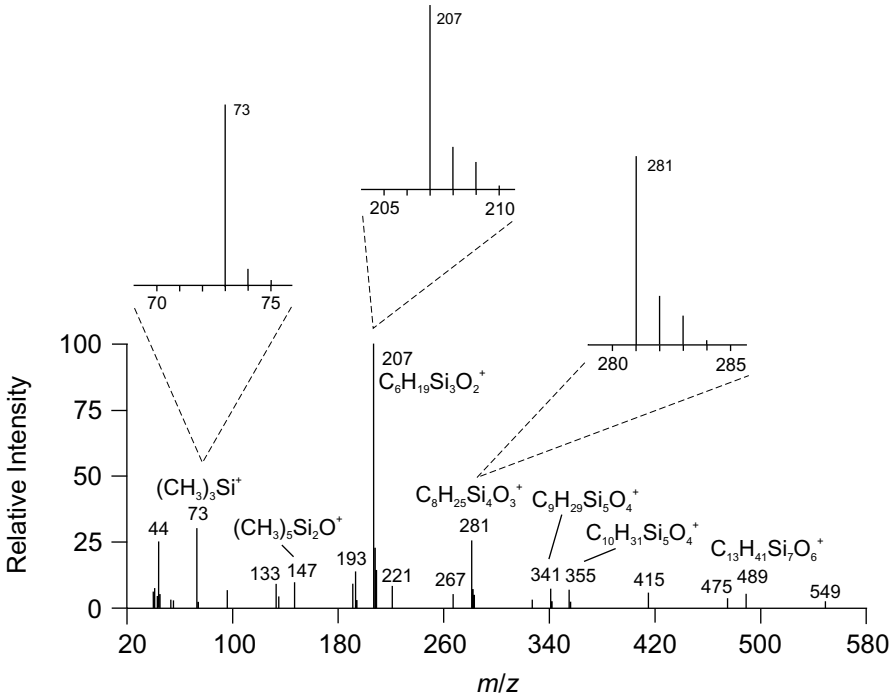

Figure 2.11. Mass spectrum of background from a GC/MS run with the GC oven at 260°C. The peak clusters beginning at *m*/*z* 73, 207, and 281 have been expanded to emphasize the contributions of higher mass isotopes of Si.

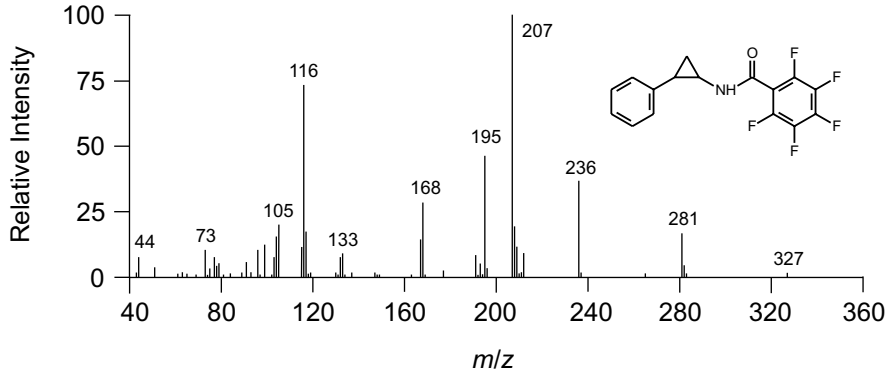

Figure 2.12. Mass spectrum of 1-pentafluorobenzamido-2-phenylcyclopropane (Problem 2.7). (Reprinted by permission of Elsevier Science from Ausloos et al., 1999. Copyright by the American Society of Mass Spectrometry.)

2.7. Review the criteria for good spectra found in Section 1.6. Then comment on whether the spectrum in Figure 2.12 should be included in a library of standard mass spectra (Ausloos et al., 1999).

2.2.2 Complex Isotope Clusters

2.2.2.1. Sulfur Dioxide. Most compounds of interest to organic chemists contain one or more elements in addition to C and H. The presence of two or more elements having higher mass isotopes in the same molecule complicates the isotopic peak intensity situation. Two specific examples should serve as an illustration.

In the spectrum of sulfur dioxide (SO_2; see Figure 2.13), the M + 2 peak at *m/z* 66 is larger than the M + 1. These intensities are inconsistent with the presence of C alone, but the peak at *m/z* 66 is not intense enough to indicate Cl. The presence of an X + 2 peak whose intensity lies in between those for C and Cl, and whose X + 1 peak is less intense than the X + 2, is characteristic of the presence of S. Because the relative intensities of the X + 2 peaks for S and Si are somewhat similar, an ion containing several C atoms and one or more S atoms can be confused with one containing Si under some circumstances.

Sulfur dioxide contains two elements, each having more than one naturally occurring stable isotope—S as ^{32}S, ^{33}S, and ^{34}S, and O as ^{16}O, ^{17}O, and ^{18}O. A cluster of peaks above the $M^{+\bullet}$ peak at *m/z* 64 is therefore expected. Calculating the relative sizes of the peaks at *m/z* 65 and 66, as shown in Table 2.4, follows by analogy from previous discussions, because it involves only the contributions of $^{33}S^{16}O_2$ and $^{32}S^{16}O^{17}O$ for *m/z* 65 and $^{34}S^{16}O_2$ and $^{32}S^{16}O^{18}O$ for *m/z* 66.[4] Because the two ions at each *m/z* value have different absolute masses (the mass defects of S and O are different), their contributions at low resolution are calculated independently and then added together (see Table 2.2).

DropBooks

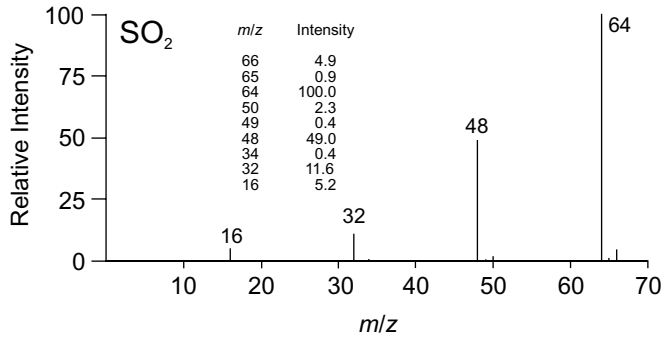

Figure 2.13. Mass spectrum of SO_2 shows isotope peak intensities from contributions of two different elements.

[4] The isotopic composition of the ion with *m/z* 66 can also be $^{32}S^{17}O_2$ or $^{33}S^{16}O^{17}O$. However, the contributions from these two combinations are small enough to ignore when compared to the others.

For the very low intensity peaks at *m/z* 67 and 68, a different principle applies. In these cases, both elements contribute higher mass isotopes to each ion at the same time. The probability for each contributing ion is calculated by multiplying the probabilities of the individual isotopic abundances together (Section 2.2.1.1). Thus, to produce a peak at *m/z* 67, the presence of ^{33}S demands the additional presence of exactly one ^{18}O (^{33}S and ^{34}S cannot occur together because there is only one S). The relative size of the *m/z* 67 peak in the SO_2 spectrum, then, is found by multiplying the relative probability of finding ^{33}S (0.76/95.0) by the relative probability of finding one ^{18}O (which, in this case, is $2 \times 0.2/99.8$, since there are two O atoms in the molecule). The overall probability is very small, because multiplying the individual probabilities together produces a number much smaller than either of them.

The relative size of the *m/z* 68 peak is determined using a combination of both of these methods. Two separate entities, $^{34}S^{16}O^{18}O$ and $^{32}S^{18}O^{18}O$, contribute to *m/z* 68, each containing two isotopes of higher atomic mass. Calculating the total probability for this combination is analogous to calculating the probability of rolling two dice so that the sum of the upper faces is 4. There are two ways to accomplish this—with either a 1 and 3 or two 2's. The probability of obtaining a 1 and 3 in a single roll of two dice is $2 \times 1/6 \times 1/6 = 2/36 = 1/18$, because the probability of obtaining either a 1 or 3 is 1/6, and there are two different orientations (1 and 3, or 3 and 1) that produce a sum of 4. In addition to rolling a 1 and 3, rolling two 2's also will produce a sum of 4. The probability of rolling two 2's is the same as rolling two 1's, which is $1/6 \times 1/6 = 1/36$. Thus, the overall probability of rolling two dice so that the sum of their upper faces is 4 is the sum of the probability of rolling a 1 and 3 plus the probability of rolling two 2's, or $1/18 + 1/36 = 3/36 = 1/12$.

The relative intensity of the peak at *m/z* 68, then, is determined by the sum of the contributions of $^{34}S^{16}O^{18}O$ and $^{32}S^{18}O^{18}O$, which in turn are calculated from the products of the relative abundances of the individual isotopes contained therein:

$$[m/z\,68]/[m/z\,64] = \{[P(^{34}S) \times 2P(^{18}O)] + [P(^{18}O)]^2\}/[P(^{32}S^{16}O_2)]$$

This peak is larger than the one at *m/z* 67 simply because the probability of having ^{34}S is greater than that of having ^{33}S (Table 2.4). The contributions of ^{18}O are so small that they can be ignored.

Table 2.4. Calculated relative intensities in the $M^{+\bullet}$ peak cluster of SO_2

m/z 64	$^{32}S^{16}O^{16}O$	100%
m/z 65	$^{33}S^{16}O^{16}O \Rightarrow (0.75/95.0) \times 100\%$ (for 1 S) +	
	$^{32}S^{16}O^{17}O \Rightarrow 2(0.04/99.9) \times 100\%$ (for 2 O) $= 0.76 + 0.08 =$	0.84%
m/z 66	$^{34}S^{16}O^{16}O \Rightarrow (4.2/95.0) \times 100\%$ (for 1 S) +	
	$^{32}S^{18}O^{16}O$ $2(0.2/99.8) \times 100\%$ (for 2 O) $= 4.4 + 0.4 =$	4.8%
m/z 67	$^{33}S^{18}O^{16}O \Rightarrow (0.75/95.0) \times 2(0.2/99.8) \times 100\% =$	0.0032%
m/z 68	$^{34}S^{18}O^{16}O \Rightarrow (4.2/95.0) \times 2(0.2/99.8) \times 100\% +$	
	$^{32}S^{18}O^{18}O$ $(0.2/99.8)^2 \times 100\% = 0.0177 + 0.0004 =$	0.018%

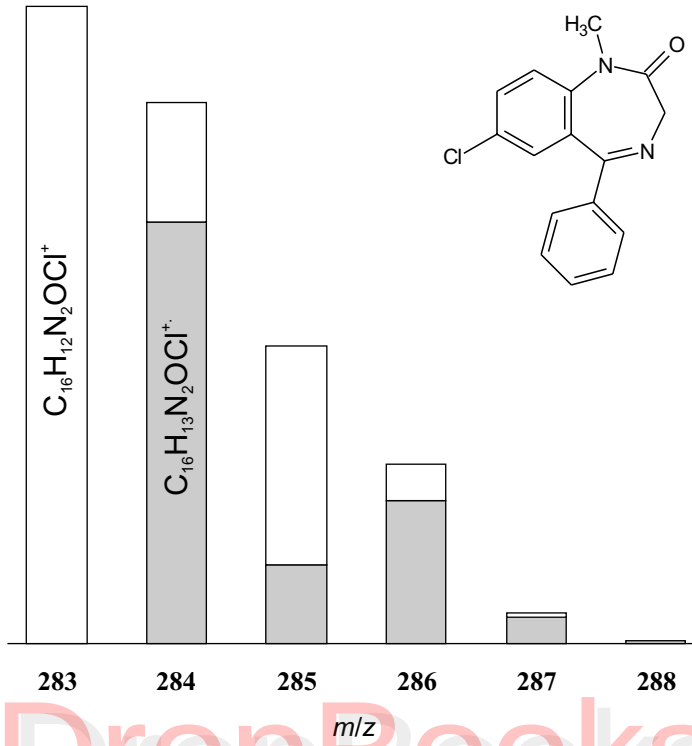

DropBooks

Figure 2.14. Overlapping peak clusters with contributions from several isotopes; the $M^{+\bullet}$ region from the mass spectrum of diazepam.

2.2.2.2. Diazepam. Larger molecules may contain several heteroatoms in addition to C. In these cases, calculating relative intensities for the isotopic contributions to the peaks in various ion clusters at low *m/z* discrimination will reflect the contributions of several different isotopes to the same peak. To illustrate, consider the $M^{+\bullet}$ region for the tranquilizer diazepam ($C_{16}H_{13}N_2OCl$; one popular brand name is Valium). The cluster begins at *m/z* 283 (Figure 2.14 and Table 2.5) and is complicated by the fact that two separate peak clusters overlap one another—one corresponding to $(C_{16}H_{13}N_2OCl)^{+\bullet}$ (the $M^{+\bullet}$ peak) starting at *m/z* 284 and one due to $(C_{16}H_{12}N_2OCl)^+$ at *m/z* 283 (the fragment ion that results from the loss of $^{\bullet}H$). Sorting through this array is tedious but illustrates the application of principles that have been discussed earlier in this chapter.

m/z 283. The most intense peak in this cluster is *m/z* 283, and its size is determined solely by the energy processes that govern the fragmentation of the $M^{+\bullet}$, not by isotope considerations.

Table 2.5. Overlapping peak clusters from diazepam (contributions from several isotopes)

m/z	$C_{16}H_{12}N_2OCl^+$		$C_{16}H_{13}N_2OCl^{+\bullet}$	Intensity
283	100.0^o			$=100.0^o$
284	$^{13}C\ 17.6^c$ $^{15}N\ 0.7^c$	+	67.6^o	$=85.9^o$
285	$^{37}Cl\ 32.6^c$ $^{18}O\ 0.2^c$ $2^{13}C\ 1.5^c$	+	$^{13}C\ 11.9^c$ $^{15}N\ 0.5^c$	$=45.7^c\ (47.1^o)$
286	$^{13}C^{37}Cl\ 5.7^c$ $^{13}C^{18}O\ 0.03^c$ $^{15}N^{37}Cl\ 0.2^c$	+	$^{37}Cl\ 22.0^c$ $^{18}O\ 0.1^c$ $2^{13}C\ 1.0^c$	$=29.0^c\ (28.3^o)$
287	$2^{13}C^{37}Cl\ 0.5^c$ $^{18}O^{37}Cl\ 0.1^c$	+	$^{13}C^{37}Cl\ 3.9^c$ $^{15}N^{37}Cl\ 0.2^c$ (etc.)	$=4.7^c\ (5.0^o)$

^{o}= observed intensity.
^{c}= calculated intensity.

m/z 284. Because the ion at *m/z* 283 contains 16 C and 2 N atoms, the peak at *m/z* 284 must show independent contributions from $(^{13}C^{12}C_{15}H_{12}{}^{14}N_2{}^{16}O^{35}Cl)^+$ and $(^{12}C_{16}H_{12}{}^{15}N^{14}N^{16}O^{35}Cl)^+$—or, for brevity and clarity, the contributions of ^{13}C and ^{15}N. For 16 C atoms, the *calculated* contribution is substantial ($16 \times 1.1\% = 17.6\%$), while that for 2 N atoms is much smaller ($2 \times 0.37\% = 0.7\%$). The total contribution from these ions to the *m/z* 284 peak is $17.6\% + 0.7\% = 18.3\%$. The *observed* intensity of *m/z* 284 is 85.9%, indicating that $85.9 - 18.3 = 67.6\%$ of this peak comes from the monoisotopic molecular ion $(^{12}C_{16}H_{13}{}^{14}N_2{}^{16}O^{35}Cl)^{+\bullet}$.

m/z 285. At *m/z* 285, the situation becomes complicated. The *m/z* 283 ion not only makes ^{13}C and ^{15}N contributions to its X + 1 peak at *m/z* 284, but two elements also make significant contributions to the X + 2 peak at *m/z* 285: ^{18}O and ^{37}Cl. Furthermore, because of the relatively large number of C atoms in this ion, the contribution of two ^{13}C's to the X + 2 peak also must be considered. All these contributions are independent of one another (all the contributors have different absolute masses), so that their effects are calculated separately and then added together:

$$P(^{37}Cl) = 32.6\% \times 100\%\,(\text{the size of } m/z\ 283)/100\% = 32.6\%$$

$$P(^{18}O) = 0.2\% \times 100\%/100\% = 0.2\%$$

$$P(2^{13}C) = (0.006 \times 16^2)\% \times 100\%/100\% = 1.5\%$$

$$\text{Total contributions from } (C_{16}H_{12}N_2OCl)^+ \text{to } m/z\ 285 = 34.3\%$$

Contributions to the M + 1 peak at *m/z* 285 from ^{13}C and ^{15}N in the $M^{+\bullet}$ are also significant:

$$P(^{13}C) = (16 \times 1.1\%) \times 67.6\% \text{ (the intensity of } m/z \text{ 284 due to the } M^{+\bullet})/100\% = 11.9\%$$

$$P(^{15}N) = (2 \times 0.37\%) \times 67.6\%/100\% = 0.5\%$$

$$\text{Total contributions from } (C_{16}H_{13}N_2OCl)^{+\bullet} \text{ to } m/z \text{ 285} = 12.4\%$$

Based on the observed intensities of the peaks at *m/z* 283 and 284, the *calculated* intensity of the *m/z* 285 peak due to the isotopic contributions from all these ions is 34.3 + 12.4 = 46.7%. This is well within the 10% experimental error of measurement when compared to the *observed* intensity of 47.1%.

m/z 286. At *m/z* 286 the contributions of coupled higher mass isotopes from the *m/z* 283 ion begin to take effect. Because one of these elements is Cl, the effects are not negligible, as they were with the higher mass ions in the $(SO_2)^{+\bullet}$ cluster. As with SO_2, the probability of each combination is calculated using the product of the individual isotope probabilities, and the total contribution from all these combinations to *m/z* 286 is obtained by adding them together. Thus,

$$P(^{13}C^{37}Cl) = P(^{13}C)P(^{37}Cl) = (16 \times 1.1\%) \times (1 \times 32.6\%) \times 100\% \text{ (the size of } m/z \text{ 283)}/(100)^2\% = 17.6\% \times 32.6\% \times 100\%/(100)^2\% = 5.7\%$$

$$P(^{13}C^{18}O) = P(^{13}C)P(^{18}O) = (16 \times 1.1\%) \times (1 \times 0.2\%) \times 100\%/(100)^2\% < 0.1\%$$

$$P(^{15}N^{37}Cl) = P(^{15}N)P(^{37}Cl) = (2 \times 0.37\%) \times (1 \times 32.6\%) \times 100\%/(100)^2\% = 0.2\%$$

$$\text{Total contributions from } (C_{16}H_{12}N_2OCl)^{+} \text{ to } m/z \text{ 286} = 5.9\%$$

DropBooks

[The $(100)^2\%$ factor found in the denominator of these expressions, as well as the $(100)^3\%$ factor in some of the calculations below, is necessary to adjust for the fact that percentages, rather than actual probabilities (all of which would be less than 1), are being used.]

Isotope contributions to the M + 2 peak from the $M^{+\bullet}$ are more important than the double isotope contributions above:

$$P(^{37}Cl) = (1 \times 32.6\%) \times 67.6\% \text{(the actual size of the } M^{+\bullet} \text{peak)}/100\% = 22.0\%$$

$$P(^{18}O) = (1 \times 0.2\%) \times 67.6\%/100\% = 0.1\%$$

$$P(2^{13}C) = (0.006 \times 16^2)\% \times 67.6\%/100\% = 1.0\%$$

$$\text{Total contributions from } (C_{16}H_{13}N_2OCl)^{+\bullet} \text{ to } m/z \text{ 286} = 23.1\%$$

The total *calculated* relative intensity of the *m/z* 286 peak is the sum of all these contributions, or 5.9% + 23.1% = 29.0%. This agrees remarkably well with the *observed* intensity of 28.3% for this peak.

m/z 287. For the peak at *m/z* 287, all contributing species involve *at least* two different isotopes. Although the list of contributors is long, only some of the ions containing ^{37}Cl actually make a significant contribution to the size of the *m/z* 287 peak:

Contributors from $(C_{16}H_{12}N_2OCl)^+$:

$$P(2^{13}C^{37}Cl) = P(2^{13}C)P(^{37}Cl) = (0.006 \times 16^2)\% \times [1 \times 32.6\%] \times 100\%/100^2\% = (1.5\%)\,(32.6\%) \times 100\%/100^2\% = 0.5\%$$

$$P(2^{13}C^{18}O) = P(2^{13}C)P(^{18}O) = (1.5\%) \times (1 \times 0.2\%) \times 100\%/100^2\% \ll 0.1\%$$

$$P(^{18}O^{37}Cl) = P(^{18}O)P(^{37}Cl) = (0.2\%) \times (32.6\%) \times 100\%/100^2\% = 0.1\%$$

$$P(2^{15}N^{37}Cl) = P(2^{15}N)P(^{37}Cl) = (0.37\%)^2 \times 32.6\% \times 100\%/(100)^3\% \ll 0.1\%$$

$$P(2^{15}N^{18}O) = P(2^{15}N)P(^{18}O) = (0.37\%)^2 \times 0.2\% \times 100\%/(100)^3\% \ll 0.1\%$$

$$P(^{13}C^{15}N^{37}Cl) = P(^{13}C)P(^{15}N)P(^{37}Cl) = (17.6\%)\,(2 \times 0.37\%)\,(32.6\%) \times 100\%/(100)^3\% < 0.1\%$$

$$P(^{13}C^{15}N^{18}O) = P(^{13}C)P(^{15}N)P(^{18}O) = (17.6\%)\,(2 \times 0.37\%)\,(0.2\%) \times 100\%/(100)^3\% \ll 0.1\%$$

Contributors from $(C_{16}H_{13}N_2OCl)^{+\bullet}$:

$$P(^{13}C^{37}Cl) = P(^{13}C)P(^{37}Cl) = (16 \times 1.1\%) \times (1 \times 32.6\%) \times 67.6\%/(100)^2\% = (17.6\%)\,(32.6\%) \times 67.6\%/(100)^2\% = 3.9\%$$

$$P(^{15}N^{37}Cl) = P(^{15}N)P(^{37}Cl) = (2 \times 0.37\%) \times (32.6\%) \times 67.6\%/(100)^2\% = (0.7\%)\,(32.6\%) \times 67.6\%/(100)^2\% = 0.2\%$$

$$P(^{13}C^{18}O) = P(^{13}C)P(^{18}O) = (16 \times 1.1\%) \times (1 \times 0.2\%) \times 67.6\%/(100)^2\% = (17.6\%)\,(0.2\%) \times 67.6\%/(100)^2\% \ll 0.1\%$$

Thus, the *calculated* intensity for the *m/z* 287 peak is $0.5 + 0.1 + 3.9 + 0.2 = 4.7\%$, close to the *observed* value of 5.0%.

m/z 288 and Above. Although the peak at *m/z* 288 is small, it is still not below the limits of detectability. The number of isotopic contributors from the ion at *m/z* 283 is now considerable and includes such combinations as $^{13}C_2{}^{15}N^{18}O$, $^{13}C^{15}N_2{}^{37}Cl$, and $^{13}C^{18}O^{37}Cl$. Calculation of these intensities follows directly from previous discussions and is not pursued further.

2.3. OBTAINING ELEMENTAL COMPOSITIONS FROM ISOTOPE PEAK INTENSITIES

Information about the elemental composition of an ion is contained in the isotope peak intensities for that ion. Although the elemental composition for both

molecular and fragment ions can be determined from peak intensity data, it is important to remember that, for fragment ions, the presence of peaks due to other fragment ions at *m/z* values immediately above or below that of the ion of interest may complicate, and in some cases render impossible, this determination. Also, because of the inherent experimental error in measuring mass spectral peak intensities, this determination will become less and less useful at higher *m/z* values. The information presented in this chapter can be summarized in the following guidelines, which should be followed in sequence, at least at first, in order to determine the elemental composition of an ion from its isotope peak intensities.

1. Determine the nominal *m/z* value for the ion in question. This will be the most intense peak in the *isotope* cluster (Section 2.2.1.2) unless the ion contains several Br and/or Cl atoms, or has $m/z > \sim 1,000$. Be aware that peaks due to other fragment ions may occur at immediately adjacent *m/z* values.
2. Normalize peak intensities in the isotope cluster by assigning a value of 100% to the nominal mass peak, then dividing the observed intensities for the remaining peaks by the observed intensity for the nominal mass peak.
3. Use the nitrogen rule (Section 3.5) to identify the probable presence of N in the compound. Of all the elements commonly seen in organic compounds, only N has both an odd valence (3) and an even mass (14). The result is that compounds containing an odd number of N atoms will have an odd nominal MM, and a compound containing an even number of (or no) N atoms will have an even nominal MM. If the nominal MM is odd, it is usually expedient to assume at first that there is one N atom present. Similarly, if the compound has an even nominal MM, the assumption that no N atoms are present is most often warranted. However, these assumptions are sometimes incorrect, and evidence that they are incorrect should not be discounted.
4. Ignoring O for the moment, determine the number and types of A + 2 elements that are present. The intensity patterns due to the presence of Cl and Br are shown in Figure 2.6. Determining whether Si or S is present may not be straightforward, especially if several C atoms are also involved. Try different combinations of elements using the equation in Table 2.2 until the best fit is established.
5. Assign the number and types of A + 1 elements. It is important to identify all contributors to the X + 1 peak before calculating the number of C atoms that might be present. The presence of N can usually be determined using the nitrogen rule (step 3 above), whereas Si and S are identified by their contributions to the X + 2 peak. Once the contributions of these elements to the X + 1 peak are calculated using the equation in Table 2.2, this value is subtracted from the normalized intensity of the X + 1 peak. The number of C atoms can now be calculated using Equation 2.2.[5]

[5] Because these calculations are limited mostly to $m/z < \sim 300$, any contributions of ^{2}H and ^{17}O to the X + 1 peak will be ignored.

DropBooks

6. After the number of C atoms has been determined in step 5, the contribution of C to the X + 2 peak can be calculated using Equation 2.3. Any remaining intensity in the X + 2 peak must be due to O. Calculate the number of O atoms using Equation 2.4.
7. Any remaining mass not accounted for by A + 1, and A + 2 elements must be due to A elements. Most often, the presence of H will account for this mass, but losses of 19 and 127 *m/z* units from the $M^{+\bullet}$ peak that lead to significant peaks in the spectrum may indicate the presence of F or I, respectively. The presence of P may be more difficult to determine.
8. Using the *rings plus double bonds* formula in Equation 2.5 below, calculate the total number of rings plus double bonds in the $M^{+\bullet}$ or other odd-electron ions (Section 3.2). For ions that have the general formula $C_xH_yN_zO_n$, this value is given by the equation

$$\text{Total rings plus double bonds} = x - 1/2y + 1/2z + 1 \qquad (2.5)$$

   This equation applies only to elements in their lowest valence state, but it can be expanded to include other elements that have the same valence as those given above. Thus, C in the general formula can be either C or Si or a mixture thereof, H can be either H or any halogen, N can be N or P, and so forth. Notice that the numbers of O or S atoms in the ion do not enter into this calculation.
9. If possible, postulate a structure for the ion.

EXAMPLES

In the following examples, isotope peak intensity data are given for the $M^{+\bullet}$ peak from the mass spectra of four unknown compounds. From this data the elemental composition of each compound will be determined, and possible structures corresponding to these elemental compositions will be proposed.

Example 2.1

m/z	Observed Rel. Int.	Normalized Rel. Int.
122	77.5	100.0 (=77.5/77.5 × 100)
123	6.0	7.8 (=6.0/77.5 × 100)
124	0.6	0.8 (=0.6/77.5 × 100)

Answer: The $M^{+\bullet}$ peak has a nominal *m/z* value of 122. This value is an even number, indicating that the compound probably does not contain N. The observed intensities for these peaks (relative to an unspecified base peak of 100% somewhere else in the spectrum) must be normalized relative to the most intense peak in the cluster. These are reflected in the values shown in the right-hand column above.

The intensity of the M + 2 peak is inconsistent with the presence of any of the A + 2 elements, with the possible exception of O. Therefore, the intensity of the M + 1 peak (N is not present) must be due solely to the contributions of ^{13}C. The number of C atoms in the ion is calculated using Equation 2.2:

$$(\text{No. of C atoms}) \times 1.1\% = 7.8\%$$

Therefore,

$$(\text{No. of C atoms}) = 7.8\%/1.1\% = 7.1 \approx 7$$

The contribution of seven C atoms to the M + 2 peak is given by Equation 2.3:

$$[0.006 \times (\text{No. of C atoms})^2]\% = [0.006 \times 7^2]\% = [0.006 \times 49]\% = 0.29\%$$

This value accounts for only 0.3% of the 0.8% normalized intensity of the M + 2 peak, leaving 0.8% − 0.3% = 0.5% that could be contributed by O. The number of O atoms in the ion can be calculated using Equation 2.4:

$$(\text{No. of O atoms}) \times 0.2\% = 0.5\%$$

and

$$(\text{No. of O atoms}) = 0.5\%/0.2\% = 2.5$$

DropBooks

This number falls exactly between two and three O atoms. However, the mass of seven C atoms and two O atoms is $(7 \times 12) + (2 \times 16) = 84 + 32 = 116$ u, which leaves only 6 u to account for. The presence of a third O atom is thus impossible, and the remaining mass must be due to the presence of six H atoms.

The elemental composition of this ion (and, because this is the $M^{+\bullet}$ peak, of the compound itself) is thus $C_7H_6O_2$. The rings plus double bonds formula shows that this elemental composition generates

$$(\text{No. of C atoms}) - \tfrac{1}{2}(\text{No. of H atoms}) + \tfrac{1}{2}(\text{No. of N atoms}) + 1$$
$$= 7 - \tfrac{1}{2}(6) + \tfrac{1}{2}(0) + 1 = 5$$

unsaturations in the molecule as a mixture of rings and/or double bonds. A value of four unsaturations or higher often indicates the presence of an aromatic ring (a benzene ring has three double bonds and one ring for four unsaturations). Several structures are consistent with these data, including benzoic acid ($C_6H_5CO_2H$) and the three isomeric hydroxybenzaldehydes (*o*-, *m*-, and *p*-HO-C_6H_4CHO). The fifth unsaturation in each of these molecules is the carbonyl double bond.

Example 2.2

m/z	Obs. Rel. Int.	Normalized Rel. Int.
99	12.3	100.0 (=12.3/12.3 × 100)
100	0.9	7.3 (= 0.9/12.3 × 100)
101	Too small to be measured	

Answer: The nominal *m/z* value for the $M^{+\bullet}$ peak is 99. This is an odd number, which means that, because it reflects the MM of the compound, there must be an odd number of N atoms in the compound. At the outset the presence of one N atom will be assumed. As in the previous example, the observed peak intensities must be normalized relative to the most intense peak in the cluster. Notice in this case that the intensity of the M + 2 peak was too small to be recorded. Also notice that, because the observed intensity of the M + 1 peak is so small, the relative experimental error in measuring the intensity of this peak is large. If the observed intensity were 0.8 or 1.0, rather than 0.9, the normalized relative intensities for this peak would be 6.5% or 8.1%, respectively.

Because data for the M + 2 peak are missing, the presence of any A + 2 elements must be determined by logic. Chlorine and Br are clearly absent, and the presence of even one Si or S would produce a peak of about 0.4–0.6% observed intensity. Unless the entire spectrum is extremely weak and peaks under about 1% relative intensity are not recorded, a peak of this magnitude should be observed. Thus, it appears that only the presence of O cannot be ruled out at this point.

The presence of one N atom in the compound produces a contribution of 0.4% to the M + 1 peak, which must be subtracted from the normalized intensity for that peak before calculating the number of C atoms. This leaves $7.3 - 0.4 = 6.9\%$ that must come from the presence of $6.9\%/1.1\% = 6.3 \approx 6$ C atoms in the molecule.

The mass of six C atoms and one N atom is $(6 \times 12) + (1 \times 14) = 72 + 14 = 86$ u. There is not enough missing mass to accommodate an O atom or any other A + 2 element. Instead, 13 H atoms make up the remainder, giving an elemental composition of $C_6H_{13}N$. The rings plus double bonds formula shows that there is $6 - \frac{1}{2}(13) + \frac{1}{2}(1) + 1 = 1$ unsaturation in the molecule. Without further information, it is difficult to choose between many possible structures. Cyclohexylamine (C_6H_{11}-NH_2), having a saturated cyclohexane ring, is one structure that satisfies the requirement.

Example 2.3

m/z	Obs. Rel. Int.
84	100.0
85	5.1
86	4.4

Answer: The nominal *m/z* value for this ion is even (84). Unless other information in the spectrum were to prove contradictory, it should be assumed initially that no N atoms are present. The largest peak in the cluster is also the base peak in the spectrum, so that normalization of the other intensities is not necessary.

Because the molecular mass is <100, the relative intensity of the M + 2 peak (4.4%) is too large to come from C or O alone, but not large enough to come from either Cl or Br. The observed intensity for the M + 2 peak does not correlate well with that expected for ^{30}Si (3.4%), but does match that for one S atom[6]:

$$(\text{No. of S atoms}) \times 4.4\% = 4.4\%$$
$$(\text{No. of S atoms}) = 4.4\%/4.4\% = 1$$

Because N appears to be absent from this molecule, the only A + 1 element to be considered is C. In order to determine the number of C atoms in this ion, however, the contribution of one S atom to the M + 1 peak (0.8%) must first be subtracted from the observed intensity: 5.1% − 0.8% = 4.3%. The number of C atoms is then calculated from Equation 2.2:

$$(\text{No. of C atoms}) \times 1.1\% = 4.3\%$$
$$(\text{No. of C atoms}) = 4.3\%/1.1\% = 3.9 \approx 4$$

Four C atoms plus one S atom adds up to $(12 \times 4) + (32) = 80$ u, 4 u short of the MM. The addition of four H atoms satisfies this requirement, giving an elemental composition of C_4H_4S.

DropBooks

The rings plus double bonds formula indicates that there are

$$(4) - \tfrac{1}{2}(4) + \tfrac{1}{2}(0) + 1 = 4 - 2 + 0 + 1 = 3$$

unsaturations in the molecule. Although the combination of one double and one triple bond cannot be ruled out, a structure containing a ring plus two double bonds is also possible. Thiophene, whose structure is shown below, fits this description.

[6] Although the isotopic peak intensity data are consistent with one Si and three or four O atoms, these combinations do not fit the observed *m/z* values. The mass of SiO_4 (MM 94) is too large, whereas SiO_3 (MM 76) must accommodate eight H atoms, producing an untenable structure:

m/z	Obs. Int.	Calc. for SiO_4	Calc. for SiO_3
84	100.0	100.0	100.0
85	5.1	5.1	5.1
86	4.4	4.2 (=3.4 + 0.8)	4.0 (=3.4 + 0.6)

Example 2.4

m/z	Obs. Rel. Int.
115	27.9
116	7.3
117	100.0
118	63.6
119	5.7
120	0.2

Two fragment ion peaks in the spectrum of this compound are useful in helping determine the elemental composition. They occur at *m/z* 103 (8.2%) and 91 (28.4%, which corresponds to the $C_7H_7^+$ ion; see Chapter 5).

Answer: Although the most intense peak in the cluster is found at *m/z* 117, this peak clearly cannot represent the $M^{+\bullet}$. The only A + 1 element that contributes more than 1.1% to the M + 1 peak is Si, and even four Si atoms ($4 \times 28 = 112$ u) will produce an M + 1 contribution of only $4 \times 5.1 = 20.4\%$. The peaks at *m/z* 115 and 116 are too small to represent the $M^{+\bullet}$ because the MM is not great enough to accommodate more than one Br or 3 Cl atoms (see Figure 2.6). Because a characteristic C-containing fragment ion peak is observed at *m/z* 91, it is safe to assume that this compound contains mostly C atoms. The true $M^{+\bullet}$ peak is therefore the one at *m/z* 118, and the peak at *m/z* 117 represents the $(M - 1)^+$ ion. The small fragment ion peak at *m/z* 103, which is 15 below *m/z* 118, represents the loss of $^{\bullet}CH_3$ and corroborates this assignment. Because *m/z* 118 is an even value, N is assumed to be absent.

The M + 2 peak at *m/z* 120 is quite small, ruling out the presence of any of the obvious A + 2 elements. Under the assumption that most of the mass of this compound consists of C atoms, the number of C atoms can be roughly approximated by dividing the observed intensity of the *m/z* 119 peak by that of the peak at *m/z* 118. This gives $5.7/63.6 \times 100 = 8.9\%$, or about $8.9/1.1 \approx 8$ C atoms. However, the fact that the *m/z* 117 peak is so intense means that it will produce ^{13}C contributions at both *m/z* 118 and *m/z* 119 which cannot be ignored. If the assumption is made for the moment that the $(M - 1)^+$ ion also contains eight C atoms, these contributions would be $8 \times 1.1 = 8.8\%$ and $0.006 \times (8)^2 = 0.006 \times 64 = 0.4\%$, respectively. These values do not have to be normalized because the *m/z* 117 peak is already the base peak in the spectrum. This leaves a $63.8 - 8.8 = 54.8\%$ intensity at *m/z* 118 that is due to the $M^{+\bullet}$ and $5.7 - 0.4 = 5.3\%$ at *m/z* 119 for the M + 1 peak in the $M^{+\bullet}$ peak cluster.

The number of C atoms present in this compound is more accurately calculated using these latter figures. This leads to a value of $5.3/54.8 \times 100 = 9.7\%$, which is closer to $9.7/1.1 = 8.8 \approx 9$ C atoms than eight. If there are nine C atoms in the $M^{+\bullet}$, there must also be nine C atoms in the $(M - 1)^+$ ion.

If contributions from the smaller peaks at *m/z* 115 and 116 are ignored, the following intensities can be calculated for the peaks at *m/z* 117–120:

m/z	$(M-1)^+$	$M^{+\bullet}$	Total Calc. Int.
117	100.0	—	100.0
118	9.9	53.7 (= 63.6 − 9.9)	63.6
119	0.5	5.3 (= 53.7 × 9.9%)	5.8
120	—	0.3 (= 0.006 × 9^2 × 53.7%)	0.3

These values match the observed intensities well.

The combined mass of nine C atoms is $9 \times 12 = 108$ u, which leaves only 10 u to be made up by other elements. The presence of 10 H atoms satisfies this requirement, producing an elemental composition of C_9H_{10}. The rings plus double bonds formula shows that there are $9 - \frac{1}{2}(10) + \frac{1}{2}(0) + 1 = 5$ unsaturations. As in Example 2.1, the presence of an aromatic ring can account for four of these unsaturations, leaving an additional ring or double bond for the remaining unsaturation. There are a number of similar structures that meet this description, including several methylstyrenes and cyclopropylbenzene. The mass spectra of many of these compounds are similar to one another.

ADDITIONAL PROBLEMS

DropBooks

2.8–2.12. The mass spectra of five unknown compounds are shown in Figures 2.15 through 2.19. Isotope peak intensity data for the $M^{+\bullet}$ peak are provided in each figure, and data for important fragment ions are given in a few cases. Determine the elemental composition for each ion for which data are given. If possible, propose structures for the unknowns.

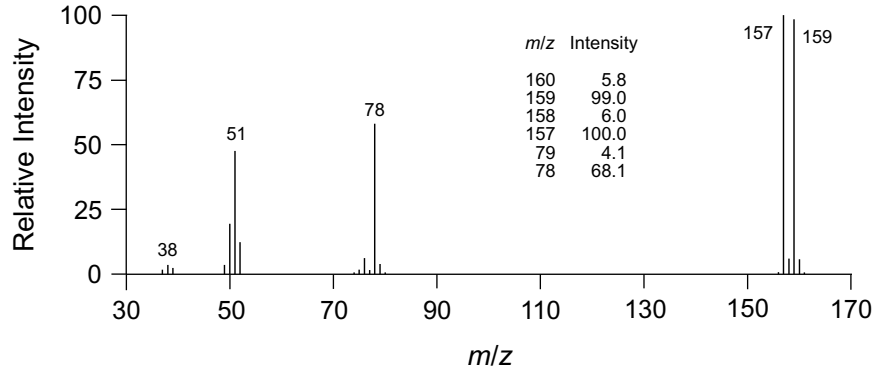

Figure 2.15. Mass spectrum for Problem 2.8.

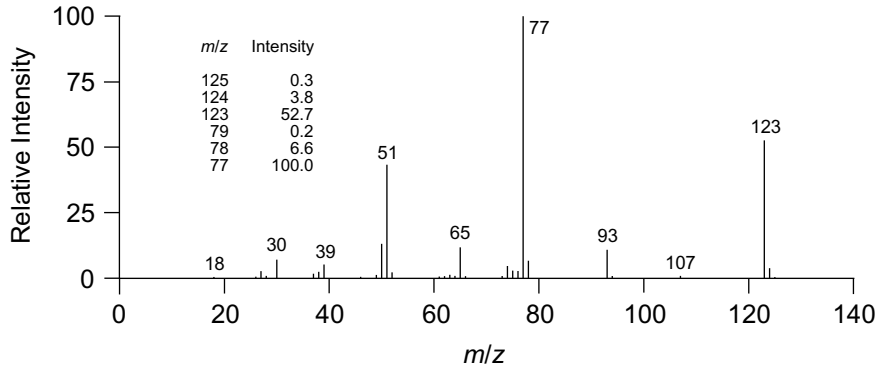

Figure 2.16. Mass spectrum for Problem 2.9.

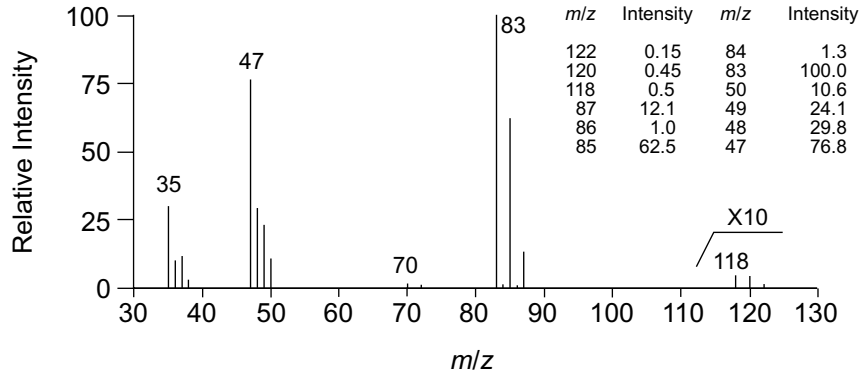

Figure 2.17. Mass spectrum for Problem 2.10.

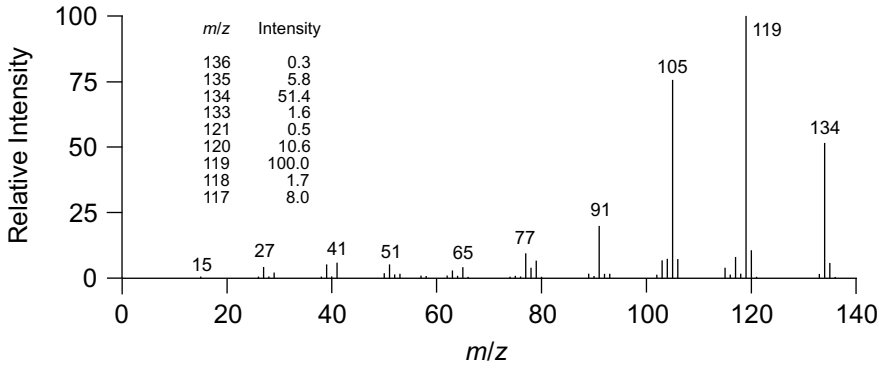

Figure 2.18. Mass spectrum for Problem 2.11.

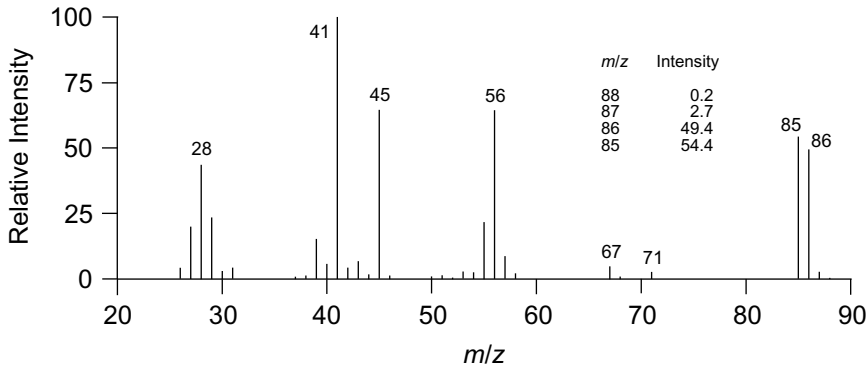

Figure 2.19. Mass spectrum for Problem 2.12.

2.13. Using the data in Table 1.3, try to calculate the elemental composition of the ion that produced the *m/z* 299 peak in the spectrum of THC. How useful are these data, which were produced using a transmission quadrupole during the course of a routine capillary GC/MS analysis?

REFERENCES

DropBooks

P. Ausloos, C. L. Clifton, S. G. Lias, A. I. Mikaya, S. E. Stein, D. V. Tchekhovskoi, O. D. Sparkman, V. Zaikin, and D. Zhu, "The Critical Evaluation of a Comprehensive Mass Spectral Library," *J. Amer. Soc. Mass Spectrom.*, **10**, 287–299 (1999).

J. R. Ehleringer, J. F. Casale, M. J. Lott, and V. L. Ford, "Tracing the Geographical Origin of Cocaine," *Nature*, **408**, 311–312 (2000).

F. W. McLafferty and F. Tureček, *Interpretation of Mass Spectra*, 4th edition, (University Science Books, Mill Valley, CA, 1993), frontispiece.

D. R. Rubenstein, C. P. Chamberlain, R. T. Holmes, M. P. Ayres, J. R. Waldbauer, G. R. Graves, and N. C. Tuross, "Linking Breeding and Wintering Ranges of a Migratory Songbird Using Stable Isotopes," *Science*, **295**, 1062–1065 (2002).

O. D. Sparkman, *Mass Spec Desk Reference* (Global View Publishing, Pittsburgh, PA, 2000), pp. 108–109.

3

IONIZATION, FRAGMENTATION, AND ELECTRON ACCOUNTING

3.1. A BRIEF REVIEW OF ORBITALS AND BONDING

The electrons in chemical elements are found in orbitals that occupy the space surrounding the nucleus. These orbitals have discrete energies and shapes that are defined by quantum mechanics. Two types of atomic orbitals are of interest in organic mass spectrometry: *s*-orbitals, which are spherically symmetrical about the nucleus, and a set of three *p*-orbitals, which lie along each of the Cartesian axes and are symmetrical to rotation around the axis along which they are found. Figure 3.1*a* illustrates the shape and location of *s*- and *p*-orbitals.

For most common elements, only electrons in the outermost shell of orbitals are used in forming chemical bonds. When these elements form chemical bonds with other atoms, ''pure'' *s*- and *p*-orbitals are rarely used. Instead, lower-energy configurations are achieved by ''mixing'' the *s*- and *p*-orbitals to varying degrees, depending on the types of bonds that are formed. When the outermost *s*- and all three *p*-orbitals are mixed, the result is a set of four hybrid sp^3 suborbitals that point toward the vertices of a tetrahedron (Figure 3.1*b*). Carbon uses sp^3 hybrid suborbitals in forming compounds such as methanol. Mixing the *s*- and two *p*-orbitals leads to a set of three hybrid sp^2 suborbitals, all of which lie in the same plane and point toward the vertices of an equilateral triangle (Figure 3.1*c*). The axis of the remaining *p*-orbital is perpendicular to the plane of the three sp^2 suborbitals. This configuration is adopted by the C atoms that make up a molecule of ethene

Understanding Mass Spectra: A Basic Approach, *Second Edition*. By R. Martin Smith
ISBN 0-471-42949-X © 2004 John Wiley & Sons, Inc.

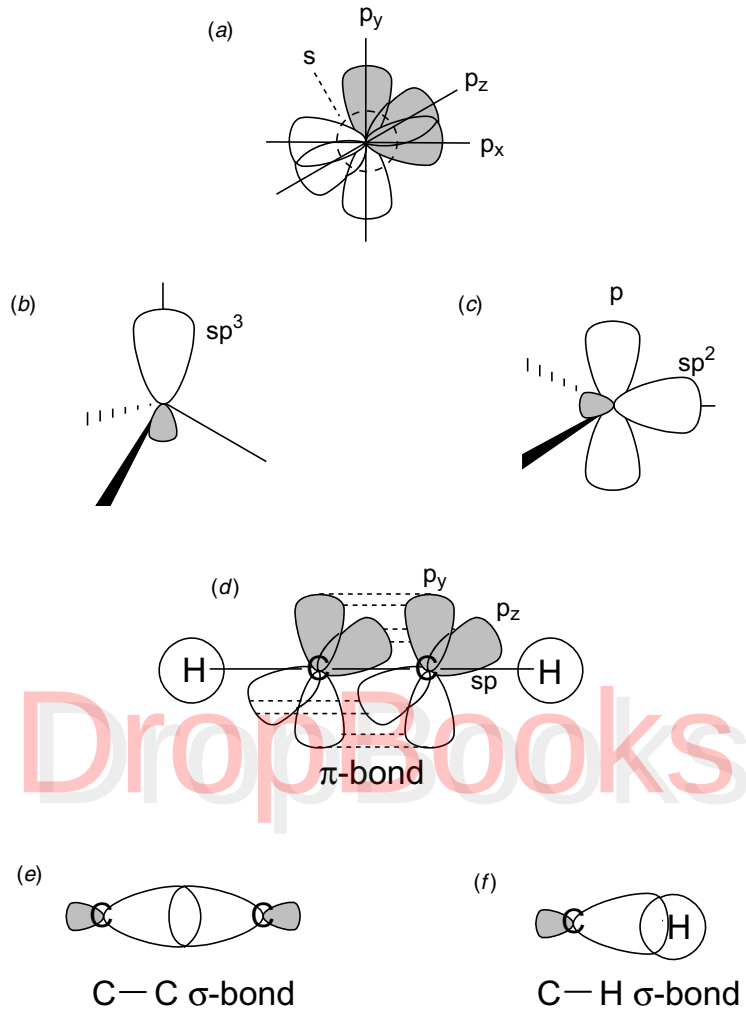

DropBooks

Figure 3.1. Orbitals and bonds in organic molecules. (*a*) The outermost *s*- and *p*-orbitals of a second-row element; (*b*) sp^3-hydrid suborbital; (*c*) sp^2-hydrid suborbital and remaining *p*-orbital; (*d*) acetylene, showing *sp*-hybrid geometry at C and two π-bonds between *p*-orbitals on adjacent C atoms; (*e*) C–C σ-bond formed by overlap between two hybrid suborbitals; (*f*) C–H σ-bond formed by overlap between a hybrid suborbital on C and the *s*-orbital of H.

(ethylene). Finally, mixing the *s*- and one *p*-orbital leads to a set of two hybrid *sp* suborbitals that lie on a straight line and point in opposite directions from one another (Figure 3.1*d*). The C atoms in a molecule of ethyne (acetylene) use this configuration. The axes of the two *p*-orbitals remaining on each C atom are perpendicular to the axis of the *sp* suborbitals and to each other.

Atomic orbitals and hybrid suborbitals on one atom can combine with those on neighboring atoms to produce molecular orbitals that, when filled with two

electrons each, describe chemical bonds. An atomic orbital or hybrid suborbital can also be filled with two electrons that do not enter into chemical bonding. These are called nonbonding electrons and nonbonding orbitals.

When the electron cloud of two orbitals or hybrid suborbitals overlap in a ''head-on'' manner, a σ-bond is formed. Figure 3.1*e* shows a C—C σ-bond formed by overlap between two hybrid suborbitals, and Figure 3.1*f* depicts a C—H σ-bond formed by overlap between a hybrid suborbital on C and the *s*-orbital on H. If no other bonds are formed between the two atoms, this σ-bond is called a single bond.

Overlap between two *p*-orbitals that are located on adjacent atoms already joined by a σ-bond cannot occur in a ''head-on'' manner because the orbitals are parallel to one another. Instead, overlap occurs in a ''side-by-side'' fashion. When the resulting molecular orbital is filled with two electrons, a π-bond is formed. Because compression of the σ-bond between the two atoms is limited by nuclear repulsions, the amount of overlap between the two *p*-orbitals is also limited. As a result, most π-bonds are weaker than most σ-bonds.

Figure 3.1*d* illustrates the two π-bonds in acetylene that are formed by overlap of adjacent pairs of *p*-orbitals. The two C atoms in this molecule have a total of three bonds connecting them: a σ-bond formed by overlap of *sp* hybrid suborbitals and the two π-bonds. Taken together, this combination is called a triple bond. In ethylene the two C atoms are joined by a double bond, which is the combination of a σ-bond formed by overlap of sp^2 hybrid suborbitals and a π-bond between the adjacent *p*-orbitals. Double bonds are stronger than single bonds because they consist of two bonds: a σ-bond and a π-bond. However, π-bonds are still generally weaker than σ-bonds.

3.2. EVEN- AND ODD-ELECTRON SPECIES

When an electrically neutral molecule interacts with high-energy electrons in the electron ionization source, the molecule absorbs energy. In an effort to reach a lower-energy state, one of the molecule's electrons is expelled. Because nearly all atomic and molecular orbitals in organic molecules contain pairs of electrons, this process leaves one unpaired electron and a positive charge where the lost electron used to be. The radical ion concept may be unfamiliar, but keeping track of each electron is important when writing mechanisms for mass spectral fragmentations.

Both ions and neutral fragments can have either an odd or even number of electrons. Writing out complete valence electronic (Lewis) structures for these species may make this easier at first. A few simple examples are shown in Figure 3.2.

Even-Electron Neutral Species (EE^0). Nearly all electrically neutral organic molecules have an even number of electrons in their ground state. To denote their electrical neutrality, even electron (EE) species may be given the superscript ^{0} following their formulas. Most EE^0 species have all their electrons paired either in single,

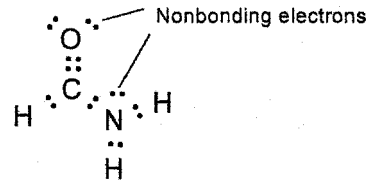

Even-electron Neutral Molecule

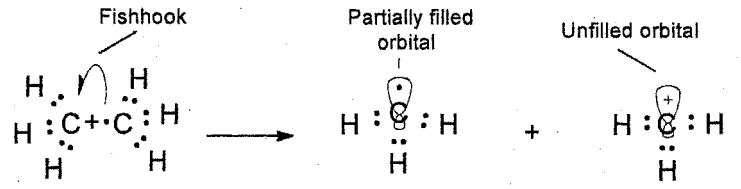

Figure 3.2. Electronic structures of some simple molecules, radicals, and ions.

DropBooks

double, or triple bonds or as nonbonding (lone) pairs. Some EE^0 fragments can exist as diradicals, that is, with two unpaired electrons located on different atoms. However, because additional energy is needed to keep the electrons from pairing up and forming a bond, diradicals tend to occur infrequently. The valence electronic structure for the ground state of formamide ($HCONH_2$), a molecule containing a C—O double bond and two atoms with nonbonding electrons, is shown at the top of Figure 3.2.

Odd-Electron Ion (Radical Ion; $OE^{+\bullet}$). Ejection of one electron from an EE^0 molecule forms an odd-electron ion (the molecular ion; $M^{+\bullet}$) in which the single electron remaining in the now partially filled orbital is unpaired. Because only EE^0 molecules will be considered in this book, the $M^{+\bullet}$ formed by EIMS are odd-electron ions. Odd-electron ions are denoted by the symbol$^{+\bullet}$, placed either after the formula or at the actual charge site. If the radical site and the site of positive charge are located on separate atoms, the $^\bullet$ may be placed next to the atom having the radical site, and a + sign placed next to the atom having the positive charge. If the charge and radical are not associated with the same or adjacent atoms, these ions are called distonic ions. The $M^{+\bullet}$ for ethane (C_2H_6) is seen at the left of the equation at the bottom of Figure 3.2.

Odd-Electron Neutral Fragment (Radical; $^\bullet OE$). When an $OE^{+\bullet}$ fragments, it must produce at least one odd-electron fragment in order to balance the total number of

electrons. If exactly two products are formed, which is the case for most fragmentations, then one of the products will be an OE species and the other an EE species. In Figure 3.2, the central bond of the $M^{+\bullet}$ of ethane, weakened by the loss of an electron from the C—C σ-bond, breaks apart. One electron, whose movement is denoted in Figure 3.2 by a single-headed arrow or ''fishhook,'' moves away with one of the methyl groups (arbitrarily assigned the left one in Figure 3.2) to produce a methyl radical ($^{\bullet}CH_3$). A methyl radical contains one unpaired electron, located in a nonbonding sp^3 orbital on the C atom.

A methyl radical is electrically neutral. The valence shell for C contains four electrons, so that it will remain electrically neutral if it has four electrons associated with it. In $^{\bullet}CH_3$ the C atom shares an electron pair with each of the three H atoms and in the process ''owns'' one electron from each bonding pair, for a total of three bonding electrons. The fourth electron is the nonbonded unpaired electron, which completes the requirements for the electrical neutrality of C. Each H atom is electrically neutral because it also owns one electron (one-half of an electron pair shared with a C atom), thus fulfilling its normal valence requirement. Because $^{\bullet}CH_3$ is electrically neutral and not a charged species, it is not detected by the mass spectrometer.

Even-Electron Ion (EE^+). The other product resulting from the fragmentation of ethane is a methyl carbenium ion ($^{+}CH_3$), shown at the right of the equation at the bottom of Figure 3.2. The main difference between a methyl carbenium ion and a methyl radical is the absence of the unpaired electron in the nonbonding orbital associated with the C atom. Because this orbital contains no electron, the C atom is one electron short of electrical neutrality, and the species is thus positively charged. At the same time, all the valence electrons in a methyl carbenium ion are paired in the bonds between the C atom and H atoms, rendering the ion an even-electron species.

3.3. SITE OF INITIAL IONIZATION

Ionization in EIMS occurs by a complex process in which enough energy from the ionizing electron beam is transferred to the sample molecule that the ionization potential of the molecule is exceeded and the molecule ejects an electron to form a positive ion. In fact, the energy of the ionizing electrons (traditionally, 50–70 eV) so far exceeds the ionization potential of the molecule that, if a substantial proportion of this energy is transferred to the molecule, additional ionization (formation of double and triple charged ions) and/or fragmentation can occur. How much energy is transferred depends on how the ionizing electrons and the electron cloud of the molecule interact.

The electrons most susceptible to ejection are those in molecular orbitals having the highest energy (the highest occupied molecular orbitals, or HOMOs). Figure 3.3 shows the relative energies of different types of molecular orbitals found in organic compounds. Basically, these molecular orbitals fall into five categories—σ, π, n, π^*,

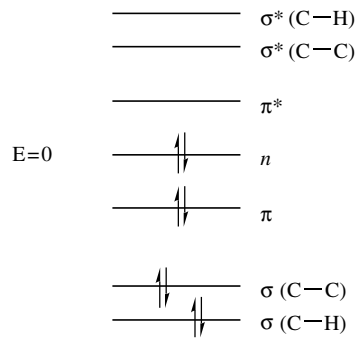

Figure 3.3. Relative energies of molecular orbitals in organic compounds.

and σ^*. Molecular orbitals that describe σ-bonds in the molecule are called σ-orbitals (Section 3.1), and molecular orbitals describing the π-bonds in a molecule are denoted as π-orbitals. The strongest bonds in the molecule are σ-bonds. Because π-bonds are generally weaker than σ-bonds (Section 3.1), π-orbitals are usually found at higher energies than σ-orbitals.

Unlike C and H, most heteroatoms in neutral molecules do not share all their valence electrons with other atoms in chemical bonds. Instead, they have one or more orbitals that each contain a pair of nonbonding electrons. These molecular orbitals are called *n*-orbitals, and because they are not involved in bonds with other atoms, no bonding energy is gained. These orbitals are found near the "zero" of energy for the molecule. In contrast to the σ- and π-orbitals, which may describe bonding that extends over several atoms at the same time, *n*-orbitals remain essentially localized on the individual heteroatoms.

DropBooks

Located at even higher energies are antibonding σ^*- and π^*-orbitals. These orbitals are nearly always empty in the ground state of the molecule because they describe a situation in which some atoms are not bonded together.

Electron ionization causes ejection of an electron from one of the uppermost molecular orbitals in the molecule. The order of orbital energy shown in Figure 3.3 indicates that, if the molecule contains heteroatoms, ionization should occur preferentially at one of the *n*-orbitals on the heteroatoms. On the other hand, if a molecule contains no heteroatoms, but does have C—C double or triple bonds, the ejected electron should come from the highest-energy π-orbital(s). Saturated hydrocarbons, lacking both *n*- and π-orbitals, must lose an electron from one of the σ-orbitals. The symbolism shown in Figure 3.4 will be used to designate these various types of ionization.

This simplistic picture is complicated by three factors. First, there is considerable variation in the strengths of different σ- and π-bonds, so that some π-bonds are stronger than some σ-bonds (which means that the orbitals for these π-bonds occur at lower energies than those for the σ-bonds). Second, although nonbonding orbitals occur near a zero of energy for a given molecule, these zeros are not the same from molecule to molecule because electrons associated with more electronegative

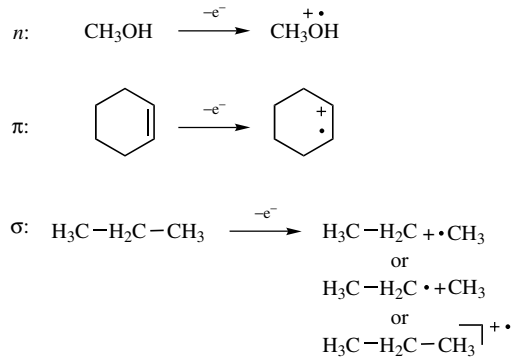

Figure 3.4. Examples showing notation for localization of initial ionization site. When a σ-bond is ionized, the charge can remain with either side of the bond, so that the $M^{+\bullet}$ is often best represented as $(R–H)^{]+\bullet}$.

atoms are generally more difficult to remove than those associated with atoms that are less electronegative. Finally, because so much energy is available from the ionizing electron, electrons from molecular orbitals below the HOMO(s) may be ejected, especially if the difference in energy between the HOMO(s) and the orbital at lower energy is fairly small.

The energy required to remove one electron from a molecule is called the ionization energy (IE) or ionization potential of the molecule. A list of ionization energies for a number of molecules and radicals is found in Table 3.1, which is also located inside the front cover of this book. This table will be used repeatedly during subsequent discussions because, in order to devise realistic mechanisms for how molecules fragment, the site of initial ionization must be defined. Table 3.1 will assist in that task.

The data in Table 3.1 illustrate some concepts that have been discussed previously, as well as some new ones. First, the IEs for groups containing electronegative atoms are higher than those for other species. For example, IEs for both the halogen radicals and alkyl halides decrease as one proceeds down the Periodic Table from the highly electronegative F to the much less electronegative I. Also, those of alkyl N-containing compounds are lower than those of the corresponding O compounds, but comparable to those of the corresponding S compounds.

Second, the addition of a double or triple bond in a structure generally lowers the IE, because π-orbitals are generally found at higher energies than σ-orbitals. This is seen, for example, by comparing the IEs for cyclohexane (9.9 eV) and cyclohexene (8.8 eV) or *n*-alkanes (10.4 eV) and *n*-alkenes (9.6 eV).

Third, the IEs for the radicals listed at the right side of the table reflect the stabilities of the ions that are formed by removal of the unpaired electron—that is, the lower the IE, the more stable the resulting ion. For example, the benzyl radical has a lower IE than does the phenyl radical because benzyl ion ($C_6H_5—C^+H_2$) is stabilized by delocalization of the charge over the entire aromatic ring (Figure 3.5). In the phenyl ion ($^+C_6H_5$), the positive charge is located in an empty sp^2 orbital that

Table 3.1. Ionization energies of selected compounds and radicals (in eV)

Hydrocarbons		O/S Compounds		N/Halogen Compounds		Radicals	
HC≡CH	11.4	CO	14.0	N_2	15.6	$F^{\bullet}$	17.4
CH_2=CH_2	10.5	CO_2	13.6	HCN	13.6	$Cl^{\bullet}$	13.0
n-Alkanes	~10.4	H_2O	12.5	NH_3	10.2	$Br^{\bullet}$	11.8
$R_2CHCHR'_2$	~10.2[a]	H_2C=O	10.9	$RCONH_2$	~9.8	$I^{\bullet}$	10.5
Cyclohexane	9.9	RCO_2R'	~10.2	RCH=NH	~9.6	$SH^{\bullet}$	10.4
Benzyne	9.7	*n*-ROH	~10.1	Pyridine	9.3	$CH_3^{\bullet}$	9.8
n-Alkenes	~9.6	RCHO	~9.8	RCH=NR′	~9.1	CH_2=$CH^{\bullet}$	8.8
Benzene	9.2	CH_3COCH_3	9.7	$RCONR'_2$	~8.8	$ROCO^{\bullet}$	8.6
RCH=CHR′	~9.1	$ArCO_2H$	9.7	*n*-RNH_2	~8.7	$CH_3O^{\bullet}$	8.6
1,3-Butadiene	9.1	CH_2C=O	9.6	Pyrrole	8.2	$Ar^{\bullet}$	8.1[b]
$ArCH_3$	8.9	R_2O	~9.5	R_2NH	~8.0	CH_2=$CHCH_2^{\bullet}$	8.1
Cyclohexene	8.8	ArCOR	~9.4	$ArNH_2$	7.7	$HCO^{\bullet}$	8.1
Ar-CH=CH_2	8.4	*n*-RSH	~9.1			*n*-$Bu^{\bullet}$	8.0
Naphthalene	8.1	Thiophene	8.9			$HOCH_2^{\bullet}$	7.6
		Furan	8.9	*n*-RF	~12.5	$HSCH_2^{\bullet}$	7.5
		ArOH	8.5	*n*-RCl	~10.7	*s*-$Bu^{\bullet}$	7.3
		R_2S	~8.4	*n*-RBr	~10.1	$ArCH_2^{\bullet}$	7.1
		ArOR	~8.2	*n*-RI	~9.2	$CH_3CO^{\bullet}$	7.0
		CH_3SSCH_3	7.4	ArCl	9.1	$ROCH_2^{\bullet}$	~6.9
				ArBr	9.0	*t*-$Bu^{\bullet}$	6.7
						Cyclic $C_3H_3^{\bullet}$	6.6
						Cyclic $C_7H_7^{\bullet}$	6.2
						$H_2NCH_2^{\bullet}$	6.1
						$R_2NCH_2^{\bullet}$	~5.7
						$H_2NCR_2^{\bullet}$	~5.4

DropBooks

[a]R and R′ stand for alkyl groups. Approximate values based on averages for two or more similar compounds.
[b]Ar = C_6H_5–.
Source: Reprinted in part by permission from F. W. McLafferty and F. Tureček, *Interpretation of Mass Spectra, 4th Edition*, pp. 343–345. Copyright University Science Books, Sausalito, CA, 1993.

lies within the plane of the ring and does not overlap with the *p*-orbitals that form the π-bonds of the ring. The IEs for isomeric alkyl radicals also conform to this trend, with that of the *tert*-butyl radical being the lowest, that of *n*-butyl the highest, and that for *sec*-butyl falling in between.

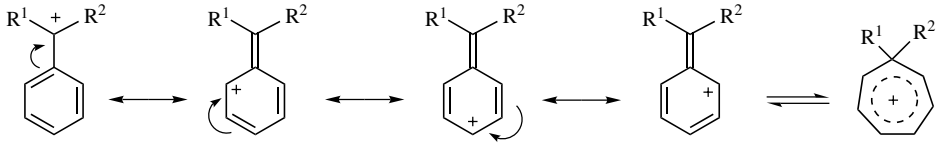

Figure 3.5. Stabilization of the benzyl ion by the aromatic ring.

The low IEs for the various alkyl N-containing radicals in Table 3.1 may seem surprising. As will be seen in Chapter 6, the ions formed from these radicals are produced in great abundance from the $M^{+\bullet}$ of appropriate compounds, sometimes to the near exclusion of all other ions.

Finally, the IEs of small double and triple bonded molecules such as CO, CO_2, N_2, and HCN are all quite high, so that these molecules resist taking a positive charge. As a result, they are frequently lost as neutral species in the fragmentation of appropriate compounds, as will become apparent in subsequent chapters.

Example 3.1

Determine the most likely initial ionization site for cocaine, whose structure is given below.

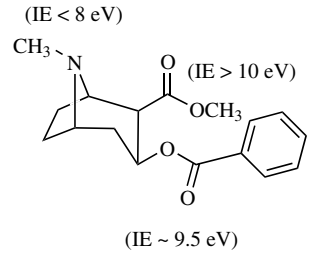

Answer: In order to solve this problem, appropriate model compounds must be found in Table 3.1 that will provide approximate IEs for the functional groups present in cocaine. The N in cocaine is a tertiary aliphatic amine; the closest model in Table 3.1 is a secondary amine (R_2NH), whose IE is approximately 8.0 eV. The carbomethoxy group is an aliphatic ester of an aliphatic acid, which is best approximated by RCO_2R' (with an IE of 10.2 eV). The last group is an aliphatic ester of benzoic acid, for which the closest model in Table 3.1 is benzoic acid itself, with an IE of 9.7 eV. The IEs for the C—C σ-bonds in the ring system are best approximated by that for cyclohexane, about 9.9 eV.

Even if there is some inaccuracy in estimating the IEs of the functional groups in cocaine based on those of the models, it seems clear that the IE of the amine group is considerably lower than those of either the ester groups or the σ-bonds in the ring system. If the large difference in the IEs of the models is truly reflective of the situation in cocaine, initial ionization in this molecule should occur almost exclusively at the N atom. In other molecules the differences may not be as large, and initial ionization may occur at two or more sites in the molecule.

3.4. TYPES OF FRAGMENTATION

The fragmentation depicted at the bottom of Figure 3.2 shows an odd-electron ion dissociating to give an odd-electron neutral fragment (radical) and an even-electron

ion, a process that can be symbolized by the equation

$$OE^{+\bullet} \rightarrow OE^{\bullet} + EE^{+}$$

All single-bond cleavages of the $M^{+\bullet}$ produce an $OE^{\bullet}$ and an EE^{+}.

Odd-electron ions can also fragment to give a second $OE^{+\bullet}$, but in that case the other product must be an EE^{0} because the unpaired (odd) electron is now found in the ionic fragment:

$$OE^{+\bullet} \rightarrow OE^{+\bullet} + EE^{0}$$

Whereas formation of an $OE^{\bullet}$ and an EE^{+} from an $OE^{+\bullet}$ occurs with cleavage of a single bond (as illustrated in Figure 3.2), formation of a second $OE^{+\bullet}$ and an EE^{0} is a more complex process and must involve both bond breaking and new bond formation, often with rearrangement of the atoms in the original ion. This type of fragmentation is sometimes useful for determining molecular structure (see Chapter 7, e.g.).

Even-electron ions, formed by fragmentation of either $OE^{+\bullet}$ or other EE^{+}, also have two ways of distributing valence electrons during their own dissociation. In either case, the two products must both be of the same type—either even- or both odd-electron:

$$EE^{+} \rightarrow EE^{+} + EE^{0}$$

or

$$EE^{+} \rightarrow OE^{+\bullet} + OE^{\bullet}$$

DropBooks

The first process is commonly observed. The second is less common because of the additional energy required to separate the previously paired electrons. As with the formation of EE^{0} from $OE^{+\bullet}$, the first process often proceeds with some structural rearrangement. The formation of double- and triple-bond small molecules (such as $CH_2{=}CH_2$, $CH_2{=}O$, $HC{\equiv}CH$, $HC{\equiv}N$, $C{\equiv}O$, or N_2) can be a strong driving force for this type of fragmentation. Subsequent chapters contain many examples.

The simplest type of fragmentation is σ-*bond cleavage*, which occurs in saturated hydrocarbons. An example is shown at the bottom of Figure 3.2. In this example, the initial charge and odd electron in the $M^{+\bullet}$ are both initially located between the same pair of atoms, and the odd electron leaves with the neutral fragment. The C atom that is best able to stabilize the charge will determine which product ion is the most abundant. In this case, both potential ion products are methyl carbenium ions. In other alkanes, however, σ-bond cleavage may produce secondary or tertiary carbenium ions that, because of their greater stability, will be more abundant (Sections 3.3 and 3.6.4).

Other fragmentation processes occur either by having the charge remain in the same part of molecule in which it originally resided (*charge retention*) or by neutralizing the original charge site and moving the charge to a new site in the

molecule (*charge migration*). Single-step charge retention fragmentations occur by *homolytic cleavage* of a single bond, in which a bonding electron moves to pair with the radical-site electron in the $M^{+\bullet}$. These fragmentations are said to occur by radical-site initiation (McLafferty and Tureček, 1993). α-Cleavage (Chapter 6) is a good example of a fragmentation that is initiated by the radical site.

Single-step charge migration fragmentations, on the other hand, occur by *heterolytic cleavage*, in which two electrons move in response to the charge site on the $M^{+\bullet}$. This neutralizes the original charge site and moves the charge to another atom. These are called charge-site initiated fragmentations. Different notations are used to distinguish between radical-site and charge-site initiated fragmentations. In this book, the movement of an individual electron will be denoted by a single-headed arrow or fishhook (⇀) and the movement of an electron pair by a full-headed arrow (→).

3.5. THE NITROGEN RULE

The nitrogen rule was introduced briefly in Section 2.3 to help generate elemental composition information about the $M^{+\bullet}$. Because any fragmentation of the $M^{+\bullet}$ that produces an $OE^{+\bullet}$ and EE^0 is sometimes useful in determining molecular structure, it is important to be able to identify peaks in the mass spectrum that represent $OE^{+\bullet}$. The nitrogen rule can help identify $OE^{+\bullet}$ fragments in some spectra. It is worthwhile to examine the derivation and utility of this rule a little more closely.

All but one of the elements normally encountered in organic mass spectrometry have an odd valence and odd nominal mass (H, F, P, Cl, Br, and I) or an even valence and even nominal mass (C, O, Si, and S). The exception is N, which has an odd valence and even nominal mass. Because of this, molecules (M^0) that contain an odd number of N atoms have an odd nominal mass. The $M^{+\bullet}$ differs in mass from the M^0 by only the mass of an electron, so that the $M^{+\bullet}$ has the same nominal mass as the M^0. Further, because most of the $M^{+\bullet}$ encountered in EIMS are single-charge ions, the *m/z* values for these ions are going to be the same as the nominal masses of the molecules. Therefore, the *m/z* value for an $M^{+\bullet}$ that contains an odd number of N atoms will be odd. Conversely, all $M^{+\bullet}$ that contain either zero or an even number of N atoms will produce peaks having even *m/z* values. Finally, because all $OE^{+\bullet}$ have the same valence requirements as the $M^{+\bullet}$, the nitrogen rule can be applied to all $OE^{+\bullet}$.

When a single bond in the $M^{+\bullet}$ of an organic molecule is cleaved, an EE^+ and $OE^\bullet$ are produced. Because both product species are one substituent short of fulfilling the valence requirements for an $OE^{+\bullet}$, an EE^+ that contains an odd number of N atoms will have an *even* nominal *m/z* value, and an EE^+ that contains an even number of N atoms (including 0) will have an *odd* nominal mass (Figure 3.6).

As a result, if the $M^{+\bullet}$ peak occurs at an even *m/z* value in the spectrum of an unknown compound, and the peaks that represent logical losses from the $M^{+\bullet}$ appear at odd *m/z* values, it is likely that the compound contains no N atoms and that all the peaks at odd *m/z* values are due to EE^+ resulting from single-bond

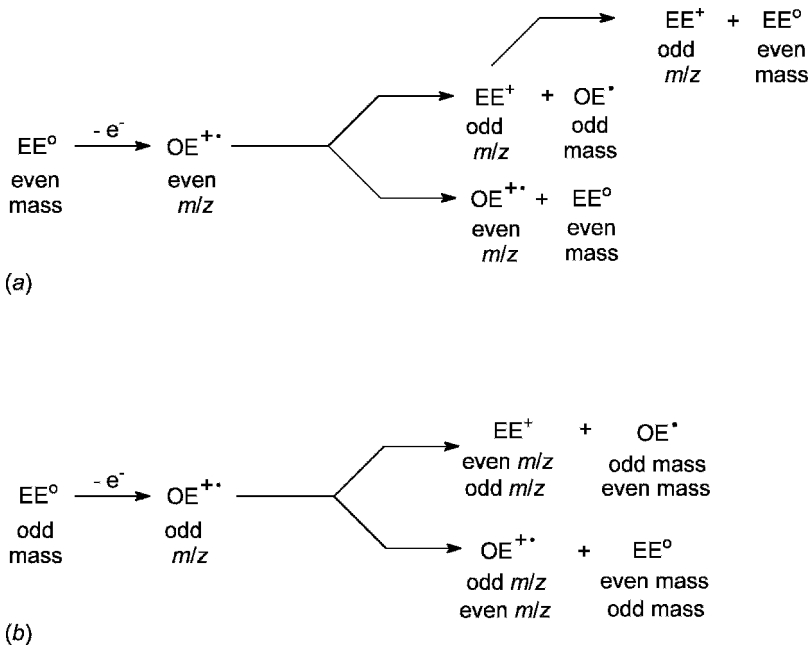

Figure 3.6. Application of the nitrogen rule to the ionization and fragmentation of even- and odd-mass molecules. (*a*) Fragmentation of an even-mass $M^{+\bullet}$ containing no N atoms leads to EE^+ fragments having odd *m*/*z* values and $OE^{+\bullet}$ fragments having even *m*/*z* values. (*b*) The *m*/*z* values for odd- and even-electron fragments that result from an odd-mass $M^{+\bullet}$ are less predictable. (From Sparkman and Watson, 2002.)

DropBooks

cleavage. If in the middle of these peaks there are a few peaks at even *m*/*z* values, these peaks probably represent $OE^{+\bullet}$ (Figure 3.6*a*).

The situation is more complex if the $M^{+\bullet}$ peak occurs at an odd *m*/*z* value. In that case, whether an $OE^{+\bullet}$ and EE^+ fragment ion has an odd or even *m*/*z* value depends on whether it contains a N atom or not (Figure 3.6*b*). Without knowing the fragmentations of the $M^{+\bullet}$ beforehand, these assignments cannot be made with certainty. In general, however, if the $M^{+\bullet}$ peak occurs at an odd *m*/*z* value, and the peaks that represent logical losses from the $M^{+\bullet}$ appear at even *m*/*z* values, it is likely that the compound which produced the spectrum contains an odd number of N atoms.

3.6. ENERGY CONSIDERATIONS IN FRAGMENTATION PROCESSES

3.6.1. Fragmentation Rates

The course of any chemical reaction is governed either by thermodynamic factors, in which the relative amounts of reactants and products in the final mixture are

determined by their relative stabilities, or by kinetic factors, in which product distribution is determined by the relative rates of possible reactions of the starting material. To be governed by thermodynamic control, the reactants and products must reach a state of equilibrium in which all products can revert to starting materials by reversing the reaction pathways that led to their formation. The strong electric fields present in the ion source of a mass spectrometer make equilibrium between fragmenting ions and their products difficult, because one of the main functions of the ion source is to *remove* the ion products as rapidly as they are formed. It is a reasonable assumption, then, that mass spectral fragmentations are controlled by the relative rates at which they occur.

Rates of chemical reactions are given by the Arrhenius equation

$$k = Ae^{-\Delta G^{\ddagger}/RT} \tag{3.1}$$

where k is the rate constant for the reaction, A is a "frequency factor" determined by the nature of the reaction, $\Delta G^{\ddagger}$ is the free energy of activation, R is the gas constant, and T is the temperature at which the reaction takes place. The larger the value of k, the faster the reaction. At constant T, $e^{-\Delta G^{\ddagger}/RT}$ approaches $e^0 = 1$ as $\Delta G^{\ddagger}$ decreases, and k increases toward a limiting value of A—that is, the reaction occurs more readily. On the other hand, as $\Delta G^{\ddagger}$ increases, $e^{-\Delta G^{\ddagger}/RT}$ approaches $e^{-\infty} = 0$, and k becomes smaller and smaller. In other words, the reaction occurs more slowly.

Those fragmentations in the ion source that have the largest values of k generate the most product ions per unit time. The actual timing of various fragmentation processes is critical because ions leave the ion source within about 10^{-5} s of being formed. Ions that are relatively stable (i.e., have large $\Delta G^{\ddagger}$'s for further fragmentation) react only slowly and tend to remain intact until they reach the detector. Less stable ions dissociate to varying degrees before they leave the ion source, thereby decreasing the number of these ions that reach the detector. Ions having $\Delta G^{\ddagger}$'s so low that they fragment completely before leaving the ion source are not detected directly at all.

Determining the relative rates of various fragmentation reactions hinges mostly on estimations of $\Delta G^{\ddagger}$, the energy needed to boost an ion to the transition state for the reaction. The transition state is a configuration of maximum energy in which breaking bonds are severely stretched and any new bonds are starting to form (Figure 3.7). For fragmentations that involve only a single step of bond breaking (no new bond formation), this energy will be the same as the dissociation energy for the bond that is being broken. The transition state occurs at an energy maximum and thus is differentiated from a reaction intermediate, which occurs at an energy minimum (even if that minimum is shallow and lies substantially above the energies of the reactants and products; see Figure 3.7). Because some energy is required to change the configuration of the intermediate, an intermediate has a finite lifetime, whereas a transition state does not.

The equation for determining $\Delta G^{\ddagger}$ is

$$\Delta G^{\ddagger} = \Delta H^{\ddagger} - T\Delta S^{\ddagger} \tag{3.2}$$

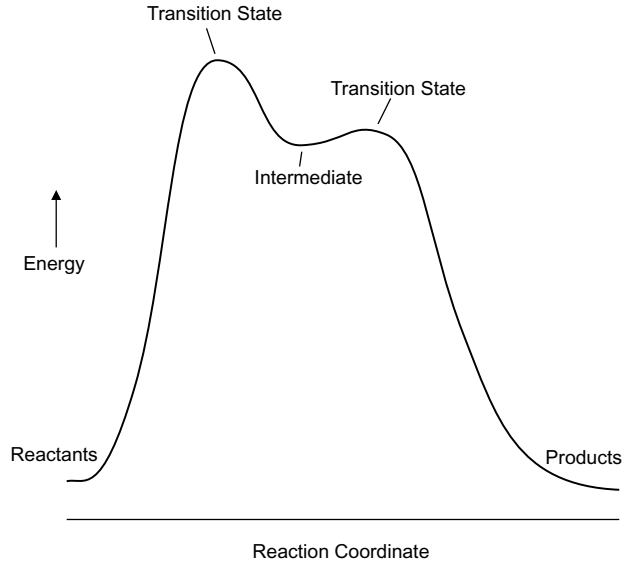

Figure 3.7. Energy diagram for a hypothetical reaction having an intermediate and two transition states.

where $\Delta H^{\ddagger}$ is the change in enthalpy or heat of activation (the energy needed to stretch and twist bonds toward their breaking point) and $\Delta S^{\ddagger}$ is the change in entropy (or orderliness) of the entire system (the more order required, the more *negative* the value of $\Delta S^{\ddagger}$). The term $\Delta H^{\ddagger}$ is affected by bond strengths and the relative stabilities of reactants and products. Although breaking bonds in the reactants obviously requires an input of energy (raising $\Delta H^{\ddagger}$), the simultaneous formation of bonds in the products (as happens during rearrangement reactions) or the formation of particularly stable ion products can lower $\Delta H^{\ddagger}$ at the same time.

$\Delta S^{\ddagger}$ is a measure of how difficult it is to get atoms to align themselves so that the reaction can take place. A reaction in which a bond simply stretches until it breaks should have a small value for $\Delta S^{\ddagger}$ because the alignment of atoms in the transition state is, if anything, more random than in the reactant. On the other hand, the need to arrange several atoms in a specific pattern, as occurs during rearrangement reactions, leads to a large negative value for $\Delta S^{\ddagger}$ and increases the overall energy of activation. All other things being equal, the change in entropy required to form five- and six-membered rings during rearrangement reactions is less than that needed to form other-sized rings. Nonetheless, rearrangements involving three-, four-, and seven-membered ring transition states also occur, especially if $\Delta H^{\ddagger}$ is particularly favorable.

3.6.2. Metastable Ions

A few fragmentations have reaction rates that fall in a narrow range around 10^{-5} s. When this happens, the precursor ion does not fragment before leaving the ion

source, but the resulting product ion is formed before it reaches the detector. The ability to detect these ions, which are called metastable ions, depends on the *m*/*z* analyzer used. For example, the motions of ions in the transmission quadrupole are unaffected by conditions that the ions experience prior to their arrival at the filter because the equations of motion involve only fields that are present in the filter itself (Section 1.3.3). Therefore, whether the precursor ion fragments before leaving the ion source or before entering the filter does not alter the fact that the ion actually passing through the filter is the product ion, which is the ion that will be detected.

In a magnetic sector instrument a precursor ion having an *m*/*z* value of m_1 may decompose just after leaving the ion source, but prior to arriving at the magnet, to form a product ion having an *m*/*z* value of m_2. The motions of the ions in this case (Section 1.3.2) are dependent on both the accelerating voltage that the precursor ion experienced as it left the ion source as well as the magnetic field strength and path radius when the product ion reaches the magnet. As a result, the ion is not detected at either m_1 or m_2, but rather at an *m*/*z* value that is determined by the equation

$$m^* = m_2^2/m_1 \tag{3.3}$$

Ions that fragment during their passage either through the analyzer or mass filter itself will develop motions that cause them to be undetectable.

The mass spectral peaks that result from metastable ions in magnetic sector instruments are generally weak and poorly resolved. They also occur most often at nonintegral *m*/*z* values due to the relationship in Equation 3.3. This is another reason why they may not be detected by lower resolution instruments (Section 1.5.2). When detected, however, metastable ions can be useful in determining fragmentation pathways. The precursor and product ions are often prominent ions in the spectrum, and their relationship as a precursor/product ion pair can be established because their *m*/*z* values must satisfy Equation 3.3.

3.6.3. Energy Diagrams

The energy diagram in Figure 3.8 describes the hypothetical fragmentation of an $M^{+\bullet}$ to give three *observed* product ions. The final product ions $^{+}F^{2}$ and $^{+}F^{3}$ in this illustration are arbitrarily shown to be more stable than the $M^{+\bullet}$. This is not always the case, even if one or both product ions produce prominent peaks in the spectrum.

During ionization, individual molecules absorb varying amounts of energy from the ionizing electrons. After absorbing enough energy for ionization, the $M^{+\bullet}$ have a fairly wide range of internal energy left over, which results in differing propensities toward further fragmentation. If $\Delta G^{\ddagger}$'s for one or more fragmentations of the $M^{+\bullet}$ are fairly low, many (or most) of the $M^{+\bullet}$ will have sufficient energy to fragment, and the $M^{+\bullet}$ will only be present in low concentrations by the time ions leave the ion source. This is typical of the behavior of aliphatic alcohols (Section 6.4.1), whose spectra often exhibit no $M^{+\bullet}$ peak.

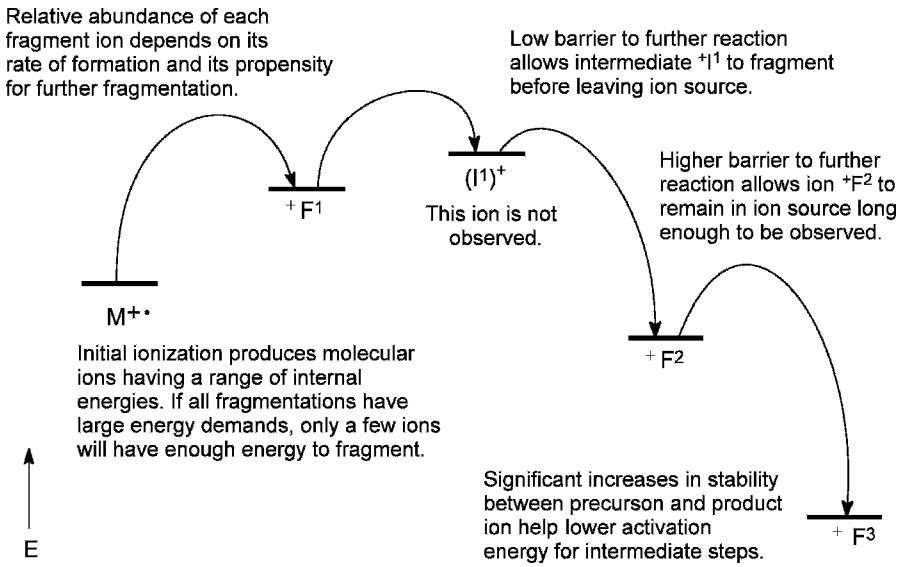
Relative abundance of each fragment ion depends on its rate of formation and its propensity for further fragmentation.
Low barrier to further reaction allows intermediate $^{+}I^{1}$ to fragment before leaving ion source.
$(I^{1})^{+}$
This ion is not observed.
Higher barrier to further reaction allows ion $^{+}F^{2}$ to remain in ion source long enough to be observed.
$^{+}F^{1}$
$M^{+\bullet}$
Initial ionization produces molecular ions having a range of internal energies. If all fragmentations have large energy demands, only a few ions will have enough energy to fragment.
$^{+}F^{2}$
Significant increases in stability between precurson and product ion help lower activation energy for intermediate steps.
$^{+}F^{3}$
E

Figure 3.8. Diagram illustrating various energy considerations during the fragmentations of a hypothetical $M^{+\bullet}$ and its resulting fragment ions.

DropBooks

On the other hand, if $\Delta G^{\ddagger}$'s for all fragmentations are fairly large, few $M^{+\bullet}$ will have the extra energy needed to fragment, and most of the observed peaks will be due to unfragmented $M^{+\bullet}$. Large $\Delta G^{\ddagger}$'s can result either from the precursor ion being very stable relative to all the product ions or from the fact that the fragmentation must proceed through several high-energy steps before a stable fragment can be lost. Aromatic compounds that lack easily fragmentable substituents, as well as compounds that have complex ring systems in which several bonds must be broken before a stable fragment can be lost, often show the $M^{+\bullet}$ peak as the base peak in the spectrum.

In order to be detected in reasonable abundance, product ions must be formed by pathways that produce significant numbers of ions. In addition, $\Delta G^{\ddagger}$'s for further fragmentation of these ions must be fairly high; otherwise, they will fragment before they accumulate to any significant degree. Indeed, if $\Delta G^{\ddagger}$ toward further fragmentation is extremely low, the intermediate ion will not be observed despite the fact that it is formed initially. Section 9.4 provides an example of a compound that fragments via an expected intermediate ion which is not observed in the spectrum.

Examining the α-cleavage fragmentations of 1-phenyl-2-aminopropane (amphetamine; see Section 6.3.1) should help clarify these concepts. The energy diagram for these fragmentations is shown in Figure 3.9. As illustrated in the center of Figure 3.9, initial ionization can occur either at the N atom (with an IE of ~8.7 eV; see Table 3.1) or in the aromatic ring (with an IE of ~8.9 eV). Initial ionization is followed by homolytic cleavage of bonds to the C atom next to the N (C2)

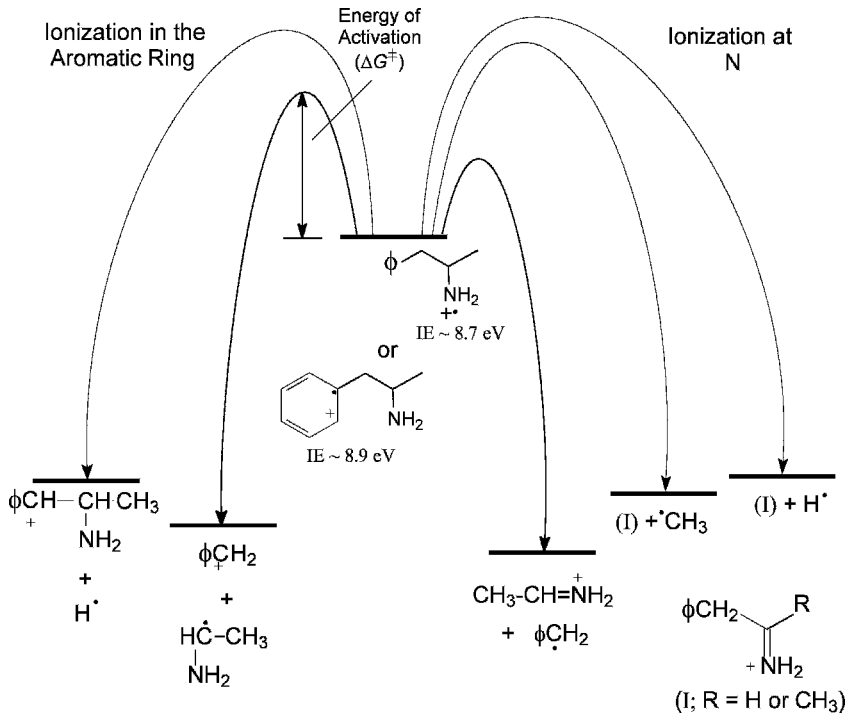

Figure 3.9. Energy diagram showing relative transition-state energies for α-cleavage fragmentations of 1-phenyl-2-aminopropane (not drawn to scale).

or to the one next to the aromatic ring (C1), respectively. The five different ways in which the $M^{+\bullet}$ of this compound can undergo α-cleavage are shown in Figure 3.9 and listed in Table 3.2. The product ions formed in these reactions are all fairly stable with respect to further fragmentation.

Because the base peak in the spectrum occurs at *m/z* 44, the fragmentation that forms the ion having this *m/z* value must have the lowest $\Delta G^{\ddagger}$. Why? With the exception of the broken bonds, the arrangements of atoms in all the product ions and radicals are the same as that in the $M^{+\bullet}$. It thus seems safe to assume that entropy factors play a relatively minor role in determining values for $\Delta G^{\ddagger}$. Instead,

Table 3.2. α-Cleavage fragmentations of 1-phenyl-2-aminopropane

Cleavage After Ionization at N		Cleavage After Ionization in Ring	
Loss of $H^{\bullet}$	(*m/z* 134; <1%)	Loss of $H^{\bullet}$	(*m/z* 134; <1%)
Loss of $^{\bullet}CH_3$	(*m/z* 120; 1–2%)	Loss of H_2N-$^{\bullet}CH$–CH_3	(*m/z* 91; 5–15%)
Loss of $\phi C^{\bullet}H_2$	(*m/z* 44; 100%)	(Formation of $\phi C^{+}H_2$)	

differences in $\Delta G^{\ddagger}$ are determined by enthalpy factors that help stabilize the transition states for such reactions. In this case, these enthalpy factors appear to be the same ones that help stabilize the products.

Consider first the fragmentations that occur after initial ionization on the N atom (right side of Figure 3.9). In each case, the product ion contains a new π-bond formed between C2 and the amine N atom. The methyl and benzyl ($\phi-CH_2$) groups attached to the doubly bonded C atom only offer a small amount of inductive stabilization of the incipient product ions in the transition state. The π-system of the aromatic ring in the benzyl group is not conjugated with the C=N bond and therefore cannot provide resonance stabilization. As a result, these three ions should all have similar stabilities.

The incipient radicals, on the other hand, have significantly different stabilities, with $^{\bullet}CH_3$ somewhat more stable than $^{\bullet}H$, but substantially less stable than benzyl radical (ϕ-$C^{\bullet}H_2$), which is resonance-stabilized (see Figure 3.5; the benzyl radical is stabilized by similar resonance structures). For this reason, the transition state of the fragmentation that forms benzyl radical is stabilized (i.e., has the lowest $\Delta G^{\ddagger}$ relative to the other pathways) by the resonance energy of the incipient benzyl radical. Ions having *m*/*z* 44, which are formed by this pathway, will be formed more rapidly, and thus in greater abundance, than ions formed via the other pathways.

Because the IEs for the amine group and the aromatic ring are similar, initial ionization can also occur by loss of one of the π-bond electrons from the ring. Homolytic cleavage of the bonds to the substituents on C1, and subsequent charge stabilization in the ring, leads to the formation of two benzyl carbenium ions as shown on the left side of Figure 3.9. One of these is the benzyl ion itself, formed by loss of a radical that contains the N atom and its attached C atoms; the other is a substituted benzyl ion produced by the loss of $^{\bullet}H$. As above, the two product ions should have similar stabilities, but the difference in stability between a secondary radical and $^{\bullet}H$ is substantial. This difference in stability is reflected in a corresponding difference in $\Delta G^{\ddagger}$ for these two fragmentations, so that the peak at *m*/*z* 91 due to loss of the secondary radical is more intense.

DropBooks

3.6.4. Stevenson's Rule

Although the explanation in the previous section explains why the peak at *m*/*z* 44 is larger than the peaks at *m*/*z* 120 and 134, and why peak at *m*/*z* 91 is also larger than the peak at *m*/*z* 134, it still does not explain why the *m*/*z* 44 peak is more intense than the one at *m*/*z* 91. To understand this, look at what happens when the σ-bond breaks between C1 (the benzylic C atom) and C2 (the C atom next to the N).

As the bond between these two atoms stretches (see below), this bond can break either homolytically, with neutralization of the radical site in either the aromatic

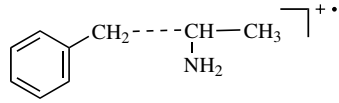

ring or on the N atom (depending on where initial ionization occurred), or heterolytically with neutralization of the initial charge. Determining which combination is more likely to form—benzyl ion and N-containing radical, or benzyl radical and N-containing ion—is accomplished using the IEs listed for radical fragments in Table 3.1. This is an example of the application of Stevenson's rule (Stevenson, 1951): If two fragments compete for possession of the charge during σ-bond cleavage, the incipient fragment that has the lower IE will primarily end up with the charge. In this case, the IE for benzyl radical is 7.1 eV, while that for the N-containing fragment is approximately 6.0 eV (Table 3.1 does not provide an exact model). Stevenson's rule predicts that the charge will reside primarily on the N-containing fragment (*m*/*z* 44), which is what is observed.

ADDITIONAL EXAMPLES

Although the material in this chapter has been rather theoretical in nature, it has some important applications that will be used throughout the rest of the book. In particular, writing mechanisms for fragmentation reactions depends on these concepts. Chapter 8 is devoted entirely to the subject of postulating mechanisms that account for how ions fragment.

Example 3.2

Write a mechanism that shows the loss of a methyl group from the $M^{+\bullet}$ of isopropanol. In doing so, determine (a) the site of initial ionization, (b) where the charge ends up after fragmentation, and (c) how the electrons from all the bonds that are broken contribute to formation of the final products.

Answer

(a) The IEs for loss of the electrons in the σ-bonds in the $M^{+\bullet}$ of this compound are slightly higher than those for loss of the nonbonding electrons in the OH group (Table 3.1). Therefore, initial ionization will occur preferentially on the O atom.

(b) After cleavage of the bond between C1 and C2, the location of the charge will be determined by Stevenson's rule (Section 3.6.4). The IE for a radical on a C atom located next to O is about 6.9 eV (Table 3.1), whereas the IE for a methyl radical is 9.8 eV. This means that the charge will end up primarily on the O-containing fragment (oxonium ion).

(c) A mechanism showing this fragmentation is given in Equation 3.4.

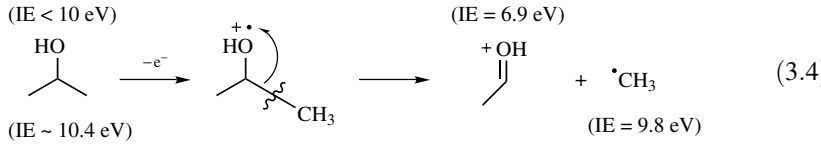

(3.4)

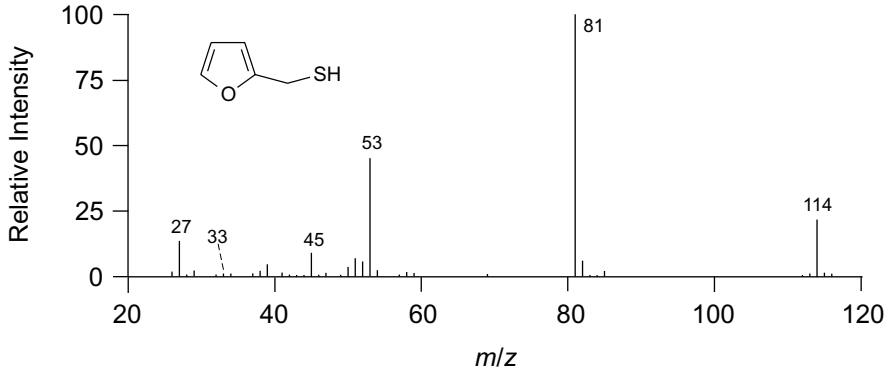

Figure 3.10. Mass spectrum of 2-furanmethanethiol (Example 3.3).

Example 3.3

2-Furanmethanethiol is an important constituent in the aroma of coffee. The base peak in the mass spectrum of this compound occurs at *m/z* 81 (Figure 3.10). Write a mechanism that accounts for the formation of this peak using the steps listed in the previous example.

DropBooks

Answer: The $M^{+\bullet}$ (*m/z* 114) must lose 33 u to produce the ion having *m/z* 81. The most likely group of atoms to account for this loss is SH. That SH is actually the group which is lost is corroborated by the fact that the *m/z* 83 peak is too small to accommodate the presence of S in the ion having *m/z* 81 (Section 2.2.2.1).

(a) The initial ionization site can be determined from Table 3.1. The two most likely sites are the S in the thiol group (with an IE of ~9.1 eV) and the O in the furan ring (with an IE of ~8.9 eV or lower; note that the IE for toluene is lower than that for benzene). Although ionization will occur to some extent at both sites because this difference is relatively small, initial ionization on the O atom in the furan ring should be preferred.

(b) Breaking the bond between the S atom and the ''benzylic'' C atom will generate either $^{\bullet}$SH and a benzylic type ion, or $^{+}$SH and a benzylic type radical. Stevenson's rule predicts that the resulting charge will reside on the fragment whose radical has the lowest IE. The IE for $^{\bullet}$SH is 10.4 eV (Table 3.1), whereas that for a benzylic-type radical (Ar—C$^{\bullet}$H$_2$) is about 7.1 eV. Even if this latter value is off by as much as 20%, the IE for the benzylic fragment is substantially lower than that for the SH group. Therefore, this fragmentation should occur by loss of $^{\bullet}$SH and formation of the furfuryl ion (Ar-C^{+}H$_2$). The spectrum of this compound (Figure 3.10) shows that the peak at *m/z* 33 (due presumably to $^{+}$SH) is only about 1% in intensity compared to the base peak.

(c) If initial ionization occurs on the furan O and the resulting fragmentation involves loss of the relatively distant thiol group, an alternate resonance form for the $M^{+\bullet}$ places the radical site near the departing $^{\bullet}SH$ (Equation 3.5). The ability of the $M^{+\bullet}$ to redistribute the electron density in this manner is important if two apparently distant sites participate in fragmentation reaction.

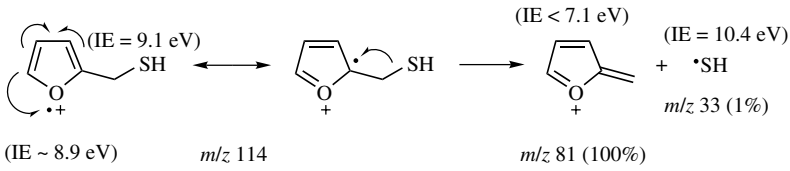

(3.5)

PROBLEMS

3.1. The relative intensity of the *m/z* 15 peak due to $^{+}CH_3$ in the mass spectrum of 1-phenyl-2-aminopropane is quite small. Why?

3.2. Write detailed mechanisms for the following simple fragmentations. Start by determining the initial ionization site using Table 3.1. Then write out structures for all the reactants and products, paying particular attention to which ones are ions, which radicals, and which neutral molecules. Show as many valence electrons as necessary. Next, determine what bond in the precursor ion must break in order to form the products, and decide whether formation of these products occurs by homolytic or heterolytic cleavage (i.e., does the charge site stay in the same place or move to another location?). Finally, show the electron movement needed to accomplish these fragmentations using fishhooks or full-headed arrows.

(**a**) Formation of ethyl radical and $H_2C{=}N^{+}H_2$ from *n*-propylamine

(**b**) Formation of methyl radical and allyl carbenium ion ($H_2C{=}CH{-}C^{+}H_2$) from 1-butene

(**c**) Loss of chlorine from isopropyl chloride

(**d**) Loss of a methyl group from acetone (H_3CCOCH_3)

(**e**) Loss of carbon monoxide from cyclohexanone (this fragmentation involves more than one step)

3.3. The base peak in the mass spectrum of 3,3-dimethyl-2-butanone (*t*-butyl methyl ketone; see Figure 3.11) is formed when the bond between the carbonyl group and the *t*-butyl group is broken. Predict the initial ionization site for this molecule and the group that will end up with the charge. Finally, write a mechanism for this fragmentation, showing appropriate electron movement with either fishhooks or full-headed arrows.

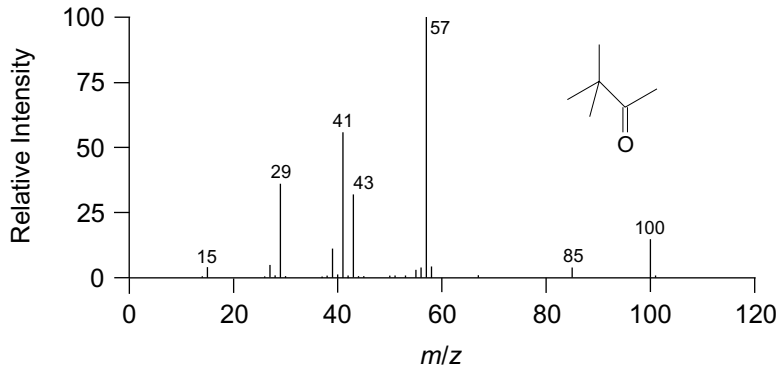

Figure 3.11. Mass spectrum of 3,3-dimethyl-2-butanone (Problem 3.3).

REFERENCES

F. W. McLafferty and F. Tureček, *Interpretation of Mass Spectra*, 4th edition, (University Science Books, Mill Valley, CA, 1993), pp. 57–65.

O. D. Sparkman and J. T. Watson, *Interpretation of Mass Spectra*: *An American Chemical Society Short Course* (American Chemical Society, Washington, DC, 2002).

D. P. Stevenson, "Ionization and Dissociation by Electron Impact," *Disc. Faraday Soc.*, **10**, 35 (1951).

DropBooks

4

NEUTRAL LOSSES AND ION SERIES

4.1. NEUTRAL LOSSES

4.1.1. Losses from the Molecular Ion

An unknown mass spectrum usually cannot be identified unless the $M^{+\bullet}$ peak is correctly identified. Assessing what neutral fragments are lost directly from the $M^{+\bullet}$ helps identify the correct choice of the $M^{+\bullet}$ peak in the spectrum and provides clues about what substructural groups are present in the molecule. Table 4.1, which is also located inside the front cover of this book, lists some neutral losses that are commonly encountered in EIMS. More extensive lists may be found in reference texts such as McLafferty and Tureček (1993).

Several aspects of this table deserve comment. First, this list is not all-inclusive. It specifically does not include combinations of losses. The spectra of many steroids, for example, exhibit peaks representing the loss of 33 from the $M^{+\bullet}$ (see Figure 9.1). These spectra also have peaks that indicate the losses of H_2O at $M - 18$ and $^{\bullet}CH_3$ at $M - 15$, so the peak at $M - 33$ undoubtedly is due to consecutive losses of $^{\bullet}CH_3$ *and* H_2O from the $M^{+\bullet}$ (not necessarily in that order).

Second, although Table 4.1 can potentially be used for determining losses from any ion represented in the mass spectrum, it is most useful *only for losses from the* $M^{+\bullet}$. For example, when two peaks separated by 15 *m/z* units are observed in the

Understanding Mass Spectra: A Basic Approach, *Second Edition*. By R. Martin Smith
ISBN 0-471-42949-X © 2004 John Wiley & Sons, Inc.

Table 4.1. Common neutral losses

M − 1	$H^{\bullet}$	M − 32	CH_3OH; S[a]
M − 15	$^{\bullet}CH_3$	M − 33	$HS^{\bullet}$[a]
M − 16	O (rare; N → O cmpds.);	M − 35	$Cl^{\bullet}$[a]
	$^{\bullet}NH_2$ (amides)	M − 36	HCl[a]
M − 17	$^{\bullet}OH$; NH_3 (rare)	M − 42	$H_2C{=}C{=}O$;
M − 18	H_2O		$H_2C{=}CH\text{-}CH_3$
M − 19	$F^{\bullet}$	M − 43	$CH_3C^{\bullet}O$; $^{\bullet}C_3H_7$
M − 20	HF	M − 44	CO_2
M − 26	HCCH, $^{\bullet}CN$	M − 45	$CH_3CH_2O^{\bullet}$; $^{\bullet}CO_2H$
M − 27	HCN; $H_2C{=}C^{\bullet}H$	M − 46	NO_2 (nitro cmpds.)
M − 28	CO; $H_2C{=}CH_2$	M − 57	$CH_3CH_2C^{\bullet}O$; $^{\bullet}C_4H_9$
M − 29	$CH_3C^{\bullet}H_2$; $HCO^{\bullet}$	M − 77	$^{\bullet}C_6H_5$ (phenyl)
M − 30	NO (nitro cmpds.);	M − 79	$Br^{\bullet}$[a]
	H_2CO	M − 91	$C_6H_5C^{\bullet}H_2$ (benzyl)
M − 31	$CH_3O^{\bullet}$	M − 127	$I^{\bullet}$

[a] Check for loss of or change in isotope peak intensity pattern.

middle of a spectrum, it is tempting to assume that the higher-mass ion loses $^{\bullet}CH_3$ to produce the lower mass ion. However, unless the precursor for the lower-mass ion is known by some independent means, there is no assurance that the ions are related to one another through a common fragmentation pathway.

Third, it is important to remember that there are no common organic fragments between $^{\bullet}H$ and $^{\bullet}CH_3$ that can be lost. This means that **ions do not lose 14 u fragments**. Because of the instability of atomic nitrogen (N) and methylene (CH_2), these groups are not lost from the $M^{+\bullet}$ or any fragment ion. This is not to say that peaks are never observed in the spectrum between the M − 1 and M − 15 peaks. In the spectra of aromatic compounds, for example, it is not uncommon to see peaks representing consecutive losses of several H atoms. In such cases, however, peaks corresponding to each of these losses are observed (see Figure 4.8, e.g.). An M − 6 peak, without the intervening peaks at M − 1, M − 2, and so forth, being present as well, should be viewed with suspicion.

In addition to the gap between 1 and 15, there are two other noteworthy gaps in Table 4.1: between 20 and 26, and between 36 and 42. These gaps are useful when evaluating the choice for the $M^{+\bullet}$ peak in an unknown spectrum. Although consecutive losses can account for peaks at some of these *m/z* values under some circumstances, peaks in these areas not accompanied by relevant smaller losses indicate either that the spectrum is not that of a pure compound or that the postulated choice for the $M^{+\bullet}$ peak is not correct.

Some losses listed in Table 4.1 are very common and sometimes occur even from the $M^{+\bullet}$ of compounds that do not contain the specific functional group which is lost. These include the losses of $^{\bullet}H$ and $^{\bullet}CH_3$, H_2O (from certain oxygenated compounds), HC≡CH (acetylene; from aromatic compounds), HC≡N (hydrogen

DropBooks

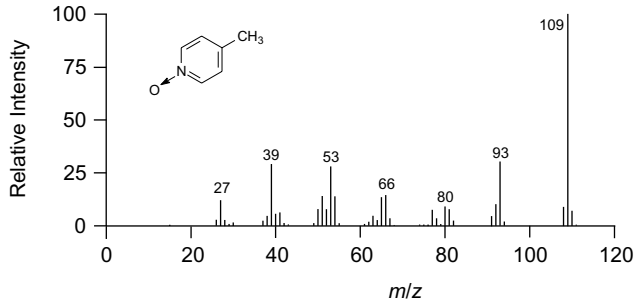

Figure 4.1. Mass spectrum of 4-methylpyridine-*N*-oxide. The peak at *m*/*z* 93 represents the loss of atomic O from the N–O bond in the $M^{+\bullet}$.

cyanide; from aromatic compounds containing N in or on the ring),[1] C≡O (carbon monoxide) and $CH_2{=}CH_2$ (ethylene) (both have a molecular mass of 28, making it difficult at low *m*/*z* discrimination to tell which has been lost), $CH_3C^{\bullet}H_2$ (ethyl radical), and $^{\bullet}C_3H_7$ (propyl or isopropyl radical).

Other losses reflect the presence of specific functional groups, such as $^{\bullet}F$, $CH_3O^{\bullet}$ (methoxy radical), atomic sulfur (S) and $^{\bullet}SH$ from certain S-containing compounds, $^{\bullet}Cl$ and HCl from chlorinated compounds, and NO and NO_2 from nitro compounds. Higher mass losses in this category include $CH_3CO^{\bullet}$ (acetyl radical) from methyl carbonyl compounds, $^{\bullet}C_6H_5$ (phenyl radical) and $C_6H_5C^{\bullet}H_2$ (benzyl radical) from appropriately substituted benzenes, as well as the halogen radicals $^{\bullet}Br$ and $^{\bullet}I$. Although the loss of H_2O (18) from O-containing compounds is commonplace, the corresponding loss of NH_3 (17) from amines occurs much less frequently. Thus, the loss of 17 from the $M^{+\bullet}$ should be assumed initially to be that of $^{\bullet}OH$ (hydroxyl radical) unless independent evidence dictates otherwise.

One loss occurs infrequently but is characteristic enough to deserve particular mention. This is the loss of 16, which is nearly specific either for primary amides (where the loss is $^{\bullet}NH_2$; see, e.g., Figure 6.20*b*) or for certain formally polar N–O bonds such as those found in nitrogen oxides and nitro groups. In the latter case, atomic O is lost with its *six* valence electrons (Figure 4.1).

Example 4.1

Identify the compound whose mass spectrum is shown in Figure 4.2.

Answer: The peak in this spectrum with the highest *m*/*z* value is the one at *m*/*z* 114. One way to determine whether or not this peak represents the $M^{+\bullet}$ is to calculate

[1] The loss of 27 as vinyl radical ($CH_2{=}C^{\bullet}H$) is much less common and tends to occur only with certain compounds that have terminal double bonds.

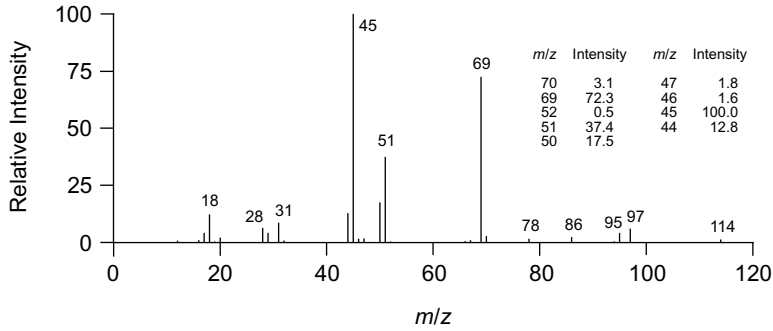

Figure 4.2. Mass spectrum for Example 4.1.

the losses that are indicated by the observed fragment ion peaks. The smallest observed losses are 17 to produce the peak at *m/z* 97, 19 to give the peak at *m/z* 95, and 28 to produce the *m/z* 86 peak. Losses corresponding to these masses are all listed in Table 4.1. In addition, the two most intense peaks in the spectrum, *m/z* 45 and 69, represent ions whose combined masses add up to 114 u. The peak at *m/z* 114 thus appears to represent the $M^{+\bullet}$. Because the MM is even and many of the fragment ion peaks in the spectrum occur at odd *m/z* values, the absence of N seems likely (see Section 3.5).

DropBooks

All the peaks above *m/z* 69 are too small to produce elemental compositions. Therefore, the elemental composition of the $M^{+\bullet}$ will have to be inferred from the other information contained in the spectrum. With the possible exception of O, the presence of A + 2 elements are not indicated. The normalized intensity of the *m/z* 70 peak relative to the peak at *m/z* 69 is 4.3%, which indicates the presence of 4.3/1.1 ≈ 4 C atoms. The normalized intensity of the *m/z* 52 peak (1.3% relative to the peak at *m/z* 51) shows that the ion having *m/z* 51 contains only one C atom.

The *m/z* 45 ion also has only one C atom because the *m/z* 46 peak has a relative intensity of 1.6%. Unfortunately, the intensity of the peak at *m/z* 47 is not due to isotope contributions alone and thus cannot be used to determine if O is present. The size of this peak is too small to be due to S, but it is also too large to result from a combination of one C atom and two O atoms (the largest number of O atoms that can be accommodated by the mass).

The losses from the $M^{+\bullet}$ must now be attributed to specific functional groups. The loss of 17 is most likely $^{\bullet}OH$ (Table 4.1 and Section 4.1.1). The loss of 19 is a characteristic one and strongly suggests the presence of F. Either CO or $CH_2{=}CH_2$ could cause the loss of 28, but the loss of 36 is trickier. There is no indication from any of the peak clusters in the spectrum that Cl is present; therefore, the loss of 36 is unlikely to be that of HCl. On the other hand, this compound does exhibit losses of both 17 and 19, which together add up to 36. This seems the most reasonable explanation for formation of the peak at *m/z* 78. Finally, the loss of 45 could be either that

of $^{\bullet}CO_2H$ or $^{\bullet}OCH_2CH_3$, but because the base peak in the spectrum occurs at *m/z* 45, and the ion at this *m/z* value contains only one C atom, the former choice looks more appealing.

It is helpful at this point to summarize what has been determined so far:

- The nominal MM is 114.
- The molecule does not appear to contain N or any A + 2 elements, with the probable exception of O.
- The presence of O and F is strongly suggested by the losses of 17 and 19, respectively, from the $M^{+\bullet}$.
- The ions having *m/z* 45 and 51 contain only one C atom, and the ion having *m/z* 69 appears to have four C atoms.
- The *m/z* values of the two largest peaks in the spectrum add up to the nominal MM, which is often a strong indication that the molecule has one bond that, when broken, can lead to retention of the charge by either fragment.
- The elemental composition of the fragment having *m/z* 45 is probably CO_2H for two reasons: It contains only one C atom and the $M^{+\bullet}$ shows losses of both $^{\bullet}OH$ and 28 (possibly as CO).

If the elemental composition of *m/z* 45 is indeed CO_2H, then determining the structure of the ion having *m/z* 69 will complete the identification of the unknown. Although the isotope peak intensities for this peak indicate the presence of four C atoms, this still does not account for the presence of F in the molecule. The combined mass of four C atoms and one F atom is $48 + 19 = 67$, which is 2 u short of the observed mass for this ion. Although an elemental composition of C_4H_2F for this ion is possible, it would be highly unsaturated and have an unusual structure. It is worthwhile, therefore, so search for an alternative solution.

In Figure 1.29 an intense *m/z* 69 peak was observed in the spectrum of PFTBA, the compound commonly used for tuning and calibration. In that case, the structure of the corresponding ion was seen to be $^{+}CF_3$ (Problem 1.2). If the peak at *m/z* 69 in the spectrum of this unknown also corresponds to $^{+}CF_3$, then the intensity of the *m/z* 70 peak must contain contributions from an unknown fragment ion and therefore cannot provide reliable elemental composition information. This structural assignment, however, must fit with other observed peaks in the spectrum.

The spectrum of PFTBA also shows weak-intensity peaks at *m/z* 50 and 31, both of which are also observed in this spectrum. Because it contains one C atom, the ion having *m/z* 51 is probably the $^{+}CF_2H$ ion. An elemental composition of $^{+}CF_3$ for the *m/z* 69 ion, then, adequately explains most of the remaining peaks that are observed in the spectrum.

Possible fragmentations for this compound—trifluoroacetic acid (CF_3CO_2H)—are shown in Equation 4.1. The IEs for $^{\bullet}CO_2H$ and $^{\bullet}CF_3$ are 8.6 and 8.9 eV, respectively, so that the charge should be shared almost equally between the two fragments as the C–C bond breaks. The intensities of the two peaks that represent

the ions formed from such radicals reflect these values (Stevenson's rule; Section 3.6.4).

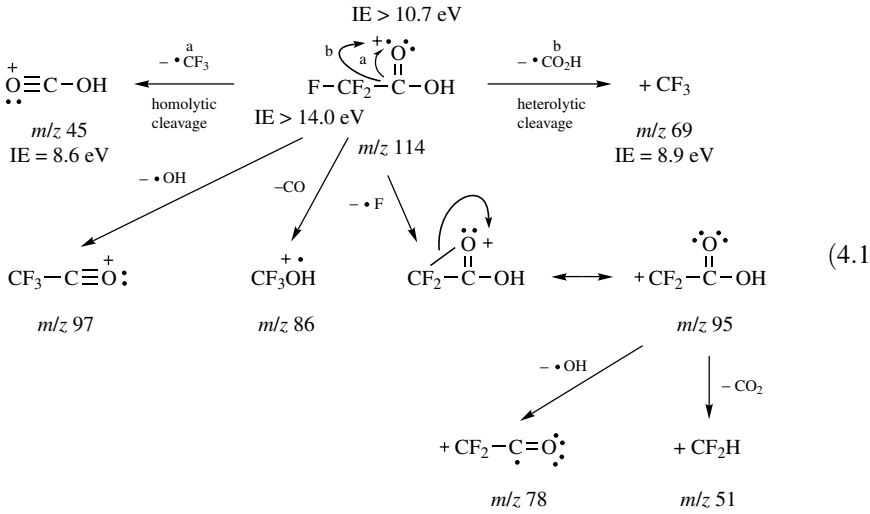

(4.1)

4.1. Review the criteria for good-quality mass spectra listed in Section 1.6. Then evaluate the spectra in Figure 4.3 and decide whether they are suitable for inclusion in a mass spectral library. What reasons can be offered in support of this decision?

4.2. A young man died after apparently inhaling an unknown substance. Several autopsy specimens were collected, and GC/MS analysis of a brain tissue extract produced the mass spectrum shown in Figure 4.4. The concentration of this compound in the brain tissue and other specimens indicated that it might well have been responsible for causing the young man's death. What is the structure of this compound? (Tranthim-Fryer et al., 2001)

4.1.2. Loss of Small Molecules from Aromatic Ions

Even in the ground state, compounds that contain adjacent N atoms tend to lose N_2, sometimes explosively. It should not be surprising, then, that the following molecules, which are all isoelectronic with N_2 and also have relatively high IEs (Table 3.1), are lost as neutral species from highly energetic ions:

$$H:C\equiv C:H$$
$$H:C\equiv N:$$
$$:N\equiv N:$$
$$^{-}:C\equiv O:^{+}$$

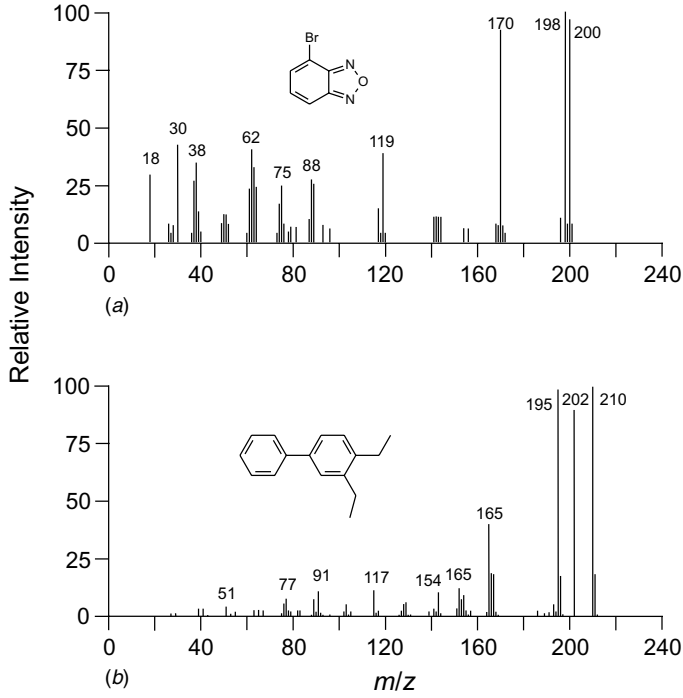

Figure 4.3. Mass spectra for Problem 4.1. (Reprinted by permission of Elsevier Science from Ausloos et al., 1999. Copyright by the American Society of Mass Spectrometry.)

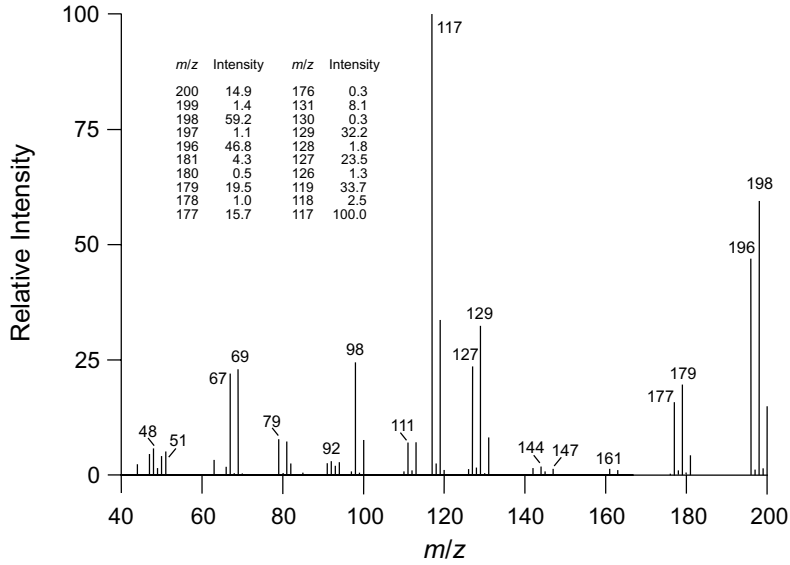

Figure 4.4. Mass spectrum for Problem 4.2.

The structure of CO deserves brief comment. Although the molecule itself is electrically neutral, the C atom, with three electrons donated to bonds with the O and two more in the nonbonding pair, carries a formal negative charge. The O, also with five electrons, carries a formal positive charge. This relative unusual structure must be kept in mind when attempting to write mechanisms for fragmentations in which CO is lost.

Aromatic molecular and fragment ions, through rearrangement of their π-electronic structure, routinely lose small molecules like those listed above. For example, the spectra of benzene (Figure 4.15*a*), naphthalene (Figure 4.8*a*), and phenanthrene (Figure 4.8*c*) all have significant fragment ions peaks that correspond to the loss of HCCH from the $M^{+\bullet}$.

Figure 4.5 outlines several fragmentations that produce characteristic peaks in the spectra of many aromatic compounds. The first of these, Figure 4.5*a*, shows the loss of HCCH by the benzyl ion ($^{+}C_7H_7$; *m/z* 91) to form the cyclopentadienyl ion ($^{+}C_5H_5$; *m/z* 65), which in turn loses acetylene to yield the cyclopropenium ion ($^{+}C_3H_3$; *m/z* 39). As illustrated, the structure of the benzyl ion is not static. Rather, it is in equilibrium with the cycloheptatrienyl (tropylium) ion and has a number of resonance structures as well (Figure 3.5).

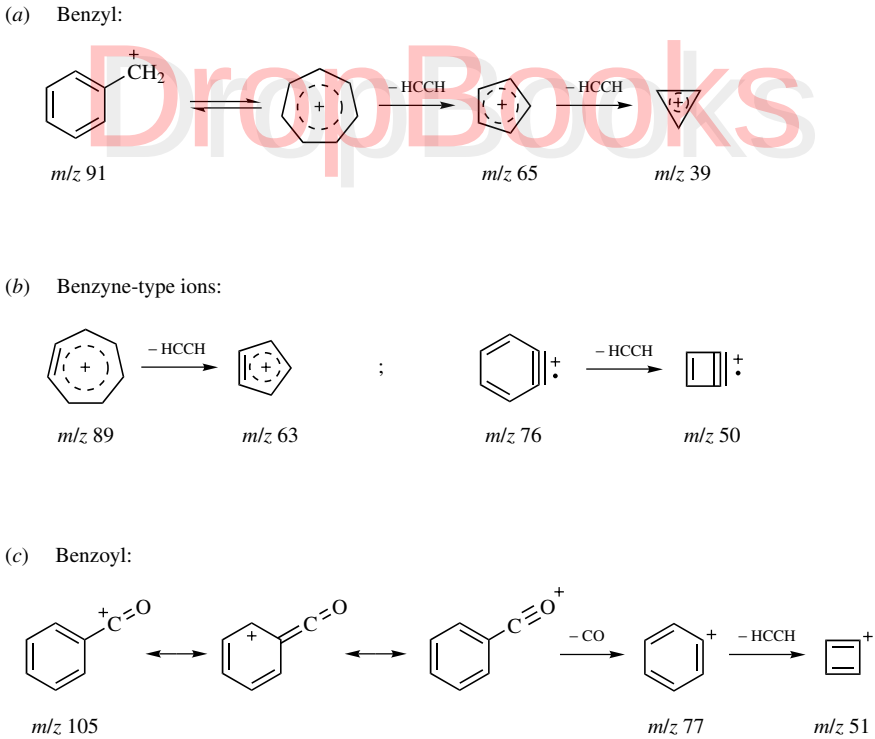

DropBooks

Figure 4.5. Structures and fragmentations of prominent low-mass aromatic ions.

The cyclic $^{+}C_7H_7$ and $^{+}C_3H_3$ structures are examples of nonbenzenoid aromatic systems. Hückel's rule states that cyclic systems of contiguously overlapping *p*-orbitals which contain $(4n + 2)$ π-electrons (where $n = 0, 1, 2 \ldots$) are more stable than expected due to a lowering of the energy of the π molecular orbitals. In the cases of benzene and the tropylium ion, $n = 1$ and $4(1) + 2 = 6$; for the cyclopropenium ion, $n = 0$ and $4(0) + 2 = 2$. Both the tropylium and cyclopropenium ions are very stable; in fact, their salts can be isolated in the laboratory.

Cyclic systems containing $4n$ electrons, on the other hand, do not delocalize electron density as well and are less stable than expected (Deniz et al., 1999). These systems are said to be antiaromatic. Because it has antiaromatic properties, the abundance of the cyclopentadienyl ion ($^{+}C_5H_5$; *m/z* 65; $n = 1$) is always less than that of $^{+}C_7H_7$ and usually is less than that of $^{+}C_3H_3$, both of which are aromatic. This is true even though energy is gained during the formation of $^{+}C_5H_5$ from the new π-bond that is formed in the expelled HCCH.

Aromatic $M^{+\bullet}$ that have electronegative substituents attached to the ring fragment to form ions in which the ring contains a triple bond (benzyne-type ions; Figure 4.5*b*). Benzyne itself is an unstable intermediate that can be formed in the laboratory by the decomposition of aromatic compounds containing electronegative substituents. Ions of this type also fragment by the loss of HCCH.

Compounds that contain an aromatic ring with an attached carbonyl group—whether as a ketone, ester, amide, and so forth—show a strong tendency to fragment so that the benzoyl ion ($C_6H_5CO^{+}$; *m/z* 105) produces a prominent peak in the spectrum. As shown in Figure 4.5*c*, the benzoyl ion loses CO to form the phenyl ion ($^{+}C_6H_5$; *m/z* 77). Like other aromatic ions just discussed, $^{+}C_6H_5$ loses HCCH to produce the ion with *m/z* 51.

The $M^{+\bullet}$ of aromatic compounds that have heteroatoms either in or attached directly to the ring also fragment by losing small, multiple-bonded molecules that usually contain the heteroatom. The spectra of three examples are shown in Figure 4.6.

Other than the sequential loss of $H^{\bullet}$ and H_2, the first major loss from the $M^{+\bullet}$ observed in the spectrum of pyridine (Figure 4.6*a*) is 27 to give the peak at *m/z* 52. This is the loss of HCN, which is analogous to the loss of HCCH in aromatic compounds that do not contain N (Equation 4.2). This fragmentation will be discussed in more detail in Section 8.2.1.

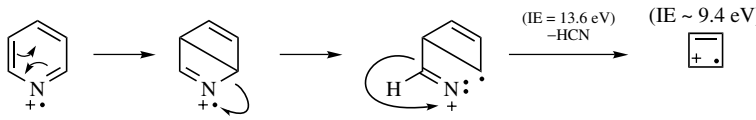

m/z 79 *m/z* 52 (4.2)

The spectrum of phenol (Figure 4.6*b*) exhibits two peaks that deserve comment. The first of these, at *m/z* 47, has an unusual *m/z* value because the range from *m/z* 46 – 49 is usually devoid of fragment ion peaks, with the exception of spectra of compounds containing sulfur (CH_3S^{+} at *m/z* 47) or chlorine (CCl^{+} at *m/z* 47 and

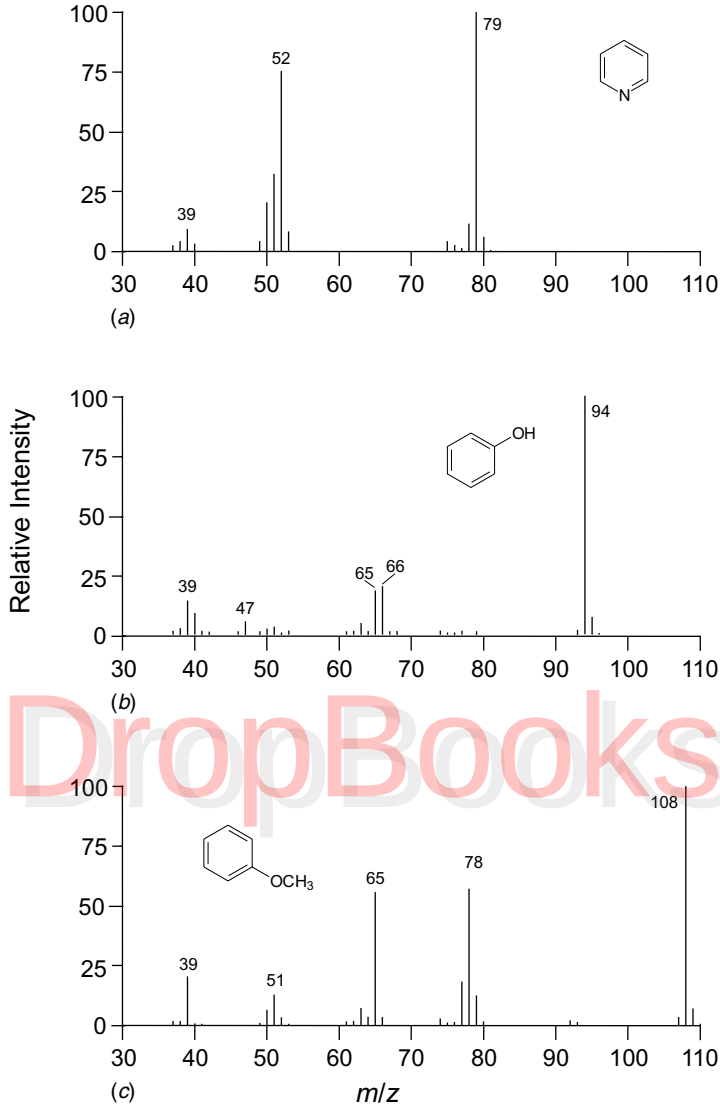

DropBooks

Figure 4.6. Mass spectra of aromatic compounds with heteroatoms: (*a*) pyridine, (*b*) phenol, and (*c*) anisole.

49). In the case of phenol, no reasonable combination of elements can account for this ion. However, the MM for this compound is 94, which is exactly twice 47. Thus, the peak at *m*/*z* 47 can be ascribed to the double-charge molecular ion ($C_6H_6O^{2+}$). Peaks due to double-charge ions are usually of low intensity and occur more frequently in the spectra of compounds that have low second IEs, such as

aromatic compounds, which also often have few low-energy fragmentation modes open to them. Double-charge ions may also be formed by compounds containing large heteroatoms such as Cl, Br, or S.

The other peak of interest in this spectrum is the one at *m/z* 66, resulting from the loss of 28 from the $M^{+\bullet}$. The loss of 28 u can be either that of CO or $CH_2{=}CH_2$ (Table 4.1); both losses occur frequently. However, loss of $CH_2{=}CH_2$ from an aromatic ring would involve substantial rearrangement of H and the electronic structure. In the examples discussed earlier in this section, two-carbon fragments were lost from aromatic ions exclusively as HCCH. Although the loss of CO must also be accompanied by H rearrangement, the mechanism shown in Equation 4.3 has its basis in ground-state chemistry (Beynon et al., 1968). The individual steps in this mechanism will be discussed in Section 8.2.1.

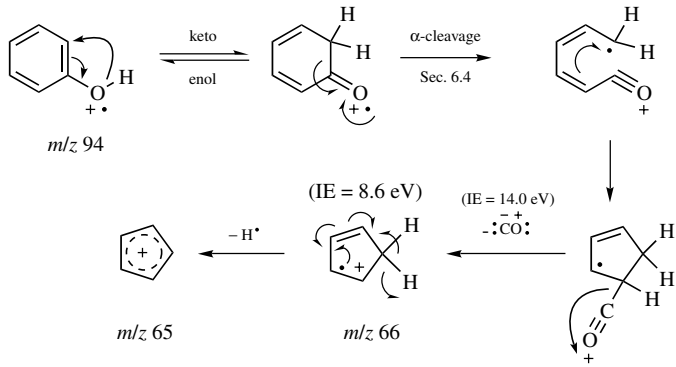

(4.3)

The spectrum in Figure 4.6*c* is that of anisole (phenyl methyl ether). What is striking about this spectrum is the intense peak at *m/z* 78, which corresponds to the loss of 30 u from the $M^{+\bullet}$. Studies have shown that the *m/z* 78 peak represents $C_6H_6^{+\bullet}$, so the fragment lost is formaldehyde ($H_2C{=}O$; Beynon et al., 1968). This loss involves both a preliminary four-center H migration and subsequent loss of a small multiple-bonded molecule, shown schematically in Equation 4.4. The loss of $H_2C{=}O$ in this manner is characteristic of anisoles.

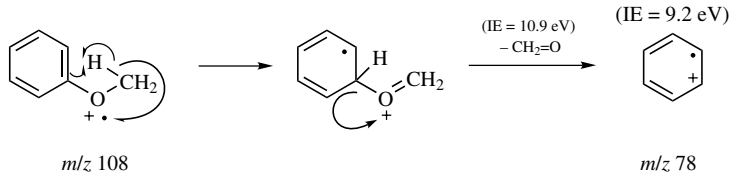

(4.4)

4.2. LOW-MASS ION SERIES

The mass spectra of saturated aliphatic hydrocarbons (e.g., *n*-decane; Figure 4.7) are visually quite different from those of the polynuclear aromatic compounds

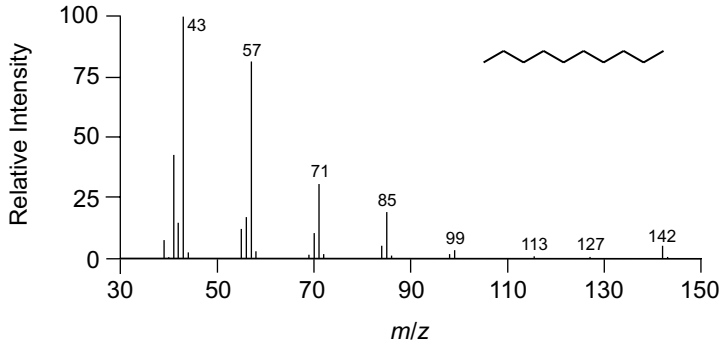

Figure 4.7. Mass spectrum of *n*-decane.

shown in Figure 4.8. The aliphatic hydrocarbon spectrum exhibits an abundance of peaks at low *m*/*z* values, making it look as if the $M^{+\bullet}$ has a tendency to fall apart in an almost random manner. The spectra of the aromatic compounds, on the other hand, show little evidence of fragmentation. In each case, the $M^{+\bullet}$ peak is also the base peak in the spectrum. The overall appearance of the mass spectrum, along with isotopic peak intensity patterns (Chapter 2) and neutral losses from the $M^{+\bullet}$ (Section 4.1), can help characterize the type of compound giving rise to the spectrum.

DropBooks

4.2.1. *n*-Alkane Spectra

The spectrum of *n*-decane is typical of the spectra of unbranched alkanes. These compounds all produce an $M^{+\bullet}$, although the relative abundance of this ion decreases with increasing chain length. *n*-Alkanes exhibit little or no loss of $^{\bullet}CH_3$, but then appear to lose progressively larger alkyl radicals in a pattern in which the most intense peaks in each group are separated by 14 *m*/*z* units, with peaks of lesser intensity one or two units below the main peak in each cluster. The base peak in these spectra most often occurs at *m*/*z* 43 or 57.

At first it might seem strange that these compounds lose alkyl radicals of virtually every size except methyl. In Figure 4.7 peaks are seen at (M − 29), (M − 43), (M − 57), and so on, appearing to represent the losses of ethyl, propyl, butyl, and larger-mass alkyl radicals, respectively. This is deceptive, however. It is true that all the C—C bonds in these molecules are of similar strength, so that initial ionization can occur at virtually any of the σ-bonds along the chain. In addition, all primary fragmentations of these $M^{+\bullet}$ form an alkyl radical and a primary carbenium ion (Equation 4.5).

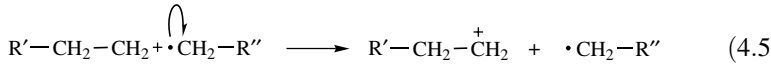

(4.5)

Because all the primary carbenium ions are similar in stability, the relative stability of the various radicals formed will determine what fragments are lost

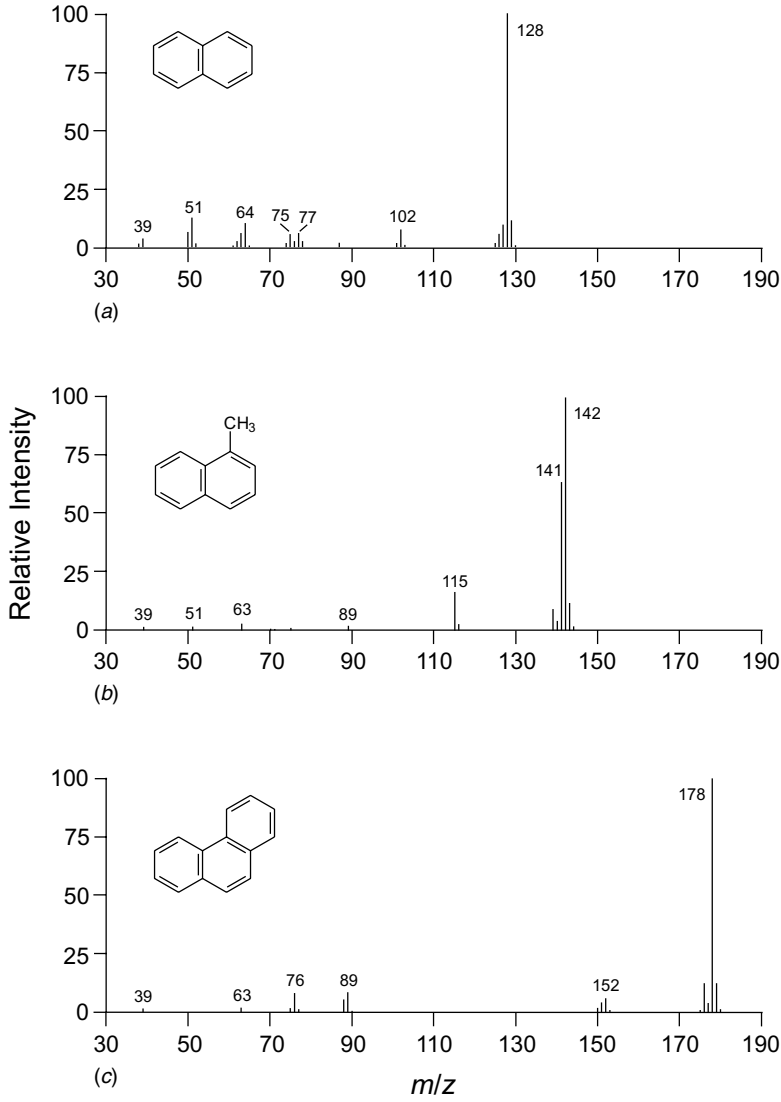

Figure 4.8. Mass spectra of three polynuclear aromatic compounds: (*a*) naphthalene, (*b*) 1-methylnaphthalene, and (*c*) phenanthrene.

(Section 3.6.3). The stability of these radicals is related to the inductive stabilization of added alkyl groups and follows the pattern

$$\text{Hydrogen} < \text{methyl} < \text{ethyl} < n\text{-propyl} < \text{isopropyl} < t\text{-butyl}$$

Isopropyl and *t*-butyl radicals are more stable because they are, respectively, secondary and tertiary radicals.

These mass spectra, by seeming to depict the loss of larger and larger alkyl radicals, do not adequately reflect the complexity of the actual fragmentations that occur. In particular, because primary radicals larger than *n*-propyl gain no further stability from increasing chain length (even the energy gain from ethyl to propyl is slight), the energy needed to produce the mixtures of primary carbenium ion and radical products is essentially the same whether these compounds lose ethyl, propyl, butyl, or pentyl radicals. This seems to contradict the fact that the peaks at lower *m*/*z* values are more intense.

The lower-mass ions result from secondary (and further) fragmentations in which heterolytic cleavage relocates the charge on a site of similar stability (all the ions formed are primary carbenium ions) and eliminates an olefin ($CH_2{=}CH_2$) (Equation 4.6).

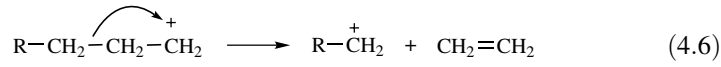

(4.6)

The driving force for this fragmentation, which lowers its $\Delta G^{\ddagger}$ (Section 3.6.1), is formation of the new π-bond in the expelled $CH_2{=}CH_2$ molecule. This is one of many examples in which loss of a small, multiple-bonded molecule relocates the charge to a site that causes the product ion to have stability similar to that of the precursor ion. Thus, although the ion with *m*/*z* 113 in Figure 4.7 is indeed formed by loss of $^{\bullet}CH_2CH_3$ from the $M^{+\bullet}$, the *m*/*z* 85 ion arises from a combination of butyl radical loss *and* loss of $CH_2{=}CH_2$ from the ion having *m*/*z* 113. Similarly, the ion with *m*/*z* 57 can form by loss of $CH_2{=}CH_2$ from the *m*/*z* 85 ion.

PrepBooks

Another reason for the abundance of low-mass ions represented in these spectra is that the $M^{+\bullet}$ of *n*-alkanes rearrange easily before fragmentation occurs (Holmes et al., 1982). The energies required for H and CH_3 migration in these ions is about the same as or lower than the energy needed for bond dissociation. Although the originally formed $M^{+\bullet}$ are unbranched, a percentage of them rearrange rapidly to branched structures that can dissociate to produce secondary and tertiary ions and radicals. As a result, the spectra of these compounds truly result from a large number of competing processes, so that the peaks observed in the spectrum have only an indirect relationship to the original structure. Fortunately, that is not true for all classes of compounds.

4.2.2. Effect of Chain Branching on the Spectra of Aliphatic Hydrocarbons

Although the spectra of saturated aliphatic hydrocarbons have many features in common, their fragmentation patterns are still different enough to provide structural information. At the same time, it is important to realize that, for compounds containing more than seven or eight C atoms, the number of possible isomers is large enough that making a one-to-one assignment of structures to spectra will usually be precluded.

The spectra of the three octanes in Figure 4.9 illustrate the differences caused by increasing the amount of branching. While the spectrum of *n*-octane (Figure 4.9*a*)

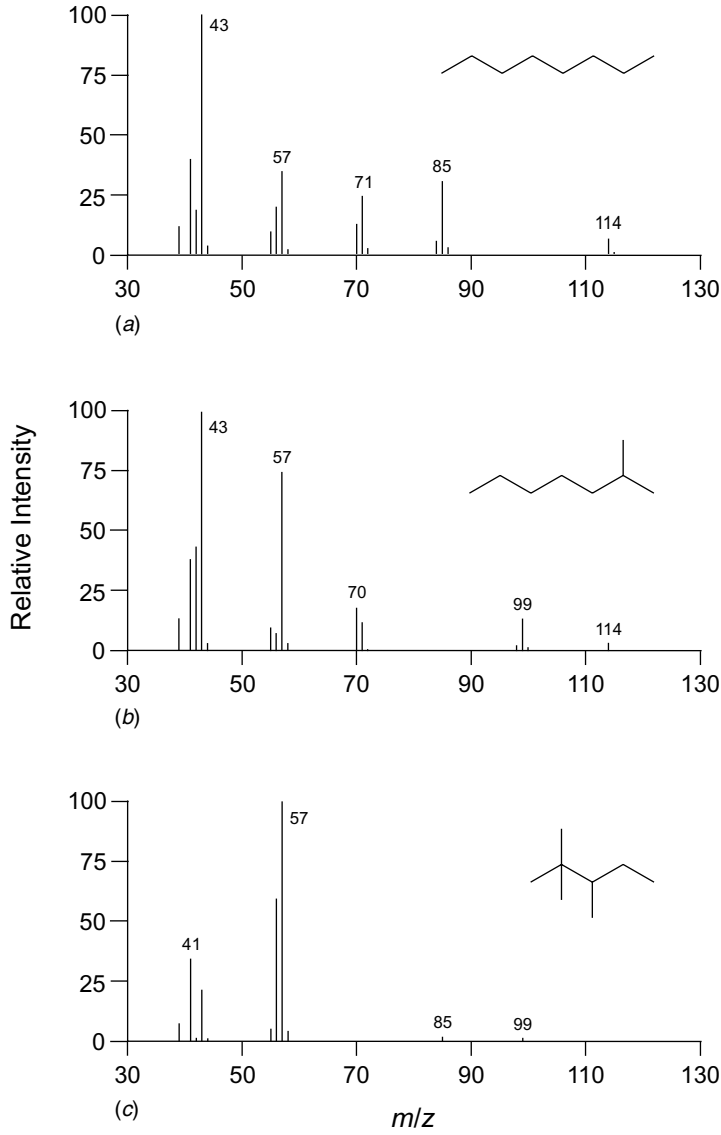

Figure 4.9. Mass spectra of three alkanes showing the effects of chain branching: (*a*) *n*-octane, (*b*) 2-methylheptane, and (*c*) 2,2,3-trimethylpentane.

shows a typical *n*-alkane pattern, that of 2-methylheptane (Figure 4.9*b*) has a sizable M − 15 peak. Although *n*-alkanes do not lose $^{\bullet}CH_3$ for reasons discussed in the previous section, loss of $^{\bullet}CH_3$ from the 2-methylheptane $M^{+\bullet}$ forms a *secondary* carbenium ion, thereby lowering $\Delta G^{\ddagger}$ for this fragmentation over those in which primary carbenium ions are formed. Loss of a pentyl radical from the

$M^{+\bullet}$ also leads to a secondary carbenium ion having *m/z* 43. However, the formation of low-mass ions by complex rearrangements and fragmentations obscures this effect, underscoring the difficulty of predicting structure based on the intensities of peaks at low *m/z* values.

Figure 4.9*c* shows the spectrum of 2,2,3-trimethylpentane, one of the most highly branched octane isomers. In this case, *m/z* 57 is not only the base peak, it is also much larger than every other peak in the spectrum except the one at *m/z* 56. A careful look at the structure should indicate why this is so. The bond between C2 and C3 must be weakened even in the neutral molecule because of steric interactions between the three methyl groups. Initial ionization at this already weakened bond is therefore likely (molecular orbitals for weaker bonds occur at higher energy and therefore have *lower* IEs). Breaking this bond to form a *secondary*-butyl radical and a *tertiary*-butyl carbenium ion should be very favorable energetically (Equation 4.7).

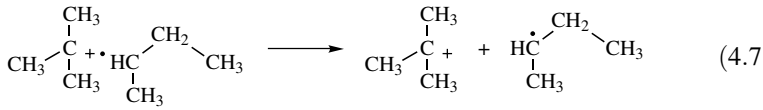

(4.7)

The alternative loss of $^{\bullet}CH_3$ to form the tertiary 2,3-dimethyl-2-pentyl ion (*m/z* 99) does not compete well because of the significant difference in stabilities between methyl and *sec*-butyl radicals. The only other fragmentation indicated by the peaks at higher *m/z* values is loss of $^{\bullet}CH_2CH_3$ to give the secondary 3,3-dimethyl-2-butyl ion (*m/z* 85). Other peaks at low *m/z* values in this spectrum do not follow the usual pattern for saturated aliphatic compounds—for example, *m/z* 56 represents $C_4H_8^{+\bullet}$ and *m/z* 41 represents $^{+}C_3H_5$, the allyl ion.

PropBooks

Ion stability appears to be far more important in determining what fragments are formed from saturated alkanes than does radical stability. That is, secondary carbenium ions will be formed preferentially over primary ions, and tertiary carbenium ions over secondary. When ion stabilities are approximately equal, however, radical stability becomes the determinative factor, following the sequence given in the previous section.

4.3. Figure 4.10 shows the spectra of three C_7H_{16} isomers. Assign structures to these spectra. (*Hint*: First draw the nine possible structures and try to predict fragmentation patterns for each structure based on the discussion above. Then look at the spectra to see which ones most closely match the predicted fragmentation patterns.)

4.2.3. Ion Series for Nonaromatic Compounds

Although the intensities of peaks at low *m/z* values in aliphatic hydrocarbon spectra may not directly reflect the structure of the original molecule, the overall appearance of the spectrum is still characteristic of this class of compounds. As observed in the spectra shown in Figures 4.7, 4.9, and 4.10, the series of intense peaks at *m/z* 43, 57,

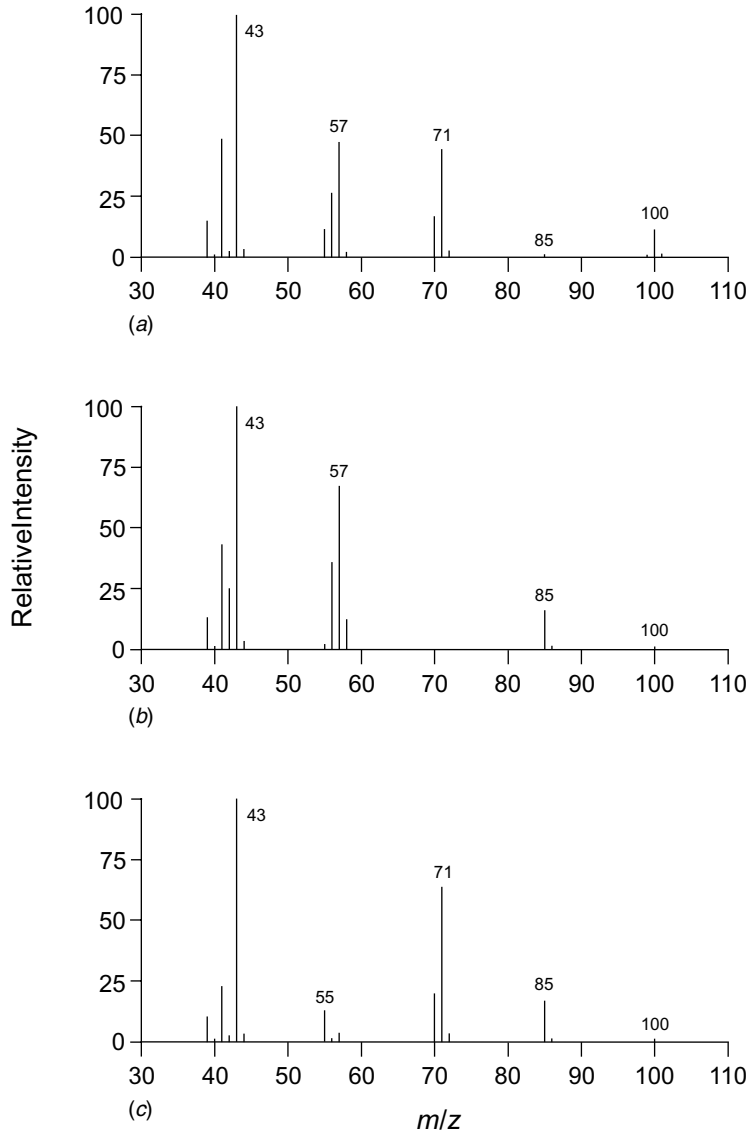

Figure 4.10. Mass spectra for Problem 4.3.

71, 85, 99, and so forth is characteristic of the spectra of saturated aliphatic hydrocarbons in general. A group of peaks at low *m*/*z* values that appears consistently in the spectra of a class of compounds is called a **low-mass ion series**, which is one of the first things to look for when trying to solve an unknown spectrum (see Chapter 5 and Table 5.1).

Table 4.2. Common ion series at low *m/z* values

1. General (of little or no value in determining specific structural features).
   a. Saturated aliphatics [$(C_nH_{2n+1})^+$]:

   $$27, \mathbf{29}; 41, \mathbf{43}; 55, \mathbf{57}; 69, \mathbf{71}; 83, \mathbf{85} \ldots$$

   b. Unsaturated aliphatics and cycloalkanes [$(C_nH_{2n-1})^+$ plus rearrangement ions $(C_nH_{2n})^{+\bullet}$]:

   $$\mathbf{27}, 29; \mathbf{41}, 43; \mathbf{55}, (\mathbf{56}), 57; \mathbf{69}, (\mathbf{70}), 71; \mathbf{83}, (\mathbf{84}) \ldots$$

2. α-Cleavage (may be highly specific; one peak often dominates spectrum).
   a. Ketones ($R{-}C{\equiv}O^+$); do not show full aliphatic pattern:

   $$\mathbf{43}; \mathbf{57}; \mathbf{71}; \mathbf{85} \ldots$$

   b. Ethers and alcohols ($R_2C{=}O^+R$):

   $$\mathbf{31}; \mathbf{45}; \mathbf{59}; \mathbf{73}; \mathbf{87} \ldots$$

   c. Amines ($R_2C{=}N^+R_2$):

   $$\mathbf{30}; \mathbf{44}; \mathbf{58}; \mathbf{72}; \mathbf{86}; \mathbf{100} \ldots$$

3. Aromatic (usually gives general information only; may be specific for benzyl and benzoyl).
   a. With electron-donating substituents (alkylbenzenes, ethers, etc.):

   $$\mathbf{39}; 50, \mathbf{51}, 52; 63, 64, \mathbf{65}; 76, \mathbf{77}, 78; 89, 90, \mathbf{91}; (\mathbf{105})$$

   b. With electron-withdrawing substituents (nitro, halogens, etc.):

   $$\mathbf{38}, \mathbf{39}; 49, \mathbf{50}, 51; 62, \mathbf{63}, 64; \mathbf{75}, \mathbf{76}, 77; 88, \mathbf{89}, 90, 91$$

   c. Benzyl ($C_6H_5C^+H_2$; may be specific if *m/z* 91 is very intense):

   $$\mathbf{39}, \mathbf{65}, \mathbf{91}$$

   d. Benzoyl ($C_6H_5CO^+$; may be specific if *m/z* 105 is intense):

   $$\mathbf{51}, \mathbf{77}, \mathbf{105}$$

DropBooks

Aliphatic compounds that have attached functional groups may have their own distinctive low-mass ion series. These series, in addition to those for some aromatic compounds to be discussed below, are listed in Table 4.2, which is also found inside the back cover of this book. Each ion series in Table 4.2 has some *m/z* values highlighted in **boldface** type. These peaks tend to be more intense than other peaks *in that area of the spectrum*. This does not necessarily mean that they are the most intense peaks in the spectrum or even that they are intense peaks.

The insertion of one or more double bonds into an aliphatic compound, or cyclization into a saturated ring system, leads to a spectrum in which peaks at lower *m/z* values still tend to predominate (Figure 4.11). The most intense peaks in each

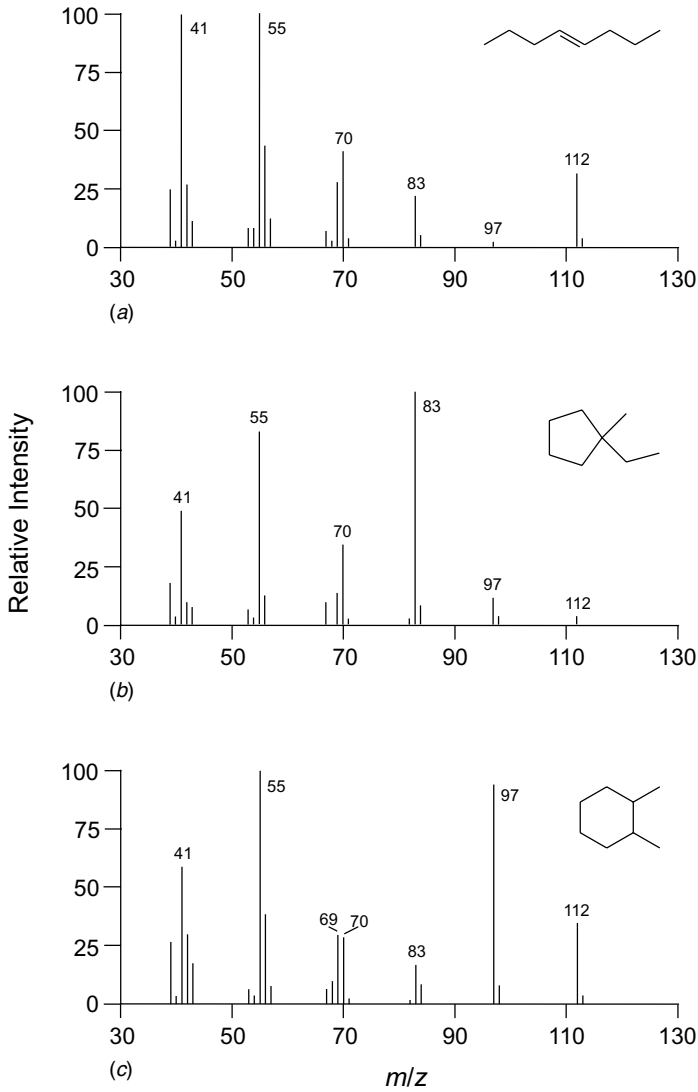

Figure 4.11. Mass spectra of olefinic and alicyclic compounds: (*a*) 4-octene, (*b*) 1-methylethylcyclopentane, and (*c*) 1,2-dimethylcyclohexane. Note the $OE^{+\bullet}$ at *m*/*z* 70.

cluster in these spectra, however, are not the same as those for saturated aliphatic compounds. Most are found two *m*/*z* units lower, reflecting stabilization of the charge by a double bond (see Chapter 6). Thus, *m*/*z* 41 corresponds to the allyl carbenium ion ($CH_2{=}CH\text{-}C^+H_2 \leftrightarrow {}^+CH_2\text{-}CH{=}CH_2$), *m*/*z* 55 to the methylallyl ion, and so forth.

The peaks at *m*/*z* 56 in the top and bottom spectra, and *m*/*z* 70 in all three spectra, represent $OE^{+\bullet}$ (Section 3.2). Studies have shown that the $M^{+\bullet}$ of olefins, like those

of alkanes, rearrange to cyclic structures at energies below that at which fragmentation occurs (van der Hart, 1999). Formation of common intermediates and fragmentation by pathways that are not directly related to the original structure occur with relative ease within this class of compounds.

The addition of groups containing heteroatoms—such as carbonyl, ether, alcohol, halogen, or amine groups—to a saturated aliphatic structure dramatically

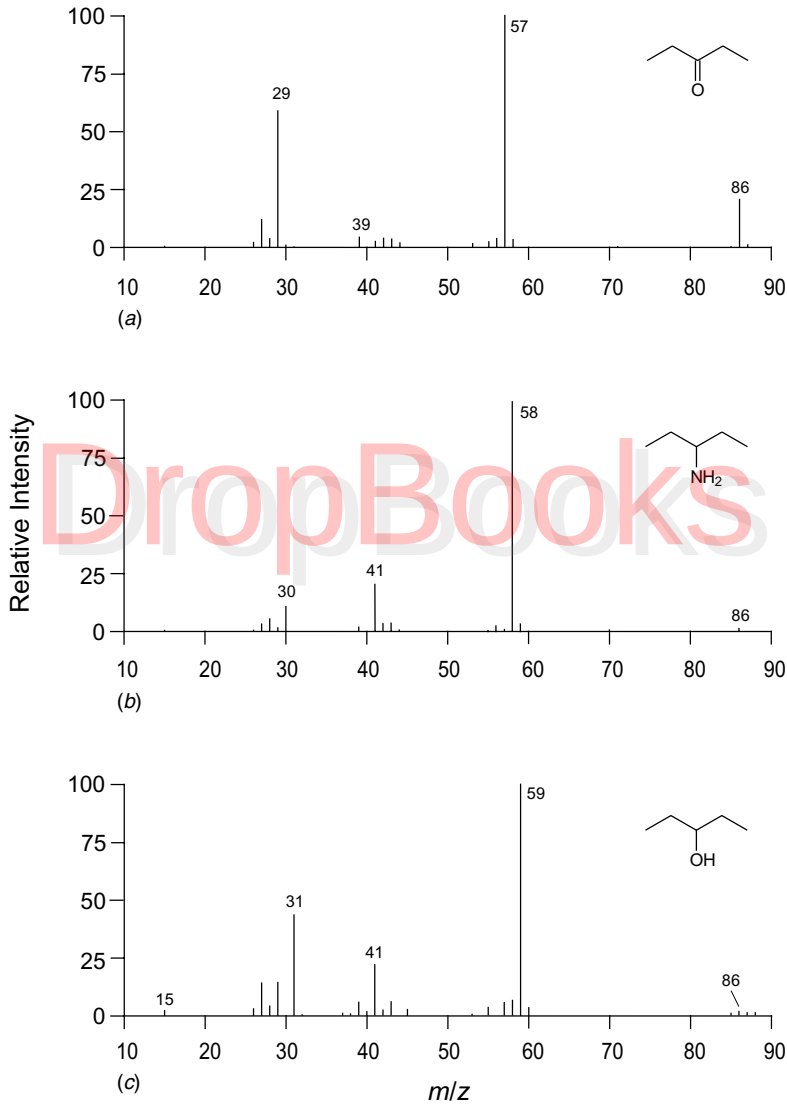

DropBooks

Figure 4.12. Mass spectra of aliphatic compounds with functional groups containing heteroatoms: (*a*) 3-pentanone, (*b*) 3-pentylamine, and (*c*) 3-pentanol.

changes the appearance of the spectrum (Figure 4.12). For one thing, initial ionization in these compounds occurs preferentially at the heteroatom, not at the σ-bonds in the molecule (Section 3.3). Also, the electronegativity of the added groups tends to weaken the bonds in the vicinity of the heteroatom in these molecules so that fragmentation is centered almost entirely on these bonds, in many cases producing one or two ions of unusual abundance and stability. This type of fragmentation, which will be discussed in detail in Chapter 6, is very characteristic of these compounds.[2]

The list of low-mass ion series given in Table 4.2 is by no means complete. Distinctive ion series characterize other types of compounds and become obvious after the spectra of several examples from the family have been studied and compared. For example, alkylsilanes may show a series of peaks at *m/z* 45, 59, and 73, corresponding to $CH_3Si^+H_2$, $(CH_3)_2Si^+H$, and $(CH_3)_3Si^+$ (Figure 4.13). This series may occur in the mass spectra of silyl derivatives of alcohols and amines, for example. Aliphatic sulfur compounds may show peaks at *m/z* 33, 47, or 61, which occur in areas of the spectrum that are usually devoid of peaks. Some compounds, such as aliphatic carboxylic acids and esters, display characteristic $OE^{+\bullet}$ peaks at *m/z* 60, 74, 88,... due to prominent rearrangement fragmentations (see Figure 7.3). More extensive lists of ion series may be found in references such as McLafferty and Tureček (1993).

Other ion series can result from everyday laboratory experience. Terpenes, for example, are isomeric unsaturated cyclic hydrocarbons found in many natural products. The spectra of the three terpenes shown in Figure 4.14 have a surprising number of similarities, despite substantial differences in structure. The peaks at *m/z* 77, 79, 93, 107, 121, and 136 are widespread among the spectra of this family of compounds. They appear to be so characteristic, in fact, that rearrangement to common intermediates prior to fragmentation seems likely.

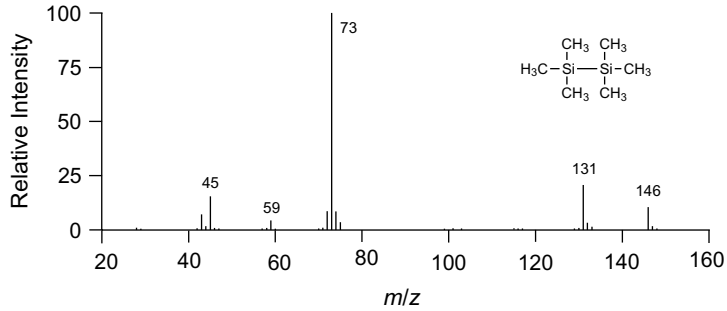

Figure 4.13. Mass spectrum of hexamethyldisilane. The low-mass ion series occurs at *m/z* 45, 59, and 73, which is the same as that for aliphatic ethers and alcohols. Note, however, the intense peak at *m/z* 73 due to the trimethylsilyl ion and the characteristic isotope pattern of Si.

[2] The spectrum of 3-pentylamine shown in Figure 4.12*b* does not exhibit an $M^{+\bullet}$ peak and therefore does not violate the nitrogen rule (Section 3.5). The peak at *m/z* 86 is due to the $(M - 1)^+$ ion.

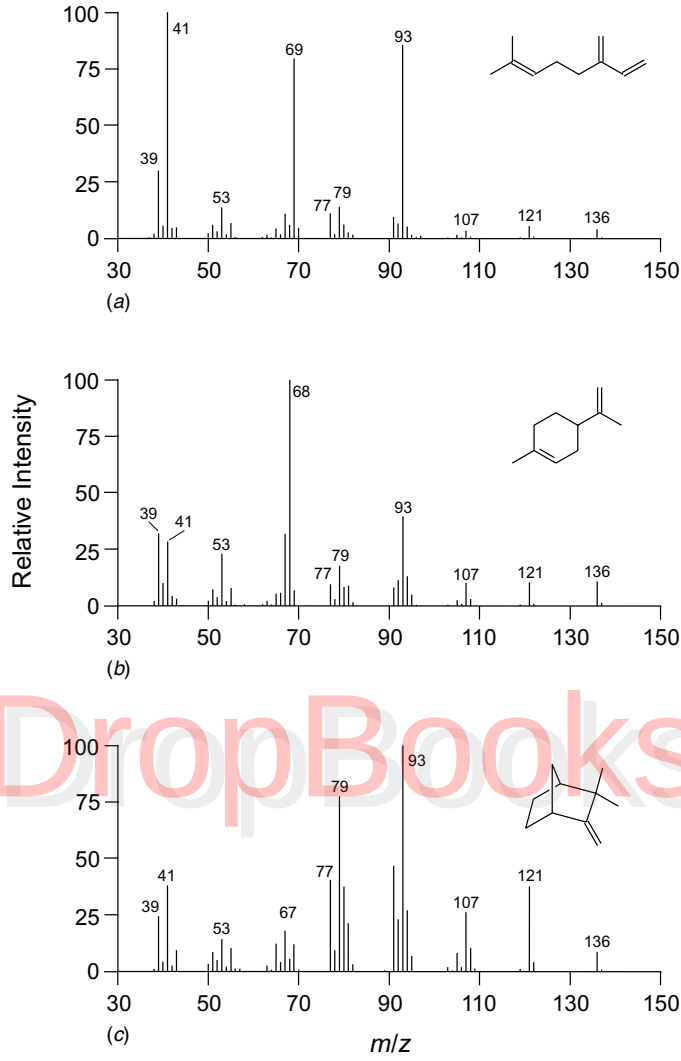

DropBooks

Figure 4.14. Mass spectra of many terpenes are very similar, despite substantial differences in structure: (*a*) 7-methyl-3-methylene-1,6-octadiene (myrcene; oil of bay), (*b*) 1-methyl-4-(2-propenyl)-cyclohexene (limonene; odor of lemons), and (*c*) 2-methylene-3,3-dimethylbicyclo[2.2.1]heptane (camphene; oil of ginger and citronella).

4.2.4. Aromatic Ion Series

Aromatic compounds produce spectra in which many of the peaks at low *m*/*z* values are weak and vary in relative intensity from spectrum to spectrum (see Figure 4.8, e.g.). The corresponding fragment ions are of relatively low abundance because the $M^{+\bullet}$ are comparatively stable, and significant energy barriers (large $\Delta G^{\ddagger}$s) must be

overcome in order for fragmentation to occur (Section 3.6.1). Despite the fact that the low-mass ion series for aromatic compounds are not restricted to specific *m/z* values, they are nonetheless consistent enough to be useful for the characterization of these compounds.

In the spectrum of naphthalene in Figure 4.8*a*, the aromatic low-mass ion series consists of the peaks at *m/z* **39**, 50, **51**, 63, **64**, **75**, and **77**. The ion series listed for aromatic compounds having electron-withdrawing groups attached to the ring (Table 4.2, series 3b) compares well with that for naphthalene. This reflects the fact that in naphthalene one aromatic ring withdraws electron density from the other.

The low-mass ion series for aromatic compounds having electron-donating substituents (Table 4.2, series 3a) is slightly different. In this case, the more intense peaks in each group tend to occur one to two *m/z* units higher (see Figure 4.15). This difference can be rationalized if possible structures for the corresponding ions are considered (Figure 4.5). The ions having *m/z* 91, 77, 65, 51, and 39, which are typical of compounds with electron-donating substituents, show the degree of unsaturation expected for aromatic compounds. On the other hand, those at *m/z* 89, 76, 63, and 50 have structures with triple bonds in the aromatic rings (benzyne-type ions; see Section 4.1.2).

The presence of a fragment ion peak at *m/z* 63 in the spectrum of benzene (Figure 4.15*a*) is unexpected. After ruling out the presence of an impurity, it is challenging to rationalize the contortions through which the benzene $M^{+\bullet}$ must go in order to lose $^{\bullet}CH_3$. One possible rationalization for this fragmentation is shown in Figure 4.16. This obviously complex fragmentation has significant energy demands, which accounts for the low abundance of the *m/z* 63 ion. All the fragmentation pathways open to the benzene $M^{+\bullet}$ apparently require large inputs of energy, so that even highly unusual fragmentations compete for the available energy. The loss of $^{\bullet}CH_3$ from an aromatic ring is not unique to benzene.

Two sets of fragmentations of aromatic ions are so characteristic as to be classified as separate series in Table 4.2. When an unsubstituted benzyl group is present in a molecule, the benzyl ion ($^{+}C_7H_7$; *m/z* 91) is often abundant and may account for the base peak in the spectrum. This is seen in the spectra of toluene and propylbenzene in Figures 4.15*b* and *c*, respectively. However, because of the ability of the benzyl ion to stabilize the transition states of fragmentations, even aromatic compounds lacking a $C_6H_5CH_2$ group may fragment with H rearrangement just so that the benzyl ion can be formed. An example is the hallucinogenic drug phencyclidine (structure below), in whose mass spectrum the *m/z* 91 peak is the most intense peak below *m/z* 200 (25–50% relative intensity) even though two H atoms must be rearranged to the benzylic C atom during the formation of this ion. As described in

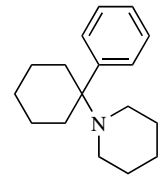

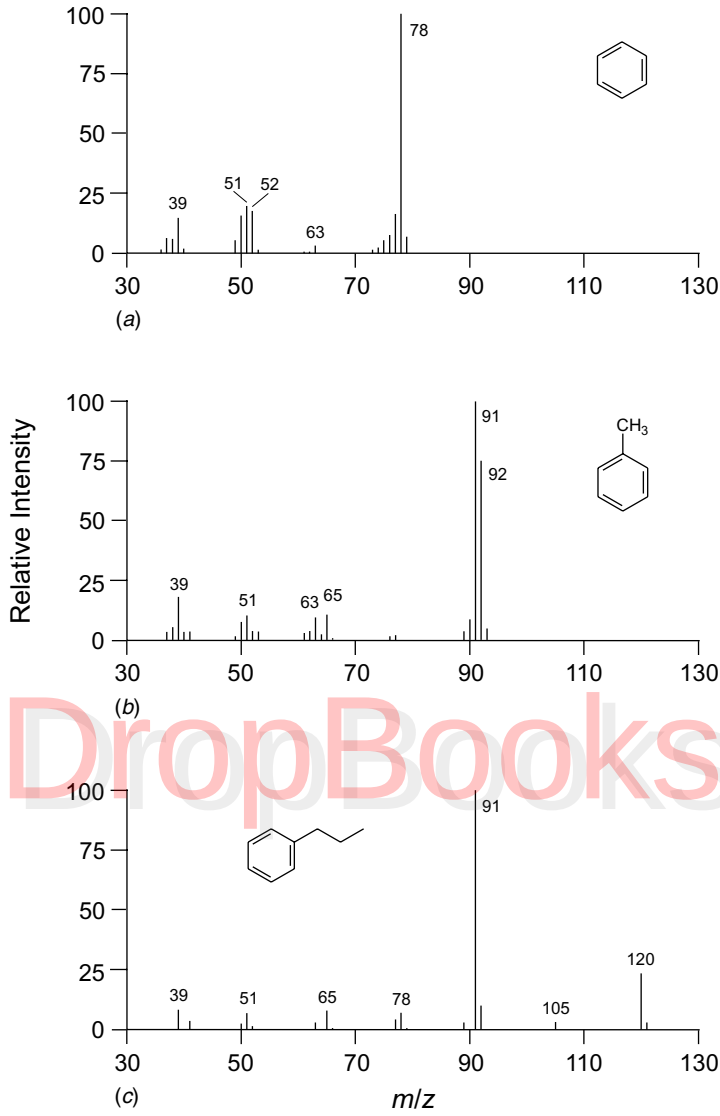

DropBooks

Figure 4.15. Mass spectra of some simple alkylbenzenes: (*a*) benzene, (*b*) toluene, and (*c*) *n*-propylbenzene.

Section 4.1.2 and Figure 4.5 (top), the benzyl ion fragments by sequential losses of HCCH to produce ions having *m*/*z* 65 and 39, with the peak at *m*/*z* 65 usually being the least intense of the three peaks.

The benzoyl ion series (Figure 4.5, bottom) is highly characteristic of aromatic compounds that have a carbonyl group attached directly to the ring. For simple

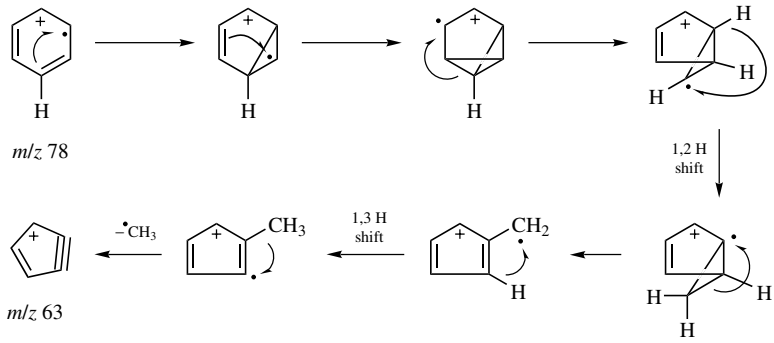

Figure 4.16. Plausible mechanism for the loss of $^{\bullet}CH_3$ from the benzene $M^{+\bullet}$.

aromatic carbonyl compounds, the benzoyl ion series may account for nearly all the most intense peaks in the spectrum (see Figures 6.19– 6.21). A more subtle example is seen in the spectrum of the stimulant drug cocaine (Figure 9.4). As with other aromatic ions, the benzoyl ion fragments through the loss of small, triple bonded molecules—first CO to produce the phenyl ion (*m*/*z* 77), then HCCH to give an ion having *m*/*z* 51 (Figure 4.5).

4.2.5. Use of Ion Series: Mass Chromatograms

Low-mass ion series can be used as a basis for producing mass chromatograms that may help simplify the analysis of complex mixtures. One example is the forensic analysis of arson residues (ASTM, 1994; Bertsch et al., 1990; Nowicki, 1990; Smith, 1982, 1983, 1987; Wallace, 1999).

The spectra of saturated aliphatic hydrocarbons exhibit characteristic intense peaks at *m*/*z* 43, 57, 71, and 85. Similarly, unsaturated and alicyclic compounds show characteristic peaks at *m*/*z* 41, 55, 69, and 83 (Table 4.2). Although aromatic compounds might be characterized in general terms by any of the appropriate ion series in Table 4.2, the aromatic compounds actually present in the petroleum distillates found in fire debris can be broken down further into separate families, each with their own distinctive set of ions (Table 4.3).

Table 4.3. Aromatic ions characteristic of petroleum distillate constituents

Type of Compound	Characteristic Ions
Alkylbenzenes	91, 105, 119, 133 (fragment ions) 78, 92, 106, 120, 134, etc. ($M^{+\bullet}$)
Alkylnaphthalenes	128, 142, 156, 170 ($M^{+\bullet}$)
Alkylstyrenes and indenes	104, 118, 132, 146 ($M^{+\bullet}$)
Alkylanthracenes and phenanthrenes	178, 192, 206 ($M^{+\bullet}$)

The data system can retrieve information about the abundances of these ions from the consecutively acquired spectra that constitute the data file from a GC/MS analysis. These data are presented as mass chromatograms, in which the detector current recorded for an individual m/z value or small group of m/z values is plotted against time (Section 1.5.4). Mass chromatograms appear to enhance sensitivity because they sometimes identify the presence of very-low-concentration components buried in complex chromatograms. However, only SIM, in which the analyzer spends an increased amount of time monitoring the m/z values of specific ions (Section 1.3.3.1), actually lowers the limits of detection.

Summed mass chromatograms for some of the hydrocarbon families found in evaporated gasoline are shown in Figure 4.17. Most striking is the pattern of peaks shown in the "naphthalenes" chromatogram, where the individual homologs are easily discernible. The locally intense and evenly spaced peaks in the "alkanes" chromatogram represent the *n*-alkanes from C_6 up to about C_{18}. With experience the trained analyst can gain insight into the composition of a sample based on this type of information.

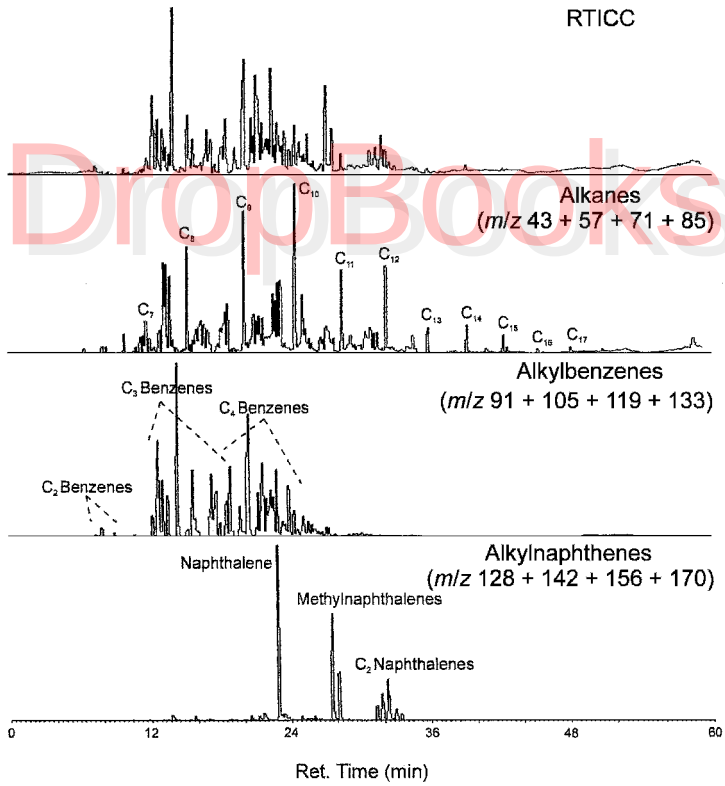

Figure 4.17. Mass chromatograms for this evaporated gasoline sample help locate individual components. Summed chromatograms here are based on characteristic ion series like those in Table 4.3.

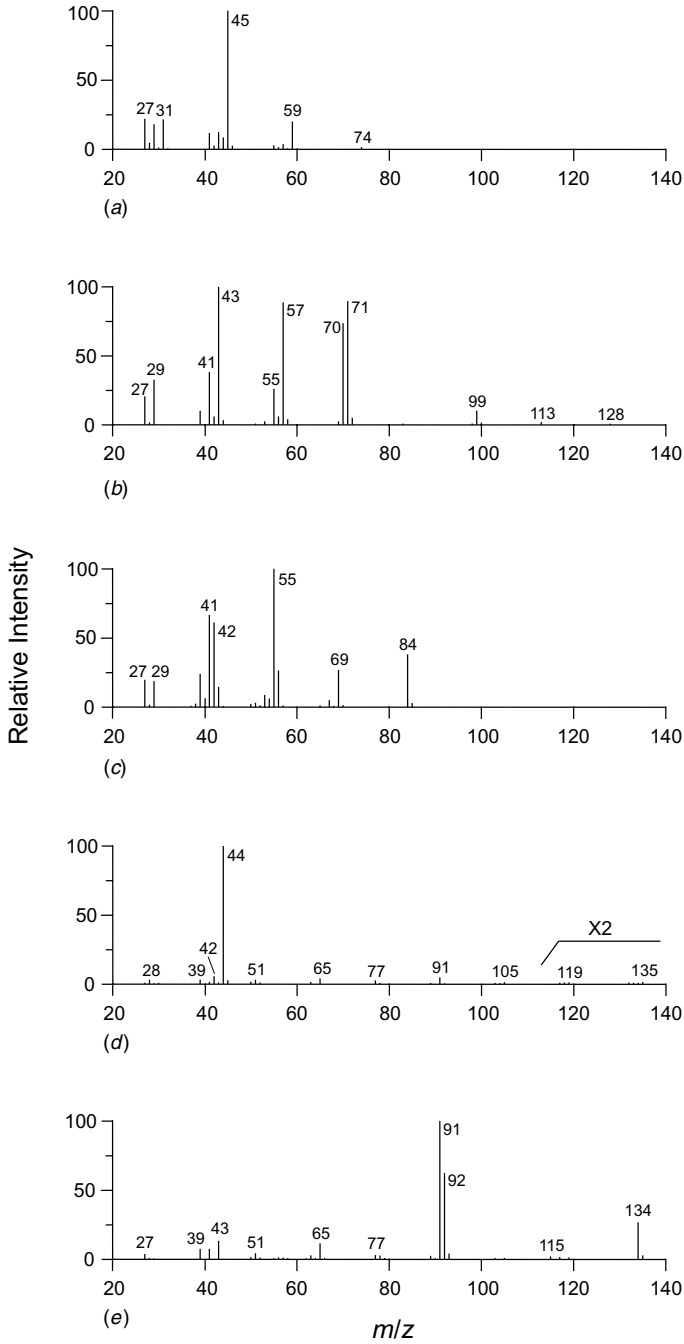

Figure 4.18. Mass spectra for Problem 4.4. In spectrum *d* the intensities of the peaks above *m*/*z* 110 are twice as large as they appear in the original spectrum.

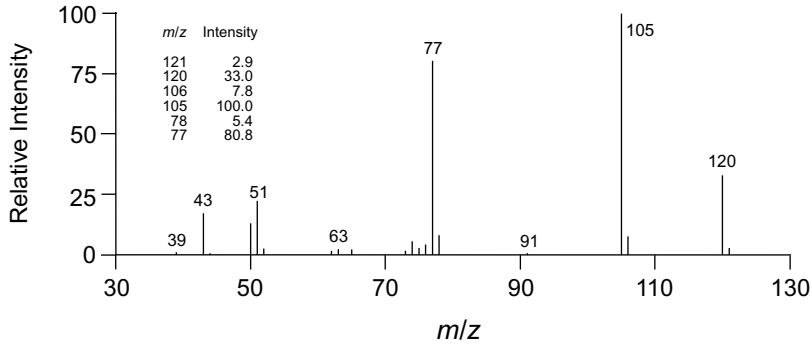

Figure 4.19. Mass spectrum for Problem 4.5.

ADDITIONAL PROBLEMS

4.4. Using Table 4.2, identify the low-mass ion series that are represented in each of the spectra in Figure 4.18. (*Caution*: There may be more than one!)

4.5. Use the information presented in this chapter, as well as isotope peak intensities for selected ions as given, to identify the compound that produced the spectrum in Figure 4.19.

DropBooks

REFERENCES

ASTM Committee E-30 on Forensic Sciences, "ASTM E 1618-94, Standard Guide for the Identification of Ignitable Liquid Residues from Fire Debris Samples by Gas Chromatography/Mass Spectrometry," *Annual Book of ASTM Standards*, Vol. 14.02 (West Conshohocken, PA, 1994).

P. Ausloos, C. L. Clifton, S. G. Lias, A. I. Mikaya, S. E. Stein, D. V. Tchekhovskoi, O. D. Sparkman, V. Zaikin, and D. Zhu, "The Critical Evaluation of a Comprehensive Mass Spectral Library," *J. Amer. Soc. Mass Spectrom.*, **10**, 287–299 (1999).

W. Bertsch, Q. W. Zhang, and G. Holzer, "Using the Tools of Chromatography, Mass Spectrometry, and Automated Data Processing in the Detection of Arson," *J. High Res. Chrom.*, **13**, 597–605. (1990).

J. H. Beynon, R. A. Saunders, and A. E. Williams, *The Mass Spectra of Organic Molecules* (Elsevier, New York, 1968), pp. 158, 172.

A. A. Deniz, K. S. Peters, and G. J. Snyder, "Experimental Determination of the Antiaromaticity of Cyclobutadiene," *Science*, **256**, 1119–1122 (1999).

J. L. Holmes, P. C. Burgers, Y. A. Mollah, and P. Wolcoff, "Isomerization of Alkane Molecular Ions," *J. Am. Chem. Soc.*, **104**, 2879–2884. (1982).

F. W. McLafferty and F. Tureček, *Interpretation of Mass Spectra*, 4th edition (University Science Books, Mill Valley, CA, 1993), frontispiece, pp. 351–354.

J. Nowicki, ''An Accelerant Classification Scheme Based on Analysis by Gas Chromatography/Mass Spectrometry (GC/MS),'' *J. Foren. Sci.*, **35**, 1064–1086. (1990).

R. M. Smith, ''Arson Analysis by Mass Chromatography,'' *Anal. Chem.*, **54**, 1399A (1982).

R. M. Smith, ''Arson Analysis by Mass Spectrometry,'' in J. Yinon, ed., *Forensic Mass Spectrometry* (CRC Press, Boca Raton, FL, 1987), pp. 30–60.

R. M. Smith, ''Mass Chromatographic Analysis of Arson Accelerants,'' *J. Foren. Sci.*, **28**, 318 (1983).

D. J. Tranthim-Fryer, R. C. Hansson, and K. W. Norman, ''Headspace/Solid Phase Microextraction/Gas Chromatography-Mass Spectrometry: A Screening Technique for the Recovery and Identification of Volatile Organic Compounds (VOC's) in Postmortem Blood and Viscera Samples,'' *J. Foren. Sci.*, **46**, 934–946 (2001).

W. J. van der Hart, ''Ab Initio Calculations on the Isomerization of Alkene Radical Cations,'' *J. Amer. Soc. Mass Spectrom.*, **10**, 575–586 (1999).

J. R. Wallace, ''GC/MS Data from Fire Debris Samples: Interpretation and Applications,'' *J. Foren. Sci.*, **44**, 996–1012. (1999).

5

A RATIONAL APPROACH TO MASS SPECTRAL PROBLEM SOLVING

In the preceding chapters, several tools were presented that can be used for solving the mass spectra of unknown compounds. However, even with an understanding of how ions fragment, solving mass spectral unknowns is a complex process and is especially difficult if little information beyond the mass spectrum is available with which to narrow the number of possible structures. The process can be compared to solving a logic puzzle.

DropBooks

It is important to have a rational plan for approaching an unknown mass spectrum. Without one there is a tendency to place disproportionate weight on some clues and to ignore others that may actually be more important. In fact, a common dilemma facing the mass spectral problem solver is not the lack of available clues but rather the abundance, and often seemingly contradictory nature, of those clues. The guidelines presented in this chapter provide a logical method for sorting through mass spectral data so that useful information is obtained. It is applicable not only for the problems in this book but also for the unknowns encountered during daily laboratory work in mass spectrometry.

5.1. GUIDELINES FOR SOLVING MASS SPECTRAL PROBLEMS

The first two guidelines listed below—doing a library search and using chemical information—are generally of more use in solving laboratory unknowns than

Understanding Mass Spectra: A Basic Approach, *Second Edition*. By R. Martin Smith
ISBN 0-471-42949-X © 2004 John Wiley & Sons, Inc.

Table 5.1. Solving mass spectral unknowns

1. Do a **library search** on the spectrum.
2. Obtain a **chemical history** of the sample.
3. Try to identify the $\mathbf{M}^{+\bullet}$ peak or decide whether it is present in the spectrum.
4. Is the nominal molecular mass even or odd? Remember the **nitrogen rule**.
5. Determine, when possible, elemental compositions for ions using **isotope peak intensities**.
   a. Determine the **nominal mass** of the ion.
   b. **Normalize** peak intensities.
   c. Look for **A + 2 element** patterns (except O).
   d. Use X + 1 peak intensity to determine numbers and types of **A + 1 elements**.
   e. Calculate **number of O atoms** from X + 2 peak intensities.
   f. Account for remaining mass with **A elements**.
6. What does the **overall appearance of the spectrum** indicate?
7. Look for **low-mass ion series** (there may be more than one).
8. List first **losses from the $\mathbf{M}^{+\bullet}$** and try to make a pattern of them.
9. Look for intense **odd-electron ions** in the spectrum.
10. Compile all this information and speculate on a structure. Calculate the total number of **rings plus double bonds** in the $M^{+\bullet}$ of the general formula $C_xX_yN_zO_n$, where X can be either H or halogen, or a mixture of both:

$$\text{Total rings plus double bonds} = x - 1/2y + 1/2z + 1$$

they are in solving the problems in this book. In a few cases, chemical information will be provided (and should not be ignored!) with the problems in this book. A condensed version of this list is found in Table 5.1, which is also reproduced inside the back cover of this book.

1. Perform a library search on the spectrum, using all the mass spectral library resources that are available. *Obtain actual graphic and tabular printouts* of the spectra picked by the library and *compare them carefully* to those of the unknown spectrum. The importance of doing an actual visual comparison of the unknown and standard spectra cannot be overemphasized. If the match is not extremely good, the spectrum picked by the library may not be the correct one.

2. Obtain a chemical history of the compound, if that is possible. Where did the compound come from? What types of compounds are likely to come from such a source? The more information that is available, the narrower the list of possible structures will be.

3. Try to identify the $M^{+\bullet}$ peak, or decide whether it is even present in the spectrum. This is often the most critical step in solving an unknown—the structure cannot be determined unless the MM of the compound is known. Unfortunately, this is also one of the most difficult steps because some compounds do not produce $M^{+\bullet}$ by EIMS. The following criteria can be used to evaluate whether a choice for the $M^{+\bullet}$ peak is reasonable or not:

a. Check isotope peak intensities. If the M + 1 peak is too large to be accommodated by a reasonable number of C atoms, the peak that appears to be the M + 1 peak itself may be the $M^{+\bullet}$ peak (Section 2.2.1.7 and Example 2.4).

b. Determine the first losses from the proposed $M^{+\bullet}$ (Table 4.1). Some losses are virtually impossible or occur so infrequently that they can be discounted (Section 4.1). The presence of peaks at *m*/*z* values representing unlikely losses means either that the spectrum contains peaks due to a contaminant or that the choice for the $M^{+\bullet}$ peak is not the correct one.

c. Minimize the amount of unwanted background in the spectrum. If the spectrum appears to be ''dirty'' (i.e., there are lots of small, extraneous peaks, even at very high *m*/*z* values), the possibility of missing a low-intensity $M^{+\bullet}$ peak becomes a real problem.

d. If GC data for the compound are available (e.g., by GC/MS), compare the proposed MM of the unknown with that of compounds which elute at similar retention times. For GC columns that separate compounds roughly by MM, a compound having a MM of 175 would not be expected to elute at a retention time near that of one with a MM of 300.

e. If the $M^{+\bullet}$ peak cannot be clearly identified from the EI spectrum, consider using less energetic ionization methods such as CI (Section 1.2.2) or ESI (Section 1.2.3.1). These techniques usually reduce the amount of fragmentation so that the $M^{+\bullet}$ (or the protonated molecule, MH^+) can be observed.

f. If alternative ionization methods are not available, try to form a chemical derivative of the compound. Derivatization may allow the MM to be determined even when the $M^{+\bullet}$ peak of the underivatized compound is absent. At the least, derivatization usually increases the volatility of high MM compounds so that potentially more sensitive GC analysis can be carried out at lower column temperatures, where thermal decomposition is less likely to occur. Remember to account for the mass(es) of the added derivatizing group(s) when calculating the MM of the original compound. Also be aware that the addition of derivatizing groups can significantly alter the fragmentation pattern of the $M^{+\bullet}$ (e.g., see Section 6.3.2).

DropBooks

4. Is the MM even or odd? Do the fragment ion peaks in the spectrum occur primarily at odd or even *m*/*z* values? Use the nitrogen rule (Section 3.5) to determine the probable presence of N in the molecule. The nitrogen rule states that any $OE^{+\bullet}$ which has an odd number of N atoms and contains only C, H, N, O, Si, S, P, or halogen will have an odd nominal mass. Similarly, any $OE^{+\bullet}$ having an even number of N atoms (including no N atoms) will have an even nominal mass. If most of the fragment ion peaks occur at odd *m*/*z* values, the absence of N is more likely.

5. Analyze the isotope peak intensity information in the $M^{+\bullet}$ peak cluster and other major peak clusters in the spectrum using the procedure outlined in Section 2.3. Look for patterns from the A + 2 elements or the lack of patterns produced by the A elements (F, P, and I). Try to calculate the number of C atoms, O atoms,

and so forth, recognizing the limitations of such calculations (Section 2.2.1.4). Keep in mind that not only must the elements present fit the isotope peak intensity pattern, but their combined masses must also add up to the observed nominal m/z value. Also remember that no fragment ion can contain more atoms of any element than were present in the $M^{+\bullet}$.

6. What does the overall appearance of the spectrum indicate (Section 4.2)? Is the $M^{+\bullet}$ peak the most intense peak in the spectrum, indicating that the compound might be aromatic? Are there many peaks at low m/z values, making it appear as if the $M^{+\bullet}$ falls apart almost randomly? Does one fragment ion peak completely dominate the spectrum?

7. Look for low-mass ion series (Section 4.2 and Table 4.2). Do the library search results give any clues as to the family of compounds in question?

8. Compile a list of suggested losses from the $M^{+\bullet}$ (Section 4.1 and Table 4.1) and try to make a pattern of them. Has a similar pattern of losses been encountered in the spectra of other compounds?

9. Look for intense peaks in the spectrum that represent $OE^{+\bullet}$ (this is more difficult with compounds containing N; see Section 3.5). These peaks may provide clues about structural arrangements that fragment in a specific manner (see, e.g., the γ-hydrogen rearrangement and retro Diels–Alder fragmentation in Chapter 7).

10. Compile the information from all the preceding steps and speculate on a structure. Calculate the number of rings plus double bonds in the $M^{+\bullet}$ or other $OE^{+\bullet}$ in the spectrum using the formula given in Section 2.3. For ions that have the general formula $C_xH_yN_zO_n$, this value is given by the equation

$$\text{Total rings plus double bonds} = x - 1/2y + 1/2z + 1$$

Each element in this formula can be replaced by other elements that have the same valence—for example, any halogen can be substituted for H, and so on.

Does the postulated structure explain all the major peaks observed in the spectrum? Is it possible to write reasonable mechanisms for fragmentations leading to particularly stable ion products (see Chapter 8)? If not, be skeptical. Try different arrangements of the same functional groups, if necessary. Sometimes an isomer of the originally proposed structure contains a key element that causes the whole spectrum to make sense.

11. Above all, do not give up—even if success seems elusive. Solving mass spectral unknowns is rarely easy (even for mass spectrometrists who have many years of experience) and may be nearly impossible without chemical information and/or additional spectral or physical data.

EXAMPLES

The examples and problems that constitute the rest of this chapter illustrate how the guidelines given in the preceding section can be applied to the spectra of various

types of compounds. Explanations accompanying the answers to the unknown spectra in the remaining examples and the problems follow the order of these guidelines. Not all steps will be discussed in each case. The purpose of rigidly following this order is to develop a method for focusing on those aspects of the spectrum that will yield the most useful information. It may be possible to omit some of the steps after a lot of practice and experience, but most new students of mass spectral interpretation struggle with organizing an approach to problem solving.

Example 5.1

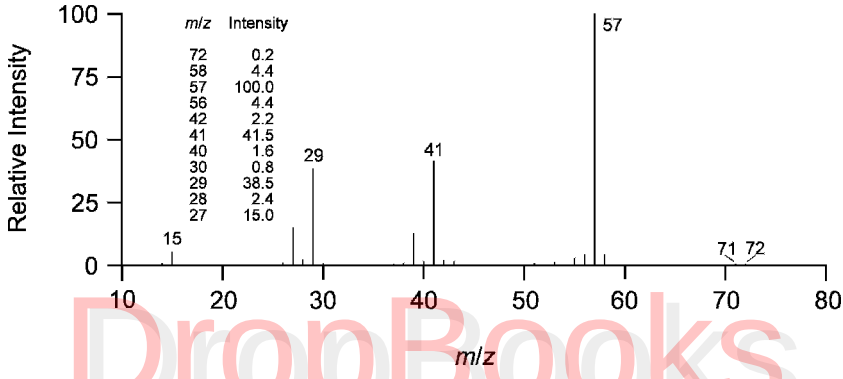

DropBooks

Figure 5.1. Mass spectrum for Example 5.1.

Answer 5.1

(*Steps 1 and 2*) There are no library search results and no chemical history provided for this, or for most of the remaining examples and problems in this chapter.

(*Step 3*) At first glance, the base peak at *m/z* 57 might appear to be the $M^{+\bullet}$ peak, because there are only two very weak-intensity peaks in the spectrum at higher *m/z* values. It would be easy to dismiss these as background peaks. Before doing so, however, all the information available in the spectrum must be used to evaluate the choice for the $M^{+\bullet}$ peak. One of the best places to begin is the analysis of losses from the proposed $M^{+\bullet}$. If the peak at *m/z* 57 corresponds to the $M^{+\bullet}$, then—other than losses of $^{\bullet}H$—the first major loss is that of 16 to produce the peak at *m/z* 41. As indicated in Table 4.1, the loss of 16 is not common and is characteristic of certain types of compounds—most notably primary amides ($-CONH_2$) and compounds having polarized N—O bonds. The smallest two primary amides are formamide ($HCONH_2$, MM 45) and acetamide (CH_3CONH_2, MM 59), and the smallest aliphatic nitro compound is nitromethane (CH_3NO_2, MM 61). None of these structures should produce a large peak at *m/z* 57. On the other hand, if the small peak at *m/z* 72 is the $M^{+\bullet}$ peak, the peaks at *m/z* 71 and 57 would correspond to losses

of 1 ($^{\bullet}H$) and 15 ($^{\bullet}CH_3$), respectively. The choice of *m/z* 72 as the $M^{+\bullet}$ peak thus seems more reasonable than the peak at *m/z* 57. However, the rest of the spectrum must support this choice.

(*Step 4*) The choice of *m/z* 72 as the $M^{+\bullet}$ peak means that the nominal MM is even. All the major fragment ion peaks in the spectrum occur at odd *m/z* values, which is consistent with the absence of N (Section 3.5). Notice that, if *m/z* 57 were the $M^{+\bullet}$ peak, the compound would have to contain an odd number of N atoms.

(*Step 5*) The weak intensity of the *m/z* 72 peak precludes obtaining information about the elemental composition of the $M^{+\bullet}$. The isotope peak intensities in the *m/z* 57 peak cluster are free of interferences from other fragment ions because, other than the loss of $^{\bullet}H$, the mass of the smallest fragment that can be lost from the $M^{+\bullet}$ is 15 u. The ion represented by the *m/z* 57 peak appears to have no A + 2 elements (including O—the intensity of the peak at *m/z* 59 is too small). Because N is probably absent as well, the only contribution to the X + 1 peak should be that of C. The number of C atoms in this ion is $4.4/1.1 = 4$. If four atoms of C are present, the remaining mass $\{[57 - (4 \times 12)] = 57 - 48 = 9\}$ must be due to nine H atoms. This gives an elemental composition of C_4H_9, a butyl ion.

Analysis of isotopic peak intensities for the *m/z* 41 peak does not yield useful results. The [X + 1]/[X] intensity ratio is $2.2/41.5 = 5.3\%$, which implies the presence of about five C atoms. This is clearly impossible and means that one of the contributors to the *m/z* 42 peak is a fragment ion having that nominal *m/z* value. The peak cluster beginning at *m/z* 29 reveals more information. In this case, the *m/z* 30 peak has a normalized intensity of 2.1% relative to the *m/z* 29 peak, indicating the presence of $2.1/1.1 \approx 2$ C atoms. The combined mass of two C atoms is 24 u, leaving five H atoms to make up the remaining mass. The *m/z* 29 peak thus represents the ethyl ion, $^{+}CH_2CH_3$.

(*Step 8*) As stated above, the peaks at *m/z* 71 and 57 represent the losses of $^{\bullet}H$ and $^{\bullet}CH_3$, respectively, from the $M^{+\bullet}$. If the assumption were made that the peak at *m/z* 41 was produced by the loss of 31 directly from the $M^{+\bullet}$, this would lead to the conclusion that the molecule contains a methoxy group (CH_3O; see Table 4.1). The presence of O in the molecule has already been ruled out, however, indicating that the peak at *m/z* 41 is undoubtedly produced by a combination of losses. This underscores the problem of attempting to assign precursor ions for fragment ion peaks that occur in the middle of the spectrum.

(*Step 9*) The rearrangement fragmentations that are useful in Step 9 have not yet been discussed. This step will be omitted until Chapter 7.

(*Step 10*) The *m/z* 57 peak represents a butyl ion ($^{+}C_4H_9$), and this ion is produced by the loss of $^{\bullet}CH_3$ from the $M^{+\bullet}$. This means that the elemental composition of the $M^{+\bullet}$ is C_5H_{12}. There are $5 - \frac{1}{2}(12) + \frac{1}{2}(0) + 1 = 0$ rings plus double bonds in the molecule; therefore, this is a saturated aliphatic hydrocarbon. There are three C_5H_{12} isomers: *n*-pentane, 2-methylbutane, and 3,3-dimethylpropane. Based on the discussions in Sections 4.2.1 and 4.2.2, both *n*-pentane and 2-methylbutane would be expected to lose $^{\bullet}CH_2CH_3$ to some degree, producing a significant peak at *m/z* 43. Instead, the peak at *m/z* 43 is very small, and the loss of $^{\bullet}CH_3$ is the

most important fragmentation that the $M^{+\bullet}$ of this compound undergoes. This is consistent with the behavior expected from 3,3-dimethylpropane (Equation 5.1).

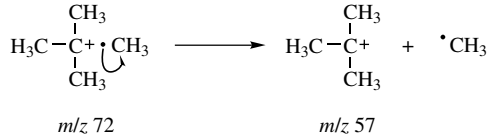

(5.1)

Example 5.2

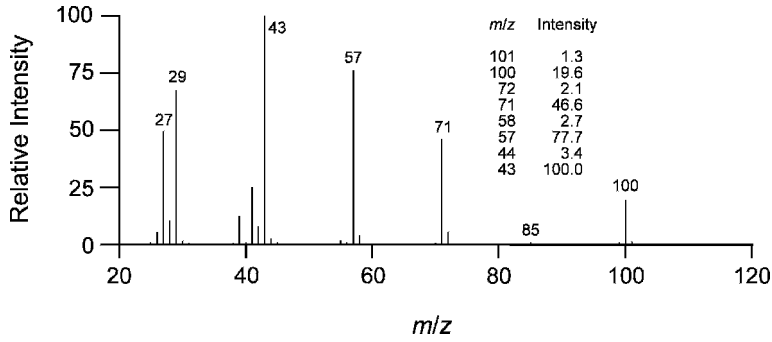

Figure 5.2. Mass spectrum for Example 5.2.

DropBooks

Answer 5.2

(*Step 3*) The peak at *m/z* 100 appears to be the $M^{+\bullet}$ peak, showing initial losses of 1, 15, and 29.

(*Step 4*) This, coupled with the fact that all the major fragment ion peaks occur at odd *m/z* values, makes the presence of N seem unlikely (Section 3.5).

(*Step 5*) None of the obvious A + 2 element patterns are present in either the $M^{+\bullet}$ or any of the major fragment ion peak clusters. The isotope peak intensities in the *m/z* 43, 57, 71, and 100 peak clusters show the presence of 3, 3, 4, and 6 C atoms, respectively, in the corresponding ions. This means that the peak at *m/z* 43 represents a propyl ion, but the ions having *m/z* 57, 71, and 100 all contain too few C atoms to account for all the observed mass (the elemental compositions for aliphatic hydrocarbon ions having masses of 57, 71, and 100 u are C_4H_9, C_5H_{11}, and C_7H_{16}, respectively). Because the compound does not seem to contain N, this makes the presence of O likely.

(*Steps 6 and 7*) The spectrum contains a number of intense peaks at low *m/z* values and appears to have a saturated aliphatic low-mass ion series at *m/z* 43, 57, and 71. However, the isotopic peak intensity information belies this. Another low-mass ion series that occurs at the same *m/z* values is that for ketones (Table 4.2, series 2*a*). Although the isotope peak data are insufficient to confirm the presence of O, elemental compositions of $C_6H_{10}O^{+\bullet}$ for the $M^{+\bullet}$, $C_4H_7O^+$ for the *m/z* 71 ion, and $C_3H_5O^+$ for the *m/z* 57 ion seem reasonable at this point. It is also instructive to compare this spectrum with that of *n*-decane (Figure 4.7) and *n*-octane

(Figure 4.9*a*). Despite the presence of major peaks at *m/z* 43, 57, and 71 in all three spectra, the spectra of the *n*-alkanes also contain important peaks at *m/z* 70, 56, and 55—peaks that are completely absent from the spectrum of this compound. The lack of peaks at *m/z* values one and two units below intense fragment ion peaks is more typical of RCO^+ ions than R^+ ions.

(*Steps 8 and 10*) Although losses of $H^\bullet$ and $^\bullet CH_3$ are recorded in the spectrum, the primary losses from the $M^{+\bullet}$ are 29 ($^\bullet CH_2CH_3$) to produce $C_4H_7O^+$ (*m/z* 71), 43 (a propyl radical) to form $C_3H_5O^+$ (*m/z* 57), and 57 ($^\bullet C_3H_5O$) to give the propyl ion (*m/z* 43). The fragments represented by these peaks are therefore propyl and C_3H_5O or ethyl and C_4H_7O. Because the compound appears to be a ketone from the low-mass ion series, the structures of the fragment ions having *m/z* 57 and 71 must be $CH_3CH_2CO^+$ and $C_3H_7CO^+$, respectively (Equation 5.2). Without further information, the nature of the propyl group (*n*-propyl or isopropyl) cannot be determined. In this case, 3-hexanone, it is an *n*-propyl group.

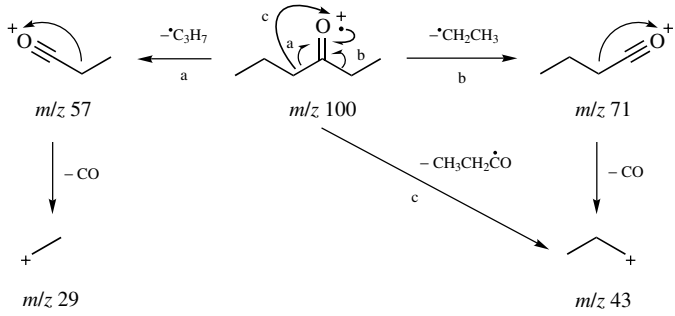

(5.2)

Example 5.3

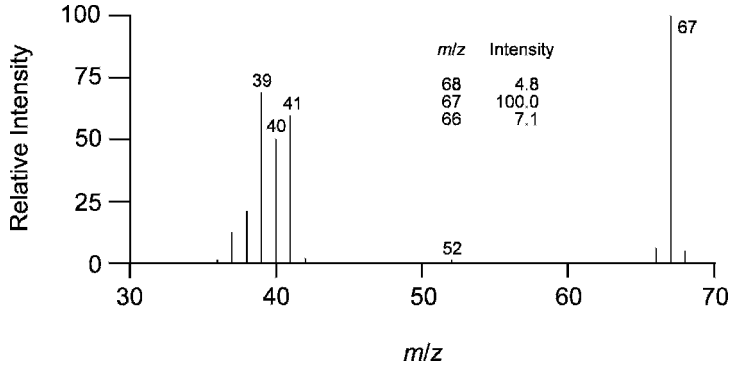

Figure 5.3. Mass spectrum for Example 5.3.

Answer 5.3

(*Steps 3 and 4*) The MM of this compound appears to be 67, indicating that the compound contains an odd number of N atoms. The presence of one N atom will be assumed initially.

(*Step 5*) None of the obvious A + 2 element patterns are present, and isotopic peak intensity information from the *m/z* 67 peak cluster indicates that four C atoms are present in the corresponding ion. This leads to an elemental composition of C_4H_5N.

(*Steps 6 and 8*) The $M^{+\bullet}$ peak is the base peak, and the only major losses observed are 26 (HC≡CH or $^{\bullet}$C≡N), 27 (HCN), and 28 (to form $^{+}C_3H_3$). This pattern is consistent with that expected of an aromatic compound, although (*Step 7*) the MM is so low that a typical aromatic low-mass ion series is not produced.

(*Step 10*) The rings plus double bonds formula determines that the elemental composition C_4H_5N contains $4 - \frac{1}{2}(5) + \frac{1}{2}(1) + 1 = 3$ unsaturations. A structure that fits these criteria is pyrrole, which, in addition to the four π-electrons from the two double bonds, also has a pair of nonbonding electrons associated with the N atom that forms a cyclic system of overlapping *p*-type orbitals containing six electrons. This conforms to Hückel's rule for determining aromaticity (Section 4.1.2). Pyrrole exhibits other spectroscopic characteristics and chemical behavior consistent with this definition. The small peak at *m/z* 52 must represent an ion resulting from the loss of $^{\bullet}CH_3$ from the $M^{+\bullet}$. Remember that benzene exhibits similar behavior (Figure 4.15*a*). Rationalizations for the primary losses from the $M^{+\bullet}$ are shown in Equation 5.3.

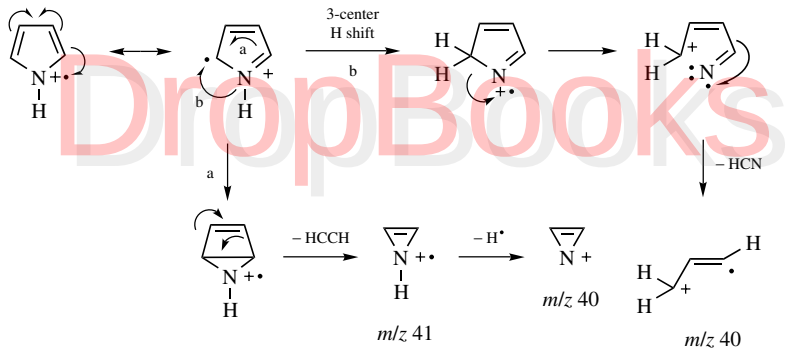

(5.3)

DropBooks

Example 5.4

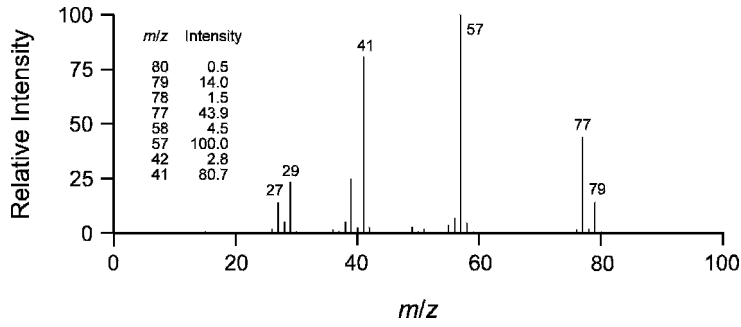

Figure 5.4. Mass spectrum for Example 5.4.

Answer 5.4

(*Step 3*) The first step in solving any mass spectral unknown is identifying the $M^{+\bullet}$ peak. Up to this point, one peak in the spectrum of each example or problem has always seemed like a logical choice for the $M^{+\bullet}$ peak. In this spectrum, however, neither of the peaks at *m/z* 77 or 79 can represent the $M^{+\bullet}$ because, barring severe contamination by some extraneous material, the base peak would lie 20 or 22 *m/z* units lower at *m/z* 57. The loss of 22 is forbidden (Table 4.1), and the loss of 20 as HF is highly unlikely here (see Step 5 below). There are no peaks in the spectrum above *m/z* 80; therefore, the $M^{+\bullet}$ peak cannot be identified directly. The only hope is that it might be possible to *infer* it from the available information.

(*Step 4*) Not knowing the MM precludes determining the presence or absence of N. It is important to concentrate on what can be learned from the spectrum.

(*Step 5*) The peaks at *m/z* 77 and 79 appear to indicate the presence of one Cl atom (the intensity of the *m/z* 79 peak is about $\frac{1}{3}$ that of *m/z* 77) and three C atoms, although these assumptions are tenuous because the mass of the $M^{+\bullet}$ is unknown. The peaks at *m/z* 77 and 79 could just as easily represent individual fragment ions that come from different precursors.

(*Steps 6 and 7*) The peaks at *m/z* 27, 29, 41, and 57 all fall into the aliphatic and olefinic low-mass ion series, and the relative intensities of *m/z* 42 and 58 indicate the presence of three and four C atoms, respectively, in the ions having *m/z* 41 and 57. The *m/z* 41 peak therefore represents the allyl ion ($^{+}CH_2{-}CH{=}CH_2$) and *m/z* 57 one of the saturated butyl ions ($^{+}C_4H_9$).

(*Steps 8 and 10*) There appear to be no hydrocarbon ions above *m/z* 57 (the next member of the low-mass ion series would be at *m/z* 71) and the *m/z* 77 ion seems to contain a Cl and three C atoms. It is therefore conceivable that the compound consists of a butyl group and a Cl atom. This would lead to a MM of 92, and the *m/z* 77 peak could be produced by the loss of $^{\bullet}CH_3$ from the $M^{+\bullet}$.

The nature of the butyl group remains to be determined. The lack of a peak at *m/z* 43 in the hydrocarbon ion series indicates that neither an *n*-propyl nor, especially, an isopropyl group is present in the molecule. This leaves only *t*-butyl chloride (2-methyl-2-chloropropane) and *sec*-butyl chloride (2-chlorobutane) as possible answers. Spectra of both compounds would be needed for comparison in order to distinguish conclusively between them, although the fragmentations discussed in the next chapter make *t*-butyl chloride the most reasonable choice (Equation 5.4).

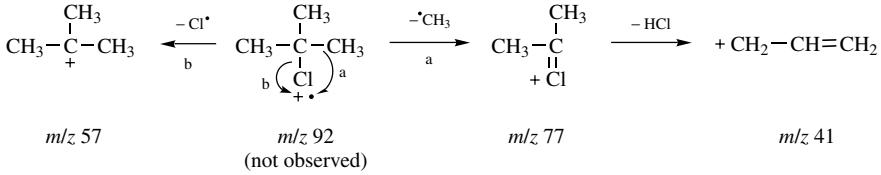

(5.4)

Example 5.5

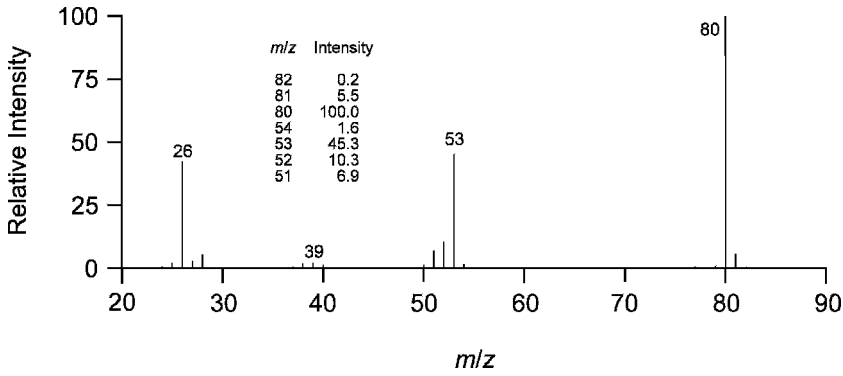

Figure 5.5. Mass spectrum for Example 5.5.

Answer 5.5

(Steps 3 and 4) The peak at *m/z* 80 appears to be the $M^{+\bullet}$ peak, which means that the compound has an even nominal MM. This is consistent with an even number of N atoms. Up to this point, the assumption has always been made that this number is zero. However, a strong piece of evidence contradicts that assumption in this case: Other than a very small peak at *m/z* 79 representing the loss of $^{\bullet}H$, the fragment ion corresponding to the first loss from the $M^{+\bullet}$ peak is the peak at *m/z* 53 *(Step 8)*. This represents the loss of 27, which is most commonly that of HCN (the loss of a vinyl radical is much less common), indicating that N may be present in the molecule. Because the MM is even, this means that there have to be at least two N atoms. There are few fragment ion peaks in the spectrum as a whole, so whether these peaks occur at even or odd *m/z* values is of little use here. The assumption will be made that there are two N atoms in this compound.

(Step 5) There are no obvious A + 2 elements in this compound. The intensity of the M + 1 peak shows that, in addition to two N atoms, the $M^{+\bullet}$ contains $5.5 - (2 \times 0.4) = 5.5 - 0.8 = 4.7\% \rightarrow 4$ C atoms. The ion having *m/z* 53 appears to have, in addition to a *single* N atom (if the assumption is correct that HCN is lost in producing this peak), $(1.6/45.3) - 0.4 = 3.5 - 0.4 = 3.1\% \rightarrow 3$ C atoms.

It is worth mentioning that the isotope peak intensity data for the $M^{+\bullet}$ are more consistent with the presence of N than the lack of it. The presence of O seems unlikely because the relative intensity of the M + 2 peak is only slightly greater than that calculated from the presence of the four C atoms $(0.006 \times 4^2 = 0.1\%)$. If O is absent, then the intensity of the M + 1 peak predicts the presence of only five C atoms, which would have to be accompanied by 20 H atoms in order to arrive at the observed MM. This is impossible.

(Steps 6 and 7) The fact that the $M^{+\bullet}$ peak is the base peak in the spectrum and the presence of a truncated aromatic low-mass ion series at *m/z* 38–39 and 50–53 both indicate that this is the spectrum of an aromatic compound.

DropBooks

(Step 10) The combined mass of four C atoms and two N atoms is $(4 \times 12) + (2 \times 14) = 48 + 28 = 76$ u. The remaining 4 u must be due to H. The number of rings plus double bonds calculated for $C_4H_4N_2$ is $4 - \frac{1}{2}(4) + \frac{1}{2}(2) + 1 = 4$, which is indicative of an aromatic ring. If the ring has six members, it must contain both the C and N atoms. Three isomers (in which the N atoms are in the 1 and 2, 1 and 3, and 1 and 4 positions) are possible. These compounds are likely to produce similar spectra and might not be easy to distinguish by mass spectrometry. In this case, the spectrum is that of 1,4-diazabenzene (pyrazine). Formation of the m/z 53 ion is rationalized in Equation 5.5.

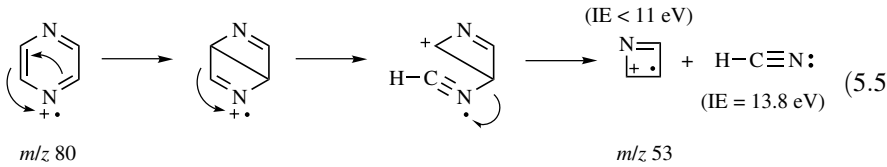

(5.5)

PROBLEMS

5.1–5.4. The spectra for these unknowns are given in Figures 5.6 through 5.9. Determine elemental compositions and assign possible structures for the compounds that produced these spectra. As in the examples above, follow the guidelines in Section 5.1 in the order they are given in order to derive your answer.

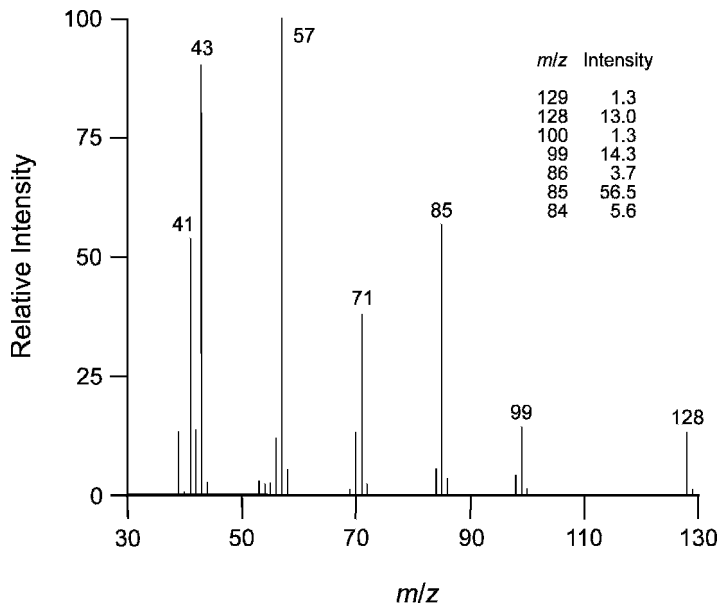

Figure 5.6. Mass spectrum for Problem 5.1.

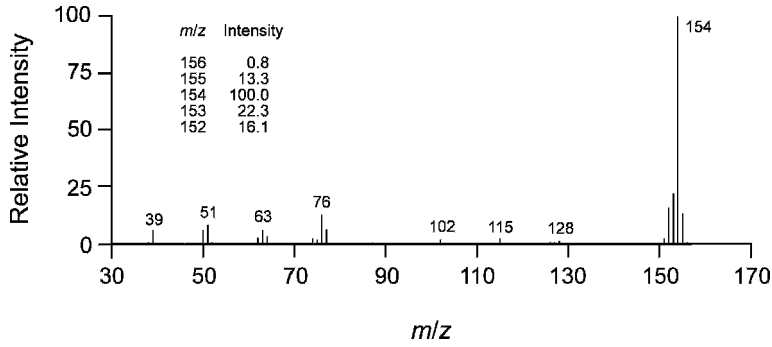

Figure 5.7. Mass spectrum for Problem 5.2.

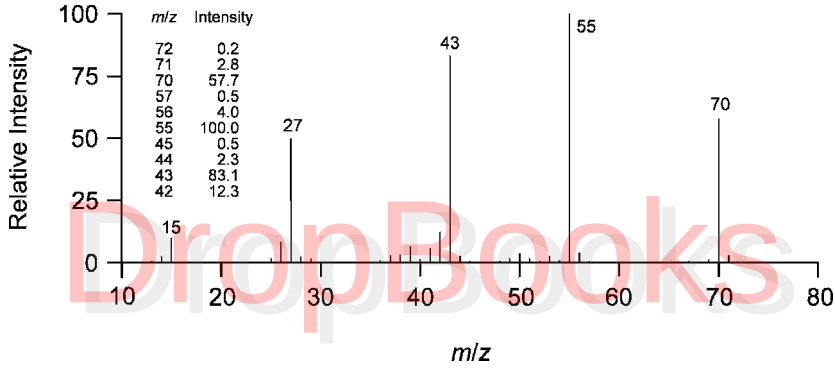

DropBooks

Figure 5.8. Mass spectrum for Problem 5.3.

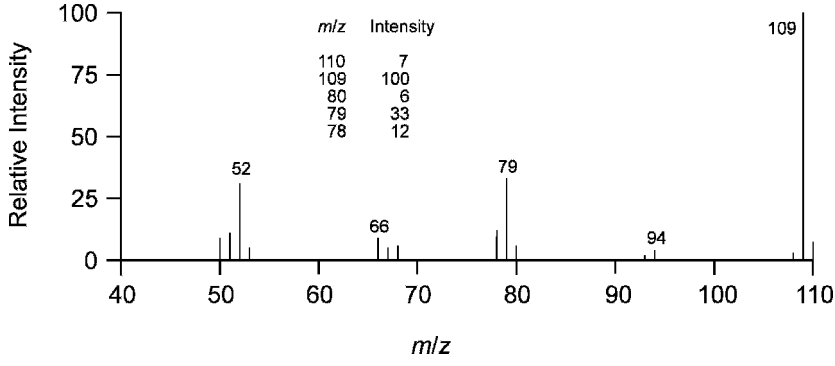

Figure 5.9. Mass spectrum for Problem 5.4.

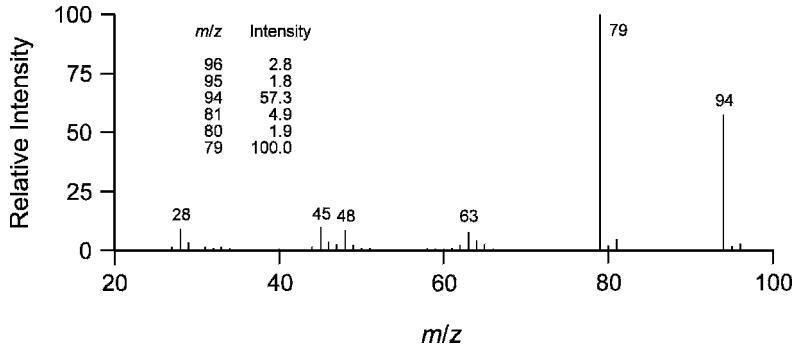

Figure 5.10. Mass spectrum for Problem 5.5.

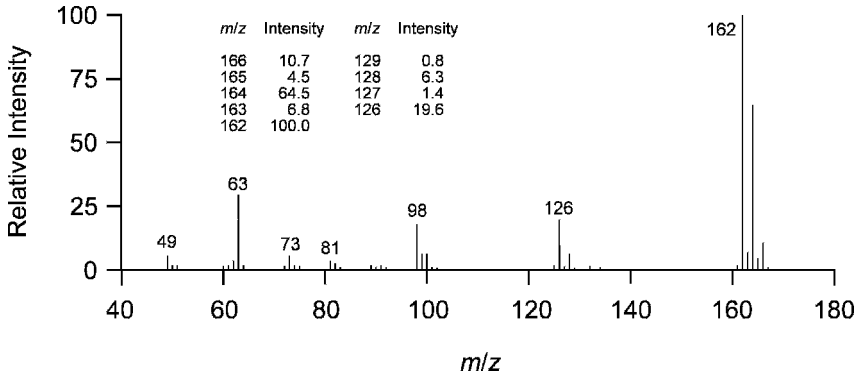

Figure 5.11. Mass spectrum for Problem 5.6.

5.5. The mass spectrum shown in Figure 5.10 was obtained from a compound that is found in some "natural" remedies for joint pain. What is the structure of this compound?

5.6. The compound whose spectrum is shown in Figure 5.11 was identified as a sex pheromone of the female Lone Star tick (*Amblyomma americanum*) (Berger, 1972). What is the structure of this compound?

REFERENCE

R. S. Berger, "Sex Pheromone of the Lone Star Tick," *Science*, **177**, 704–705 (1972).

6

α-CLEAVAGE AND RELATED FRAGMENTATIONS

6.1. INTRODUCTION

DropBooks

The simplest fragmentations involve inonization of a σ-bond in an aliphatic hydrocarbon, followed by cleavage of the ionized bond to produce an alkyl radical and an alkyl carbenium ion (Equations 4.5 and 4.7; see also Figure 3.2). In this chapter the primary focus will be on a fragmentation in which a σ-bond is cleaved and electron density shifts in order to help stabilize the charge. This fragmentation can occur either when one of the electrons in the breaking bond moves to pair up with a radical site (homolytic cleavage; see Section 3.4) or the pair of electrons from the breaking bond moves to neutralize a charge site (heterolytic cleavage). Homolytic cleavage occurs with charge retention, whereas heterolytic cleavage results in charge migration.

α-Cleavage is a special case of this type of homolytic cleavage. α-Cleavage is given this name because, after initial ionization at a heteroatom or a group that can act like a heteroatom, bond breaking occurs by moving one of the electrons from a σ-bond to the C atom that is α (i.e., adjacent) to the heteroatom or group in order to neutralize the initially formed radical site (Figure 6.1). In the representation shown in Figure 6.1, the heteroatom or heteroatom-like group is denoted by X. The R groups may be alkyl groups, H, or any other functional group that can be lost easily as a radical.

Understanding Mass Spectra: A Basic Approach, *Second Edition*. By R. Martin Smith
ISBN 0-471-42949-X © 2004 John Wiley & Sons, Inc.

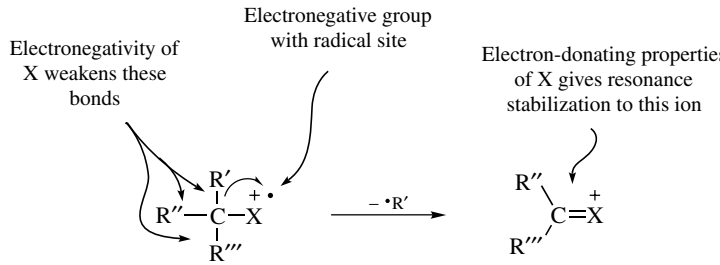

X = NR_2, OR, double bond or aromatic ring; or X, R‴ = =O.
R group forming most stable radical will be lost preferentially.

Figure 6.1. Generalized representation of α-cleavage fragmentation.

As discussed in Section 3.3, molecules containing heteroatoms usually undergo initial ionization at the heteroatom through loss of a nonbonding (*n*) electron. If X is an aromatic ring or double bond, a π-electron may be lost during initial ionization. Fragmentation occurs when a σ-bond to the α C atom (arbitrarily shown here as the C—R′ bond) is cleaved homolytically, and one of the electrons from this breaking bond moves to pair with the radical site on the adjacent X group. The R′ group leaves as a radical, and the α C atom rehybridizes to form a *p*-orbital containing the remaining σ-bonding electron. The *p*-orbital overlaps with the unpaired, nonbonding electron on the ionized X group to form a new π-bond between the α C atom and the X group. If all the R groups are alkyl groups or H, the ions formed from the loss of the various R groups have similar stabilities. In that case, the R group forming the most stable radical is lost preferentially (Section 4.2.1).

In α-cleavage the electronegative X group withdraws σ electron density away from the other bonds to the α C atom, thereby weakening them relative to other bonds in the $M^{+\bullet}$. If cleavage occurs away from the initially formed radical site (i.e., not at the α C atom), the site of cleavage and the radical site must be linked by contiguous overlapping orbitals (Section 6.4.2).

The ability of X to stabilize the charge at first may seem to be at odds with the fact that X is also fairly electronegative. Indeed, groups that best support homolytic cleavage are those whose electronegativities are closest to that of C. Nitrogen is so well adapted to this role that this is nearly always the primary mode of fragmentation for molecules containing aliphatic N atoms. When the N is contained in a complex saturated ring system, many of the most intense peaks in the spectrum typically result from rearrangements in which the charge is stabilized by the N atom (e.g., see Sections 6.3.3 and 9.3).

Several common X groups meet the two criteria shown in Figure 6.1—the O atom in alcohols and ethers, the N atom in amines, and most aromatic rings. The double bonded O atom of a carbonyl group is also included (but not the entire carbonyl group). In this case, the symbolism in Figure 6.1 necessitates the presence of

only two R groups on the carbonyl C atom. As with other X groups, the nonbonding electrons on the carbonyl O atom stabilize the charge by forming an additional π-bond to the carbonyl C atom (R^2—C≡O^+). α-Cleavage also occurs at C atoms next to halogens, S atoms in thiols (RSH) and sulfides (RSR), and even isolated double bonds (allylic cleavage; X = R_2C=CR—).

6.2. BENZYLIC CLEAVAGE

When initial ionization occurs in an aromatic ring (X = C_6H_5), homolytic cleavage can occur at a C atom attached directly to the ring (Equation 6.1).

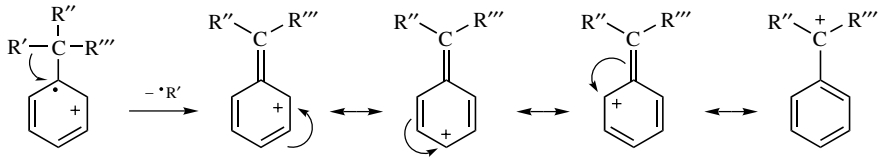

(6.1)

DropBooks

With the exception of its bond to the ring, any of the bonds to this benzylic C atom may be broken. The spectra in Figure 6.2 illustrate this type of fragmentation, which is known as benzylic cleavage, for three isomeric alkylated benzenes. In each case, the largest alkyl radical is lost (isopropyl, ethyl, and methyl, respectively) in order to produce the base peaks at *m/z* 91, 105, and 119. The only other loss by benzylic cleavage that is possible in these molecules is $H^{\bullet}$. In the mass spectrum of isobutylbenzene (Figure 6.2*a*), the stability of $H^{\bullet}$ cannot compete with that of $CH_3C^{\bullet}HCH_3$, so that the M − 1 peak is not observed. On the other hand, loss of any of the eight benzylic H atoms on the three benzylic C atoms of 3,5-dimethylethylbenzene (Figure 6.2*c*) competes somewhat more effectively with loss of the single methyl group, so that the M − 1 peak is observed. Loss of $^{\bullet}CH_3$ from the $M^{+\bullet}$ of this compound is still preferred by a factor of about 20. Benzylic cleavage is the most important fragmentation these $M^{+\bullet}$ undergo, reflecting the much smaller activation energies required for α-cleavage than for other fragmentations of aromatic rings.

When more than one methyl group is attached to the ring, the greater stability of $^{\bullet}CH_3$ compared to $H^{\bullet}$ leads to preferential loss of a $^{\bullet}CH_3$ directly from the ring (Figures 6.3 and 1.23*c*). This is true even though the resulting phenyl ions are less stable than the corresponding benzylic ions (the IE for phenyl radical is 8.1 eV, whereas that of benzyl radical is 7.1 eV; Table 3.1). The incipient phenyl ions formed during these fragmentations may also rearrange by H migration to produce the isomeric benzyl ions, further lowering the activation energies for these

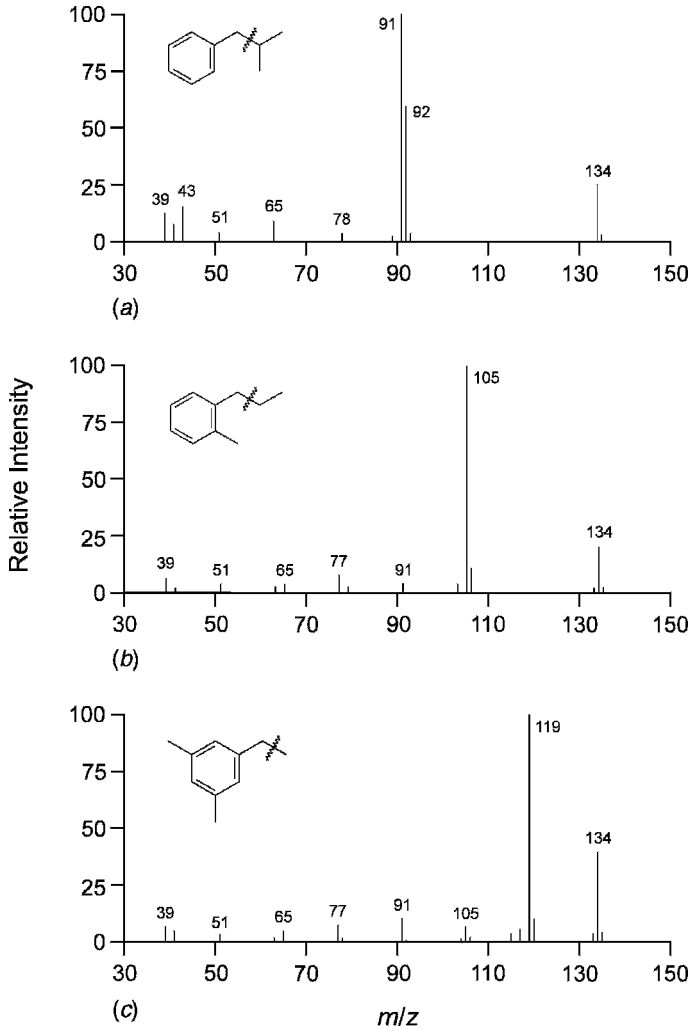

Figure 6.2. Mass spectra of three C_4-benzenes: (*a*) isobutylbenzene, (*b*) 2-methyl-*n*-propylbenzene, and (*c*) 3,5-dimethylethylbenzene. In each case, the largest alkyl group is lost by benzylic cleavage from a C atom next to the ring.

fragmentations. In cases where methyl groups are attached to three or more adjacent C atoms on the ring, steric interactions may lower the activation energy for $^{\bullet}CH_3$ loss even further.

Loss of $H^{\bullet}$ is significant, however, when the benzylic C atom is located *between* two aromatic rings. In the spectrum of diphenylmethane ($C_6H_5CH_2C_6H_5$), the M − 1 peak at *m*/*z* 167 has an intensity of 90% relative to that of the $M^{+\bullet}$ peak (*m*/*z* 168; 100%).

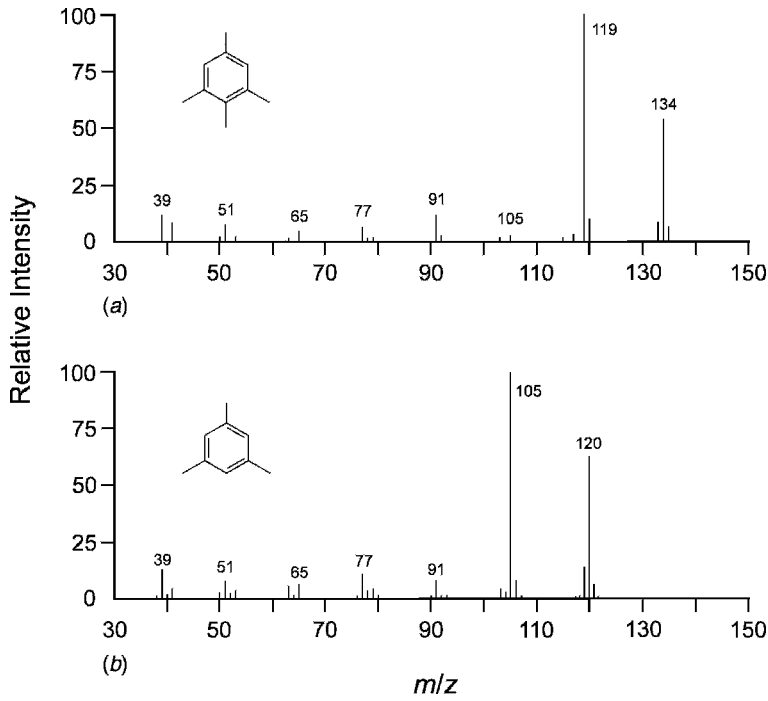

Figure 6.3. The mass spectra of polymethylated benzenes show the loss of $^{\bullet}CH_3$ directly from the aromatic ring: (*a*) 1,2,3,5-tetramethylbenzene and (*b*) 1,3,5-trimethylbenzene.

DropBooks

6.1. The two compounds whose spectra are shown in Figure 6.4 have the same nominal MM. Relative peak intensities for the $M^{+\bullet}$ and base peak clusters in each spectrum are as follows:

a		b	
m/z	Rel.Int.	*m/z*	Rel.Int.
121	2.3	121	2.4
120	22.8	120	23.6
92	10.5	106	9.2
91	100.0	105	100.0

Identify the compounds that gave rise to these spectra.

6.2. The chromatogram in Figure 6.5 was obtained from methanolic dilution of the contents of a spray canister labeled CS Tear Gas (*ortho*-chlorobenzalmalononitrile). The small peaks at the longer retention times come from the mineral

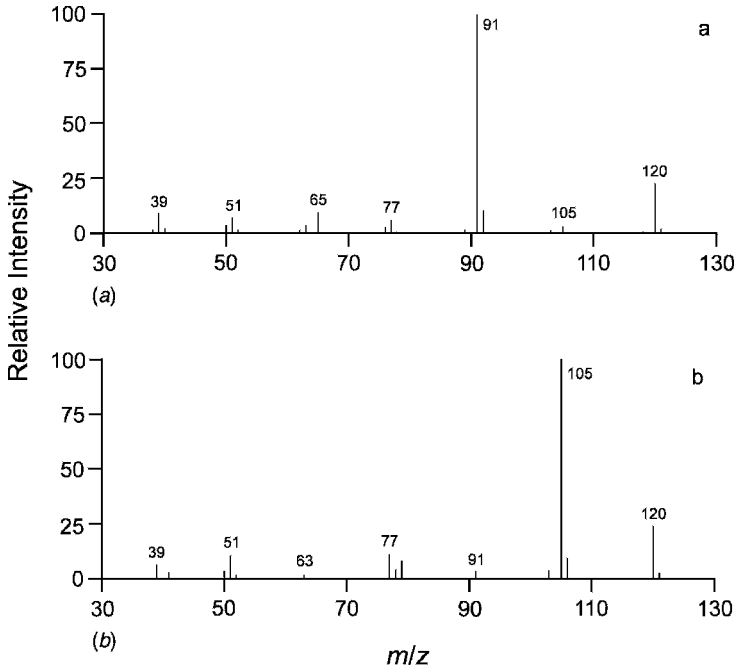

Figure 6.4. Mass spectra for Problem 6.1.

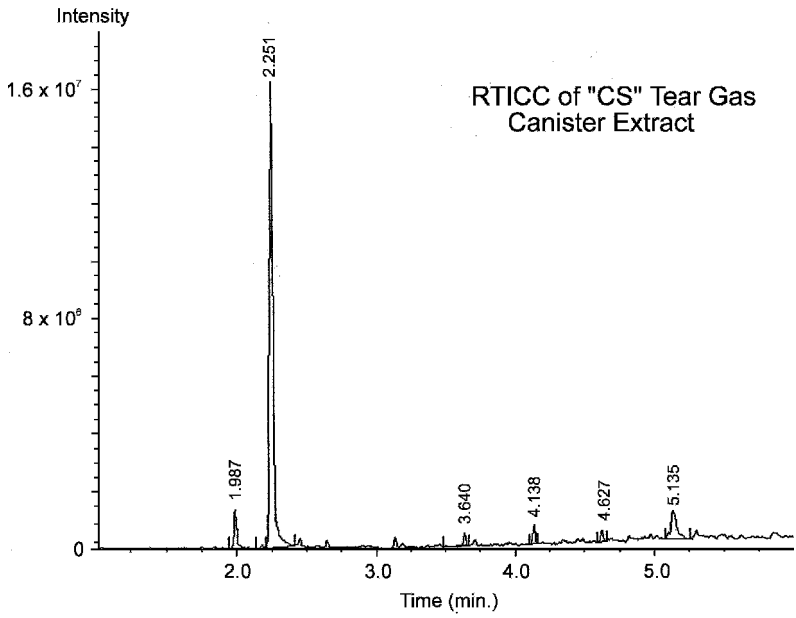

Figure 6.5. RTICC of an extract of the contents of a CS tear gas canister (Problem 6.2).

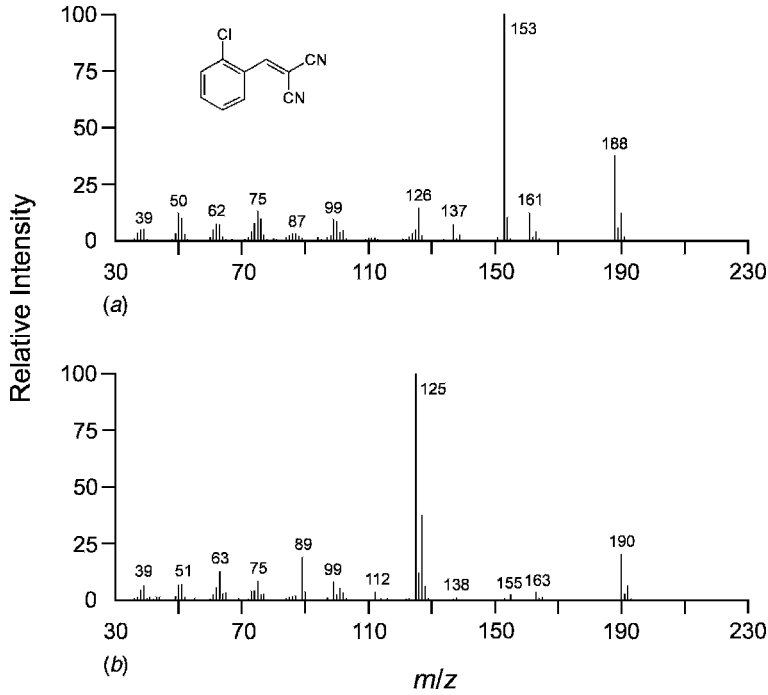

Figure 6.6. Mass spectra of (*a*) *o*-chlorobenzalmalononitrile (CS tear gas; top) and (*b*) an unknown impurity (Problem 6.2).

DropBooks

oil carrier in the can. Mass spectra for the compounds having retention times of 1.987 and 2.251 min are shown in Figure 6.6. The peak at 2.251 min was identified by a library search as CS, but the smaller peak gave no computer matches. Identify the major losses in the CS mass spectrum and convince yourself that the library search results are correct. Then determine the structure of the compound that produced the other spectrum.

6.3. CLEAVAGE NEXT TO ALIPHATIC NITROGEN

Two characteristics are worth remembering about the mass spectra of compounds containing aliphatic N. First, cleavage of the C—N bonds usually accounts for only a small fraction of the total fragmentation. Second, the base peak in the spectra of most of these compounds arises either directly via homolytic cleavage or, when the N is contained in a ring system, by initial homolytic cleavage and subsequent rearrangement that keeps the charge on the N.

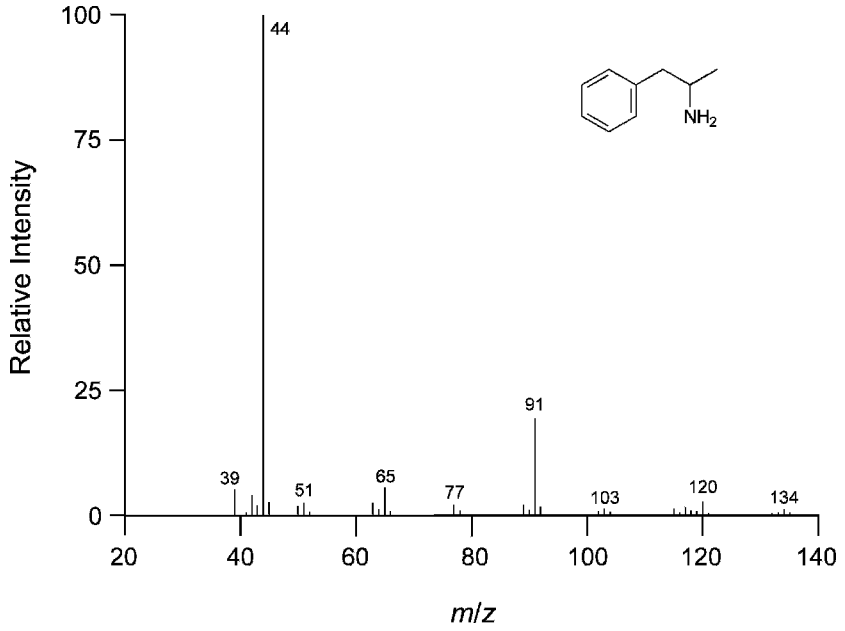

Figure 6.7. Mass spectrum of amphetamine. The presence of one intense peak at low *m/z* values, and few other peaks of significant size, is characteristic of the spectra of many aliphatic amines.

6.3.1. Structural Relationships: α-Cleavage in 1-Phenyl-2-aminopropanes

The mass spectrum of amphetamine, a central nervous system stimulant, illustrates both these phenomena. The outstanding feature in this spectrum (Figure 6.7) is the base peak (*m/z* 44). Depending on the origin of the spectrum, this peak is usually 5–10 times more intense than any other peak in the spectrum. The peaks at *m/z* 39, 50–52, 63–65, 77–78, and 89–91 constitute the aromatic low-mass ion series, with a benzyl ion series at *m/z* 39, 65, and 91. Of the remaining peaks, none are greater than about 3% relative intensity. The M − 1 peak at *m/z* 134 is larger than the $M^{+\bullet}$ peak at *m/z* 135.

The small peaks in the regions between *m/z* 102–104 and 115–119 correspond to alkylbenzene ions arising from loss of radicals containing the NH_2 group, but the ions that give rise to the peaks at *m/z* 134, 120, 91, and 44 are all produced by α-cleavage. The three ions having the charge stabilized on the N atom (*m/z* 44, 120, and 134) should have similar stabilities because the substituents on the α C atom are either alkyl groups or H (Equation 6.2). The aromatic ring is isolated electronically from the α C atom and cannot stabilize by conjugation. The only factor remaining to explain the differences in the ion abundances is the relative stabilities of the

radicals formed in these reactions (Section 4.2.1).

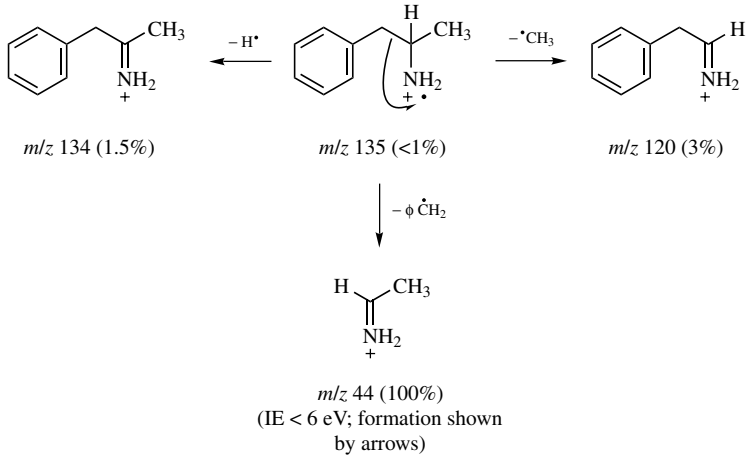

(6.2)

Because the IE for the aromatic ring (8.8 eV) is comparable to that of the amine group (ca. 8.7 eV), the benzyl ion (*m*/*z* 91) can arise either through the type of mechanism depicted in Equation 6.1 or by initial ionization at N, followed by heterolytic cleavage and charge migration (Equation 6.3). In either case, Stevenson's rule predicts that the charge should remain primarily on the N-containing fragment, as discussed previously in Sections 3.6.3 and 3.6.4.

DropBooks

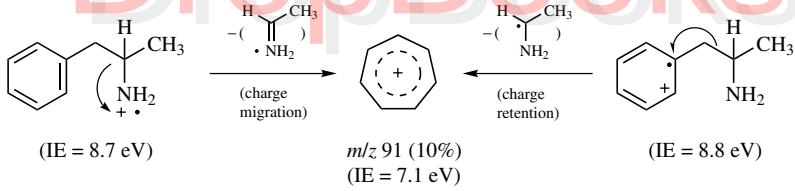

(6.3)

Except for the ions represented by the peaks at *m*/*z* 44 and 91 in Figure 6.7, the other α-cleavage ions are of such low abundance as to be easily overlooked. However, the intensities of the small peaks representing these ions do, in fact, reflect the structural differences that occur in this family of compounds. The spectra of phentermine and methamphetamine, two isomeric stimulants that are similar in structure to amphetamine, illustrate this point well. In Figure 6.8 the base peak in each spectrum (*m*/*z* 58) is actually five times larger than shown, denoted by the (X5) located next to the 58 in each spectrum. Note that the *y*-axis in each spectrum only goes up to 20% relative intensity. Using this format for presentation accentuates the differences in intensity between the less intense peaks in the spectra (Steeves et al., 2000).

Although there are several differences between these spectra at low *m*/*z* values, only the difference in the intensities of the peaks at *m*/*z* 134 (relative to the peak at

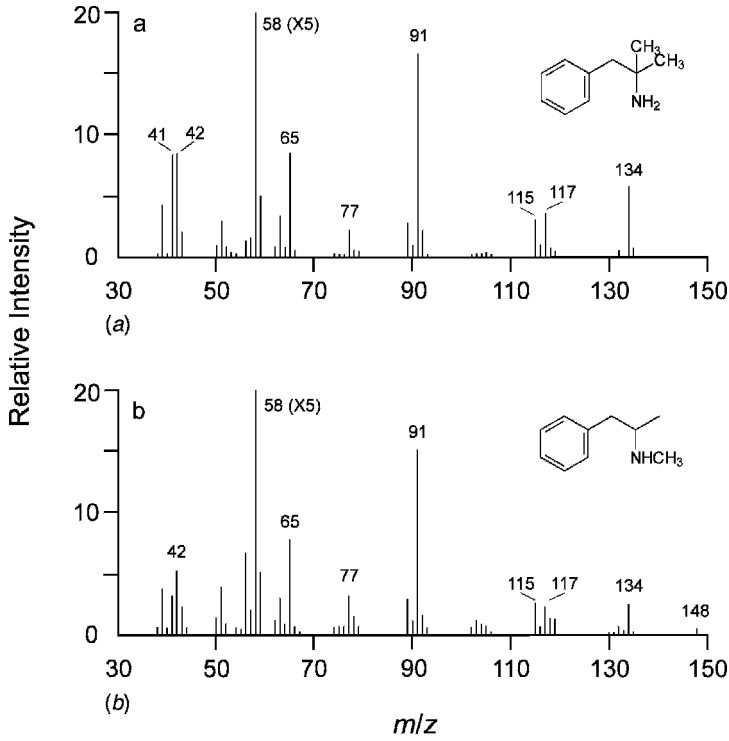

Figure 6.8. Mass spectra of (*a*) phentermine and (*b*) methamphetamine. Although these compounds have similar structures and mass spectra, they are distinguishable by subtle differences in the peaks that result from α-cleavage. In the actual mass spectra, the *m*/*z* 58 peaks are five times larger than shown.

m/*z* 91) and the presence of a tiny peak at *m*/*z* 148 in the methamphetamine spectrum distinguish the two at high *m*/*z* values. These differences are reproducible, and as such are indicative of the structural differences between the two molecules.

When α-cleavage occurs with the radical site located on the N atom, phentermine can lose either of the *geminal* methyl groups to produce the ion having *m*/*z* 134 (Equation 6.4) or a benzyl radical to give the ion represented by the base peak at *m*/*z* 58.

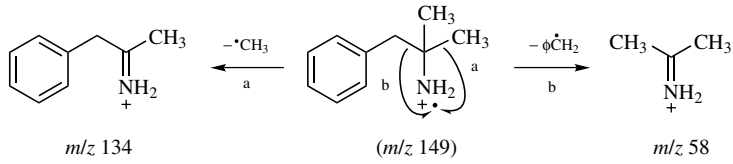

m/*z* 134 (*m*/*z* 149) *m*/*z* 58 (6.4)

The benzyl ion (*m*/*z* 91) can be formed either by heterolytic cleavage when the charge is on the N atom or through benzylic cleavage when ionization occurs

initially in the aromatic ring (see Equation 6.3). Although the H atoms associated with the benzylic C atom could theoretically be lost by benzylic cleavage, these losses are observed only when several H atoms of this type are present, and then only if other fragmentations are not more highly favored (Section 6.2). Charge stabilization on the benzylic C is not favored over stabilization by N (Section 3.6.4), and formation of the much less stable $H^{\bullet}$ makes this fragmentation even less likely.

Methamphetamine, in contrast, has two C atoms next to the N—one having three H atoms (the *N*-methyl group), the other with a single H atom, a CH_3 group, and a benzyl group. Loss of any of the four H atoms produces an ion with *m/z* 148 (Equation 6.5).

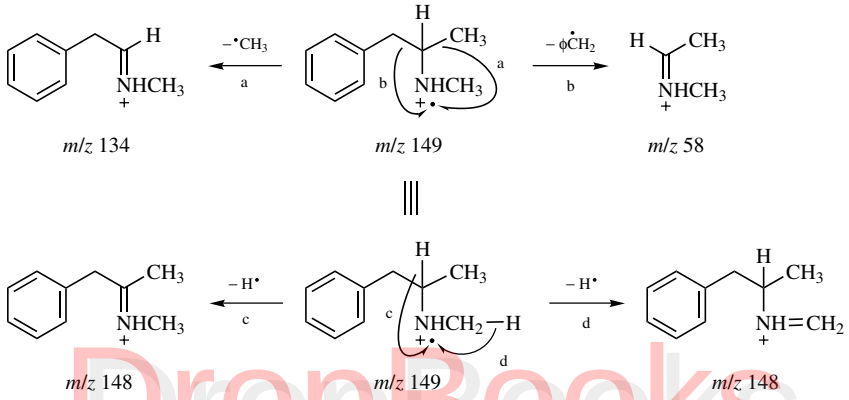

(6.5)

DropBooks

Loss of the aliphatic CH_3 group leads to the *m/z* 134 peak, and loss of the benzyl radical produces the ion having *m/z* 58. Heterolytic or benzylic cleavage as described in Equation 6.3 leads to the benzyl ion (*m/z* 91). The presence of the tiny peak at *m/z* 148 in the methamphetamine spectrum, then, is not accidental; it is predicted by the molecular structure and knowledge of how α-cleavage occurs.

If the two spectra in Figure 6.8 are compared, the relative intensity of the *m/z* 134 peak in the spectrum of phentermine is seen to be approximately 6%, whereas in the methamphetamine spectrum its intensity is only about 3%. This seems to reflect the fact that phentermine has two CH_3 groups that can be lost by α-cleavage as opposed to only one for methamphetamine (both spectra were obtained on the same instrument under similar conditions). Although it is easy to push this point too far, the intensities recorded for the *m/z* 91 peak and numerous other peaks, relative to the peak due to primary α-cleavage at *m/z* 58, are similar in the two spectra. This indicates that similar amounts of energy are needed for comparable fragmentation processes in the two $M^{+\bullet}$, and that the relative intensities of the *m/z* 134 peaks may be related solely to probability, not energy distribution, factors.

Loss of the methylamino group by cleavage of the C–N bond leads to the ions having *m/z* 115–119, but this fragmentation does not compete well with α- and benzylic cleavages (see Equation 8.10).

The origin of the low-mass ion series for aliphatic amines (Table 4.2, series 2c) should now be clear. In the spectra of amphetamine, methamphetamine, and phentermine, the peaks at *m/z* 44 and 58 dwarf all other peaks in the spectra. Compounds having more, or larger, aliphatic groups attached to the N atom still fragment so as to lose the largest aliphatic radical and produce an intense peak (usually the base peak) in which the charge is located on the N. Thus, the spectrum of 3,4,5-trimethoxy-β-phenethylamine (mescaline) shows a base peak at *m/z* 30 (produced at least in part by heterolytic cleavage after initial ionization on one of the O atoms; Equation 6.6); *N*,*N*-dimethylamphetamine [$C_6H_5CH_2CH(CH_3)N(CH_3)_2$] produces a base peak at *m/z* 72 (Equation 6.7); and *N*,*N*-dimethylphentermine [$C_6H_5CH_2C(CH_3)_2N(CH_3)_2$] gives a base peak at *m/z* 86 (Equation 6.8).

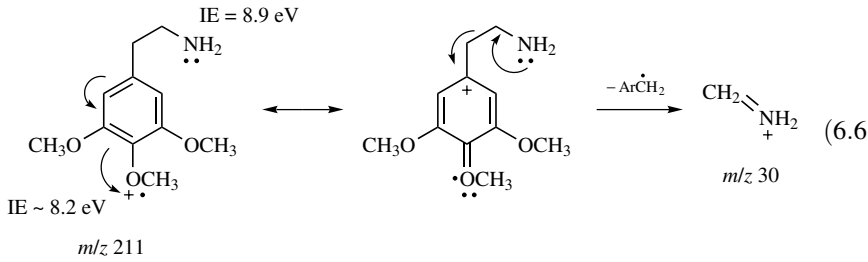

(6.6)

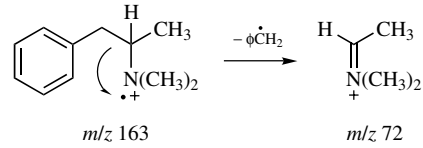

(6.7)

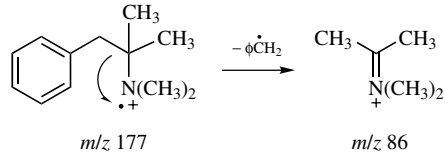

(6.8)

The presence of an intense peak at any of these *m/z* values—30, 44, 58, 72, 86, 100, 114,. . .—is almost an immediate clue that somewhere in the molecule there is an aliphatic group containing a N atom. This is true even for fairly complex molecules such as lidocaine, a local anesthetic, and amitriptyline, an antidepressant drug (Figure 6.9).

6.3. Methamphetamine and four of its isomers produced the spectra shown in Figure 6.10.

(a) The base peak in each spectrum occurs at *m/z* 58. What does this say about the distribution of alkyl groups in these molecules? In particular, what does this indicate about the possibility of substitution on the aromatic

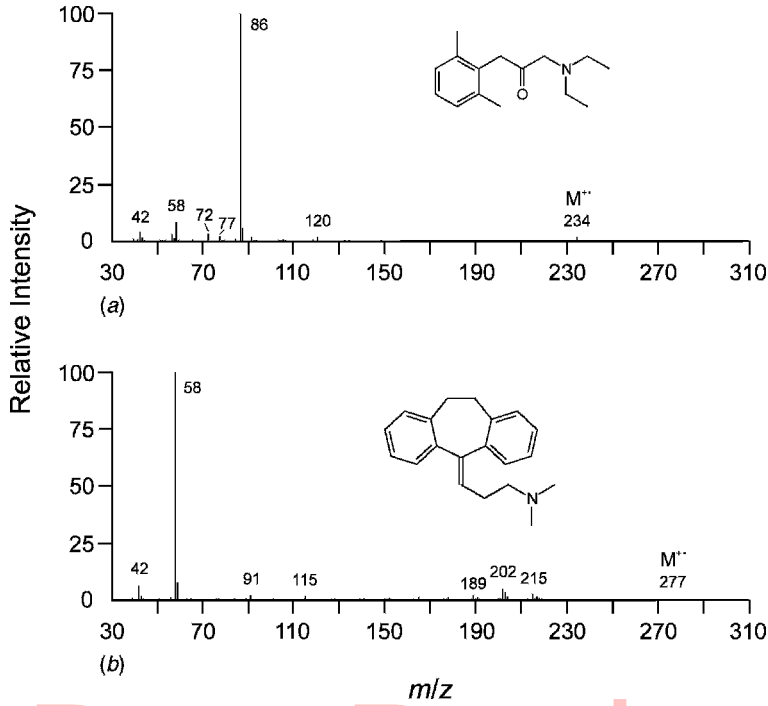

Figure 6.9. Mass spectra of two aliphatic amines attached to complex aromatic groups: (*a*) lidocaine and (*b*) amitryptilene. Peaks due to α-cleavage dominate the spectra of these compounds.

DropBooks

rings? What would happen to this peak if any of these compounds had additional alkyl groups attached to the benzylic C atom?

(b) Draw out all the possible isomeric structures that meet the criteria in part (a). Determine which spectrum is that of methamphetamine by comparison with Figure 6.8. Then, predict what ions would be formed by α-cleavage for each of these structures. Finally, match the predicted fragmentation patterns with those observed in the spectra in Figure 6.10.

6.3.2. Cleavage Next to Electron-Deficient Nitrogen

In order for α-cleavage to occur, the X group in Figure 6.1 must serve as the initial radical and charge site and must also be able to help stabilize the charge after fragmentation has taken place. The attachment of strong electron-withdrawing groups to the X group will severely compromise both of these abilities—first by raising the IE of the X group and then by destabilizing the resultant positive charge through electron withdrawal. As an example, compare the spectra of the antidepressant

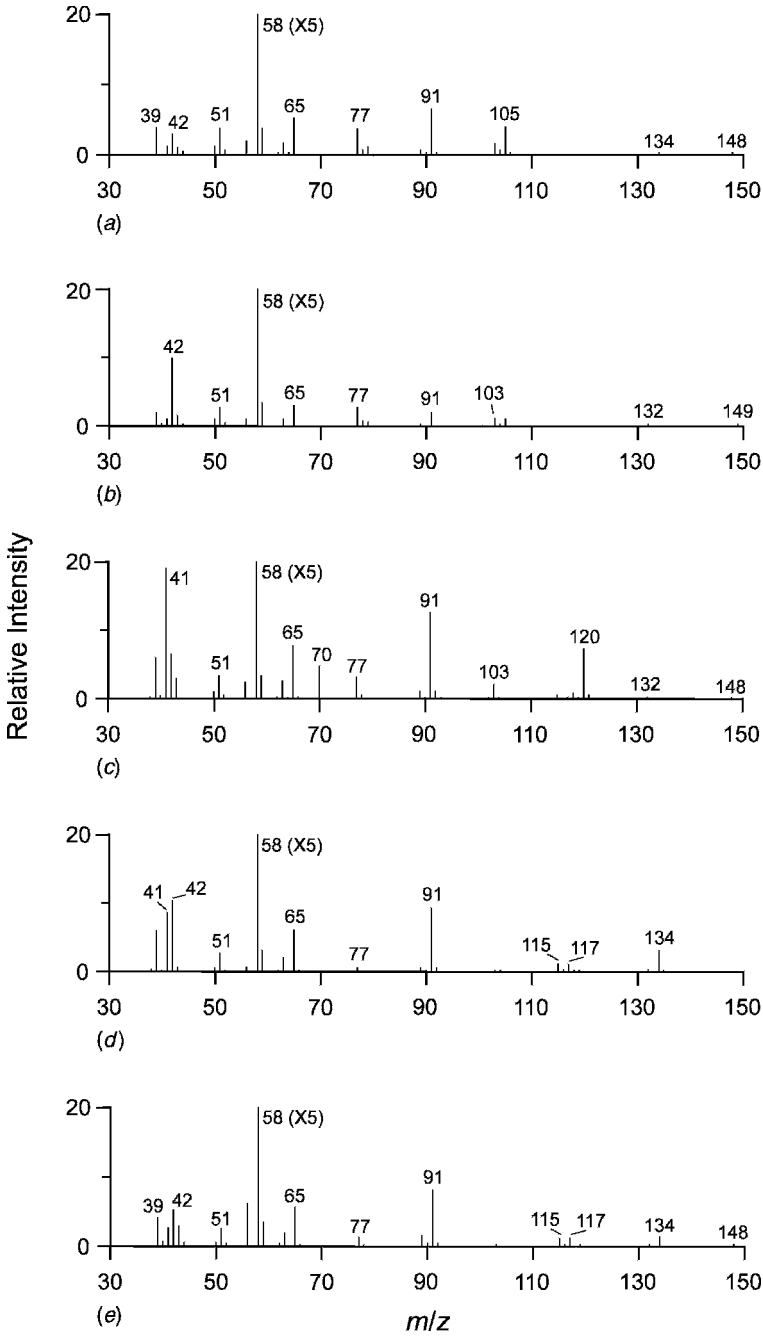

Figure 6.10. Mass spectra for Problem 6.3. The intensities of the *m/z* 58 peaks are actually five times greater than shown.

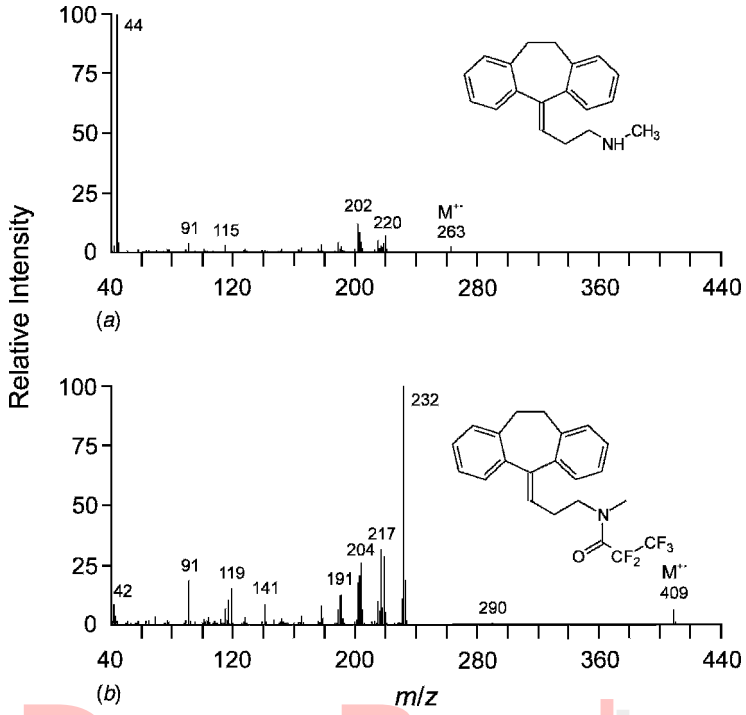

Figure 6.11. Mass spectra of (*a*) nortriptylene and (*b*) its *N*-pentafluoropropionyl derivative. A strongly electronegative group attached to N greatly increases the IE at that site and reduces the N atom's ability to support the charge during α-cleavage.

DropBooks

drug nortriptylene with that of its *N*-pentafluoropropionyl derivative (Figure 6.11). Whereas the peak representing α-cleavage dominates the spectrum of nortriptylene (*m*/*z* 44, 100%; Equation 6.9), the corresponding peak in the spectrum of the pentafluoropropionyl derivative is relatively small (*m*/*z* 190, 12%). Notice that the IE for the amide group in the derivative is significantly higher than that of the aromatic rings (the IE for the F atoms is even higher at >12.5 eV), so that initial ionization will occur preferentially in the ring, not on the N atom. The base peak in the spectrum of the derivative appears to come from loss of the amide group (Equation 6.10).

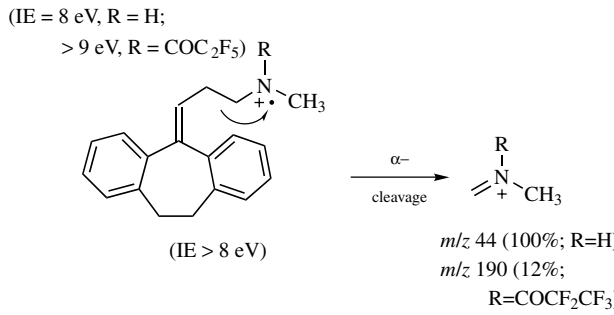

(6.9)

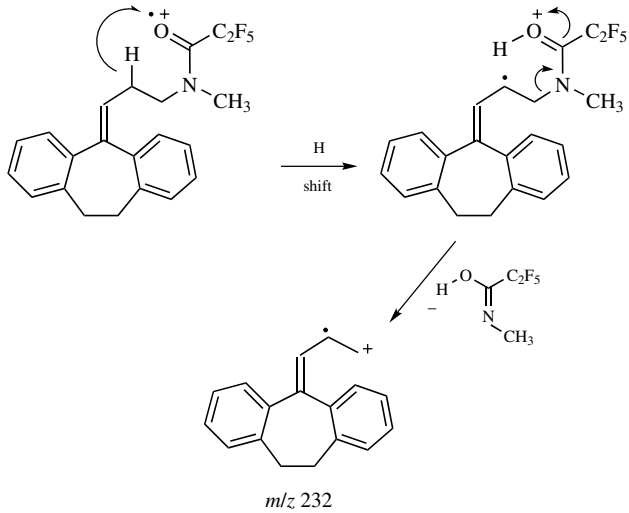

(6.10)

Even transformation of an amine to a formyl amide substantially reduces the relative abundance of α-cleavage ions (Figure 6.12 and Equation 6.11). In this case, initial ionization shifts from the N atom to one of the O atoms on the ring, and other fragmentation options become more important here as with the example above.

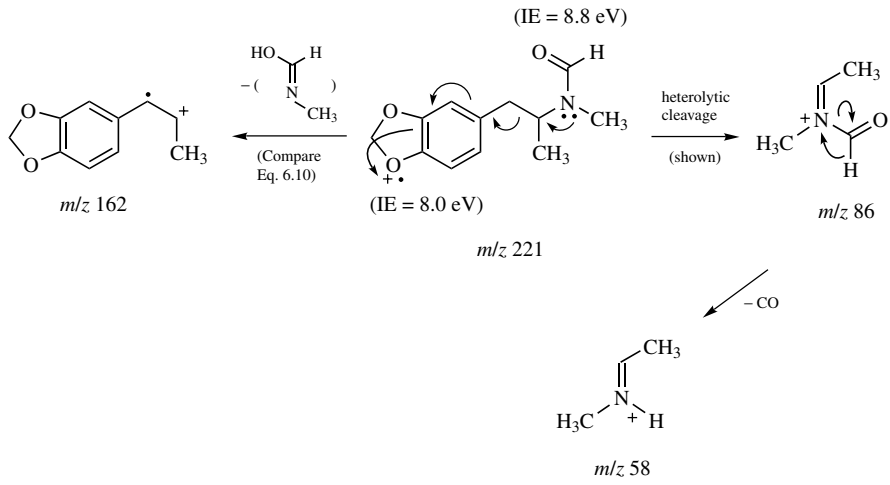

(6.11)

6.3.3. α-Cleavage in Complex Nitrogenous Ring Systems

Locating a N atom within a saturated ring system does not preclude α-cleavage—it merely modifies the results. This is seen in the fragmentation of many naturally occurring alkaloids, where initial bond breaking by α-cleavage may not lead

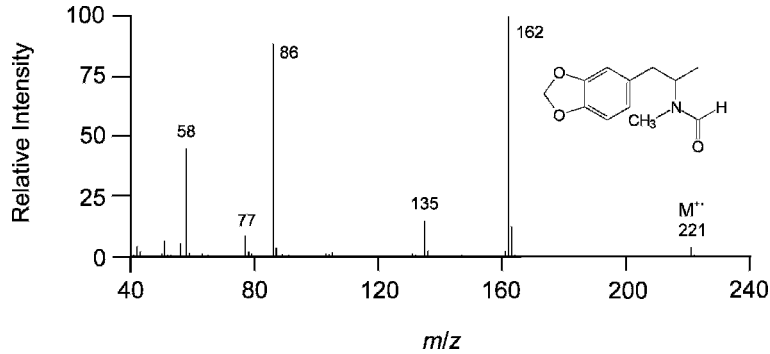

Figure 6.12. Mass spectrum of *N*-formyl-3,4-methylenedioxymethamphetamine. Compare this spectrum with that of the underivatized amine shown in Figure 9.2*b*.

directly to any neutral loss from the molecule. Instead, an assortment of bond rearrangements and H migrations must take place before a neutral fragment that can be lost is eventually produced. During these intermediate steps, the charge remains on the N atom.

A good example is formation of the base peak (*m*/*z* 136) in the spectrum of ibogaine, a stimulant found in the central African plant *Tabernanthe iboga*. The elemental composition of the product ion is known (Beynon et al., 1968), and the complex mechanism shown in Figure 6.13 offers a rationalization for its formation using steps that are discussed in this book. Note the formation of a benzylic radical intermediate, the presence of conjugation in the product ion, and the formation of new π-bonds in both the third and final steps. Such processes should help lower $\Delta G^{\ddagger}$'s for the overall fragmentation scheme. Further examples of α-cleavage fragmentations of alkaloids having complex structures are found in Chapter 9.

DropBooks

6.4. CLEAVAGES OF ALIPHATIC OXYGENATED COMPOUNDS

6.4.1. α-Cleavage

Like the N atom in amines, O atoms in aliphatic alcohols and ethers also direct α-cleavage. However, because O is more electronegative than N, it supports a positive charge less well—both during initial ionization and in the product ion. This is seen in the IEs in Table 3.1 for O-containing compounds and for radicals such as $ROC^{\bullet}H_2$; both are significantly higher than those of their nitrogenous counterparts. As a result, other fragmentations of the $M^{+\bullet}$ often compete favorably with α-cleavage in these compounds, and the resulting mass spectra may not be dominated by peaks reflecting this fragmentation, as is the case with the spectra of amines.

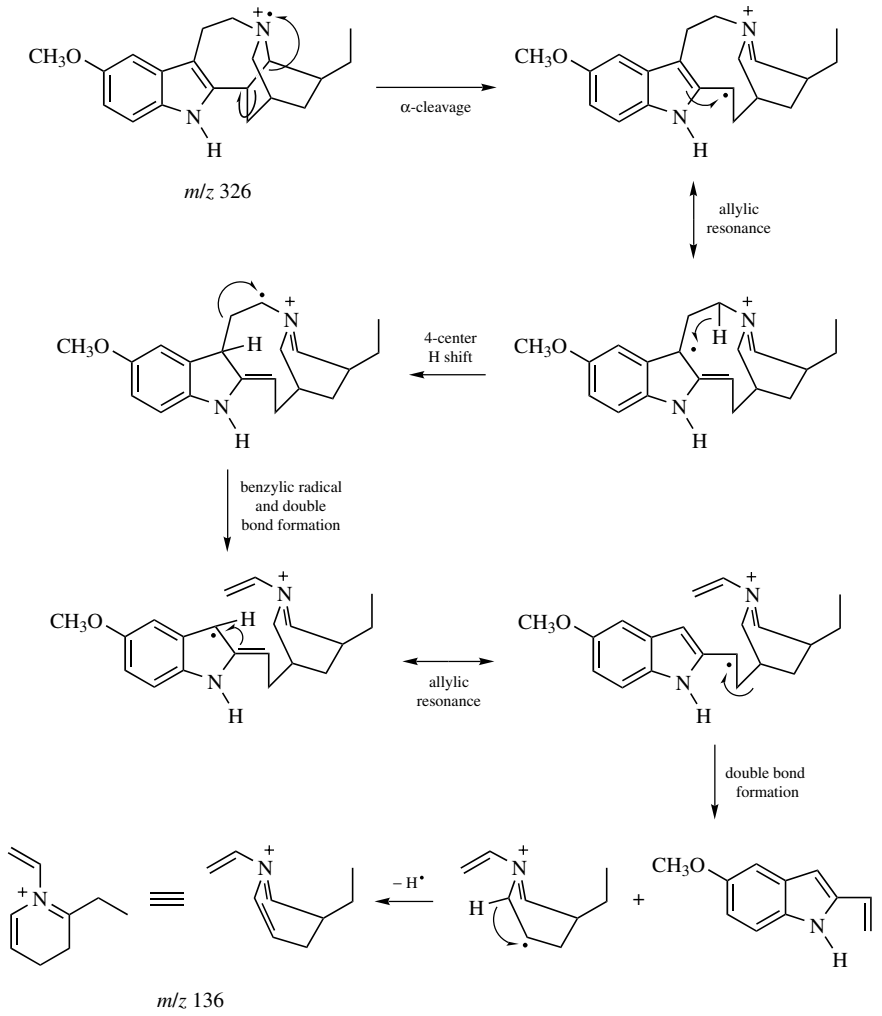

Figure 6.13. Possible mechanism for formation of the base peak (*m*/*z* 136) in the spectrum of ibogaine. After initial α-cleavage, the resulting distonic ion must undergo significant rearrangement before a suitable leaving group is formed.

The spectrum of 1,1-dimethoxyethane does not show a $M^{+\bullet}$ peak at *m*/*z* 90 (Figure 6.14; the apparent loss of 14 from *m*/*z* 89 to 75 is inconsistent with *m*/*z* 89 being the $M^{+\bullet}$ peak). This behavior is not unusual for aliphatic oxygenated compounds. Based on the discussion so far in this chapter, probable α-cleavage fragmentations for this compound can now be predicted (Equation 6.12). There are actually three C atoms next to the two O atoms in this molecule; two of

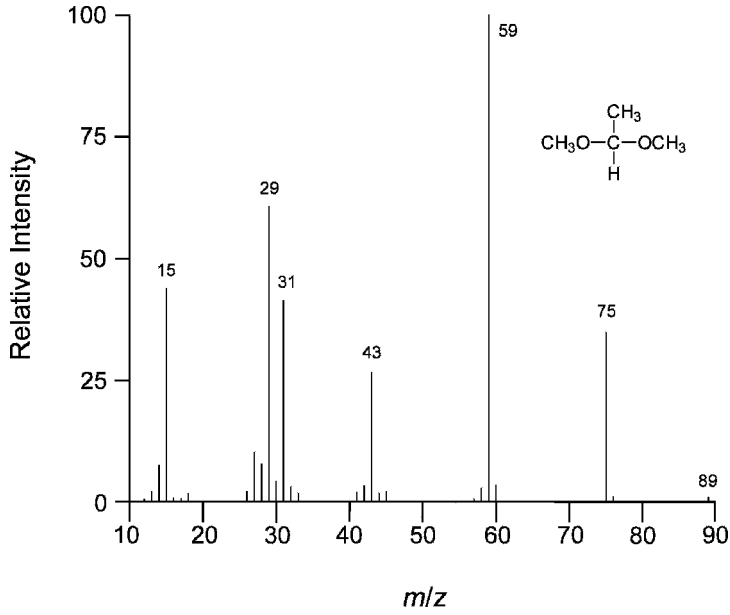

Figure 6.14. Mass spectrum of 1,1-dimethoxyethane. Although an aliphatic O atom also directs α-cleavage, the effect on the spectrum is often not as noticeable as with N.

DropBooks

these contain only H atoms. The presence of seven H atoms that can be lost by α-cleavage increases the likelihood that the M − 1 peak, which is barely visible at *m/z* 89, will be observed.

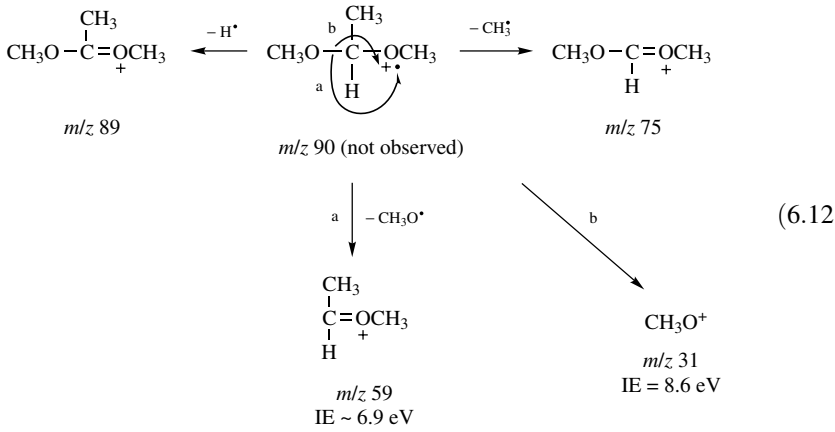

(6.12)

Of the two groups remaining on the central C atom, it is not clear beforehand which will likely be lost. On the basis of size and the fact that there are two methoxy groups as opposed to one methyl group, loss of $^{\bullet}OCH_3$ might seem more reasonable. However, the O provides no obvious additional stability to $^{\bullet}OCH_3$ that

would account for the 3-fold difference in intensity between the peaks at *m/z* 59 and 75 observed in Figure 6.14. A more likely explanation is that the ion resulting from loss of $^{\bullet}CH_3$ still contains two O atoms, and whereas one O atom stabilizes the positive charge, the other withdraws electron density from the same region because of its electronegativity. This overrides any stability gained from having two O atoms share the charge by resonance, so that formation of the $(M - 15)^+$ ion (*m/z* 75) is *destabilized* relative to the $(M - 31)^+$ ion (*m/z* 59). The peak at *m/z* 31 corresponds to the $^{+}OCH_3$ ion, which is formed by heterolytic cleavage (Equation 6.12).

It is instructive at this point to return to the spectrum in Figure 4.18*a* (Problem 4.4). In the context of Chapter 4, the large *m/z* 45 peak and low-mass ion series only allowed classification of this compound as either an aliphatic alcohol or ether. Seven isomeric structures can be written for aliphatic alcohols and ethers having the elemental composition $C_4H_{10}O$. The number of possible structures that could have produced this spectrum can be limited by considering α-cleavage fragmentations for each structure.

The $M^{+\bullet}$ (*m/z* 74) apparently loses $^{\bullet}CH_2CH_3$ to produce the base peak at *m/z* 45. Only two of these structures can lose $^{\bullet}CH_2CH_3$ by α-cleavage: *sec*-butanol [$\mathbf{CH_3CH_2}$CH(OH)CH_3] and methyl *n*-propyl ether ($\mathbf{CH_3CH_2}CH_2OCH_3$). The compound responsible for the spectrum in Figure 4.18*a* must be chosen from these two possibilities. The fact that the *m/z* 59 peak, resulting from loss of $^{\bullet}CH_3$, is of moderate intensity in this spectrum suggests that *sec*-butanol is the answer to this problem. This compound is expected to lose $^{\bullet}CH_3$ by α-cleavage, whereas methyl

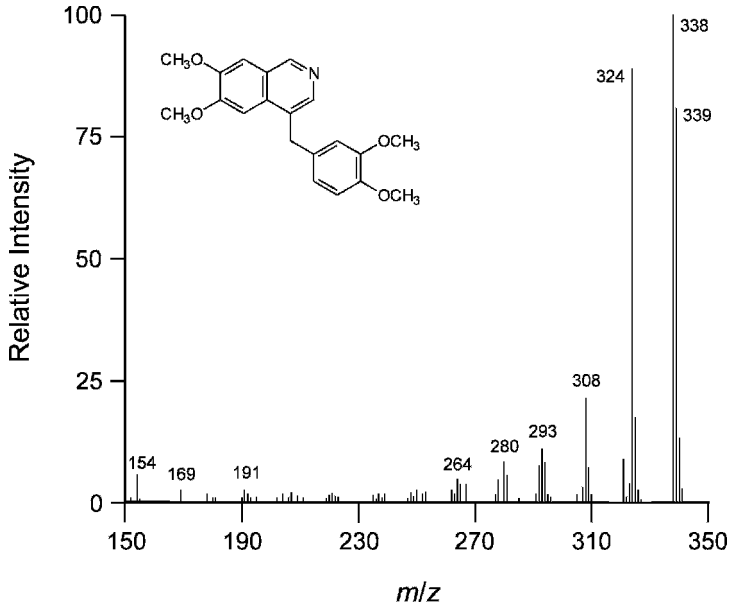

Figure 6.15. Mass spectrum of papaverine. Formation of the $[(M - 1)^+]$ and $[(M - 15)^+]$ ions occur by single bond cleavages away from the initial ionization site.

n-propyl ether cannot. Nevertheless, only a comparison of the spectra of these two compounds can answer this question unambiguously (see Problem 6.8 at the end of this chapter).

6.4.2. Bond Cleavage Away from the Ionization Site

Papaverine is a nonnarcotic alkaloid found in the seedpods of the opium poppy, *Papaver somniferum*, as well as in the opium that is extracted from these pods. In addition to an intense $M^{+\bullet}$ peak at *m*/*z* 339, the mass spectrum of papaverine exhibits a base peak at *m*/*z* 338 due to loss of $H^{\bullet}$ and an intense peak at *m*/*z* 324 from the loss of $^{\bullet}CH_3$ (Figure 6.15). The facile loss of $H^{\bullet}$ might be expected because this compound, like diphenylmethane (Section 6.2), has a "doubly benzylic" C atom. In this case, however, the site of initial ionization should be located on any of the O atoms associated with the aromatic methoxy groups (Table 3.1 and Equation 6.13). The intensity of the M − 15 peak is not expected, because breaking a carbon-heteroatom bond usually accounts for only a small percentage of the overall fragmentation.

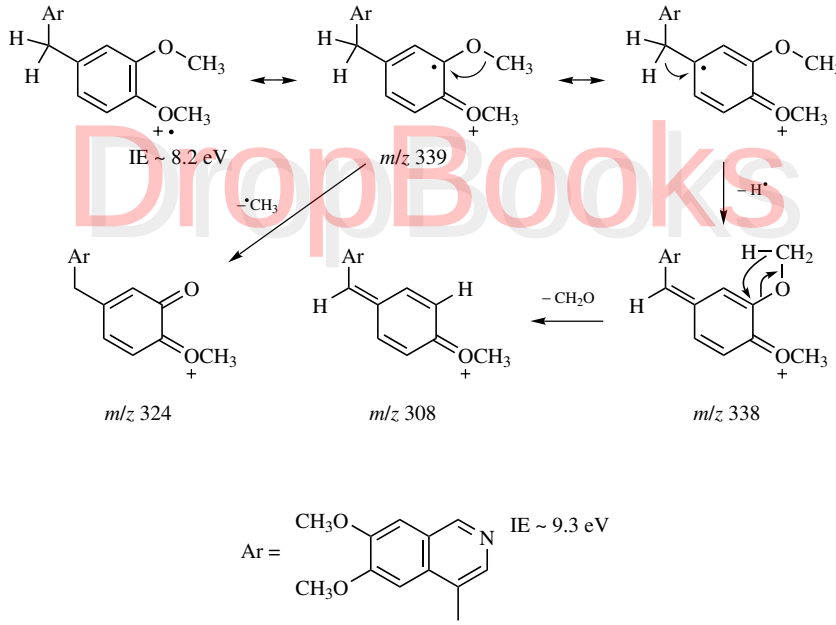

DropBooks

(6.13)

In both these cases, the C atom from which the radical fragment leaves is not attached directly to the initially ionized heteroatom, but rather to another group that is connected to the heteroatom by a series of *p*-orbitals. Rearrangement of the electronic structure occurs during these fragmentations (Equation 6.13), producing ions in which the charge is stabilized both by the initially ionized O atom and

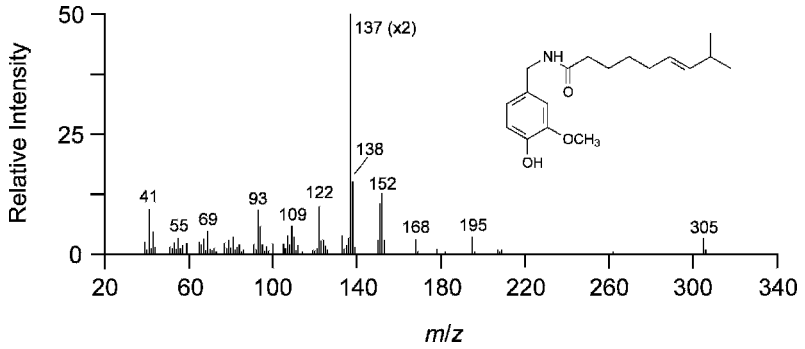

Figure 6.16. Mass spectrum of capsaicin. The *m/z* 137 peak results from cleavage at the benzylic C atom after initial ionization at the phenolic O atom (Equation 6.14).

by the extended aromatic system. Notice that the lost $^{\bullet}CH_3$ is not the one attached to the initially ionized O, and that fragmentation occurs by breaking a carbon-heteroatom bond. The peak at *m/z* 308 may result from loss of $CH_2{=}O$ from the ion having *m/z* 338 (compare Equation 4.4).

Capsaicin is a skin irritant that produces the hot sensation experienced when eating jalapeños, habaneros, and other peppers of the genus *Capsicum*. Formation of the base peak in the spectrum of this compound (Figure 6.16) also occurs by cleavage of a single bond that is removed from the initial ionization site (Equation 6.14).

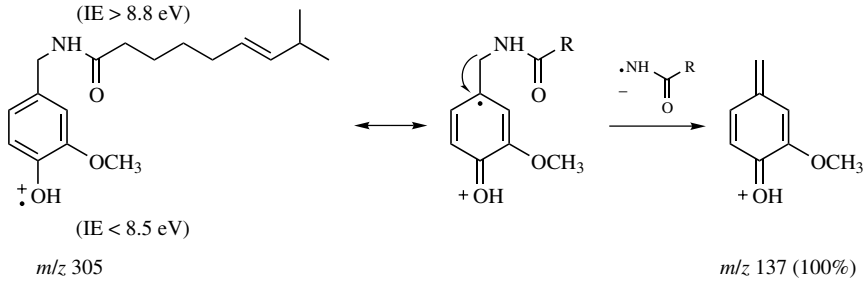

(6.14)

6.4. Eugenol, whose mass spectrum is shown in Figure 6.17, is the compound primarily responsible for the odor and taste of cloves. The two most intense peaks in its mass spectrum are due to the $M^{+\bullet}$ (*m/z* 164) and the $(M - 15)^+$ ion (*m/z* 149). A less intense, but still important, fragment ion peak occurs at *m/z* 137 due to the loss of 27 u from the $M^{+\bullet}$. Because the compound contains no N atoms, this loss cannot be due to HCN. Based entirely on fragmentations that have been discussed so far, write mechanisms that account for both of these losses.

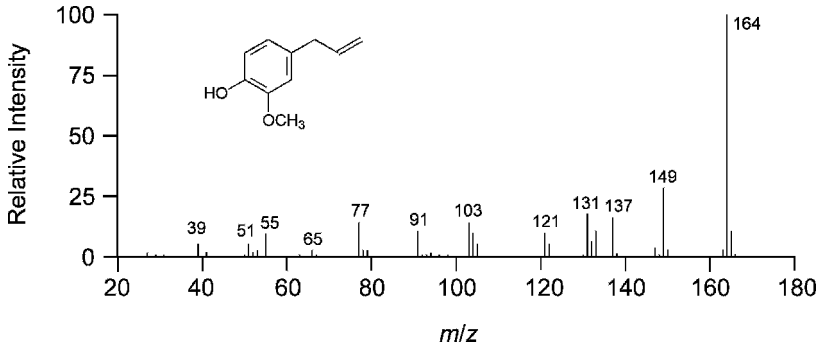

Figure 6.17. Mass spectrum of eugenol (Problem 6.4).

6.5. Figure 6.18 shows the mass spectra for the three methoxyphenol isomers. From the peaks at high *m/z* values, identify the major first losses from the $M^{+\bullet}$ in each spectrum. Explain why the spectra of the *o*- and *p*- isomers are different from that of the *m*-isomer.

6.4.3. Cleavage at Carbonyl Groups

Ketones. Initial ionization at the O atom of a carbonyl group also leads to α-cleavage at the adjacent C atom, which in this case is the carbonyl C atom. Because only two groups are bonded to this C atom (the third "group" is the C—O π-bond), cleavage can occur on either side of the carbonyl C atom. For aliphatic ketones, both losses are usually observed. Loss of the larger alkyl radical leads to the more intense fragment ion peak, in keeping with previous discussions (Equation 6.15). The spectrum of 3-pentanone (Figure 4.12*a*) illustrates the situation when both alkyl groups are the same. The peak at *m/z* 57, which is due to $CH_3CH_2C{\equiv}O^+$ formed by α-cleavage, is the most intense peak in the spectrum. Other examples are seen in Figures 4.19, 5.2, and 7.2.

The IE of an acyl radical is about 7 eV (Table 3.1), whereas those of primary alkyl radicals are considerably higher. Ionization energies for secondary and tertiary radicals, on the other hand, are closer to those of acyl radicals, so that formation of secondary and tertiary carbenium ions (Equation 6.15) often competes successfully with the formation of acylium ions for some aliphatic ketones (Stevenson's rule; see Section 3.6.4). An example of this behavior is seen in Problem 3.3. As a result, interpretation of the spectra of suspected ketones is complicated and, because the low-mass ion series for both alkyl and acylium ions is the same (Table 4.2), must include careful examination of the isotopic peak intensity data for as many of the major peaks in the spectrum as possible.

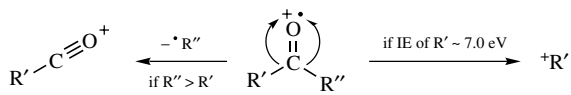

(6.15)

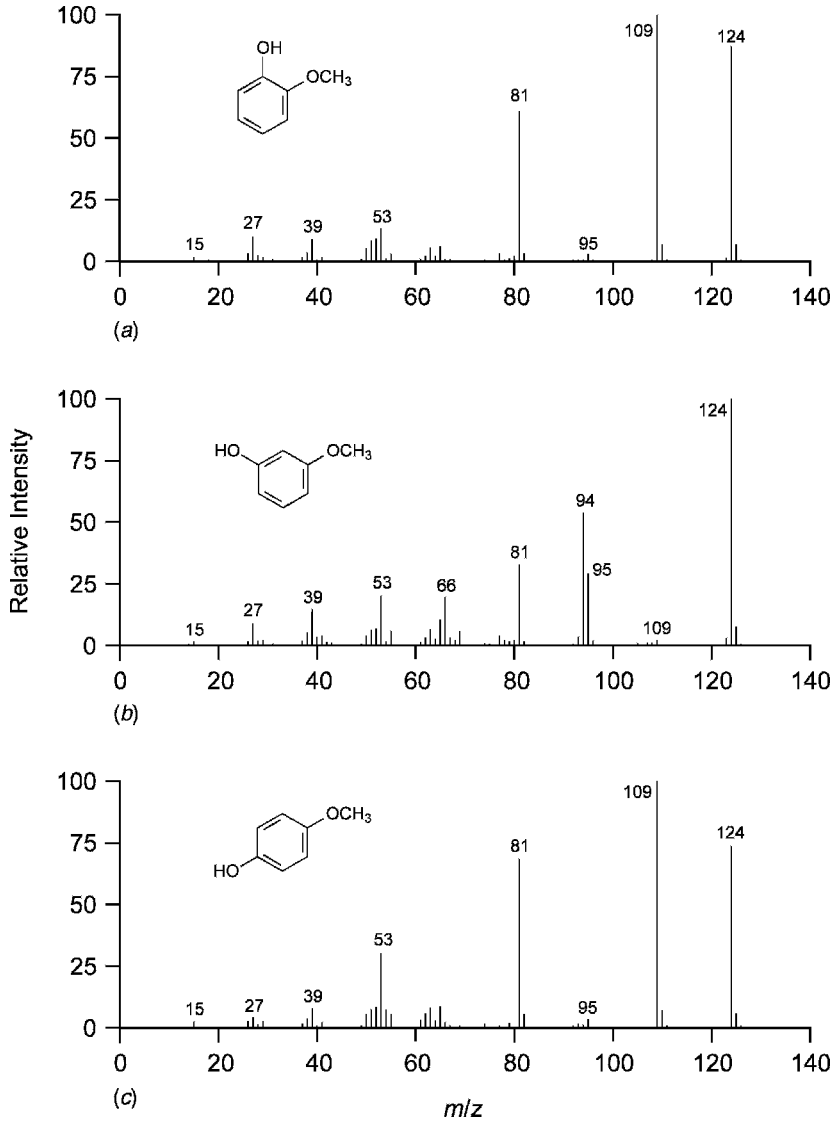

Figure 6.18. Mass spectra of the three methoxyphenols (Problem 6.5).

Esters. Other types of carbonyl compounds undergo α-cleavage as well, with aliphatic and aromatic compounds sometimes exhibiting markedly different behaviors because of differences in the energies needed to form aliphatic and aromatic ion products. When the bonds between the carbonyl C atom and its adjacent atoms in the $M^{+\bullet}$ of an ester are broken (Equation 6.16), the IE of the incipient formyl

radical is considerably higher than that of the corresponding acylium radical because the additional O atom in the formyl ion has a destabilizing effect due to its electronegativity (Section 6.4.1).

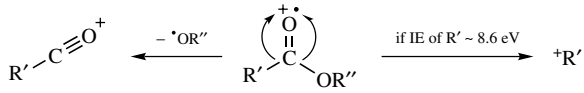

(6.16)

Therefore, the peak due to the acylium ion is usually more intense than that for the formyl ion. Because the IE of the formyl radical is as high as it is, even primary alkyl carbenium ions can compete successfully for the charge.

In the spectrum of methyl acetate, the simplest aliphatic ester (Figure 6.19*a*), losses of both groups attached to the carbonyl C atom are seen: $^{\bullet}CH_3$ to produce the *m*/*z* 59 peak and $^{\bullet}OCH_3$ to give the peak at *m*/*z* 43. The preferred loss of the $^{\bullet}OCH_3$ follows the logic discussed in the previous paragraph.

Ethyl butanoate (Figure 6.19*b*) shows a more complex fragmentation pattern, with peaks due to low-mass alkyl carbenium ions predominating. The peaks at *m*/*z* 71 and 73 arise from α-cleavage on either side of the carbonyl group. Again, loss of the alkoxy radical (here $^{\bullet}OCH_2CH_3$) is preferred. The peak at *m*/*z* 88 is due to a McLafferty-type γ-hydrogen rearrangement (Section 7.2.1). Because of the structural requirements of the McLafferty rearrangement, a similar fragmentation is not observed in the spectrum of methyl acetate.

In the spectrum of methyl benzoate (Figure 6.19*c*), loss of a phenyl radical to produce a peak at *m*/*z* 59 is not observed. Rather, $^{\bullet}OCH_3$ loss leads to the more stable benzoyl ion ($\phi C{\equiv}O^+$), which fragments to give the prominent benzoyl ion series at *m*/*z* 51, 77, and 105. Ions due to other fragmentations of the $M^{+\bullet}$ of this compound are of low abundance.

On the other hand, α-cleavage at the carbonyl group is only one of several important fragmentations of the $M^{+\bullet}$ of 2-acetoxymethylfuran (Figure 6.19*d*). The peak at *m*/*z* 43 is due to the acylium ion ($CH_3C{\equiv}O^+$), but the base peak at *m*/*z* 81 is the result of benzylic-type cleavage (furan is another example of a non-benzenoid aromatic compound, Section 4.1.2; see also Example 3.3). The loss of 42 from the $M^{+\bullet}$ to produce the *m*/*z* 98 peak is due to the loss of ketene ($CH_2{=}C{=}O$). This is similar to the behavior of some aromatic acetates (Section 6.5.2; see Problem 6.13).

Amides. Amides also undergo cleavage at either side of the carbonyl group (Figure 6.20). Indeed, loss of 16 u as $^{\bullet}NH_2$ from the $M^{+\bullet}$ of primary amides is nearly characteristic of losses of this mass (Table 4.1). Both aliphatic and aromatic primary amides exhibit this behavior, as shown in the spectra of *n*-butyramide and benzamide. This loss is more pronounced in the spectrum of the aromatic compound because the benzoyl ion is resonance-stabilized and the *n*-butyryl ion is not.

The spectrum of *n*-butyramide also shows a peak at *m*/*z* 44 due to loss of propyl radical from the $M^{+\bullet}$. An argument could be made that propyl radical should be lost because it is larger than $^{\bullet}NH_2$. However, comparison of radical size is not

DropBooks

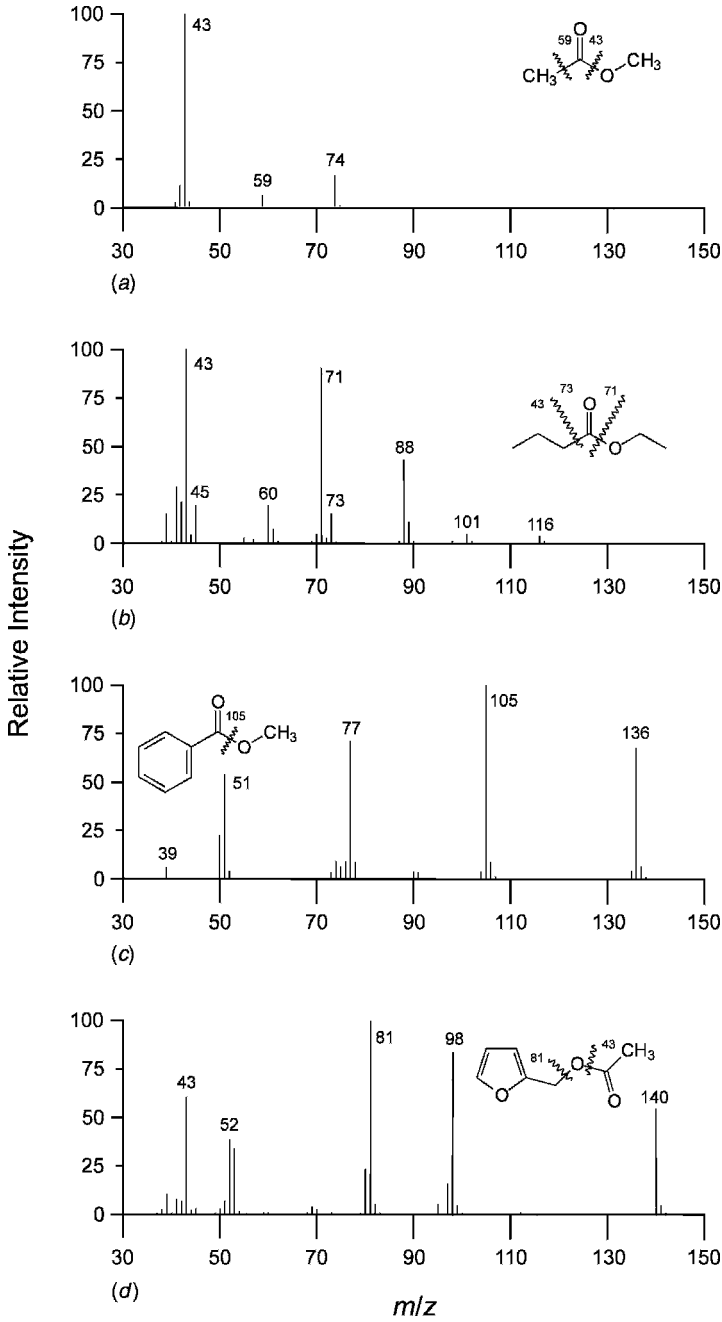

Figure 6.19. Mass spectra of aliphatic and aromatic esters: (*a*) methyl acetate, (*b*) ethyl butanoate, (*c*) methyl benzoate, and (*d*) 2-acetoxymethylfuran. Note the intense benzoyl low-mass ion series in (*c*).

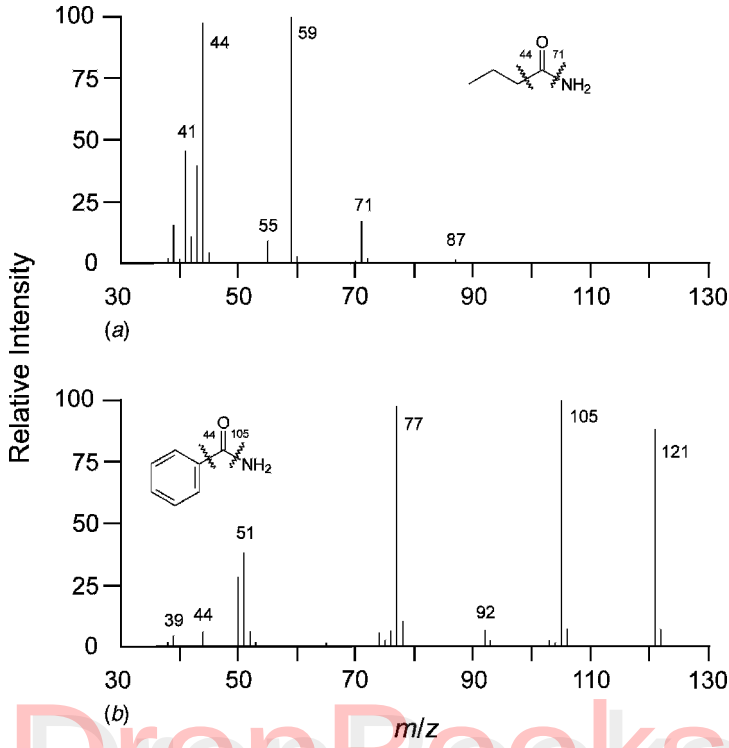

Figure 6.20. Mass spectra of an aliphatic and aromatic amide: (*a*) *n*-butyramide and (*b*) benzamide.

DropBooks

applicable when comparing radical sites on different elements because the ions formed may have significantly different stabilities. In this case, the ion formed after propyl radical loss is resonance-stabilized (Equation 6.17), where it is not with the loss of $^{\bullet}CH_3$ from 1,1-dimethoxyethane (Section 6.4.1), because the lower electronegativity of the N atom does not so severely destabilize the resonance form having the charge located on the carbonyl O atom. In fact, N stabilizes the charge better than O does.

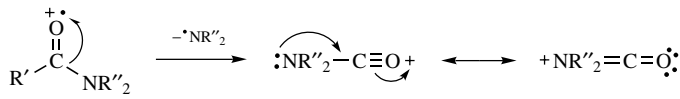

(6.17)

The other intense peak in the *n*-butyramide spectrum (*m*/*z* 59) arises from the McLafferty-type γ-hydrogen rearrangement—a common fragmentation of aliphatic carbonyl compounds (Section 7.2.1).

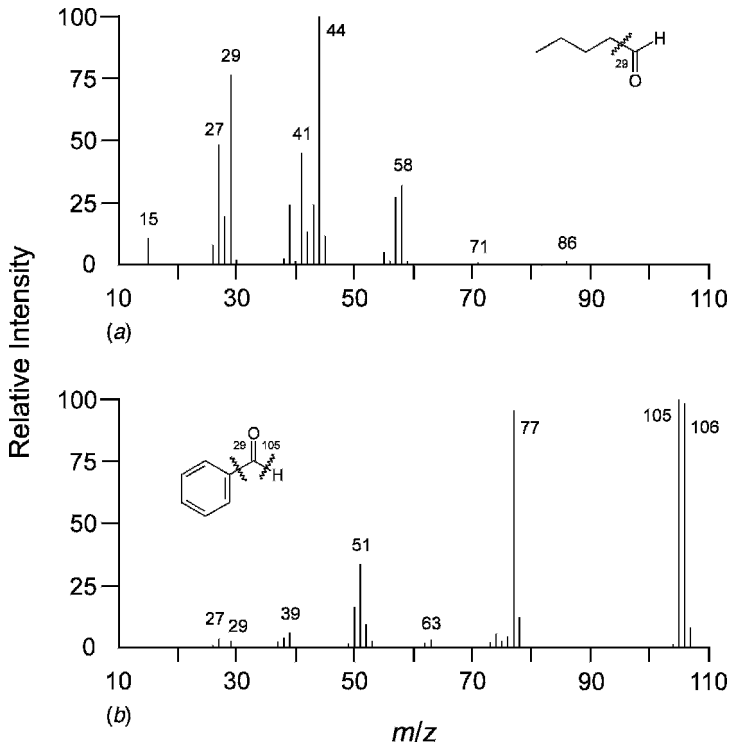

Figure 6.21. Mass spectra of an aliphatic and aromatic aldehyde: (*a*) *n*-pentanal and (*b*) benzaldehyde.

The mass spectrum of benzamide, like that of methyl benzoate, is dominated by the benzoyl ion series. The small, but noticeable, peak at *m/z* 44 results from loss of phenyl radical. Although the N atom helps support the charge in the NH_2-C≡O^+ ion, the aromatic ring, which has an even lower electronegativity and a greater capacity to stabilize by resonance, does a better job.

Aldehydes. The mass spectra of the aliphatic and aromatic aldehydes shown in Figure 6.21 are very different. Loss of $H^\bullet$ from the carbonyl C atom in *n*-pentanal cannot compete with loss of butyl radical (*m/z* 29). Because of the high IE for $^\bullet$CHO (Table 3.1), even the *n*-butyl ion (*m/z* 57) competes favorably for the charge. The base peak in this spectrum (*m/z* 44) is due to a McLafferty rearrangement ion (Section 7.2.1).

In contrast, the benzoyl low-mass ion series, resulting from the loss of $H^\bullet$ from the $M^{+\bullet}$, dominates the spectrum of benzaldehyde. Loss of phenyl radical leads to the weak intensity peak at *m/z* 29 (<5% relative intensity), which reflects the greater stability of the benzoyl ion vs. the HC≡O^+ ion, not the relative stabilities of the phenyl and H radicals.

6.5. ELIMINATION FRAGMENTATIONS IN OXYGEN AND NITROGEN COMPOUNDS

6.5.1. Secondary Elimination from Initial α-Cleavage Ions

α-Cleavage alone does not explain the mass spectrum of ethyl isopropyl ether (Figure 6.22). Loss of any of the three methyl groups attached to the two α C atoms in this compound is expected to lead to a base peak at *m/z* 73. Instead, the spectrum implies, on the basis of what was discussed in previous sections, that this $M^{+\bullet}$ loses either propyl or isopropyl radical by α-cleavage.

Certain ions formed by α-cleavage undergo a secondary fragmentation that eliminates an olefin and gives product ions that are nearly as stable as the precursor ions. This elimination occurs via a cyclic four-atom intermediate; therefore, certain structural features must be met. *If an ion formed by α-cleavage contains, on the side of the heteroatom* opposite *the double bond, an alkyl group having two or more C atoms and an available H atom on the second C from the heteroatom, this alkyl group will be lost as an olefin to produce an important ion due to secondary elimination*. Evidence of this fragmentation is more prominent in the spectra of ethers than in those of amines, probably because the greater electronegativity of O more easily induces H migration. In the spectra of ethers, peaks representing secondary elimination ions are more intense than the peaks due to the original α-cleavage ions. In the spectra of amines, the secondary elimination peaks are usually 50–70% as intense as the peaks resulting from α-cleavage. The ions formed by α-cleavage from alcohols and primary amines do not meet the structural

DropBooks

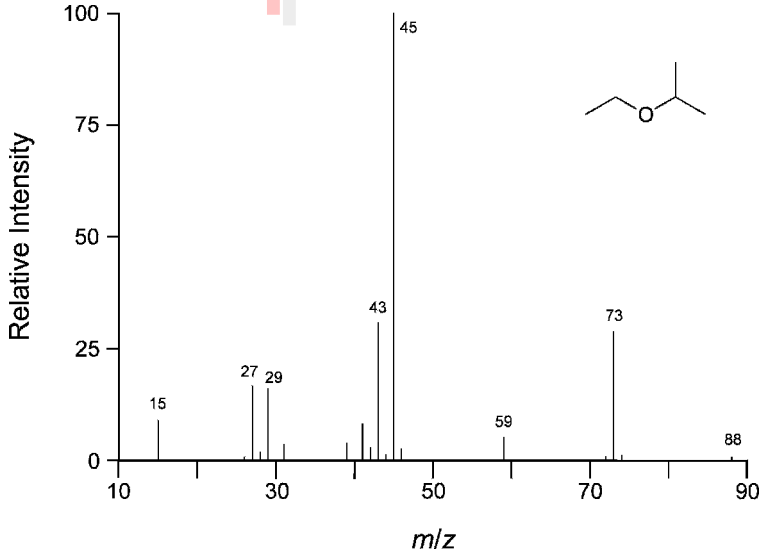

Figure 6.22. Mass spectrum of ethyl isopropyl ether. Peaks resulting from secondary elimination after α-cleavage are more intense than peaks due to the initially formed α-cleavage ions.

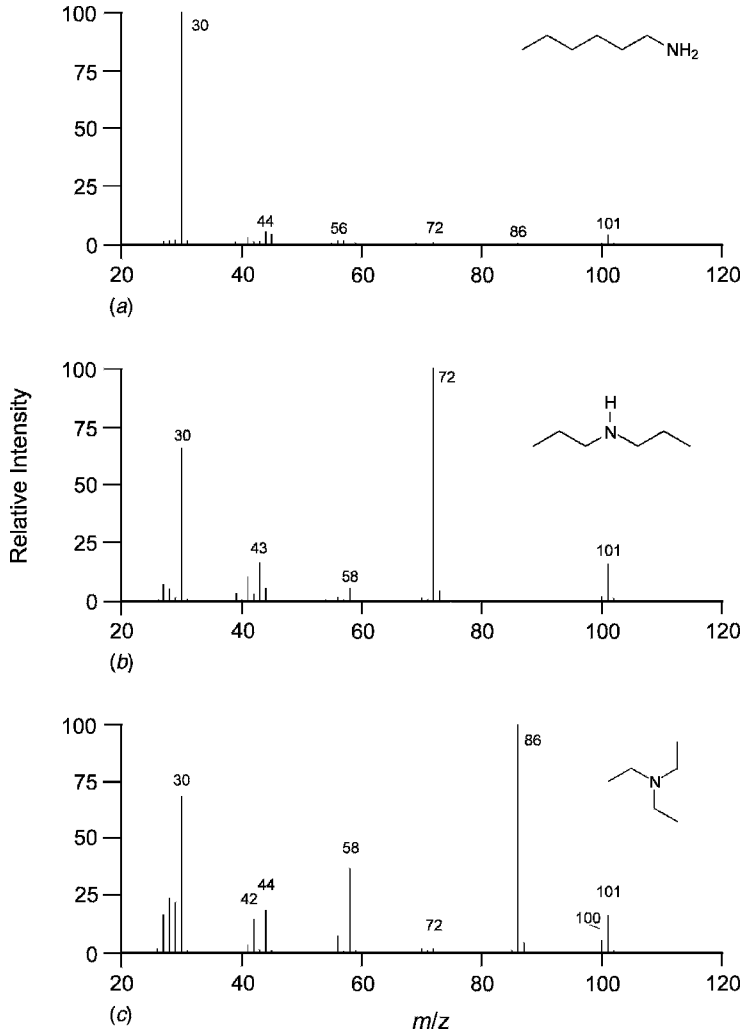

Figure 6.23. Mass spectra of three isomeric amines: (*a*) *n*-hexylamine, (*b*) *N,N*-di-*n*-propylamine, and (*c*) triethylamine. Secondary eliminations from α-cleavage ions account for the peaks at *m*/*z* 58 and 30 in (*b*) and at *m*/*z* 72, 58, and 44 in (*c*). The peak at *m*/*z* 30 in (*c*) results from an additional secondary loss from the *m*/*z* 58 ion.

requirements given above and therefore do not undergo the elimination (Equation 6.18 and Figure 6.23*a*).

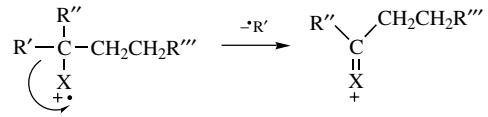

(X = OH, NH_2) (6.18)

For ethyl isopropyl ether, α-cleavage indeed leads to loss of $^{\bullet}CH_3$ to give the ion having *m/z* 73. This ion has an ethyl group located on the side of the O atom opposite the double bond and therefore meets the structural requirement for secondary elimination (Equation 6.19).

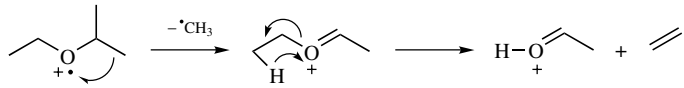

m/z 88 *m/z* 73 *m/z* 45 (6.19)

In fact, three other combinations of α-cleavage and subsequent secondary elimination are possible from the $M^{+\bullet}$ of this molecule (Equations 6.20–6.22). The elimination shown in Equation 6.20 accounts for the small peak at *m/z* 59, which is otherwise hard to explain because cleavage of the C—O bond is not expected.

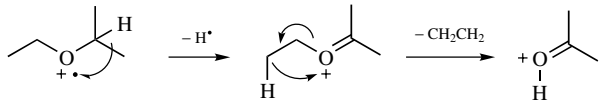

m/z 88 *m/z* 87 *m/z* 59 (6.20)

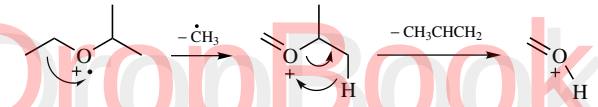

m/z 88 *m/z* 73 *m/z* 31 (6.21)

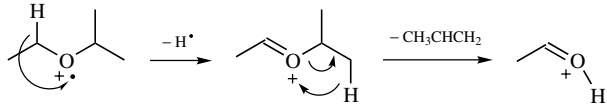

m/z 88 *m/z* 87 *m/z* 45 (6.22)

DropBooks

Many secondary and tertiary amines also undergo this elimination; in fact, some tertiary amines contain two alkyl groups that can undergo the elimination sequentially. The spectra of *n*-hexylamine and di-*n*-propylamine exhibit the expected peaks from α-cleavage at M – 73 (*m/z* 30) and M – 29 (*m/z* 72), respectively (Figures 6.23*a* and *b*). In the case of di-*n*-propylamine, an intense fragment ion peak also occurs at M – 29 – 42 (*m/z* 30) due to secondary elimination of the second propyl group as a molecule of propylene (Equation 6.23).

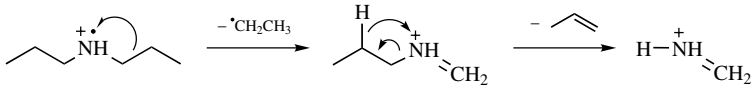

m/z 101 *m/z* 72 *m/z* 30 (6.23)

The spectrum of triethylamine (Figure 6.23*c*) shows not only the expected loss of $^{\bullet}CH_3$ to produce the base peak at *m*/*z* 86, but also elimination of ethylene from one of the remaining ethyl groups to produce the fairly abundant ion having *m*/*z* 58. This ion, in turn, loses ethylene from the final ethyl group to produce the peak at *m*/*z* 30 (Equation 6.24). A similar sequence of losses following initial loss of $H^{\bullet}$ accounts for the peaks at *m*/*z* 100, 72, and 44.

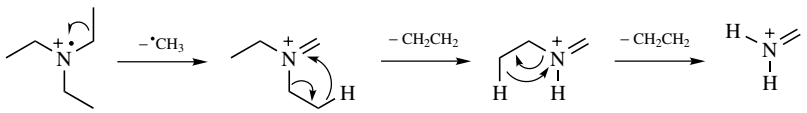

m/*z* 101 *m*/*z* 86 *m*/*z* 58 *m*/*z* 30

(6.24)

6.6. The compound whose structure is given below was reported as a by-product of methamphetamine synthesis, but no EI mass spectrum of the compound was included.

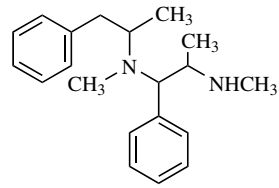

(a) After determining the most likely site for initial ionization, make a list of all the ions and radicals that could result from the various α-cleavage fragmentations at that site. Next, rank the ions from least stable to most stable based on such factors as conjugation or inductive effects. Finally, for ions in the most stable group, rank the corresponding radical products from least stable to most stable. The base peak in the spectrum should be determined by the fragmentation that forms the most stable pair of products. What will be the base peak in this spectrum?

(b) Examine the structures of all the product ions from the first part of this problem. Which structures meet the criteria for secondary elimination from the initial α-cleavage ion? What will the structures of these secondary product ions be?

6.5.2. Hydride Shifts

The base peaks in the spectra of 3-pentanamine and 3-pentanol (Figures 4.12*b* and *c*) are those expected from α-cleavage. Peaks that are not expected in these spectra are those at *m*/*z* 30 in the 3-pentanamine spectrum and *m*/*z* 31 in the spectrum of 3-pentanol—peaks that appear to be the result of secondary elimination of ethylene from the primary α-cleavage ions. However, as stated in the previous section,

neither of these α-cleavage ions has the correct structural requirements for this elimination to occur (Equation 6.18).

Although primary alcohols and amines still follow this precept, the primary α-cleavage ions of some secondary alcohols, as well as some secondary and tertiary amines, undergo a similar elimination that involves the formal shift of a hydride ion ($:H^-$) back to the charged α C atom, not to the charged heteroatom (Equation 6.25). This rearrangement appears to require more energy than the secondary elimination discussed in the previous section, because the peaks that result from this fragmentation are smaller than those observed after secondary elimination. The reason for this might be that the H is not drawn as strongly to the less electronegative C atom. The hydride shift/elimination has structural requirements that are similar to those of secondary elimination, except that in this case the two-carbon chain containing the migrating H is on the same side of the heteroatom as the double bond.

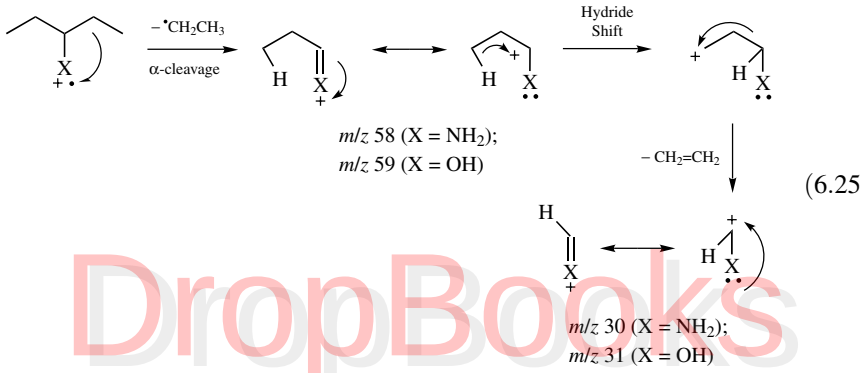

(6.25)

DropBooks

6.5.3. Elimination Fragmentations of Some Aromatic Compounds

When the O atom of an ester or the N atom of an amide is attached directly to an aromatic ring, an alternate mode of fragmentation may take precedence over α-cleavage. This fragmentation, which involves olefin elimination and a four-atom cyclic intermediate, is similar to the rearrangements discussed in the previous sections and in Section 4.1.2.

The spectrum of acetylacetaminophen, the O-acetylated derivative of the analgesic acetaminophen (a common brand name is Tylenol), illustrates this well (Figure 6.24). The peak at *m/z* 43 arises from α-cleavage at either carbonyl group, forming $CH_3C{\equiv}O^+$. The loss of $^\bullet CH_3$ by α-cleavage (*m/z* 178) is not observed because both the ions and radicals formed during this fragmentation are less stable than those leading to the peak at *m/z* 43 (Section 6.4.3). Instead, the only two high-mass ions other than the $M^{+\bullet}$ are seen at *m/z* 151 $[(M-42)^+]$ and *m/z* 109 $[(M-42-42)^+]$. These ions are produced by the sequential losses of ketene ($CH_2{=}C{=}O$) as shown in Equation 6.26. The first step in each of these eliminations is best explained by radical-site-induced migration of a H atom via a four-atom intermediate. Once again, the fragment ions formed in this manner are

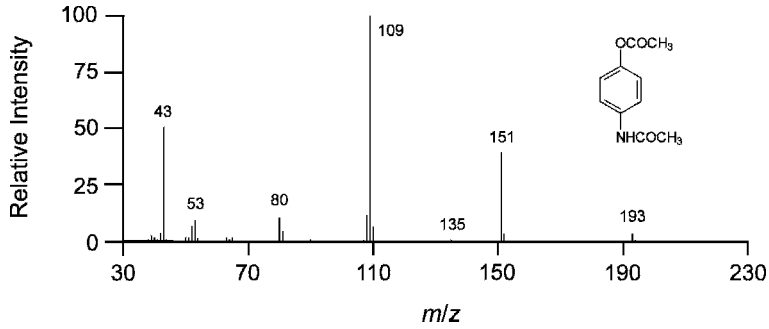

Figure 6.24. Mass spectrum of acetylacetaminophen. Acylated derivatives of phenols and aromatic amines lose ketene in addition to undergoing α-cleavage at the carbonyl group.

essentially as stable as their precursor ions. They also form by a H migration that has minimal energy requirements, followed by elimination of a small molecule containing a newly formed π-bond.

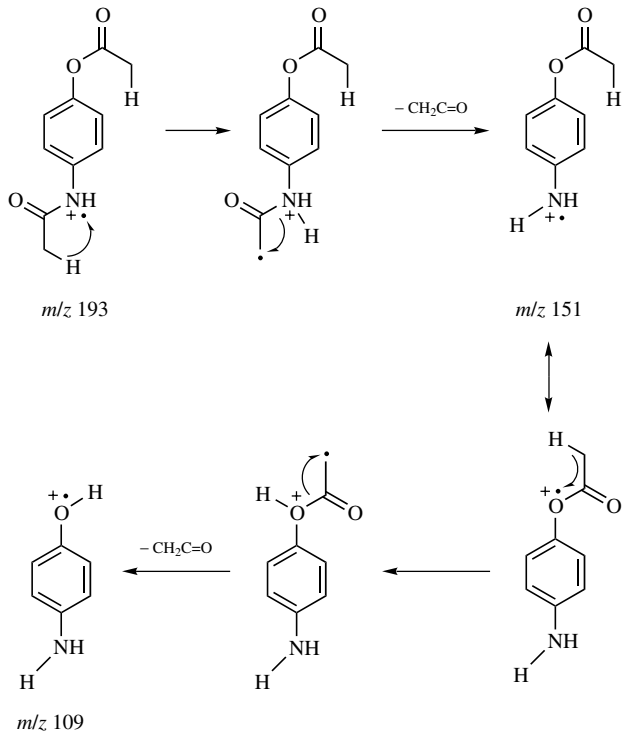

(6.26)

A similar type of elimination also explains the behavior of phenylalkylethers such as ethoxybenzene, whose $M^{+\bullet}$ loses ethylene (*m/z* 94; 100%) to the near exclusion of all other fragmentation (Equation 6.27). The controversial herbicide

atrazine eliminates both ethylene and propylene in an analogous manner, although in this case these eliminations are overshadowed by the expected α-cleavage loss of $^{\bullet}CH_3$ (Equation 6.28).

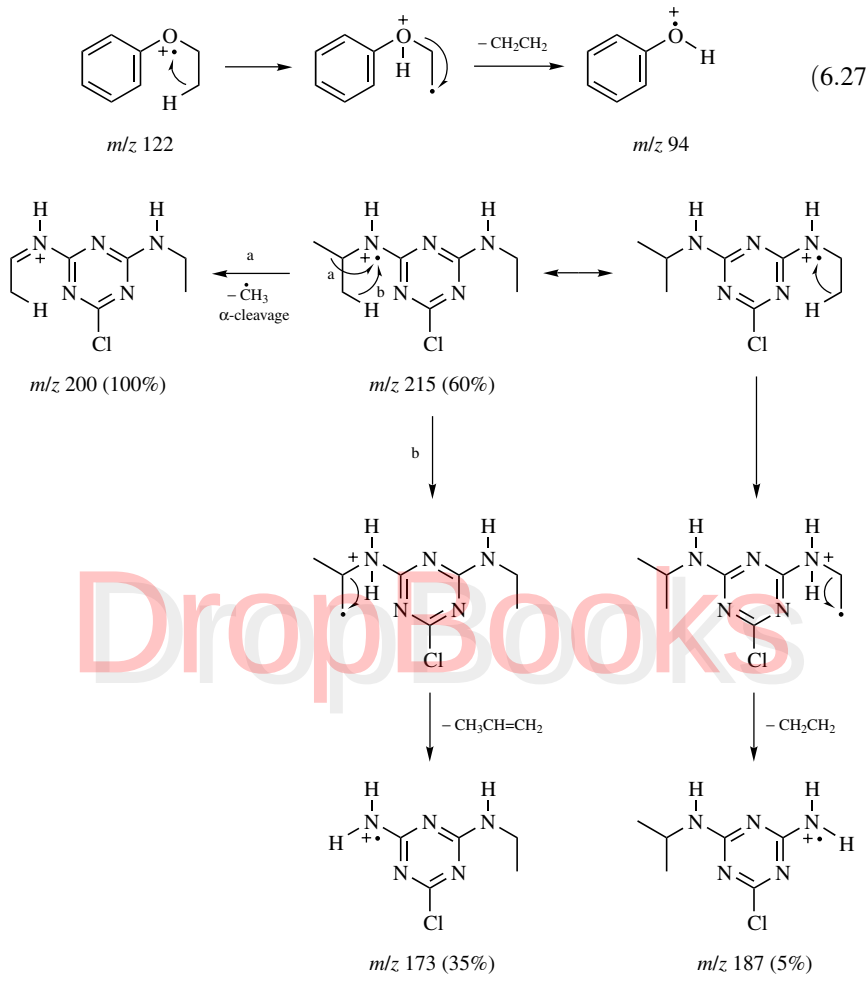

(6.27)

(6.28)

DropBooks

6.5.4. Water Elimination in Aliphatic Alcohols

The spectrum of *n*-pentanamine shows a base peak at *m/z* 30 from α-cleavage, an $M^{+\bullet}$ peak at *m/z* 87 (about 7% relative intensity), and no other fragment ion peaks having intensities greater than 1–2%. In contrast, the spectrum of *n*-pentanol (Figure 6.25) exhibits a base peak at *m/z* 42 and other important fragment ion peaks at *m/z* 55 and 70—none of which are expected if α-cleavage is the primary mode of

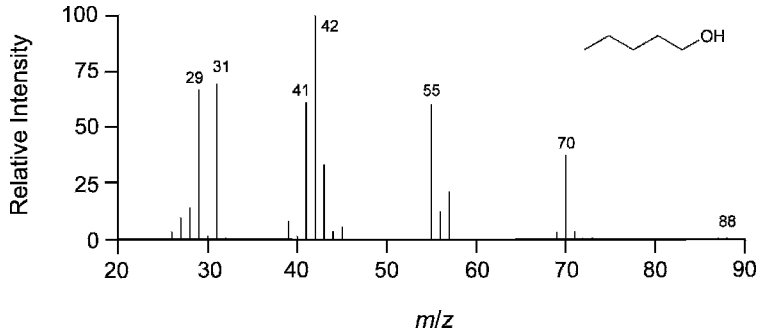

Figure 6.25. Mass spectrum of *n*-pentanol, which contains intense peaks that represent fragmentations related to the initial loss of water by the $M^{+\bullet}$.

fragmentation. The peak resulting from α-cleavage in this spectrum occurs at *m/z* 31 with a relative intensity of only about 70%.

What is the origin of these unexpected peaks? Primary alcohols with a chain length of four C atoms or longer are prone to lose water from the $M^{+\bullet}$ by formation of a cyclic intermediate. It is important to understand that loss of water by aliphatic alcohols during mass spectral fragmentation is different from that observed in solution under acid-catalyzed conditions. In the latter case (Equation 6.29), secondary and tertiary alcohols are more likely to lose water than are primary alcohols because the carbenium ions formed are more stable. In the mass spectrometric fragmentation of aliphatic alcohols, on the other hand, mainly primary alcohols undergo this loss. Furthermore, the H atom lost in this fragmentation comes not from an adjacent C atom but rather from a position several C atoms removed, typically through formation of a six-atom cyclic intermediate such as that shown in Equation 6.30.

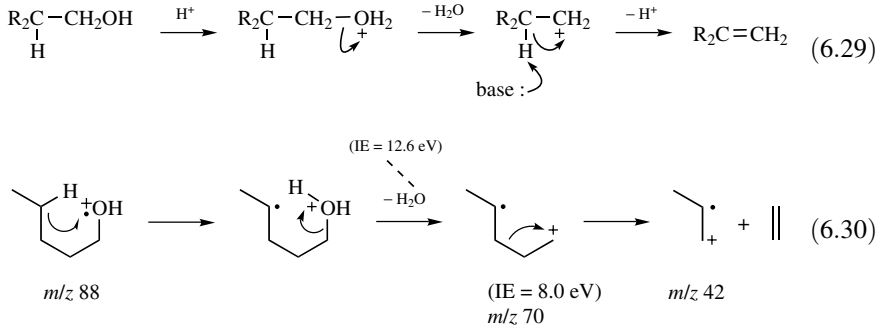

This fragmentation appears to be driven by the attraction of the migrating H atom to the radical site on the initially ionized O atom, as well as by its electronegativity. In aliphatic amines, ammonia loss occurs much less easily because the less electronegative N is not as attractive to H and is also better able to stabilize the charge in the ion resulting from α-cleavage. In secondary and tertiary alcohols, the $R_2C{=}O^{+}H$ ions formed by α-cleavage are stabilized by the additional alkyl

substituents (IE <6.9 eV; Table 3.1), making α-cleavage a more attractive mode of fragmentation.

Once water loss has occurred, the distonic fragment ion having *m/z* 70 behaves like a primary carbenium ion in a straight-chain environment (Section 4.2.1), losing ethylene to produce the more abundant ion having *m/z* 42 (Equation 6.30). The ions represented by the peaks at *m/z* 41 and 55 are, respectively, the allyl and methylallyl ions.

EXAMPLES

Examples 6.1 and 6.2

Identify the compounds whose spectra are shown in Figures 6.26 and 6.27.

Answer 6.1

(*Step 3*) The peak at *m/z* 59 cannot represent the $M^{+\bullet}$ because the first loss to produce the *m/z* 45 peak would then be only 14. The tiny peak at *m/z* 60 seems a more reasonable candidate for the $M^{+\bullet}$ peak.

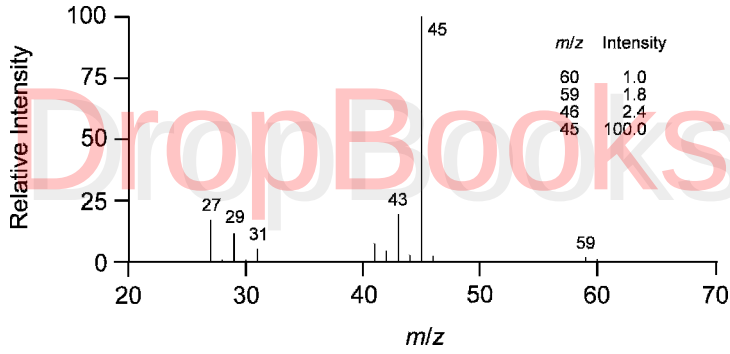

Figure 6.26. Mass spectrum for Example 6.1.

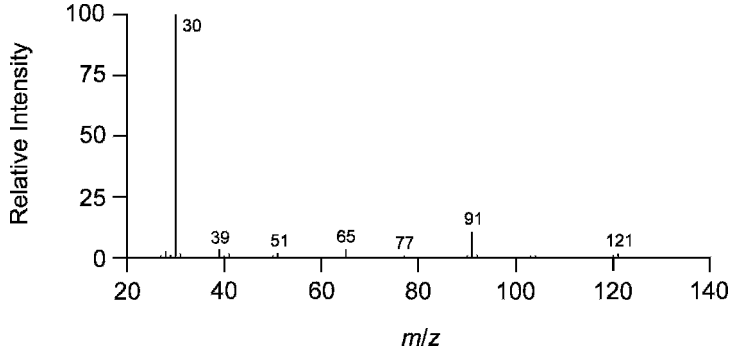

Figure 6.27. Mass spectrum for Example 6.2.

(*Step 4*) The apparent even MM and presence of fragment ion peaks at odd *m/z* values indicate that N is not present.

(*Step 5*) The lack of obvious A + 2 heteroatom patterns indicates that C and H, and possibly O, are the only elements present. The $M^{+\bullet}$ peak is too small to provide isotope information, but the isotope cluster for the peak at *m/z* 45 shows that this ion contains two C atoms. Because the difference between *m/z* 45 and *m/z* 60 is 15 (a $^{\bullet}CH_3$), it is likely that the $M^{+\bullet}$ contains three C atoms.

(*Step 6*) The spectrum shows no signs of aromaticity, but the base peak at *m/z* 45 plus the small peaks at *m/z* 31 and 59 are indicative of an aliphatic ether or alcohol (Table 4.2).

(*Steps 8 and 10*) Three structures are possible: *n*-propanol, isopropanol, and methylethylether. Only the latter two compounds are consistent with the spectrum because *n*-propanol should produce an intense peak at *m/z* 31 by α-cleavage. Although it is tempting to speculate on which of these two compounds produces this spectrum, only comparison of this spectrum with known standards will settle the issue unambiguously. Actually, the spectra of these two compounds are very similar. Methylethylether shows a larger $M^{+\bullet}$ peak, an enhanced M − 1 peak because it has five H atoms on the α C atoms, and a more intense *m/z* 31 peak due to secondary elimination of ethylene from one of the ions having *m/z* 59 (Equation 6.31). Isopropanol, which gave rise to the spectrum in Figure 6.26, has a more intense *m/z* 43 peak due to stabilization of the charge by the isopropyl group (Equation 6.32).

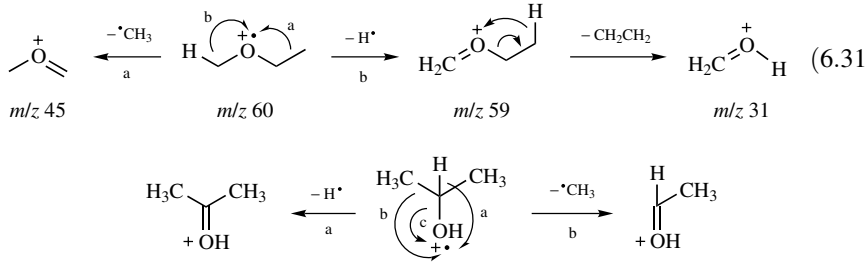

(6.31)

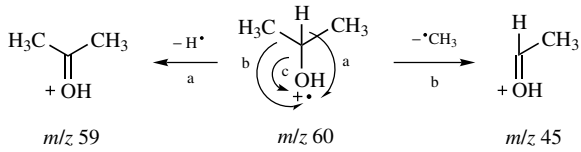

(6.32)

Answer 6.2

(*Steps 3 and 4*) The MM (121) appears to be odd. In combination with the base peak at *m/z* 30 (*Steps 6 and 7*), this strongly suggests an aliphatic amine.

(*Step 7*) These features are accompanied by a weak, but significant, benzyl low-mass ion series (*m/z* 39, 65, and 91). There are no other peaks of significance in the spectrum. The combination of benzyl ($C_6H_5C^+H_2$; *m/z* 91) and $CH_2{=}N^+H_2$ (*m/z* 30) leads to β-phenethylamine ($C_6H_5CH_2CH_2NH_2$), which has a MM of 121. This is consistent with the postulated $M^{+\bullet}$ peak. You should convince yourself that no other isomeric structure could produce the intense *m/z* 30 peak by α-cleavage (Equation 6.33).

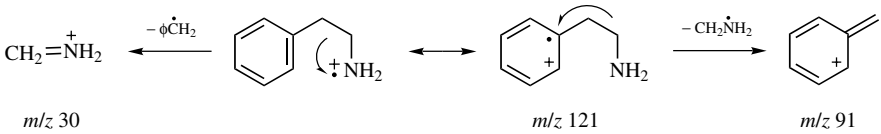

(6.33)

ADDITIONAL PROBLEMS

6.7. The compound whose spectrum is shown in Figure 6.28 was recovered from the residue of an illicit drug lab in which methamphetamine was being manufactured. What is the structure of this compound? [*Hint*: The fact that methamphetamine was the intended final product can be used to determine possible structures for this unknown.]

6.8. Figure 6.29 contains the spectra of the seven $C_4H_{10}O$ isomers. Draw the structures for each of these compounds and predict important modes of fragmentation for each. Then match the structures with the spectra.

6.9. Starting on the next page, the structures of eight compounds are given along with one or more important peaks in the EIMS of each compound. The base peak in each spectrum is identified by an asterisk (*); if the base peak is more than 10 times more intense than any other peak in the

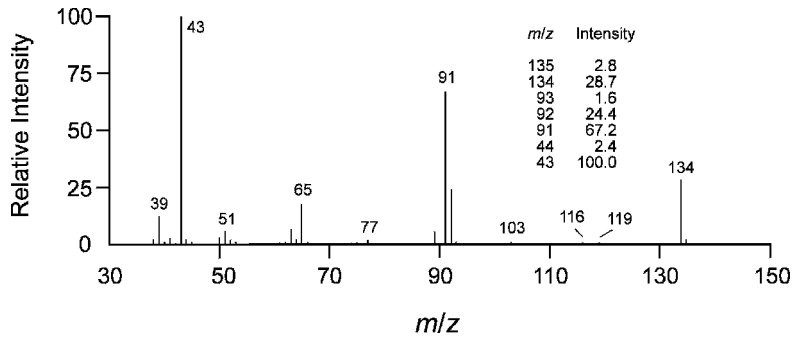

Figure 6.28. Mass spectrum for Problem 6.7.

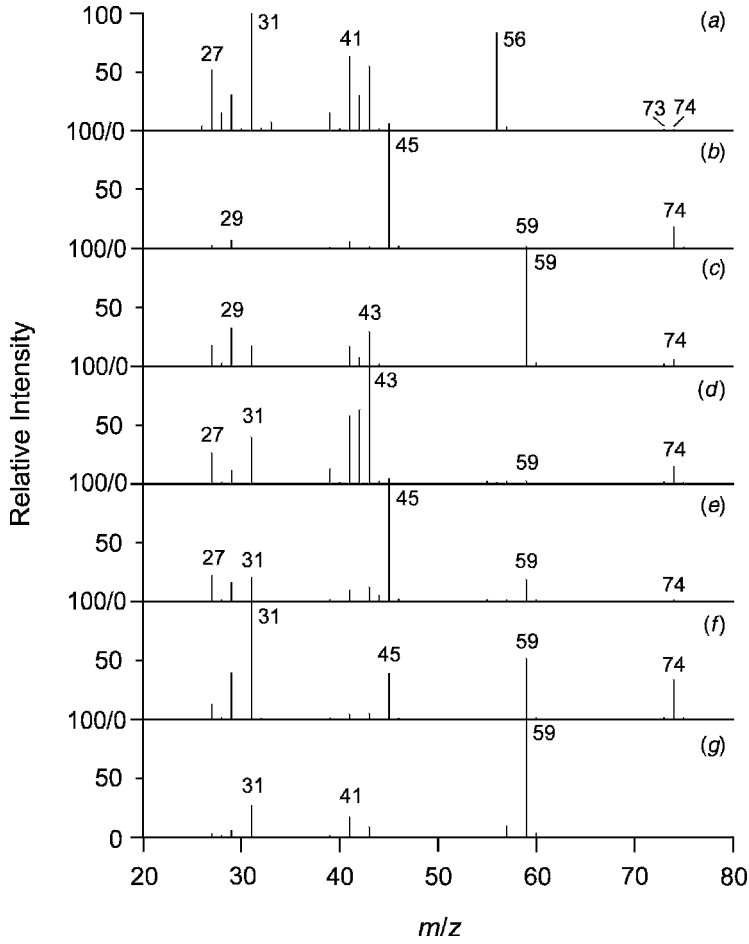

Figure 6.29. Mass spectra of the seven $C_4H_{10}O$ isomers (Problem 6.8).

spectrum, it is denoted by a double asterisk (**). Identify in each structure the most likely site for initial ionization. Then account for formation of the base peak, and other peaks as indicated, in each spectrum.

(a) *N*-Pentylpiperidine (*m/z* 98**)

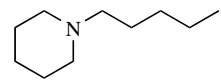

(b) 2-Furancarboxylic acid, propyl ester (*m/z* 95*)

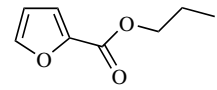

(c) *s*-Butylisopropylsulfide (*m/z* 103, 61*)

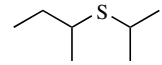

(d) 1-(1-Cyclohexenyl)-2-propanone (*m/z* 95*, 43)

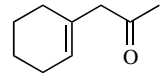

(e) Doxepin, an antidepressant drug (*m/z* 58**)

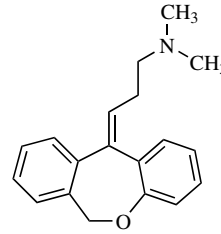

(f) α-Methylfentanyl, "China White," a potent narcotic drug (*m/z* 259*)

DropBooks

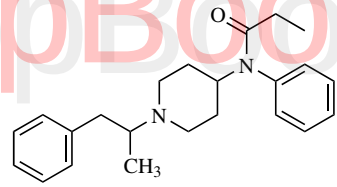

(g) Benzocaine, a topical anesthetic (*m/z* 120*)

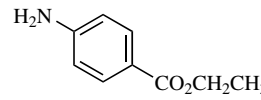

(h) *N*,*N*-Diethylamphetamine (*m/z* 100*, 91, 72, 44)

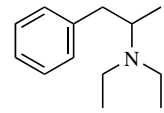

6.10–6.11. Identify the compounds for which spectra are shown in Figures 6.30 and 6.31.

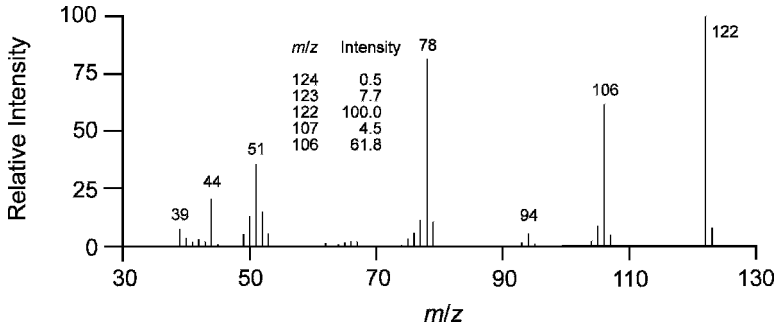

Figure 6.30. Mass spectrum for Problem 6.10.

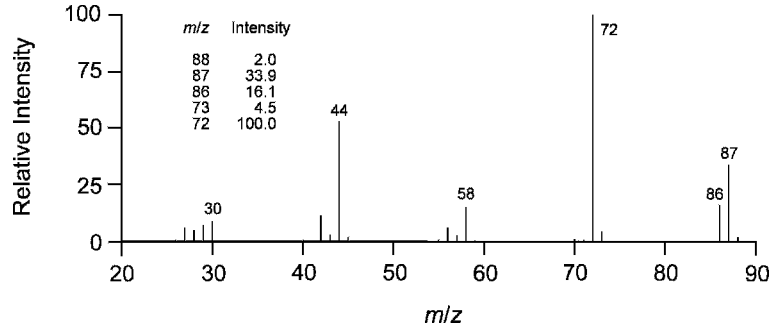

Figure 6.31. Mass spectrum for Problem 6.11.

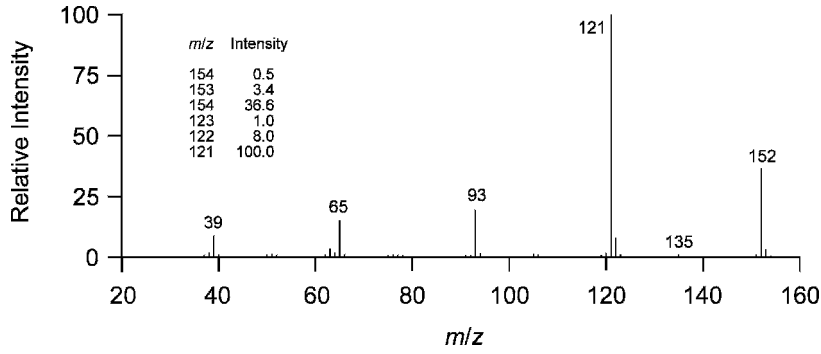

Figure 6.32. Mass spectrum for Problem 6.12.

6.12. The mass spectrum shown in Figure 6.32 is from a compound that was isolated from vaginal secretions of female dogs in estrus and was subsequently shown to elicit sexual arousal in male dogs (Goodwin et al., 1979). What is the structure of this compound?

6.13. Write mechanisms for the formation of the following ions in the spectrum of 2-acetoxymethylfuran (Section 6.4.3; Figure 6.19*d*): (**a**) *m*/*z* 98 from loss of ketene ($CH_2{=}C{=}O$); (**b**) *m*/*z* 81 from benzylic-type cleavage (*Hint*: Where is initial ionization likely to occur?); and (**c**) *m*/*z* 43 ($CH_3C{\equiv}O^+$).

REFERENCES

—, *Forensic and Analytical Chemistry of Clandestine Phenethylamines* (CND Analytical, Inc., Auburn, AL, 1994), pp. 31–50.

J. H. Beynon, R. A. Saunders, and A. E. Williams, *The Mass Spectra of Organic Molecules* (Elsevier, New York, 1968), pp. 348–350.

M. Goodwin, K. M. Gooding, and F. Regnier, "Sex Pheromone in the Dog," *Science*, **203**, 559–561 (1979).

J. B. Steeves, H. M. Gagné, and E. Buel, "Normalization of Residual Ions After Removal of the Base Peak in Electron Impact Mass Spectrometry," *J. Foren. Sci.*, **45**, 882–885 (2000).

DropBooks

7

IMPORTANT MASS SPECTRAL REARRANGEMENTS

7.1. INTRODUCTION

Chapters 4 and 6 contained examples of fragmentations that involved rearrangement of the atoms and electron density in certain types of ions. In each of these fragmentations, the rearrangements were facilitated by elimination of a small neutral molecule (EE^0) and formation of a fragment ion that was approximately as stable as the precursor ion.

In this chapter, four specific types of mass spectral rearrangements will be discussed: the γ-hydrogen shift rearrangement, cyclohexanone-type rearrangement, retro Diels–Alder fragmentation, and double-hydrogen rearrangement. These fragmentations do not occur unless certain structural requirements are met. As a result, they can provide specific structural information about the parts of the molecule in which they occur.

Unimolecular rearrangements occur through formation of cyclic intermediates or transition states. The size of the rings formed as intermediates is not accidental. Although rearrangements involving rings of three or four atoms are expected to proceed easily because the atoms are close to one another, rings of five or six atoms are easier to form for entropic and structural reasons and are preferred intermediates for many rearrangements in organic molecules (Section 3.6.1). Rearrangements involving larger ring intermediates occur less frequently. The first two rearrangements discussed in this chapter involve cyclic intermediates that involve six atoms.

Understanding Mass Spectra: A Basic Approach, *Second Edition*. By R. Martin Smith
ISBN 0-471-42949-X © 2004 John Wiley & Sons, Inc.

None of the fragmentations described in this chapter occur routinely by concerted mechanisms. Although a few exceptions exist, it is safe to assume that all occur in a step-wise manner.

7.2. γ-HYDROGEN REARRANGEMENT

7.2.1. McLafferty-Type Rearrangement

Figure 7.1 summarizes a rearrangement in which a H atom that is four atoms distant from a C atom containing the functionality that has the charge migrates to the radical site created in the initial ionization. Subsequent breaking of the bond between the α and β atoms and pairing of one of those electrons with the new radical site lead to loss of an olefin. Because the H atom that migrates is located on the γ C atom and the bond to the β C atom is broken, this fragmentation is known as the γ-hydrogen rearrangement with β-cleavage; the name is usually shortened to simply the γ-H rearrangement. Within this general framework several combinations are possible. When the X group in Figure 7.1 is O (i.e., for carbonyl compounds), this fragmentation is called the *McLafferty rearrangement*, named after Fred McLafferty of Cornell University, a pioneer in mass spectral interpretation.

The individual steps in the mechanism shown in Figure 7.1 are all analogous to processes discussed previously. Initial ionization occurs at the heteroatom or heteroatom-like group through loss of a nonbonding or π-bonding electron. Transfer of a H atom occurs via a cyclic six-atom intermediate. This γ-H shift moves the radical site from its initial location to a position not associated with the atom that has the charge and results in a distonic ion (Section 3.2). Pairing of the odd electron in the distonic ion with one of the electrons from the bond between the α and β atoms results in the ejection of an olefin and formation of an ion whose stability is similar to that of the precursor ion. The fragmentation is facilitated by the energy gained in forming a new π-bond in the olefinic product.

DropBooks

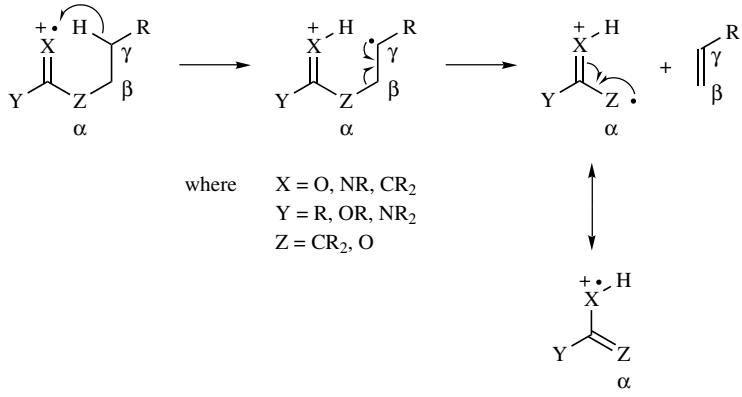

Figure 7.1. Generalized representation of the γ-hydrogen shift rearrangement resulting in a β-cleavage.

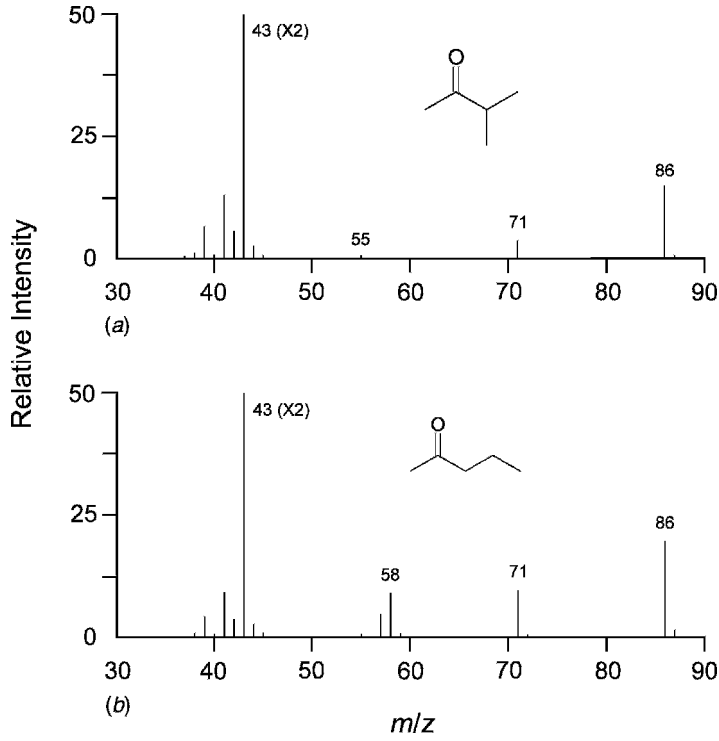

Figure 7.2. Mass spectra of two aliphatic ketones: (*a*) 3-methyl-2-butanone and (*b*) 2-pentanone. The peak at *m/z* 58 in the spectrum of 2-pentanone is the result of a γ-hydrogen (McLafferty) rearrangement.

The position of the H atom in this rearrangement is critical; the reaction does not occur unless a H atom is available on the γ C atom. Consider the two spectra in Figure 7.2. 3-Methyl-2-butanone (Figure 7.2*a*) undergoes α-cleavage, as expected, to give fragment ions represented by the peaks at *m/z* 71 and 43 (cleavage on either side of the carbonyl group). The peak at *m/z* 43 is more intense because isopropyl radical is more stable than methyl radical.

In addition to peaks representing the ions formed by α-cleavage, the spectrum of 2-pentanone (Figure 7.2*b*) shows a peak at *m/z* 58 that does not occur in the spectrum of 3-methyl-2-butanone. This peak stands out because it occurs at an even *m/z* value; values for all the other important fragment ion peaks in both spectra are odd. Because neither of these compounds contains N, the nitrogen rule (Section 3.5) predicts that any peaks occurring at even *m/z* values will be due to $OE^{+\bullet}$. This means that the *m/z* 58 ion is a likely candidate for formation by a rearrangement process.

The structure of this ion and the mechanism for its formation cannot be determined from this information alone. Instead, a method of labeling atoms is needed. Deuterium (D) is the isotope of H having an atomic mass of 2. Replacement of

Table 7.1. McLafferty rearrangement in 2-pentanone and its deuterated derivatives

Compound	$M^{+\bullet}$	$PrCO^+$	CH_3CO^+	Rearrangement Ion
$CH_3COCH_2CH_2CH_3$	86	71	43	58
$CD_3COCH_2CH_2CH_3$	89	71	46	61 (∴all D retained)
$CH_3COCD_2CH_2CH_3$	88	73	43	60 (∴all D retained)
$CH_3COCH_2CD_2CH_3$	88	73	43	58 (∴all D lost)
$CH_3COCH_2CH_2CD_3$	89	74	43	59 (∴2 D lost, 1 D retained)

some of the H atoms in a molecule with D increases the MM by 1 u for each H atom replaced—a shift readily apparent in the mass spectrum. If one or more H atoms at a specific location in a molecule are replaced with D atoms, the presence or absence of that site in various ions can be tracked by studying whether or not the peaks in the spectrum due to those ions shift in *m/z* value. Deuterium is preferred in these studies, rather than alkyl derivatives, for example, because the effect of D on the relative $\Delta G^{\ddagger}$'s of various fragmentation reactions should be negligible compared with those of the undeuterated compounds. In contrast, competing fragmentations in alkyl or other derivatives can obscure the effects being studied.

In this case, four deuterated derivatives of 2-pentanone were synthesized unambiguously. Synthesis of these compounds was not trivial because simply exchanging H with D in 2-pentanone by reaction with most deuterated reagents would lead to an inseparable mixture of compounds. In one derivative all the H atoms on C1 were replaced with D, in another all the H atoms on C3, and so forth. Important peaks in the mass spectra of these compounds, and of 2-pentanone itself, are listed in Table 7.1.

DropBooks

In the spectrum of the first derivative, 1-d_3-2-pentanone, the $M^{+\bullet}$ peak is not observed at *m/z* 86 for $^{12}C_5H_{10}{}^{16}O$, but rather is found at *m/z* 89 for $^{12}C_5D_3H_7{}^{16}O$.[1] The peak at *m/z* 71 in the 2-pentanone spectrum, which represents the loss of $^{\bullet}CH_3$ from next to the carbonyl group, also occurs at *m/z* 71 in this spectrum, because C1 and all its H atoms (or D atoms) are lost in this fragmentation. α-Cleavage on the other side of the carbonyl group produces the isopropyl radical and the acylium ion, which is represented by the peak at *m/z* 43 in the spectrum of 2-pentanone. The corresponding peak appears at *m/z* 46 in the spectrum of 1-d_3-2-pentanone because all the D atoms remain with the fragment that has the charge. Finally, the rearrangement ion peak moves from *m/z* 58 to *m/z* 61 in the 1-d_3-2-pentanone spectrum, indicating that, whatever the mechanism, C1 and its attached H atoms are still present in the resulting ion.

In the spectrum of 3-d_2-2-pentanone, the $M^{+\bullet}$ peak is found at *m/z* 88 because of the addition of two D atoms. The ion arising from the α-cleavage loss of $^{\bullet}CH_3$ now has *m/z* 73 because the D atoms are present in the fragment ion. The acylium ion peak stays at *m/z* 43. The peak that occurs at *m/z* 58 in the spectrum of 2-pentanone

[1] The nitrogen rule (Section 3.5) does not apply here. Because the nominal mass of the ion is used in the nitrogen rule, it only applies to ions containing the most abundant naturally occurring stable isotopes of the constituent elements.

moves to *m/z* 60 in this spectrum, indicating that C3 and both its D atoms are retained during the rearrangement fragmentation.

The spectrum of 4-d_2-2-pentanone is similar, except that the rearrangement ion peak remains at *m/z* 58. This is consistent with the *loss* of C4 and its attached H atoms.

The peak due to the rearrangement ion moves to *m/z* 59 in the spectrum of 5-d_3-2-pentanone, a change of 1 from the spectrum of 2-pentanone. This means that only

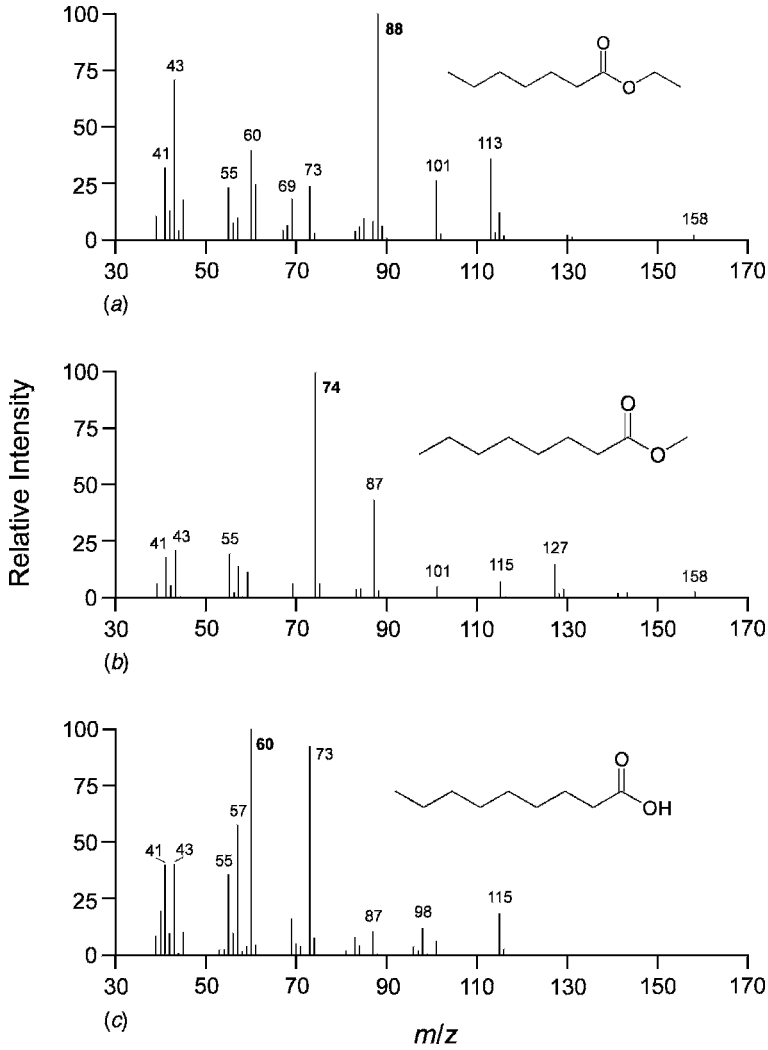

Figure 7.3. Mass spectra of three long-chain fatty acid derivatives: (*a*) ethyl heptanoate, (*b*) methyl octanoate, and (*c*) nonanoic acid. In each case, the McLafferty rearrangement ion produces the base peak in the spectrum.

one of the three D atoms on C5 is *retained* in the fragment ion. Because the 58 u in the fragment ion have already been accounted for as C_3H_6O, the neutral fragment that is lost must be C_2H_4, an ethylene molecule.

These findings are compatible with the mechanism shown in Figure 7.1: One H atom from the γ C atom (C5, in this case) migrates to the part of the molecule that contains C atoms 1, 2 and 3, while the β and γ C atoms (C4 and C5) and four of the five groups attached to them are lost. As long as the γ C atom has at least one H atom, the β and γ C atoms can have a variety of substituents. Generalizing beyond alkyl groups is dangerous, however, because the electronic structure of some molecules may permit other fragmentation processes to occur more readily. 3-Methyl-2-butanone (Figure 7.2*a*) does not have a γ C atom and does not undergo the rearrangement.

The McLafferty rearrangement is not limited to aliphatic ketones. Aliphatic carboxylic acids and their derivatives also undergo this fragmentation, which sometimes produces the most intense fragment ion peak in the spectrum (Figure 7.3 and Equation 7.1). Nor is the rearrangement limited to the aliphatic portion of the molecule ($Z = CH_2$ in Figure 7.1). Butyl palmitate, for example, exhibits two peaks of nearly equal intensity due to McLafferty rearrangements involving the ester ($Z = O$ in Figure 7.1) and aliphatic portions of the molecule, respectively (Equation 7.2).

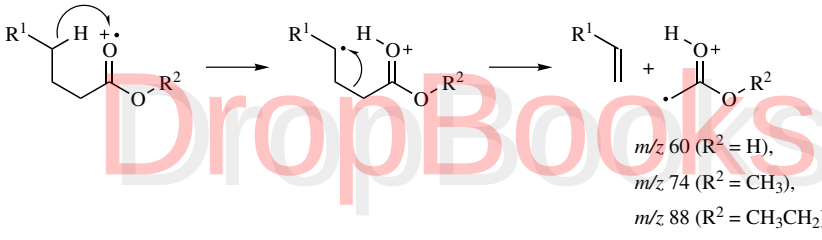

(7.1)

m/z 60 (R^2 = H),
m/z 74 (R^2 = CH_3),
m/z 88 (R^2 = CH_3CH_2)

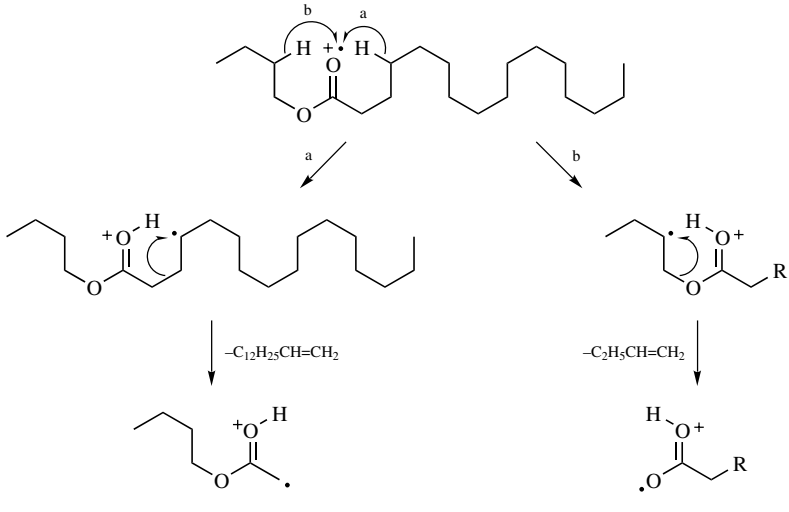

(7.2)

m/z 116 (12%)

m/z 256 (15%)

DropBooks

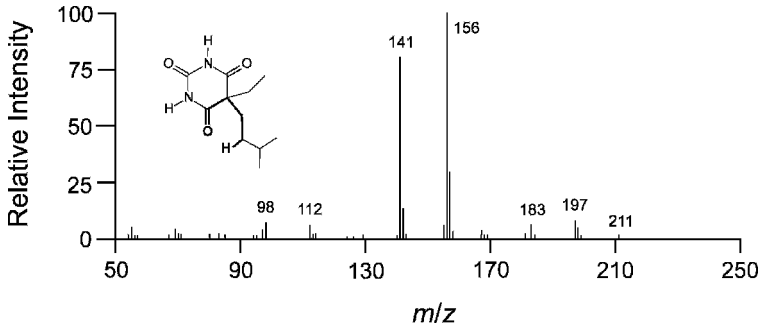

Figure 7.4. The McLafferty rearrangement ion accounts for the base peak in the mass spectrum of amobarbital.

If the $OE^{+\bullet}$ fragment resulting from the McLafferty rearrangement gains aromatic resonance energy unavailable to the precursor ion, the peak representing the rearrangement ion may be strikingly intense (Figure 7.4 and Equation 7.3).

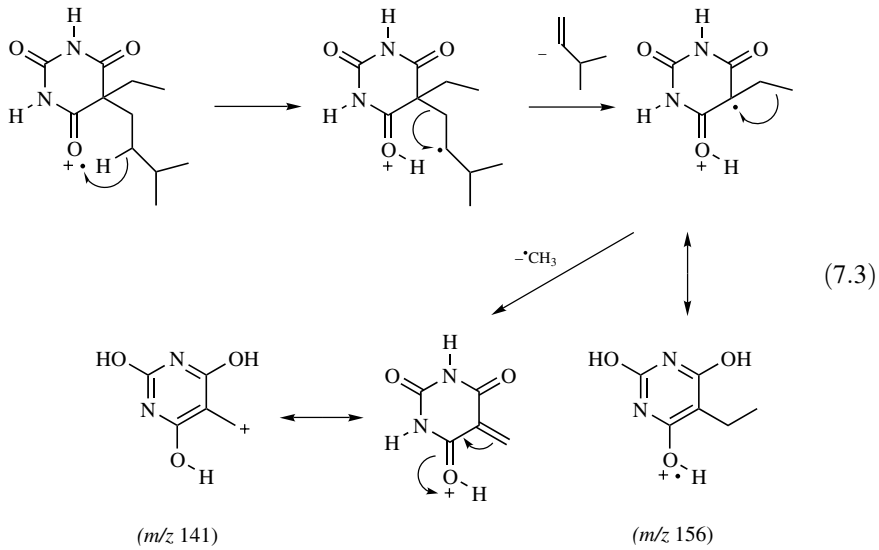

(7.3)

7.2.2. γ-Hydrogen Rearrangement in Alkylbenzenes

As expected, the alkylbenzene spectra in Figure 7.5 show aromatic and benzylic low-mass ion series as well as a base peak at *m/z* 91 due to benzylic cleavage (Section 6.2). However, the *m/z* 92 peak in the spectrum of *n*-butylbenzene (Figure 7.5*c*) is much too large to be due to contributions from ^{13}C in the *m/z* 91 ion. In fact, the *m/z* 92 peak in the spectrum of *n*-propylbenzene has an intensity

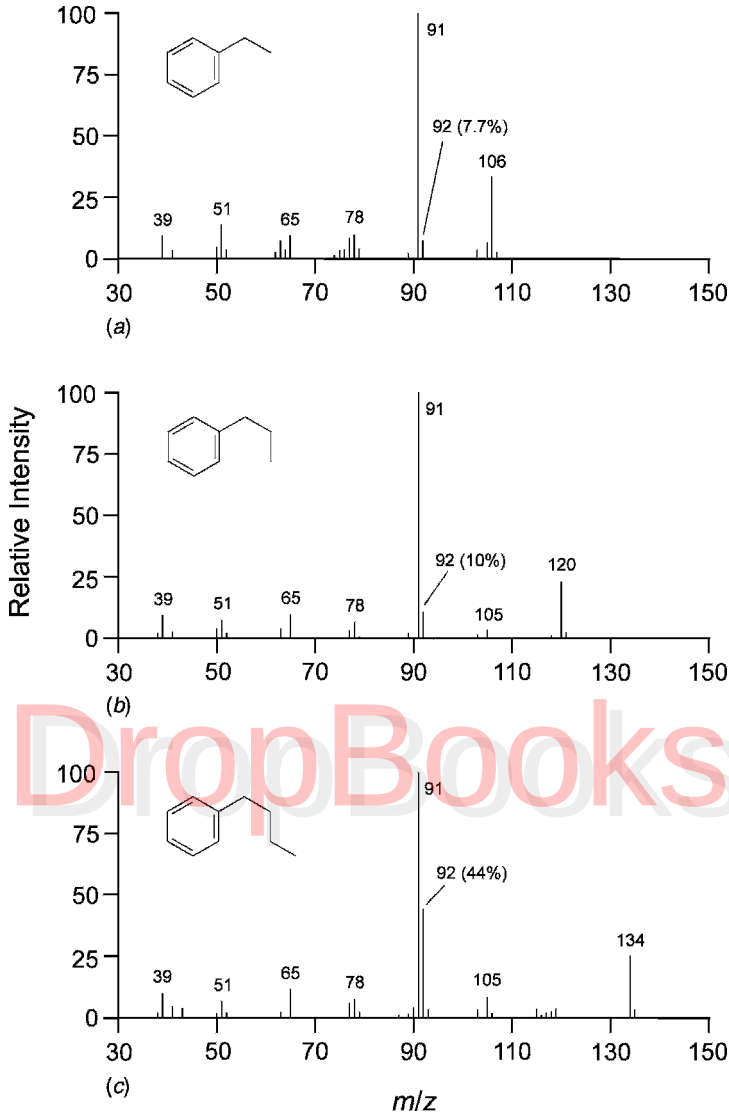

DropBooks

Figure 7.5. Mass spectra of three alkylbenzenes: (*a*) ethylbenzene, (*b*) *n*-propylbenzene, and (*c*) *n*-butylbenzene. The intensity of the *m*/*z* 92 peak increases with increasing facility of the γ-hydrogen rearrangement.

of about 10%, slightly larger than the 7.7% calculated for ^{13}C contributions from the *m*/*z* 91 ion. Although this difference might easily be overlooked in the case of *n*-propylbenzene, errors in intensity measurement cannot possibly account for the size of the *m*/*z* 92 peak in the butylbenzene spectrum.

Because the peak at *m/z* 92 represents an $OE^{+\bullet}$ fragment (it has an even *m/z* value in the spectrum of a compound that contains no N atoms), its formation by a rearrangement process seems likely. If initial ionization occurs with loss of one of the π-electrons associated with the aromatic ring, this site could cause an appropriately situated H atom to migrate to one of the ring positions. Ethylbenzene (Figure 7.5*a*) does not appear to produce the *m/z* 92 ion at all, so that H atoms attached to the C atom which is γ to the ring seem a likely source (Equation 7.4).

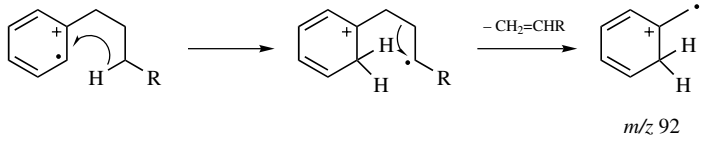

m/z 92

(7.4)

Table 7.2 lists the ratios of the relative intensities of the *m/z* 92 and 91 peaks in the spectra of a variety of alkylbenzenes. (For those compounds having an additional methyl group on the benzylic C atom, peaks for the benzylic cleavage and

Table 7.2. Measure of the γ-H rearrangement in various alkylbenzenes

	m/z 92/91		*m/z* 92/91		*m/z* 92/91
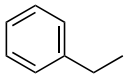 A	0.08	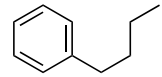 F	0.6	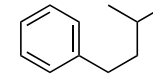 K	1.2
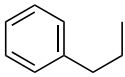 B	0.10	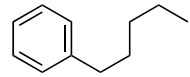 G	0.7	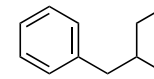 L	1.3
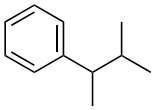 C	0.1*	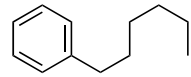 H	0.8	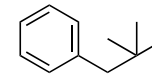 M	1.6
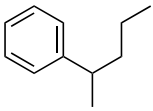 D	0.1*	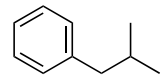 I	0.6	(*−*m/z* 106/105)	
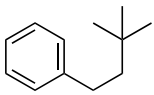 E	0.1	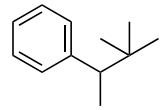 J	1.0*		

γ-H rearrangement ions occur at *m/z* 105 and 106, respectively). The data in this table support the hypothesis that a γ-H atom is involved in this fragmentation. First, compounds such as 1-phenyl-3,3-dimethylbutane (Table 7.2, Structure E), which lack γ H atoms, do not appear to undergo this rearrangement. The spectrum of this compound shows a peak at *m/z* 92 that is due almost exclusively to ^{13}C contributions from the *m/z* 91 ion. At the other extreme, in the spectrum of 1-phenyl-2,2-dimethylpropane (neopentylbenzene; Table 7.2, Structure M), the *m/z* 92 peak is over one and a half times the size of the *m/z* 91 peak, reflecting the fact that this compound has nine H atoms which are γ to the ring.

One variable affecting the activation energy for this rearrangement seems to be the strength of the incipient double bond in the resulting olefin. Thus, $M^{+\bullet}$ that result in the formation of substituted olefins undergo the rearrangement more readily than those that do not. For example, propylbenzene (Table 7.2, Structure B) generates ethylene as the olefin product and shows minimal evidence for fragmentation via γ-H rearrangement. But 1-phenyl-3-methylbutane (Table 7.2, Structure K) undergoes this fragmentation more easily than the isomeric *n*-pentylbenzene (Table 7.2, Structure G) because the olefin formed has two attached alkyl groups rather than one. This happens even though Structure K contains only one γ H atom.

The presence of an alkyl group on the benzylic C atom increases the relative stability of the benzyl ion and thereby diminishes the importance of the γ-H rearrangement. Even in cases where several H atoms can migrate (1-phenyl-1,2-dimethylpropane; Table 7.2, Structure C), benzylic cleavage is the preferred fragmentation because it does not have the entropic requirements of the γ-H rearrangement (Section 3.6.1). Only in the case of 1-phenyl-1,2,2-trimethylpropane (Table 7.2, Structure J) does the availability of many migratable H atoms and the stability of the product olefin allow the γ-H rearrangement to compete favorably with benzylic cleavage.

DropBooks

Because of its inherent basicity and electronegativity, a N atom in the ring enhances a preference for the γ-H rearrangement. The spectra of 2- and 4-propylpyridine illustrate this point (Figure 7.6). Both compounds undergo the γ-H rearrangement to produce ions having *m/z* 93. This happens more easily in 2-propylpyridine because the migrating H atom is attracted directly to the initial ionization site by means of a 6-atom intermediate and the resulting distonic ion retains the aromatic character of the ring (Equations 7.5 and 7.6). Indeed,

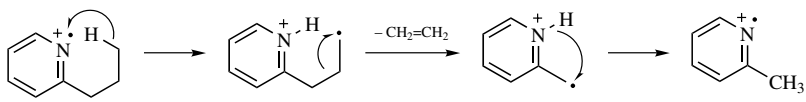

m/z 121 *m/z* 93 (7.5)

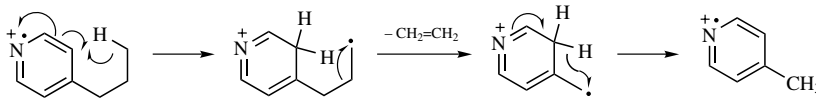

m/z 121 *m/z* 93 (7.6)

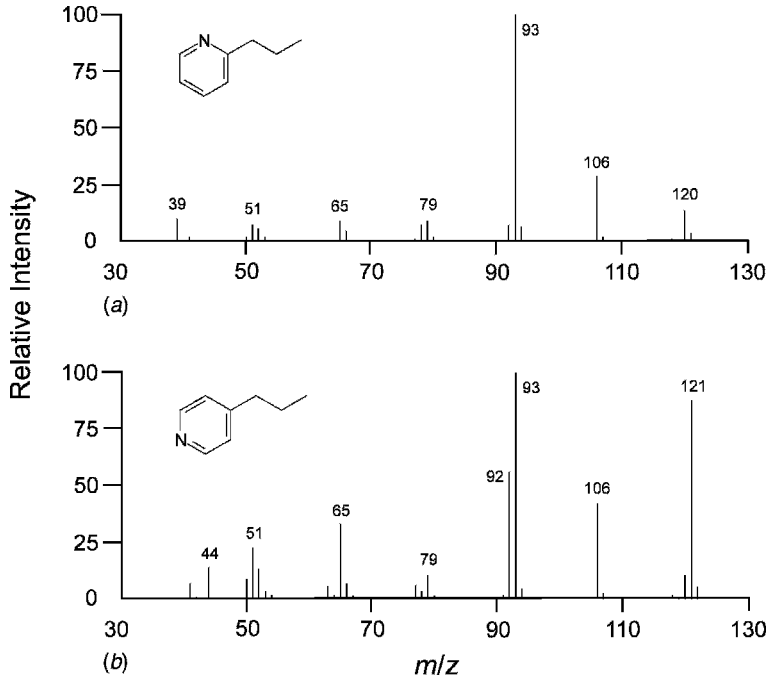

Figure 7.6. Mass spectra of (*a*) 2-propylpyridine and (*b*) 4-propylpyridine.

this pathway requires so little energy in 2-propylpyridine that the $M^{+\bullet}$ peak is extremely weak in intensity. In contrast, the $M^{+\bullet}$ of the 4-propyl isomer lacks an efficient mechanism for accepting the migrating H atom without creating highly strained bonds within the ring. The result is that the $M^{+\bullet}$ peak for the 4-propyl isomer is one of the most intense peaks in the spectrum.

The difference in fragmentation patterns exhibited by 2- and 4-propylpyridine is a variation of the *ortho effect*, which is the tendency of aromatic compounds having substituents located *ortho* to one another to undergo reactions that are different from those where the same substituents are *meta* or *para* to one another. *Ortho* substituents can interact via cyclic intermediates in ways that *meta* and *para* substituents cannot. A more thorough discussion of the *ortho* effect will be given in Section 8.4.

7.2.3. γ-Hydrogen Rearrangement Initiated by a Remote Ionization Site

Fragmentation of the $M^{+\bullet}$ can occur at a location several atoms removed from the initial ionization site if the electron density in the intervening bonds can be rearranged easily to stabilize the charge. This is true for the γ-H rearrangement as well as for α-cleavage (Section 6.4.2). For example, the *m/z* 258 ion in the spectrum of Δ^9-tetrahydrocannabinol (THC, the biologically active constituent of

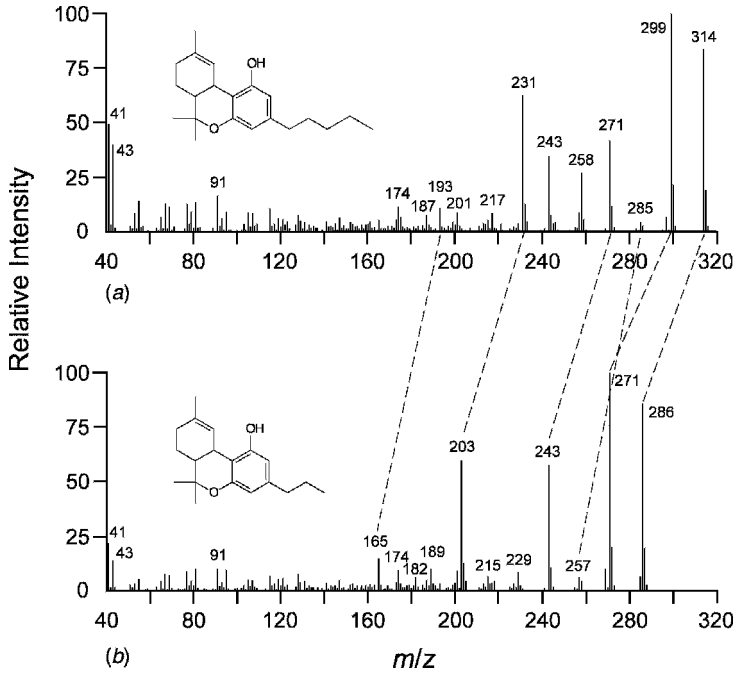

Figure 7.7. Mass spectra of (*a*) Δ^9-tetrahydrocannabinol and (*b*) tetrahydrocannabivarin. Note the correspondence between peaks in (*a*) that occur 28 *m/z* units lower in (*b*). All the ions represented by these peaks contain the entire alkyl side chain. The ion having *m/z* 258 in (*a*), which is due to the γ-hydrogen rearrangement, is not represented in (*b*).

DropBooks

marijuana) arises from just this type of fragmentation (Figure 7.7*a* and Equation 7.7). Initial ionization occurs preferentially at one of the O atoms, and the γ-H rearrangement involves substantial redistribution of the π-electron density.

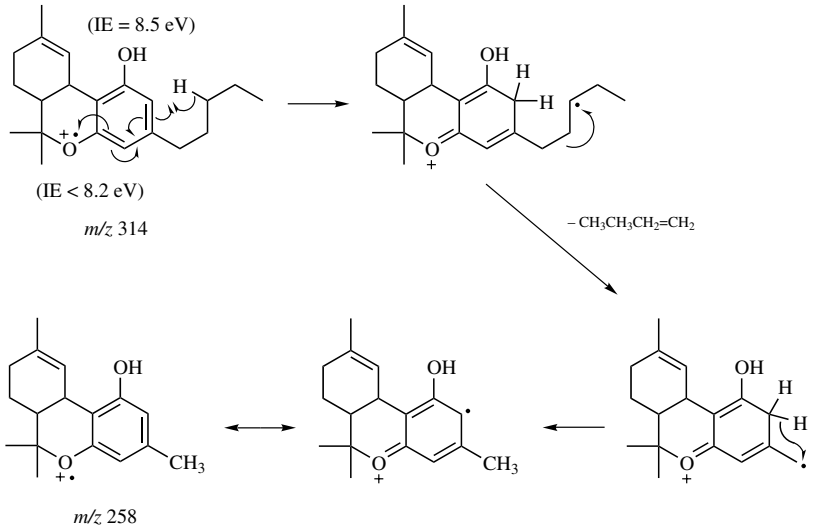

(7.7)

Support for the mechanism shown in Equation 7.7 comes from the spectrum of Δ^9-tetrahydrocannabivarin, a homolog of THC having a propyl side chain (Figure 7.7*b*; Smith, 1997). Most of the peaks at high *m/z* values in the spectrum of this compound occur at values 28 units below those observed in the spectrum of THC. These pairs of peaks, which are linked by the dotted lines in Figure 7.7, all represent ions in which the aliphatic side chain on the aromatic ring remains intact. The peak due to the γ-H rearrangement, however, should occur at the same *m/z* value in both spectra because all except one C atom of the aliphatic chain is lost in this fragmentation.

In the spectrum of Δ^9-tetrahydrocannabivarin, the peak at *m/z* 258 is much less intense than it is in the THC spectrum, consistent with the decreased propensity for propylbenzenes to undergo this rearrangement (Section 7.2.2). Indeed, the pattern of the weak peaks at *m/z* 257 and 258 in Figure 7.7*b* appears to correspond to that for the peaks at *m/z* 285 and 286 in the spectrum of THC.

A similar mechanism accounts for formation of the second largest fragment ion peak in the spectrum of capsaicin (Equation 7.8; see also Figure 6.16). In this case, the ''normal'' McLafferty rearrangement, which leads to the smaller peak at *m/z* 195, is less important because initial ionization should occur preferentially at the ring O atoms, rather than at the amide group.

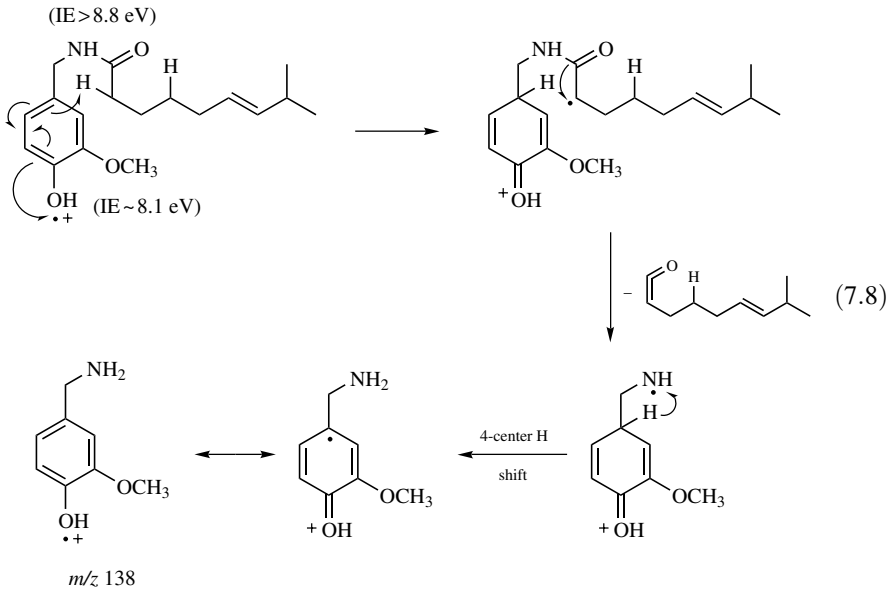

Example 7.1

Identify the compound that produced the spectrum shown in Figure 7.8.

Answer

(*Step 3*) The presence of a significant fragment ion peak at *m/z* 87 (M – 15) is consistent with the small peak at *m/z* 102 being the $M^{+\bullet}$ peak.

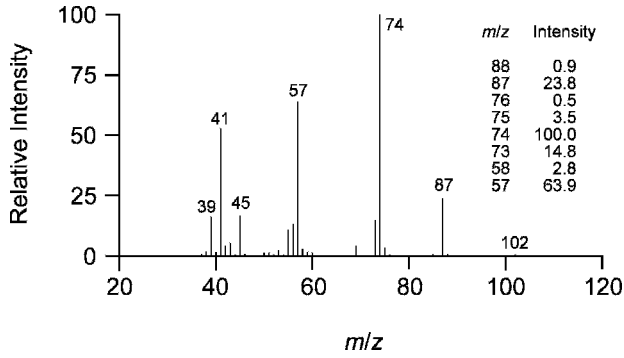

Figure 7.8. Mass spectrum for Example 7.1.

(*Step 4*) The apparent even MM and the fact that most of the important fragment ion peaks in the spectrum occur at odd *m/z* values indicates that N is absent.

(*Step 5*) It is unclear from the isotope peak intensities whether the ion having *m/z* 87 contains three or four C atoms ($0.9/23.8 = 3.8 \rightarrow 3.5$ C atoms). The fragment ion that produces the base peak at *m/z* 74 in the spectrum contains three C atoms. The ion having *m/z* 57 has four C atoms, which means that this ion is a butyl ion ($^{+}C_4H_9$). The lack of obvious A + 2 elements, as well as the apparent lack of N, indicates that the *m/z* 74 ion probably contains O in addition to C. Indeed, the contribution of three C atoms to the X + 2 peak at *m/z* 76 is only 0.05%, far less than the observed 0.5%. The presence of two O atoms in this ion, calculated from the isotope peak intensities ($2 \times 0.2\%$ per O atom = 0.4%), seems likely from an arithmetical standpoint [$(12 \times 3$ C atoms$) + (16 \times 2$ O atoms$) = 68$ u].

DropBooks

(*Steps 6 and 7*) The spectrum looks more like that of an aliphatic, rather than an aromatic, compound. The most consistent low-mass ion series is the one at *m/z* 43, 57, and 71, although the peaks at *m/z* 45, 59, 73, and 87 (all indicative of ions containing O; see Table 4.2) should not be overlooked.

(*Step 8*) The $M^{+\bullet}$ appears to lose $^{\bullet}CH_3$ fairly easily to produce the ion with *m/z* 87, which means that the location of this CH_3 group may be structurally significant. The peak at *m/z* 74 results from the loss of 28 u. In theory, this loss could be that of either CO or $CH_2{=}CH_2$, but the presence of a saturated butyl group as well as two O atoms in the molecule (which accounts for 89 u) makes the loss of $CH_2{=}CH_2$ more likely because the ion with *m/z* 74 still contains both O atoms.

(*Step 9*) The absence of N in the molecule means that the peak at *m/z* 74 is an $OE^{+\bullet}$ fragment ion and therefore must arise by means of a rearrangement fragmentation. A review of the material in this chapter will show that aliphatic carboxylic acids and their esters can produce intense $OE^{+\bullet}$ fragment ion peaks at *m/z* 60, 74, 88, and so on, due to the McLafferty rearrangement (Figure 7.3 and Equation 7.1). The presence of the base peak in this spectrum at *m/z* 74 not only indicates that the McLafferty rearrangement occurs and is important in the fragmentation of the $M^{+\bullet}$ of this unknown, but it also provides information about what arrangement of atoms is needed in order to produce a peak at that *m/z* value.

In order for the McLafferty rearrangement to take place as depicted in Equation 7.1 in the "acid half" of the $M^{+\bullet}$ of an aliphatic carboxylic acid, the aliphatic chain must contain at least three C atoms *in addition to* the carbonyl C atom.[2] This fact alone eliminates from consideration esters of acetic acid (CH_3CO_2R) and propanoic acid ($CH_3CR_2CO_2R'$, where R is H or CH_3) and leaves only derivatives of butanoic and pentanoic acids as possible structures. These possibilities can be limited further by their predicted behavior in the McLafferty rearrangement (Table 7.3). Two of these structures (pentanoic acid and 3-methylbutanoic acid) should produce peaks at *m/z* 60 during this fragmentation and thus can be eliminated. Other aspects of the spectrum must be used to distinguish the remaining two structures.

(*Step 10*) The second most intense peak in the spectrum shown in Figure 7.8 is the one at *m/z* 57, which was identified in Step 5 as representing a $^+C_4H_9$ ion. Of the two remaining structures, only 2-methylbutanoic acid has a butyl group that could account for the formation of this peak (Equation 7.9). The fact that this group is a *sec*-butyl group (IE − 7.3 eV) means that it will compete favorably for the charge during α-cleavage at the carbonyl group (the IE for the formation of $^+CO_2H$ is 8.6 eV).

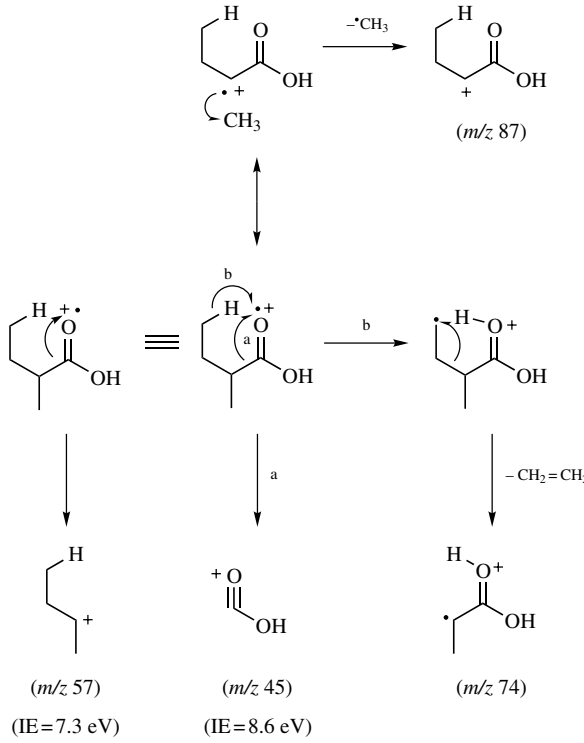

(7.9)

[2] Although the McLafferty rearrangement can involve H atoms in the "alcohol half" of the ester group, this is not a favored mode of fragmentation and does not lead to an intense peak in the spectrum (see Section 7.5).

Table 7.3. McLafferty rearrangement in possible structures for Example 7.1

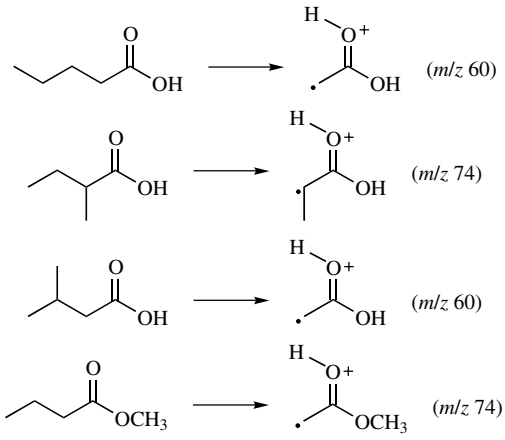

Based on the apparent structure, the loss of $^{\bullet}CH_3$ by the $M^{+\bullet}$ of this compound is somewhat unexpected. A more likely fragmentation would seem to be the loss of $^{\bullet}OH$ by α-cleavage to produce an ion having *m/z* 85. However, none of the acids having this MM produce a significant peak at *m/z* 85, yet all show a peak due to the loss of $^{\bullet}CH_3$. This behavior can be explained by the fact that the IEs for aliphatic carboxylic acids and alkanes are both in the range of 10–10.5 eV. Therefore,

DropBooks

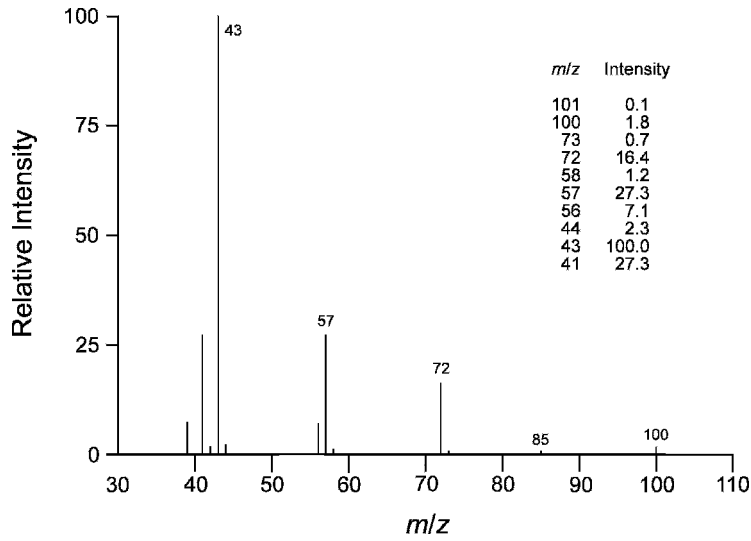

Figure 7.9. Mass spectrum for Problem 7.1.

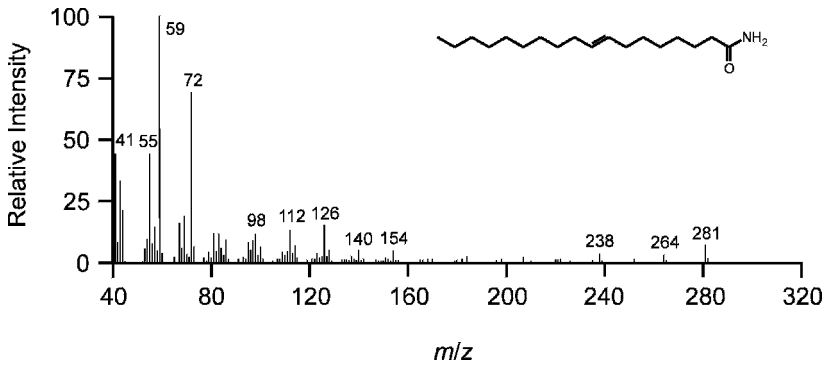

Figure 7.10. Mass spectrum of 8-octadecenamide (Problem 7.2).

ionization at one of the σ-bonds in the alkane portion of molecule competes well with ionization at the carbonyl group, and loss of $^{\bullet}CH_3$ by σ-bond cleavage leads to formation of a secondary carbenium ion.

7.1. Identify the compound that produced the spectrum shown in Figure 7.9.

7.2. 8-Octadecenamide, whose spectrum is shown in Figure 7.10, is one of several long-chain, unsaturated amides that are found when plastic bags are extracted with methanol. Account for formation of the base peak (*m/z* 59) in this spectrum.

7.3. CYCLOHEXANONE-TYPE REARRANGEMENT

The spectrum of cyclohexanone (Figure 7.11) has some features that may seem surprising. These include the peak at *m/z* 83, representing the loss of $^{\bullet}CH_3$, as well as those at *m/z* 80 (loss of water), *m/z* 70 (losses of $CH_2{=}CH_2$ and CO; as it turns out, *both* are lost), *m/z* 69 ($^{\bullet}CH_2CH_3$), and *m/z* 55 (either a propyl or an acetyl radical).

Cyclohexanone is a ketone in which the γ-H atoms are constrained by the ring structure from undergoing the McLafferty rearrangement. Hence, the most likely fragmentation to occur after initial ionization at the O atom is α-cleavage on either side of the carbonyl group. But because the carbonyl C atom is part of the ring, this cleavage involves no loss of mass. Other fragmentations must occur before ions are formed that are detectable by MS.

As with the McLafferty-type rearrangement (Section 7.2.1), determining a mechanism for formation of the base peak at *m/z* 55 involved studying the mass spectra of labeled derivatives—in this case, the three deuterated derivatives shown in Table 7.4. In interpreting the results of this study, it was assumed that, if all the D atoms were lost from a C atom during fragmentation, that C atom was lost as well.

In the spectrum of 2,2,6,6-tetradeuteriocyclohexanone, the base peak was found at *m/z* 56, a shift of 1, indicating that three of the four D atoms were lost in the

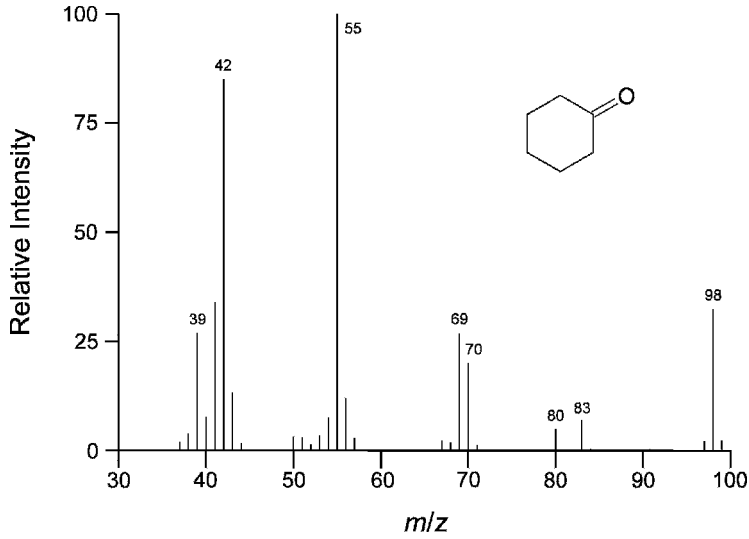

Figure 7.11. Mass spectrum of cyclohexanone.

fragmentation leading to its formation. At this point, it could not be determined if one or both of the C atoms containing these D atoms was lost as well. The spectrum of 3,3,5,5-tetradeuteriocyclohexanone had a base peak at *m/z* 57, consistent with the loss of two of the four D atoms. This indicated that either C3 or C5 (it does not matter which one; they are equivalent by symmetry) and its attached deuteriums were lost from the $M^{+\bullet}$ of this compound. Finally, the base peak in the spectrum of 4,4-dideuteriocyclohexanone occurred at *m/z* 55, signaling the loss of C4 and its attached D atoms.

DropBooks

The data in Table 7.4 support the following scenario: In forming the ion having *m/z* 55, C6 (or C2; they are equivalent) and its H atoms, C5 and its H atoms, C4 and

Table 7.4. Cyclohexanone rearrangement—deuterium labeling studies

	Base Peak		Base Peak
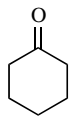	*m/z* 55	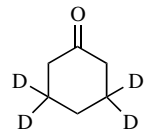	*m/z* 57 (2 of 4 D's retained)
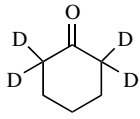	*m/z* 56 (only 1 of 4 D's retained)	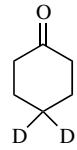	*m/z* 55 (both D's lost)

its H atoms, and one of the H atoms from C2 are lost—a total of three C atoms and seven H atoms. Carbon atoms 4, 5, and 6 and their attached H atoms are all contiguous, but loss of the H atom from C2 must still be explained. By analogy with fragmentations discussed previously, migration of •H from C2 to the primary radical site on C6 in the initially formed distonic ion can proceed through a six-atom cyclic intermediate to form a more stable secondary radical (Equation 7.10). The bond between C3 and C4 then breaks to form a propyl radical and an α-cleavage type ion that is stabilized by conjugation with the newly formed double bond.

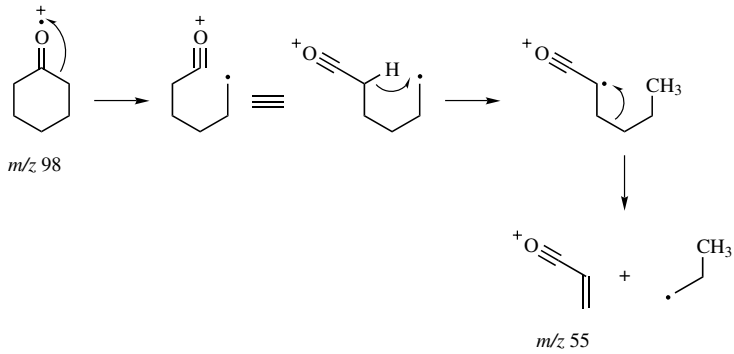

(7.10)

The remaining major fragmentations of cyclohexanone are also consistent with this mechanism (Figure 7.12). At the right of this figure, the radical formed after H rearrangement also can lose either $^{\bullet}CH_3$ or $^{\bullet}CH_2CH_3$ to produce the ions having *m/z* 83 and 69, respectively. Although the structures for the resulting ions are not known with certainty, both ion and radical products are less stable than those resulting from loss of propyl radical.

The distonic ion formed after α-cleavage can lose CO (path *a* in Figure 7.12) to give one of the ions having *m/z* 70 (two ions are seen at high resolution). This ion,

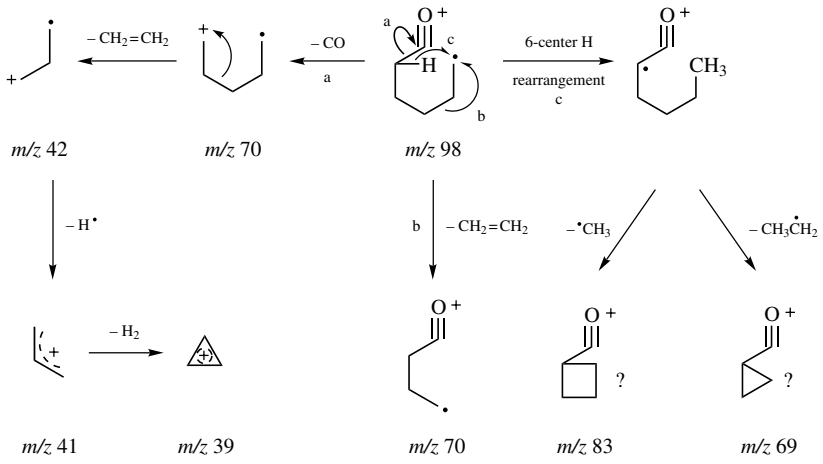

Figure 7.12. Fragmentations of cyclohexanone.

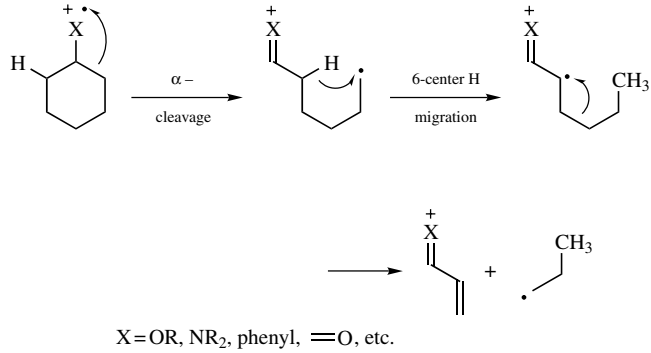

Figure 7.13. Generalized mechanism for the cyclohexanone-type rearrangement.

in turn, loses $CH_2{=}CH_2$ like other primary aliphatic ions (Equation 4.6) to produce the ion with *m/z* 42. Loss of $H^{\bullet}$ from the *m/z* 42 ion can produce the allyl ion (*m/z* 41), and loss of additional H atoms forms the aromatic cyclopropenium ion (*m/z* 39). An alternate fragmentation of the initially formed distonic ion involves direct loss of $CH_2{=}CH_2$ to form a second ion at *m/z* 70 (path *b* in Figure 7.12), which is nearly as stable as the initial intermediate. Once again, elimination of a small unsaturated molecule facilitates this fragmentation.

The cyclohexanone-type rearrangement also occurs in other cyclohexane derivatives. Because the initial step in this fragmentation is simply α-cleavage and the remaining steps do not involve direct involvement of the carbonyl O atom per se, any functional group capable of causing α-cleavage to occur within the ring should also initiate this rearrangement (Figure 7.13). The spectra of two other cyclohexane derivatives, methoxycyclohexane and dimethylaminocyclohexane (Figure 7.14), show base peaks resulting from cyclohexanone-type rearrangements (Equations 7.11 and 7.12).

DropBooks

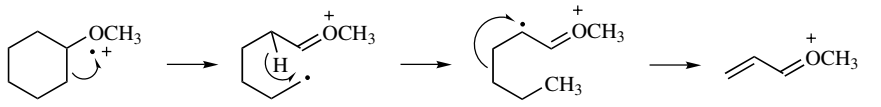

m/z 114 *m/z* 71

(7.11)

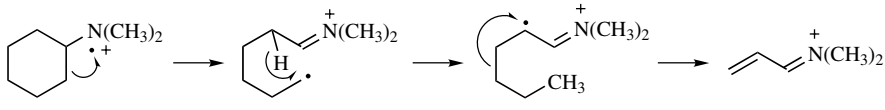

m/z 127 *m/z* 84

(7.12)

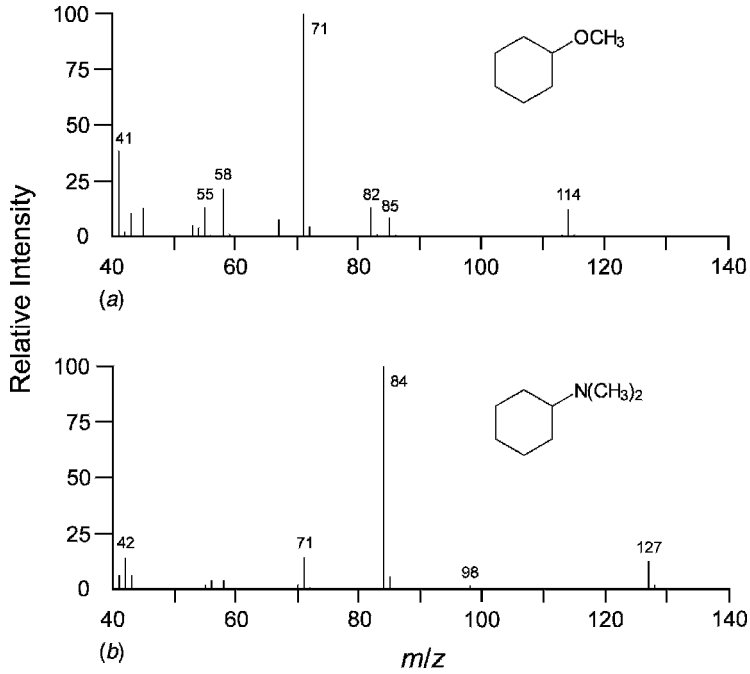

Figure 7.14. Mass spectra of two cyclohexane derivatives in which peaks resulting from the cyclohexanone-type rearrangement are the dominant feature: (*a*) methoxycyclohexane and (*b*) *N,N*-dimethylaminocyclohexane.

7.3. The mass spectrum of 4-methylcyclohexanol is shown in Figure 7.15. Write a mechanism to account for the formation of the base peak at *m/z* 57.

7.4. Except for the location of the $M^{+\bullet}$ peaks, the spectra of *N*-methyl- and *N*, 7-dimethyldecahydroquinoline (Figure 7.16) are extremely similar. Explain.

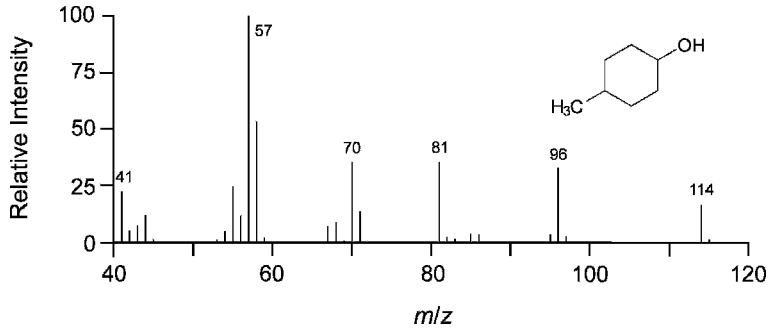

Figure 7.15. Mass spectrum of 4-methylcyclohexanol (Problem 7.3).

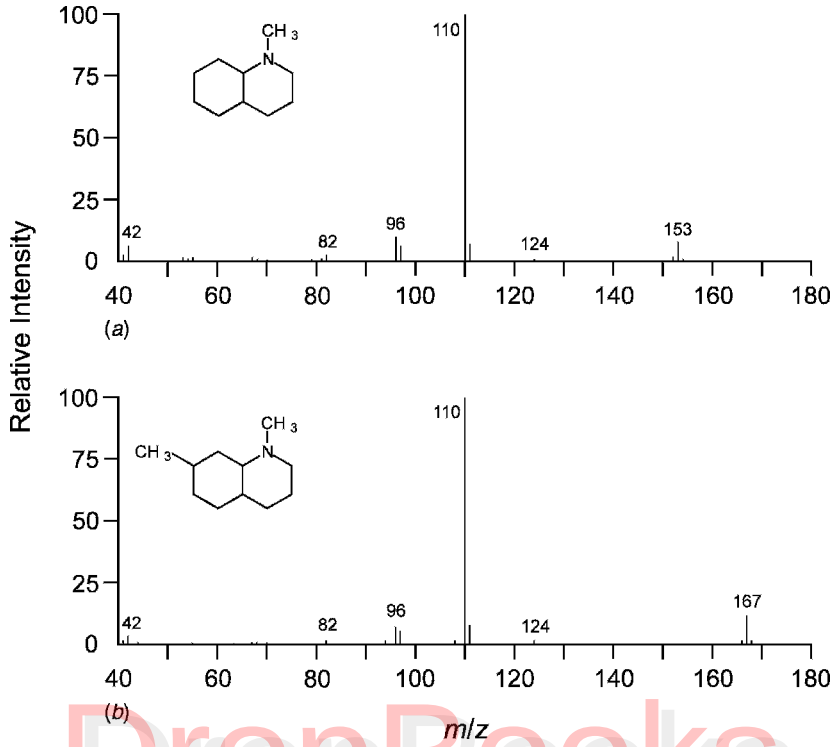

DropBooks

Figure 7.16. Mass spectra of *N*-methyl- and *N*,7-dimethyldecahydroquinoline (Problem 7.4).

7.4. RETRO DIELS–ALDER FRAGMENTATION

During the γ-hydrogen and cyclohexanone-type rearrangements, six-atom cyclic intermediates or transition states are formed. Compounds that already have six-membered rings containing one double bond (cyclohexene derivatives) may undergo a fragmentation in which the ring is cleaved to produce an olefin and a diene. The Diels–Alder reaction—the approximate reverse of this reaction in neutral molecules (Equation 7.13)—was named after the two chemists who won the Nobel Prize in 1950 for its utility in synthetic organic chemistry for constructing six-membered ring systems from noncyclic compounds.

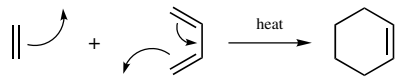

(7.13)

The retro Diels–Alder fragmentation may occur in compounds having hetero-atoms and complex ring structures. The energy factors that control this reaction

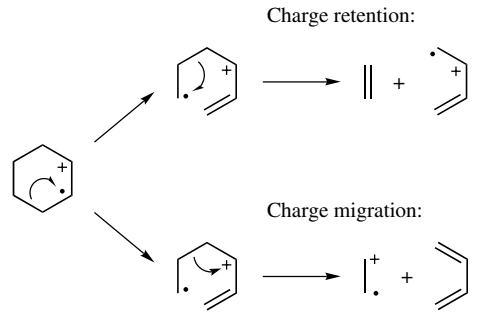

Figure 7.17. The retro Diels–Alder fragmentation can proceed either by charge retention or charge migration.

are sensitive to subtle structural changes and may produce a large peak in the spectrum of one compound, while a closely related compound may show little or no evidence at all for this fragmentation.

The retro Diels-Alder fragmentation can proceed via two different mechanisms (Figure 7.17). In both cases, initial ionization occurs at the double bond, followed by electron density redistribution in which the charge either is retained on the incipient diene fragment (charge retention) or transferred to the olefin product (charge migration). It is tempting to write out this fragmentation using double-headed arrows as a shorthand notation (Equation 7.14). Although the Diels-Alder reaction often proceeds in a concerted manner without the formation of intermediates, the retro Diels-Alder fragmentation nearly always does not. Understanding the outcome of this fragmentation for a specific compound may be difficult if both mechanisms and all possible intermediates are not considered.

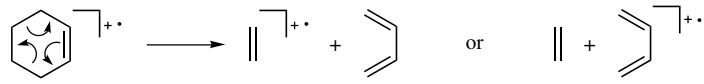

(7.14)

Limonene [1-methyl-4-(2-propenyl)cyclohexene], a terpene that is largely responsible for the characteristic odor of lemons, contains a cyclohexene ring having only alkyl substituents. The retro Diels-Alder fragmentation accounts for the base peak in its mass spectrum (Figure 7.18 and Equation 7.15). Because the $M^{+\bullet}$ essentially splits in half during this fragmentation, both the charge retention and charge migration mechanisms predict the same products.

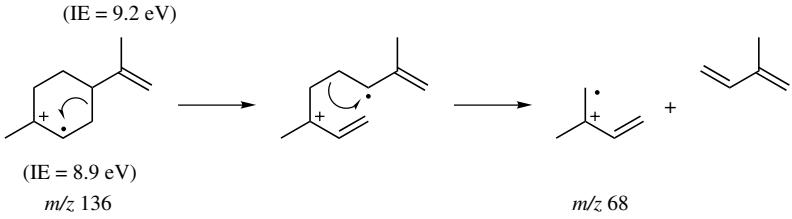

(7.15)

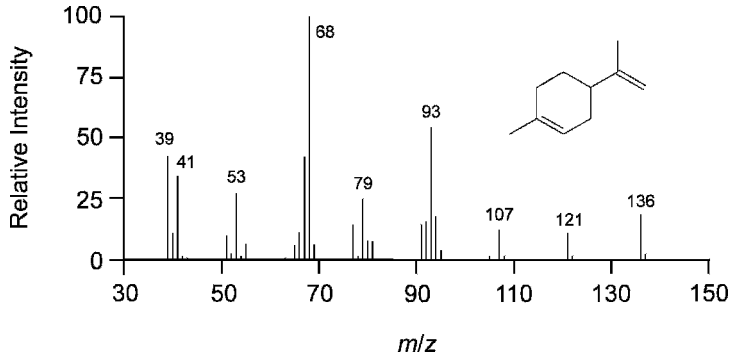

Figure 7.18. Mass spectrum of limonene. The retro Diels-Alder fragmentation accounts for the base peak in the spectrum.

The mass spectra of 3- and 4-phenylcyclohexene, on the other hand, show quite different responses to the retro Diels–Alder reaction (Figure 7.19). If mechanisms for these fragmentations were written only in shorthand form, one would predict that the 4-phenyl isomer should produce either butadiene (*m*/*z* 54) or styrene

DropBooks

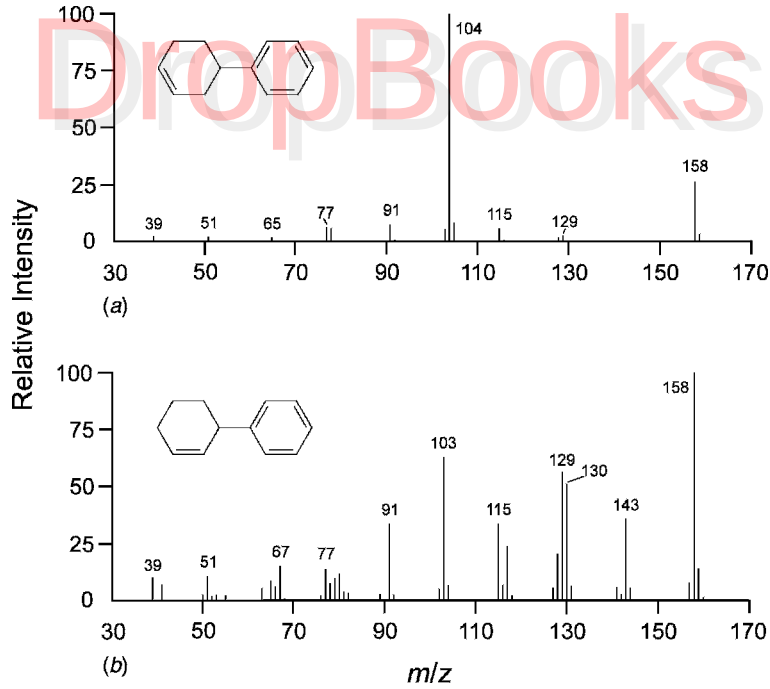

Figure 7.19. Mass spectra of (*a*) 4- and (*b*) 3-phenylcyclohexene. These compounds respond in different ways to the retro Diels–Alder fragmentation.

(*m*/*z* 104) $OE^{+\bullet}$ fragments, with the latter preferred because of its lower IE (Equation 7.16; see Stevenson's rule, Section 3.6.4).

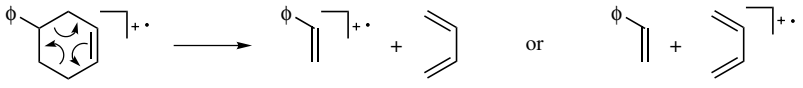

m/*z* 158 — *m*/*z* 104 (IE = 8.4 eV) — *m*/*z* 54 (IE = 9.1 eV) (7.16)

3-Phenylcyclohexene, on the other hand, should produce either ethylene (*m*/*z* 28) or 1-phenylbutadiene (*m*/*z* 130) $OE^{+\bullet}$ fragments, with the latter ion predominating (Equation 7.17). It is puzzling, then, why the *m*/*z* 104 peak dwarfs almost all the other peaks in the spectrum of the 4-phenyl isomer, but the *m*/*z* 130 peak in the spectrum of the 3-phenyl isomer is only one of many fragment ion peaks.

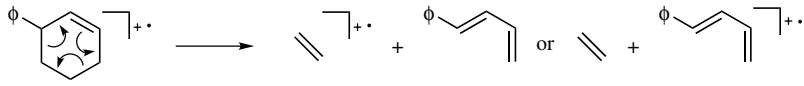

m/*z* 158 — *m*/*z* 28 (IE = 10.5 eV) — *m*/*z* 130 (IE < 8.4 eV) (7.17)

A closer examination of the fragmentation mechanisms helps clear up this confusion. Because the double bonds are not conjugated with the aromatic ring, ionization can occur in the cyclohexene ring (Table 3.1). In the case of 4-phenylcyclohexane, *m*/*z* 104 forms by charge migration because the charge in the product ion must be transferred from the double bond (the site of original ionization) to the opposite side of the cyclohexane ring. A charge retention mechanism is needed to account for the formation of the *m*/*z* 130 ion from the 3-phenyl isomer.

Ionization of the double bond can be written so that the charge is located on either C atom. Initial ionization as depicted in Equations 7.18 and 7.19 facilitates writing these mechanisms. In Equation 7.18, the first step of the rearrangement involves neutralization of the originally formed charge by heterolytic cleavage and relocation of the charge on the benzylic C atom. The other product formed in this step is an allylic radical, which also is resonance-stabilized.

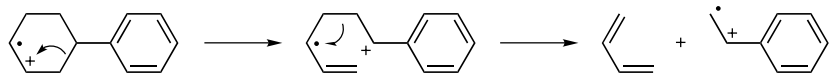

m/*z* 158 — *m*/*z* 104 (7.18)

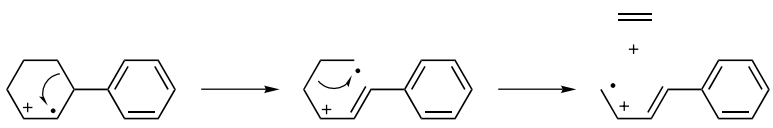

m/*z* 158 — *m*/*z* 130 (7.19)

On the other hand, the first step in the fragmentation of 3-phenylcyclohexene in Equation 7.19 produces an ion that is resonance-stabilized by extended conjugation, but it also produces a primary radical. Evidently the small amount of additional stabilization energy gained by extending the conjugation does not adequately compensate for the difference in energy between an allylic and a primary radical, so that formation of the *m/z* 104 ion from the $M^{+\bullet}$ of 4-phenylcyclohexene has a smaller energy requirement than formation of the ion at *m/z* 130 by the 3-phenyl isomer. Notice that, while Stevenson's rule predicts which fragment will retain the charge for each compound, it cannot predict the relative facility of the fragmentations between the two compounds. Only a comparison of the mechanisms can do that.

The retro Diels–Alder fragmentation can also be initiated by a remote ionization site, which often occurs in more complex molecules. The spectrum of cannabidiol, the biosynthetic precursor to Δ^9-THC in marijuana, exhibits few intense fragment ion peaks at high *m/z* values (Figure 7.20). Like limonene above (note the similarities in structure), the ion having *m/z* 246 results from the loss of 68 u from the $M^{+\bullet}$ by what formally appears to be charge retention retro Diels–Alder fragmentation. In this case, however, initial ionization should occur preferentially at one of the O atoms on the aromatic ring (Equation 7.20). The intermediate in this fragmentation is stabilized both by the charge on the O atom and the allylic radical. The $OE^{+\bullet}$ formed after loss of the molecule of isoprene should have stability at least comparable to that of the starting ion.

DropBooks

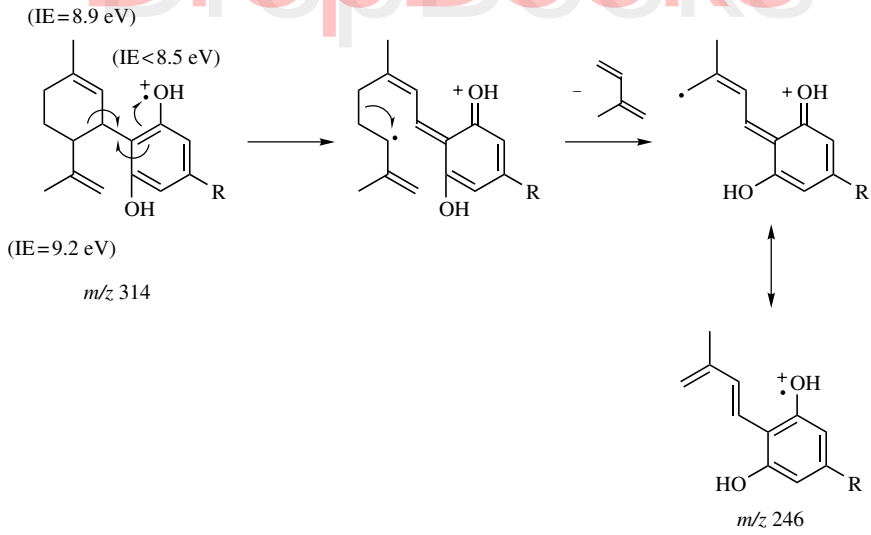

(7.20)

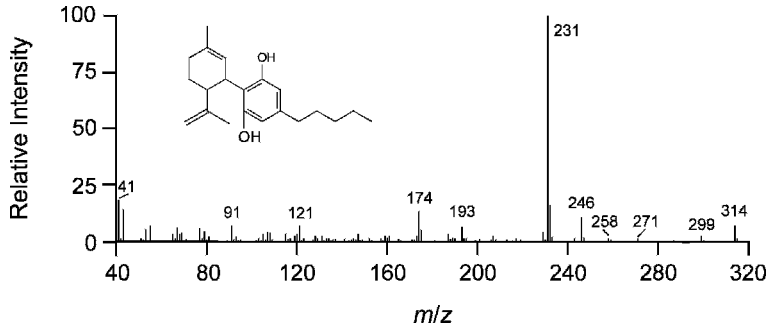

Figure 7.20. Mass spectrum of cannabidiol. The ion having *m/z* 246 results from a modified retro Diels–Alder fragmentation in which initial ionization probably occurs at one of the O atoms on the aromatic ring.

7.5. The spectra of 3- and 4-hydroxycyclohexene (Figure 7.21) are very different. Which spectrum goes with which isomer? Give a reason for your answer.

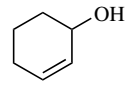

3-Hydroxycyclohexene

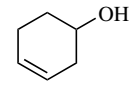

4-Hydroxycyclohexene

7.6. The first significant fragment ion peak observed in the mass spectrum of lysergic acid diethylamide (LSD; structure below) occurs at *m/z* 280, corresponding to the loss of 43 u from the $M^{+\bullet}$. Studies have shown that the fragmentation involves the loss of $H_2C{=}N{-}CH_3$ by what is formally a retro Diels-Alder fragmentation (Nigam and Holmes, 1969). However, the IE for ionization at the tertiary amine group (<8.0 eV) is lower than that for the double bond in the cyclohexene ring (which is conjugated with the aromatic ring; IE ~8.4 eV). Assuming that initial ionization occurs at the N atom of the tertiary amine group, write a mechanism that accounts for this loss.

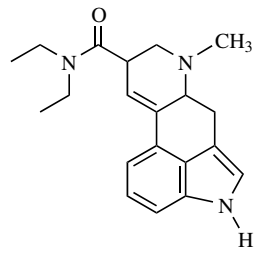

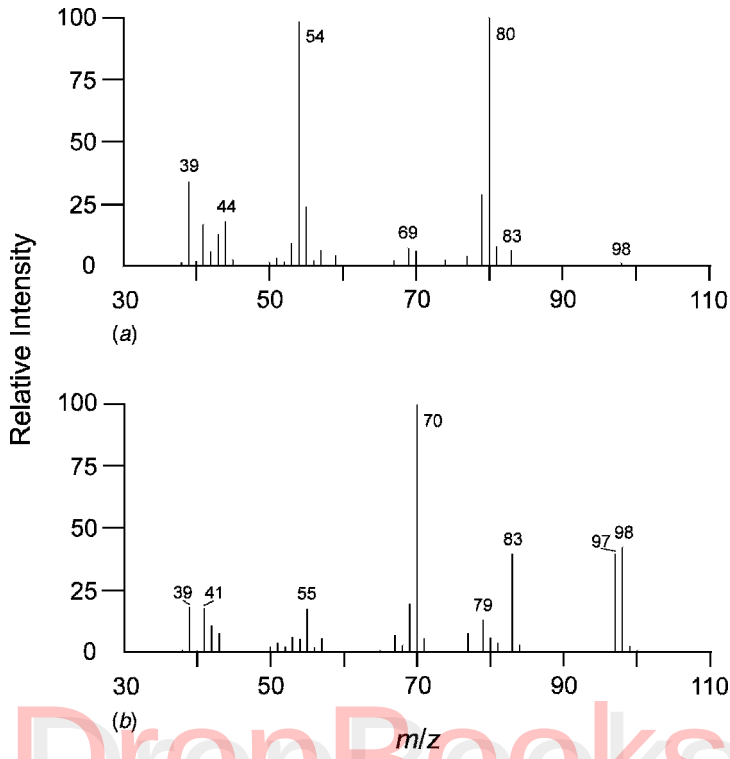

Figure 7.21. Mass spectra for Problem 7.5.

DropBooks

7.5. DOUBLE-HYDROGEN (McLAFFERTY + 1) REARRANGEMENT

Not all mass spectral rearrangements proceed via transition states or intermediates that involve rings of four or six atoms. In the spectrum of butyl palmitate (Figure 7.22), the ions resulting from the McLafferty rearrangement (*m/z* 116 and 256; Equation 7.2) account for only a small proportion of the total fragmentation. Instead, the major fragment ion at high mass has *m/z* 257, one *m/z* unit higher than that of the ion produced by the McLafferty rearrangement on the ester side of the carbonyl group.

The fragmentation that produces this ion is characteristic of esters and amides that are derived from alcohols and amines having aliphatic chains at least three C atoms long. Because it involves the migration of *two* H atoms and proceeds through the same distonic ion intermediate as that formed during the McLafferty rearrangement, it is known both as the double-hydrogen rearrangement and the

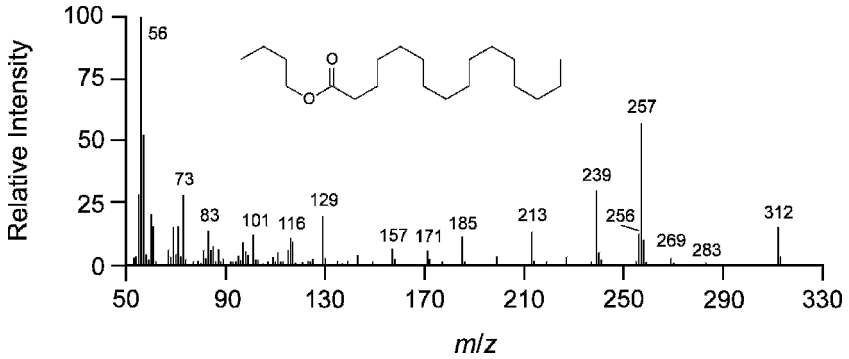

Figure 7.22. Mass spectrum of butyl palmitate. The peak at *m/z* 257 results from the double-H (McLafferty + 1) rearrangement.

McLafferty + 1 rearrangement (McLafferty and Tureček, 1993). The migration of the second H atom is somewhat unusual in that it involves formation of a five-atom cyclic transition state (Equation 7.21). Both the ion and radical products are resonance-stabilized. The base peak in the spectrum at *m/z* 56 is the result of heterolytic cleavage from the intermediate distonic ion.

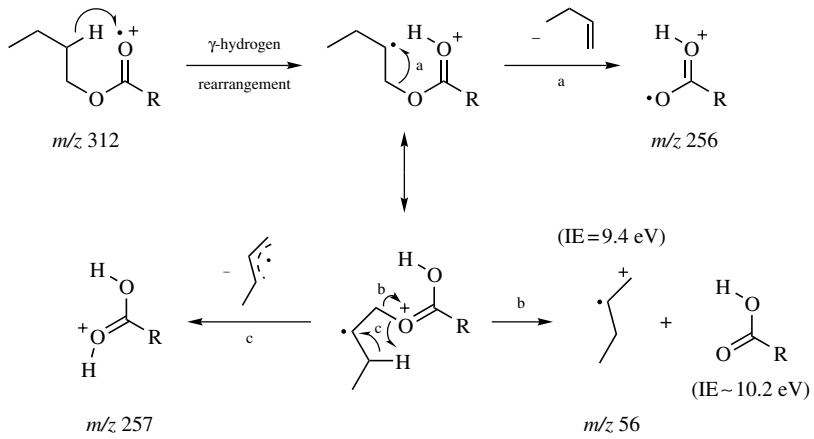

(7.21)

In the spectra of acetate esters of aliphatic alcohols, this rearrangement produces a characteristic, if not particularly intense, peak at *m/z* 61. This is seen in the spectrum of isoamyl acetate (Figure 7.23 and Equation 7.22), a compound well known for its characteristic banana odor. The peak at *m/z* 43 in this spectrum represents the

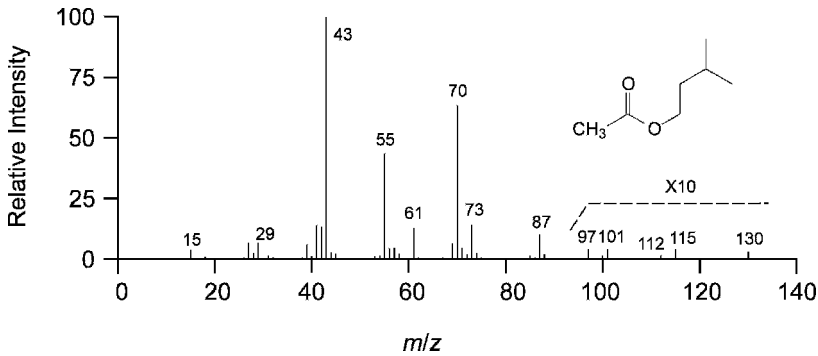

Figure 7.23. Mass spectrum of isoamyl acetate. The intensities of the peaks at high *m*/*z* values are increased by a factor of 10.

acylium ion, formed by α-cleavage at the carbonyl group. The peak at *m*/*z* 70 is the result of heterolytic cleavage from the intermediate distonic ion.

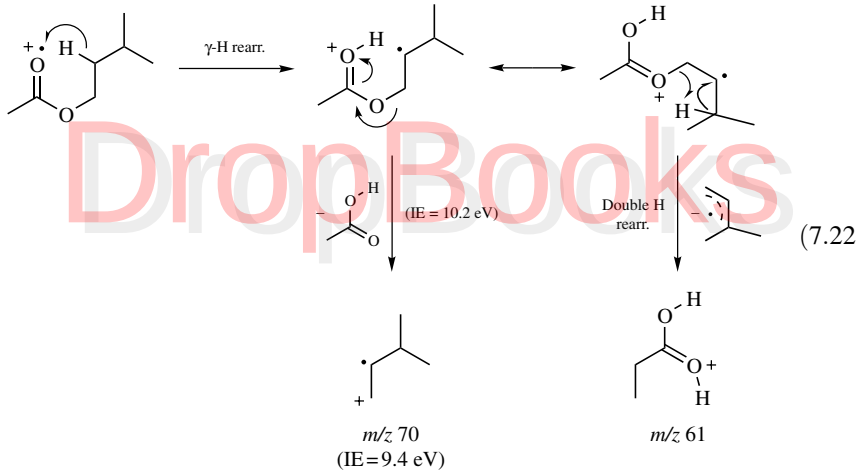

(7.22)

DropBooks

ADDITIONAL PROBLEMS

7.7. Identify the compound whose spectrum is shown in Figure 7.24. (*Hint*: The peak at *m*/*z* 94 corresponds to the $M^{+\bullet}$. The peak at *m*/*z* 91 in this spectrum is unusual in that it occurs at M − 3.)

7.8. The spectrum of *N*,*N*-dicyclohexylamine (Figure 7.25) exhibits primarily two fragment ion peaks: at *m*/*z* 138 and 56. Write mechanisms showing how these ions, as well as the ion represented by the weak peak at *m*/*z* 152, are formed.

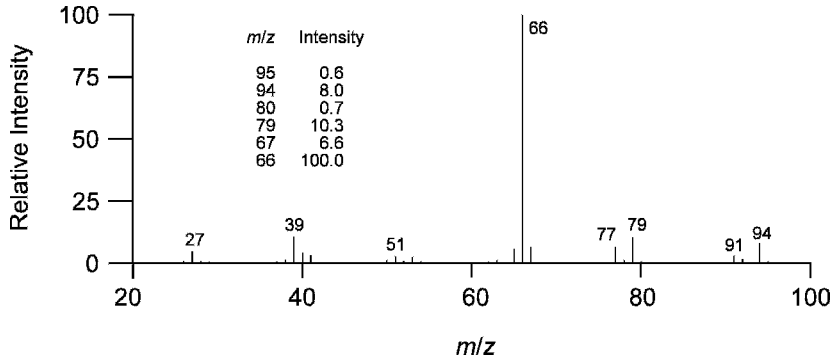

Figure 7.24. Mass spectrum for Problem 7.7.

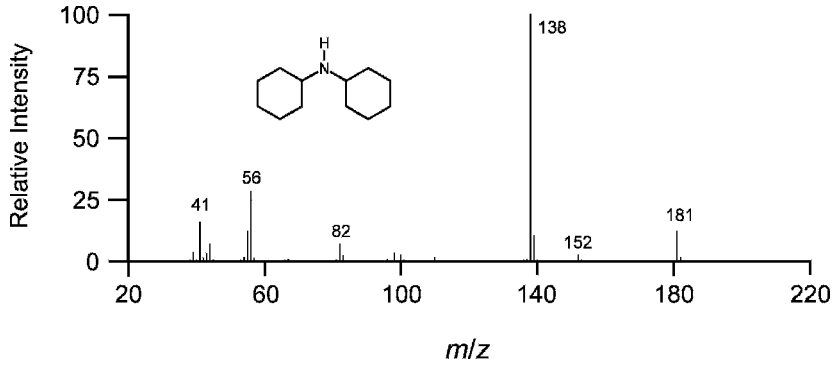

Figure 7.25. Mass spectrum of *N,N*-dicyclohexylamine (Problem 7.8).

REFERENCES

F. W. McLafferty and F. Tureček, *Interpretation of Mass Spectra*, 4th edition (University Science Books, Mill Valley, CA, 1993), p. 81.

I. C. Nigam and J. L. Holmes, "Mass Spectrometry of Lysergic Acid Diethylamide," *J. Pharm. Sci.*, **58**, 506–507 (1969).

R. M. Smith, "Identification of Butyl Cannabinoids in Marijuana," *J. Foren. Sci.*, **42**, 610–618 (1997).

8

RATIONALIZING MASS SPECTRAL FRAGMENTATIONS

8.1. GENERAL GUIDELINES

DropBooks

The fragmentation of an organic compound in EIMS results from the excess energy left over after formation of the $M^{+\bullet}$ (Section 3.3). Because initial ionization can take place at different sites in many molecules, more than one $M^{+\bullet}$ for a compound may be formed. Fragmentation of these $M^{+\bullet}$ can occur through several different reaction pathways.

In most cases, it is difficult to predict what the mass spectrum of a given compound is going to look like. There are simply too many factors to be taken into account. Most mass spectra contain peaks from unexpected fragmentations. These must be rationalized after the fact, and nearly always without help from independent studies such as deuterium labeling. Writing mechanisms for simple mass spectral fragmentations can be straightforward; many examples have been presented so far in this book. Rationalizing the fragmentations of ions having complex structures, however, can demand insight and ingenuity.

It is possible, nonetheless, to set down some general guidelines for devising creative, yet realistic, fragmentation mechanisms. Most of these concepts have been developed in previous chapters (e.g., see the examples and problems in Chapter 3), but it is worthwhile to summarize them here. A condensed version of these

Understanding Mass Spectra: A Basic Approach, *Second Edition*. By R. Martin Smith
ISBN 0-471-42949-X © 2004 John Wiley & Sons, Inc.

Table 8.1. Guidelines for writing fragmentation mechanisms

1. Verify the masses of precursor and product ions as well as those of each intermediate.
2. Identify atom groupings in the precursor ion that can generate the observed loss.
3. Locate a reasonable site for initial ionization.
4. Postulate only intramolecular reactions.
5. Break the most labile (electron-poor) bonds first.
6. Do not overlook electronic arrangements that allow bond cleavage at locations removed from the initial ionization site.
7. Balance charges and electrons for each step of the fragmentation sequence.
8. Remember that mechanisms for forming abundant ions (especially those with high mass) usually involve few steps and result in a single fragment ion and a neutral particle (radical or molecule).
9. Rank ion products according to their relative stabilities. If ionic products have similar stabilities, then rank the stabilities of radical products. Relative stability in both cases follows the approximate order

$$H < CH_3 < CH_3CH_2 < n\text{-alkyl} < \text{secondary} < \text{allyl} < \text{tertiary} < \text{benzyl}$$

10. Start with the fragmentations discussed in this book, especially those that can produce small unsaturated molecules or in which the charge can be stabilized by conjugation or on a heteroatom.
11. Look for H atoms that can migrate easily.
12. Use different resonance structures if one structure does not work.

guidelines is found in Table 8.1, which is duplicated inside the back cover of this book. In the remainder of this chapter, these guidelines will be applied to several specific examples.

1. Verify the masses of precursor and product ions as well as those of each intermediate. Errors in arithmetic may account for more mistakes in mass spectral interpretation than any other single factor. From the difference in mass between the precursor and product ions, determine the numeric value of the neutral loss. Compare this value with those for common neutral losses listed in Table 4.1. If more than one group can account for the observed numeric loss, try to determine which loss seems more reasonable, based on the expected behavior of the precursor ion.

2. Look carefully at the precursor ion for structural arrangements that can produce the group of atoms that is lost. Sometimes these may be obvious (as with the loss of CO, e.g.). In other cases, more resourcefulness may be necessary.

3. Locate the most likely site for initial ionization. Consult a table of IEs such as that in Table 3.1. If the difference in IE between competing sites in a molecule is small, ionization will occur at more than one site. Compounds with heteroatoms tend to ionize by loss of an electron from the *n*-orbital(s) of the heteroatom(s), and compounds having double bonds or aromatic rings by loss of one of the π-electrons. Initial ionization by loss of σ-electrons will occur only in

saturated alkanes or if highly electronegative groups are present in an aliphatic molecule (Chapter 3).

4. Remember that only *intramolecular* reactions (those involving unimolecular decomposition of the precursor ion) are allowed in EIMS.

5. Bonds that are electron-poor (located in the vicinity of electronegative atoms) are broken most easily. α-Cleavage (Chapter 6) is an excellent example of a fragmentation that takes advantage of this fact.

6. If the group that appears to be lost is relatively distant from the charge or radical site, look for ways to reorganize electrons in order to allow the proposed fragmentation to occur. For this to happen, the ionization and cleavage sites must be connected by one or more double bonds or through the σ-bonds of a complex ring system. Some examples are shown in Equations 6.13, 6.14, 7.7, 7.8, and 9.6.

7. Balance charges and electrons for each step of a fragmentation sequence. Losing or gaining an electron is an easy way to get off the correct reaction path. Determine which fragment ends up with the charge, and note whether a charge retention or charge migration mechanism must be invoked to account for the charge location (Chapter 3).

8. As a general rule, the formation of abundant ions (especially those with high *m*/*z* values) involves few steps. Exceptions may occur if the ring structure of the molecule is so complex that simple fragmentations lead only to isomeric ionic structures, not to actual fragmentation (Figure 6.13, e.g.). Mechanisms that require many intermediates usually have greater energy demands than those that do not, and are therefore less likely to occur (Chapter 3).

DropBooks

9. The relative stability of ionic products, which can be predicted using Stevenson's rule (Section 3.6.4), tends to be more important than that of radical products. However, if ionic products have similar stabilities, the relative stability of the radicals takes precedence. In both cases, relative stability follows the approximate order

$$H < CH_3 < CH_3CH_2 < n\text{-alkyl} < \text{secondary} < \text{allyl} < \text{tertiary} < \text{benzyl}$$

10. The fragmentations and rearrangements discussed in this book, because of their simplicity and general applicability, should be considered as starting points and patterns for mechanism writing. Two prominent categories include

a. Loss of small, unsaturated molecules with concurrent formation of an ion that is at least as stable as the precursor ion (Section 6.5, e.g.); and

b. Fragmentations in which the charge is stabilized either by conjugation with one or more double bonds or an aromatic system, or on a heteroatom.

11. Hydrogen atoms migrate easily. The energy demands of rearranging a H atom from one site to another is often so low that short-term decreases in ion stability are tolerated if the overall sequence forms stable ion and radical products. Although H migration occurs preferably via five- and six-atom cyclic transition states for entropic reasons, other ring sizes are tolerated if the enthalpy gain is large enough (Chapter 3).

12. When one resonance structure does not give the desired result, try another one. This can include ring openings and closings that have parallels in solution chemistry, such as

a. Benzyl → tropylium

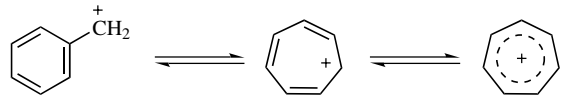

(8.1)

b. Benzene $OE^{+\bullet}$ → bicyclo[2.2.0]hexadiene (“Dewar” benzene) $OE^{+\bullet}$

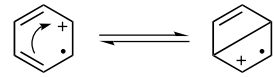

(8.2)

c. Unsaturated seven-membered rings → bicyclo[4.1.0]heptyl systems

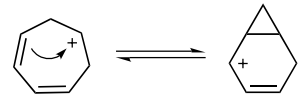

(8.3)

d. Unsaturated eight-membered rings → bicyclo[4.2.0]octyl systems

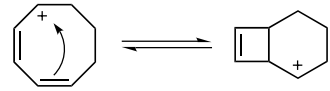

(8.4)

e. Keto/enol equilibrium

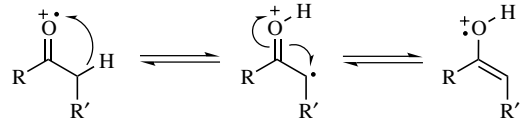

(8.5)

8.2. LOSS OF SMALL MOLECULES

8.2.1. Loss of Small Molecules from Aromatic Ions Revisited

The examples in the rest of this chapter will apply the guidelines in the previous section to a number of specific examples. One place to begin is to look closer at the mechanisms by which small molecules are lost from aromatic ions (Section 4.1.2).

Benzyl Ion Series. The benzyl low-mass ion series consists of peaks representing the benzyl ion (*m*/*z* 91), cyclopentadienyl ion (*m*/*z* 65), and cyclopropenium ion (*m*/*z* 39). Each of the lower-mass ions is formed by loss of HC≡CH from the

next higher-mass ion (Figure 4.5). Five of the C atoms in the benzyl ion have only one H atom attached to them, so it is fairly easy to envisage the loss of HC≡CH as a contiguous two-carbon unit from the ring with the attached H atoms. However, it is easier to account for the structures of the resulting ion products if the loss is depicted as occurring from a cycloheptatrienyl (tropylium) ion, which can be attained using the equilibrium shown in Equation 8.1.

The losses of HC≡CH can then be rationalized as a series of steps involving isolation of a H—C—C—H unit within a cyclobutene ring using equilibria similar to those shown in Equations 8.2 through 8.4, followed by charge-induced fragmentation with loss of HC≡CH (Equation 8.6). The overall sequence is driven by formation of the aromatic cyclopropenium ion and the two new π-bonds in the expelled molecules of HC≡CH.

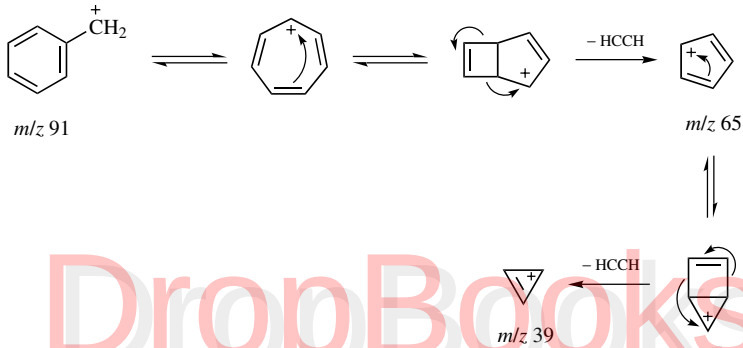

(8.6)

DropBooks

Pyridine. A similar mechanism can be envisioned for the loss of HCN from the $M^{+\bullet}$ of pyridine (Equation 8.7; see Figure 4.6*a*). As in the example just discussed, the H—C—N sequence of atoms already exists in the precursor ion, so that no rearrangement of atoms is needed to account for the loss. After initial ionization at the N atom, the first step in this mechanism serves to isolate the H—C—N linkage from the rest of the molecule. This is accomplished by formation of a bicyclo[2.2.0]hexa-2,5-diene (''Dewar benzene'') intermediate (Equation 8.2). Subsequently, homolytic cleavage of the bond between the N and C2 of the ring keeps the charge on the N, but moves the radical site to the cyclobutene ring. Heterolytic cleavage of the bond between C5 and C6 of the original ring completes the loss of a neutral molecule of HCN (IE = 13.6 eV; Table 3.1) and moves the charge to the resulting cyclobutadiene ring (IE ~ 9.4 eV).

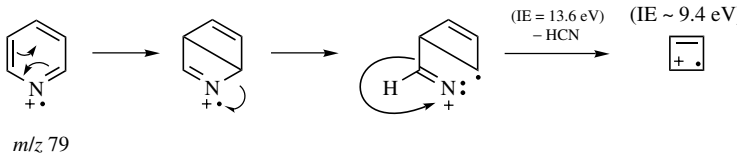

(8.7)

Phenol. The loss of CO from the phenol $M^{+\bullet}$ can be rationalized as shown in Equation 8.8 (Beynon et al., 1968; see Figure 4.6*b*). In order to lose CO, the H atom must be removed from the phenolic O, and the aromatic ring must be opened. The first step can be accomplished by interconversion between the *enol* form of phenol and its tautomeric *keto* form via a 4-center H migration (Equation 8.5). This equilibrium normally lies far to the left (>99% enol) due to the resonance energy of the aromatic ring. However, any reaction that disturbs the equilibrium by removing the keto form (such as the proposed fragmentation) will cause further formation of the keto form, driving the fragmentation until the enol form is consumed (LeChatlier's principle).

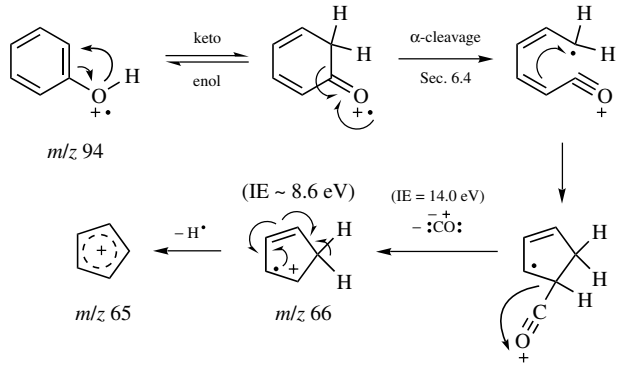

(8.8)

The second step in this fragmentation involves α-cleavage next to the carbonyl group, with stabilization of the charge on the carbonyl O atom and formation of an allylic radical. Although CO could arguably be lost at this point, generation of a potentially more stable ion in a ring seems more appealing. To accomplish this, the double bond nearest the carbonyl group donates one electron to form a new C—C single bond, the five-membered ring closes, and an equally stable allylic radical site is generated. The charge remains on the carbonyl O. Finally, heterolytic cleavage of the C—C bond between the ring and the carbonyl group moves the electron pair onto the carbonyl C atom, expelling a neutral molecule of CO (IE = 14.0 eV; Table 3.1) and forming the cyclopentadiene $OE^{+\bullet}$ (*m*/*z* 66; Equation 8.8; IE = 8.6 eV). The cyclopentadienyl ion (*m*/*z* 65) can form by $H^{\bullet}$ loss from the ion having *m*/*z* 66.

8.2.2. γ-Butyrolactone

γ-Butyrolactone (GBL) is formed by reversible dehydration of 4-hydroxybutyric acid (γ-hydroxybutyric acid; GHB). GBL occurs naturally at low concentrations in various wines (Vose et al., 2001) and is used as an industrial cleaning solvent. It is also a metabolic precursor of the "date rape" drug GHB. The mass spectrum of GBL is shown in Figure 8.1.

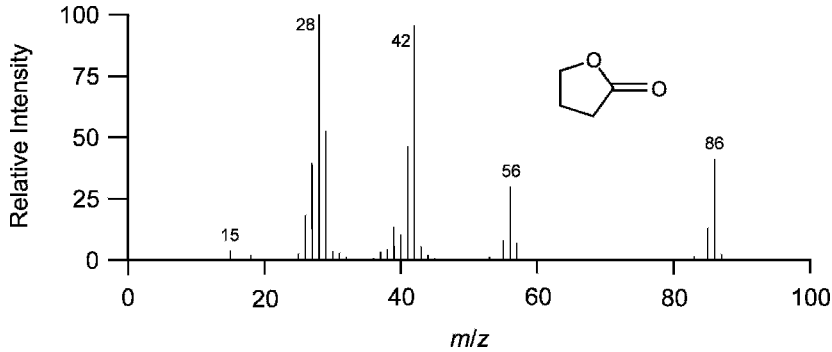

Figure 8.1. Mass spectrum of γ-butyrolactone (GBL; adapted with permission from Vose et al., 2001. Copyright ASTM International).

The mass spectrum of GBL shows major fragment ion peaks at *m/z* 85, 56, 42, and 28, corresponding to neutral losses of 1, 30, 44, and 56, respectively. By referring to Table 4.1 and the structure of this compound, the first three losses appear to be those of $^{\bullet}H$, formaldehyde ($H_2C{=}O$), and CO_2. The ion(s) having *m/z* 28 could be either $H_2{}^{\bullet}C{-}C^{+}H_2$ or $CO^{+\bullet}$ or both. Because all four functionalities occur in GBL without rearrangement of any atoms (see structure below), their formation could be fairly straightforward.

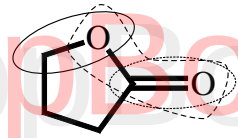

DropBooks

A good way to begin rationalizing this or any fragmentation scheme is to ask the question, "What is this molecule expected to do?" Because GBL contains a carbonyl group, initial ionization should occur by loss of one of the *n* electrons on the carbonyl O. α-Cleavage on either side of the carbonyl group (Figure 8.2) produces two isomeric distonic ions. Both distonic ions have the charge on the carbonyl O atom—one having the radical site on the α C atom (path *a*), the other with the radical site on the ring O atom (path *b*). These ions each contain groups whose facile loss explains the major fragmentations.

The distonic ion formed by path *a* has the radical site located on the α C atom. In order for CO_2 to be lost from this ion, the charge must be moved from the O atom to the ring C atoms. To accomplish this, heterolytic cleavage between the γ C atom and the ring O atom must occur as shown at the left of Figure 8.2. This produces the ion with *m/z* 42, which in turn can lose $^{\bullet}H$ to generate the resonance-stabilized allyl ion having *m/z* 41. This behavior is typical of ions containing only C and H (look, e.g., at peaks at low *m/z* values in the spectra in Figures 4.7 and 4.9).

The distonic ion formed by path *b* in Figure 8.2 has two options that are reasonable. First, the loss of $^{\bullet}H$ from the γ C atom forms a new C—O π-bond and produces the ion having *m/z* 85 (path *c*). In the second option, $H_2C{=}O$ is lost through homolytic cleavage of the bond between the β and γ carbons, forming the ion with *m/z* 56

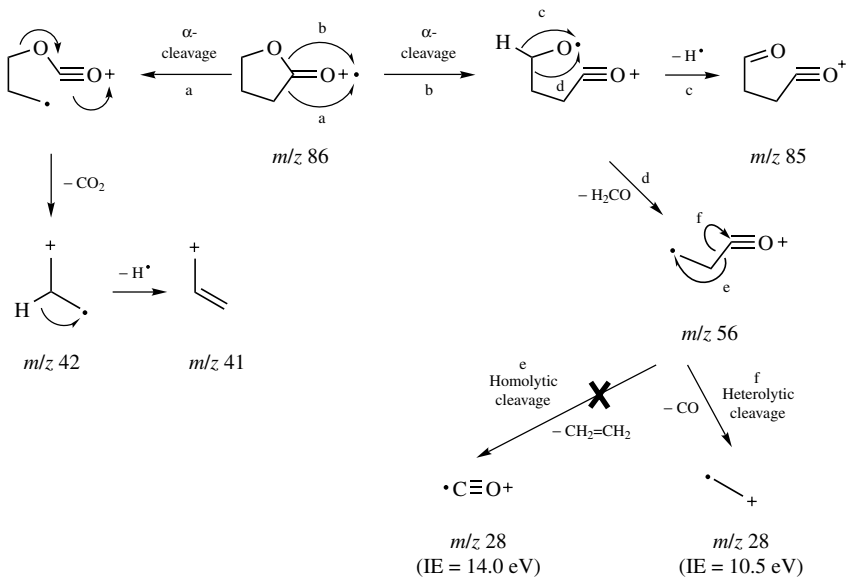

Figure 8.2. Proposed fragmentations of γ-butyrolactone (GBL).

and a new π-bond in the expelled molecule of $H_2C{=}O$ (Figure 8.2, path *d*). The resulting *m/z* 56 ion, in turn, can cleave the bond between the carbonyl and α C atoms either homolytically or heterolytically to form an $OE^{+\bullet}$ fragment having *m/z* 28. In the first case ethylene and $CO^{+\bullet}$ are formed (Figure 8.2, path *e*), whereas in the second case CO and $H_2{}^{\bullet}C{-}C^{+}H_2$ are produced (Figure 8.2, path *f*). Because the IE of ethylene is substantially lower than that of CO, Stevenson's rule predicts that CO and $H_2{}^{\bullet}C{-}C^{+}H_2$ should be formed.

8.1. The mass spectrum of bicyclo[2.2.2]oct-2-en-5-ol (Figure 8.3) shows only two major fragment ion peaks at *m/z* 80 (100%) and 79 (64%). Rationalize the formation of the two ions represented by these peaks.

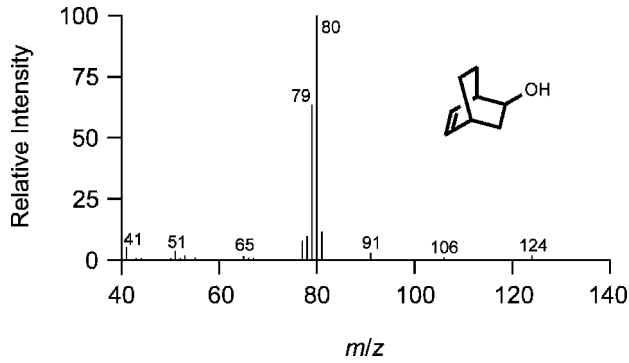

Figure 8.3. Mass spectrum of bicyclo[2.2.2]oct-2-en-5-ol (Problem 8.1).

8.3. EPHEDRINE

A more complex example is ephedrine, a stimulant and a precursor in the illicit manufacture of methamphetamine. The mass spectrum of ephedrine (Figure 8.4*a*) is similar to those of the more potent stimulants methcathinone and methamphetamine (Figures 8.4*b* and *c*, respectively), with which it shares a common carbon skeleton.

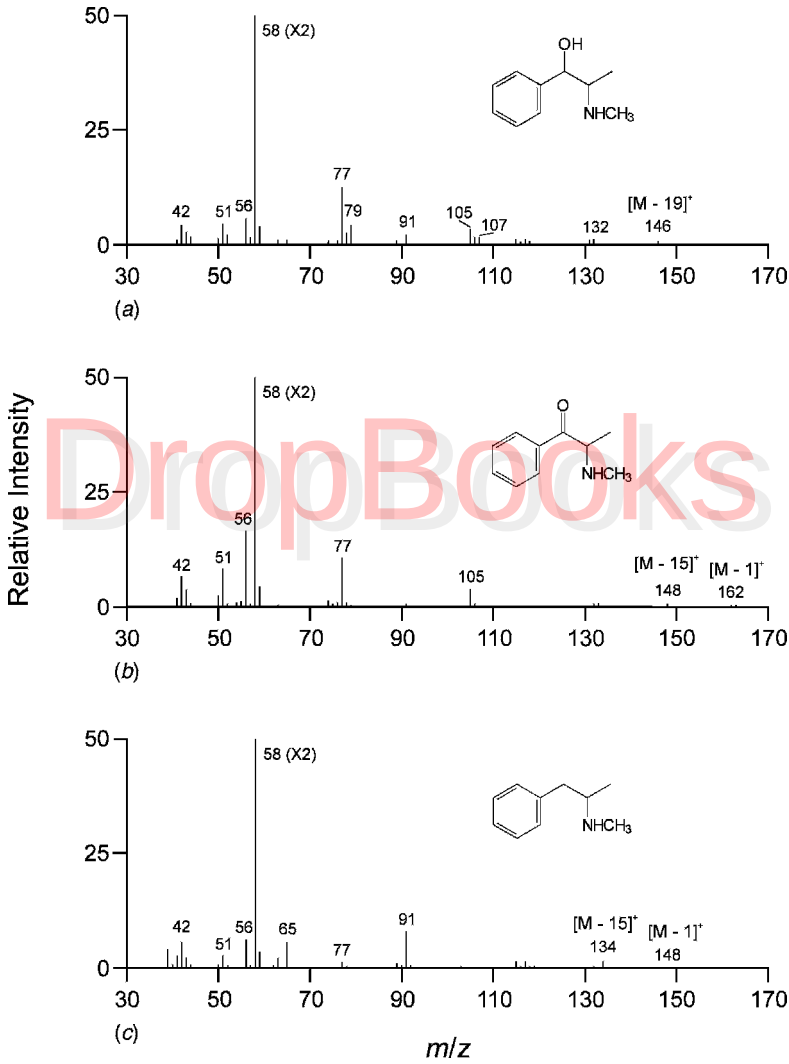

DropBooks

Figure 8.4. Mass spectra of three closely related stimulants: (*a*) ephedrine, (*b*) methcathinone, and (*c*) methamphetamine. The intensity scales in all three spectra have been expanded by a factor of 2.

The fragmentation of all three compounds is dominated by α-cleavage next to the N atom to give the intense peak at *m/z* 58 (Equation 8.9). At high *m/z* values, however, these spectra are quite different from one another. None of the three spectra exhibit a $M^{+\bullet}$ peak, and the α-cleavage losses of $^{\bullet}H$ and $^{\bullet}CH_3$ that are represented in the methcathinone and methamphetamine spectra (see Equation 6.5) are not observed in the ephedrine spectrum. Instead, the small peak at *m/z* 146, which is reproducible from spectrum to spectrum, represents a loss of 19(!!) from the $M^{+\bullet}$. The other peak resulting from α-cleavage (*m/z* 107) is somewhat overshadowed by the peaks at *m/z* 106 and 105 as well as by those at *m/z* 77–79.

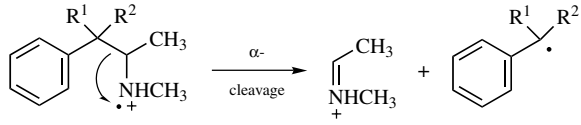

(8.9)

R^1 = OH, R^2 = H (ephedrine) *m/z* 58
R^1, R^2 = O (methcathinone)
R^1 = R^2 = H (methamphetamine)

m/z 146 and 132. Ephedrine does not contain fluorine, so that the loss of 19 u is not likely to occur easily in one step. Two losses are worth considering—one involving the loss of $^{\bullet}NH_2$ or NH_3 combined with the loss of either three or two H atoms, and the second involving loss of $^{\bullet}OH$ and two H atoms. Although methamphetamine loses $CH_3NH^{\bullet}$ to produce the low abundance ions at *m/z* 115–119 (Equation 8.10), the loss of $^{\bullet}NH_2$ or NH_3 (which would involve multiple rearrangements) is not observed. Therefore, there is no reason to think that ephedrine would lose either of these fragments.

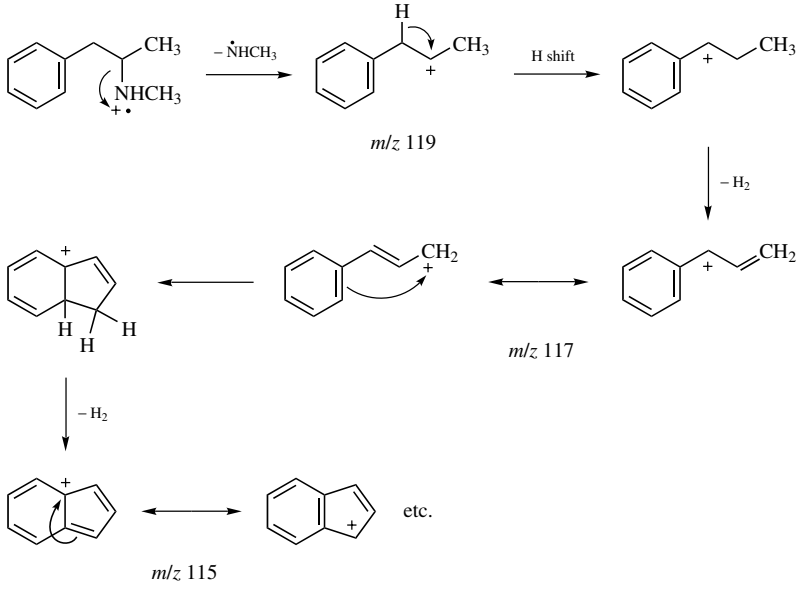

(8.10)

Ephedrine has alternatives for fragmentation that methamphetamine and methcathinone do not have because the OH group on the benzylic C atom is a better candidate for loss than either the similarly located H atoms in methamphetamine or the carbonyl O atom in methcathinone. What happens after initial ionization, however, is not immediately clear because several scenarios for loss of $^{\bullet}OH$ or H_2O are plausible. What has to be kept in mind is that there must be some energetic inducement for ephedrine to deviate from the fragmentation paths taken by methamphetamine and methcathinone. This probably means that the ion resulting from any alternate path has a more stable structure than those that can be formed easily by the other two compounds.

Such a structure can be achieved through initial loss of $^{\bullet}OH$ by benzylic cleavage after ionization in the aromatic ring, followed by ring formation and charge stabilization on the N (Equation 8.11). The resulting ion (*m/z* 148) is not observed in the spectrum, but instead loses $^{\bullet}H$ in order to restore aromaticity to the ring. The ion with *m/z* 147 then can lose either $^{\bullet}H$ or $^{\bullet}CH_3$ from the C atom adjacent to the N atom to produce the ions having *m/z* 146 and 132, respectively. Both these ions have the charge on a quaternary N atom and also contain a double bond in the five-membered ring that is conjugated with the π-system in the aromatic ring. The relative intensities of the *m/z* 146 and 132 peaks reflect the relative stabilities of the $^{\bullet}H$ and $^{\bullet}CH_3$, respectively, that are lost.

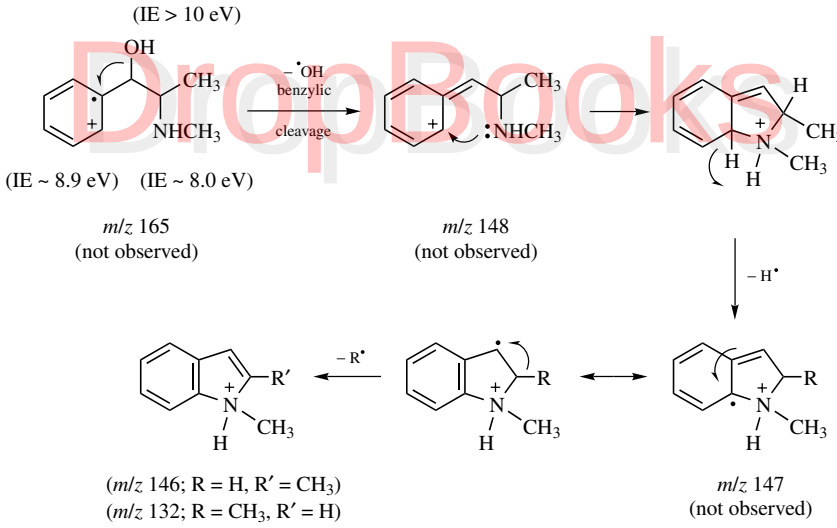

(8.11)

Why is this path followed in the fragmentation of ephedrine instead of the "normal" α-cleavage losses of $^{\bullet}H$ and $^{\bullet}CH_3$? The answer seems to lie in the benzylic OH group, which because of its electronegativity should *destabilize* the ions formed if $^{\bullet}H$ or $^{\bullet}CH_3$ are lost from the C atom next to the N atom. Methcathinone also has an O atom on the benzylic C atom, but this O atom cannot be lost because it is tied up in a carbonyl group. As a result, the intensities of the peaks that are produced by

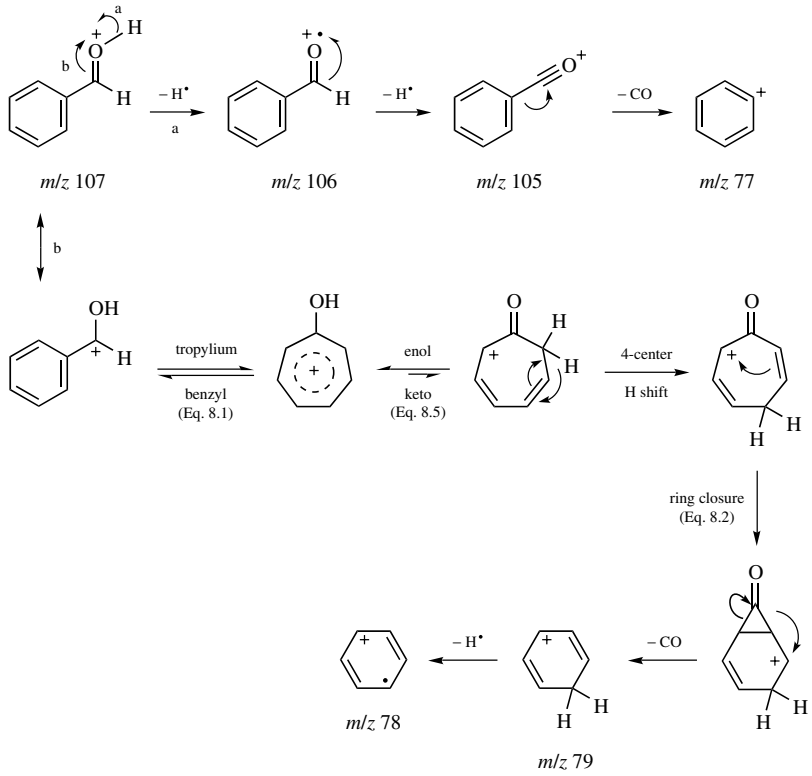

Figure 8.5. Proposed fragmentations of the hydroxybenzyl ion (*m/z* 107) from ephedrine.

losses of •H and •CH_3 in the spectrum of methcathinone are weaker in intensity than the corresponding peaks in the methamphetamine spectrum, which lacks the electronegative substituent on the benzylic C atom.

m/z 107 and 79. The hydroxybenzyl ion (*m/z* 107) can be formed by benzylic cleavage after initial ionization in the aromatic ring (Equation 8.12). Loss of •H from this ion produces the benzaldehyde radical ion (*m/z* 106), which can in turn lose another •H to form the benzoyl ion (*m/z* 105; Figure 8.5). Although formation of the phenyl ion (*m/z* 77) by loss of CO from the benzoyl ion is an expected fragmentation (see Figure 4.5), the ions with *m/z* 78 and 79 are more difficult to explain because the spectrum of benzaldehyde (Figure 6.21*b*) does not contain peaks representing either of these ions.

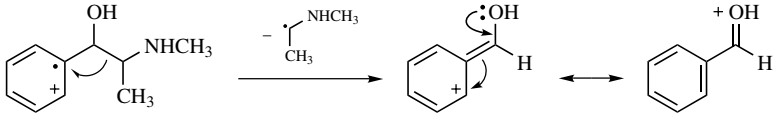

(8.12)

The ion having *m/z* 79 can be produced by the loss of CO from the *m/z* 107 ion, although rearrangement of H atoms from both the O and adjacent C atoms must occur prior to this loss. Loss of ethylene from the *m/z* 107 ion seems unlikely because aromatic ions prefer to lose acetylene instead; see Figure 4.5). Three rearrangements described in Section 8.1 help rationalize this loss. First, the *m/z* 107 ion has two other forms that are useful. One is a resonance form that has the charge located on the benzylic C atom, and the second, because of the equilibrium that exists between benzylic ions and their cycloheptatrienyl counterparts (Equation 8.1), is the hydroxytropylium ion (Figure 8.5). The hydroxytropylium ion, containing an ''aromatic'' hydroxyl group, is similar to phenol and, as such, is in equilibrium with its keto form by means of a 4-center H shift (compare Equations 8.5 and 8.8). These equilibria effectively transfer the H atoms away from the O atom and its adjacent C atom to other parts of the ion. Even though the keto form is much less stable than the enol form due to the loss of aromatic resonance energy, this equilibrium will constantly be disturbed by the irreversible formation of other ion products.

Loss of CO might proceed directly from the keto form or as shown in Figure 8.5. The 4-center shift of a H atom, followed by closure of the unsaturated seven-membered ring to form a bicyclo[4.1.0]heptenyl ion (compare Equation 8.3), isolates the CO-producing moiety. Cleavage of the strained cyclopropanone ring then yields the desired result. The ion with *m/z* 79 is unstable toward $^{\bullet}H$ loss to give $C_6H_6^{+\bullet}$ (*m/z* 78). Further loss of $^{\bullet}H$ to produce the more abundant phenyl ion seems unlikely because $C_6H_6^{+\bullet}$ does this inefficiently (see Figure 4.15*a*).

DropBooks

8.2. Write mechanisms for formation of the ions that correspond to the peaks at *m/z* 148, 105, 77, 58, and 51 in the spectrum of methcathinone (Figure 8.4*b*). Are the mass spectra of methamphetamine, methcathinone, and ephedrine different enough to allow their identification by mass spectrometry?

8.3. Cathine, one of the alkaloids from the plant *Catha edulis*, has the structure and spectrum shown in Figure 8.6. Write mechanisms for formation of the ions represented by the peaks at *m/z* 134, 132, 118, 107, 105, 79, 78, 77, and 44. Some alternative schemes for explaining the fragmentations of ephedrine fail because they cannot explain the similarities in the spectra of these two compounds.

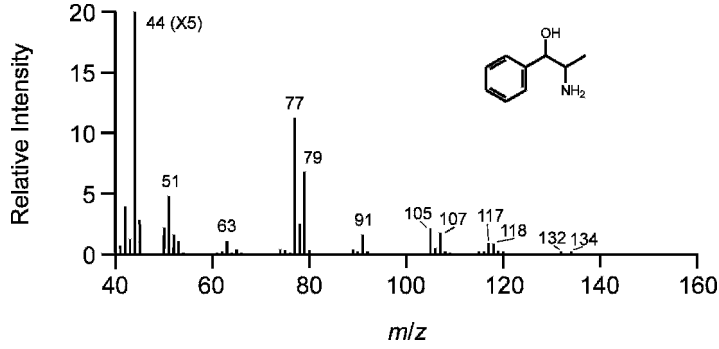

Figure 8.6. Mass spectrum of cathine (Problem 8.3).

8.4. *ORTHO* EFFECT: THE HYDROXYBENZOIC ACIDS

The spectra of *m*- and *p*-hydroxybenzoic acid (Figures 8.7*b* and *c*) are similar to one another. Although there are small differences in the relative intensities of peaks throughout the spectra, all the major peaks occur at the same *m*/*z* values. The same is not true for the spectrum of *o*-hydroxybenzoic acid (salicylic acid; Figure 8.7*a*).

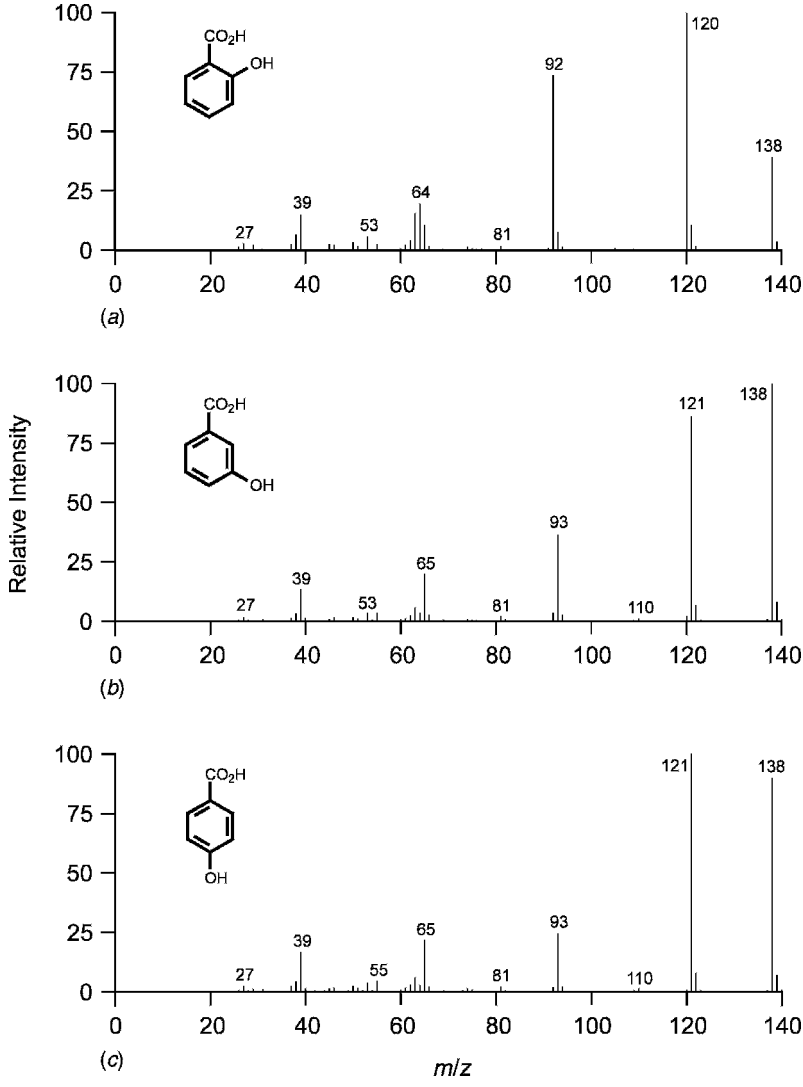

Figure 8.7. Mass spectrum of *o*-hydroxybenzoic acid (*a*) is different from those of *m*- (*b*) and *p*-hydroxybenzoic acid (*c*), due to interactions that are possible between the substituents in the *ortho*-isomer (*ortho* effect).

Whereas all the major peaks in the spectra of the *m*- and *p*-isomers occur at odd *m/z* values, indicating that they correspond to EE^+, *m/z* values for the high-mass peaks in the spectrum of the *o*-isomer are even, which means that these peaks correspond to $OE^{+\bullet}$. The reason for this difference is that the proximity of two functional groups which are *ortho*- to one another allows them to interact in ways that are not possible in the *meta*- and *para*-isomers. This *ortho effect* frequently occurs in benzene derivatives that have more than one substituent.

The spectra of *m*- and *p*-hydroxybenzoic acid are explainable in terms of previously discussed fragmentations (Equation 8.13). Although the values in Table 3.1 predict that initial ionization should occur at the O atom of the OH group, the orbitals on all three O atoms are interconnected through the π-electron system of the aromatic ring and the carbonyl group. Therefore, initial ionization can be depicted as occurring on any of the O atoms. For convenience, the carbonyl O atom is chosen. The ion having *m/z* 121 is formed by α-cleavage loss of $^{\bullet}OH$ from next to the carbonyl group. In the *p*-isomer, the charge in the resulting ion is stabilized not only on the carbonyl O atom, but also by the O atom in the OH group (Equation 8.13, Structure A). A resonance form similar to structure A is not possible if the OH group is in the *meta* position, which may explain why the relative intensities of the $M^{+\bullet}$ peak and the peak at *m/z* 121 in the spectra of the *m*- and *p*-isomers are reversed. The *m/z* 121 ion loses CO by heterolytic cleavage to yield the phenolic ion having *m/z* 93, which in turn loses CO in a manner analogous to that observed for phenol to give the cyclopentadienyl ion (*m/z* 65; see Equation 8.8).

DropBooks

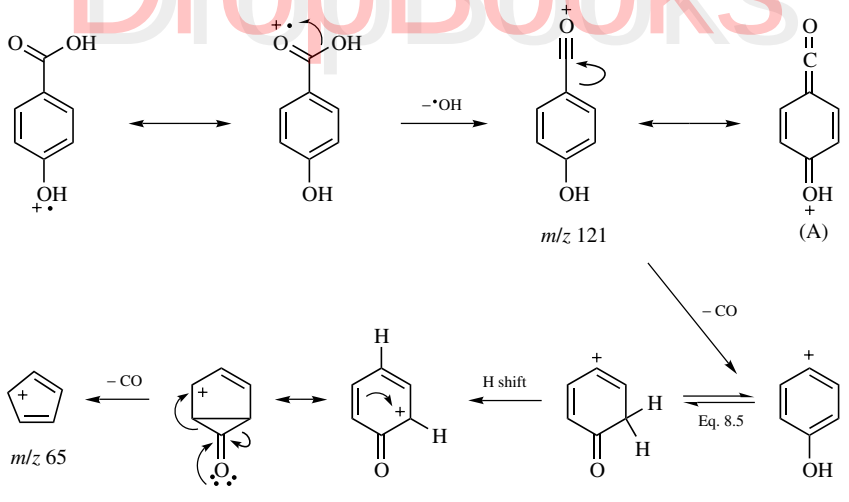

(8.13)

As with the other two isomers, initial ionization for the *o*-isomer can be depicted as occurring on any of the O atoms. In this case, it is convenient to place the initial

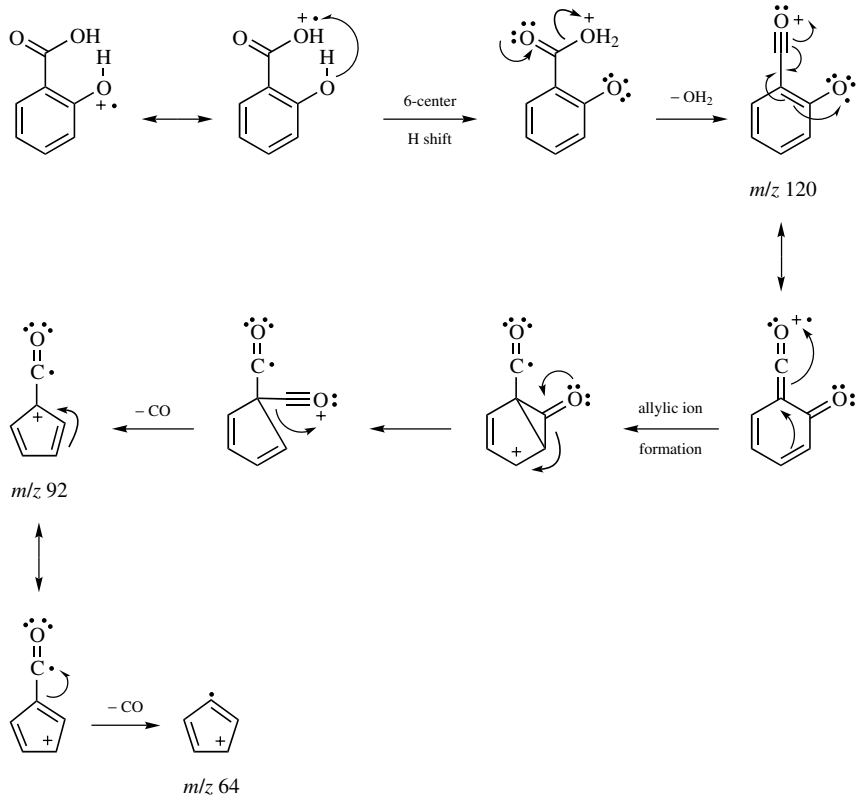

Figure 8.8. Proposed high-mass fragmentations of *o*-hydroxybenzoic acid.

charge and radical sites on the O atom in the OH of the acid group (Figure 8.8). The loss of 18 u from the $M^{+\bullet}$ of the *o*-isomer to produce the ion with *m*/*z* 120 is that of a molecule of water (Beynon et al., 1968). Because the acid and hydroxy groups are close to one another in this compound, it is possible to transfer a H atom from the OH group on the ring to the initial radical site by means of a six-atom cyclic intermediate. Heterolytic cleavage, with charge stabilization on the carbonyl O atom, causes the loss of a molecule of water.

The resonance form that is shown at the upper right of Figure 8.8 for the ion with *m*/*z* 120 is not convenient for rationalizing subsequent losses from this ion. Relocation of the radical site to the carbonyl O atom, followed by formation of a bicyclo[3.1.0]hexane ring structure in which the charge is stabilized as an allylic ion (compare Equation 8.3), serves to isolate both of the groups that can potentially be lost as CO. Loss of the first molecule of CO as shown in the middle of Figure 8.8 produces the $OE^{+\bullet}$ fragment ion having *m*/*z* 92. This ion, in turn, loses a second molecule of CO to yield another $OE^{+\bullet}$ ion—this one with *m*/*z* 64. Although other rationalizations can be used to explain the loss of the two molecules of CO, those

illustrated in Figure 8.8 are similar to fragmentations that have been discussed previously in this book.

Examples of losses due to the *ortho* effect are seen in other compounds as well. For instance, the intense *m/z* 149 peak observed in the spectra of phthalate plasticizers is formed in this way (Equation 8.14; Beynon et al., 1968). The loss of $^{\bullet}OH$ from the $M^{+\bullet}$ to produce the base peak in the spectrum of the explosive 2,4,6-trinitrotoluene (TNT) offers an example from perhaps a more exciting compound (Equation 8.15). Notice that, despite the presence of a formal positive charge on the N atom and a formal negative charge on the O atom in the nitro group (this is true for each of the nitro groups), the ion has a net overall single positive charge and one unpaired electron. The production of this highly delocalized ion is so favored energetically that the $M^{+\bullet}$ peak is not observed in the spectrum.

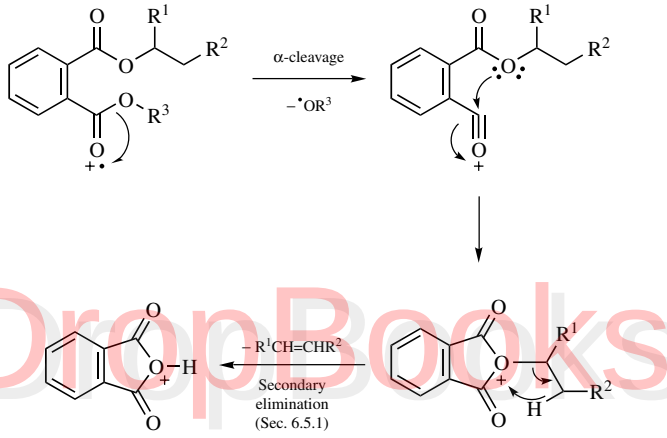

(8.14)

(*m/z* 149)

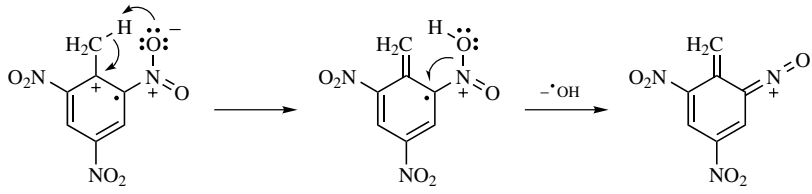

(8.15)

(*m/z* 227; not obs.)

(*m/z* 210; 100%)

DropBooks

ADDITIONAL PROBLEMS

8.4. Identify the common pain reliever whose spectrum is shown in Figure 8.9.

8.5. The spectra of methyl 3,5-dimethylbenzoate and methyl 2,5-dimethylbenzoate (Figure 8.10) both have base peaks at *m/z* 133 that represent the loss of $^{\bullet}OCH_3$

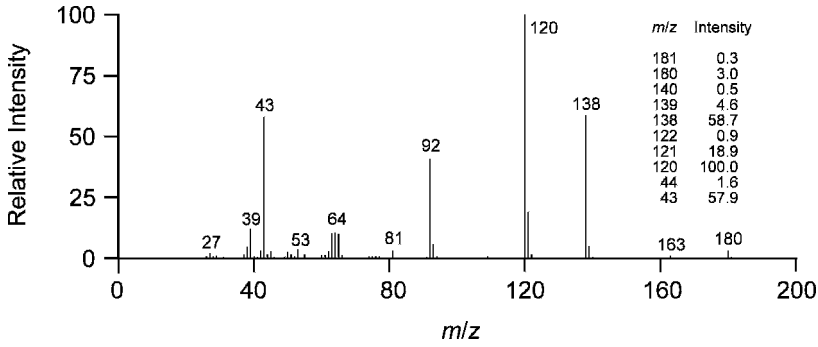

Figure 8.9. Mass spectrum for Problem 8.4.

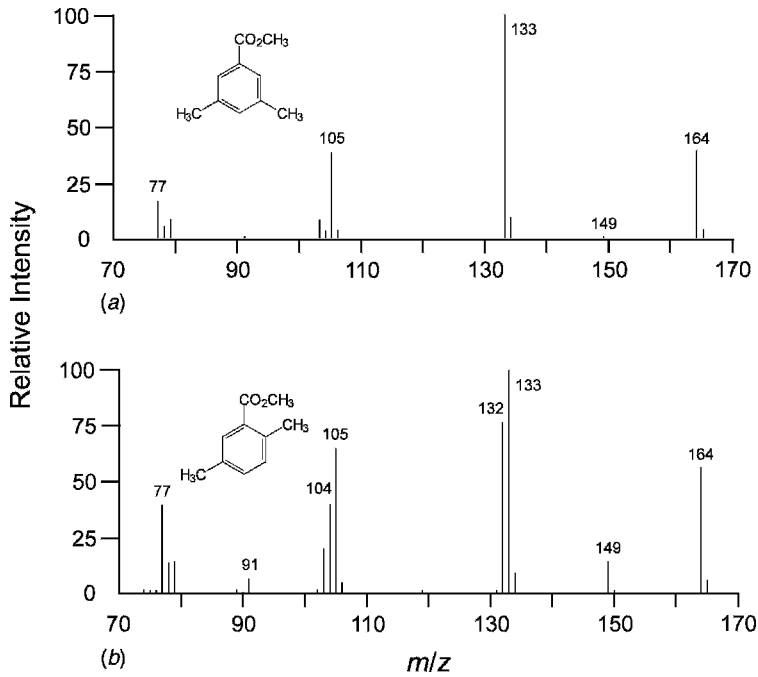

Figure 8.10. Mass spectra of (*a*) methyl 3,5-dimethylbenzoate and (*b*) methyl 2,5-dimethylbenzoate (Problem 8.5).

from the $M^{+\bullet}$ by α-cleavage. The ions having *m*/*z* 133 then lose CO to produce ions represented by the intense peaks at *m*/*z* 105. However, the spectrum of methyl 2,5-dimethylbenzoate also has intense peaks at *m*/*z* 132 (from the loss of a molecule of methanol) and *m*/*z* 104 (from an additional loss of CO) that are not present in the spectrum of the 3,5-isomer. Rationalize this difference.

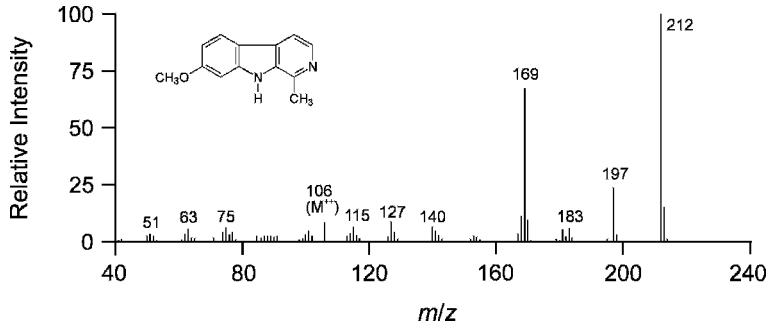

Figure 8.11. Mass spectrum of harmine (Problem 8.6).

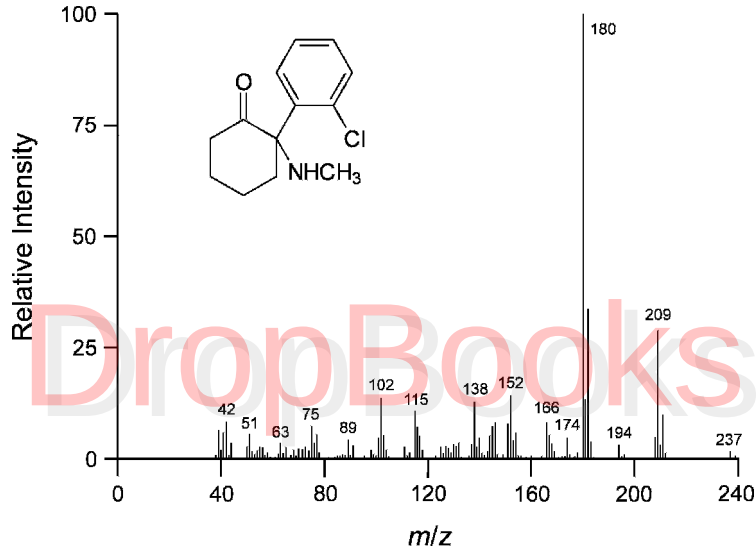

Figure 8.12. Mass spectrum of ketamine (Problem 8.7).

8.6. The mass spectrum of the indole alkaloid harmine is shown in Figure 8.11. Write reasonable mechanisms for formation of the two fragment ions with *m/z* 197 and 169. (*Hint*: Which methyl group is most likely to be lost?)

8.7. Ketamine, whose structure and mass spectrum are shown in Figure 8.12, is a veterinary tranquilizer that produces hallucinogenic effects in humans. Account for formation of the peaks at *m/z* 209, 194, and 180 in this spectrum.

REFERENCES

J. H. Beynon, R. A. Saunders, and A. E. Williams, *The Mass Spectra of Organic Molecules* (Elsevier, New York, 1968), pp. 235–236.

J. Vose, T. Tighe, M. Schwartz, and E. Buel, "Detection of Gamma-Butyrolactone (GBL) as a Natural Component of Wine," *J. Foren. Sci.*, **46**, 1164–1167 (2001).

9

STRUCTURE DETERMINATION IN COMPLEX MOLECULES USING MASS SPECTROMETRY

9.1. INTRODUCTION

The mass spectra of complex molecules usually defy complete interpretation. More often than not, all that can be done with them is to rationalize formation of some of the high-mass ions and other ions of significant abundance. Even this may not always be possible. The mass spectra of some steroids, for example, have so many intense peaks that the $M^{+\bullet}$ of these molecules seem to break apart just about everywhere (Figure 9.1). Because most of the molecules encountered in day-to-day organic analysis have complex structures, an approach to interpreting the mass spectra of these molecules is necessary.

As should be apparent from the examples presented up to this point, the fragmentations discussed in this book are applicable to complex molecules. But a different approach to structure determination is needed when dealing with the mass spectra of these compounds. The primary reason is that it is nearly impossible to determine a unique structure for an unknown complex molecule solely on the basis of its mass spectrum, unless the structure of the compound has been determined previously by independent means and a known mass spectrum already exists.

Many approaches to interpreting the spectra of large molecules are possible. Some of the tools that help identify specific fragmentation processes—preparation

Understanding Mass Spectra: A Basic Approach, *Second Edition*. By R. Martin Smith
ISBN 0-471-42949-X © 2004 John Wiley & Sons, Inc.

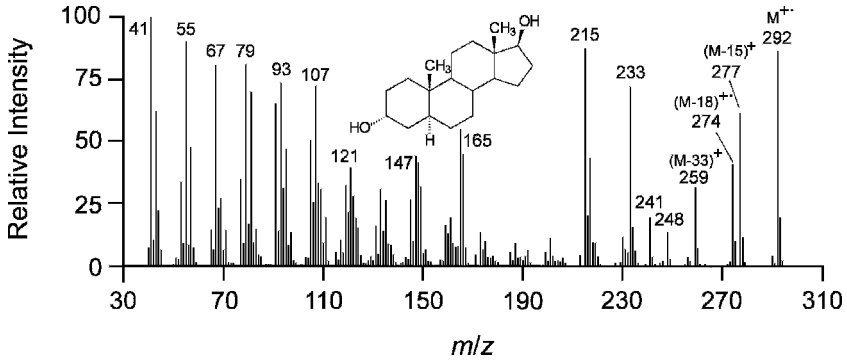

Figure 9.1. Mass spectra of some complex molecules, such as that of the steroid shown here, contain so many intense peaks that only the formation of a few ions can be rationalized.

of deuterated derivatives (Sections 7.2 and 7.3), high resolution MS, and MS/MS (Section 1.3.5)—are either time-consuming or demand instrumentation beyond the resources or goals of many analytical labs. A more practical approach is to study the spectra of related compounds that possess the same basic molecular skeleton but differ in the functional groups attached to it. This is similar to studying the spectra of deuterated derivatives, except that, in some cases, the work of characterizing the derivatives may already have been done—either in our own laboratories or by others working within the same narrow field of organic analysis. A disadvantage of this approach is that, because other functional groups are involved, the derivatives may fragment in ways that differ significantly from those of the original compound.

DropBooks

In this chapter, the mass spectra of three families of drugs of abuse will be discussed in order to illustrate how such a process might be undertaken. There is nothing so inherently unique about these compounds that the methods described here cannot be applied to other types of compounds. In each instance, the spectra of different family members are compared and contrasted so that their fragmentations can be understood as well as possible. This information is then used in a predictive manner to determine unique structures for other members of the family solely by means of their mass spectra. In the process, there will be further examples of the fragmentations and guidelines for rationalizing fragmentation mechanisms that were discussed in previous chapters.

9.2. "DESIGNER DRUGS" RELATED TO MDA

3,4-Methylenedioxyamphetamine (MDA) is a hallucinogen whose mass spectrum (Figure 9.2*a*) is similar to that of amphetamine (Figure 6.7). Prominent peaks due to low-mass aromatic ions occur at *m/z* 51 and 77, and α-cleavage accounts

for the base peak in the spectrum (Equation 9.1, path *a*). The peak at *m/z* 135 is produced by benzylic cleavage after ionization at one of the ring O atoms (Equation 9.1, path *b*). The weak intensity peaks at *m/z* 178 and 164 are the result of losses of $H^{\bullet}$ and $^{\bullet}CH_3$, respectively, after initial ionization at the N atom (Equation 9.2).

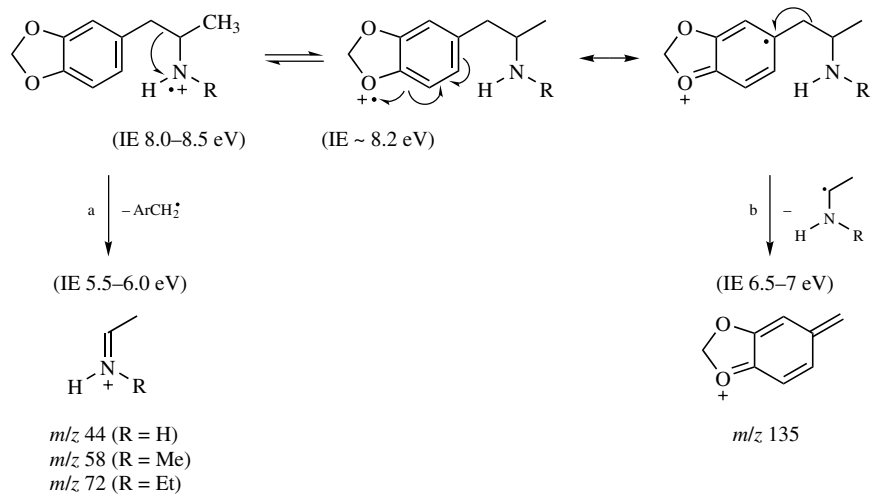

(9.1)

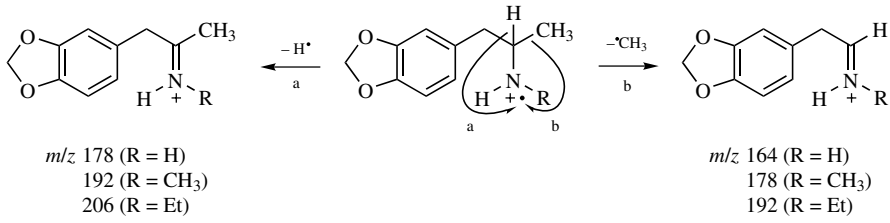

(9.2)

Formation of the ion having *m/z* 136 is similar to the γ-H rearrangement observed with alkylbenzenes (Section 7.2.2). In this case, however, ionization occurs initially at a location removed from the site of the rearrangement (compare Equation 7.7). Furthermore, the migrating H probably does not come from the terminal methyl group on the alkyl side chain because propylbenzenes do not undergo this rearrangement to any significant degree (Sections 7.2.2 and 7.2.3). Migration of one of the amine H atoms seems more likely because the intensity of the *m/z* 136 peak in the spectra of the *N*-alkyl derivatives of

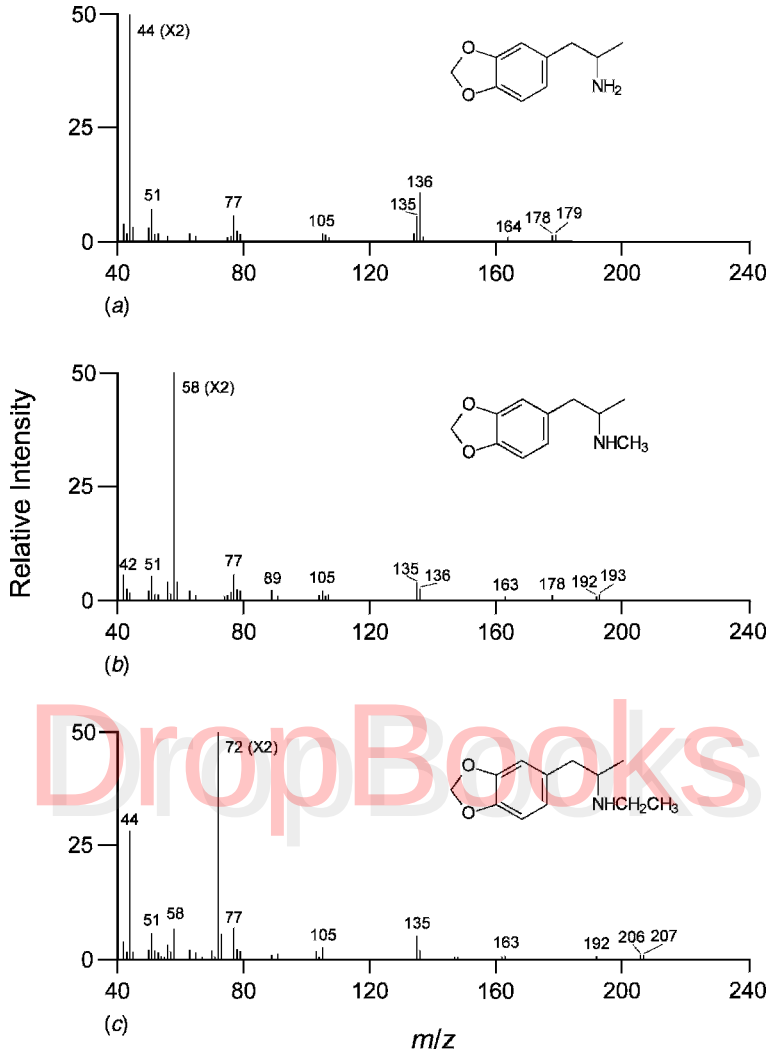

DropBooks

Figure 9.2. Mass spectra of (*a*) 3,4-methylenedioxyamphetamine (MDA) and two of its *N*-alkylated derivatives: (*b*) *N*-Methyl MDA (MDMA) and (*c*) *N*-ethyl MDA (MDE). The intensity of the base peak in each spectrum is actually twice that shown.

MDA (which contain one fewer H atom that can migrate; see below) decreases relative to that for MDA (Figure 9.2). Amphetamine and methamphetamine show a little propensity to undergo this fragmentation (compare the relative intensities of *m*/*z* 77 and 78 in Figures 6.7 and 6.8), so that the methylenedioxyphenyl

ring appears to provide an electron-rich site that attracts the migrating H (Equation 9.3).

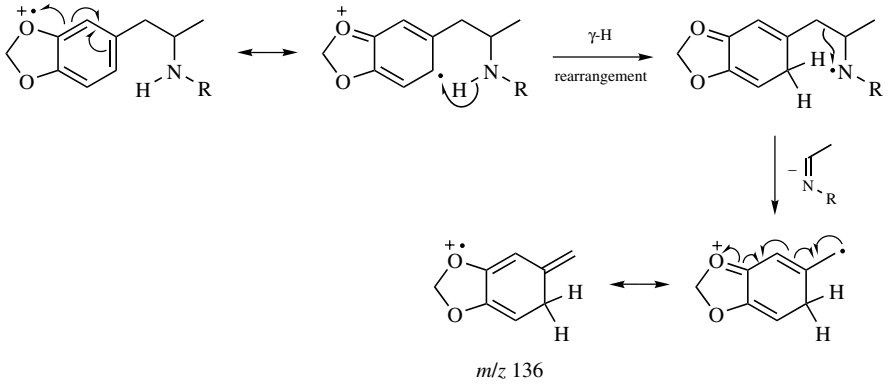

m/z 136

(9.3)

Illicit drug manufacturers repeatedly attempt to thwart prosecution by synthesizing new compounds called "designer drugs" that have the same basic chemical structures as controlled drugs, but are "legal" because they have different functional groups attached to them. Two such compounds are *N*-alkyl homologs of MDA: 3,4-Methylenedioxymethamphtamine (MDMA; "Ecstasy"; Figure 9.2*b*) and 3,4-methylenedioxy-*N*-ethylamphetamine (MDE; "Eve"; Figure 9.2*c*).

The most obvious difference between the mass spectra of these two compounds and that of MDA is the position of the base peak (Figure 9.2). This shift is predictable and is consistent with α-cleavage loss of the methylenedioxybenzyl radical after initial ionization on the N atom (Equation 9.1). Both compounds also show minor losses of $H^{\bullet}$ and $^{\bullet}CH_3$ as in Equation 9.2 and formation of the *m/z* 135 ion by benzylic cleavage (Equation 9.1). The spectrum of MDE also exhibits an intense *m/z* 44 peak, resulting from the loss of ethylene via secondary elimination from the initially formed α-cleavage ion (Equation 9.4; see Section 6.5.1). The small peaks at *m/z* 163 in the spectra of MDMA and MDE are undoubtedly due to loss of the *N*-alkylamino radical, which is similar to the behavior of methamphetamine (Equation 8.10).

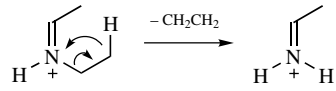

m/z 72 *m/z* 44

(9.4)

9.1. A compound suspected of being a new MDA analog produced the mass spectrum in Figure 9.3. Assign a unique structure to this compound based on this spectrum.

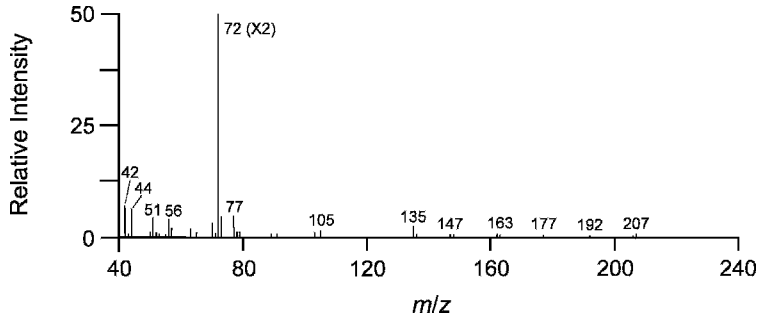

Figure 9.3. Mass spectrum for Problem 9.1.

9.3. COCAINE AND ITS METABOLITES

There are only two important fragmentation reactions that characterize the mass spectrum of MDA: α-cleavage and the γ-H rearrangement. This makes interpreting the spectrum straightforward and predicting the behavior of new analogs relatively easy. Interpreting the mass spectrum of cocaine (Figure 9.4) is considerably more difficult because it has a more complex structure.

Determining how cocaine fragments is facilitated by the substantial literature on the metabolism of this drug. These studies contain a comparative wealth of mass spectra that provide information about the mass spectrometric behavior of this

DropBooks

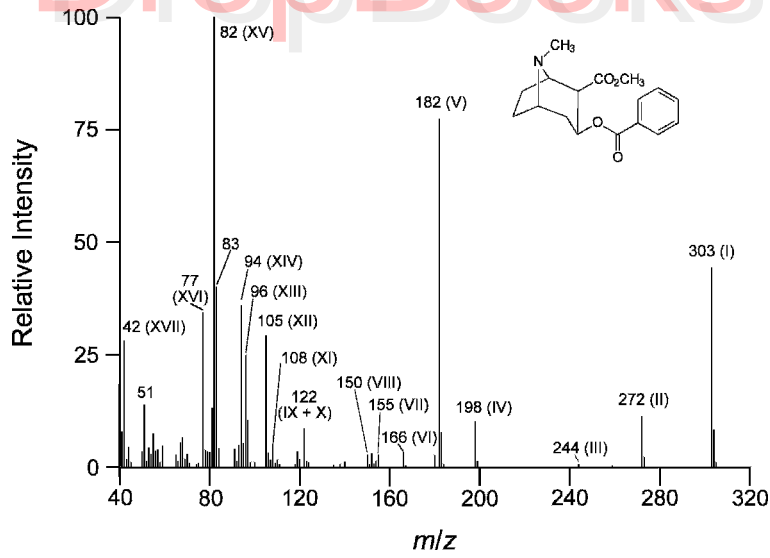

Figure 9.4. Mass spectrum of cocaine. Roman numerals refer to ion structures listed in Table 9.1 and shown in Figure 9.7 and Equations 9.5–9.11. (Reprinted with permission from Smith, 1997. Copyright ASTM International.)

family of compounds. In addition, a high-resolution mass spectrum of cocaine was published by Shapiro and coworkers in 1983, providing empirical formulas for the major ions represented in the spectrum.

9.3.1. Peak Correlations

As with the deuterated derivatives of 2-pentanone and cyclohexanone discussed in Chapter 7, the correlation of fragment ion peaks in metabolite and derivative spectra with their corresponding peaks in the spectrum of cocaine identifies how changes in attached functional groups alter the *m*/*z* values for various fragment ion peaks. This, in turn, helps identify what parts of the original $M^{+\bullet}$ are still present in those fragment ions. When functional groups in the derivatives differ significantly from those in the parent compound, these correlations are sometimes difficult to make. For example, although the spectra of cocaethylene, *p*-hydroxycocaine, and hydroxymethoxycocaine (Figure 9.5) appear to have almost a peak-for-peak correspondence to that of cocaine, those of methyl ecgonine, benzoylecgonine, and norcocaine (Figure 9.6) are quite different, making correlation patterns harder to determine.

Mass spectral correlations for several cocaine metabolites, as well as the ion elemental compositions determined by Shapiro et al. (1983), are given in Table 9.1[1]. This table, found on pages 266–267, also includes data for a deuterated derivative, *N*-trideuteriomethylnorcocaine (d_3-cocaine), an internal standard used for the GC/MS quantitation of cocaine by SIM (Section 1.3.3.1). Some preliminary comments need to be made about this table. First, these compounds differ from one another by substitution at three different sites—the alkyl group attached to the N atom (R^1), the alkyl ester group (R^2), and the aromatic ring (Ar = aryl). Second, the Roman numerals refer to postulated structures of various ions in the fragmentation of the $M^{+\bullet}$ of these compounds, assigned on the basis of peak correlations (Figures 9.4 and 9.7 and Equations 9.5–9.11). Third, uncertain correlations are denoted in the table by question marks. Dashes in the table signify the absence of peaks either because appropriate functional groups are not present in the derivative or because the peak is so small that it was not observed. Finally, peaks for which no correlations could be determined are not represented in this table.

When the *N*-methyl group of cocaine is replaced with a CD_3 group, only three of the peaks listed in Table 9.1 *do not move* by 3 *m*/*z* units when compared to the spectrum of cocaine. Thus, the *N*-methyl group (and presumably the N atom itself) must be retained in all but those three fragment ions. This constitutes most of the important ions represented in the spectrum and reflects, as stated on a number of occasions before, the propensity for an aliphatic N atom to direct ionization, fragmentation, and stabilization of the charge. The only peaks that do not shift are one of the peaks at *m*/*z* 122 (there are two; see below) and those in the benzoyl low-mass ion series at *m*/*z* 77 and 105.

[1]A more complete list of mass spectral correlations of cocaine derivatives may be found in R. M. Smith (1997).

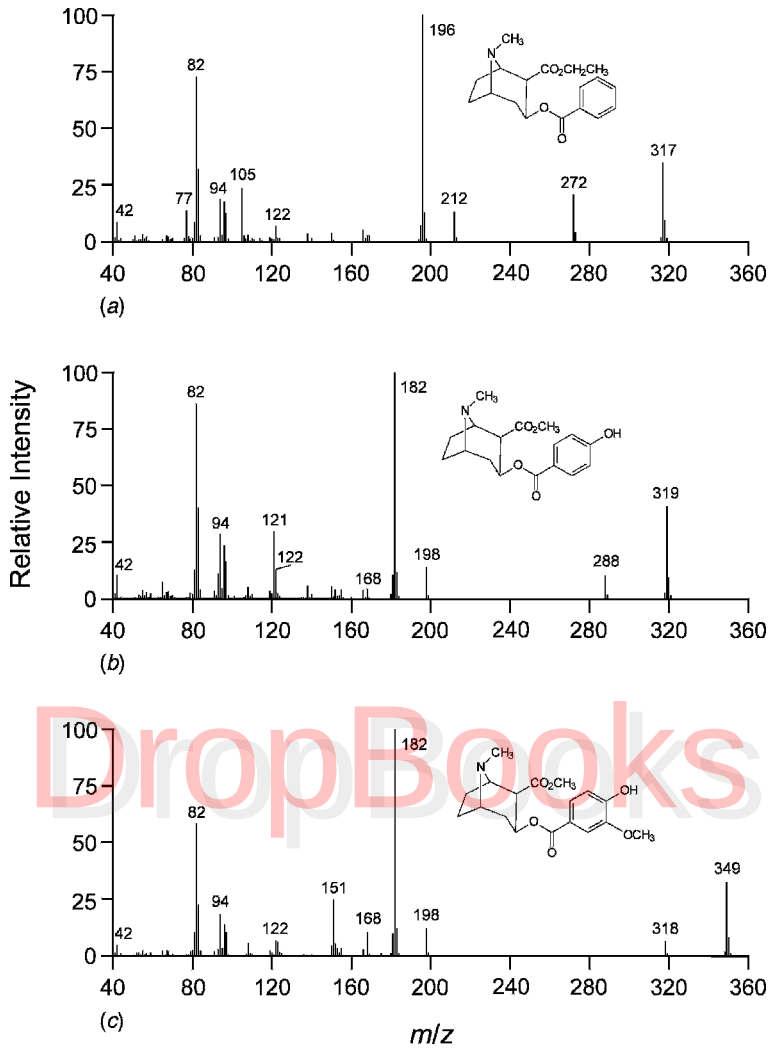

DropBooks

Figure 9.5. Mass spectra of three cocaine metabolites: (*a*) cocaethylene, (*b*) *p*-hydroxycocaine, and (*c*) hydroxymethoxycocaine. In contrast to those in Figure 9.6, the spectra of these compounds are visually very similar to that of cocaine.

m/z 272. When the methyl ester group of cocaine is exchanged for an ethyl group (cocaethylene; compare the data in Table 9.1 with the spectrum for this compound in Figure 9.5*a*), ion II, which is seen at *m/z* 272 for cocaine, does not shift. This indicates that ion II is formed by loss of the alkoxy radical ($^{\bullet}OR^2$) from the alkyl ester group. This is also consistent with the elemental composition for this ion

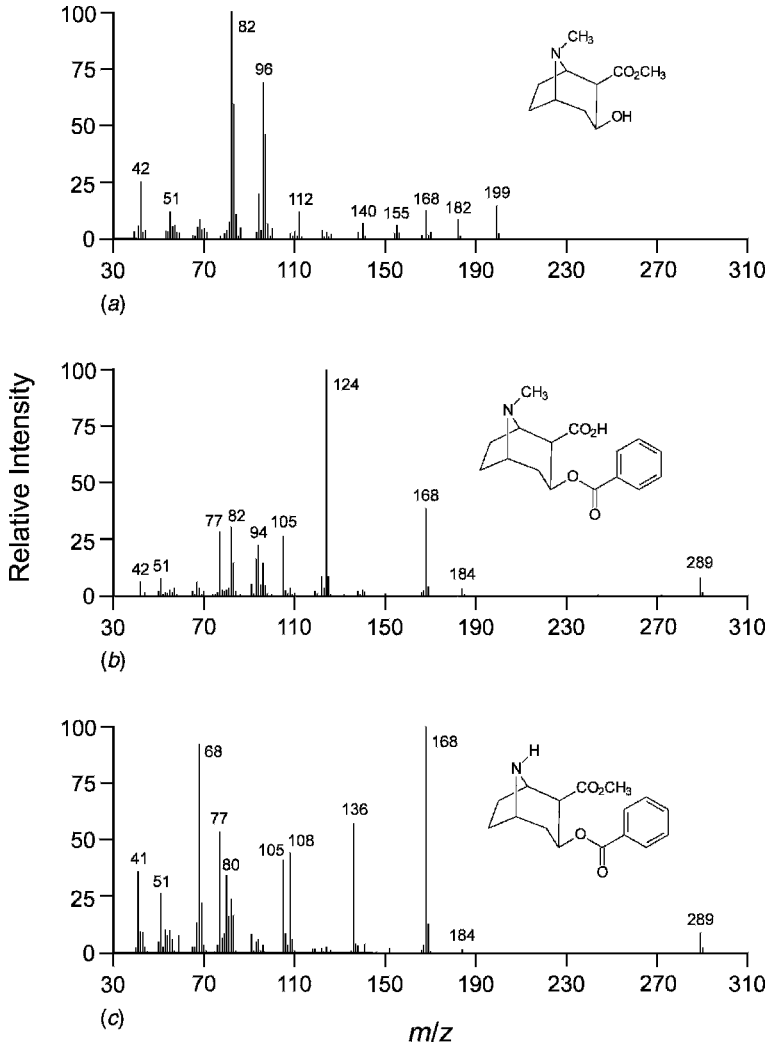

Figure 9.6. Mass spectra of three cocaine metabolites: (*a*) methyl ecgonine, (*b*) benzoylecgonine, and (*c*) norcocaine. Although these spectra have peaks in common with that of cocaine, correlation of peaks with functional group changes is not straightforward.

determined by the high-resolution data. Thus, the spectrum of *any* cocaine derivative in which *only* the methoxy group has been replaced by a different alkoxy group should exhibit a peak at *m/z* 272. Conversely, ion II should always occur at M − 31 in the spectra of other cocaine derivatives where $R^2 = CH_3$ (e.g., hydroxycocaine; see Table 9.1 and Figure 9.5*b*).

Table 9.1. Prominent ions in the mass spectra of substituted cocaines

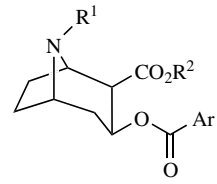

	Functional Group			Ion Structure/Elemental Composition[a]						
				I	II	III	IV	V	VI	VII
	R^1	R^2	Ar	$C_{17}H_{21}NO_4$	$C_{16}H_{18}NO_3$	—	$C_{10}H_{16}NO_3$	$C_{10}H_{16}NO_2$	$C_9H_{12}NO_2$	$C_8H_{10}NO_2$
Cocaine	CH_3	CH_3	ϕ	303	272	244	198	182	166	152–155
D_3-cocaine	CD_3	CH_3	ϕ	306	275	—	201	185	169	155–158
Norcocaine	H	CH_3	ϕ	289	—	—	184	168	?	138–141?
Benzoylecgonine	CH_3	H	ϕ	289	272	—	184	168	?	?
Cocaethylene	CH_3	CH_3CH_2	ϕ	317	272	244	212	196	166	166–169
Arylhydroxy-cocaine	CH_3	CH_3	[b]	319	288	260	198	182	166?	152–155
Hydroxy-methoxycocaine	CH_3	CH_3	[c]	349	318	—	198	182	166?	152–155?
Hydroxy-cocaethylene	CH_3	CH_3CH_2	[b]	333	288	260	212	196	166?	166–169?

[a] Elemental composition from Shapiro et al., 1983.
[b] Ar = C_6H_4OH.
[c] Ar = $C_6H_3(OMe)(OH)$.
Adapted with permission from Smith, 1997. Copyright ASTM International.

DropBooks

m/z 244. Another high-mass ion whose peak does not shift in the spectrum of cocaethylene is the one having *m/z* 244 (ion III). Because the difference in mass between 272 and 244 is 28 u, the methyl ester carbonyl group is a likely source for this loss by analogy with fragmentations of other carbonyl compounds (Section 6.4.3). Indeed, the peak representing ion III occurs 28 *m/z* values below that for ion II in every spectrum in which both ions are observed.

m/z 198 and 182. Ions IV and V shift to higher *m/z* values by 14 units in the spectrum of cocaethylene, indicating that, in contrast to ions II and III, both of these ions retain the R^2 ester group. This is also in contrast to the spectrum of *p*-hydroxycocaine (Figure 9.5*b*), in which the aromatic ring now bears the additional functional group. In that case, the peaks for ions IV and V remain at *m/z* 198 and 182, indicating that both these ions lose the aromatic ring during their formation. Because 105 u is lost from the $M^{+\bullet}$ during formation of the ion having *m/z* 198 and 121 u is lost in forming the *m/z* 182 ion, it seems reasonable to assume that these losses are due to benzoyl and benzoate radicals, respectively. The elemental compositions determined by the high-resolution data bear this out.

Table 9.1 (*Continued*)

Ion Structure/Elemental Composition[a]									
VIII	IX	X	XI	XII	XIII	XIV	XV	XVI	XVII
$C_9H_{12}NO$	$C_8H_{12}N$	$C_7H_6O_2$	$C_7H_{10}N$	C_7H_5O	$C_6H_{10}N$	C_6H_8N	C_5H_8N	C_6H_5	—
150	122	122	108	105	96–97	94	82	77	42
153	125	122	111	105	99–100	97	85	77	45
136?	?	?	94?	105	82–83	80	68	77	—
150?	?	122?	108	105	96–97	94	82	77	42
150	122	122	108	105	96–97	94	82	77	42
150	122	138	108	121	96–97	94	82	93	42
150?	122	168	108	151	96–97	94	82	123	42
150	122?	138	?	121	96–97	94	82	93?	42

m/z 122 (Two Ions) and 105. At the low *m*/*z* end of the hydroxycocaine spectrum, peaks representing ions XII and XVI (the benzoyl ion series) shift from *m*/*z* 77 and 105 to *m*/*z* 93 and 121, respectively, in keeping with the presence of an additional O atom on the aromatic ring. Also, there are peaks at both *m*/*z* 122 and 138. The former corresponds to ion IX, and, because it does not shift in the spectra of either cocaethylene or hydroxycocaine, must not contain either the carboalkoxy or aromatic ester group. The elemental composition reported for ion IX is consistent with this observation. The ion with *m*/*z* 138 (ion X) corresponds to the hydroxybenzoic acid $OE^{+\bullet}$. Confirmation of these assignments can be seen in the spectrum of hydroxymethoxycocaines (Figure 9.5*c*), in which the benzoyl/benzoic acid ion series shifts to *m*/*z* 123, 151, and 168, while the peak for ion IX remains at *m*/*z* 122.

Other Ions. Structures for some of the remaining ions cannot be determined with certainty, and in fact may be formed by more than one mechanism. Particularly intriguing are the low abundance ions VI (*m*/*z* 166) and VIII (*m*/*z* 150). Ion VI appears to contain neither the R^2 group nor the aromatic ring (Table 9.1), and ion VIII not only contains neither the R^2 group nor the aromatic ring, but it is also

structurally distinct from ions VII (*m/z* 152–155), which still contain the R^2 group. Ions XIII–XV (*m/z* 94–97 and 82–83) all contain the N atom and its substituents. The number of C atoms remaining in these ions indicates that the former contain either the five- or six-membered ring of the tropane skeleton, whereas the latter probably contain the five-membered ring. Ion XVII contains only the N atom and its substituents, plus an additional C atom.

9.3.2. Proposed Fragmentations

Devising mechanisms that account for the losses observed during the fragmentation of cocaine derivatives is no trivial matter. In addition to the peak correlations given in Table 9.1, the spectra of other 8-aza-bicyclo[3.2.1]octane (tropane) derivatives must be studied in order to provide a more complete picture. Presentation of all of these data is beyond the scope of this book. It is worthwhile, however, to look briefly at how some of the more important ions that are represented in the cocaine spectrum might be formed.

Of the three functional groups in cocaine, the IE of the amine group is considerably lower than those of the ester groups (Equation 9.5; see also Example 3.1). Therefore, it is possible that initial ionization takes place almost exclusively at this site. Excluding the losses of $H^{\bullet}$, there are four possible α-cleavage fragmentations that can occur on either side of the two bridgehead C atoms, all of which lead to stabilization of the charge on the N atom. Only one of these four modes produces a secondary radical site, however, and thus should be the favored mode of cleavage (ion Ia; Equation 9.5). This distonic ion is postulated as the intermediate for many of the fragmentations of this ring system.

DropBooks

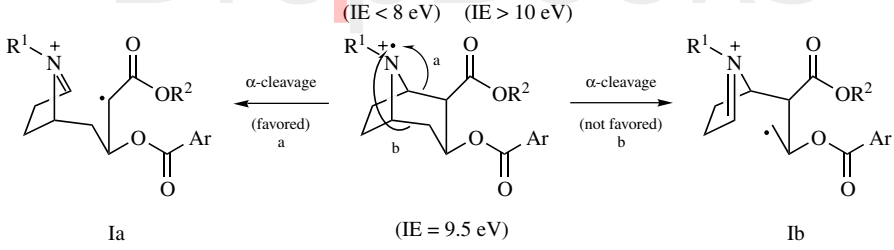

(9.5)

Loss of $^{\bullet}OR^2$ from ion Ia to produce ion II (*m/z* 272) can proceed with formation of a new π-bond (Figure 9.7, path *a*), which should lower the overall $\Delta G^{\ddagger}$ for this fragmentation. Cyclic loss of benzoic acid and formation of an additional π-bond that is conjugated with the C=C bond in the ketene group could then produce the low abundance ion VIII (*m/z* 150; Figure 9.7).

Although ion III (*m/z* 244) formally arises from loss of CO from ion II, this loss seems unlikely to occur directly from the structure for ion II shown in Figure 9.7. An alternative pathway involves loss of the entire CO_2R^2 group from ion Ia, which can occur if a H atom is transferred from C3 to C2 to form a second intermediate ion Ic (Figure 9.7, path *b*). Ion Ic can also lose $ArCO^{\bullet}$ to produce ion IV (*m/z* 198),

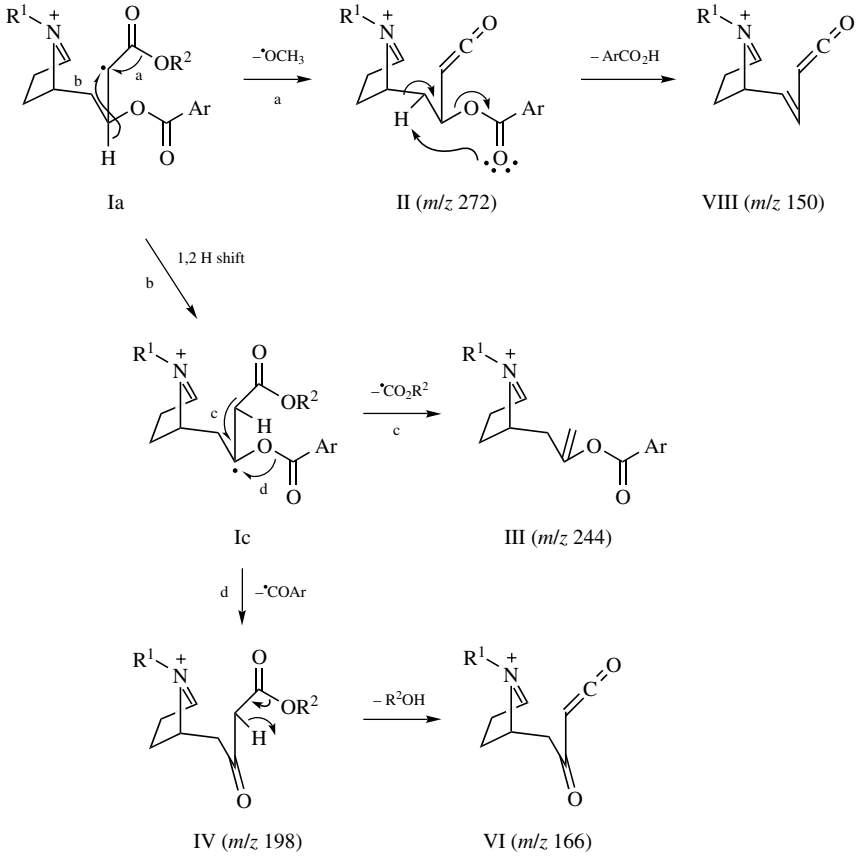

Figure 9.7. Proposed high-mass fragmentations of cocaine.

which in turn can expel a molecule of R^2OH to form ion VI (*m*/*z* 166). Each of these steps generates a new π-bond—indeed the structure proposed for ion VI contains an α,β-unsaturated ketone.

Formation of ion V (*m*/*z* 182) can occur by loss of benzoate radical directly from ion Ia (Equation 9.6). An alternative route leads to the isomeric ion Va, which could produce, by additional formal loss of HCO_2R^2, the N-containing ion IX (*m*/*z* 122; Equation 9.7).

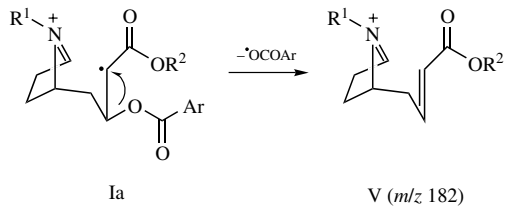

(9.6)

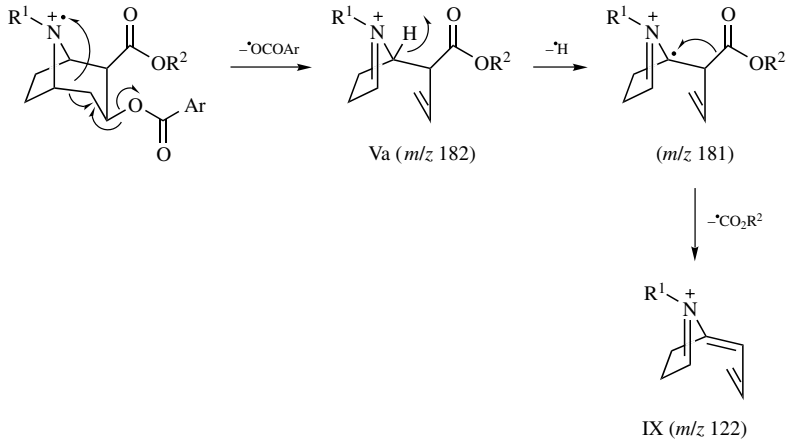

(9.7)

Other fragmentations of ion Ia also can produce ions XIII and XIV (*m/z* 94–97; Equation 9.8) and ions XV (*m/z* 82 and 83; Equation 9.9). Both these proposed

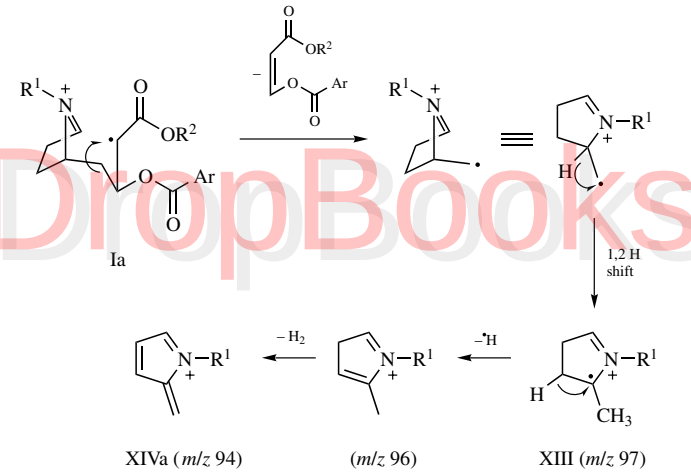

DropBooks

(9.8)

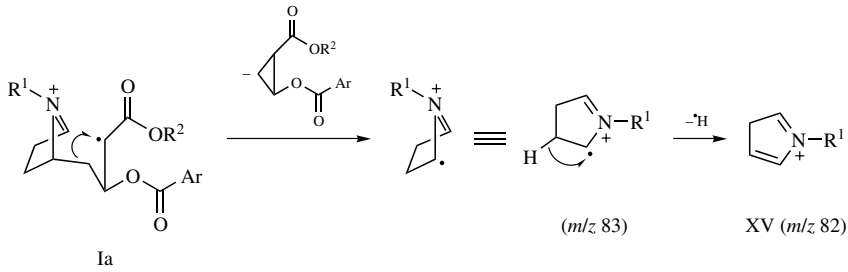

(9.9)

fragmentations involve new bond formation in the neutral product as well as the generation of delocalized ion products. An alternative—possibly additional—pyridinium structure for ion XIV (*m/z* 94) is shown on the next page.

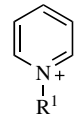

It is challenging to write charge migration mechanisms that account for formation of the benzoic acid (ion X; *m/z* 122) and benzoyl ions (ion XII; *m/z* 105) (Equations 9.10 and 9.11, respectively). Indeed, these ions may result from a small amount of ionization at the benzoate ester group. On the other hand, the proposed fragmentations have some merit in that they retain the most likely ionization site, maintain the charge on the N atom, and lead to new bond formation in the products. The H transfer shown in Equation 9.10 can occur if the side chain containing the benzoate group has rotational freedom.

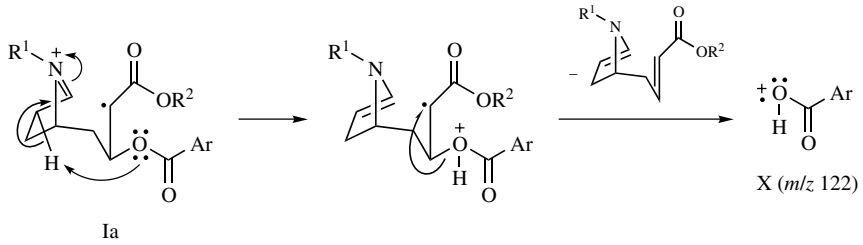

Ia

X (*m/z* 122)

(9.10)

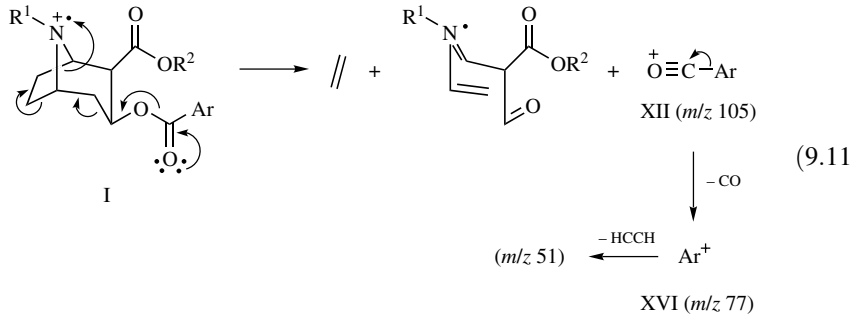

I

XII (*m/z* 105)

(9.11)

9.3.3. Application

If the peak correlations portrayed in Table 9.1 are generally correct, it should be possible to predict the mass spectrum of phenylacetylmethylecgonine, whose structure (shown below) is different from all the derivatives listed in Table 9.1.

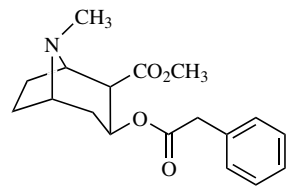

This compound is isomeric with cocaethylene, but has the extra methylene group between the phenyl ring and the "benzoyl" carbonyl group. Approximate peak intensities can be assigned to the various fragment ion peaks (and their accompanying isotope peaks) based on the intensities of corresponding peaks in the spectrum of cocaine.

The $M^{+\bullet}$ peak for this compound will occur at *m/z* 317. Ion II is formed by loss of $^{\bullet}OR^2$ from the $M^{+\bullet}$, which in this molecule is $^{\bullet}OCH_3$. Therefore, the peak corresponding to ion II will occur at *m/z* 286 (M – 31). The peak for ion III, formed by the additional loss of CO, will be observed at *m/z* 258 (M – 59). Because ions IV and V involve loss of the aromatic ring and its attached carbonyl group, their peaks will not shift from the values observed in the spectrum of cocaine, but will remain at *m/z* 198 and 182, respectively. Ions VI–VIII all have lost the aromatic ring as well, so that peaks for these ions will not shift either.

Although ion IX, having lost both ester groups, still produces a peak at *m/z* 122, the peaks representing ions X, XII, and XVI, which constitute the aromatic acid and its fragments, all will shift. The peak for the acid $OE^{+\bullet}$ (ion X) will move to *m/z*

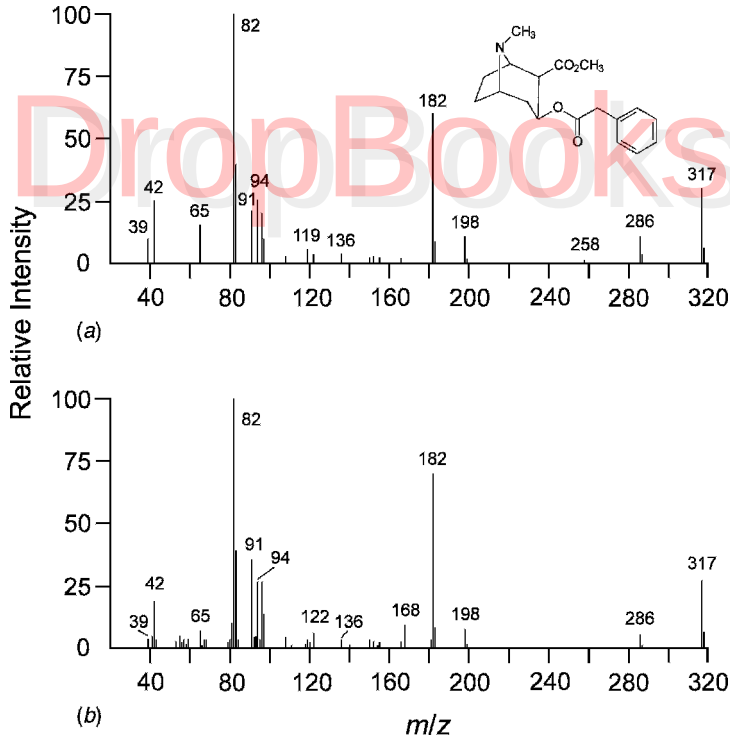

Figure 9.8. (*a*) Mass spectrum of phenylacetylmethylecgonine predicted by analogy to fragmentations of other cocaine derivatives (see text), and (*b*) actual mass spectrum of phenylacetylmethylecgonine.

136, while that for the phenylacetyl ion (ion XII) will appear at *m/z* 119. What happens during the decomposition of ion XII is less clear because it should lose CO to form the benzyl ion (*m/z* 91), rather than phenyl (*m/z* 77), and the benzyl ion has its own ion series at *m/z* 39 and 65. How energy will be apportioned in the fragmentation of these ions is not predictable, so that their actual relative intensities may differ from those expected.

Peaks corresponding to the major N-containing ion clusters at *m/z* 94–97 (XIII and XIV), *m/z* 82 and 83 (XV), and *m/z* 42 (XVII) will remain at these *m/z* values because only the unchanged core of the cocaine molecule is left.

Figure 9.8 shows the spectrum based on these predictions and an actual spectrum of phenylacetylmethylecgonine for comparison. Although there are numerous differences between the spectra (as there should be since not all the ions from the cocaine spectrum were even considered), the predicted spectrum is remarkably accurate.

9.2. What differences would you expect between the spectra of phenylacetylmethylecgonine (Figure 9.8) and that of toluylmethylecgonine (structure below), a recently synthesized cocaine analog?

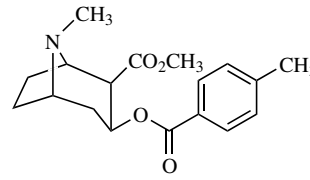

9.3. Using the information in this section, identify the compound that gave rise to the spectrum in Figure 9.9.

9.4. The chromatogram shown in Figure 9.10 was obtained after derivatization of a urine extract designed to isolate cocaine and its metabolites. The derivatizing reagent used for this sample replaced all HO- groups with $CH_3CH_2CH_2O$- groups. In addition to cocaine and propylbenzoylecgonine, which resulted from propylation of the cocaine metabolite benzoylecgonine (Equation 9.12),

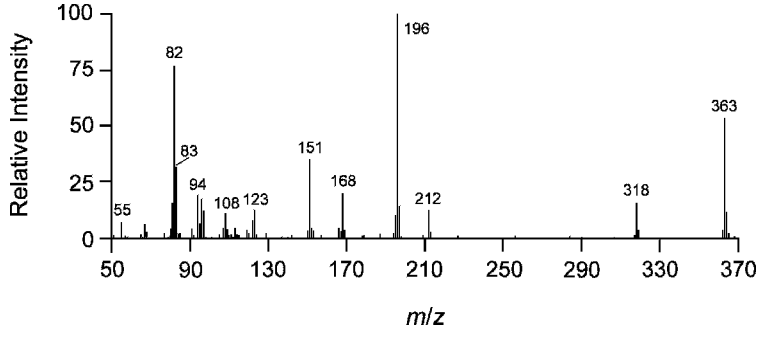

Figure 9.9 Mass spectrum for Problem 9.3.

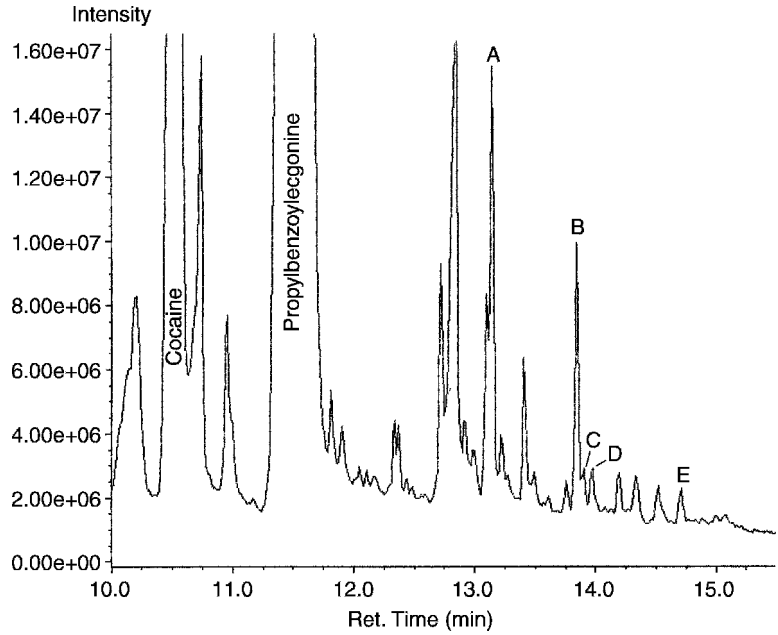

Figure 9.10 Partial RTICC from a urine sample that was extracted for basic drugs and derivatized by propylation (Problem 9.4).

DropBooks

five other apparent cocaine metabolites were observed. These are labeled as peaks A, B, C, D, and E in Figure 9.10. The spectra for these compounds are shown in Figure 9.11. Assign structures to these derivatives based on these spectra. (*Note*: Some of these spectra are so weak that only the major peaks in the spectrum can be counted on to provide reliable information.)

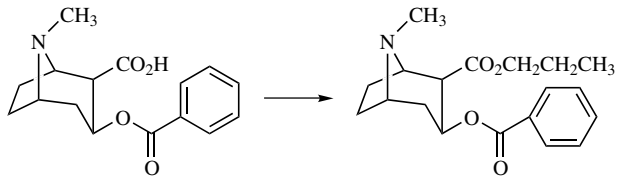

Benzoylecgonine Propylbenzoylecgonine (9.12)

9.4. PHENCYCLIDINE AND ITS ANALOGS

9.4.1. Fragmentations of Phencyclidine

Phencyclidine is a veterinary tranquilizer that produces hallucinogenic effects in humans. Also known as PCP (an acronym for the chemical name 1-phenylcyclohexylpiperidine), this drug and its analogs have enjoyed sporadic periods of illicit

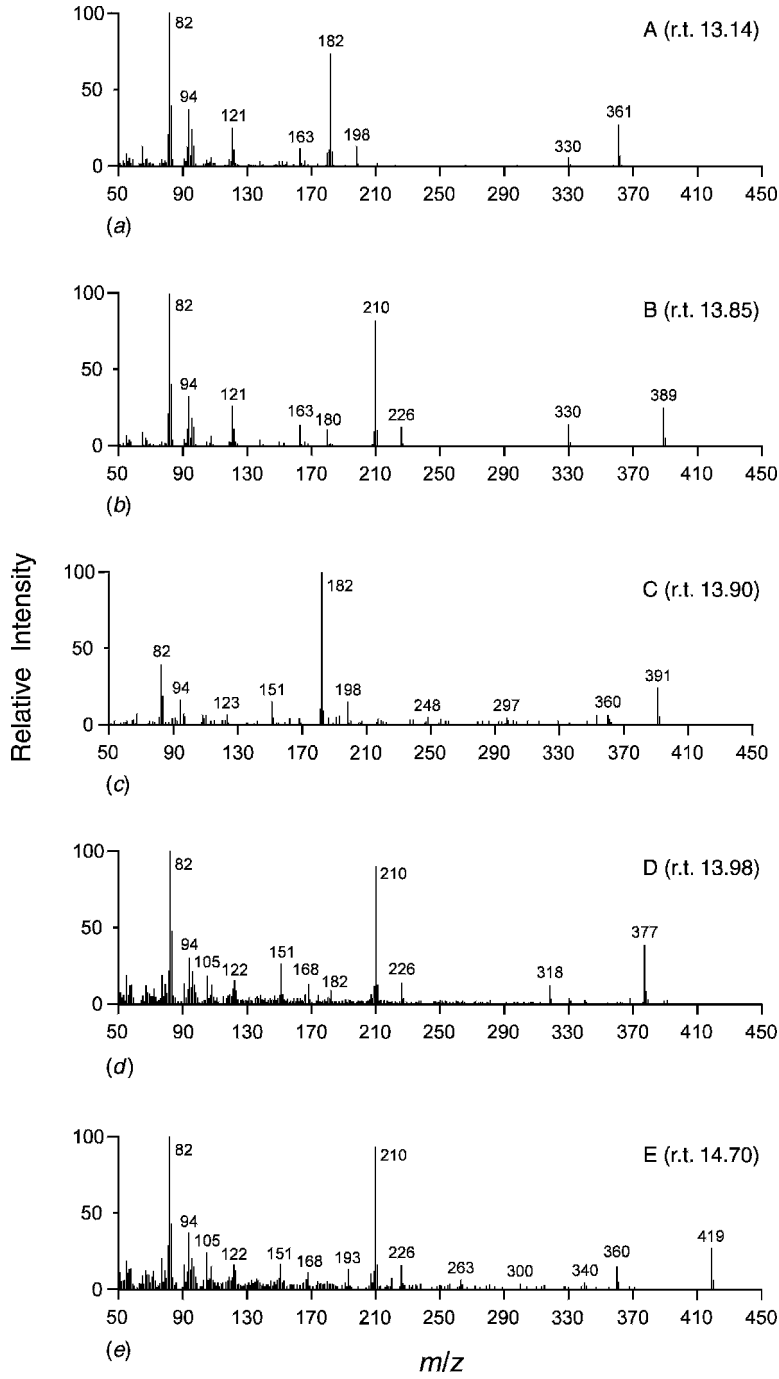

Figure 9.11. Mass spectra for Problem 9.4.

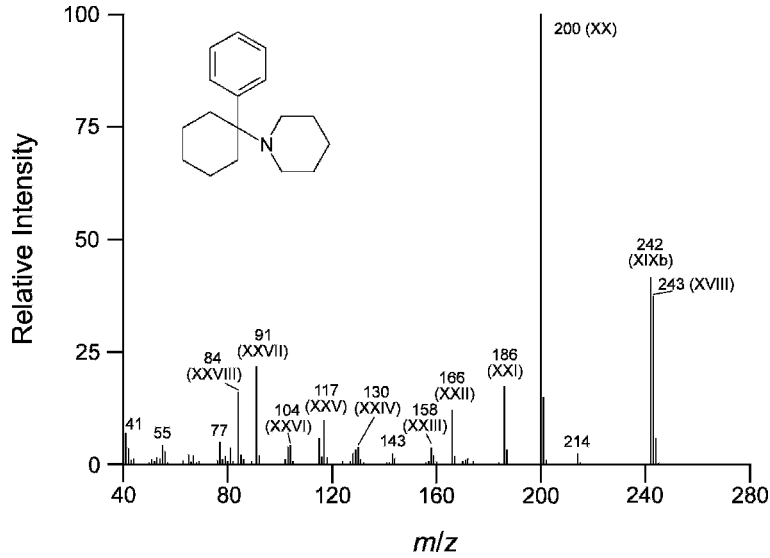

Figure 9.12. Mass spectrum of phencyclidine. Roman numerals refer to ion structures in Table 9.2 and Figures 9.13–9.15.

popularity for over three decades. At first glance, the losses observed in the mass spectrum of phencyclidine (Figure 9.12) might seem surprising. Facile loss of $H^{\bullet}$ usually occurs only from highly activated positions—for example, from C atoms directly attached to two aromatic rings (see Section 6.2 and Equation 6.13). The apparent loss of a propyl radical to produce the base peak at *m/z* 200 might not have been predicted, given the lack of aliphatic groups in the molecule.

DropBooks

Although the mass spectra of several phencyclidine analogs are available from various literature sources, chemists at the Drug Enforcement Administration (DEA) studied the mass spectra of phencyclidine and three of its deuterated derivatives to gain insight into the fragmentation of this molecule (Clark, 1986). The derivatives used were those in which:

1. All the H atoms on the aromatic ring had been replaced with D (this compound will be denoted here as the d_5 derivative).
2. All the H atoms on the cyclohexyl ring were replaced with D (the d_{10} derivative).
3. All the H atoms on both the phenyl and cyclohexyl rings were replaced with D (the d_{15} derivative).

The d_5 derivative was synthesized by initially combining the Grignard reagent of d_5-bromobenzene with cyclohexanone. The d_{10} derivative was made by using decadeuteriocyclohexanone as one of the starting materials, while synthesis of the d_{15} compound used a combination of both these methods. The results of this study are summarized in Table 9.2. As in Table 9.1, the Roman numerals refer to ions

Table 9.2. Important ions in the mass spectra of some substituted phencyclidines

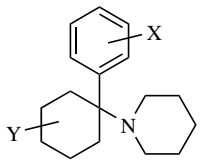

Name	X	Y	XVIII	XIX	XX	XXI	XXII	XXIII	XXIV	XXV	XXVI	XXVII	XXVIII
Phencyclidine	—	—	243	242	200	186	166	158	130	117	104	91	84
d_5-Phencyclidine	d_5	—	248	246	205	190, 191	166	163	135	122	109	96	84
d_{10}-Phencyclidine	—	d_{10}	253	252	203	188	176	167	135	120+	104, 105	92, 93	85
d_{15}-Phencyclidine	d_5	d_{10}	258	256	208	192, 193	176	172	140	125+	109, 110	97, 98	85
Arylmethyl-PCP	CH_3	—	257	256[a]	214	200	166	172	144	131	?	105	84

[a] *ortho*-Methylphencyclidine also shows a peak at *m/z* 242 (10%) from loss of the aryl methyl group.

associated with the peaks in Figure 9.12 and the corresponding structures in Figures 9.13–9.15.

m/z 242. Not only is the facile loss of $H^{\bullet}$ from the $M^{+\bullet}$ of phencyclidine unexpected, but the data in Table 9.2 reveal that the source of this H atom is even more surprising. In the spectrum of the d_5 derivative, the peak corresponding to ion XIX shifts not from *m/z* 242 to 247 (as would be expected if the $H^{\bullet}$ were lost via α-cleavage from one of the C atoms next to the N atom in the piperidine ring), but rather to *m/z* 246. The intensity of the peak at *m/z* 247 in this spectrum is consistent only with the ^{13}C contribution from the *m/z* 246 ion. There is only one possible interpretation to this data: The $H^{\bullet}$ is lost from the phenyl ring! This loss can be rationalized if, after initial ionization at the N atom, one of the *ortho* H atoms on the phenyl ring is lost and a C—N bond is formed that retains the charge on the N atom (Figure 9.13, path *a*). Additional support for this mechanism comes from the mass spectra of arylmethyl analogs of phencyclidine, in which the *meta*- and *para*-isomers show virtually no loss of the arylmethyl group (as expected), but the *ortho*-isomer produces a 10% peak corresponding to the loss of this group (Lodge et al., 1992; Equation 9.13). The remaining data for the ion XIX

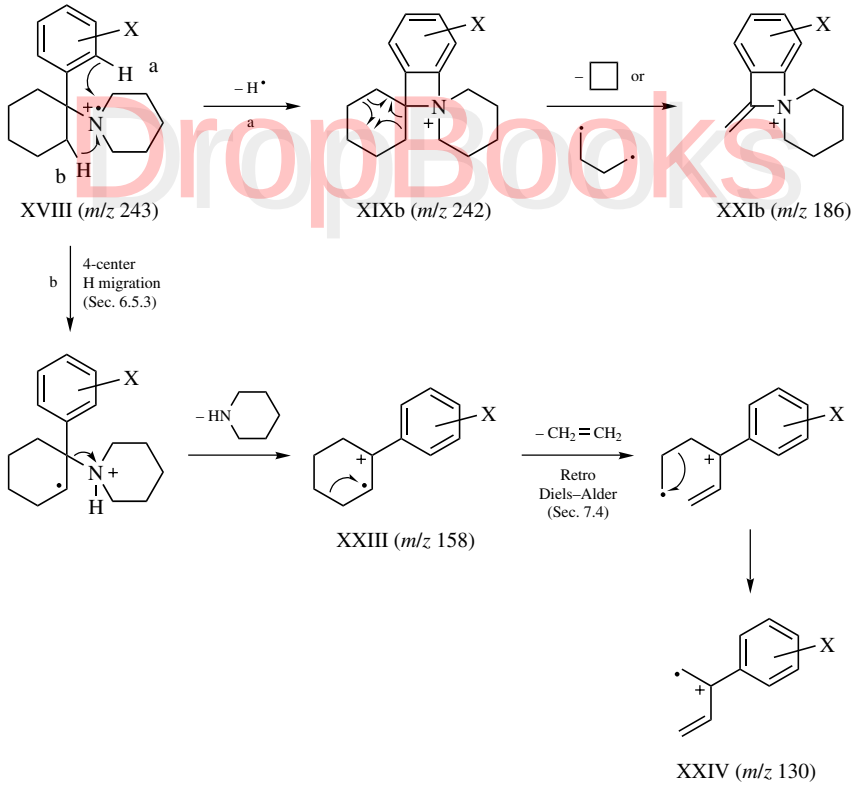

DropBooks

Figure 9.13. Fragmentation of phencyclidine showing losses of a phenyl H atom and piperidine.

in Table 9.2 are also consistent with this interpretation because the d_{10} derivative shows no loss of D and the d_{15} derivative loses only one D.

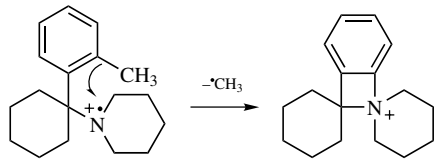

m/*z* 242 (9.13)

m/z 200. Formation of ion XX (*m*/*z* 200) can occur via a cyclohexanone-type rearrangement (Section 7.3), which is supported by the data in Table 9.2. In particular, the deuterated aromatic ring of the d_5 derivative shows no loss of D, while the d_{10} derivative loses 7 of the 10 D atoms in the cyclohexane ring. The same pattern of losses is reflected in the spectrum of the d_{15} compound. Such losses are expected if a propyl radical ($^{\bullet}C_3H_7$) is lost entirely from the cyclohexane ring (Figure 9.14).

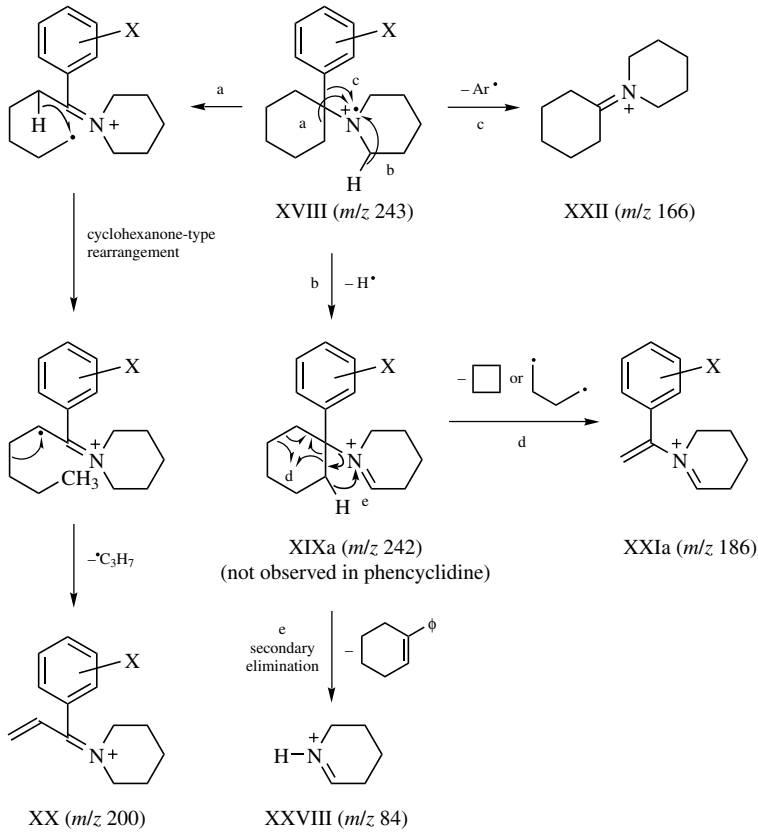

Figure 9.14. Some primary fragmentation modes of phencyclidine. In this figure Ar = aryl.

The weak peak at *m/z* 214 results from loss of an ethyl, rather than a propyl, radical from the distonic ion intermediate in this rearrangement (Equation 9.14; compare Figure 7.12).

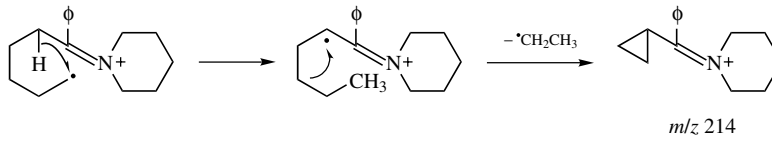

(9.14)

m/z 214

m/z 186. Ion XXI, which occurs at *m/z* 186 in the phencyclidine spectrum, appears as a pair of peaks in the spectra of the d_5 and d_{15} derivatives. In the spectrum of the d_5 derivative, these peaks are seen at *m/z* 190 and 191 in a ratio of approximately 4:3, indicating a nearly equal tendency to lose either one or no D atom from the phenyl ring. At the same time, the spectrum of the d_{10} compound shows the loss of eight D atoms from the cyclohexane ring. For the d_{15} derivative, the pair of peaks appears at *m/z* 192 and 193 in an approximate ratio of 2:1, corresponding to losses of eight cyclohexyl D atoms *plus* either one or no phenyl D atom.

These observations can be explained only if formation of ion XIX occurs via two different pathways—one involving the loss of a phenyl H atom, the other by the loss of a H atom from the piperidine ring (Figures 9.13 and 9.14, paths *b* plus *d*). The remaining step in this fragmentation involves the loss of four C and eight H atoms from the cyclohexane ring. Although the ions formed in this fragmentation (XXIa and XXIb) are stabilized by extended conjugation, the nature of the lost fragment is not clear. Formation of an additional σ-bond to form cyclobutane is a tempting rationalization, but a C_4H_8 diradical cannot be ruled out.

DropBooks

m/z 166. The peak for ion XXII occurs at *m/z* 166 in the phencyclidine spectrum, 77 units below the $M^{+\bullet}$ peak. Loss of phenyl radical by α-cleavage is expected to occur in this molecule (Figure 9.14, path *c*). The data in Table 9.2 bear this out because the d_5 derivative shows the loss of all five phenyl D atoms, while the d_{10} derivative loses no D atoms.

m/z 158 and 130. The low abundance ion having *m/z* 158 (ion XXIII) shows no loss of D from the phenyl ring and only one D atom from the cyclohexane ring. This is consistent with loss of a molecule of piperidine from the $M^{+\bullet}$ (Figure 9.13). Although such fragmentations usually do not compete well with α-cleavage, the product ion formed here is stabilized by conjugation with the aromatic ring. This fragmentation is similar to those discussed earlier in Section 6.5.3, but in this case the charge ends up on the olefin fragment. Ion XXIII, which is formally the $M^{+\bullet}$ of 1-phenylcyclohexene, undergoes the retro Diels–Alder fragmentation (Section 7.4) to give ion XXIV (*m/z* 130) through loss of $CH_2{=}CH_2$ (Figure 9.13). Consistent with this proposal, Table 9.2 shows that, in the spectra of the deuterated derivatives, ion XXIII loses an additional four D atoms from the cyclohexane ring and none from the phenyl ring in forming ion XXIV.

m/z 84. Ion XXVIII is the only other ion whose peaks show a simple pattern of D loss. Formation of this ion involves the loss of all the phenyl H atoms, as well as all

but one of the cyclohexane H atoms. This is consistent with the loss of phenylcyclohexene via secondary rearrangement of the initially formed α-cleavage ion from the unobserved ion XIXa at *m/z* 242 (Figure 9.14, path *e*). Interestingly, this ion can be formed *only* via ion XIXa. Ion XIXb, which is not an α-cleavage ion, must break bonds to both the cyclohexane and aromatic rings, in addition to rearranging H, in order to generate ion XXVIII. The behavior of ion XXVIII in the spectra of the deuterated derivatives provides impressive evidence for the formation of ion XIXa in the fragmentation of phencyclidine despite the fact that no peak corresponding to the ion itself is observed. Because ion detection is determined in part by the relative $\Delta G^{\ddagger}$'s of further fragmentation reactions (and thus to the lifetime of that ion in the ion source; Section 3.6.1), these results indicate that ion XIXa reacts too rapidly to reach the detector. Higher $\Delta G^{\ddagger}$'s for further fragmentation of ion XIXb, on the other hand, allow it to be detected.

Other Ions. The ions having *m/z* 117, 104, and 91 give patterns of D loss that are actually more complex than the data in Table 9.2 indicate, implying that all three are formed via several different pathways and that their stabilities probably play a more important role in their formation than the mechanisms by which they are formed. Ion XXV, which arises primarily via loss of seven H atoms from the cyclohexane ring while retaining the H atoms on the aromatic ring, could have either of the two structures shown in Figure 9.15, provided both C atoms in the aziridine ring of structure XXVa and the H atom on the N originate on the cyclohexane ring. The ion with *m/z* 115 is probably related structurally to *m/z* 117 by loss of additional H (see, e.g., Equation 8.10).

Although the *m/z* 104 ion also can have at least two structures, XXVIa (which might seem more likely on a purely intuitive basis) is not consistent with the deuterium labeling data. Barring migration of H *from* the piperidine ring to the cyclohexane ring (which is not observed for any of the other ions), this structure would result from loss of seven of the cyclohexane H atoms. Instead, the most prominent peaks in the cluster ascribable to this ion in the spectrum of the d_{10} derivative show the loss of 9 or 10 cyclohexane D atoms, which is more consistent with structure XXVIb (Figure 9.15). Notice that this ion has the charge located on the N atom.

Finally, ion XXVII (*m/z* 91; $C_7H_7^+$) arises primarily via the loss of eight cyclohexyl H atoms, with a small contribution (10–15%) from the loss of a phenyl H atom *and* eight cyclohexane H atoms. This behavior is similar to that of ion XXI, which was formed via pathways involving each of the *m/z* 242 ions. Although the two H atoms

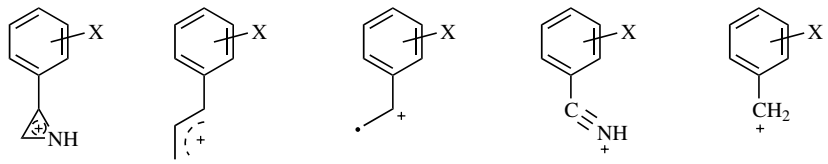

XXVa XXVb XXVIa XXVIb XXVII (*m/z* 91)

(*m/z* 117) (*m/z* 104)

Figure 9.15. Possible structures for three low-mass ions in the mass spectrum of phencyclidine.

that end up on the benzylic C atom come from the cyclohexane ring, mechanisms that attempt to account for these rearrangements are not straightforward.

9.4.2. Phencyclidine Analogs

In contrast to the spectra of cocaine and many of its derivatives (see Figure 9.5, e.g.), spectra of the analogs of phencyclidine lack superficial resemblance to one another (Figure 9.16). This lack of similarity arises because none of the major high-mass ions have the same masses. Yet if the pattern of losses from the $M^{+\bullet}$ of these compounds is considered (Table 9.3), a different picture emerges. For

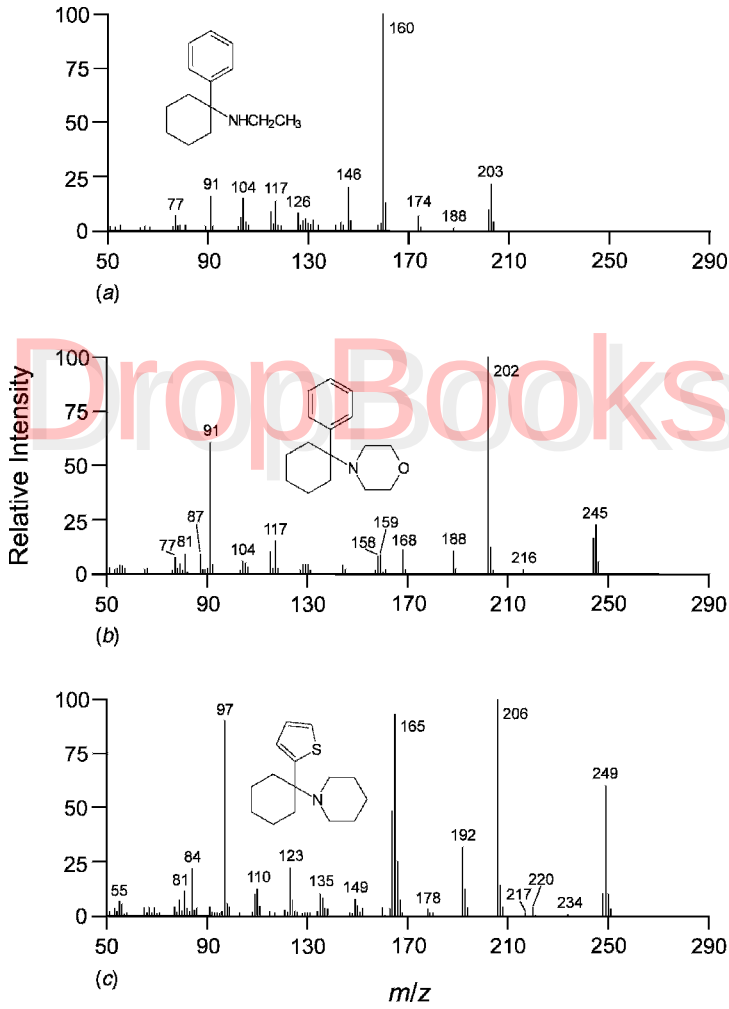

Figure 9.16. Mass spectra of three phencyclidine analogs: (*a*) *N*-Ethyl-1-phenylcyclohexylamine, (*b*) *N*-(1-phenylcyclohexyl)morpholine, and (*c*) *N*-[1-(2-thienyl)cyclohexyl]piperidine.

Table 9.3. Pattern of fragmentation losses in phencyclidine analogs

Ion	*m/z* in a[a]	*m/z* in b[a]	*m/z* in c[a]
$M^{+\bullet}$	203	245	249
$(M-1)^+$	202	244	248
$(M-43)^+$	160	202	206
$(M-1-56)^+$	146	188	192
$(M-Ar)^{+}$[b]	126	168	166
$ArCH{=}CHC^+H_2$[b]	117	117	123
$ArC^+H{-}{}^\bullet CH_2$[b]	104	104	110
ArC^+H_2[b]	91	91	97

[a]From mass spectra for compounds shown in Figure 9.16.
[b]Ar = Aryl

example, two of the three compounds shown form an abundant $(M-1)^+$ ion. The thiophene analog, Figure 9.16*c*, has only one *ortho* H atom to lose from the aromatic ring and thus exhibits a less abundant $(M-1)^+$ ion. In addition, the spectra of all three compounds show a small but detectable M − 29 peak from loss of an ethyl radical, a base peak at M − 43 due to loss of a propyl radical, a peak of moderate intensity at M − 57 (actually M − 56 − 1; see Figures 9.13 and 9.14), and a peak due to α-cleavage loss of the aryl group. In addition, the phencyclidine "low-mass ion series" at *m/z* 91, 104, 115, and 117 is reproduced in Figures 9.16*a* and *b*. In the spectrum of the thiophene analog, this series is displaced to higher *m/z* values by six units, reflecting the higher mass of the thiophene ring.

The thiophene analog loses the piperidine ring much more readily than either phencyclidine or the other two analogs shown here. In this case, stabilization of the charge can occur on S (whose electronegativity is comparable to that of N) either via charge migration cleavage removed from the ionization site after ionization at the N atom or by "benzylic" cleavage after initial ionization at S (Equation 9.15). The corresponding ions having *m/z* 159 in the spectra of phencyclidine and the other two analogs lack this additional stabilization.

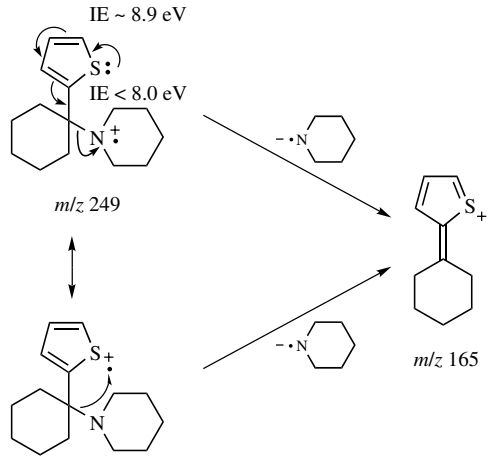

(9.15)

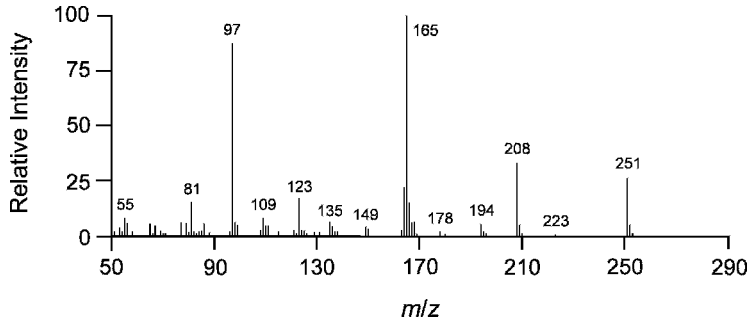

Figure 9.17. Mass spectrum for Problem 9.6.

9.5. Using the fragmentation pattern for phencyclidine and its analogs as a model, predict the major features of the mass spectrum of *N*,*N*-diethyl-1-phenylcyclohexylamine (structure below). Predict approximate relative intensities for the ions using those in Figure 9.12 as a guide.

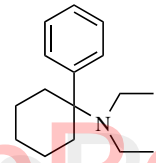

DropBooks

9.6. Identify the compound that gave rise to the spectrum in Figure 9.17.

9.7. In contrast to the spectra of the tolyl analogs of phencyclidine (see data in Table 9.2), the spectrum of 1-benzylcyclohexylpiperidine (structure below) has a base peak at *m*/*z* 166 and a peak of only 1–2% relative intensity at *m*/*z* 214 due to the cyclohexanone-type rearrangement. Explain this difference in behavior.

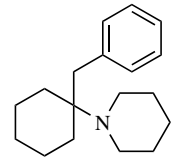

9.5. A PRACTICAL PROBLEM

9.8. Sometimes the mass spectrum of a single derivative contains enough information to identify major losses from the $M^{+\bullet}$ of a compound. Such is the case with diazepam (a popular brand name is Valium) and its pentadeuterio derivative. The derivative was purchased as an internal standard for the SIM quantitation (Section 1.3.3.1) of diazepam in biological fluids. The spectra of these two compounds are shown in Figure 9.18, with peak correlations

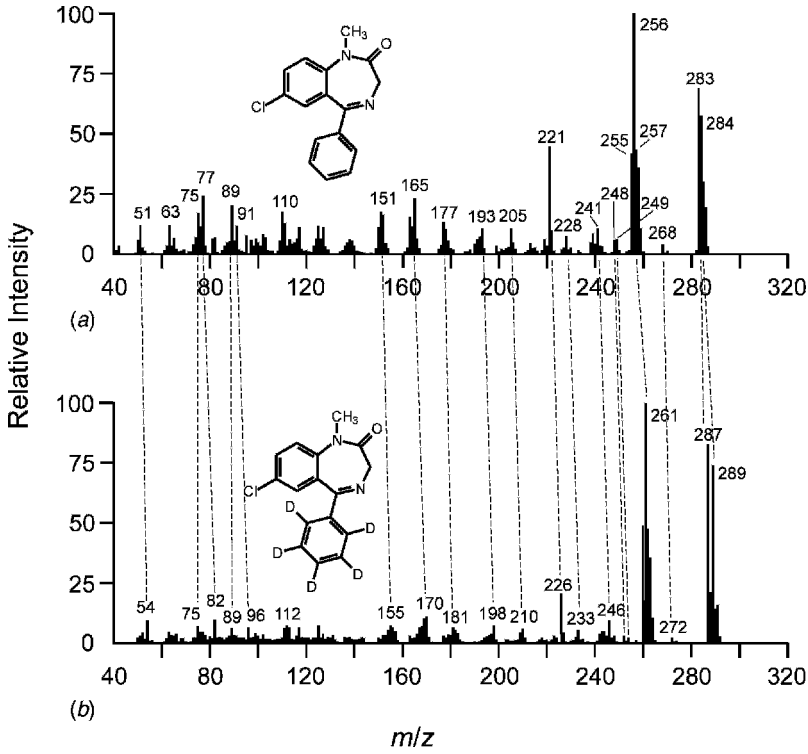

Figure 9.18. Mass spectra for Problem 9.8.

between the two spectra indicated by the dotted lines. Notice that, in addition to D atoms on the otherwise unsubstituted phenyl ring, the second aromatic ring contains a Cl atom whose presence or absence also can be followed.

(**a**) List how much mass is lost from the $M^{+\bullet}$ in producing important ions whose peaks occur at *m*/*z* values of 205 or above in the diazepam spectrum.

(**b**) From the shifts in *m*/*z* values observed in the spectrum of the deuterated derivative, calculate how many D atoms are lost and retained in the formation of each of these ions, as well as whether the Cl atom is present or not in the ion.

(**c**) Postulate what functional groups might be lost in order to account for the ions whose peaks appear in the spectrum of the derivative.

(**d**) Propose mechanisms that would account for these losses.

REFERENCES

C. C. Clark, "Electron Impact Mass Spectrometry for Identification of Phencyclidine," *J. Assoc. Off. Anal. Chem.*, **69**, 814–820 (1986).

B. A. Lodge, R. Duhaime, J. Zamecnik, P. MacMurray, and R. Brousseau, "New Street Analogs of Phencyclidine," *Foren. Sci. Int.*, **55**, 13–26 (1992).

R. H. Shapiro, D. S. Amenta, M. T. Kinter, and K. B. Komer, "Mass Spectral Analysis of Cocaine and Pseudococaine," *Spectroscopy: Int. J.*, **2**, 227–231 (1983).

R. M. Smith, "Arylhydroxy Metabolites of Cocaine in the Urine of Cocaine Users," *J. Anal. Toxicol.*, **8**, 35–37 (1984*a*).

R. M. Smith, "Ethyl Esters of Arylhydroxy- and Arylhydroxymethoxycocaines in the Urines of Simultaneous Cocaine and Ethanol Users," *J. Anal. Toxicol.*, **8**, 38–42 (1984*b*).

R. M. Smith, "The Mass Spectrum of Cocaine," *J. Foren. Sci.*, **42**, 475–480 (1997).

R. M. Smith, M. A. Poquette, and P. J. Smith, "Hydroxymethoxybenzoylmethylecgonines: New Metabolites of Cocaine From Human Urine," *J. Anal. Toxicol.*, **8**, 29–34 (1984).

DropBooks

10

ANSWERS TO PROBLEMS

Chapter 1

1.1. In order to scan from high to low *m*/*z* values in the QIT, initial values of *q* would have to be high. At these values for *q*, only ions having high *m*/*z* values would be trapped.

1.2. The structures proposed for some of these ions will seem more logical after the discussion of α-cleavage in Chapter 6.

m/*z*

31: ^{+}CF

69: $^{+}CF_3$

100: $F_2C^{+}-{}^{\bullet}CF_2 \quad (C_2F_4)^{+\bullet}$

114: $F_2C{=}N^{+}{=}CF_2 \quad (C_2F_4N^{+})$

119: $CF_3C^{+}F_2 \quad (^{+}C_2F_5)$

131: $CF_2{=}CFC^{+}F_2 \quad (^{+}C_3F_5)$

219: $CF_3CF_2CF_2C^{+}F_2 \quad (^{+}C_4F_9)$

Understanding Mass Spectra: A Basic Approach, *Second Edition*. By R. Martin Smith
ISBN 0-471-42949-X © 2004 John Wiley & Sons, Inc.

264: $CF_3CF_2CF_2CF{=}N^+{=}CF_2$ $(C_5F_{10}N^+)$

414: $CF_3CF_2CF_2CF{=}N^+{=}CFCF_2CF_2CF_3$ $(C_8F_{16}N^+)$

464:
$$\begin{array}{l} CF_3CF_2CF_2CF_2{-}N^+{=}CF_2 \\ \qquad\qquad\qquad\quad | \\ \qquad\qquad\qquad\quad CF{=}CF{-}CF_2CF_3 \end{array} \quad (C_9F_{18}N^+)$$

502: $(CF_3CF_2CF_2CF_2)_2{-}N^+{=}CF_2$ $(C_9F_{20}N^+)$

576:
$$\begin{array}{l} CF_3CF_2CF_2CF_2{-}N^+{=}CF{-}CF{=}CF{-}CF_3 \\ \qquad\qquad\qquad\quad | \\ \qquad\qquad\qquad\quad CF{=}CF{-}CF_2CF_3 \end{array} \quad (C_{12}F_{22}N^+)$$

614: $(CF_3CF_2CF_2CF_2)_2{-}N^+{=}CF{-}CF{=}CF{-}CF_3$ $(C_{12}F_{24}N^+)$

1.3. 3-Ethylcyclohexene has the elemental composition C_8H_{14}, which has a molecular mass of 110. The peak at *m/z* 96 in the spectrum shown in Figure 1.30 appears to correspond to the $M^{+\bullet}$, especially because the first observed fragment ion peak occurs at *m/z* 81 (M − 15, which corresponds to the loss of a methyl radical, $^\bullet CH_3$). Therefore, the apparent $M^{+\bullet}$ peak does not correspond to the molecular mass. The peak at *m/z* 96 cannot result from fragmentation of the $M^{+\bullet}$ of 3-ethylcyclohexene because ions do not lose fragments of 14 u (110 − 96 = 14; see Section 4.1). This spectrum undoubtedly is not that of 3-ethylcyclohexene.

DropBooks

Chapter 2

2.1. If *m/z* 44 is the $M^{+\bullet}$ peak, the peaks at *m/z* 45 and 46 might arise from ions that contain ^{13}C instead of ^{12}C, or ^{15}N instead of ^{14}N. (It is also possible that this unknown does not produce an $M^{+\bullet}$, and that *all* the observed ions are fragment ions. Detecting this possibility is discussed in Chapter 5.) There are only a limited number of organic compounds that contain C and also have a molecular mass of 44:

$$CO_2 \qquad CH_3CHO \qquad (CH_2)_2O \qquad CH_3CH_2CH_3$$
$$FC{\equiv}CH \qquad CH_3N{=}NH \qquad CH_2NNH_2$$

The observed losses from the *m/z* 44 peak are almost exclusively multiples of 12 and 16, 16 to give the peak at *m/z* 28, 28 (16 + 12) to produce the *m/z* 16 peak, and 32 (16 + 16) to give the peak at *m/z* 12. This, coupled with the fact that loss of hydrogen radicals ($H^\bullet$) is not observed (i.e., there are no peaks at *m/z* 43, 42, 27, etc.), makes most of the listed possibilities seem unlikely. If those structures that contain H are eliminated, only CO_2 remains. The peak at *m/z* 22 may be puzzling at first, but it is due to the M^{2+} ion. This supports the assumption that *m/z* 44 is the $M^{+\bullet}$ peak. [*Answer*: carbon dioxide;

CO_2 (Equation 10.1)]

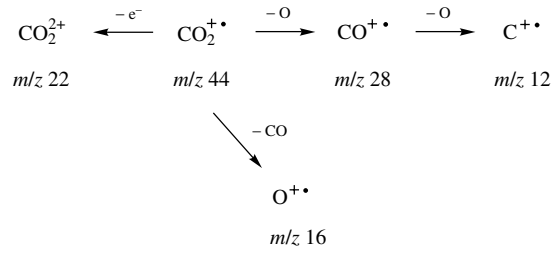

(10.1)

2.2. Atomic weight of Br $= [(78.918)\,(50.69\%) + (80.916)\,(49.31\%)]/100\%$
$= 79.903 \approx 80$

Average molecular mass of $Br_2 = 79.90 \times 2 = 159.80 \approx 160$

The $M^{+\bullet}$ region in the mass spectrum for Br_2 will show peaks at *m/z* 158 for ions containing two atoms of ^{79}Br, *m/z* 160 for those containing one atom of ^{79}Br and one of ^{81}Br, and *m/z* 162 for those having two atoms of ^{81}Br.

2.3. The probabilities representing various combinations of Cl isotopes in an ion that contains three Cl atoms are as follows:

$$P(3^{35}Cl) = (0.758)^3 = 0.436,\ P(2^{35}Cl)\,(^{37}Cl) = (0.758)^2\,(0.242) = 0.139$$
$$P(^{35}Cl)\,(2^{37}Cl) = (0.758)\,(0.242)^2 = 0.044,\quad P(3^{37}Cl) = (0.242)^3 = 0.014$$

When both isotopes are present at the same time, three different orientations are possible, so that

$$[X]/[X+2]/[X+4]/[X+6]$$
$$= P(3^{35}Cl)/[3 \times P(2^{35}Cl)\,(^{37}Cl)]/[3 \times P(^{35}Cl)\,(2^{37}Cl)]/P(3^{37}Cl)$$
$$= (0.436)/[3 \times (0.139)]/[3 \times (0.044)]/(0.014)$$
$$= 0.436/0.417/0.132/0.014$$
$$= 100.0/95.6/30.2/3.2$$

2.4. (**a**)

$[m/z\ 234]/[m/z\ 236]/[m/z\ 238] = 51/100/47 \approx 51/100/49 \rightarrow$ 2 Br atoms
$[m/z\ 155]/[m/z\ 157] = 36/35 = 100/97 \approx 100/98 \rightarrow$ 1 Br atom

(**b**) $[m/z\ 270]/[m/z\ 272]/[m/z\ 274]/[m/z\ 276]/[m/z\ 278] = 6/12/10/3.5/1 = 50/100/83/30/8 \rightarrow$ Does not fit any pattern in Figure 2.6, but because $270 - 235 = 35$ and the ion with *m/z* 235 has five Cl atoms (see

below), one can infer that this ion contains six Cl atoms.

$[m/z\ 235]/[m/z\ 237]/[m/z\ 239]/[m/z\ 241]/[m/z\ 243]$
$= 61/100/64/21/< 1 \approx 61/100/65/21/4$
$\rightarrow$ 5 Cl atoms (best fit, even though peak at m/z 243 is too small)

$[m/z\ 200]/[m/z\ 202]/[m/z\ 204]/[m/z\ 206]$
$= 5/7/3/1 = 71/100/43/14 \approx 77/100/48/11$
$\rightarrow$ 4 Cl atoms
(best fit; because peaks are small, relative errors are large)

$[m/z\ 165]/[m/z\ 167]/[m/z\ 169] = 14/14/4 = 100/100/29$
$\approx 100/98/32/3.5 \rightarrow$ 3 Cl atoms

(c) $[m/z\ 128]/[m/z\ 130]/[m/z\ 132] = 69/89/21 = 77/100/24$
$\approx 77/100/24.5 \rightarrow$ BrCl combination

$[m/z\ 91]/[m/z\ 93]/[m/z\ 95] = 5/23/18 = 22/100/78 \rightarrow$ Does not match any pattern in Figure 2.6. The mass of this ion is too low to contain more than one Br atom or two Cl atoms. Therefore, it is likely that this cluster consists of overlapping clusters from two different fragment ions. If the ion with m/z 91 (rel. int. = 5.3%) contains 1 ^{79}Br atom, then there must be a corresponding peak with the same intensity at m/z 93 for the ion containing a ^{81}Br atom. But the m/z 93 peak is much larger than that, so the remaining intensity (23.0 − 5.3 = 17.7%) must be due to the presence of some other ion. The peak at m/z 95 also has an intensity of 17.7%, so that the ion corresponding to the m/z 93 − m/z 95 pair also contains one Br atom.

$[m/z\ 79]/[m/z\ 81] = 7/7 = 100/100 \approx 100/98 \rightarrow$ 1 Br atom
$[m/z\ 49]/[m/z\ 51] = 100/32 \approx 100/33 \rightarrow$ 1 Cl atom

2.5. Size of M + 1 peak for $C_{60} = 60 \times 1.1\% = 66\%$
Size of M + 2 peak for $C_{60} = (60 \times 1.1\%)^2/200 = 21.8\%$
Size of M + 3 peak (see Sections 2.2.1.3 and 2.2.1.5)

$$= C(n, 3)\frac{(0.989)^{60-3}(0.011)^3}{(0.989)^{60}} = \frac{n(n-1)(n-2)}{6}\frac{(0.011)^3}{(0.989)^3}$$

$$= \frac{(60)(59)(58)}{6}\frac{(0.011)^3}{(0.989)^3} = 0.047 \rightarrow 4.7\%$$

$$\text{Size of M} + 4 \text{ peak} = C(n, 4)\frac{(0.989)^{60-4}(0.011)^4}{(0.989)^{60}}$$

$$= \frac{(60)(59)(58)(57)}{(1)(2)(3)(4)}\frac{(0.011)^4}{(0.989)^4} = 0.0075 \rightarrow 0.75\%$$

DropBooks

2.6. **(a)** Because the ions having *m/z* 235, *m/z* 237, and *m/z* 239 all contain the same number of A + 1 elements, calculation of the number of C atoms by using any of these pairs should lead to the same result:

$[m/z\ 235]/[m/z\ 234] = 3.5/50.9 = 6.9\% \approx [m/z\ 237]/[m/z\ 236] = 6.5/100 = 6.5\% \approx [m/z\ 239]/[m/z\ 238] = 3.3/47.3 = 7.0\%$. The average intensity of the M + 1 peaks for these pairs is 6.8%, which is consistent with the presence of $6.8/1.1 = 6.2 \approx 6$ C atoms.

$[m/z\ 156]/[m/z\ 155] = 2.6/35.7 = 7.3\% \approx [m/z\ 158]/[m/z\ 157] = 2.4/34.8 = 6.9\%$. The average intensity of the X + 1 peak for these pairs is 7.1%, which is also consistent with the presence of $7.1/1.1 = 6.4 = \approx 6$ C atoms. This result is expected because $234 - 155 = 79$, the mass of one Br atom. Therefore, the ions having *m/z* 155 and 234 both must contain the same number of C atoms.

The compound that produced the spectrum in Figure 2.8*a* thus contains two Br atoms (Problem 2.4) and six C atoms. The combined mass of these atoms is $(2 \times 79) + (6 \times 12) = 158 + 72 = 230$ u. This is 4 u short of the observed MM; therefore, the remaining mass must be due to four H atoms. [*Answer*: $C_6H_4Br_2$]

(b) The intensities of the peaks in the cluster beginning at *m/z* 270 are too small to have their M + 1 peaks recorded. But because $270 - 235 = 35$ (the mass of one Cl atom) the number of C atoms in the $M^{+\bullet}$ can be deduced by determining the number of C atoms in the ion having *m/z* 235. For these peaks,

$$[m/z\ 236]/[m/z\ 235] = 4.0/61.1 = 6.5\% \approx [m/z\ 238]/[m/z\ 237] = 5.3/100 = 5.3\% \approx [m/z\ 240]/[m/z\ 239] = 4.0/63.7 = 6.3\%$$

The average intensity for the X + 1 peak for these pairs is 6.0%, indicating the presence of 5.5 C atoms. This is just at the limit of the ±10% error in determining the relative intensities of mass spectral peaks, and underscores the difficulty in determining the precise number of C atoms in an ion by this method. The remaining peaks in the spectrum do not have X + 1 intensities recorded.

The ion having *m/z* 235 contains five Cl atoms (Problem 2.4), which have a combined mass of $5 \times 35 = 175$ u. An additional five C atoms have a combined mass of $5 \times 12 = 60$ u. The combination of five Cl and five C atoms adds up to the observed ionic mass, so that the elemental composition for this ion is $^{+}C_5Cl_5$. The $M^{+\bullet}$ contains an additional Cl atom (Problem 2.4), resulting in an elemental composition of C_5Cl_6. [*Answer*: C_5Cl_6]

(c) $[m/z\ 129]/[m/z\ 128] = 0.7/69.0 = 1.0\% \approx [m/z\ 131]/[m/z\ 130] = 1.0/89.4 = 1.1\%$. The average intensity for the M + 1 peak in this cluster is 1.1%, consistent with the presence of one C atom.

$[m/z\ 50]/[m/z\ 49] = 1.3/100 = 1.3\% \rightarrow 1$ C atom

The $M^{+\bullet}$ contains one Br atom, one Cl atom (Problem 2.4), and one C atom for a combined mass of $79 + 35 + 12 = 126$ u. The presence of two H atoms completes the mass requirement for the $M^{+\bullet}$. The ion having *m/z* 49 contains one Cl atom (Problem 2.4) and one C atom, giving $35 + 12 = 47$ u. The remaining mass for this ion is also made up of two H atoms, producing an elemental composition of $^{+}CH_2Cl$. [*Answer*: CH_2ClBr]

2.7. The peak clusters at *m/z* 207 and, especially, at *m/z* 281 have X + 2 peaks that are inconsistent with the atoms present in this molecule. A comparison of this spectrum with the one in Figure 2.11 shows that these clusters are due to silicones that are present as impurities, not to the compound whose structure is shown. This spectrum should not be included in any collection of standard spectra.

2.8. The cluster of peaks that appears to represent the $M^{+\bullet}$ contains a doublet of equally intense peaks separated by 2 *m/z* units. The first (and most intense) peak in this cluster occurs at an odd *m/z* value (157), meaning that the MM must be odd also. Because of the nitrogen rule, this compound must contain at least one N atom. The intense doublet at *m/z* 157 and 159, with a ratio of intensities of 100/99, is consistent with the presence of one Br atom. No other A + 2 elements are obviously present.

The fragment ion peak at *m/z* 78 in Figure 2.15 does not have a corresponding X + 2 peak, showing that the Br atom is lost when this peak is produced ($157 - 78 = 79$, the mass of one Br atom). The peaks at *m/z* 158 and 160 represent the $(M + 1)^+$ ions for the peaks corresponding to the two isotopes of Br. Both provide the same information concerning the number of C and N atoms in the compound. In fact, so does the *m/z* 79 peak since this ion does not contain Br. If one N atom is assumed to be present, the ^{15}N contribution to the *m/z* 158 peak is 0.4%. The remaining intensity of the *m/z* 158 peak ($6.0 - 0.4 = 5.6\%$) is due to the ^{13}C contribution and is consistent with the presence of $5.6/1.1 = 5.1$ or 5 C atoms. The peak at *m/z* 79 has an intensity of $4.1/68.1 = 6.0\%$ relative to the *m/z* 78 peak, which is also consistent with the presence of one N atom (0.4%) and five C atoms (5.5%) in the corresponding ion. Five C atoms, a N atom, and a Br atom add up to $(5 \times 12) + (1 \times 14) + (1 \times 79) = 153$ u, leaving 4 u to be accounted for by four H atoms. The elemental composition of the $M^{+\bullet}$ is thus C_5H_4NBr.

The rings plus double bonds formula determines that this elemental composition gives rise to $5 - \frac{1}{2}(4 + 1) + \frac{1}{2} + 1 = 4$ rings plus double bonds—an unsaturated molecule that is likely to contain an aromatic ring. (Note that the Br atom counts as a H atom in this equation; see Section 2.3.) A simple structure that fulfills these requirements is bromopyridine. Three isomeric structures are possible, and they cannot be easily distinguished without comparing the standard spectra of all three compounds. [*Answer*: 3-bromopyridine (Equation 10.2)]

DropBooks

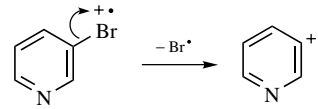

m/z 157 *m/z* 78 (10.2)

2.9. The $M^{+\bullet}$ peak occurs at *m/z* 123, which means that the compound has an odd nominal MM. As in the previous problem, the presence of an odd number of N atoms is indicated, and the presence of one N atom will be assumed initially. To facilitate determination of isotopic peak intensities, the relative intensities for the $M^{+\bullet}$ peak cluster must be normalized so that the intensity of the $M^{+\bullet}$ peak is 100%. This is done by dividing each intensity by the observed intensity of the $M^{+\bullet}$ peak (52.7%) and multiplying by 100:

	Obs. Int.	Normalized Int.
m/z 123	52.7%	100.0%
124	3.8%	7.2%
125	0.3%	0.6%

Because the normalized intensity of the M + 2 peak is <1%, none of the obvious A + 2 elements can be present.

The intensity of the M + 1 peak must account for the presence of both N and C. Subtracting the contribution of one N atom from the normalized observed intensity leads to $7.2 - 0.4 = 6.8\%$ for the contributions of 6.8/1.1 ~ 6 C atoms.

Determining the elemental composition of the ion having *m/z* 77 is not as straightforward because the presence of the N atom in this ion cannot be determined using the nitrogen rule (it is uncertain whether or not this ion is an odd-electron ion; Section 3.5). The observed intensity for the X + 1 peak at *m/z* 78, however, seems more consistent with the presence of six C atoms ($6 \times 1.1 = 6.6\%$) than with five C atoms and a N atom [$(5 \times 1.1) + 0.4 = 5.9\%$]. If the ion contains six C atoms, then its elemental composition must be $^{+}C_6H_5$.

Six C atoms and one N atom account for $(6 \times 12) + (1 \times 14) = 86$ u, so that 37 u remain to be assigned. Although the molecule could theoretically contain two more N atoms (just *one* more would cause the MM to be even), this seems unlikely because these atoms would add $2 \times 0.4 = 0.8\%$ to the intensity of the M + 1 peak. This is inconsistent with the observed intensity. Instead, the intensity of the M + 2 peak provides possible clues. Nitrogen contributes nothing to the intensity of the M + 2 peak, and six C atoms contribute only $(6.6)^2\%/200 = 0.2\%$, well short of the observed intensity. Since the obvious A + 2 elements are absent, the only choice remaining is O. Two O atoms would contribute not only $0.2 \times 2 = 0.4\%$ to the M + 2 peak (giving a total of $0.2 + 0.4 = 0.6\%$), but also 32 of the 37 missing units of

mass. The remaining 5 u are attributable to H, producing an elemental composition of $C_6H_5NO_2$.

The number of rings plus double bonds in this molecule is $6 - 1/2(5) + 1/2 + 1 = 6 - 2.5 + 0.5 + 1 = 5$. An aromatic compound would be a good starting place for postulating a structure, and the peak at *m/z* 77 ($^+C_6H_5$; the phenyl ion) is consistent with that assumption. This accounts for three double bonds and one ring; the remaining double bond must be exterior to the ring. The N and two O atoms constitute a nitro group, which contains that double bond. [*Answer*: nitrobenzene; $C_6H_5NO_2$ (Equation 10.3)]

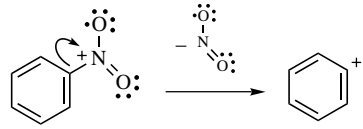

m/z 123 *m/z* 77 (10.3)

2.10. The small cluster of peaks between *m/z* 118 and 122 offers the best choice for locating the $M^{+\bullet}$ peak. These peaks are all separated by 2 *m/z* units, so that the presence of more than one Br and/or Cl atom seems likely. This makes the peak at *m/z* 118 the most likely choice for the $M^{+\bullet}$ peak. This peak occurs at an even *m/z* value, indicating that N probably is not present. The relative intensities of the peaks at *m/z* 118, 120, and 122 are 0.5/0.45/0.15 ~ 100:90:30, but because they are so weak, their intensities are known imprecisely. By comparison with Figure 2.6, this pattern most closely fits that for three Cl atoms.

DropBooks

The peak cluster at *m/z* 83 to 87 also strongly suggests the presence of Cl. Comparison of relative intensities of the peaks at *m/z* 83, 85, and 87 with those in Figure 2.6 indicates that this ion contains two Cl atoms (100/62/12 vs. 100/65/11). If so, then *m/z* 118, being 35 units above *m/z* 83, must contain three Cl atoms, as indicated above.

The weak intensities of the peaks in the *m/z* 118–122 cluster precludes obtaining information about other elements that might be present. Therefore, the cluster beginning at *m/z* 83 must be used to determine elemental compositions. The peak at *m/z* 84 has an intensity of 1.3%, which is consistent with the presence of one C atom in the ion having *m/z* 83. Because 83 u is 13 more than the combined mass of two Cl atoms, its structure must be $^+CHCl_2$. Adding a Cl atom to this formula gives $CHCl_3$ as the elemental composition for the $M^{+\bullet}$.

The cluster of peaks beginning at *m/z* 47 is complex and contains two overlapping clusters: *m/z* 47 and 49 due to CCl^+ and *m/z* 48 and 50 from $CHCl^{+\bullet}$. The normalized intensity of the *m/z* 49 peak is 31.3% relative to that of *m/z* 47, and that of *m/z* 50 is 35.6% of the intensity of the peak at *m/z* 48. The peaks at *m/z* 35 and 36 (with isotope peaks at *m/z* 37 and 38,

respectively) correspond to $Cl^+$and $HCl^{+\bullet}$. [*Answer*: chloroform; $CHCl_3$ (Equation 10.4)]

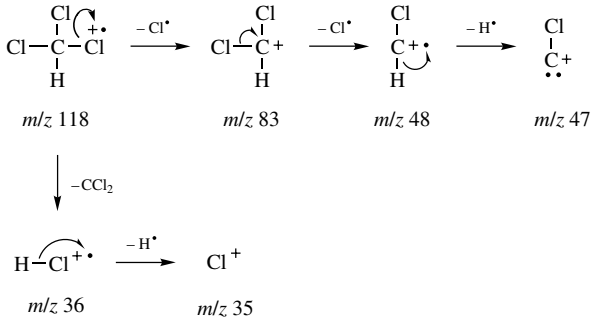

(10.4)

2.11. The peak at *m/z* 134 appears to represent the $M^{+\bullet}$, giving an even nominal MM. An even number of N atoms is indicated; an assumption that there are none will be made initially. Normalized intensities for the $M^{+\bullet}$ peak cluster are as follows:

m/z 134	100.0%
m/z 135	11.3%
m/z 136	0.6%

These intensities are inconsistent with the presence of any of the obvious A + 2 elements. If no N atoms are present, the normalized intensity of the M + 1 peak indicates the presence of $11.3/1.1 = 10.3 \approx 10$ C atoms. (Notice that the answer is 10 C atoms, not 11, because each C atom contributes 1.1%, not 1.0%, to the intensity of the M + 1 peak.)

Ten C atoms contribute 120 u of mass, leaving only 14 u to account for. The presence of O, as well as the presence of only one N atom, is impossible, and the intensity of the M + 2 peak can be accounted for solely by the 10 C atoms: $(0.006 \times 10^2)\% = (0.006 \times 100)\% = 0.6\%$. The remaining mass, therefore, must be due to H, leading to an elemental composition of $C_{10}H_{14}$.

From the intensity of the *m/z* 120 peak, the ion having *m/z* 119 appears to have $10.6/1.1 = 9.6$ C atoms. Although this rounds up to 10 C atoms, such a number is clearly impossible because the combined mass of 10 C atoms is 120. The presence of 9 C atoms in this ion is more likely, arising from loss of a methyl radical ($^{\bullet}CH_3$) from the $M^{+\bullet}$.

The rings plus double bonds formula yields $10 - \frac{1}{2}(14) + 0 + 1 = 4$ unsaturations. As in previous problems, an aromatic ring structure seems likely. Many isomeric structures are possible, and the mass spectra of many of these compounds are similar. [*Answer*: 1,4-diethylbenzene

(Equation 10.5)]

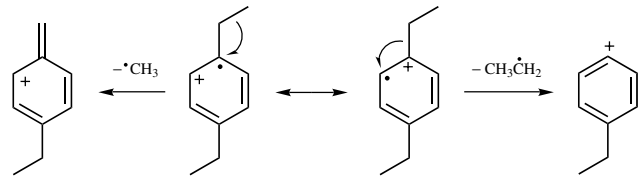

(10.5)

m/z 119 *m/z* 134 *m/z* 105

2.12. Although there are two peaks of nearly equal intensity in the region of the spectrum where the $M^{+\bullet}$ peak might occur, these peaks are *not* separated by 2 *m/z* units. Therefore, they do not imply the presence of an A + 2 element. If one of these peaks corresponds to the $M^{+\bullet}$, which one is it? The answer is the peak at *m/z* 86, because it is far too intense to be due to isotope contributions from the *m/z* 85 ion by any of the common A + 1 elements. Most likely, the $M^{+\bullet}$ peak is the peak at *m/z* 86, and the *m/z* 85 peak is the M − 1 peak. This is corroborated by the fact that the first fragment ion peak observed below these peaks is the one at *m/z* 71, which would correspond to the M − 15 (M − $^{\bullet}CH_3$) peak. The nominal MM is thus even, and the presence of N is not suspected initially.

The number of C atoms in the $M^{+\bullet}$ can be *estimated* by calculating the intensity of the the peak at *m/z* 87 peak relative to that of the peak at *m/z* 86: 2.7/49.4 = 5.5%, or five C atoms. If there are five C atoms in the $M^{+\bullet}$, there must also be five C atoms in the $(M-1)^+$ ion, because this ion is produced by loss of •H from the $M^{+\bullet}$. The observed intensity for the *m/z* 85 peak is 54.4%, so that a contribution of 54.4% × 5.5% = 3.0% is expected for the *m/z* 86 peak due to the five C atoms present in the *m/z* 85 ion. This leaves 49.4 − 3.0 = 46.4% of the *m/z* 86 peak intensity that is due to the actual $M^{+\bullet}$. The number of C atoms in the $M^{+\bullet}$ must be calculated based on this number, 2.7/46.4 = 5.8%, which is still consistent with five C atoms.

Five C atoms will also produce a peak having $(0.006 \times 5^2)\% = 0.15\%$ normalized intensity at *m/z* 88. The actual normalized intensity for this peak is 0.2/46.4 = 0.4%, which *may be* significantly larger than that calculated for C alone. (Remember that the intensities of weak intensity peaks sometimes have large errors in measurement.) Nonetheless, the presence of a single O atom would account for the difference.

The combined mass of five C atoms and one O atom is (5 × 12) + 16 = 76 u, 10 u short of the observed MM. The difference must be made up by 10 H atoms, leading to an elemental composition of $C_5H_{10}O$. The rings plus double bonds formula predicts $5 - \frac{1}{2}(10) + 0 + 1 = 1$ unsaturation. This could be due either to a ring or double bond, and, without further knowledge of how compounds like this fragment (Equation 10.6), determining a unique structure is impossible. [*Answer*: tetrahydropyran]

DropBooks

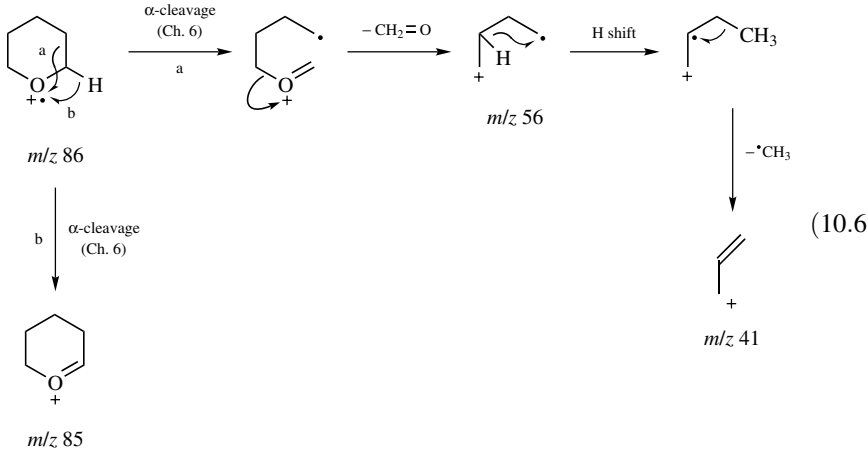

(10.6)

2.13. The observed peak intensities are

m/z 299	100.0%
m/z 300	22.0%
m/z 301	2.5%

From the intensity of the m/z 300 peak, the calculated number of C atoms is $22.0/1.1 = 20.0$; this value is correct. Twenty C atoms will contribute $(20 \times 1.1)^2\%/200 = 2.4\%$ to the size of the m/z 301 peak, which is close to the observed value. However, 20 C atoms accounts for only $20 \times 12 = 240$ u of the mass of this ion—59 u short of the observed mass. No obvious $A + 2$ elements are present (nor is N, because the nominal MM, 314, is even; see Table 1.3), so that O probably makes up some of this difference. The presence of 2 O atoms and 27 H atoms seems likely just from an arithmetic standpoint (20 C atoms cannot accommodate either 59 H atoms or 43 H atoms and 1 O atom), but the number of O atoms cannot be determined directly from the observed intensity of the m/z 301 peak.

These values are actually quite good considering that no attempt was made to produce a spectrum in which the peak intensities were known precisely. Nonetheless, it should be apparent that if the data were not this good, it would be nearly impossible to determine a unique elemental composition for this ion.

Chapter 3

3.1. The IE for the formation of $^+CH_3$ is much higher (9.8 eV) than that for the benzyl ion (7.1 eV), so that reactions leading to its formation will not be favored.

3.2. (a)

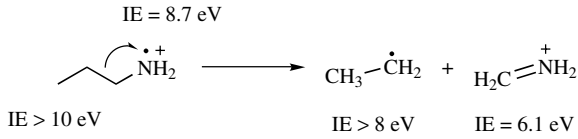

(10.7)

(b)

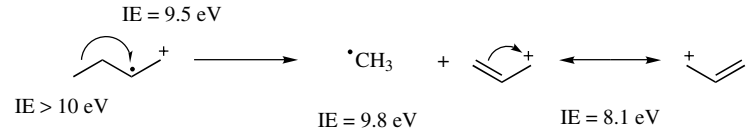

(10.8)

(c)

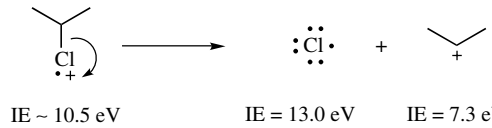

(10.9)

(d)

DropBooks

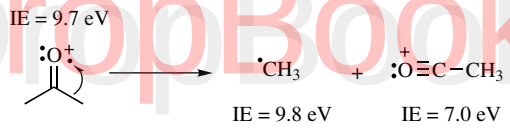

(10.10)

(e)

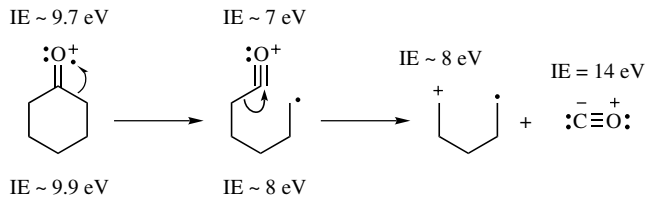

(10.11)

3.3.

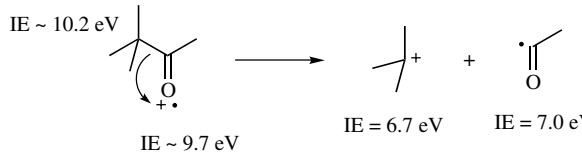

(10.12)

Chapter 4

4.1. **(a)** The MM and relative intensities in the $M^{+\bullet}$ peak cluster are consistent with the structure shown on the spectrum. The loss of 28 u from the $M^{+\bullet}$ that produces the ion having *m/z* 170, whatever its nature, cannot involve the loss of Br, yet there is no correspondingly intense peak at either *m/z* 168 or 172 to indicate the presence of Br in this ion. Either the *m/z* 170 peak is the result of some contaminant or artifact, or the intensity of the *m/z* 168 or 172 peak has been reported incorrectly. This spectrum should not be considered representative of the indicated compound.

(b) The MM of this compound is 210, and the isotope peak intensities in the $M^{+\bullet}$ peak cluster are reasonable for the structure shown. The loss of 15 as $^{\bullet}CH_3$ to produce the peak at *m/z* 195 is expected (Section 6.2.1), but the loss of 8 to give the *m/z* 202 peak is not (Table 4.1). In addition, there are no isotope peaks associated with the *m/z* 202 peak, even though all the rest of the intense peaks at high *m/z* values have these isotope peaks. This peak looks like an electronic artifact (a noise spike), not the result of a contaminant in the sample. Other spectra of this compound that were obtained during the same analysis should be examined to see if they also contain the *m/z* 202 peak. If they do not, that would confirm this peak is indeed a noise spike. Neither of these spectra should be included in any collection of standard spectra.

4.2. Despite the relatively high MM of this compound, the spectrum is approachable by focusing on the problem solving techniques that have been discussed so far. The major peaks in the $M^{+\bullet}$ peak cluster all occur at even *m/z* values, whereas most of the fragment ion peaks occur at odd *m/z* values. Barring other evidence, the presence of N is not indicated. The spectrum is replete with peak clusters in which individual peaks are separated by 2 *m/z* units, strongly implying the presence of Cl and/or Br. Although it is less intense than the *m/z* 198 peak, the peak at *m/z* 196 looks like the best choice for the $M^{+\bullet}$ peak because it occurs at the lowest *m/z* value in that cluster.

The peak intensity ratio for the M, M + 2, and M + 4 peaks in the $M^{+\bullet}$ peak cluster is 79/100/25, which is close to the 77/100/25 pattern expected for a combination of one Cl and one Br atom (Section 2.2.1.1 and Figure 2.6). This pattern is repeated in the clusters beginning at *m/z* 177 and 127. The intensities of the peaks at *m/z* 197 and 199 both indicate the presence of two C atoms in the $M^{+\bullet}$.

Because there are so many fragment ions in this spectrum, it is useful to list the apparent losses from the $M^{+\bullet}$:

m/z	*m/z* Loss	Group Lost	Observed Isotope Pattern
177	19	F	BrCl
161	35	Cl	Br?
145	51	?	BrCl?
142	54	(Cl + F)?	Br?
127	69	CF_3	BrCl
117	79	Br	C_2Cl
111	85	Cl + 50 u	Br

The first loss indicates that there is probably at least one F atom in the molecule, and the loss of 69 strongly suggests the presence of a CF_3 group (see the answer to Example 4.1).

If the masses of the atoms known or suspected to be present are added together, they come to 79 (Br) + 35 (Cl) + 24 (2C) + 57 (3F) = 195 u. This leaves only a H atom remaining. Supporting evidence for the presence of H comes from the weak intensity peak at *m/z* 176, which also makes halogen isotope contributions to the peaks at *m/z* 178 and 180. Several isomeric arrangements of these atoms are possible, but the one that places all three F atoms on the same C most easily accounts for the peaks at *m/z* 127 and 69.

Proposed fragmentations that account for the formation of all these ions is shown in Figure 10.1. [*Answer*: 1-bromo-1-chloro-2,2,2-trifluoroethane (halothane); BrClCH-CF_3]

DropBooks

4.3. There are nine isomeric C_7H_{16} structures:

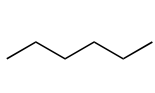

A: *n*-heptane

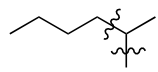

B: 2-methylhexane

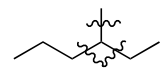

C: 3-methylhexane

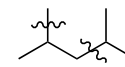

D: 2,4-dimethyl-pentane

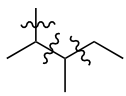

E: 2,3-dimethyl-pentane

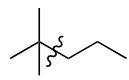

F: 2,2-dimethyl-pentane

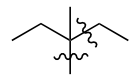

G: 3,3-dimethyl-pentane

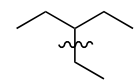

H: 3-ethylpentane

I: 2,2,3-trimethyl-butane

Based on the discussions in this section, the following features should be expected from these structures:

A: A "typical" *n*-alkane spectrum like Figure 4.7, for example, with the M − 15 peak having the lowest intensity of the fragment ion peaks resulting from loss of alkyl radicals. Spectrum *a* in Figure 4.10 is consistent with this structure.

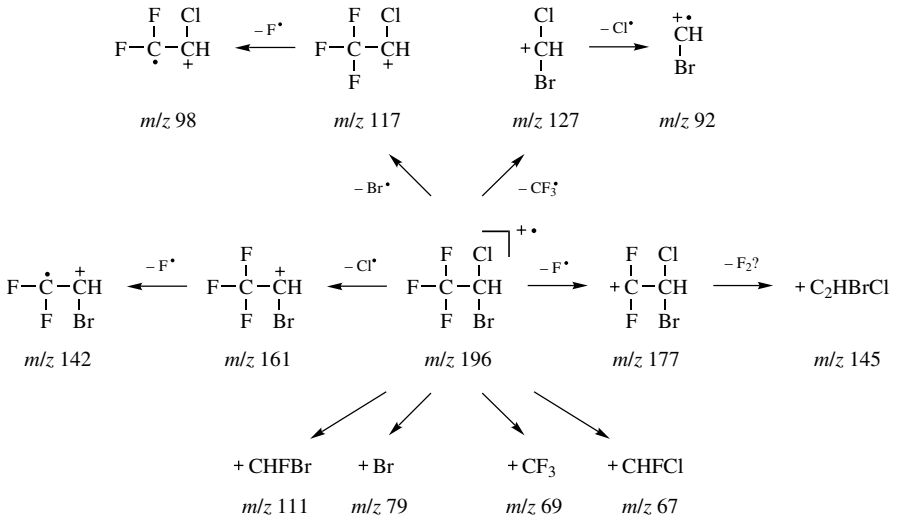

Figure 10.1. Proposed fragmentations of halothane (Problem 4.2).

B: Loss of either a methyl or butyl radical generates a secondary carbenium ion, so that peaks at *m/z* 85 and 43 should be prominent. Loss of an ethyl radical is not expected, because this would produce a primary carbenium ion and primary radical. Loss of an isopropyl radical to produce an *m/z* 57 peak might be significant due to the relative stability of the isopropyl radical. Spectrum *b* in Figure 4.10 is consistent with these expectations.

C: Loss of a methyl, an ethyl, or a propyl radical leads to a secondary carbenium ion; thus, peaks at *m/z* 85, 71, and especially *m/z* 57 should be intense. Although spectrum *a* (Figure 4.10) is a possibility, the *m/z* 85 peak in the spectrum of this compound might be expected to be larger than the $M^{+\bullet}$ peak (compare the spectrum of 2-methylheptane; Figure 4.9*b*).

D: This molecule is likely to undergo fragmentation in a manner similar to structure B, except that with this structure, production of an isopropyl carbenium ion also generates an isobutyl radical. Predicting differences between the spectra of Structures B and D is not meaningful at this point.

E: This structure can form secondary carbenium ions by loss of methyl, ethyl, isopropyl, or *s*-butyl radicals. Loss of isopropyl radical should result in an intense *m/z* 57 peak (relative to *m/z* 71 and 85). Although spectrum *a* (Figure 4.10) has peaks at the correct *m/z* values for this structure, the fact that secondary carbenium ions can be formed by several pathways means that the $M^{+\bullet}$ peak should be very weak compared to fragment ion peaks. Because formation of the *s*-butyl carbenium ion also forms a secondary radical, the *m/z* 57 peak in spectrum *a* seems too weak in intensity to fit this structure.

F: Because loss of an *n*-propyl radical leads to the *t*-butyl carbenium ion, *m*/*z* 57 should be the base peak in the spectrum (see Figure 4.9*c* and Equation 4.7). This is not observed in any of the spectra.

G: Loss of either a methyl or an ethyl radical results in a tertiary ion, so that peaks at both *m*/*z* 85 and 71 should be prominent features of the spectrum. No loss of propyl is expected. Spectrum *c* (Figure 4.10) is consistent with this structure.

H: Because loss of $H^{\bullet}$ from the central C atom leads to a tertiary carbenium ion, the presence of an M − 1 peak (even if weak in intensity) is expected. Loss of any of the three ethyl groups should produce an intense *m*/*z* 71 peak relative to the other alkyl fragment ion peaks. These features are not observed in any of the spectra.

I: Like structure F, the stability of both the *t*-butyl carbenium ion and the isopropyl radical should produce a spectrum with *m*/*z* 57 as the base peak. This is not observed in any of the spectra.

Structures F, H, and I appear to be inconsistent with the spectra in Figure 4.10 and can be eliminated. Although Structures C and E are consistent with spectrum *a*, neither one seems like the best candidate. On the other hand, Structure A seems consistent with spectrum *a*, both structures B and D with spectrum *b*, and Structure G with spectrum *c*. In fact, this is as far as one can go on the basis of the available data. Spectrum *b* was actually produced by Structure D, but without the spectrum of B for comparison, this assignment could not be made with certainty.

Spectra for the remaining structures are shown in Figure 10.2. As often happens, there are some unexpected features in the spectra. For example, the peak at *m*/*z* 85 in the spectrum of compound C is smaller than expected, although it is still not smaller than the $M^{+\bullet}$ peak. Compounds E and H both show intense peaks at *m*/*z* 56 and 70, respectively, that represent rearrangement ions. This tendency is more pronounced in compounds that can form highly substituted olefins, whose IEs are lower than those of *n*-alkenes. [*Answer*: (a) *n*-heptane, (b) 2,4-dimethylpentane, and (c) 3,3-dimethylpentane]

DropBooks

4.4. (**a**) s-Butanol [$CH_3CH_2CH(OH)CH_3$]. Ion series: aliphatic ether or alcohol (*m*/*z* 31, 45, and 59); alkane or alkene (*m*/*z* 27, 29, 41, 43, 55, and 57).

(b) 3,3,4-Trimethylhexane. Ion series: saturated alkane (*m*/*z* 29, 43, 57, 71, 99, and 113, with the presence of significant peaks at X − 1 and/or X − 2 for each of these peaks).

(c) 3-Hexene-*Z*. Ion series: unsaturated alkane or alicyclic compound (*m*/*z* 27, 41, 55, and 69).

(d) 1-Phenyl-2-(*N*-methylamino)ethane ($C_6H_5CH_2CH_2NHCH_3$). Ion series: aliphatic amine (*m*/*z* 44; it is not unusual for the remaining peaks in this series to be absent); electron-donating aromatic (*m*/*z* 39, 50 and 51, 63 and 65, 77 and 78, and 91); benzyl (*m*/*z* 39, 65, and 91; in this case, the

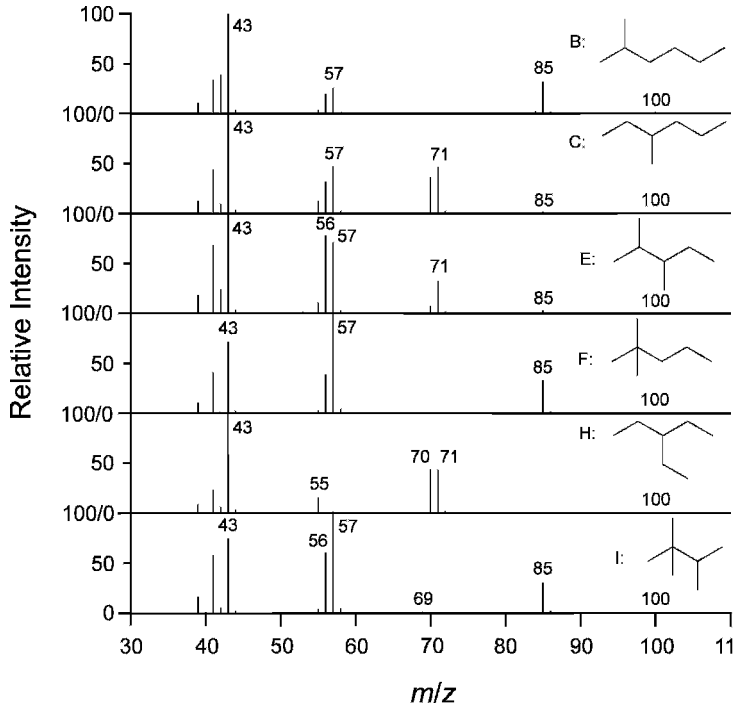

Figure 10.2. Mass spectra of the C_7H_{16} isomers not included in Problem 4.3.

spectrum is so dominated by the peak at *m/z* 44 that it is difficult to discern the presence of this ion series).

(e) 1-Phenyl-2-methylpropane (isobutylbenzene). Ion series: electron-donating aromatic (*m/z* 39, 50–52, 63 and 65, 77 and 78, and 89 and 91); benzyl (*m/z* 39, 65, and 91); alkane (*m/z* 27 and 43, as well as the extremely weak peak at *m/z* 57; in this case, the aliphatic peaks are hard to see among the peaks due to aromatic ions).

4.5. The MM appears to be even (120) and the major fragment ion peaks occur at odd *m/z* values, leading to an initial assumption that N is not present. There are no obvious patterns due to A + 2 elements in the $M^{+\bullet}$ peak cluster. From the isotope peak intensities, the ions having *m/z* 77, 105 and 120 seem to have 6, 7, and 8 C atoms, respectively. An electron-withdrawing aromatic low-mass ion series appears to be present at *m/z* 39, 50–51, 62–65, and 73–77. More important, however, notice that the three most intense ions in the spectrum other than the $M^{+\bullet}$ peak occur at *m/z* 51, 77, and 105, which is the benzoyl ion series (Table 4.2; compare also with Figures 6.19–6.21). This is consistent with the proposed elemental compositions for the *m/z* 77 and 105 ions and accounts for nearly the entire structure. The peak at *m/z* 43 could be

either a propyl ion or the acylium ion (CH_3CO^+). Without isotope peak intensity information, this cannot be determined.

The first loss from the $M^{+\bullet}$ is 15 u ($^{\bullet}CH_3$). This loss must occur from the portion of the molecule that does not contain the benzoyl group; otherwise, the benzoyl ion series would not account for the most important fragment ion peaks in the spectrum. Therefore, this compound must consist of a benzoyl group (C_6H_5CO) and a methyl group. Although several isomeric structures are possible, only the one that has the methyl group attached directly to the carbonyl group accounts for both the benzoyl ion series and the peak at *m/z* 43 (CH_3CO^+). [*Answer*: acetophenone; $C_6H_5COCH_3$ (Equation 10.13)]

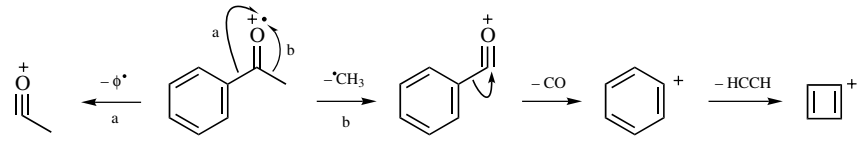

m/z 43 *m/z* 120 *m/z* 105 *m/z* 77 *m/z* 51

(10.13)

Chapter 5

5.1. *(Step 3)* The $M^{+\bullet}$ peak appears to be the one at *m/z* 128. *(Step 4)* The even nominal MM and the fact that all the major fragment ion peaks occur at odd *m/z* values means that N is probably absent. *(Step 5)* The presence of A + 2 heteroatoms is not indicated, and the isotope peak intensities for the $M^{+\bullet}$ peak are consistent with the presence of nine C atoms (*m/z* 129 is 10% ≈ 9 × 1.1% relative to *m/z* 128). If O were present, this would lead to an elemental composition of C_9H_4O and an unlikely (but not impossible) structure that would contain many unsaturations. An elemental composition of C_9H_{20} for the $M^{+\bullet}$ is more likely.

(Step 6) The spectrum contains a lot of fragment ion peaks at low *m/z* values and looks much more like the spectrum of an aliphatic compound than an aromatic one. *(Step 7)* A saturated aliphatic (or ketonic) low-mass ion series is observed at *m/z* 43, 57, 71, 85, and 99. These peaks are all accompanied by other peaks one or two *m/z* values lower, which is more typical of the spectra of saturated hydrocarbons than of ketones (see Example 5.2). *(Step 8)* The progressive losses of alkyl fragments from the $M^{+\bullet}$ indicate that this compound is a saturated alkane. *(Step 10)* The rings plus double bonds formula indicates that there are no unsaturations in the $M^{+\bullet}$, which is expected for a saturated alkane. Determining a unique structure for this compound is more difficult, especially without other spectra for comparison. Despite the fact that the peak at *m/z* 85 is larger than the one at *m/z* 71, this is a spectrum of the straight-chain isomer. [*Answer*: *n*-nonane; C_9H_{20}]

DropBooks

5.2. *(Steps 3 and 4)* The apparent $M^{+\bullet}$ peak occurs at an even *m/z* value (154). The fragment ion peaks in the spectrum occur at both even and odd *m/z* values, making it difficult to determine whether N is present or not by these criteria alone. *(Step 5)* There are no obvious A + 2 heteroatom patterns in the spectrum, and the isotopic peak intensity data from the $M^{+\bullet}$ peak cluster indicate the presence of 12 C atoms in the molecule ($12 \times 1.1\% = 13.2\%$). If this is reliable, C alone accounts for 144 u of the MM, so that the remaining 10 u must come from H. *(Steps 6 and 7)* The $M^{+\bullet}$ peak is over four times more intense than any other peak in the spectrum, typical of a highly unsaturated compound, and there is a distinctive electron-withdrawing aromatic low-mass ion series at *m/z* 39, 50–51, 62–64, and 74–77.

(Step 8) Other than H, the first loss from the $M^{+\bullet}$ is 26 (probably due to HCCH) to give the tiny peak at *m/z* 128, and the *m/z* 128 ion appears to lose 26 u to produce the ion having *m/z* 102. *(Step 10)* All this points to an aromatic compound—possibly one with more than one aromatic ring. Although several $C_{12}H_{10}$ isomers can be drawn [rings plus double bonds $= 12 - \frac{1}{2}(10) + 0 + 1 = 8$], the most common is biphenyl. In reality, the spectra of several of these compounds are similar to this one. [*Answer*: biphenyl; $C_{12}H_{10}$ (Equation 10.14)]

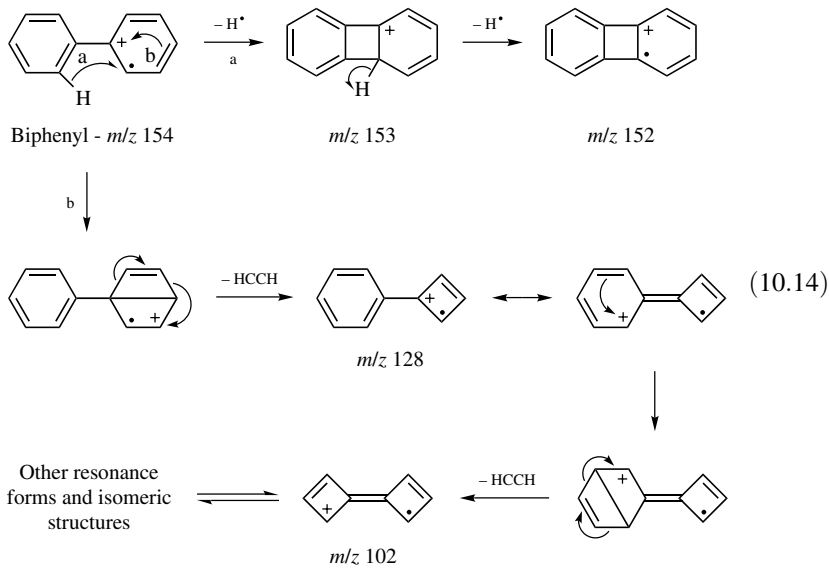

(10.14)

5.3. *(Step 3)* The peak at *m/z* 70 appears to be the $M^{+\bullet}$ peak. *(Step 4)* The compound therefore has an even nominal MM, and all the major fragment ion peaks in the spectrum occur at odd *m/z* values. It is likely that no N is present. *(Step 5)* The isotope peak clusters for the ions having *m/z* 43, 55, and 70 all have useful data for determining elemental composition. If only C, H, and O are present (isotope patterns due to other A + 2 elements are clearly

absent), the normalized relative intensity of the M + 1 peak indicates that the $M^{+\bullet}$ contains 2.8/57.7 = 4.9% → 4 C atoms. The ion having *m/z* 55 is calculated to have either three or four C atoms (4.0/1.1 = 3.6 C atoms). However, if the $M^{+\bullet}$ contains four C atoms and the peak at *m/z* 55 represents the loss of $^{\bullet}CH_3$ (which is the most probable explanation for the origin of a peak at M − 15), then the presence of three C atoms in this ion seems more likely. Finally, the X + 1 peak for the ion having *m/z* 43 has a normalized relative intensity of 2.3/83.1 = 2.8%. Although this is indicative of the presence of 2.8/1.1 = 2.5 C atoms, it is important to remember that the intensity of the X + 1 peak is more likely to predict too many C atoms than too few because of the possible (and often likely) presence of fragment ion peaks contributing to the intensity at that *m/z* value. The presence of two C atoms in the ion having *m/z* 43 therefore seems more likely than three.

The finding that the *m/z* 43 ion has two C atoms, rather than three, is important because it identifies that ion as the acylium ion ($CH_3C{\equiv}O^+$) rather than either the propyl ($CH_3CH_3C^+H_2$) or isopropyl ion ($CH_3C^+HCH_3$). It also identifies the presence of O in the compound. The presence in a spectrum of an intense peak that is due to the acylium ion usually indicates the presence of a carbonyl group in the molecule (Section 6.4). The normalized relative intensities of the *m/z* 57 and 72 peaks, both of which are 0.4–0.5%, are also consistent with the presence of four C atoms plus an O atom.

(*Steps 6 and 7)* The spectrum appears to be that of an aliphatic compound, rather than an aromatic one. The peaks at *m/z* 27 and 55 are indicative of some unsaturation (Table 4.2, series 1b). The peak at *m/z* 43 has already been identified as the acylium ion, not a propyl group.

(*Step 8)* The first observed loss from the $M^{+\bullet}$ is 15, a methyl radical. The difference between 55 and 43 is only 12, a loss forbidden by Table 4.1, and the difference between 70 and 43 is 27, which is often identified with the loss of HCN. In this case, however, the isotope peak intensities for the $M^{+\bullet}$ peak are inconsistent with an elemental composition of $C_2H_2N_2O$, which would be required to satisfy the even MM and the presence of O in the molecule. The other loss of 27 shown in Table 4.1 is that of a vinyl radical ($H_2C{=}C^{\bullet}H$), which seems more reasonable here because of the calculated elemental compositions of the major fragment ions. This is supported by the presence of a large peak at *m/z* 27, which is likely to be due to the vinyl carbenium ion ($H_2C{=}C^+H$). The IE for vinyl radical is 8.8 eV, in contrast to that of HCN, which is 13.8 eV. This means that formation of vinyl ion should compete favorably with formation of acylium ion (IE = 7.0 eV; Table 3.1), whereas formation of $HCN^{+\bullet}$ would not.

(*Step 10)* The combined mass of four C atoms and an O atom is 48 + 16 = 64 u. The remaining mass is due to the presence of six H atoms. An elemental composition of C_4H_6O for the $M^{+\bullet}$ gives rise to $4 - \frac{1}{2}(6) + 0 + 1 = 2$ rings plus double bonds. One of these unsaturations is due to the carbonyl group that was indicated by the presence of the

DropBooks

acylium ion (*m/z* 43). The other is likely to be due to the double bond in a vinyl group. The functional groups that have been identified in this compound are methyl (CH_3), vinyl ($H_2C{=}CH{-}$), and acetyl (CH_3CO, which includes a methyl group). The combined masses of a vinyl group (27) and an acetyl group (43) add up to the observed MM, leading to a molecular structure that simply links those two groups together. [*Answer*: 3-buten-2-one; methyl vinyl ketone (Equation 10.15)]

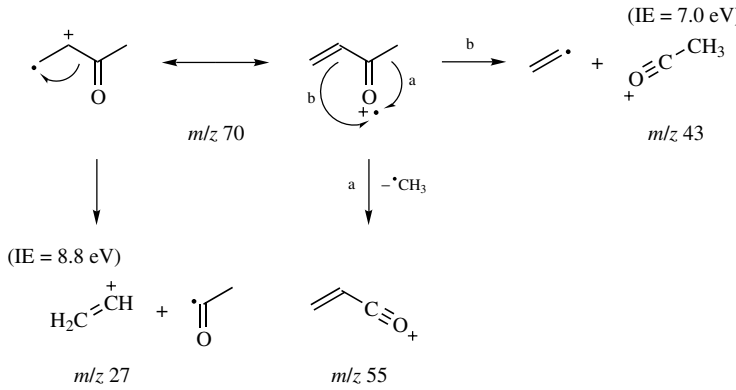

(10.15)

5.4. *(Step 3)* The peak at *m/z* 109 is the base peak and looks like a good candidate for the $M^{+\bullet}$ peak. *(Step 4)* The apparent odd MM indicates the presence of at least one N atom in the molecule. *(Step 5)* Isotope peak patterns due to A + 2 elements are clearly missing from this spectrum. The intensity of the M + 1 peak is consistent with the presence of six C atoms and one N atom (6.6% + 0.4%) in the $M^{+\bullet}$. The combined mass of these atoms is 72 + 14 = 86 u, which leaves 23 u unaccounted for. The presence of seven H atoms and one O atom could make up this difference, leading to an elemental composition of C_6H_7NO. The peak at *m/z* 80 is too large (18% relative to the peak at *m/z* 79) to provide the elemental composition of the ion having *m/z* 79.

(Steps 6 and 7) The $M^{+\bullet}$ peak is the base peak in the spectrum, indicating that this is probably the spectrum of an aromatic compound. This is substantiated by an aromatic low-mass ion series at *m/z* 50–53, 66–68, and 78–80. *(Step 8)* The first loss from the $M^{+\bullet}$ peak is 15 ($^{\bullet}CH_3$) to give the peak at *m/z* 94, a loss that is typical—if hard to explain—of aromatic compounds (Figure 4.16). The loss from *m/z* 109 to 79 is 30, which corresponds to the loss of CH_2O. Anisoles (phenyl methyl ethers) lose CH_2O from the $M^{+\bullet}$ by rearrangement of a H atom from the methyl group onto the aromatic ring (Equation 4.4). The loss from *m/z* 79 to *m/z* 52 is 27 (HCN), which is indicative of the presence of a N atom in or on an aromatic ring (Equation 4.2).

(Step 10) The number of rings plus double bonds in this molecule is $6 - \frac{1}{2}(7) + \frac{1}{2}(1) + 1 = 4$. This is the number of unsaturations in a 6-membered aromatic ring. The presence of a N atom in the ring and a methyl ether group attached to the ring is indicated by the observed pattern of losses and is consistent with the calculated elemental composition. Although the spectra of the three possible isomers are likely to be somewhat different from one another (see the *ortho* effect in Section 8.4), distinguishing between the isomers on the basis of one spectrum is not useful at this point. [*Answer*: 4-methoxypyridine (Equation 10.16)]

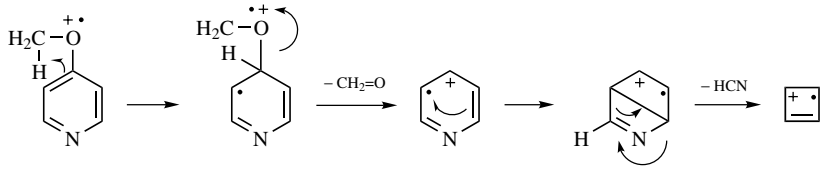

(10.16)

5.5. *(Step 2)* A chemical history of the compound is given in the text of the problem. If this were an unknown sample in a laboratory setting, it would be worthwhile to visit a pharmacy to see what compounds are present in these types of products. For this problem, however, the history is less useful (unless you are familiar with these products) because a compound of this sort is an unusual additive to a product that is advertised to be "natural".

(Step 3) The peak at *m/z* 94 appears to correspond to the $M^{+\bullet}$. *(Step 4)* The nominal MM of this compound (94) is even. The labeled fragment ion peaks occur at both even and odd *m/z* values, so that the presence of N cannot be determined with certainty at this point. *(Step 5)* Although Br and Cl are clearly absent, the X + 2 peaks in both of the clusters beginning at *m/z* 94 and 79 are larger than their respective X + 1 peaks. They are also of the right relative intensity to indicate the presence of one S atom (Table 2.1). The presence of at least one C atom is indicated by the loss of 15 ($^{\bullet}CH_3$) from the $M^{+\bullet}$ peak to produce the base peak at *m/z* 79 *(Step 8)*.

The relative intensities in the $M^{+\bullet}$ peak cluster are 1.8/57.3 = 3.1% for the M + 1 peak and 2.8/57.3 = 4.9% for the M + 2 peak. One S atom contributes 0.8% to the M + 1 peak, leaving 3.1 − 0.8 = 2.3% to be accounted for by any remaining elements. If N is not present and the presence of at least one C atom is likely, the contribution of two C atoms accounts for this intensity. For the M + 2 peak, one S atom accounts for 4.4%, leaving about 0.5% for other contributors. This value is too large for two ^{13}C's, but about right for the presence of two O atoms. An analysis of the peak cluster beginning at *m/z* 79 is consistent with this interpretation:

$$m/z\ 80: \qquad 1.9\% \approx (1 \times 0.8\%; {}^{33}S) + (1 \times 1.1\%; {}^{13}C)$$

$$m/z\ 81: \qquad 4.9\% \approx (1 \times 4.4\%; {}^{34}S) + (2 \times 0.2\%; {}^{18}O)$$

DropBooks

(Steps 6 and 7) The intensities of the two peaks at highest *m/z* values, plus the cluster of peaks between *m/z* 63 and 65, seem to indicate that this compound is aromatic. However, there do not appear to be enough atoms in this molecule to support an aromatic structure. The peak at *m/z* 45 falls into the low-mass ion series for aliphatic alcohols and ethers, but the intensity of this peak is weak and not accompanied by other peaks in that series. Overall, the information gleaned from these two steps is not decisive.

(Step 10) The combined mass of two C atoms, two O atoms, and a S atom is $(2 \times 12) + (2 \times 16) + (1 \times 32) = 88$ u, leaving six H atoms to make up the remaining mass. Although several different arrangements of these atoms are possible, the relative simplicity of this spectrum is evidence in favor of a symmetrical structure that can lose $^{\bullet}CH_3$ easily. [*Answer*: dimethylsulfone; $CH_3SO_2CH_3$ (Equation 10.17)]

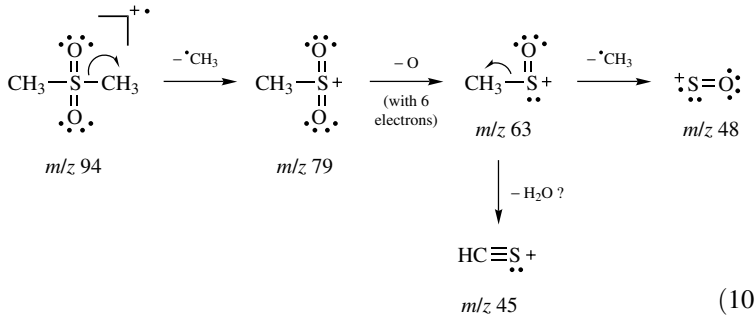

(10.17)

5.6. *(Step 2)* As with the preceding problem, a chemical history of the sample is given but is useful only if access to information in the field of insect pheromones is available. Even that information was not helpful to the original researchers, who were surprised to find this compound being used by the tick as a pheromone. *(Step 3)* The isotope peak cluster from *m/z* 162–166 indicates the presence of two Cl atoms (Figure 2.6), which means that the peak at *m/z* 162 in that cluster is the most likely candidate for the $M^{+\bullet}$ peak. *(Step 4)* The apparent nominal MM (162) is even, but the *m/z* values for fragment ion peaks have both even and odd values. Until other information in the spectrum is examined, the presence or absence of N will not be known with certainty. *(Step 5)* The intensity of the *m/z* 163 peak relative to that of *m/z* 162 is more consistent with the presence of six C atoms in the $M^{+\bullet}$, than with five C and two N atoms. If N is absent, then C and Cl account for $(6C \times 12) + (2Cl \times 35) = 72 + 70 = 142$ u, leaving 20 u unassigned. An O atom and four H atoms most easily explain this difference. *(Steps 6 and 7)* The intense $M^{+\bullet}$ peak and the electron-withdrawing aromatic low-mass ion series at *m/z* 49–51, 62–63, and 72–75(!) indicate an aromatic ring with more than one substituent.

(Step 8) The first major loss from the $M^{+\bullet}$ is 36, not 35, and the change in the isotope peak intensity pattern confirms that this loss must be HCl. The

apparent loss from *m/z* 126 to 98 is 28 u. This could be either $CH_2{=}CH_2$ or CO, but because this seems to be an aromatic compound that probably contains O, the loss of CO is more likely (see Section 4.1.2). *(Step 10)* The rings plus double bonds formula gives $6(\text{C}) - \frac{1}{2}(4\text{H} + 2\text{Cl}) + \frac{1}{2}(0) + 1 = 4$ unsaturations—in all likelihood, a substituted benzene ring. If the loss of 28 u is indeed that of CO, likely structures include several dichlorophenol isomers (see Equation 4.3). Although the spectra of several of these isomers are quite similar to one another, only those with at least one Cl atom next to the OH group show a loss of HCl from the $M^{+\bullet}$ (Equation 10.18). This phenomenon, called the *ortho* effect, will be discussed in Section 8.4. [*Answer*: 2,6-dichlorophenol; $C_6H_4OCl_2$]

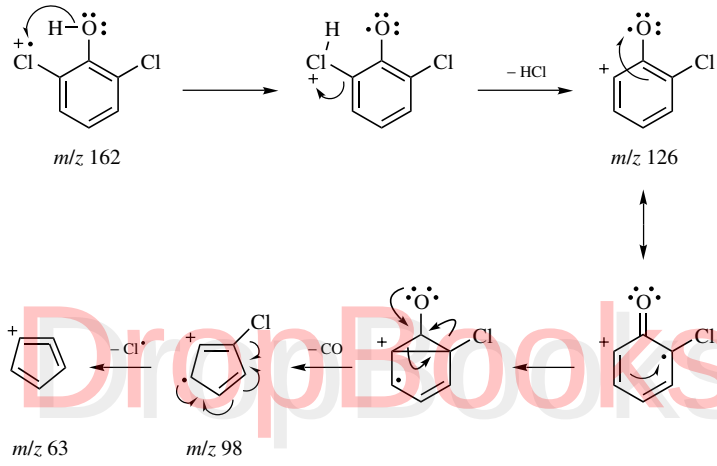

(10.18)

DropBooks

Chapter 6

6.1. *(Step 3)* The MM of both compounds is given in the problem as 120. *(Step 4)* The MMs are even, and all the important fragment ion peaks in both spectra occur at odd *m/z* values. Therefore, N is probably absent from both compounds. *(Step 5)* From the isotope peak intensity data in the $M^{+\bullet}$ peak clusters, both compounds appear to have nine C atoms and to thus be isomers of one another. The remaining 12 u in each case are undoubtedly contributed by H. Although the intensity of the *m/z* 92 peak relative to that at *m/z* 91 in Figure 6.4*a* indicates the presence of 9–10 C atoms in the *m/z* 91 ion, this is impossible for the mass of the ion. This means only that a fragment ion is also contributing to the intensity of the *m/z* 92 peak (Section 7.2.2). *(Step 6)* Both spectra, having prominent peaks at high *m/z* values and only weak intensity peaks at low *m/z* values, appear to be the spectra of aromatic compounds. *(Step 7)* Both spectra show an aromatic low-mass ion series; in fact, Figure 6.4*a* shows a benzyl ion series at *m/z* 39, 65, and 91.

(Steps 8 and 10) Four basic types of structures are possible for aromatic C_9H_{12} isomers:

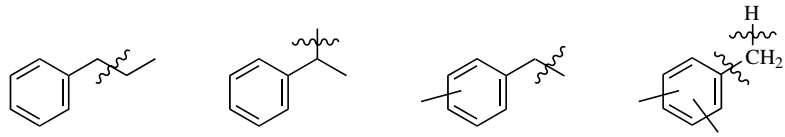

Of these, only *n*-propylbenzene is expected to lose $^{\bullet}CH_2CH_3$ by benzylic cleavage. This loss should produce an intense M − 29 peak at *m*/*z* 91, like that seen in Figure 6.4*a*. Isopropylbenzene and the isomeric methylethylbenzenes, on the other hand, should lose $^{\bullet}CH_3$ by benzylic cleavage, thereby producing an intense *m*/*z* 105 peak like that observed in Figure 6.4*b*. Although the isomeric trimethylbenzenes can lose neither methyl nor ethyl radical by benzylic cleavage, •H loss from the $M^{+\bullet}$ of these compounds is still overshadowed by the loss of $^{\bullet}CH_3$ from the ring (see Figure 6.3). In addition to a prominent peak due to the loss of $^{\bullet}CH_3$, however, the spectra in Figure 6.3 also have an M − 1 peak of at least modest intensity due to the loss of •H by benzylic cleavage. This peak is absent from both spectra in Figure 6.4.

The choice between isopropylbenzene and the methylethylbenzenes depends on more subtle criteria. Isopropylbenzene has only one H atom that can be lost by benzylic cleavage, whereas the methylethylbenzenes all have five. The latter compounds thus should exhibit at least a weak intensity *m*/*z* 119 peak (Figures 1.23 and 6.2). Because Figure 6.4*b* shows no visible peak at *m*/*z* 119, isopropylbenzene seems like a more reasonable choice. [*Answer*: (a) *n*-propylbenzene and (b) isopropylbenzene]

6.2. The $M^{+\bullet}$ peak cluster having a nominal *m*/*z* value of 188 in the spectrum of "CS" has intensities that are consistent with the presence of one Cl atom. The losses from the $M^{+\bullet}$ of CS to produce the major fragment ion peaks at high *m*/*z* values can be rationalized as follows:

m/*z*	Loss
161	HCN
153	$^{\bullet}$Cl; confirmed by the loss of the ^{37}Cl isotope peak
137	HC≡CCN, cyanoacetylene; loss of acetylenes from aromatic compounds is typical (Section 4.1.2), although loss of this particular acetylene is unexpected
126	$^{\bullet}$Cl and HCN
100	$^{\bullet}$Cl, HCN, and HCCH
99	$^{\bullet}$Cl, HCN, and HCN

An electron-withdrawing aromatic low-mass ion series is indicated by the peaks around *m/z* 39, 50, 62, and 75.

(Step 2) Given the origin of the unknown compound, it seems reasonable to assume that it might be structurally related to CS. This is the value of knowing the sample history: Several of the steps listed in Section 5.1 can be cut short in order to arrive at a structure for this unknown. *(Steps 3, 5, 8, and 10)* Because the $M^{+\bullet}$ peak of the unknown occurs at *m/z* 190 (two units higher than for CS) and the peak intensities indicate the presence of one Cl atom in the $M^{+\bullet}$, a logical choice for a structure is one in which two H atoms have been added across the C—C double bond of CS. In contrast to CS, which is highly unsaturated and fragments by losing $^{\bullet}Cl$ and small unsaturated molecules, this compound has a fragile bond that can undergo α-type cleavage (shown here after initial ionization at Cl) to produce the intense peak at *m/z* 125 (Equation 10.19):

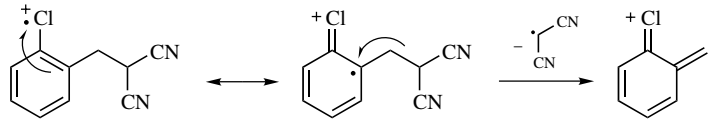

(10.19)

m/z 190 *m/z* 125

DropBooks

The remaining fragmentations of the unknown are unexceptional. Loss of HCN produces the peak at *m/z* 163, while loss of $^{\bullet}Cl$ yields the ion represented by the tiny peak at *m/z* 155. These two compounds illustrate the difference in behavior between aromatic and "aliphatic" compounds of similar structure. [*Answer*: 1-(2-chlorophenyl)-2,2-dicyanoethane]

6.3. **(a)** The base peak at *m/z* 58 limits the distribution of alkyl groups to the vicinity of the N atom and thus limits the number of structures that need to be considered as possible solutions. Moving an alkyl group from near the N to either the aromatic ring or the benzylic C atom would cause the peak due to primary α-cleavage to move to either *m/z* 44 or 30, depending on what group was moved.

(b) Only five structures, shown in Table 10.1 with their predicted α-cleavage losses, are possible. The spectrum in Figure 6.10*e* is that of methamphetamine (Structure A). Comparison of the spectra in Figures 6.8*a* and 6.10*d* reveals that the latter spectrum is that of phentermine (Structure B).

These structures can be categorized fairly easily according to their respective α-cleavage losses after initial ionization at the N atom: Structures A and E—H•, $^{\bullet}CH_3$, and $C_6H_5C^{\bullet}H_2$; Structure B—$^{\bullet}CH_3$ and $C_6H_5C^{\bullet}H_2$; Structure C—$H^{\bullet}$, $^{\bullet}CH_2CH_3$, and $C_6H_5C^{\bullet}H_2$; and

Table 10.1. Possible structures for Problem 6.3

	Structure	α-Cleavage Losses
A.	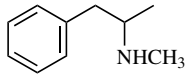	4 $H^{\bullet}$ (*m/z* 148); $^{\bullet}CH_3$ (*m/z* 134); $\phi C^{\bullet}H_2$ (*m/z* 58)
B.	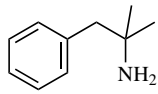	2 $^{\bullet}CH_3$ (*m/z* 134); $\phi C^{\bullet}H_2$ (*m/z* 58)
C.	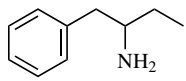	$H^{\bullet}$ (*m/z* 148); $CH_3C^{\bullet}H_2$ (*m/z* 120); $\phi C^{\bullet}H_2$ (*m/z* 58)
D.	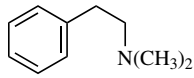	8 $H^{\bullet}$ (*m/z* 148); $\phi C^{\bullet}H_2$ (*m/z* 58)
E.	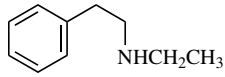	5 $H^{\bullet}$ (*m/z* 148); $^{\bullet}CH_3$ (*m/z* 134); $\phi C^{\bullet}H_2$ (*m/z* 58)

Structure D—only $H^{\bullet}$ and $C_6H_5C^{\bullet}H_2$. The spectrum in Figure 6.10*c* exhibits a relatively intense peak for loss of $^{\bullet}CH_2CH_3$, which is consistent with Structure C, and the one in Figure 6.10*d* shows loss of $^{\bullet}CH_3$, but not $H^{\bullet}$, as the spectrum for Structure B should (and does; see Figure 6.8*b*).

Because Figure 6.10*b* does not show significant losses of either $^{\bullet}CH_3$ or $^{\bullet}CH_2CH_3$, it seems most suitable for Structure D. The weak intensity of the *m/z* 91 peak in this spectrum is due to the difference in IEs for the aromatic ring and the tertiary amine group. The ring has an IE of about 8.9 eV, whereas that of the N atom is less than 8 eV (Table 3.1). Ionization is predicted to occur primarily on the N atom and not in the ring.

Assigning structures to the spectra in Figure 6.10*a* and *e* would be difficult without a known spectrum of methamphetamine for comparison. The observed spectra are nonetheless consistent with the difference between Structures A and E. The peaks at *m/z* 115 and 117 in Figure 6.10*e* are due to alkylbenzene ions from the aromatic ring and its attached 3-carbon chain (see Equation 8.10). They would not be expected in the spectrum of Structure E, which has only a 2-carbon side chain. The spectrum for this compound instead shows an enhanced

peak at *m/z* 105 (Figure 6.10*a*). [*Answer*: (a) *N*-ethyl-β-phenethylamine; (b) *N*,*N*-dimethyl-β-phenethylamine; (c) 1-phenyl-2-aminobutane; (d) phentermine; and (e) methamphetamine]

6.4. The loss of 27 u must be due to a vinyl radical from the terminal double bond in the side chain (Table 4.1) After initial ionization at the O atom in the OH group, two resonance structures place the radical site at the *ortho* and *para* positions in the ring (Equation 10.20). Loss of $^{\bullet}CH_3$ from the methoxy group in the *ortho* position (as in Equation 6.13) produces the peak at *m/z* 149. Loss of a vinyl radical by benzylic cleavage accounts for the peak at *m/z* 137.

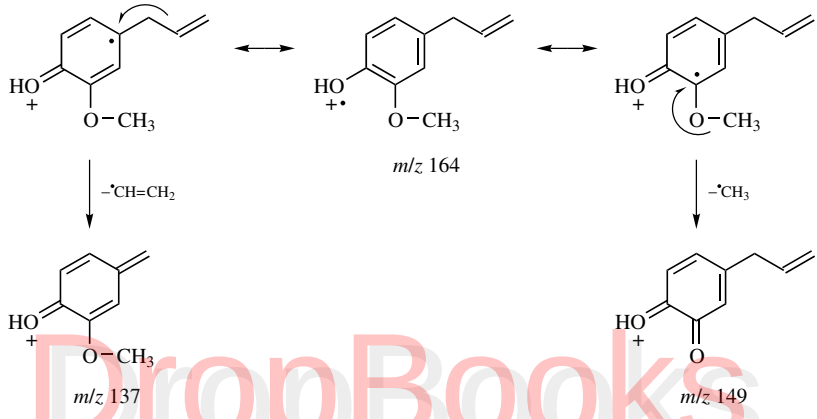

(10.20)

DropBooks

6.5. The spectra of the *o*- and *p*-isomers show large peaks reflecting the loss of $^{\bullet}CH_3$ from the $M^{+\bullet}$. The loss to form the peak at *m/z* 94 in the spectrum of the *m*-isomer is 30 (=124 − 94). Loss of $^{\bullet}CH_3$ by the $M^{+\bullet}$ of the *o*- and *p*-isomers can occur by formation of new double bonds and stabilization of the charge at the original site of ionization (see Equations 6.13 and 6.14). The corresponding loss by the $M^{+\bullet}$ of the *m*-isomer, however, results in formation of a diradical in which the electrons cannot be paired (Figure 10.3). The $M^{+\bullet}$ of the *m*-isomer, therefore, prefers the loss of $CH_2{=}O$ by rearrangement (Equation 10.21; compare Equation 4.4). In the spectra of all three isomers, the peak at *m/z* 81 is best explained by initial loss of $^{\bullet}CH_3$ followed by loss of CO from the resulting ion having *m/z* 109 (Figure 10.3).

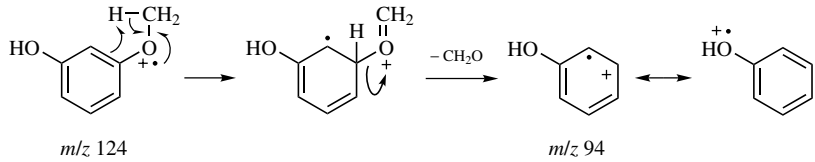

(10.21)

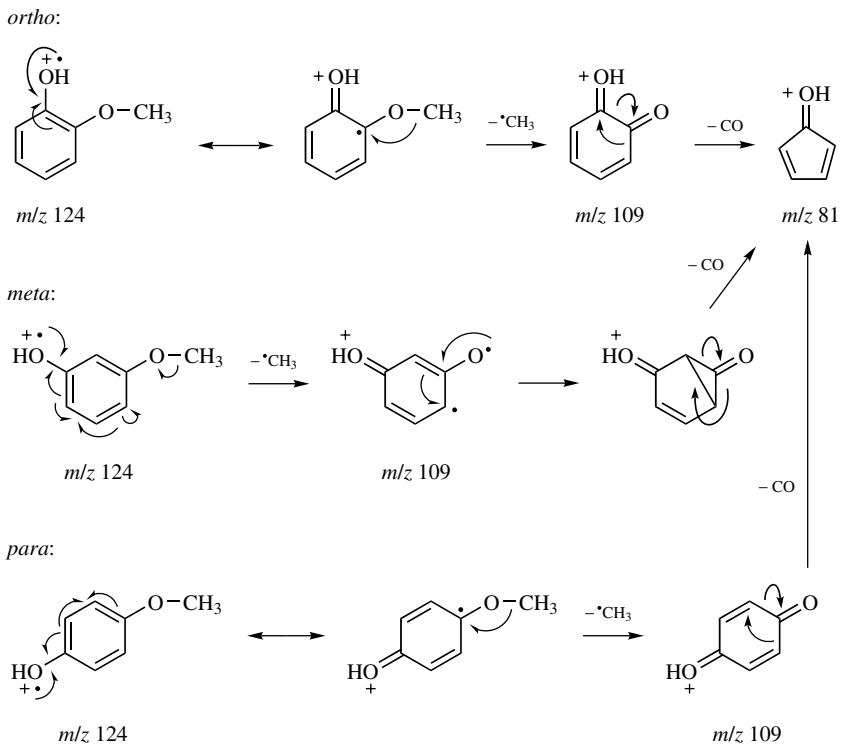

Figure 10.3. Proposed sequential losses of $^{\bullet}CH_3$ and CO from *o*-, *m*-, and *p*-methoxyphenol (Problem 6.5).

6.6. (a) There are four places to consider as possible sites for initial ionization: the two aromatic rings and the two amine N atoms. The IE for both the aromatic rings will be close to that of toluene (~8.9 eV), which is considerably higher than that for either of the N atoms. Of the two N atoms in the molecule, the tertiary N will have a somewhat lower IE (<8.0 eV) and thus should be the preferential site for initial ionization. However, the difference in IE between the N atoms is not sufficient to preclude ionization at the secondary N atom as well.

Because of the complex structure of this molecule, a number of α-cleavage fragmentations are possible at atoms next to these two sites:

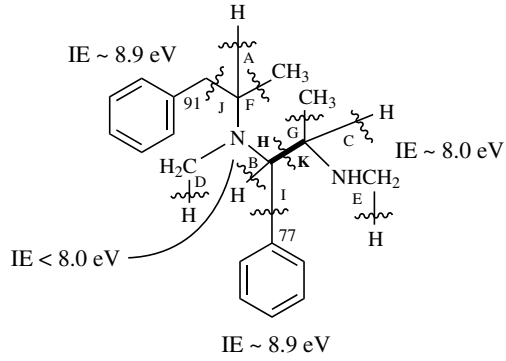

In all, five different $H^{\bullet}$ (leading to Structures A–E), two $^{\bullet}CH_3$ (leading to Structures F and G), and four other radicals (leading to Structures H–K) may be lost. In the following equations, increasing stability of the resulting ions is denoted by an increasing number of asterisks following the identification label on the structure (maximum 3). Hydrogen atoms that can be rearranged to initiate secondary elimination fragmentation are shown in boldface.

(i) *m/z* 295 (loss of $H^{\bullet}$, with formation of interior double bond; Structures A^{**}, B^{***}, and C^{*})

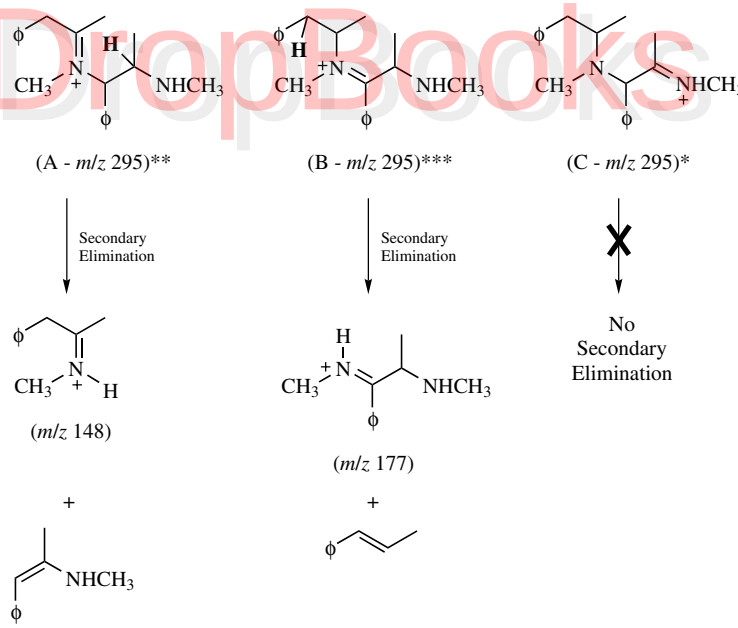

(10.22)

(ii) *m/z* 295 (loss of H•, with formation of terminal double bond; Structures D and E)

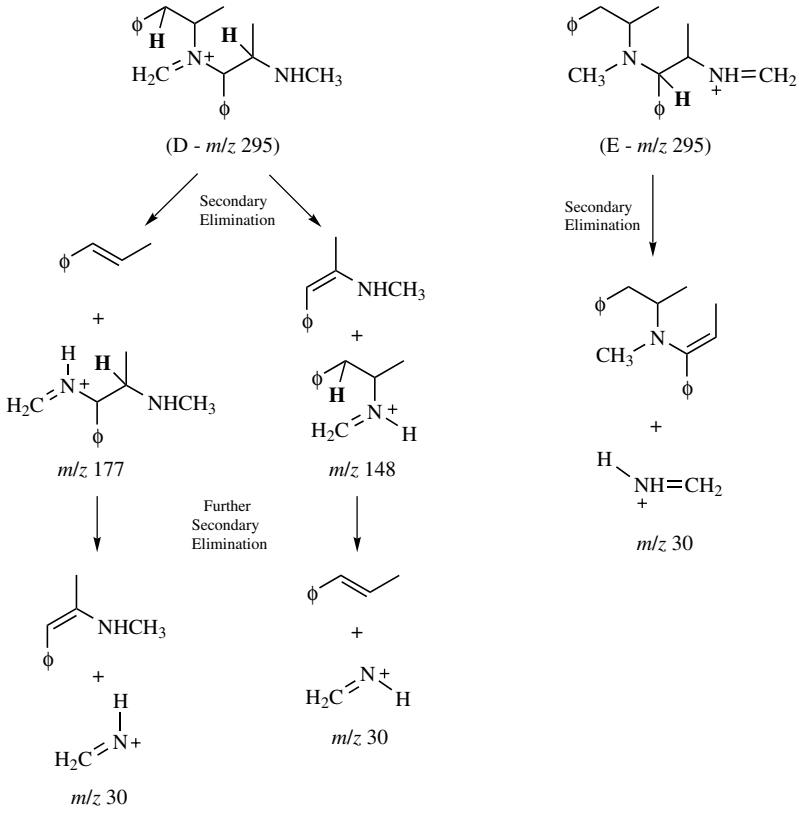

(10.23)

(iii) *m*/*z* 281 (loss of $^{\bullet}CH_3$; Structures F** and G*)

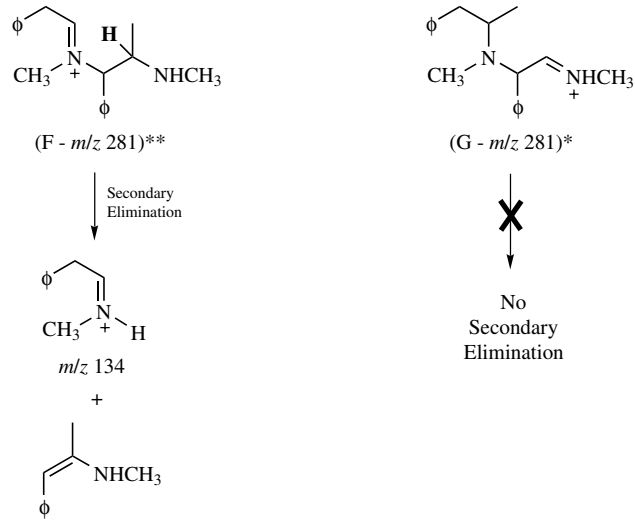

(10.24)

(iv) *m/z* 238 (loss of $CH_3C^{\bullet}HNHCH_3$; Structure H***)

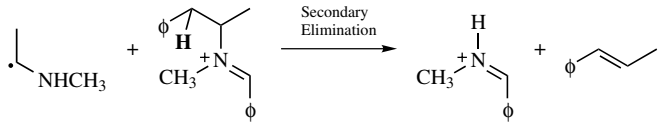

(H - *m/z* 238)*** *m/z* 120

(10.25)

(v) *m/z* 219 (loss of ϕ•; Structure I**)

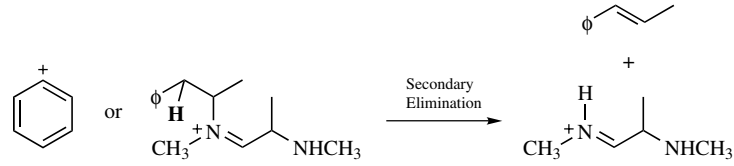

m/z 77 (I - *m/z* 219)** *m/z* 101

(10.26)

(vi) *m/z* 205 (loss of $\phi C^{\bullet}H_2$; Structure J**)

DropBooks

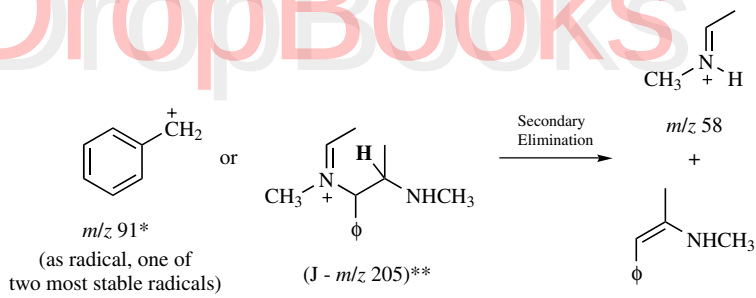

m/z 91* (as radical, one of two most stable radicals)

(J - *m/z* 205)** *m/z* 58

(10.27)

(vii) *m/z* 58 (loss of substituted benzylic radical after initial ionization at secondary N; Structure K)

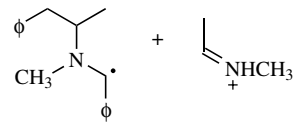

(one of two most stable radicals) (K - *m/z* 58)

Least stable of all the ion structures are Structures D and E (*m*/*z* 295) because they have terminal double bonds. Because the radical product lost during their formation is also unstable (H•), these should be the least likely to form of all the ion products. Somewhat more stable, by virtue of having an isolated, interior double bond attached to a secondary N atom and only one substituent on the α C atom end of the double bond, are Structures G (*m*/*z* 281) and K (*m*/*z* 58). The radical product lost in the formation of Structure K is a substituted benzylic radical; it is one of the two most stable radical products formed in all these fragmentations. Formation of Structure G occurs by loss of $^{\bullet}CH_3$, so that the intensity of the peak resulting from this fragmentation is expected to be low.

Slightly more stable are Structures A (*m*/*z* 295), C (*m*/*z* 295), F (*m*/*z* 281), I (*m*/*z* 219), and J (*m*/*z* 205), which have interior double bonds attached to a tertiary N atom or attached to a secondary N atom with two substituents at the α C atom end of the double bond (compare the IE for radical sites on C atoms α to an amine N atom; Table 3.1). Formation of both Structures A and C are accompanied by loss of H•, which should lead to low-intensity peaks. Formation of Structure F, which is accompanied by loss of $^{\bullet}CH_3$, is only slightly more likely. The fragmentation that leads to Structure I generates a phenyl radical and therefore has a higher probability of producing a relatively intense peak in the spectrum. Formation of a small amount of phenyl ion (*m*/*z* 77) by heterolytic cleavage is expected, but the intensity of that peak will be low because of the relatively high IE of phenyl radical.

Formation of Structure J is accompanied by loss of benzyl radical, which is one of the two most stable radical products formed in these fragmentations. The peak at *m*/*z* 219 should therefore be intense and should be accompanied by a smaller, but still significant, peak at *m*/*z* 91 due to formation of the benzyl ion.

The most stable ion structures are Structures B (*m*/*z* 295) and H (*m*/*z* 238), both of which contain interior double bonds conjugated with an aromatic ring. Because the radical product formed with Structure H is more stable than H•, it is reasonable to postulate that *m*/*z* 238 should be the base peak in the spectrum. However, the radical products formed along with Structures J and K are also resonance-stabilized. If the difference in ion stability is less than the difference between the stabilities of the corresponding radical products, it is possible that *m*/*z* 205 or 58 could become the base peak. In any case, peaks due to all three of these ions should be prominent in the spectrum. Because of the stability of Structure B (*m*/*z* 295), the peak representing this ion is expected to be fairly intense as well.

(b) Of the ion structures listed above, only Structures C, G, and K cannot undergo secondary elimination of an olefin. Structures D and E, by virtue of having a terminal double bond, can undergo two sequential secondary elimination fragmentations. The *m*/*z* values for the peaks resulting from

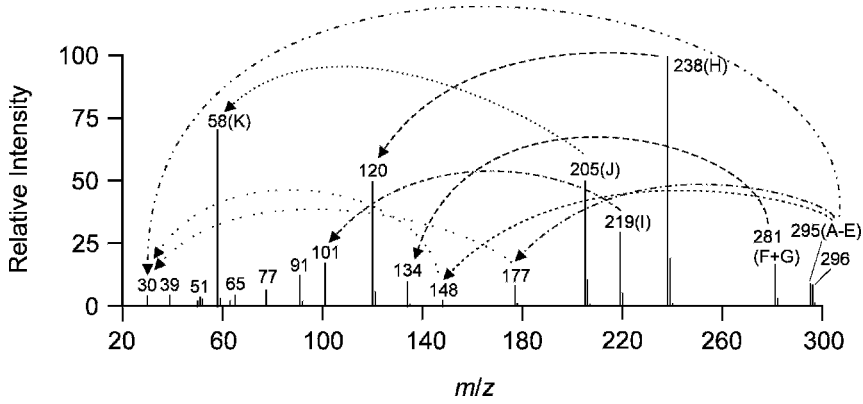

Figure 10.4. Proposed mass spectrum of 1-phenyl-2-[N-methyl-N-(1-phenyl-2-methylamino-propyl)]aminopropane (Problem 6.6).

all these fragmentations are given in Equations 10.22–10.27 above. The intensities of the peaks due to secondary elimination are generally 50–70% those of the peaks due to initial α-cleavage (Section 6.5.1).

An idea of what the spectrum of this compound might look like, based on this discussion, is shown in Figure 10.4. Appropriate isotope peaks, as well as aromatic and benzylic low- mass ion series, have been added to this spectrum. The curved arrows above the spectrum show losses due to secondary elimination fragmentations.

DropBooks

6.7. *(Step 2)* Information concerning the origin of this unknown, as noted in the hint accompanying the text of this problem, is helpful in reducing the number of possible structures. It is quite possible that the unknown structure is related to that of methamphetamine.

(Step 3) The $M^{+\bullet}$ peak in this spectrum appears to be the one at *m/z* 134. *(Step 4)* The absence of N may be inferred from the even MM and the fact that all the marked fragment ion peaks occur at odd *m/z* values.

(Step 5) The isotope peak intensity data for the peaks at *m/z* 134 and 43 in Figure 6.28 are helpful: The ion with *m/z* 134 appears to contain nine C atoms, while the one having *m/z* 43 seems to contain just two. This means it is likely that the *m/z* 43 peak represents the acylium ion ($CH_3C{\equiv}O^+$), not $CH_3CH_2CH_2^+$. *(Steps 6 and 7)* Despite the lack of reliable information concerning the elemental composition of the ion at *m/z* 91 (the *m/z* 92 peak is too intense to be due to isotope contributions alone), the peak at *m/z* 91 still seems to represent the benzyl ion (ϕC^+H_2) due to the prominent 91 → 65 → 39 low-mass ion series. *(Steps 8 and 10)* If this is true, and if the $M^{+\bullet}$ contains nine C atoms, then this molecule must be made up of just two fragments: a benzyl group and an acetyl group (91 + 43 = 134). There is only one reasonable arrangement of these fragments that fits the data: methylbenzylketone or phenyl-2-propanone, which has the 3-carbon benzene

skeleton of methamphetamine. The *m/z* 92 ion is formed by a γ-hydrogen rearrangement (Section 7.2.2). [*Answer*: phenyl-2-propanone (Equation 10.28)]

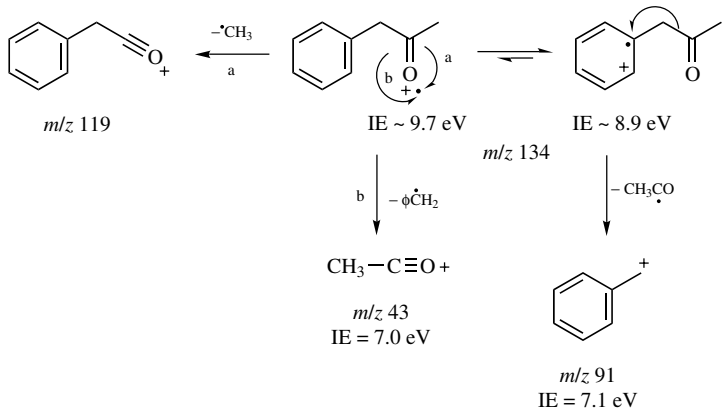

(10.28)

6.8. It is instructive first to list all possible structures and try to predict beforehand how each will fragment. Not only do primary α-cleavages need to be considered, but so do secondary eliminations of the ions produced by initial α-cleavage as well as other fragmentations that are unique to aliphatic O compounds. Seven structures, which are shown in Table 10.2, are possible.

Table 10.2. Predicted losses of $C_4H_{10}O$ isomers

Structure		Primary α-Cleavage Losses[a]	Secondary Losses
n-Butyl	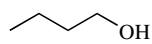	2 H• (*m/z* 73); $CH_3CH_2C^{\bullet}H_2$ (*m/z* **31**)	(Loss of H_2O)
sec-Butyl		H• (*m/z* 73); •CH_3 (*m/z* 59); $CH_3C^{\bullet}H_2$ (*m/z* **45**)	Hydride shift 59 → 31
Isobutyl	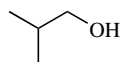	2 H• (*m/z* 73); $CH_3C^{\bullet}HCH_3$ (*m/z* **31**)	None
t-Butyl	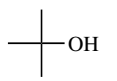	3 •CH_3 (*m/z* **59**)	None
Methylpropyl	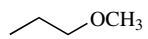	5 H• (*m/z* 73); $CH_3C^{\bullet}H_2$ (*m/z* **45**)	73 → 31
Methylisopropyl	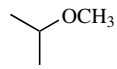	4 H• (*m/z* 73); 2 •CH_3 (*m/z* **59**)	73 → 31
Diethyl	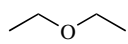	4 H• (*m/z* 73); 2 •CH_3 (*m/z* **59**)	73 → 45 59 → 31

[a]Peak representing most important α-cleavage ion is shown in **boldface**.

By comparing the information in this table with the spectra in Figure 6.29, two of the spectra should be readily identifiable. The spectrum in Figure 6.29*a* is the only one showing loss of H_2O (*m*/*z* 56) as a primary fragmentation, so it must belong to *n*-butanol. Also, only spectrum *g* in Figure 6.29 shows loss of $^{\bullet}CH_3$ with no corresponding loss of H•, consistent with behavior expected for *t*-butyl alcohol.

Of the remaining spectra, those in Figures 6.29*b* and *e* exhibit large peaks at *m*/*z* 45. Two structures are predicted to exhibit this behavior—the two proposed as solutions for Problem 4.4*a* (see discussion in Section 6.4.1). Because Figure 6.29*e* shows evidence of significant loss of $^{\bullet}CH_3$, it must correspond to *s*-butanol, and Figure 6.29*b* must be that of methyl-*n*-propylether.

Spectrum *c* (Figure 6.29) seems clearly to be associated with the group of compounds expected to have a base peak at *m*/*z* 59, and spectrum *f* with the *m*/*z* 31 group. But the base peak in spectrum *d* is *m*/*z* 43, which does not arise from α-cleavage if the compound is indeed an aliphatic alcohol or ether. The spectrum in Figure 6.29*c* seems most clearly attached to methylisopropylether, because a peak at *m*/*z* 45 is entirely absent from the spectrum.

This leaves diethylether and isobutyl alcohol as choices for the spectra in Figures 6.29*d* and *f*. Because the peaks at *m*/*z* 45 and 59 are so weak in spectrum *d*, the modest peak at *m*/*z* 31 must take precedence by default, and isobutyl alcohol becomes the answer for this spectrum. This has some merit because loss of an isopropyl radical by α-cleavage is predicted, although in this case the charge ends up primarily on the isopropyl carbenium ion. Because of the high electronegativity of O, the IE for formation of secondary isopropyl carbenium ion is lower than that for forming the unsubstituted $CH_2{=}OH^+$ ion (~7.3 eV vs. 7.6 eV). In contrast, the spectrum of isobutylamine has a base peak at *m*/*z* 30 that is over 10 times larger than any other peak in the spectrum.

DropBooks

The assignment of diethylether to Figure 6.29*f* at first seems surprising because *m*/*z* 31 is the base peak. However, this is consistent with the fact that the secondary eliminations from initial α-cleavage ions are more prominent in ethers than they are in amines (Equation 10.29). It should be clear that without having the spectra of all these isomers to compare and contrast, unique structural assignments would be much more difficult. [*Answer*: (a) *n*-butanol, (b) methylpropylether, (c) methylisopropylether, (d) isobutyl alcohol, (e) *s*-butanol, (f) diethylether, and (g) *t*-butyl alcohol]

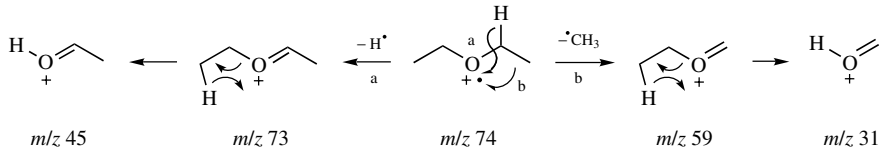

(10.29)

6.9. (a)

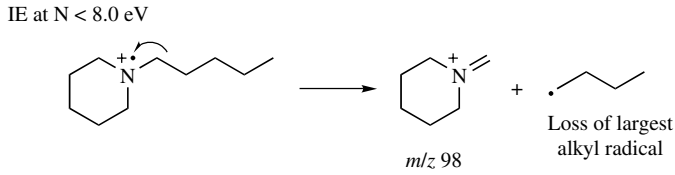

(10.30)

(b)

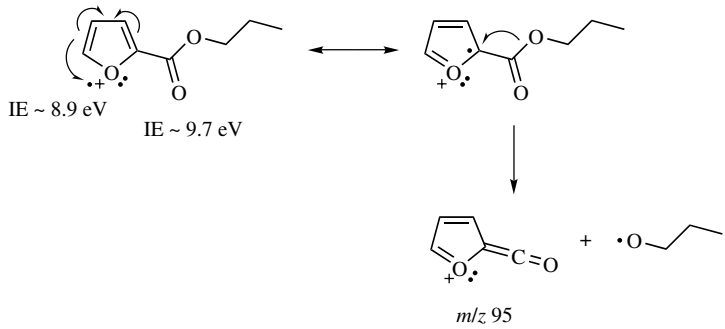

(10.31)

(c)

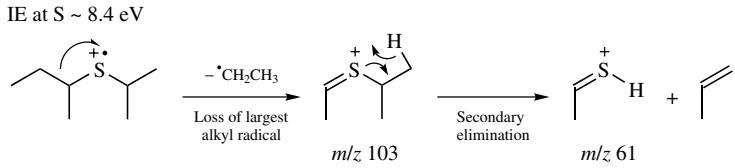

(10.32)

(d)

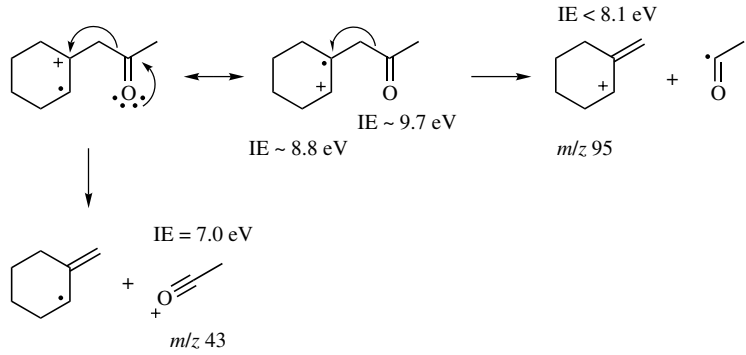

(10.33)

(e)

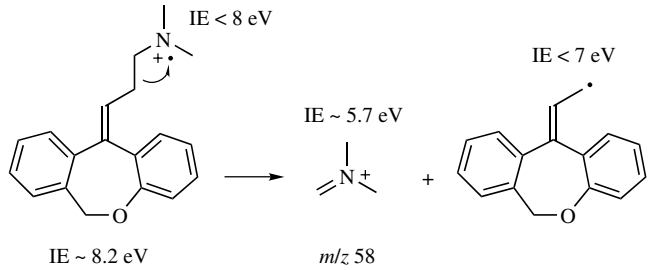

(10.34)

(f)

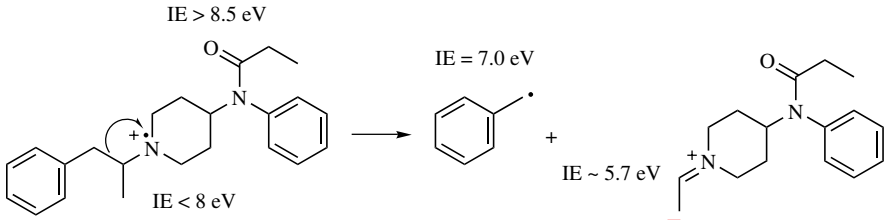

(10.35)

DropBooks

(g)

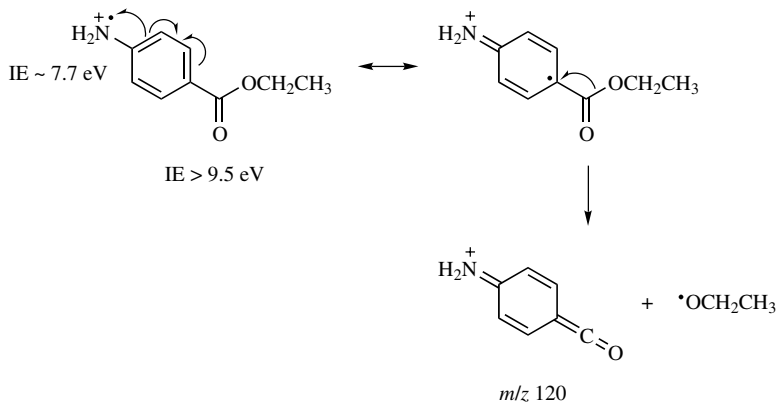

(10.36)

(h)

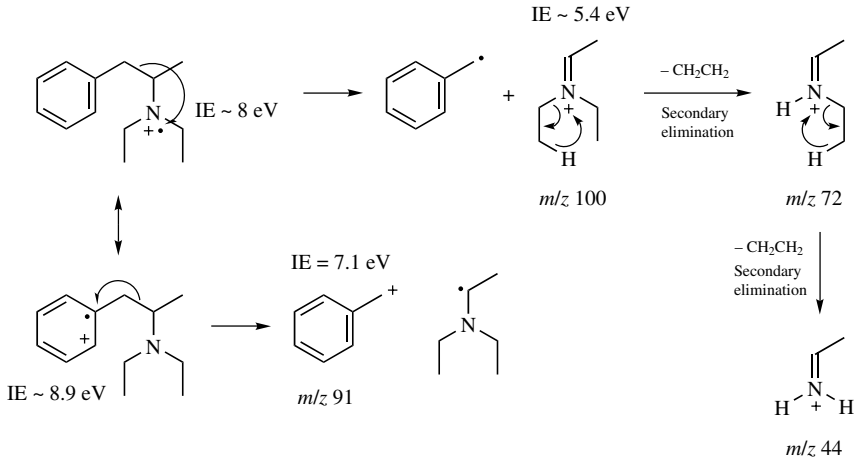

(10.37)

6.10. *(Steps 3 and 4)* Although the apparent even MM (122) might initially indicate that the compound does not contain N, the two most intense fragment ion peaks occur at even *m/z* values. If N is present, there must be at least two N atoms in the molecule. *(Step 5)* The isotope peak intensity data for the *m/z* 122 and 106 peak clusters are consistent with the presence of seven C atoms in both the corresponding ions if no N atoms are present. If two N atoms are present, then only $7.7 - 0.8 = 6.9\%$ of the peak at *m/z* 123 is due to C. This would mean that the *m/z* 122 ion would contain six C and two N atoms. Similarly, the intensity of the peak at *m/z* 107 (7.3% relative to that of the *m/z* 106 peak) would be most consistent with the presence of six C atoms and one N atom ($6.6 + 0.4 = 7.0\%$) rather than five C and two N atoms ($5.5 + 0.8 = 6.3\%$). *(Steps 6 and 7)* From the intensities of the peaks at high *m/z* values and the aromatic low-mass ion series at *m/z* 39, 51, and 78, the compound is expected to be aromatic. If the aromatic ring is a benzene ring, this leaves only one C atom and a lot of mass to account for.

(Step 8) The first loss from the $M^{+\bullet}$ (16 u) is characteristic—one observed mainly as the loss of $\bullet NH_2$ from primary amides or as atomic O from other selected N-containing compounds (Table 4.1). In either case, the presence of N is indicated by this loss, which means that the compound must contain at least two N atoms. If this compound is an aromatic primary amide, the spectrum should resemble that of benzamide (Figure 6.20*b*).

On comparison, the two spectra are seen to be nearly identical except that the intense peaks at *m/z* 77, 105, and 121 in the benzamide spectrum occur at *m/z* values one unit higher in the spectrum of this compound (Figure 6.30).

Also, a relatively weak intensity peak is observed at *m/z* 44 ($^{+}CONH_2$) that is not intense enough to be from an aliphatic amine. Further, the loss from *m/z* 78 to 51 is not the usual 26 (HCCH), but rather 27 (HCN), indicating the presence of an N atom in the aromatic ring (which accounts for the other N atom). *(Step 10)* A pyridine ring fulfills the necessary structural requirements and also accounts for all the remaining mass. The IE for the ring N atom and amide group appear to be similar (Table 3.1), so that initial ionization at either site is plausible. [*Answer*: 3-pyridinecarboxamide (nicotinamide; Equation 10.38)]

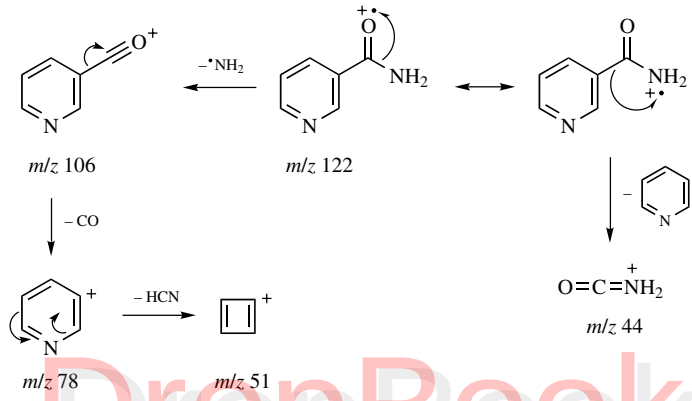

(10.38)

DropBooks

6.11. *(Steps 3 and 4)* The $M^{+\bullet}$ peak in this spectrum appears to be the one at *m/z* 87, which means that at least one N atom must be present. *(Step 5)* The isotope peak intensity data for the $M^{+\bullet}$ peak indicate the presence of five C atoms, whereas those in the *m/z* 72 peak cluster indicate that four C atoms are present in that ion. *(Steps 6 and 7)* The base peak at *m/z* 72 should be a giveaway that this is the spectrum of an aliphatic amine (see Table 4.2 and Section 6.3.1). In fact, except for the $M^{+\bullet}$ peak, nearly all the major peaks in the spectrum are at the *m/z* values expected for aliphatic amine fragment ions (*m/z* 30, 44, 58, 72, and 86).

(Steps 8 and 10) Eighteen structures are possible for the elemental composition $C_5H_{13}N$. Most of these can be eliminated quickly by considering what the base peak at *m/z* 72 really means—namely, that $^{\bullet}CH_3$ is the *largest* radical that can be lost by initial α-cleavage (secondary eliminations give rise to less intense peaks in the spectra of aliphatic amines). Therefore, the *m/z* 44 peak cannot arise from loss of a propyl radical; if this were true, the peak at *m/z* 44 would be larger than the one at *m/z* 72, because a propyl radical is more stable than a methyl radical (see Section 6.3.1). This leaves only four structures to consider: methyl *t*-butylamine, ethylisopropylamine, dimethylisopropylamine, and methyldiethylamine. (Write out at least some of the other structures to convince yourself that this is true.) These structures

Table 10.3. Possible structures for Problem 6.11

Structure	α-Cleavage Ion	Secondary Eliminations
	m/z 86 *m/z* 72	86 → 30 None
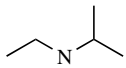	*m/z* 86 *m/z* 72	86 → 44 72 → 44 86 → 58 72 → 30
	m/z 86 *m/z* 72	86 → 44 None
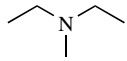	*m/z* 86 *m/z* 72	86 → 58 → 30 72 → 44

can be distinguished by looking at the pattern of secondary eliminations that the initial α-cleavage ions produce for each of these compounds (Table 10.3).

Methyl *t*-butylamine and dimethylisopropylamine can be eliminated immediately on this basis because each is predicted to produce only one peak from secondary rearrangement, instead of the three observed in this spectrum. Choosing between ethylisopropylamine and methyldiethylamine is more subtle. The ion represented by the base peak (*m/z* 72) in the case of ethylisopropylamine should produce two intense secondary rearrangement ions—at *m/z* 44 and 30 because there are two different methyl radicals that can be lost. The same is not true for methyldiethylamine. The relative intensities of the peaks due to secondary rearrangement ions for the unknown seem to indicate that, based on the relative intensities of the *m/z* 44 and *m/z* 30 peaks, the *m/z* 44 ion arises from the ion having *m/z* 72, whereas the *m/z* 30 ion probably does not. Therefore, this pattern better fits that expected of methyldiethylamine than of ethylisopropylamine. [*Answer*: methyldiethylamine]

6.12. *(Steps 3 and 4)* Based on the apparent even MM (152) and the fact that all the important fragment ion peaks occur at odd *m/z* values, it is reasonable to assume that N is not present. *(Step 5)* The $M^{+\bullet}$ appears to contain eight C atoms, whereas the ion represented by the base peak at *m/z* 121 contains seven C atoms. Although they are small, the intensities of the X + 2 peaks in both these clusters are a little larger than expected for C alone. On the other hand, they are not large enough to indicate the presence of Si or S. The presence of O would not be surprising. *(Steps 6 and 7)* The intense peaks at

high *m/z* values and the low-mass ion series at *m/z* 39 and 62–65 strongly suggest an aromatic compound.

(Step 8) Although it produces only a weak peak, the first loss from the $M^{+\bullet}$ is $152 - 135 = 17$ u. This loss is usually that of $^{\bullet}OH$ rather than NH_3 (Table 4.1). The major loss, however, is 31 u, which Table 4.1 identifies as $^{\bullet}OCH_3$. The first significant peak below *m/z* 121 occurs at *m/z* 93, indicating the further loss of CO [28 u; loss of $CH_2{=}CH_2$ in aromatic compounds is mostly restricted to compounds having aliphatic substituents external to the ring (Equations 6.27 and 6.28, and Section 7.2.2)].

(Step 10) This compound has eight C atoms (including a methoxy group and a group that can eliminate CO fairly easily) and a hydroxy group—for a potential total of three O atoms. This would lead to $(8\,C \times 12) + (3\,O \times 16) = 96 + 48 = 144$ u, with the remaining mass being made up by H. The rings plus double bonds formula gives $8 - \frac{1}{2}(8) + \frac{1}{2}(0) + 1 = 5$ unsaturations, which is consistent with an aromatic ring plus an unsaturation outside the ring. A carbonyl group would fulfill this requirement and account for the loss of CO.

Two sets of isomeric structures should be considered: the methoxybenzoic acids and the methyl hydroxybenzoate esters. Because loss of $^{\bullet}OCH_3$ by α-cleavage leads to the base peak in the spectrum of methyl benzoate (Figure 6.19*c*), the similar behavior of this compound implies the presence of a benzoate ester here as well. In contrast, methoxybenzoic acid should produce an intense peak due to the loss of $^{\bullet}OH$ by α-cleavage. In order to distinguish between isomers, known spectra for all three compounds should be compared. [*Answer*: methyl *p*-hydroxybenzoate (Equation 10.39)]

DropBooks

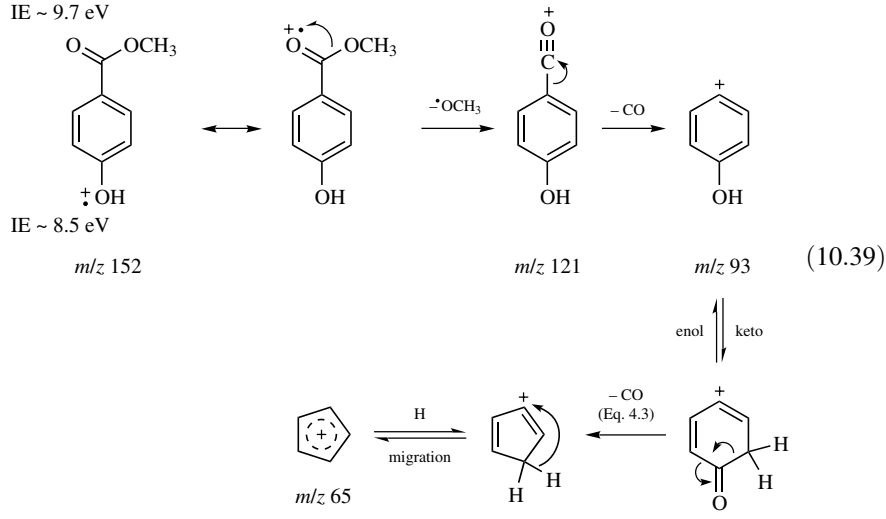

(10.39)

6.13. (a)

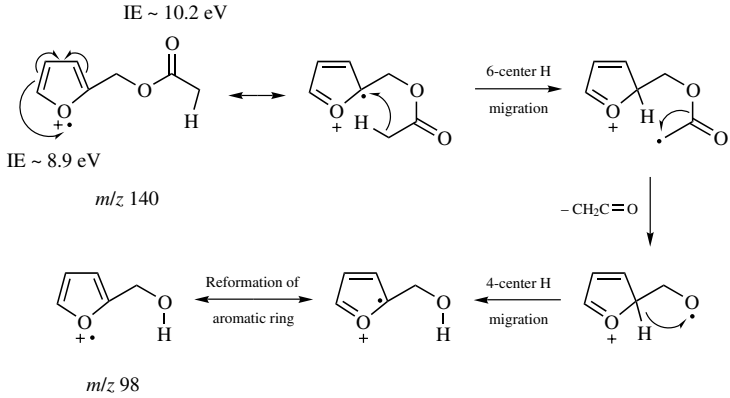

(10.40)

(b)

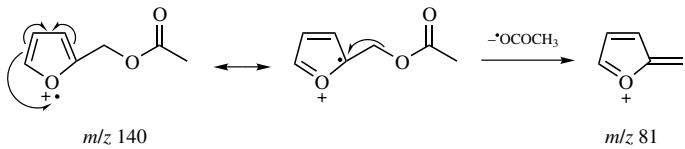

(10.41)

(c)

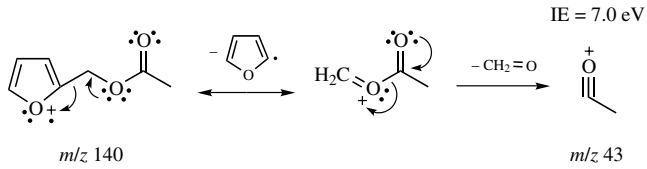

(10.42)

Chapter 7

7.1. *(Steps 3 and 4)* The apparent $M^{+\bullet}$ peak at *m/z* 100 and the presence of numerous fragment ion peaks at odd *m/z* values indicate the absence of N in this molecule. *(Step 5)* The isotope peak intensities for the *m/z* 43, 57, and 72 peaks are consistent with the presence of two, four, and four C atoms, respectively, in the corresponding ions. This means that the *m/z* 43 peak must be due to the acylium ion (CH_3CO^+), not $C_3H_7^+$, and that the peak at *m/z* 57 probably represents a butyl ion ($^+C_4H_9$). *(Steps 6 and 7)* Although this spectrum has several features of saturated aliphatic hydrocarbon spectra, including the intense peaks at *m/z* 43 and 57, the isotope peak intensities support a ketone, rather than a hydrocarbon. *(Steps 8 and 10)* Acylium ions are only observed as the base peak in the spectra of carbonyl compounds in

Table 10.4. Possible structures for Problem 7.1

Predicted McLafferty Rearrangement Ion		Predicted McLafferty Rearrangement Ion	
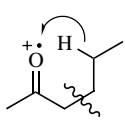	*m/z* 58	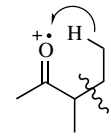	*m/z* 72
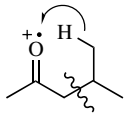	*m/z* 58	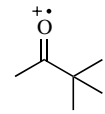	No γ-hydrogen

which they are the terminal functional group (i.e., they are formed directly by α-cleavage and not by rearrangement from interior groups in the $M^{+\bullet}$ of these molecules). Therefore, it is not unreasonable to assume that CH_3CO^+ and $C_4H_9^+$ account for the entire molecule: $CH_3COC_4H_9$.

(Step 9) Four isomeric structures can be drawn with this formula; the rest of the spectrum must be used to help distinguish between them. Aliphatic ketones undergo the γ-hydrogen (McLafferty) rearrangement under appropriate conditions. Looking at these structures and predicting the products of McLafferty rearrangement for each of them (Table 10.4) may reduce the number of possibilities. Because the observed rearrangement ion peak occurs at *m/z* 72 (the only important $OE^{+\bullet}$ peak in the spectrum other than the $M^{+\bullet}$ peak), only 3-methyl-2-pentanone is consistent with the observed spectrum. [*Answer*: 3-methyl-2-pentanone (*sec*-butyl methyl ketone)]

DropBooks

7.2.

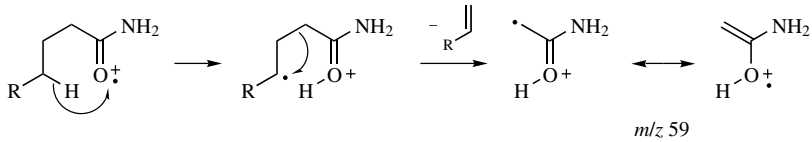

m/z 59

(10.43)

7.3. Although $^+C_4H_9$ also has a mass of 57 u and could theoretically be responsible for the base peak, cyclohexanol itself has a base peak at *m/z* 57 due to $C_3H_5O^+$.

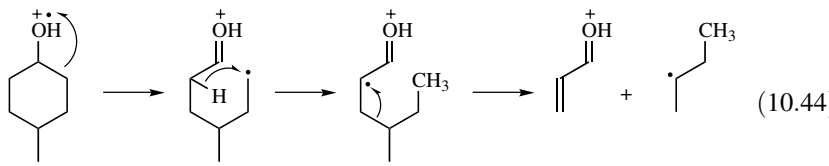

m/z 114 *m/z* 57

(10.44)

7.4. Clearly, the 7-methyl group must be lost in whatever fragmentations lead to the major ions that are represented in the spectrum. The answer to this problem becomes more apparent if the left-hand ring is viewed as a substituted aminocyclohexane (Equation 10.45; compare Equation 7.12).

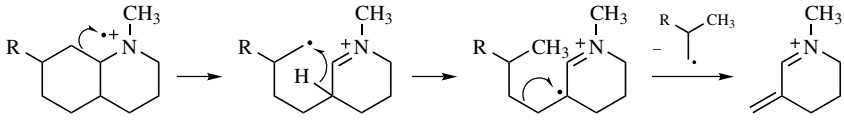

m/z 153 (R = H)
m/z 167 (R = CH_3)

m/z 110

(10.45)

7.5. These two compounds can be distinguished by identifying the products that each produces in the retro Diels–Alder fragmentation: Butadiene and vinyl alcohol $OE^{+\bullet}$ fragments (*m/z* 54 and 44, respectively) are produced in the case of 4-hydroxycyclohexene (Equation 10.46) and 1-hydroxybutadiene $OE^{+\bullet}$ fragment (*m/z* 70) from 3-hydroxycyclohexene (Equation 10.47). In addition, the 3-hydroxy isomer readily loses the H atom that is attached to the C atom next to the OH group and is also allylic to the double bond. It also loses $^{\bullet}CH_3$ by a mechanism that is similar to the loss of alkyl radicals from the cyclohexanone $M^{+\bullet}$ (Figure 7.12). The 4-hydroxy isomer loses water to form the 1,3-cyclohexadiene $OE^{+\bullet}$ fragment ion. [*Answer*: (a) 4-hydroxycyclohexene and (b) 3-hydroxycyclohexene]

4-Hydroxycyclohexene:

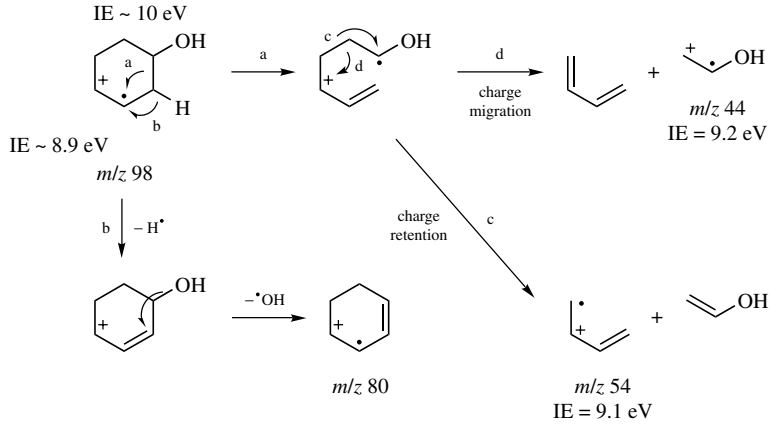

(10.46)

3-Hydroxycyclohexene:

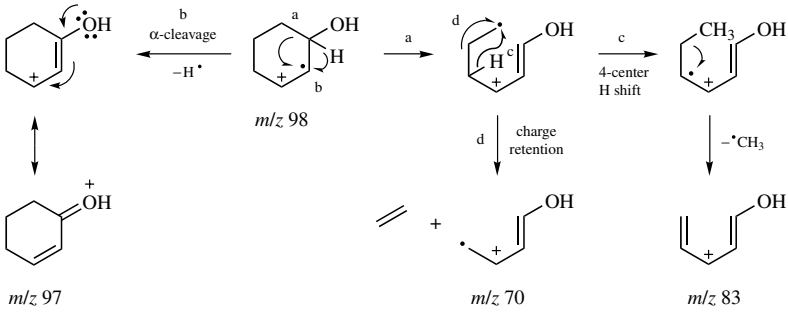

(10.47)

7.6.

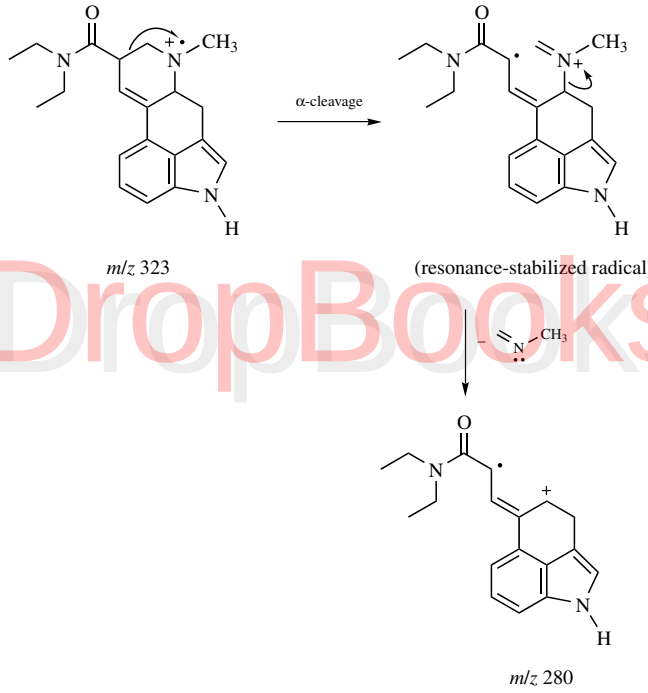

(10.48)

DropBooks

7.7. (*Steps 3 and 4*) The absence of N is indicated by the even MM and the fact that, with the exception of the peak at *m/z* 66, the most intense fragment ion peaks in the spectrum occur at odd *m/z* values. (*Step 5*) The spectrum shows no evidence of the obvious A + 2 elements. The $M^{+\bullet}$ and the ion having *m/z* 79 appear to contain seven and six C atoms, respectively, although the weak intensities of the X + 1 peaks in each case make these determinations uncertain. The ion with *m/z* 66 also appears to contain six C atoms, but this

is impossible because an ion with this mass cannot contain more than five C atoms. This means that there is a weak fragment ion peak at *m/z* 67 that also contributes to the observed intensity of this peak.

(*Steps 6 and 7*) Overall, the spectrum is not clearly either that of an aliphatic or aromatic compound. There seems to be an aromatic low-mass ion series at *m/z* 39, 51, 53, 65, and 77. Completely absent are peaks that infer the presence of O (*m/z* 31, 45, etc., for alcohols and ethers or *m/z* 43, 57, etc., for ketones). (*Step 8*) The two major losses from the $M^{+\bullet}$ are those of $^{\bullet}CH_3$ and a neutral fragment having a mass of 28 u. Because O appears to be absent, this fragment is probably $CH_2{=}CH_2$. (*Step 9*) The apparent absence of N also means that the peak at *m/z* 66 must represent an $OE^{+\bullet}$ fragment ion and therefore is probably formed by a rearrangement process. But if O is absent and the compound is not an aromatic compound, a γ-H rearrangement seems unlikely to account for the formation of this peak. In that case, a retro Diels–Alder fragmentation is a possibility.

(*Step 10*) Since N and O are absent, the elemental composition of the $M^{+\bullet}$ must be C_7H_{10}. The rings plus double bonds formula predicts that this compound will contain a total of $7 - \frac{1}{2}(10) + \frac{1}{2}(0) + 1 = 3$ rings and/or double bonds. Elemental compositions of $^{+}C_6H_7$ and $(C_5H_6)^{+\bullet}$ for the ions having *m/z* 79 and 66, respectively, seem reasonable. Because the ion with *m/z* 66 is an $OE^{+\bullet}$, the number of rings plus double bonds can be calculated for this ion as well. This ion also contains a total of three rings and/or double bonds.

There are many structures that satisfy an elemental composition of C_7H_{10}. Some structures that have highly strained bonds will not be considered. A few that might lend themselves to the cyclic loss of an olefin are shown below.

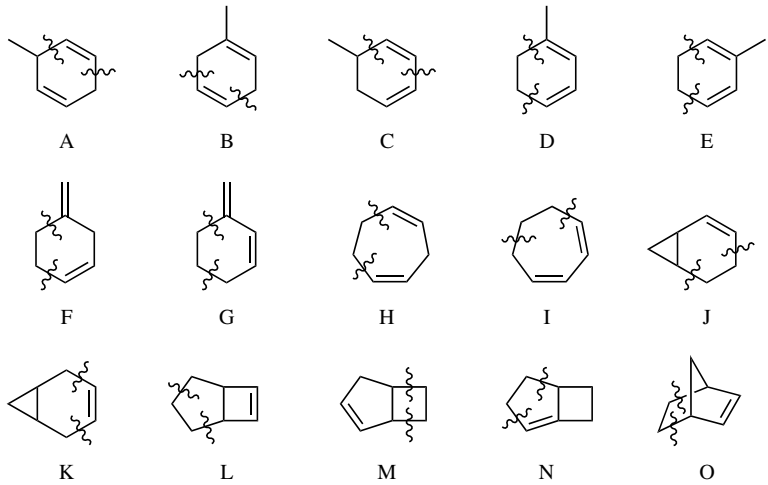

Distinguishing which structure is correct utilizes the observed fragmentation of this compound—especially the facile loss of $CH_2{=}CH_2$ to produce the ion

having *m/z* 66. Structures A, B, C, and K cannot lose $CH_2{=}CH_2$ without substantial rearrangement and, if anything, might be expected to lose $HC{\equiv}CH$ instead. Structures D–J and Structure N all contain a $-CH_2-CH_2-$ grouping, but loss of $CH_2{=}CH_2$ by mechanisms similar to that of the retro Diels–Alder fragmentation would lead to the formation of vinyl ions and therefore should be less energetically favored. Structures L and M also contain a $-CH_2-CH_2-$ grouping, but loss of $CH_2{=}CH_2$ from these structures should form distonic ion products, which would have to undergo further rearrangement in order to produce a stable ion product. Only structure O, which contains a cyclohexene ring, can lose $CH_2{=}CH_2$ by the retro Diels–Alder fragmentation to form a stable $OE^{+\bullet}$ product (Equation 10.49). [*Answer*: bicyclo[2.2.1]hept-2-ene; norbornene]

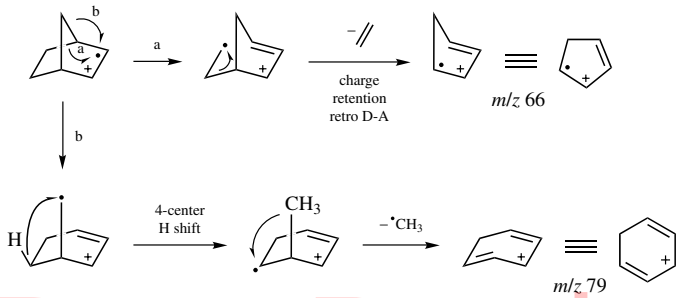

(10.49)

DropBooks

7.8. *N*,*N*-Dicyclohexylamine has two cyclohexane rings, each with a functional group that can cause α-cleavage to occur within the ring. Loss of 43 u as a propyl radical via the cyclohexanone-type rearrangement leads to the base peak at *m/z* 138, while minor loss of 29 u as an ethyl radical produces the small peak at *m/z* 152 (Equation 10.50). The *m/z* 138 ion, although it arises through a rearrangement process, has a structure that is indistinguishable from that of ions which are produced by α-cleavage. Because this ion meets the structural requirements for secondary elimination given in Section 6.5.1, loss of an olefin occurs (in this case, cyclohexene), and the ion having *m/z* 56 is produced.

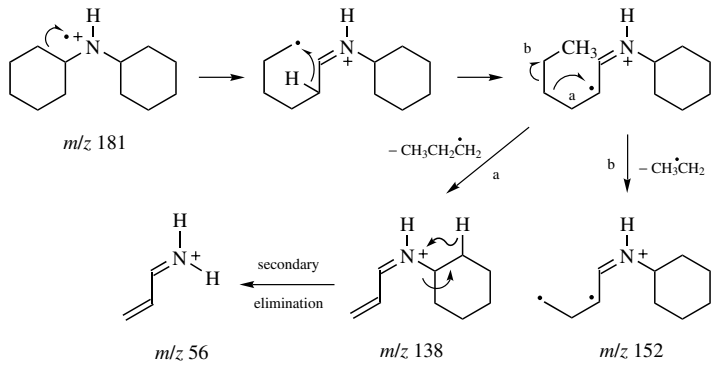

(10.50)

Chapter 8

8.1. The ion having *m/z* 80 represents a loss of 44 u from the $M^{+\bullet}$. Although loss of a molecule of propane (C_3H_8) is conceivable, this would require substantial rearrangement of both C and H and therefore would not be expected to produce the base peak in the spectrum. Another neutral fragment that has the same mass, but only two C atoms (the number of C atoms in each bridge of the structure), is C_2H_4O.

Initial ionization should occur preferentially at the double bond (Table 3.1 and Equation 10.51), so that this loss can be viewed as a retro Diels–Alder fragmentation (Section 7.4). Homolytic cleavage occurs at the C atom adjacent to the double bond with formation of a stable allylic ion. An additional homolytic cleavage with loss of vinyl alcohol produces a 1,3-cyclohexadiene $OE^{+\bullet}$ fragment (*m/z* 80). Loss of •H then gives the delocalized ion having *m/z* 79.

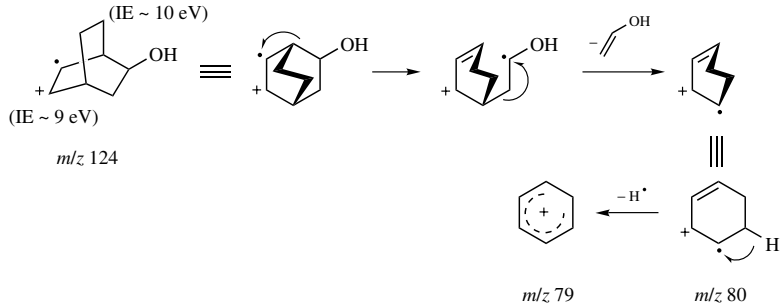

(10.51)

8.2.

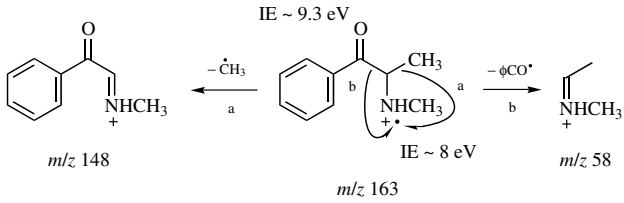

(10.52)

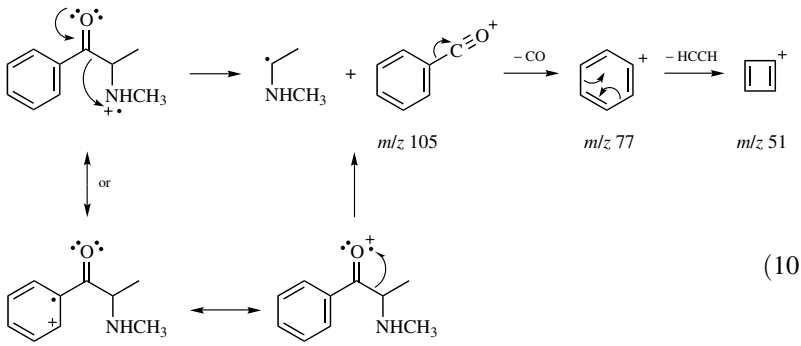

(10.53)

Formation of the benzoyl ion and fragment ions that result from its decomposition can be depicted either after initial ionization on the N atom or on the carbonyl O atom, as shown in Equation 10.53.

In spite of the fact that the peaks at *m*/*z* 58 are extremely intense relative to the remaining peaks, the spectrum of each of these compounds contains weak intensity peaks at high *m*/*z* values that are reproducible from spectrum to spectrum and are also characteristic of the compound in question. The three compounds should also have different GC retention times so that the combination of GC and MS provides an acceptable means of differentiating between them.

8.3. The fragmentations of cathine (MW 151) are entirely analogous to those of ephedrine (Figure 10.5). Ions containing the N atom all produce peaks 14 *m*/*z* units lower in the cathine spectrum than they do in the spectrum of ephedrine.

The primary difference between the two spectra at high *m*/*z* values is that the ion resulting from loss of $^{\bullet}OH$ is observed in the spectrum of cathine at *m*/*z* 134, whereas the corresponding peak at *m*/*z* 148 is not observed in the ephedrine spectrum. The difference in IE between the aromatic ring and amine group is much smaller in cathine than it is in ephedrine, which for cathine should result in an enhanced loss of $^{\bullet}OH$ by benzylic cleavage to form the ion having *m*/*z* 134. At the same time, the *n* electrons on the NH_2 group in cathine are somewhat less nucleophilic than those on the $NHCH_3$ group of ephedrine, which may decrease the propensity of this ion to form the five-membered N-containing ring. Because the ability to observe peaks in the mass spectrum is dependent on both how easily an ion is formed as well as how rapidly it fragments further (Section 3.6.1), this means that the ion produced by loss of $^{\bullet}OH$ from cathine remains in the ion source longer than does the corresponding ion from ephedrine.

DropBooks

8.4. (*Step 2*) The problem states that the unknown compound is a common pain reliever. This information narrows the choice of possible structures dramatically. In the United States, the three most commonly used pain relievers are aspirin (*o*-acetoxybenzoic acid), acetaminophen [N-(4-hydroxyphenyl)acetamide], and ibuprofen [2-(*p*-isobutylphenyl)propionic acid]. (*Step 3*) The peak at *m*/*z* 180 appears to be the $M^{+\bullet}$ peak, showing initial losses of 17, 42, and 60 to give the peaks at *m*/*z* 163, 138, and 120, respectively. (*Step 4*) The apparent even MM means that the compound must contain an even number of N atoms. Most of the important fragment ion peaks in the spectrum occur at even *m*/*z* values, which indicates either the presence of a large number of $OE^{+\bullet}$ fragment ion peaks in the spectrum, or two or more N atoms in the molecule. Of the three compounds listed in Step 2, only one of them contains a N atom.

(*Step 5*) The $M^{+\bullet}$ appears to contain nine C atoms, although the peaks at *m*/*z* 180 and 181 are too weak to produce reliable data. The ion having *m*/*z* 138 contains seven C atoms; the one with *m*/*z* 43 appears to contain only two C

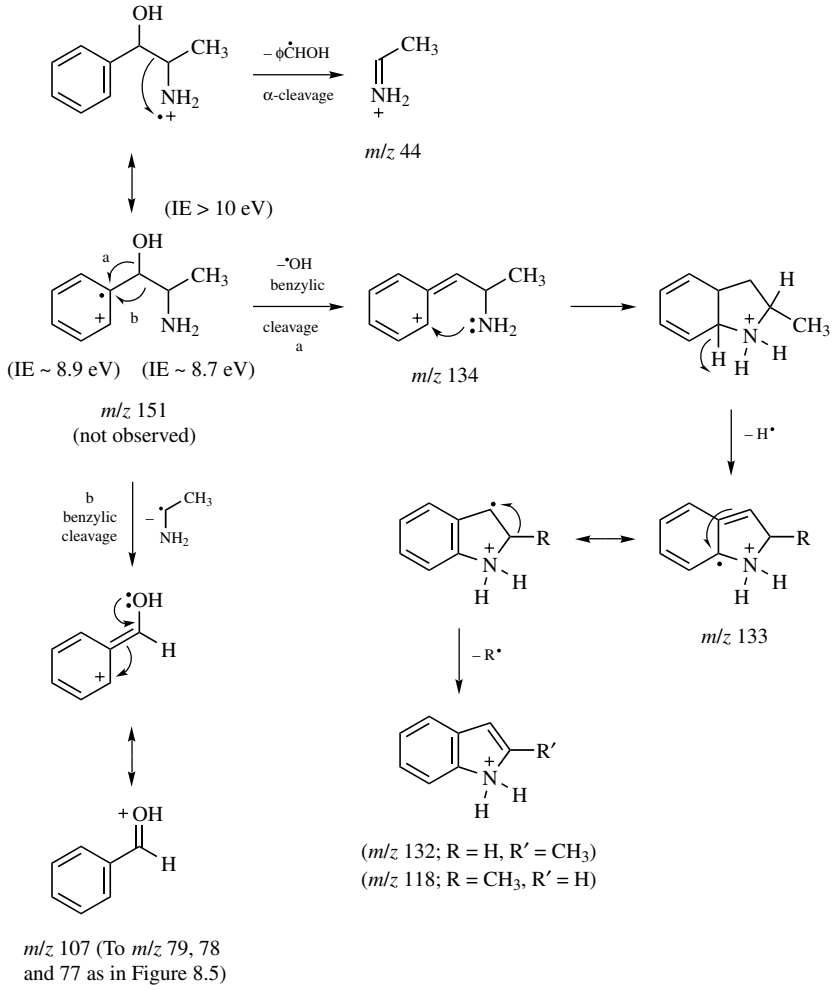

Figure 10.5. Proposed fragmentations of cathine (Problem 8.3).

atoms and is probably the acylium ion (CH_3CO^+). The presence of additional O atoms is indicated by the relatively high intensity of the X + 2 peak in the *m/z* 138 isotope cluster. The isotope peak intensity information for the *m/z* 120 ion is contaminated by the presence of a fragment ion peak at *m/z* 121; the intensity of the *m/z* 121 peak indicates the presence of more C atoms than can be accommodated by the mass of the ion.

(*Steps 6 and 7*) This spectrum bears a striking resemblance to that of salicylic acid (Figure 8.7*a*). With the exception of the peaks at *m/z* 43 and 163, all the major fragment ion peaks in the spectrum of this unknown also occur in the spectrum of salicylic acid. In fact, the MM of salicylic acid is

138, which corresponds to one of the most intense fragment ion peaks in the spectrum of the unknown. The unknown spectrum exhibits an aromatic low-mass ion series at *m/z* 38–39, 50–53, 62–65, and 74–77.

(*Steps 8 and 9*) The smallest observed loss from the $M^{+\bullet}$ is 17 u to produce the peak at *m/z* 163. This loss is most likely that of $^{\bullet}OH$ (Table 4.1). The combined loss of 42 u from the $M^{+\bullet}$ to give the ion with *m/z* 138 and the presence of a prominent fragment ion peak at *m/z* 43 that corresponds to CH_3CO^+ are often a good indication that the molecule contains an acetyl group attached to an O or N atom on an aromatic ring (Section 6.5.3). The

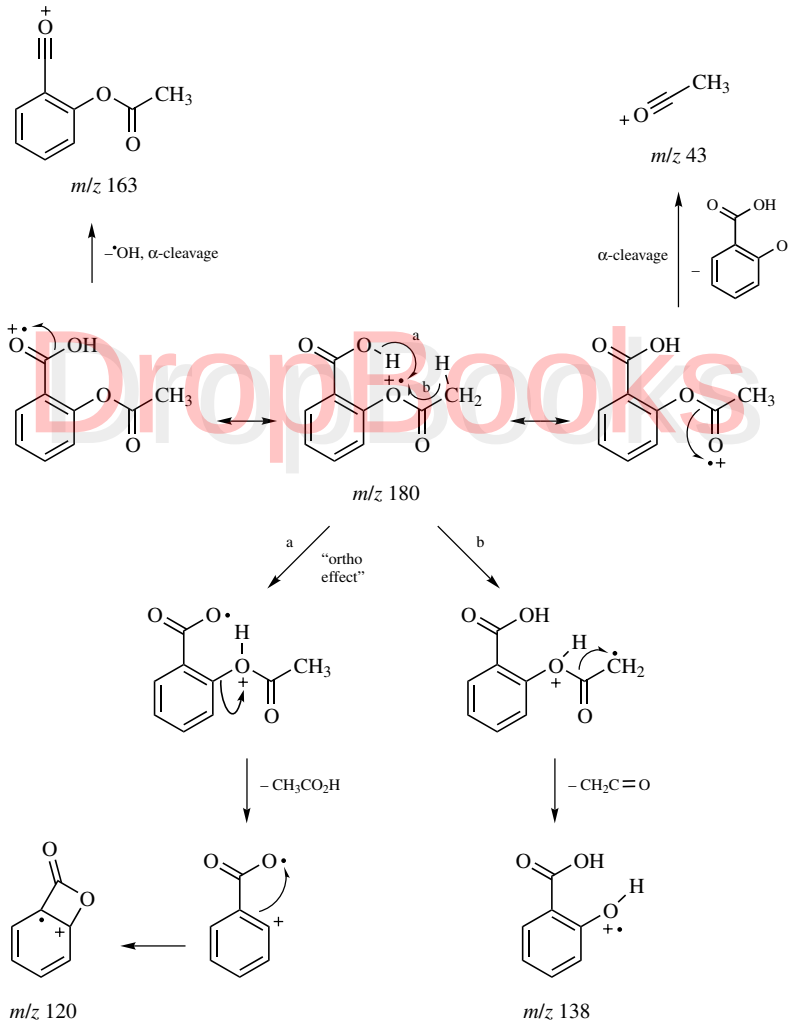

Figure 10.6. Proposed fragmentations of aspirin (Problem 8.4).

loss of 42 u in such cases is the loss of ketene ($CH_2C{=}O$). If the acetyl group were attached to an O atom, the loss of 60 u from the $M^{+\bullet}$ to produce the ion having *m/z* 120 might be the loss of a molecule of acetic acid (CH_3CO_2H). Both the *m/z* 138 and 120 peaks therefore appear to correspond to $OE^{+\bullet}$ fragment ions whose formation occurs by a rearrangement fragmentation that eliminates a neutral molecule.

(*Step 10*) The fact that this compound is a common pain reliever, the similarity between the unknown spectrum and that of salicylic acid, and the apparent presence of an acetyl group in the unknown molecule are enough information on which to postulate a structure. Aspirin is the acetate ester of salicylic acid and has the elemental composition $C_9H_8O_4$ with a MM of 180. Loss of ketene from the $M^{+\bullet}$ to produce an ion having *m/z* 138 is consistent with the presence of seven C atoms in this ion.

Rationalizations for formation of the ions having *m/z* 163, 138, 120, and 43 appear in Figure 10.6. As in the case of salicylic acid, initial ionization can be depicted as occurring by loss of an *n* electron from any of the O atoms. The ions with *m/z* 163 and 43 are both formed by α-cleavage after initial ionization at the carbonyl O atom of the benzoic acid and acetic acid groups, respectively. The loss of ketene to produce the ion having *m/z* 138 was discussed in Section 6.5.3 (see Equation 6.26). Loss of CH_3CO_2H to form the ion with *m/z* 120 occurs after transferring a H atom from the benzoic acid group to the initial radical site on the ring O atom of the acetoxy group by means of a six-atom cyclic intermediate. This is another example of the *ortho* effect. [*Answer*: 2-acetoxysalicylic acid (aspirin)]

8.5. The presence of a methyl group *ortho* to the carbomethoxy group in the 2,5-dimethyl isomer makes possible the transfer of a H atom to the initial radical site by means of a six-atom cyclic transition state (*ortho* effect). This leads to the loss of a molecule of methanol and stabilization of the charge on the carbonyl O atom (Equation 10.54). The same rearrangement is not possible in the 3,5-dimethyl isomer.

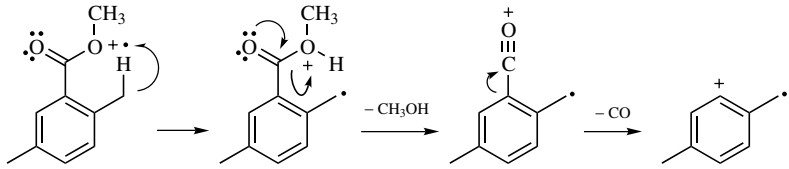

m/z 164 *m/z* 132 *m/z* 104

(10.54)

8.6. The methyl group on the pyridine ring contains a benzylic C atom; its loss is not expected (Section 6.2). Loss of $^{\bullet}CH_3$ from the methoxy group by cleavage away from the initially ionized N atom is like that seen in

papaverine (see Equation 6.13) and eugenol (Problem 6.4; see Equation 10.20). The subsequent loss of CO is analogous to that observed from phenol (see Equations 4.3 and 8.8). Loss of 28 u as ethylene, rather than as CO, seems unlikely in such a highly aromatic system (Section 4.1).

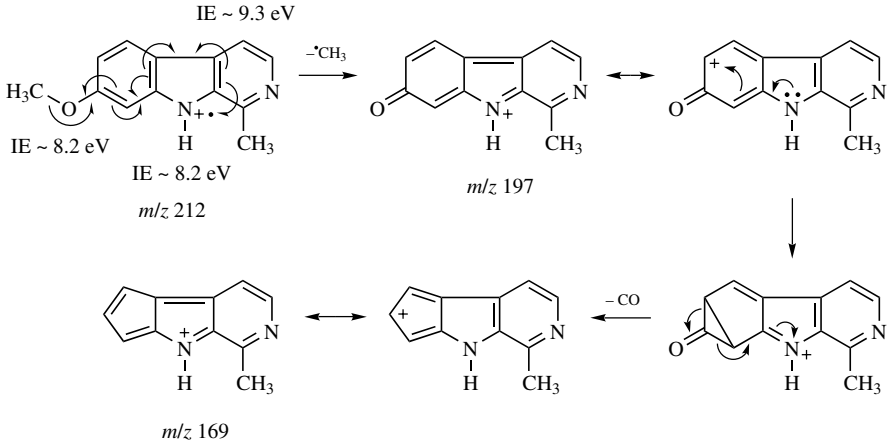

(10.55)

DropBooks

8.7. The fragment ions with *m/z* 209, 194, and 180 all show X + 2 peaks that are consistent with the presence of the Cl atom. Although loss of HCCH is possible, the only other expected fragmentations of the aromatic ring are those that involve the Cl atom. This compound is not only a cyclohexanone, but the cyclohexane ring also has two additional functional groups that can cause α-cleavage to occur within the ring. After initial ionization at the N atom (Table 3.1), the bond between the carbonyl C atom (C1) and the C atom containing both the amine and aromatic ring (C2) should break, leaving the charge stabilized on the N atom (Figure 10.7).

This leads to a situation that is similar to the one encountered after initial α-cleavage in cyclohexanone (Figure 7.12). Loss of CO to produce *m/z* 209 can occur with ring closure (path *a* in Figure 10.7) to generate an $OE^{+\bullet}$ fragment ion similar in stability to that of the $M^{+\bullet}$. Formation of a distonic ion via path *b* in Figure 10.7, however, should lead to further fragmentation. One possibility is a cyclohexanone-type rearrangement involving a 5-atom, rather than 6-atom, transfer of H to move the radical site nearer to the N atom. Subsequent loss of a methyl or an ethyl radical will lead to the ions having *m/z* 194 and 180, respectively (Figure 10.7). As in the case of cyclohexanone (Figure 7.12), loss of the larger radical is preferred because both the radical and resultant ion products are considerably more stable.

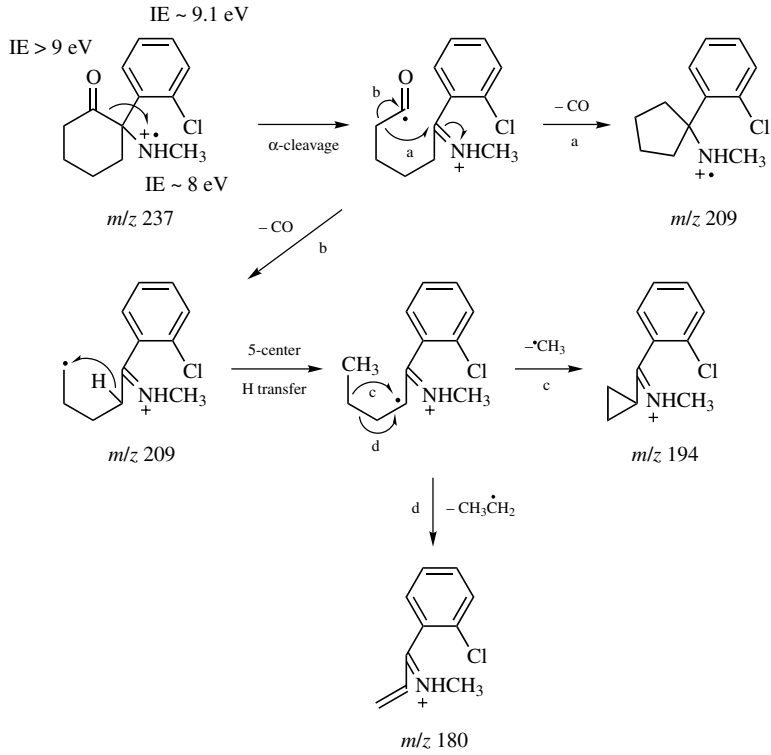

Figure 10.7. Proposed fragmentations of ketamine (Problem 8.7).

Chapter 9

9.1. This spectrum is very similar to that of 3,4-methylenedioxyethylamphetamine (MDE; Figure 9.2*c*), *but it is not identical*! (Would you have been satisfied that this *was* the spectrum of MDE if it had been identified by library search?) Most notably, the peak at *m/z* 44 is much less intense in this spectrum than it is in the MDE spectrum, where it is produced by secondary elimination from the abundant initial α-cleavage ion. Nonetheless, the presence of the *m/z* 135 peak, the base peak at *m/z* 72, and the apparent $M^{+\bullet}$ peak at *m/z* 207 strongly suggests that this compound is an isomer of MDE that differs only in the arrangement of the C atoms near the N atom (compare Problem 6.3). Eight additional structures meet these requirements. The pattern of losses observed in the unknown spectrum should help decide among these possibilities (Table 10.5).

This unknown shows loss of $H^{\bullet}$ to produce the peak at *m/z* 206 and $^{\bullet}CH_3$ to give the *m/z* 192 peak (remember that some α-cleavage losses in these compounds produce ions of extremely low abundance based on the relative

Table 10.5. Isomeric structures for Problem 9.1

		α-Cleavages	Secondary Eliminations
A	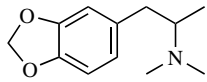	$H^{\bullet}$ $^{\bullet}CH_3$ $ArC^{\bullet}H_2$	*m/z* 44 None None
B	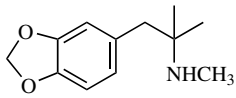	$H^{\bullet}$ $2\ ^{\bullet}CH_3$ $ArC^{\bullet}H_2$	*m/z* 30 None None
C	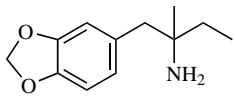	$^{\bullet}CH_3$ $CH_3C^{\bullet}H_2$ $ArC^{\bullet}H_2$	None
D	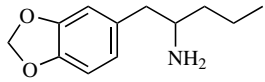	$H^{\bullet}$ $CH_3CH_2C^{\bullet}H_2$ $ArC^{\bullet}H_2$	None
E	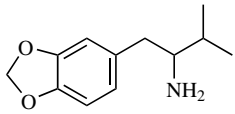	$H^{\bullet}$ $CH_3C^{\bullet}HCH_3$ $ArC^{\bullet}H_2$	None
F	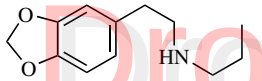	$H^{\bullet}$ $CH_3C^{\bullet}H_2$ $ArC^{\bullet}H_2$	*m/z* 58 *m/z* 30 *m/z* 30
G	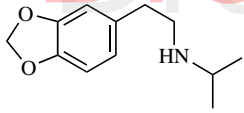	$H^{\bullet}$ $2^{\bullet}CH_3$ $ArC^{\bullet}H_2$	*m/z* 58 *m/z* 44 *m/z* 30
H	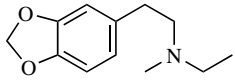	$H^{\bullet}$ $^{\bullet}CH_3$ $ArC^{\bullet}H_2$	*m/z* 58 *m/z* 30 *m/z* 44 *m/z* 44

DropBooks

stability of the radicals formed). It does not appear to lose either an ethyl or a propyl radical (the peaks at *m/z* 178 or 164 are insignificant in size), which eliminates Structures C, D, E, and F.

Although the *m/z* 44 peak is less intense than it is in the spectrum of MDE, it is still present—indicating that it may be produced by secondary elimination. On the other hand, there is no visible *m/z* 58 peak, thereby ruling out Structures G and H. The presence of another possible secondary rearrangement ion (namely, having *m/z* 30) cannot be determined because the

spectrum has not been recorded below *m/z* 40. However, Structure A is expected to produce a secondary elimination ion at *m/z* 44 after initial loss of $H^{\bullet}$ from one of the *N*-methyl groups (Equation 10.56). Structure B is not. [*Answer*: *N*,*N*-dimethyl-3,4-methylenedioxyamphetamine (Structure A)]

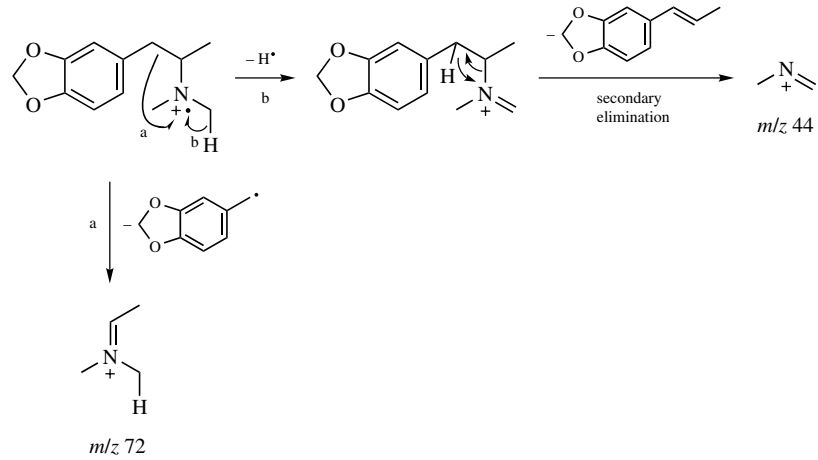

(10.56)

9.2. Phenylacetylmethylecgonine and toluylmethylecgonine should have similar spectra—in fact, they may be distinguishable only by comparing the spectra of known standards. Because the only structural difference between the two compounds occurs in the aryl groups, only the abundances of ions that directly involve fragmentation of these groups should be affected to any extent. For example, the ions having *m/z* 136 (the "benzoic acid" ion), 119 (the "benzoyl" ion), and 91 ("benzyl" ion) will have different structures when these two compounds fragment, so that they and their fragment ions will probably differ somewhat in relative intensity between the two spectra. But these differences are difficult to predict. No mass spectrum was provided for comparison.

9.3. The intense peaks at *m/z* 82 and 196 are sufficient to identify this spectrum as a derivative of cocaethylene (Table 9.1; compare Figure 9.5*a*). The loss of 45 from the $M^{+\bullet}$ peak (*m/z* 363 → *m/z* 318) also is consistent with the presence of the ethyl ester group. The presence of the *m/z* 82 peak confirms that the ring system near, and including, the *N*-methyl group is intact (Figure 10.8).

The nature of the aryl group remains to be determined. The loss of 151 from the $M^{+\bullet}$ peak to give the peak at *m/z* 212 is reflected in the presence of a peak at *m/z* 151. This corresponds, respectively, to loss of the substituted benzoyl ion and to the substituted benzoyl ion itself. Similarly, the loss of the substituted benzoate radical (167 u to give the peak at *m/z* 196) is mirrored in the presence of the benzoic acid $OE^{+\bullet}$ peak at *m/z* 168. Comparison with Figure 9.5*c* and Table 9.1 shows that *m/z* 151 and 168 are prominent peaks in

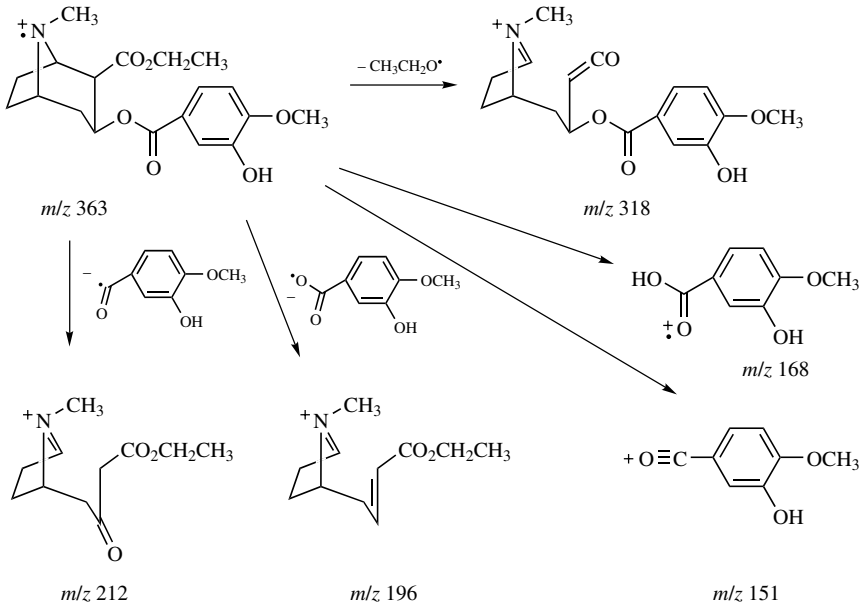

Figure 10.8. Proposed fragmentations of hydroxymethoxycocaethylene (Problem 9.3).

PrepBooks

the spectra of hydroxymethoxycocaines and correspond to the substituted benzoyl ion and benzoic acid $OE^{+\bullet}$, respectively (Figure 10.8). [*Answer*: hydroxymethoxycocaethylene]

9.4. The five unknown spectra can be arranged into two groups—those with intense *m/z* 182 peaks and those with intense *m/z* 210 peaks. By comparison with the spectra of other cocaine derivatives, it is easy to see that the first group of compounds consists of aroyl esters of methylecgonine ($R^2 = CH_3 = Me$, using the notation in Section 9.3), while the latter group comprises aroyl esters of propylecgonine ($R^2 = CH_3CH_2CH_2 = Pr$). This assignment is corroborated by first losses from the $M^{+\bullet}$ of 31 u ($MeO^{\bullet}$) for methylecgonyl esters and 59 u ($PrO^{\bullet}$) for propylecgonyl esters. Some of these spectra are so weak and filled with background peaks that identifying the first loss from the $M^{+\bullet}$ peak is difficult.

The fact that the *m/z* 82, 182, and 210 peaks are so prominent means that there are no additional groups on the tropane skeleton near the N atom. Therefore, any additional substitution must occur on the aromatic ring. The mass spectra of unknowns A and B have fairly intense *m/z* 121 peaks, while peaks at *m/z* 151 are observed in the remaining spectra. Peaks at *m/z* 121 are important in the spectra of derivatives of hydroxycocaine, whereas *m/z* 151 peaks are seen in the mass spectra of the hydroxymethoxycocaines (Table 9.1). Indeed, the $M^{+\bullet}$ peak for compound A occurs at an *m/z* value 42 units higher than that of hydroxycocaine, which corresponds to derivatization

of the aryl —OH group with a propyl group. The $M^{+\bullet}$ peak for compound B is 28 u higher still; because this is an ester of propylecgonine, not methylecgonine, the extra 28 u is accounted for by the additional $-CH_2-CH_2-$ in the propyl ester group. Compound A thus seems to have arisen from the propylation of hydroxycocaine,

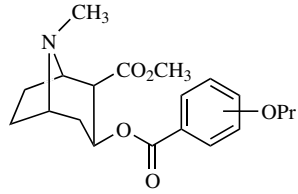

A - arylpropyloxycocaine

whereas compound B came from the propylation of hydroxybenzoylecgonine (Equation 10.57).

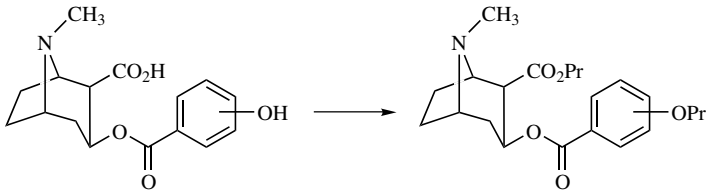

(10.57)

Hydroxybenzoylecgonine B - arylpropyloxypropylecgonine

The presence of the propyloxy group on the aromatic ring is corroborated in each of these compounds by the presence of a relatively intense *m/z* 163 peak, corresponding to the propyloxybenzoyl ion. This ion loses propylene (42 u) via a four-atom H migration to give the hydroxybenzoyl ion at *m/z* 121 (Equation 10.58; compare Equation 6.27):

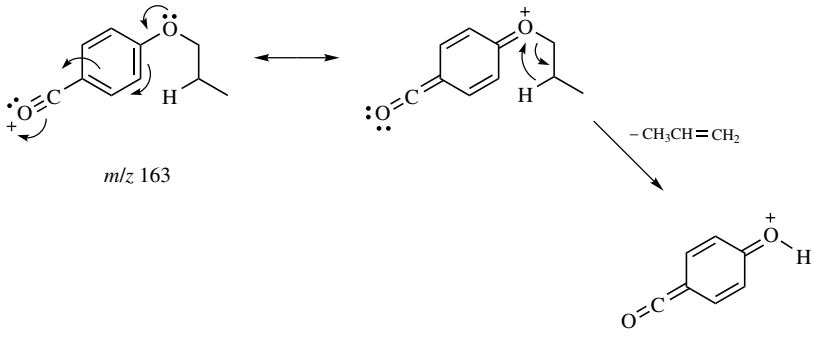

m/z 163 *m/z* 121

(10.58)

Of the remaining three compounds, unknown C is a derivative of methylecgonine, while D and E are propylated esters of benzoylecgonine derivatives. The *m/z* 151 and 168 peak combination from D is highly suggestive of the arylhydroxymethoxycocaines (Table 9.1). In fact, the apparent nominal MM of 377 is 28 u higher than that of the hydroxymethoxycocaines. This is consistent with the R^2 group being Pr, rather than Me. Unknown E has an apparent nominal MM 42 u higher than that of D, indicating not only the propylation of the carboxylic acid group, but also of the aryl hydroxy group. An isomeric methylecgonyl structure having two arylpropyloxy groups (which, from a metabolic standpoint, would have been more interesting) is inconsistent with the peak at *m/z* 210. Corroborating the presence of the arylpropyloxymethoxy group in compound E is the appearance of the corresponding benzoyl ion having *m/z* 193 (42 u higher than that shown by compound D). Like the propyloxybenzoyl ion above, it also loses propylene via rearrangement to give the hydroxymethoxybenzoyl ion seen at *m/z* 151 (see Equation 10.58).

Compound C has been left until last because of the poor quality of its spectrum. The fact that it is a derivative of methylecgonine and also has an apparent nominal MM 42 u higher than that of the hydroxymethoxycocaines strongly suggests that it is an arylpropyloxymethoxycocaine. Consistent with this is the peak at *m/z* 151 (the hydroxymethoxybenzoyl ion; the peak at *m/z* 193 corresponding to the propyloxymethoxybenzoyl ion is lost in the background clutter in that area of the spectrum). Beyond this, it is difficult to make further comments about this spectrum.

DropBooks

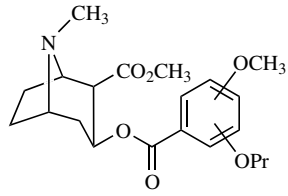

C - arylpropyloxymethoxy methylecgonine

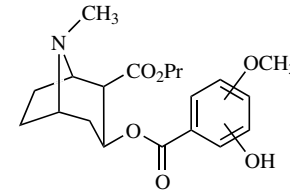

D - arylhydroxymethoxy propylecgonine

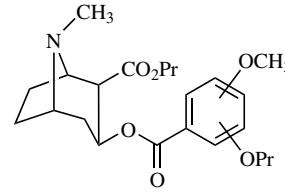

E - arylpropyloxymethoxy propylecgonine

9.5. The list of ions expected for *N*,*N*-diethyl-1-phenylcyclohexylamine is given below. The ion structure types are those in Figures 9.13–9.15. Peak intensities are assigned so that they are approximately the same as those for the corresponding peaks in the phencyclidine spectrum. The loss of an ethyl radical is a by-product of the cyclohexanone-type rearrangement (see Equation 9.14).

Ion Structure	Fragmentation	Predicted Peak
—	Isotope peak	232 (5%)
XVIII	$M^{+\bullet}$	231 (25%)
XIXb	Loss of $H^{\bullet}$ from the phenyl ring	230 (30%)
—	Loss of $^{\bullet}CH_3$ from α-cleavage in *N*-alkyl group	216 (∼1%)
—	Loss of $^{\bullet}CH_2CH_3$ from rearrangement intermediate	202 (2%)
—	Isotope peak	189 (15%)
XX	Cyclohexanone-type rearrangement	188 (100%)
—	Isotope peak	175 (3%)
XXI	Loss of $H^{\bullet} + C_4H_8$	174 (20%)
XXIII	Formation of phenylcyclohexene $OE^{+\bullet}$	158 (5%)
—	Isotope peak	155 (2%)
XXII	Loss of phenyl radical	154 (15%)
XXIV	Retro Diels–Alder from XXIII	130 (5%)
XXV	—	117 (10%)
—	Loss of H from XXV	115 (9%)
XXVI	—	104 (7%)
—	Loss of $H^{\bullet}$ from XXVI	103 (6%)
—	Isotope peak	92 (3%)
XXVII	—	91 (35%)
—	(Phenyl ion)	77 (8%)
XXVIII	Loss of phenylcyclohexene from XIXb	72 (16%)

A comparison of the predicted and actual spectra of this compound can be seen in Figure 10.9.

9.6. The intense peaks at *m*/*z* 97 and 165 and a smaller one at *m*/*z* 123 are all found in the spectrum of the thiophene analog of phencyclidine (Figure 9.16*c*). In fact, the ion series at *m*/*z* 81, 109 and 110, 135 and 136, 149 and 150 are also found in both spectra. The major loss of 43 u from the $M^{+\bullet}$, coupled with a less abundant loss of (56 + 1) u to give the peak at *m*/*z* 194, is typical of phencyclidine derivatives containing the cyclohexane ring. Thus, it seems likely that this compound differs from 1-(2-thienyl)cyclohexylpiperidine (the thiophene analog of phencyclidine) by replacement of the piperidine ring with some other group. Although the nature of the unknown group may not be obvious, the nominal MM of this compound, as well as the masses of the ions with *m*/*z* 208 and 194, all differ from those in the spectrum of 1-(2-thienyl)cyclohexylpiperidine by 2 u. A similar difference is seen between the spectra of phencyclidine and phenylcyclohexylmorpholine

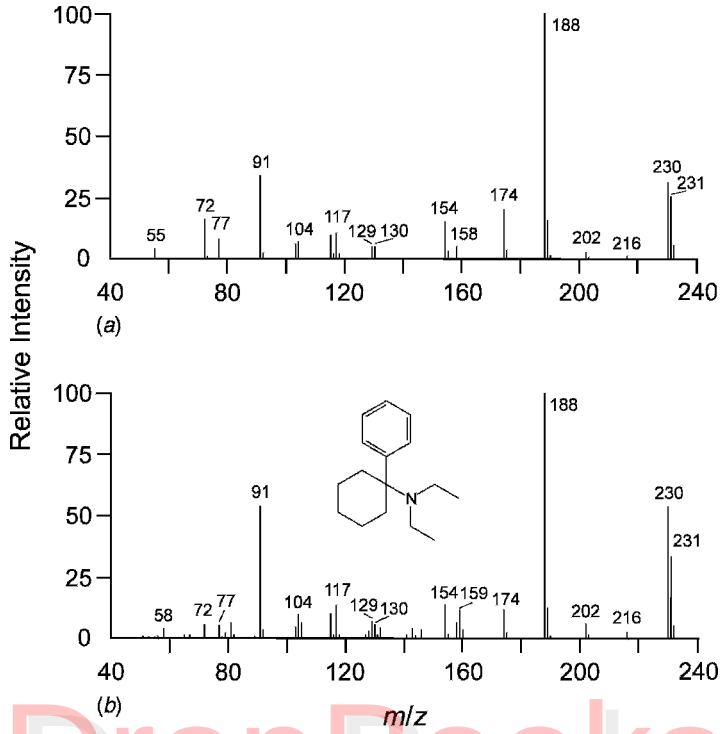

Figure 10.9. (*a*) Predicted and (*b*) actual spectra of *N,N*-diethyl-1-phenylcyclohexylamine (Problem 9.5).

DropBooks

(compare Figures 9.12 and 9.16*b*), so that a morpholine ring is a good candidate for the missing group (Figure 10.10).

Another set of structures that have the same nominal mass as 1-(2-thienyl)-cyclohexylmorpholine are *N*-alkylated 1-phenylcyclohexylamines such as that shown below:

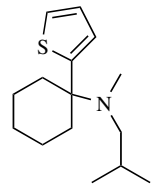

However, all these structures offer modes of α-cleavage and secondary elimination that are not possible in the morpholine derivatives, and the spectrum in Figure 9.17 shows no evidence of these losses (see Figure 10.9 and the answer to the previous problem). [*Answer*: 1-(2-thienyl)cyclo-hexylmorpholine]

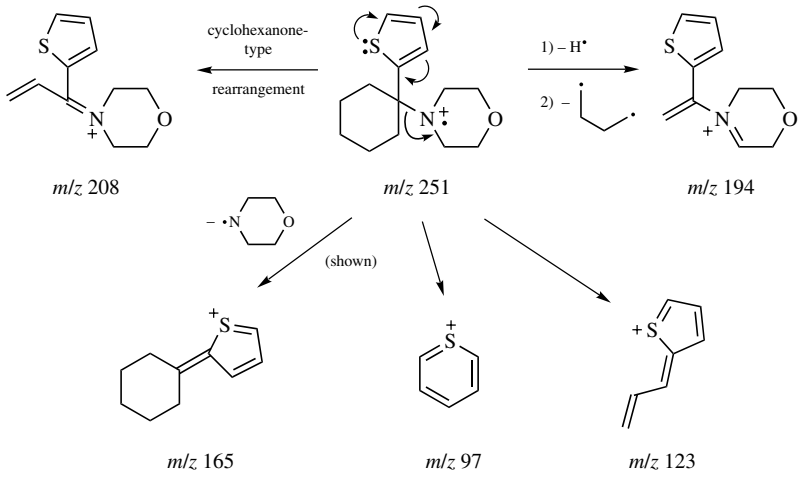

Figure 10.10. Proposed fragmentations of 1-(2-thienyl)cyclohexylmorpholine (Problem 9.6).

9.7. Instead of losing phenyl radical by α-cleavage, this compound loses a benzyl radical, thereby producing both a stable ion and very stable radical. The $\Delta G^{\ddagger}$ for this one-step loss must be substantially lower than that for the multistep cyclohexanone-type rearrangement.

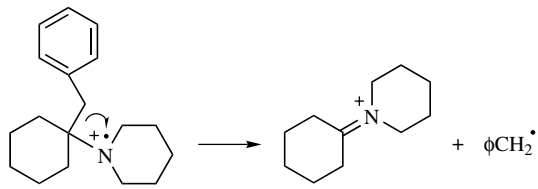

(10.59)

9.8. Losses observed in the spectra shown in Figure 9.18 are listed in Table 10.6. The postulated losses consist of only small groups: $H^{\bullet}$, $^{\bullet}CH_3$, and $^{\bullet}Cl$, and either CO or $H^{\bullet}$ plus HCN. Without high-resolution data, the loss of CO vs. $H^{\bullet}$ plus HCN cannot be distinguished, but the loss of 28 u as $CH_2{=}CH_2$ seems very unlikely in this molecule. The proposed losses reflect the high degree of unsaturation in the $M^{+\bullet}$ and resulting ions (Section 4.1.2).

What is surprising, or at least would have been surprising prior to the discussion in Section 9.4, is the loss of one D atom from the deuterated phenyl ring in several of the fragmentations of the derivative. Initial ionization at the imine N atom, loss of an *ortho* H atom from the adjacent phenyl ring, and formation of a four-membered ring parallel the similar loss from the $M^{+\bullet}$ of phencyclidine (Figure 9.13). As with phencyclidine, this

Table 10.6. Losses from the diazepam $M^{+\bullet}$

m/z	Loss (u)	Deuterium Loss	Cl Present?	Postulated Loss
283	1	1(!)	Y	$H^{\bullet}$
268	16	1(!)	Y	$H^{\bullet} + {}^{\bullet}CH_3$
257	27	0	Y	HCN
256	28	0	Y	CO or $H^{\bullet}$ + HCN
255	29	0	Y	$H^{\bullet}$ + CO or $2H^{\bullet}$ + HCN
249	35	0	N	$Cl^{\bullet}$
248	36	1(!)	N	$H^{\bullet} + Cl^{\bullet}$
241	43	0	Y?	CO + $^{\bullet}CH_3$ or $H^{\bullet}$ + HCN + $^{\bullet}CH_3$
228	56	0	Y?	$H^{\bullet}$ + HCN + CO?
221	63	0	N	CO + $Cl^{\bullet}$ or $H^{\bullet}$ + HCN + $Cl^{\bullet}$
205	79	0 (1)	N	CO (or $H^{\bullet}$ + HCN) + $^{\bullet}CH_3$ + $Cl^{\bullet}$

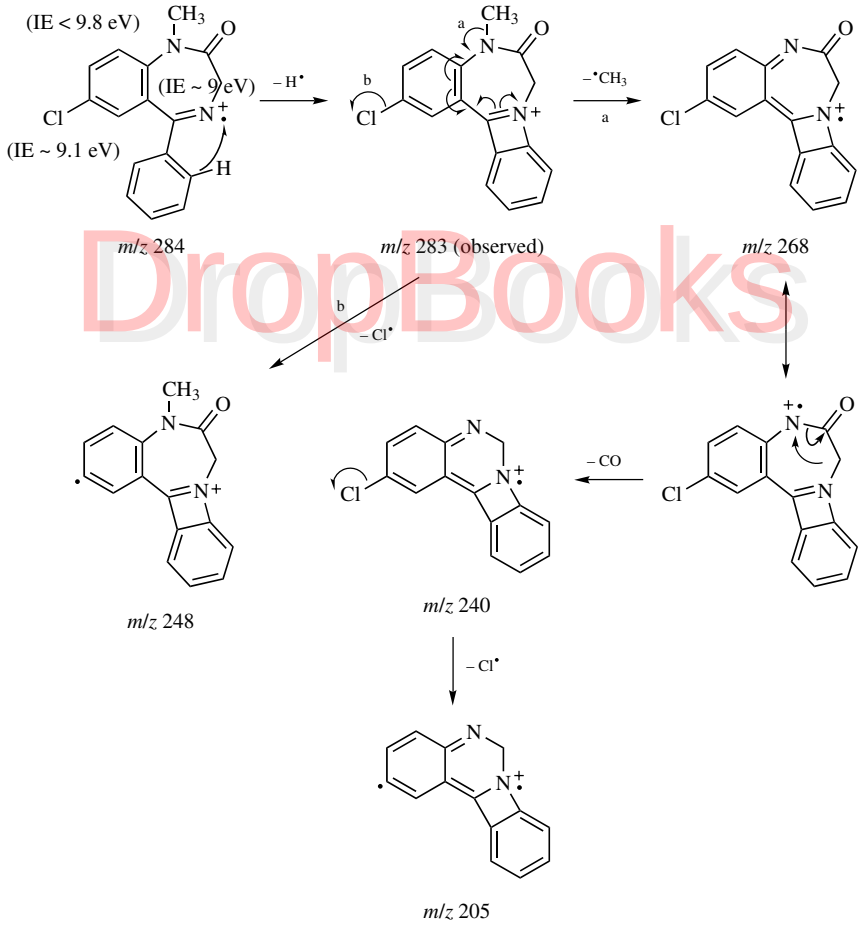

DropBooks

Figure 10.11. Proposed fragmentations of diazepam that involve initial loss of a phenyl H atom.

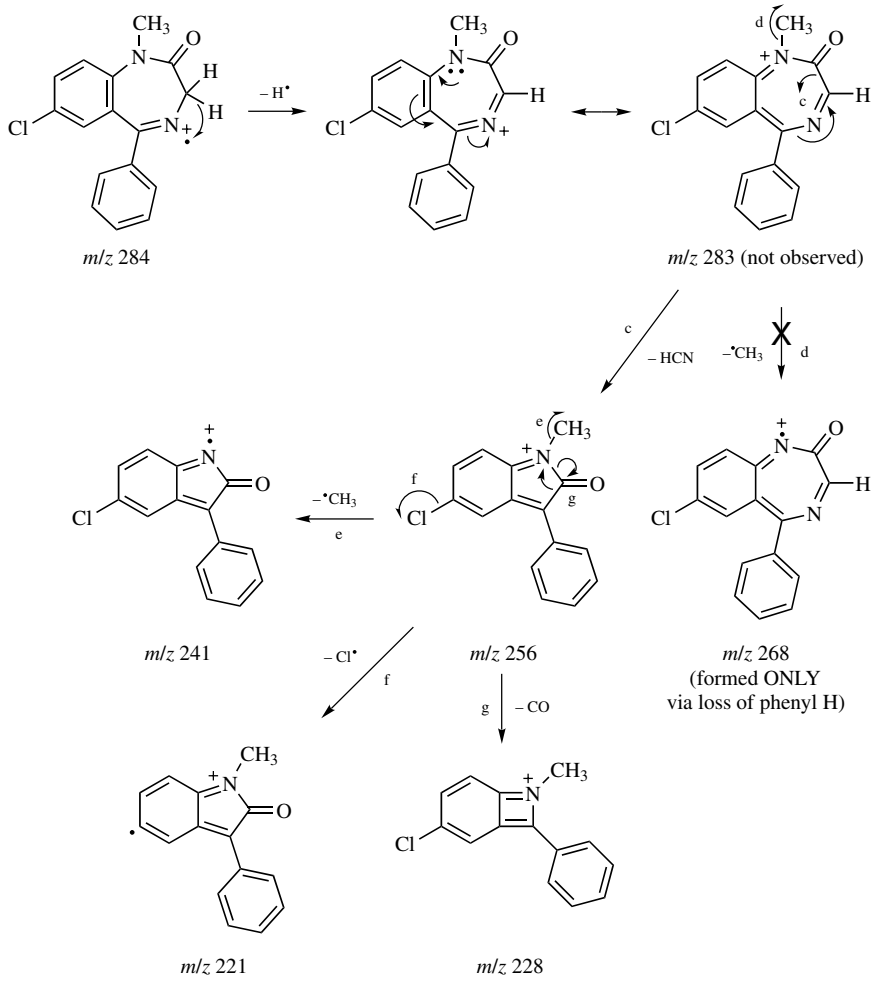

Figure 10.12. Proposed fragmentations of diazepam that involve initial loss of a H atom from the seven-membered ring.

loss alone accounts for the formation of the observed $(M - 1)^+$ ion, because the intensity of the *m/z* 288 peak is due almost entirely to isotopic contributions from the *m/z* 287 ion. A rationalization for formation of the other ions that are produced from this ion is shown in Figure 10.11.

Proposals for other losses that are consistent with these spectra are given in Figures 10.12 and 10.13. Note that formation of some of these ions may proceed through an alternative structure for the *m/z* 283 ion that has not lost the phenyl H atom. This situation is also similar to that described for phencyclidine in Section 9.4.

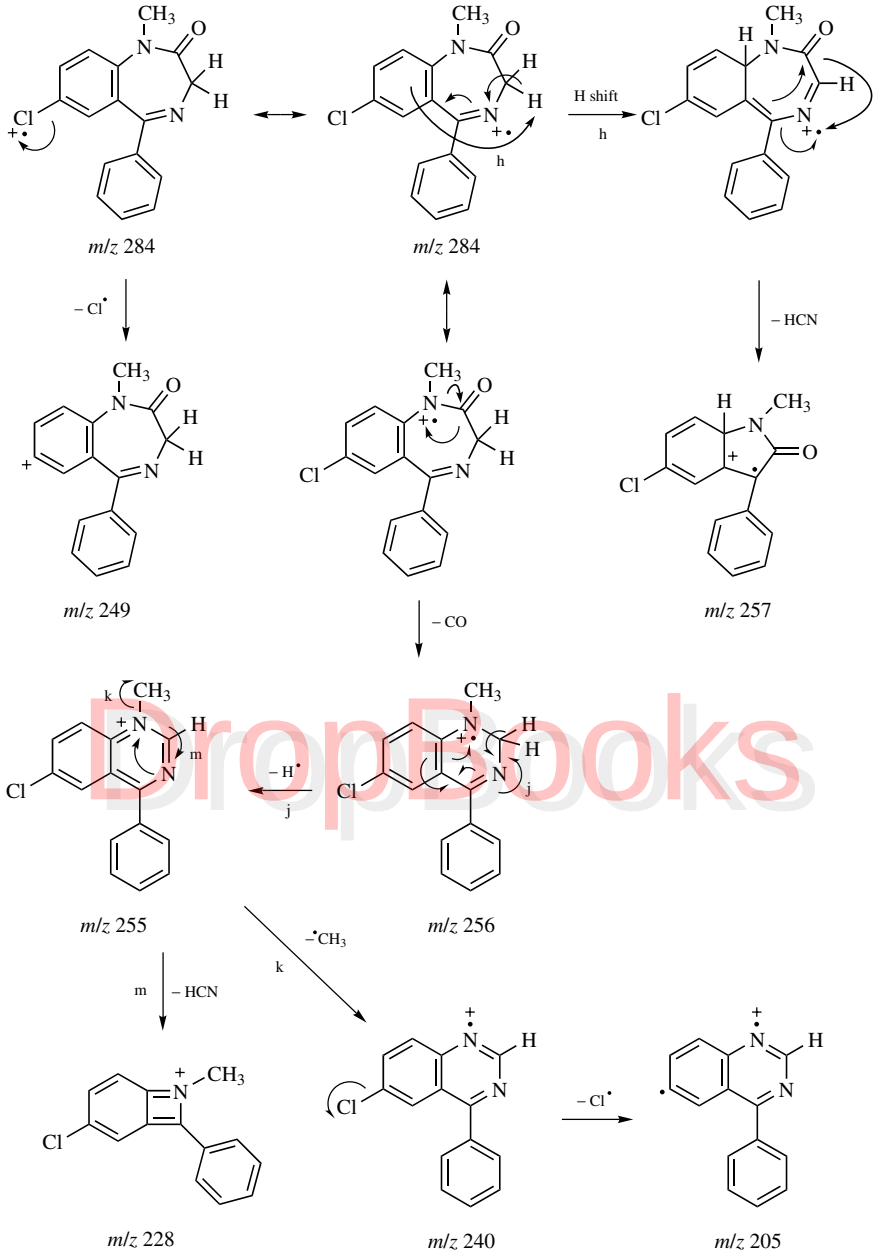

DropBooks

Figure 10.13. Additional proposed fragmentations of diazepam.

INDEX

Pages containing **representations of mass spectra** for individual compounds are shown in **boldface**; those having *interpretations of mass spectra* for individual compounds are shown in *italics.*

A, A + 1, and A + 2 elements, 77–78, 90–91, 151, 152–153
a and *q* (variables)
  for quadrupole ion trap, 21, 22–24
  for transmission quadrupole, 18–20, 21
a vs. *q* plot, *see* Stability diagram
α-Cleavage, *see* Alpha-cleavage
Abundances, ion, 41
ac generator, *see* Generator, ac
Accelerating voltage, *see* Voltage, accelerating
Acetamide,
  N-(4-acetoxyphenyl), *see* Acetaminophen, acetyl derivative
  N-(4-hydroxyphenyl), *see* Acetaminophen
  trifluoro, *N*,*N*-bis-[tris-(perfluorooctylethyl)silyl]propyl, use as calibration standard, 37
Acetaminophen, 196, 336
  acetyl derivative, 196, **197**
Acetic acid, trifluoro-, 123, **124**, 125, *126*
Acetone, 119, *298*
Acetophenone, **148**, 303, *304*
Acetylene, 100, 108
  elimination of, 122, 126, 128, 129, 145, 158, 241–242, 271, 305
  electronic structure, 126
Acids and esters, aliphatic, McLafferty rearrangement and, 212, 221, 234–236
Acquisition rates, spectral, *see* Scan, rates
Acrylonitrile, 2-cyano-3(*o*-chlorophenyl), **170**, *311–312*
Acylium ion (CH_3CO^+), distinguishing from propyl ion in spectrum, 186, 306, 320, 329
ADC, *see* Analog-to-digital converter
Agilent Technologies, 11, 21
Alcohols, aliphatic. *See also* Ethers, aliphatic
  α-cleavage and, 165, 180, 183, 321–322
  secondary elimination after α-cleavage and, 192–193
  water elimination from, 121, 122, 198–200, 321–322
  weak molecular ion peaks and, 113, 181
Aldehydes
  α-cleavage and, 191
  γ-hydrogen rearrangement and, 191, 208
Algorithm, library search, 42–43, 55
Alkanes, 132–136, 161, 304
  fragmentations of, 132–134, 157
    effect of chain branching on, 134–136, 154–155, 301–302
  in petroleum distillates, 145–146
  ionization energies, 105–106
  low mass ion series, *see* Low mass ion series, alkanes
Alkenes, 105, 106, 138–140, 147, 302
  low mass ion series, *see* Low mass ion series, alkenes
Alkylanthracenes, in petroleum distillates, 145

Understanding Mass Spectra: A Basic Approach, *Second Edition.* By R. Martin Smith
ISBN 0-471-42949-X

© 2004 John Wiley & Sons, Inc.

Alkylbenzenes
α-cleavage and, *see* Benzylic cleavage
γ-hydrogen rearrangement and, 213–216, 321
in petroleum distillates, 145–146
loss of methyl radical from ring and, 166–168, 311
Alkylnaphthalenes, in petroleum distillates, 145–146
Allyl carbenium ion, formation of, 136, 139, 159, 200, 226, 244, 245
Allylic cleavage, 166, 298, 323, 332
Alpha-cleavage (α-cleavage), 109, 114–117, 164*ff*, 240
alcohols and, *see* Alcohols, aliphatic, α-cleavage and
aldehydes and, *see* Aldehydes, α-cleavage and
amides and, *see* Amides, α-cleavage and
amines and, *see* Amines, aliphatic, α-cleavage and
aromatic rings and, *see* Benzylic cleavage
double bond and, *see* Allylic cleavage
electron withdrawing groups and, 165, 176, 178–179, 183
esters and, *see* Esters, aliphatic, α-cleavage and; Esters, aromatic, α-cleavage and
ethers and, *see* Ethers, aliphatic, α-cleavage and; Ethers, aromatic, α-cleavage and
halogen-containing compounds and, 159
hydrogen radical loss in, 171–172, 174, 182, 191, 194, 195, 249, 259, 279, 313, 347, 351. *See also* Benzylic cleavage, hydrogen radical loss via alternative loss from *o*-position of nearby aromatic ring, 278, 283, 349–350
initiated at remote ionization site, 119, 165, 184–185, 312, 314, 315, 324, 329, 339–340
ketones and, *see* Ketones, α-cleavage and
low mass ion series, *see* Low mass ion series, α-cleavage
product ion stability and, 115–116, 165, 171, 176, 180, 183, 186, 188, 190, 240, 316–319
product radical stability and, 115–116, 165, 166, 171–172, 182, 186, 191, 240, 316–319
saturated ring systems and, 179–181, 223, 226, 268*ff*
secondary elimination after, 192–195, 254, 261, 279, 316–320, 322, 323, 325, 334, 342–343, 348
relative importance in amines vs. oxygen-containing compounds, 192, 320, 322
structural requirements for, 192
sulfur-containing compounds and, *see* Sulfides, α-cleavage and; Thiols, α-cleavage and
Amblyomma americanum, 163
AMDIS, *see* Automated Mass Spectral Deconvolution and Identification System
Amenta, D.S., 286
American Society for Testing and Materials, 145, 148
Amides,
α-cleavage and, 188, 190–191, 325–326
aromatic, ketene loss and, 196–197
γ-hydrogen rearrangement and, 190, 213, 330
primary, characteristic loss of NH_2 radical by, 122, 123, 188, 325
Amines, aliphatic
α-cleavage and, 114–117, 140–141, 165, 170–180, 194–195, 198, 240, 247, 258–259, 268, 298, 315–319, 323, 324, 325, 326–327, 334, 335, 337, 340, 341–343, 348, 349
electron-poor nitrogen atom and, 176, 178–179
importance of, 165, 170
γ-hydrogen rearrangement in, 259–261
loss of alkylamino group by, 171, 174, 247
secondary elimination after α-cleavage and, 194–195, 279, 281, 316–319, 325, 327, 334
Amino acids, analysis by MS, 3
Amitryptiline, 175, **176**
Ammonia
as reagent gas in chemical ionization mass spectrometry, 8–9
loss of, 122–123
Amobarbital, **213**
Amphetamine, **12**, 119, **171**, 260
α-cleavage in, 114–117, 171, *172*, 175
4-bromo-2,5-dimethoxy-, **70**
N,N-diethyl-, 204, *325*
N,N-dimethyl-, 175

DropBooks

fragmentation, energy diagram, 114–116
α-methyl-, *see* Phentermine
N-methyl-, *see* Methamphetamine
3,4-methylenedioxy-, *see* 3,4-Methylenedioxyamphetamine
Analog-to-digital converter, 35
Anisole, *see* Benzene, methoxy-
Antiaromatic structures, 129
APCI, *see* Chemical ionization mass spectrometry, atmospheric pressure
Aperture, electron, 5
Aromatic compounds. *See also* Alkylbenzenes and individual compound types.
α-cleavage and, *see* Alpha-cleavage, initiated at remote ionization site; Benzylic cleavage
eliminations from, 126, 128–131, 241–243. *See also* Acetylene, elimination of; Amides, aromatic, ketene loss and; Carbon monoxide, elimination of; Esters, aromatic, ketene loss and; Ethers, aromatic, formaldehyde elimination and; Ethers, aromatic, olefin elimination and; Hydrogen cyanide, elimination of
intense molecular ion peaks and, 114, 132, 142, 158, 160, 305, 307, 309
low mass on series, *see* Low mass ion series, aromatic
non-benzenoid, 129, 158, 188
benzylic cleavage in, 119, 329
Aromaticity, Hückel's Rule for, 129, 158
Arrhenius equation, 111
Arrow, full-headed, use of, 109, 119, 120. *See also* Fishhook.
Arson analysis, forensic, 145–146
Aspirin, **255**, *336–338*
ASTM, *see* American Society for Testing and Materials
Atomic mass, 59–60
Atomic mass unit (amu), 3. *See also* u (Unified atomic mass unit) and Dalton.
Atomic weight, 59–60
Atrazine, *198*
Ausloos, P., 44, 54, 83, 84, 98, 127, 148
Automated Mass Spectral Deconvolution and Identification System, 29
Ayers, M.P., 98
8-Azabicyclo[3.2.1]octane, derivatives, *see* Tropane. *See also* Cocaine.
Background spectrum, subtraction of, 28–29, 47
Banana, odor of, 235
Barbituric acid, derivatives, McLafferty rearrangement and, 213
Barron, R., 54
Base peak, definition, 39
Bay, oil of, 142
Beckey, H.D., 54
Benzaldehyde, **191**, 249
Benzamide, *188*, **190**, 191, 325
Benzene, **31**, 128, 129, 143, **144**, *145*
n-butyl-, 213, **214**, 215
1,4-dibromo-, **72**, 289, 291
1,4-diethyl-, **97**, 295, *296*
ethyl-, **214**, 215
3,5-dimethyl-, 166, **167**
2-methyl-, **43**
n-hexyl-, 215
isobutyl-, **147**, 166, **167**, 215
isopropyl-, **43, 169**, 310–311
methoxy-, **130**, *131*
methyl-, *see* Toluene
methyl radical loss from, 143, 145
neopentyl-, 215, 216
n-pentyl-, 215, 216
2-pentyl-, 215
n-propyl-, 143, **144**, **169**, 213, **214**, 215, 216, 219, 259, 310–311
2-methyl-, **167**
1,2,3,5-tetramethyl-, 166–167, **168**
1,2,3-trimethyl-, **43**, 166–167, **168**
Benzocaine, 204, *324*
Benzoic acid, 92
2-acetoxy, *see* Aspirin
4-amino-, ethyl ester, *see* Benzocaine
2,5-dimethyl-, methyl ester, 254, **255**, *339*
3,5-dimethyl-, methyl ester, 254, **255**, 339
2-hydroxy-, **251**, *252–253*, 337, 339
3-hydroxy-, **251**, *252–253*
4-hydroxy-, **251**, *252–253*
methoxy-, 328
methyl ester, **205**, 327, *328*
methyl ester, 188, **189**, 191, 328
Benzoyl ion, 128–129, 145, 188, 271, 304, 335–336
low mass ion series, *see* Low mass ion series, benzoyl
Benzoylecgonine, 263, **265**, 266, 273–274
arylhydroxy derivative, 345
ethyl esters, *see* Cocaethylene
methyl esters, *see* Cocaine
propyl esters, *see* Ecgonine, propyl ester

Benzyl
ion
equilibrium with cycloheptatrienyl ion, 128, 241, 242, 249
formation of, 115–116, 117, 143, 166, 172, 173, 240, 318, 321
fragmentation of, 128, 143–144, 241–242
stability of, 105–106
low mass ion series, *see* Low mass ion series, benzyl
radical, 105, 116, 117, 240
loss of, 115–116, 122, 123, 172, 173, 175, 312–313
Benzylic cleavage, 166–167, 173–174, 188, 213, 248, 249, 311, 336–337
competition with γ-hydrogen rearrangement, 216
hydrogen radical loss via, 166–167, 174, 184, 311
initiated at remote ionization site, 259, 312, 314
nonbenzenoid aromatic compounds and, 188, 329
Benzyne, 128, 129, 143
Berger, R.S., 163
Bertsch, W., 145, 148
Beta-cleavage (β-cleavage), *see* Gamma-hydrogen rearrangement
Beynon, J.H., 131, 148, 180, 206, 243, 253, 254, 255
Bicyclo[2.2.1]heptane, 2-methylene-3,3-dimethyl-, *see* Camphene
Bicyclo[2.2.1]hept-2-ene, **237**, 332–333, *334*
Bicyclo[4.1.0]heptenyl ions, 241, 249, 250
Bicyclo[2.2.0]hexa-2,5-diene, 241, 242
Bicyclo[2.2.2]oct-2-en-5-ol, **245**, *335*
Bicyclo[4.2.0]octenyl ions, 241
Binomial expansion, use in isotope peak intensity calculations, 71–74
triangle, *see* Pascal's triangle
Biphenyl, **162**, *305*
Bond formation, driving force in fragmentation, 108, 112, 134, 180, 268
Bonding, chemical, orbitals and, 99–101
Brain tissue, extract of, 126
Bromine, isotopic peak intensities, 64–70, 289–290, 292
Bromochloromethane, **72**, 290, 291–292
4-Bromo-2,5-dimethoxyamphetamine, *see* Amphetamine, 4-bromo-2,5-dimethoxy-
Brousseau, R., 286
Buckminsterfullerene, 79–80, 290
Budde, W.L., 54
Buel, E., 206, 256
Burgers, P.C., 148
1,3-Butadiene, 106, 230–231
2-methyl-, *see* Isoprene
1-phenyl-, 231
Butane
2-methyl-, 155
2,2,3-trimethyl-, 300, 302, **303**
Butanoic acid
2-methyl-, 219, **220**, *221–223*
3-methyl-, 221, 222
methyl ester, 222
ethyl ester, 188, **189**
n-Butanol, **203**, 321–322
2-Butanol, *see sec*-Butyl Alcohol
2-Butanone
3,3-dimethyl-, 119, **120**, *298*, 330
3-methyl-, **209**, 212
1-Butene, 119, *298*
loss of, 218, 235
3-Buten–2-one, **162**, 305–306, *307*
sec-Butyl alcohol, **147**, 183, **203**, 302, 321–322
tert-Butyl alcohol, **203**, 321–322
tert-Butyl chloride, **158**, *159*
Butyl palmitate, *212*, **235**
double hydrogen rearrangement in, 234–235
McLafferty rearrangement in, 212
Butyl radicals, ionization energies of, 106
n-Butyramide, 188, **190**
Butyric acid, γ-hydroxy- (GHB), 243
γ-Butyrolactone (GBL), 243, **244**, *245*

Calibration, 34–37
standards, 34, 37; *see also* Perfluorotri-*n*-butylamine
spectra on internet, 52
Camphene, **142**
Cannabidiol, *232*, **233**
Capillary electrophoresis/mass spectrometry, 3, 4, 10
Capillary GC, use with MS, 3, 26
Capsaicin, **185**, *219*
Carbon, isotope peak intensity ratios for, 74–76, 78–79. *See also*, Isotope peak intensities, X + 1 peak; Isotope peak intensities, X + 2 peak

DropBooks

X + 1 peak, formula, 76, 78
X + 2 peak, formula, 78, 79
Carbon dioxide, **57**, 107, 288, *289*
elimination of, 244–245
Carbon monoxide, 107, 108
electronic structure, 126, 128
elimination of, 119, 123, 126, 128, 129, 130, 145, 223, 225, 243, 245, 249–250, 252–253, 339, 340
Carbonyl compounds, fragmentations of, *see* Alpha-cleavage; Gamma-hydrogen rearrangement, McLafferty-type. *See also* specific compound types.
Carrier gas, GC, for GC/MS, 3
Casale, J.F., 98
Cathine, **250**, 336, *337*
CE/MS, *see* Capillary electrophoresis/mass spectrometry
Chain branching in alkanes, factors in fragmentation of, 134–136, 300–303
Chamberlain, C.P., 98
Charge-migration fragmentation, 108–109, 164, 172, 240; *see also* Heterolytic cleavage
in retro-Diels-Alder fragmentation, 229, 231, 331
Charge-retention fragmentation, 108–109, 117, 119, 164, 240; *see also* Homolytic cleavage
in α-cleavage, 114, 164–165
in retro Diels-Alder fragmentation, 229, 232, 331–332, 334, 335
Charge site induced fragmentation, *see* Heterolytic cleavage
Charge stabilization
electronegativity and, 165, 176, 178–179, 182–183, 188, 190, 199
in product ions, *see* Stevenson's rule
Chemical history, mass spectral problem solving and, 151, 308, 309, 312, 320, 336
Chemical ionization mass spectrometry, 4, 8–9, 24, 43, 54, 152
atmospheric pressure, 4
ion-molecule reactions in, 8–9, 56–57
China White, *see* α-Methylfentanyl
Chlorine, isotope peak intensities, 64–69, 289–290, 294, 309
o-Chlorobenzalmalononitrile (''CS'' tear gas), *see* Acrylonitrile, 2-cyano-3-(*o*-chlorophenyl)
Chloroform, **97**, 294, *295*
Chromatogram, reconstructed total ion current (RTICC), 46, 47, 146, 169, 274
Chromatography, reconstructed ion, *see* Mass chromatography
CIMS, *see* Chemical ionization mass spectrometry
Citronella, oil of, 142
Clark, C.C., 276, 285
Cleaning ion source, *see* Electron ionization source, maintenance
Clifton, C.L., 54, 98, 148
Clonazepam, 62–63
Cloves, essence of, 185
Cocaethylene, 263, **264**, 266, 272, 343
arylhydroxy derivative, 266
arylhydroxymethoxy derivative, **273**, 343, *344*
Cocaine, 145, **262**, *268ff*
α-cleavage and, 268
arylhydroxy derivative, 263, **264**, 265–266, 345
arylhydroxymethoxy derivative, 263, **264**, 266, 344
cis-cinnamoyl derivative, *see* Ecgonine, methyl ester, cinnamoyl ester
derivatives, 46, 262*ff*, 343–346. *See also* Benzoylecgonine; Cocaethylene; Ecgonine, methyl ester; Ecgonine, propyl ester
deuterated derivative, 263, 266
elemental compositions of product ions, 263, 266–267
high resolution spectrum of, 263
ionization site, determination of, 107, 268
metabolites, 262*ff*
peak correlations, 263–268
Coeluting compounds, getting mass spectra for, 28–29, 49
Coffee, aroma of, 118
Cole, R.B., 12, 54
Collector, 5
Collimating magnet, 6
Collisional activation, in mass spectrometry/mass spectrometry, 25
Column bleed, 50, 82, 292
Combination, mathematical, formula, 73–75
Condensed spectrum, 42
Conjugation, fragmentation mechanisms and, *see* Fragmentation mechanisms, resonance stabilization and
Cotter, R.J., 15, 54
''CS'' tear gas, *see* Acrylonitrile, 2-cyano-3(*o*-chlorophenyl)

Curran, D.P., 54
Current, electron multiplier output, 33, 34, 35, 38–39, 41, 46
Cyanoacetylene, loss of, 311
Cycloheptatrienyl (tropylium) ion, 128–129, 241–242, 249–250. *See also* Benzyl ion, equilibrium with cycloheptatrienyl ion
Cycloheptenyl ions, 241, 249–250
Cyclohexane, **31**, 106
  1,2-dimethyl-, **139**
  N,N-dimethylamino-, *226*, **227**
  methoxy-, *226*, **227**
Cyclohexanol, 4-methyl-, **227**, *330*
Cyclohexanone, 119, **224**, *224–226*, 298, 340
  2-(2-chlorophenyl)-2-(*N*-methylamino)-, *see* Ketamine
  deuterium-labeled derivatives, 223–224
Cyclohexanone-type rearrangement, 207, 223–227, 279, 284, 330, 331, 334, 347, 349
  deuterium labeling and, 223–224
  modified, 340–341
Cyclohexene, 106
  derivatives, retro Diels-Alder fragmentation and, 228–232, 334, 335
  3-hydroxy-, **234**, *331–332*
  4-hydroxy-, **234**, *331*
  1-methyl-4-(2-propenyl)-, *see* Limonene
  1-phenyl-, 280, 347
  3-phenyl-, **230**, *231–232*
  4-phenyl-, **230**, *231*
Cyclohexylamine, 93
Cycloöctenyl ions, 241
Cyclopentadiene, 243
  hexachloro-, **72**, 289–290, 291
Cyclopentadienyl ion, 128–129, 242, 243
Cyclopentane, 1-ethyl-1-methyl, **139**
Cyclopropane, 1-pentafluorobenzamido-2-phenyl, **83**
Cyclopropenium ion, 128–129, 225, 242

DAC, *see* Digital-to-analog converter
Dalton, definition, 3
Damico, J.N., 54
Data System, 33–49
  library searches and, 41–44
  tuning and calibration and, 33–37
  use in analysis of GC/MS data, 1, 29, 46–49, 146
"Date rape drug," 243
dc generator, *see* Generator, dc
Decahydroquinoline
  N,7-dimethyl-, **228**, *331*
  N-methyl, **228**, *331*
n-Decane, 131, **132**, 156
de Hoffman, E., 24, 54
Deniz, A.A., 129, 148
Denton, M.B., 21, 55
Derivative formation; *see also* Deuterium labeling, use in determining fragmentation mechanisms
  use in molecular mass determination, 152
  use in structure determination, 262*ff*
"Designer drugs," 261
Desorption ionization, 4, 10, 12–13
Detection limit of mass spectrometry, *see* Threshold for ion detection
Detector
  electron multiplier, *see* Electron multiplier detector
  flame ionization, 46
  Mass Selective, *see* Mass Selective Detector
  photodiode array, 16
  photographic plate, 16
  photomultiplier, 16, 33
Deuterium labeling, use in determining fragmentation mechanisms, 209–212, 223–225, 258, 263, 276–278, 284–285, 349–352
Dewar benzene, *see* Bicyclo[2.2.0]hexa-2,5-diene
1,4-Diazabenzene, **160**, *161*
Diazepam, 284, **285**, 349, *350–352*
  deuterated derivative, 284, **285**, 349–350
  molecular ion peak cluster analysis, 86–89
2,2-Dicyanoethane, 1-(*o*-chlorophenyl)-, *see* Propionitrile, 2-cyano-3-(*o*-chlorophenyl)-*N,N*-Dicyclohexylamine, 236, **237**, *334*
Diels-Alder reaction, 228
N,N-Diethylamphetamine, *see* Amphetamine, *N,N*-diethyl-
Diethylether, **203**, 321, *322*
N,N-Diethyl-1-phenylcyclohexylamine, *see* Phencyclidine, *N,N*-diethyl analog
Digital-to-analog converter, 35
1,1-Dimethoxyethane, 181, **182**, *182–183*, 190
Dimethylisopropylamine, 327
Dimethylsulfone, **163**, 308, *309*

DropBooks

Diphenylmethane, 167, 184
Di-*n*-propylamine, **193**, *194*
Diradical, as fragmentation product, 102, 278, 279, 280
Distonic ion, 102, 225, 235–236, 244, 280
DNA fragments, analysis by MS, 3, 14
Double bond, definition, 101
  formation in fragmentation product, *see* Olefin elimination
Double-charged ions, *see* Ionization, multiple
Double-focusing mass spectrometer, 17, 26
Double hydrogen (McLafferty + 1) rearrangement, 207, 234–236
Doxepin, 204, *324*
Drug Enforcement Administration (DEA), 276
Duhaime, R., 286
Dwell time, in selected ion monitoring, 22
Dynode, 32

Ecgonine
  methyl ester, 263, **265**, 346
    aroyl derivatives, *see* Cocaine
    benzoyl ester, *see* Cocaine
    cinnamoyl ester, **45**
    phenylacetyl ester, *see* Phenylacetylmethylecgonine
    propylated aroyl esters, **275**, 344–346
    toluyl ester, *see* Toluylmethylecgonine
  ethyl ester, aroyl derivatives, *see* Cocaethylene
  propyl ester,
    benzoyl ester, 273, 274
    hydroxymethoxybenzoyl ester, **275**, 344–346
    propyloxybenzoyl ester, **275**, 344–346
    propyloxymethoxybenzoyl ester, **275**, 344–346
''Ecstasy'', *see* 3,4-Methylenedioxymethamphetamine
Efficiency, ionization, 6, 30
Ehleringer, J.D., 58, 98
EIMS, *see* Electron ionization mass spectrometry
Electron aperture, 5
Electron ionization mass spectrometry, 2, 4, 6. *See also* Ionization, electron.
Electron ionization source, 4, 5–8
  ion lifetimes and, 111, 114, 281
  maintenance, 8, 34
Electron multiplier detector, 15, 16, 32–33
  setting gain, 33, 34
Electron volt (eV), definition, 5
Electronegativity, charge stabilization and, *see* Charge stabilization, electronegativity and ionization and, 104–105, 176, 178
Electrospray ionization, 4, 9–12, 24, 44, 54, 152
Electrostatic analyzer in double-focusing mass spectrometer, 17
Elemental composition determination
  from exact mass, 62–63, 263
  from isotope peak intensity ratios, 52, 64*ff*
    examples, 91*ff*
    guidelines for, 89–91
    use in solving mass spectral unknowns, 151, 152–153
End caps in quadrupole ion trap, 22–23
Energy diagrams, *see* Fragmentation, energy diagrams
Energy, free, *see* Free energy of activation ($\Delta G^{\ddagger}$)
Enthalpy of activation ($\Delta H^{\ddagger}$), 111–112, 116
Entropy of activation ($\Delta S^{\ddagger}$), 111–112, 115
  effect of ring size in transition state on, 112, 207, 240
Ephedrine, **10**, **246**, *247–250*
Equation, mass spectrometric
  for magnetic sector analyzer, 16
  for quadrupole ion trap, 22
  for time-of-flight spectrometer, 14
  for transmission quadrupole, 20
Error
  arithmetic, in structure determination, 239
  experimental, in peak intensity measurement, 76, 82, 88, 214, 291
ESI, *see* Electrospray ionization
Esters
  aliphatic
    α-cleavage and, 187–189
    McLafferty rearrangement and, 188, 211–212, 221, 234–236
  aromatic
    α-cleavage and, 187–189, 196, 323, 324, 338
    ketene loss by, 196–197, 338–339
Ethane, 102–103
  1-bromo-1-chloro-2,2,2-trifluoro-, *see* Halothane

Ethers
aliphatic,
α-cleavage and, 165, 181–183, 297, 321–322. *See also* Alcohols, aliphatic, α-cleavage and
secondary elimination after α-cleavage and, 192–195, 321–322
relative importance of vs. amines, 192, 322
weak molecular ion peaks and, 181
aromatic
C-O bond cleavage and, 184–185, 314–315, 340
formaldehyde elimination and, *see* Formaldehyde, loss by phenylmethylethers
olefin elimination and, 197–198, 345
Ethoxybenzene, olefin elimination and, 197, *198*
Ethylene
loss of, *see* Alpha-cleavage, secondary elimination after; Ethoxybenzene, olefin elimination in; Gamma-hydrogen rearrangement; Olefin elimination; Retro Diels-Alder fragmentation
1,2-dichloro-, 64, **65**, 66
Ethylisopropylamine, 327
Ethylisopropylether, **192**, *194*
N-Ethyl-3,4-methylenedioxyamphetamine (“MDE”), *see* 3,4-Methylenedioxy-*N*- ethylamphetamine,
N-Ethyl-1-phenylcyclohexylamine, *see* Phencyclidine, *N*-ethyl analog
Eugenol, 185, **186**, *314*
“Eve,” *see* 3,4-Methylenedioxy-*N*-ethyl-amphetamine
Even-electron ions, 103
decomposition of, 108, 110
Excited state, 6
Extractor plate, 5, 8

Fales, H.M., 10, 54
Fast-atom bombardment (FAB), 4, 13
Fast GC, 29–30
Fenn, J.B., 10
FID, *see* Detector, flame ionization
Filament, 5, 8, 13, 24, 32, 35, 46
Fire debris, analysis by mass chromatography, 145–146
Fishhook (single-headed arrow), 102, 109, 119, 120
Fishman, V.N., 37, 54
Fluorine, as A + 1 element, 77
Focusing plate, ion, *see* Ion focusing plate
Ford, V.L., 98
Formaldehyde, 108
elimination of, 244–245, 297
loss by phenylmethylethers, 131, 184, 314
Formamide, 102
Forward library search, 42
Fragmentation, *see also* specific fragmentation reactions, such as Alpha-cleavage, etc.; Neutral losses; Olefin elimination; Rearrangement
charge-migration, *see* Charge-migration fragmentation; Heterolytic cleavage
charge-retention, *see* Charge-retention fragmentation; Homolytic cleavage
charge stabilization and, *see* Stevenson’s rule
conjugation, effects of, *see* Fragmentation mechanisms, resonance stabilization and
energy diagrams, 113–116
entropy factors and, 112, 115, 207, 240
free energy of activation ($\Delta G^{\ddagger}$) and, 111–112, 113–116, 134, 135, 142–143, 180, 281, 349
intra- *vs.* intermolecular, 2, 8–9, 56, 240
ion lifetimes and, 111, 112–113, 114, 281
kinetic factors in, 110–112
olefin formation and, *see* Olefin elimination
product ion stability and, 105–107, 132, 136, 240. *See also* Alpha-cleavage, product ion stability and; Stevenson’s rule
product olefin structure and, 216, 302, 316, 319
product radical stability and, 133, 136, 240. *See also* Alpha-cleavage, product radical stability and
rates, 111–112
thermodynamic factors in, 110–111
types, 107–109
Fragmentation mechanisms
from peak correlations, 209–211, 223–225, 263–271, 276–281, 349–352
guidelines for rationalizing, 238–241
initial ionization site and, 108–109, 239–240
resonance stabilization and, 105–106, 116, 119, 166, 184–185, 190, 213,

DropBooks

216–217, 225, 231, 235, 240, 241, 248, 254, 270, 283, 319, 329, 332. *See also* Alpha-cleavage, initiated by remote ionization site; Gamma-hydrogen rearrangement, initiated by remote ionization site
ring size for transition states and, 112, 207, 240
Free energy of activation ($\Delta G^{\ddagger}$), 111–112, 113–116. *See also* Fragmentation, free energy of activation and
Furan, 2-acetoxymethyl, 188, **189**, 206, *329*
2-Furancarboxylic acid, propyl ester, 203, *323*
2-Furanmethanethiol, **118**, *119*

$\Delta G^{\ddagger}$, *see* Free energy of activation
Gagné, H.M., 206
Gain, detector, 33, 34
Gamma-hydrogen (γ-hydrogen) rearrangement, 153, 207*ff*
in alkylbenzenes, 213–216, 218, 321
competition with α-cleavage, 216
minimal alkyl size for, 216, 219, 259
in 1-phenyl-2-aminopropanes, 259–261
initiated by remote ionization site, 217–219
McLafferty-type, 188, 190, 191, 208–213, 223, 234
aliphatic carboxylic acid derivatives and, 211–212, 213, 220–222, 234, 330
deuterium labeling and, 209–211
ketones and, 209–212, 329–330
structural requirements for, 208
Gas chromatography, 50, 152
compound separation by, 1, 3, 17, 29
retention times, compound identification and, 43, 152, 336
Gas chromatography/mass spectrometry, 35, 126
block diagram, 2
carrier gases in, 3, 32
data, computer analysis of, 46–50, 145–146
specificity of, 2, 336
spectral skewing and, 26–28
Gasoline, evaporated, mass chromatograms, 146
GBL, *see* γ-Butyrolactone
GC/MS, *see* Gas chromatography/mass spectrometry
Generator
ac, use with quadrupole ion trap, 23, 24
dc
in quadrupole ion trap, 23, 24
in transmission quadrupole, 17–18, 21
RF
in quadrupole ion trap, 22, 23
in transmission quadrupole, 17–18, 21, 25
GHB, *see* Butyric acid, γ-hydroxy-
Ginger, oil of, 142
Gooding, K.M., 206
Goodwin, M., 205, 206
Graves, G.R., 98

$\Delta H^{\ddagger}$, *see* Enthalpy of activation
Halothane, **127**, 299–300, *301*
Hansson, R.C., 149
Harmine, **256**, *339–340*
Harrison, A.G., 54
Helium
as carrier gas in GC/MS, 3, 32
as damping gas in quadrupole ion trap, 24
Henchman, M., 21, 54
n-Heptane, **137**, 300, 302
2-methyl-, **135**, 301
Heptanoic acid, ethyl ester, **211**, *212*
Hertel, R.H., 55
Heterolytic cleavage, 108–109, 117, 119, 164, 172, 231. *See also* Charge-migration fragmentation
Hexamethyldisilane, **141**
Hexane
2-methyl-, **31**, 300, **303**
3-methyl-, 300, **303**
3,3,4-trimethyl-, **147**, 302
2-Hexanone, McLafferty rearrangement in, 330
3-Hexanone, **156**, *157*
3-Hexene-(Z), **147**, 302
n-Hexylamine, **193**, 194
High-mass peaks, importance in spectral interpretation, 42, 121, 134, 153, 240
High-performance liquid chromatography/mass spectrometry, 2, 3, 4, 10, 11, 21, 54
High resolution mass spectrometry, 17, 20, 24, 258, 263. *See also m/z* Analysis, accurate
High vacuum, use in mass spectrometry, 2, 4, 8

Highest Occupied Molecular Orbital (HOMO), 103, 105
Holmes, J.L., 134, 148, 233, 237
Holmes, R.T., 98
Holzer, G., 148
Homolytic cleavage, 108–109, 114, 116, 117, 119, 164, 172. *See also* Charge-retention fragmentation
HPLC/MS, *see* High-performance liquid chromatography/mass spectrometry
Hückel's Rule, 129, 158
Hydride shifts, 195–196
Hydrocarbons
  aliphatic, 132–136, 138, 145, 146, 300, 304
    branched, 134–136, 300–303
  aromatic, 128, 131–132, 133, 142–144, 145–146, 166–168, 213–216, 295, 303, 310–311
  olefinic, 138–140, 302
  saturated cyclic, 138–140
Hydrogen
  radical, loss in α-cleavage, *see* Alpha-cleavage, hydrogen radical loss in; Benzylic cleavage, hydrogen radical loss via
  radical, loss from *o*-position of aromatic ring, 278–279, 283, 349–350
  rearrangement, *see* Rearrangement, hydrogen. *See also* Olefin elimination
  use as carrier gas in GC/MS, 3, 32
Hydrogen chloride, 64, **65**
Hydrogen cyanide, 106, 107, 108
  electronic structure, 126
  elimination of, 122–123, 126, 129, 158, 160, 161, 242, 307–308, 311–312, 326
Hydroxybenzoylecgonine, *see* Benzoylecgonine, arylhydroxy derivative
Hydroxybenzyl ion, 249–250
Hydroxycocaethylene, *see* Cocaethylene, arylhydroxy derivative
Hydroxycocaine, *see* Cocaine, arylhydroxy derivative
Hydroxymethoxycocaethylene, *see* Cocaethylene, arylhydroxymethoxy derivative
Hydroxymethoxycocaine, *see* Cocaine, arylhydroxymethoxy derivative
N-Hydroxy-3,4-Methylenedioxyamphetamine, *see* 3,4-Methylenedioxyamphetamine, *N*- hydroxy-

Ibogaine, 209, *210*
Ibuprofen, 336
Infrared spectrometry, 1, 33, 49
Intensities
  isotope peak, *see* Isotope peak intensities
  mass spectral peak, 41
    concentration dependence in GC/MS, *see* Spectral skewing
    error in measuring, *see* Error, experimental, in peak intensity measurement
Intensity, weighted, for library searches, 42
Intermediate, reaction, definition, 111–112
Internet resources for mass spectrometry, 52–53
Intra- vs. intermolecular fragmentation, 2, 8–9, 56, 240
Ion
  distonic, *see* Distonic ion
  even-electron, *see* Even-electron ions
  intermediate not observed in spectrum, 114, 248, 279, 281, 351
  lifetimes, detectability and, 111–114, 281
  metastable, 112–113
  molecular, *see* Molecular ion
  multiple-charged, 6, 7, 39, 103, 129–130, 289
  nomenclature, 70–71
  odd-electron, *see* Odd-electron species, ions
  precursor, 25, 113, 134, 155, 192, 239
  product, 26, 113, 134, 192, 239
  radical, *see* Odd-electron species, ions
  stability, fragmentation and, *see* Fragmentation, product ion stability and
Ion detection, 16, 30, 32–33. *See also* Detector
Ion focusing plate, 5, 8
Ion-molecule reactions, in chemical ionization mass spectrometry, 8–9, 56
Ion series, low mass, *see* Low mass ion series
Ion source, *see* Electron ionization source
Ion trap analyzer, *see* Quadrupole ion trap
Ionization
  chemical, *see* Chemical ionization mass spectrometry

DropBooks

electron, 2, 4, 6–7, 101–105
efficiency of, 6, 30
molecular orbitals and, 103–105
multiple, 6, 7, 39, 103, 129–130, 289
site of initial, 103–107, 165, 239–240
pulse, 13, 24, 29
resonance electron capture, 7
Ionization energy (ionization potential), 6, 105
table, 106
use in determining ionization site, 105–107, 117–119
use in determining site of charge in product ions, *see* Stevenson's rule
IR, *see* Infrared spectrometry
Isoamyl acetate, 235, **236**
Isobutane, as reagent gas in chemical ionization MS, 9, 10
Isobutyl alcohol, **203**, *321–322*
Isobutylamine, 322
Isoprene, loss of, 229, 232
Isopropanol, *see* 2-Propanol
Isopropyl chloride, *see* Propane, 2-chloro-
Isotope, definition, 58
Isotope abundances, 52, 53, 56–59
Isotope peak intensities, 64*ff*, 152–153
A, A + 1, and A + 2 elements and, 77–78
bromine and chlorine, 64–74
carbon-containing compounds, 74–76, 78–79
elemental composition from, *see* Elemental composition, from isotope peak intensity ratios
for ions having two or more elements, 68–69, 77, 83–89
internet calculators for, 52–53
molecular ion peak cluster, analysis, 76, 79, 80–82, 83–85, 86–89
normalization of, 90, 91, 93, 151, 293
overlapping peak clusters and, 80–82, 85–89, 95–96, 296
probabilities and, 66–74
silicon, 82–83
sulfur, 83–85
X + 1 peak, 76, 77–78, 90, 151
determining number of carbons from, 76
for carbon-containing compounds, 74–76
X + 2 peak, 78–79, 91, 151. *See also* Isotope peak intensities, bromine and chlorine

Kataoka, H., 12, 54
Ketamine, **256**, *340–341*
Ketene, loss of, 188, 196–197, 206, 329, 338–339
Keto-enol tautomerization, 131, 241, 243, 249–250
Ketones
α-cleavage and, 157, 186, 243, 298, 321, 329–330
McLafferty rearrangement and, 209–212, 330
Kinetic control of reactions, 111–112
Kinter, M.T., 286
Komer, K.B., 286
Kwok, K.-S., 45, 54

Laser desorption ionization (LDI), 4
matrix-assisted (MALDI), 4, 12–13, 14
Lawson, G., 54
LC/MS, *see* High performance liquid chromatography/mass spectrometry
Leary, J.J., 21, 54
LeChatlier's principle, 243
LECO, 14, 30, 31
Lemon, odor of, *see* Limonene
Lias, S.G., 54, 98, 148
Library, mass spectral
internet, 53
evaluation of, 44, 50, 54, 55
NIST/EPA/NIH, 46
Library search, 41–46
mass spectral problem solving and, 151, 170, 341
match index in, 42–43
PBM, *see* Probability Based Matching
Lidocaine, **176**
Limonene, **142**, *229*, **230**, 232
Linclau, B., 54
Lodge, B.A., 278, 286
Loh, M.J., 98
Loh, S.Y., 55
Lorazepam, **70**
Lord, H.L., 54
Losses, neutral, *see* Neutral losses
Low mass ion series, 136–145
alkanes, 136–138, 145, 302, 304
alkenes, 138–139, 145, 302
alkylsilanes, 141
alpha-cleavage, 138, 140–141, 175, 302, 326, 329

Low mass ion series (*Continued*)
aromatic, 138, 142–145, 160, 171, 213–214, 302, 305, 307, 309, 310, 312, 325, 328, 333, 338
benzoyl, 128, 138, 144–145, 148, 263, 267, 271, 303–304, 335
benzyl, 128, 138, 143–144, 171, 213–214, 241–242, 302–303, 310, 320
carboxylic acid derivatives, 141
cycloalkanes, 138, 141–142, 145
ketones vs. alkanes, 156–157, 304, 329
mass spectral problem solving and, 151, 153
mass chromatography and, 145–146
monoterpenes, 141–142
phencyclidine analogs, 283, 347
Lysergic acid diethylamide (LSD), 233, *332*

M + 1 peak intensities, *see* Isotope peak intensities, X + 1 peak
M + 2 peak intensities, *see* Isotope peak intensities, X + 2 peak
m/z Analysis, 13–26
accurate, 26
ion elemental compostions from, 26, 62–63, 263, 264–267
quadrupole ion trap and, 26
mass defects and, 62–63
m/z Discrimination (ΔM), 20, 26, 34, 37–38, 41, 61, 64, 68, 77, 78, 81, 86
sensitivity and, 21, 26, 33, 34, 63–64
tuning and, 33–34
MacMurray, P., 286
Magnet, collimating, 5–6
Magnetic sector analyzer, 15–17
accurate *m/z* analysis and, 17, 26
MALDI, *see* Laser desorption ionization, matrix-assisted
March, R.E., 22, 55
Marijuana, *see* Δ^9-Tetrahydrocannabinol; Cannabidiol
Mass
exact, 60–64
atomic, table, 52
internet calculators for, 53
elemental composition and, 62–63, 263
molecular, 59, 151
determination by chemical ionization, 9, 152
determination by electrospray ionization, 11, 152
relation to number of nitrogen atoms and, *see* Nitrogen rule
monoisotopic, 59, 60, 87
nominal, 61–62
units, 3. *See also* u (Unified atomic mass unit)
Mass chromatography, 29–31, 49, 50
comparison with selected ion monitoring, 49, 146
forensic arson analysis and, 145–146
Mass defect (Δ), 60–62, 68, 84
Mass Selective Detector (MSD), 21
Mass spectrometer, *see also m/z* Analysis, Magnetic sector analyzer, Quadrupole ion trap, Time-of-flight *m/z* analyzer, Transmission quadrupole
as GC detector, 29, 30, 46–47, 145–146
calibration, *see* Calibration
double-focusing, 17, 26
high vacuum in, 2
sample introduction modes for, 3–4
tuning, *see* Tuning
Mass spectrometry
chemical ionization, *see* Chemical ionization mass spectrometry
high resolution, *see* High resolution mass spectrometry. *See also m/z* Analysis, accurate
negative ion, 6, 7
tandem, *see* Mass spectrometry/mass spectrometry
Mass spectrometry/mass spectrometry, 9, 11, 24–26, 54, 258
quadrupole ion trap and, 24, 26
Mass spectrum, 37–41
base peak in, *see* Base peak
criteria for acceptable, 50–51, 83, 126, 292, 299
molecular ion peak in, *see* Molecular ion, peak
predicting, from spectra of related compounds, 258, 271–273, 284, 347
representations, 39–41
visual examination, importance of, 42–43, 50–51, 151
Match index, 42, 44, 45, 151
McLafferty, F.W., 42, 45, 53, 55, 68, 98, 108, 109, 120, 121, 141, 148, 208, 235, 237
McLafferty rearrangement, *see* Gamma-hydrogen rearrangement, McLafferty-type
"McLafferty + 1" rearrangement, *see* Double hydrogen rearrangement

DropBooks

MDA, *see* 3,4-Methylenedioxyamphetamine
MDE, *see* 3,4-Methylenedioxy-*N*-ethylamphetamine
MDMA, *see* 3,4-Methylenedioxymethamphetamine
Mechanism, fragmentation, *see* Fragmentation mechanisms
Mescaline, *see* β-Phenethylamine, 3,4,5-trimethoxy-
Metastable ions, 112–113
Methamphetamine, 54, 172, **173**, *174*, 175–176, **177**, 195, 202, **246**, *247*, 248, 249, 250, 312–314, 320, 321
  α-cleavage in, 173–174, 247, 312–313
  condensation product, *see* *N*-(1-Phenyl-2-methylaminopropyl)-1-phenyl-2-(*N*-methylamino)propane
Methane, 56, **57**, 58
  as reagent gas in chemical ionization mass spectrometry, 8–9
Methcathinone, **246**, *247*, 248–249, 250, *335–336*
Methyl
  carbenium ion, 102–103
  radical, 102–103, 145, 155
    electronic structure of, 102–103
    loss from polymethylated benzenes, 166, 168, 311
    loss from within aromatic rings, 143, 145, 158, 307
Methyl acetate, 188, **189**
Methyl benzyl ketone, *see* 2-Propanone, 1-phenyl-
Methyl bromide, 64, **65**, 71
Methyl *tert*-butylamine, 326–327
Methyl 2,5-dimethylbenzoate, *see* Benzoic acid, 2,5-dimethyl-, methyl ester
Methyl 3,5-dimethylbenzoate, *see* Benzoic acid, 3,5-dimethyl-, methyl ester
Methyl ethylether, 201
Methyl isopropylether, **203**, 321–322
Methyl *n*-propylether, 183, **203**, 321–322
Methyl vinyl ketone, *see* 3-Buten-2-one
Methyldiethylamine, **205**, 326–327
Methylecgonine, *see* Ecgonine, methyl ester
3,4-Methylenedioxyamphetamine (“MDA”), 47, **48**, 49, 54, 258, *259*, **260**, *261*
  N,N-dimethyl-, **262**, *341–343*
  N-ethyl-, *see* 3,4-Methylenedioxy-*N*-ethylamphetamine
  N-hydroxy-, 47, **48**, 49–50
  N-methyl-, *see* 3,4-Methylenedioxymethamphetamine
3,4-Methylenedioxy-*N*-ethylamphetamine (MDE), *259*, **260**, *261*, 341
3,4-Methylenedioxymethamphetamine (MDMA), **44**, 54, *259*, **260**, *261*
  N-formyl derivative, *179*, **180**
1-(3,4-Methylenedioxyphenyl)-2-aminopentane, 342
1-(3,4-Methylenedioxyphenyl)-2-aminopropane, *see* 3,4-Methylenedioxyamphetamine
1-(3,4-Methylenedioxyphenyl)-*N*,2-dimethyl-2-aminopropane, 342
1-(3,4-Methylenedioxyphenyl)-*N*-isopropyl-β-phenethylamine, 342
1-(3,4-Methylenedioxyphenyl)-2-methyl-2-aminobutane, 342
1-(3,4-Methylenedioxyphenyl)-3-methyl-2-aminobutane, 342
1-(3,4-Methylenedioxyphenyl)-*N*-methyl-*N*-ethyl-β-phenethylamine, 342
1-(3,4-Methylenedioxyphenyl)-2-propanone, oxime, 47, **48**, 49–50
1-(3,4-Methylenedioxyphenyl)-1-propene, 47, **48**
1-(3,4-Methylenedioxyphenyl)-*N*-propyl-β-phenethylamine, 342
α-Methylfentanyl, 204, *324*
2-Methyl-1-propanol, *see* Isobutyl alcohol
Mikaya, A.I., 54, 98, 148
Miller, P.E., 21, 55
Milne, G.W.A., 54
Molecular ion, 6, 7, 102, 103–104
  composition of, *see* Elemental Composition; Isotope peak intensities; Nitrogen rule
  losses not allowed from, 122, 152, 159, 181–182, 288
  peak
    absence in spectrum, 9, 11, 111, 113, 141, 151, 159, 181–182, 248
    determining presence in spectrum, 122, 151–152
    intensity of, in spectra of aromatic compounds, *see* Aromatic compounds, intense molecular ion peaks and
  rearrangement of, prior to bond cleavage, 134, 140, 141
  rings plus double bonds in, formula, 91, 151, 153
  stability of, 113–114, 142

Molecular orbitals, *see* Orbitals, molecular
Molecular weight, 59, 61
Molecules, protonated, in chemical ionization mass spectrometry, 9, 25, 152
Mollah, Y.A., 148
Morpholine, *N*-(1-phenylcyclohexyl)-, *see* Phencyclidine, morpholine analog
MS/MS, *see* Mass spectrometry/mass spectrometry
MS Search (NIST software), 46, 53
Multiple ionization, *see* Ionization, multiple
Myrcene, **142**

n-orbitals, *see* Orbitals, nonbonding
Naphthalene, 106, 128, **133**, 143, 146
  1-methyl-, **133**
National Institute for Standards and Technology, 29, 46, 53
Needle, nebulizing (in electrospray ionization), 10, 11
Negative ion mass spectrometry, *see* Mass spectrometry, negative ion
Neopentane, *see* Propane, 2,2-dimethyl-
Neutral losses, 53, 121–123, 126, 128–131, 151, 152, 153, 239, 240, 241–243. *See also* specific fragmentations such as Acetylene, elimination of; Hydrogen Cyanide, elimination of; Ketene, loss of; Olefin elimination; and Rearrangement
  by alkanes, 132–134
  by aromatic compounds, 126, 128–131, 143, 145, 241–243
  forbidden, 122, 152, 159, 181, 288
  molecular ion peak and, *see* Molecular ion, peak, determining presence in spectrum
  use in mass spectral problem solving, 151–153
Neutral species
  diradical, 102, 278, 279, 280
  even-electron, 101–102
  radical, 102–103
Nicotinamide, **205**, 325, *326*
Nigam, I.C., 233, 237
NIST, *see* National Institute for Standards and Technology
Nitrobenzene, **97**, 293, *294*
Nitrogen,
  as A + 1 element, 77
  as drying gas in electrospray ionization, 10
  charge stabilization by, 107, 165, 170, 175, 176, 180, 190, 191, 248, 268, 278, 281, 340
  elemental composition and, 77, 78, 90. S*ee also* Nitrogen rule
  isotope peak intensities, 86–89, 93, 292, 293, 307–308
  isotopic abundances, 58
  molecular (N_2)
    electronic structure, 126
    elimination of, 106, 107, 108, 126
Nitrogen oxides, loss of O from, 122, 123
Nitrogen rule, 90, 109–110, 151, 152, 210
  examples, 93, 157, 160, 209, 292, 293, 307
  ionic mass and, 109–110
NMR, *see* Nuclear magnetic resonance spectrometry
Nominal mass, 61–62
n-Nonane, **161**, 304
n-Nonanoic acid, **211**, *212*
Nonbonding orbitals, *see* Orbitals, nonbonding
Norbornene, *see* Bicyclo[2.2.1]hept-2-ene
Norcocaine, 263, **265**, 266
  N-trideuteriomethyl-, 263, 266
Normalization of peak intensities, *see* Isotope peak intensities, normalization of
Norman, K.W., 149
Nortriptyline, **178**, *179*
  N-pentafluroropropionyl derivative, **178**, *179*
Nowicki, J., 145, 149
Nuclear magnetic resonance spectrometry, 1
Number of carbon atoms, relation to X + 1 peak intensity, *see* Isotope peak intensities, X + 1 peak, determining the number of carbon atoms from

° (Symbol for electrical neutrality), 101
8-Octadecenamide, **223**, *330*
n-Octane, 134, **135**, 156
Octanoic acid, methyl ester, **211**, *212*
4-Octene, **139**
Odd-electron species
  ions, 101, 102
    decomposition of, 107–108
    peaks in spectrum representing, 109–110, 153, 209, 330, 333
  radicals, 102–103
    relative stability of, 132, 136, 240

DropBooks

Olefin elimination; *see also* Neutral losses; Rearrangement
π-bond formation as driving force in, 108, 112, 134, 197, 208, 242, 245, 269
from primary aliphatic ions, 134, 199, 225–226
in γ-hydrogen rearrangements, *see* Gamma-hydrogen rearrangement
in McLafferty rearrangements, *see* Gamma-hydrogen rearrangement, McLafferty type
in phenylalkylethers, *see* Ethers, aromatic, olefin elimination and
in retro Diels-Alder fragmentations, *see* Retro Diels-Alder fragmentation
in secondary elimination after α-cleavage, *see* Alpha-cleavage, secondary elimination after
ketene loss, *see* Ketene, loss of
product olefin structure and, 216, 302
Orbitals
π, 101, 103–104, 105
σ, 101, 103–104, 105
antibonding (π* and σ*), 103–104
atomic, 99–100
molecular, 101, 103–104, 105
highest occupied (HOMO), 103, 105
site of initial ionization and, 104–105
nonbonding (*n*), 101, 103–104, 158, 165, 239
subhybrid, 99–100
Ortho effect, 217, 251–254, 308, 310, 338–339
Oxygen
atomic, loss of, 122, 123, 309
charge stabilization by, 117, 119, 165, 180, 183, 190, 199, 243, 244, 253
isotope peak intensities, 77–78, 91
examples, 79, 87–89, 92, 220, 293, 296, 297, 306, 308, 337
isotopic abundances, 58

π-Bond formation, fragmentation and, *see* Olefin elimination, π-bond formation as driving force in
"P–2-P", *see* 2-Propanone, 1-phenyl
Palmitic acid, butyl ester, *see* Butyl palmitate
Papaver somniferum, 184
Papaverine, **183**, *184–185*
Pascal's triangle, binomial expansion and, 74, 75
Pawliszyn, J., 54
PBM Search, *see* Probability Based Matching
PCP, *see* Phencyclidine
Peak, mass spectral, 37–39, 41
Peak correlations,
applications, 271–272, 284, 347–348
cocaine, 263–268
diazepam, 284–285, 349–352
fragmentation mechanisms from, *see* Fragmentation mechanisms, from peak correlations
phencyclidine, 276–281
n-Pentanal, **191**
Pentane, 155
2,2-dimethyl-, 300–302, **303**
2,3-dimethyl-, **31**, 300–302, **303**
2,4-dimethyl-, **137**, 300–302
3,3-dimethyl-, **137**, 300–302
3-ethyl-, 300–302, **303**
2,2,3-trimethyl-, **135**, *136*
Pentanoic acid, 221, 222
n-Pentanol, 198, **199**, *200*
3-Pentanol, **140**, 195
2-Pentanone, **209**, *210–212*
deuterium-labeled derivatives of, 210–212
McLafferty rearrangement and, 209–212
3-methyl-, **222**, 329–330
4-methyl-, 330
3-Pentanone, **140**
n-Pentylamine, 198
3-Pentylamine, **140**, 141, 195
Peppers, *Capsicum* (hot), 185; *see also* Capsaicin
Perfluorokerosene, as calibration standard, 37
Perfluorotri-*n*-butylamine, 3, 33, 34, 37, **51**, 52, 125, 287–288
Peters, K.S., 148
Petroleum distillates, analysis of, 145–146
Peyote, *see* β-Phenethylamine, 3,4,5-trimethoxy-,
PFTBA, *see* Perfluorotri-*n*-butylamine
Pharmaceuticals, analysis by electrospray ionization MS, 11
Phenanthrene, 128, **133**
Phencyclidine ("PCP"), 143, *274ff*, **276**, 347, 349
analogs, 282–284, 347–349
arylmethyl analogs, 277, 278, *279*
benzyl analog, 284, *349*
cyclohexanone-type rearrangement and, 279–280

Phencyclidine (“PCP”) (*Continued*)
deuterium-labeled derivatives, 276–281
N,N-diethyl analog, 284, *347*, **348**
N-ethyl analog, **282**
hydrogen radical loss by, 278–279, 280, 281, 283
low mass ion series, 283, 347
morpholine analog, **282**, 283, 347
peak correlations, 276*ff*, (table) 277
retro Diels-Alder fragmentation and, 278, 280
thiophene analog, **282**, *283*, 347
thiophene morpholine analog, **284**, 347–348, *349*
o-toluyl analog, 277, 278, *279*
β-Phenethylamine, **200**, 201, *202*
N,N-dimethyl-, **177**, 312–314
N-ethyl-, **177**, 312–314
N-methyl-, **147**, 302
3,4,5-trimethoxy-, *175*
Phenol, 129, **130**, *131*, *243*
2,6-dichloro-, **163**, 309, *310*
o-, *m*-, and *p*-methoxy-, 186, **187**, *314–315*
Phentermine, 172, **173**, *174*, 175, **177**, 312–314
N,N-dimethyl-, *175*
Phenyl
ion, 105–106, 128, 129
radical, 105
Phenylacetylmethylecgonine, 271, **272**, 273, 343
1-Phenyl-2-aminobutane, **177**, 312–314
1-Phenyl-2-aminoethane, *see* β-Phenethylamine
1-Phenyl-2-aminopropane, *see* Amphetamine
1-hydroxy-, *see* Cathine
2-methyl-, *see* Phentermine
N-(1-Phenylcyclohexyl)morpholine, *see* Phencyclidine, morpholine analog
1-Phenylcyclohexylpiperidine, *see* Phencyclidine
1-Phenyl-3,3-dimethylbutane, 215, 216
1-Phenyl-1,2-dimethylpropane, 215, 216
1-Phenyl-2,2-dimethylpropane, *see* Benzene, neopentyl-
1-Phenyl-2-(*N*-methylamino)propane, *see* Methamphetamine
1-hydroxy-, *see* Ephedrine
1-Phenyl-2-(*N*-methylamino)-1-propanone, *see* Methcathinone
N-(1-Phenyl-2-methylaminopropyl)-1-phenyl-2-(*N*-methylamino)propane, 195, 315–320
1-Phenyl-2-methylbutane, 215
1-Phenyl-3-methylbutane, 215, 216
Phenylmethylethers, *see* Benzene, methoxy-; Formaldehyde, loss by phenylmethylethers
1-Phenyl-2-methylpropane, *see* Benzene, isobutyl
1-Phenyl-2-propanone, *see* 2-Propanone, 1-phenyl-
1-Phenyl-1,2,2-trimethylpropane, 215, 216
Pheromone
canine, 205, 206
insect, 163, 309
Photodiode array detector, 16
Photographic plate detector, 16
Photomultiplier detector, 16, 33
Phthalic acid, esters, *254*
Piperidine
N-(1-benzylcyclohexyl)-, *see* Phencyclidine, benzyl analog
N-pentyl-, 203, *323*
1-phenylcyclohexyl-, *see* Phencyclidine
Plate
extractor, *see* Extractor Plate
ion focusing, *see* Ion Focusing Plate
Poles (in transmission quadrupole), 17, 18, 20
Poppy, opium, 184
Poquette, M.A., 286
Potential, *see* Ionization energy; Voltages
Precursor ion, *see* Ion, precursor
Probabilities, 66
binomial expansion and, 73–74
isotope peak intensities and, 66–69, 71
Probability Based Matching, 42, 43, 55
Probe, heated, 3–4
Problems, solving mass spectral
chemical history and, 151, 308, 309, 312, 320, 336
examples, 153*ff*
guidelines for, 150–153
isotopic peak intensities and, 152–153. *See also* Intensities, isotope peak
library searches and, 151
low mass ion series and, 137, 153. *See also* Low mass ion series
neutral losses and, 121–123, 153. *See also* Neutral losses
Nitrogen rule and, 152. *See also* Nitrogen rule

DropBooks

Product ion mass spectrometry/mass spectrometry, 25–26
Propane, 2,2-dimethyl-, **154**, *155*
  2-chloro-, 119, *298*
n-Propanol, 226
2-Propanol, *117*, **200**, *201*
2-Propanone, see Acetone
  1-cyclohexenyl-, 204, *323*
  1-phenyl-, **202**, 320, *321*
Propene, loss of, 194, 198, 345
Propionic acid, 2-(*p*-isobutylphenyl)-, *see* Ibuprofen
Propionitrile, 2-cyano-3-(*o*-chlorophenyl), **170**, *312*
Propyl radical, loss, cyclohexanone-type rearrangement and, 223, 225, 279, 334
n-Propylamine, 119, *298*
Propylecgonine, *see* Ecgonine, propyl ester
Proteins, analysis by MS, 3, 11, 14
Protonated molecules, 9, 25
Pseudococaine, 286
Pseudomolecular ion, 9
Pulse ionization, 13, 24, 29
2H-Pyran, tetrahydro-, **98**, 296, *297*
Pyrazine, *see* 1,4-Diazabenzene
Pyridine, *129*, **130**, *242*
  3-bromo-, **96**, 292, *293*
  4-methoxy-, **162**, 307, *308*
  4-methyl-, *N*-oxide, **123**
  2-propyl-, *216*, **217**
  4-propyl-, *216*, **217**
3-Pyridinecarboxamide, *see* Nicotinamide
Pyrrole, **157**, *158*

q (variable in quadrupole MS), *see a* and *q*
Quadrupole ion trap, 13, 22–24, 29, 55
  high resolution mass spectra from, 24, 26
  MS/MS using, 24, 26
  scan direction in, 24, 287
Quadrupole analyzer, *see* Transmission quadrupole
Quality of spectra, criteria for, 50–51, 83, 126

Radical
  ions, *see* Odd-electron species, ions
  neutral, 6, 7, 102–103. *See also* Odd-electron species, radicals
  stability, fragmentation and, *see* Fragmentation, product radical stability and
Radical site induced fragmentation, *see* Homolytic cleavage
Radio frequency generator, *see* Generator, RF
Reagent gas, in chemical ionization mass spectrometry, 8–10, 57
Rearrangement
  π-bond formation and, *see* Olefin elimination, π-bond formation as driving force in
  cyclohexanone-type, *see* Cyclohexanone-type rearrangement
  double-hydrogen, *see* Double-hydrogen rearrangement
  hydride, *see* Hydride shifts
  hydrogen (general), 240; *see also* Olefin elimination
    3-center, examples, 145, 158, 247, 269
    4-center, examples, 131, 145, 181, 218, 219, 241, 243, 249, 252, 278, 297, 328, 329, 332, 334. *See also* Alpha-cleavage, secondary elimination after; Ethers, aromatic, olefin elimination and; Ethylene, loss of; Formaldehyde, loss by phenylmethylethers; Hydride shifts; Ketene, loss of; Olefin elimination, from primary aliphatic ions
    5-center, examples, 235, 236, 341
    6-center, examples, 253, 338, 352. *See also* Alcohols, aliphatic, water elimination from; Cyclohexanone-type rearrangement; Gamma-hydrogen rearrangement
    7-center, example, 271
    ease of, 240
  γ-hydrogen, *see* Gamma-hydrogen rearrangement
  ketene loss by aromatic compounds, *see* Ketene, loss of
  McLafferty, *see* Gamma-hydrogen rearrangement, McLafferty-type
  McLafferty + 1, *see* Double hydrogen rearrangement
  olefin elimination, *see* Olefin elimination
  product ion stability and, *see* Fragmentation, product ion stability and; Stevenson's rule
  product olefin structure and, 216, 302
  ring size of transition state and, 112, 207, 240

RECI, *see* Resonance electron capture ionization
Reconstructed ion chromatography, *see* Mass chromatography
Reconstructed total ion current chromatogram (RTICC), 46, 47, 146, 169, 274
Regnier, F., 206
Remote ionization site, initiation of fragmentation by, *see* Alpha-cleavage, initiated at remote ionization site; Gamma-hydrogen rearrangement, initiated at remote ionization site; Retro Diels-Alder fragmentation, initiated at remote ionization site
Repeller, 5, 8
Resolution
  chromatographic, peak intensities and, *see* Spectral skewing
  m/*z* (resolving power), 20. *See also* High resolution mass spectrometry; *m*/*z* Discrimination
Resonance stabilization, fragmentation mechanisms and, *see* Fragmentation mechanisms, resonance stabilization and
Resonance ejection, with quadrupole ion trap, 24
Resonance electron capture ionization, 7
Retro Diels-Alder fragmentation, 153, 207, 228–233, 331–332, 333, 334, 335, 347
  charge-retention and charge-migration mechanisms, 229, 231, 232, 331, 332, 334
  initiated at remote ionization site, 232
Reverse Nier-Johnson geometry in high resolution mass spectrometer, 17
Ring size for rearrangement transition states, entropy factors in, 112, 207, 240
Ring electrode, in quadrupole ion trap, 22, 23
Rings plus double bonds, formula, 91, 151, 153
Roboz, J., 55
Rods, quadrupole, *see* Poles (in transmission quadrupole)
RTICC, *see* Reconstructed total ion current chromatogram
Rubenstein, D.R., 58, 98

σ-bond cleavage, 102, 108, 132, 136, 156, 164
$\Delta S^{\ddagger}$, *see* Entropy of activation
Salicylic acid, *see* Benzoic acid, 2-hydroxy-
Sample introduction, modes for mass spectrometry, 3–4
Saunders, R.A., 148, 206, 256
Scan
  direction, 17, 28, 287
  lines, in stability diagrams, 19–21
  range, 14, 17, 21, 24, 35
    relation to base peak in spectrum, 39
  rates, 14, 26, 29, 35, 45
Schmidt, R.L., 21, 54
Schwartz, M., 256
Scott, D.R., 42, 55
Secondary elimination from α-cleavage ions, *see* Alpha-cleavage, secondary elimination after
Selected ion monitoring (SIM), 21–22
  mass chromatography, comparison, 49, 146
  mass defects and, 63–64
Self-Training Interpretive and Retrieval System (STIRS), 45, 54
Sensitivity
  effect of *m*/*z* discrimination on, 21, 26, 33, 34, 63–64
  pulse ionization and, 14
  selected ion monitoring and, 63–64
  tuning and, 33–34
Shapiro, R.H., 263, 266, 286
Silanes, alkyl, 147
Silicon
  isotope peak intensities, 82–83, 94
  isotopic abundances, 58
SIM, *see* Selected ion monitoring
Smith, P.J., 286
Smith, R.M., 145, 149, 219, 237, 263, 266, 286
Snyder, G.J., 149
Soft ionization, 9, 11, 24
Software, mass spectral
  general, 52
  interpretive, 45–46, 54, 55
Somayajula, K.V., 54
Source, ion, *see* Electron ionization source
Sparkman, O.D., 54, 69, 98, 110, 120, 148
Spectral skewing, over chromatographic peaks in GC/MS, 24, 26–29
Spectral variation, *see* Error, experimental, in peak intensity measurement
Stability diagram (*a* vs. *q* plot),
  for quadrupole ion trap, 23–24
  for transmission quadrupole, 19–21

DropBooks

Stability of ions and radicals, 133, 136, 239, 240. S*ee also* Fragmentation, product ion stability and; Fragmentation, product radical stability and
Stauffer, D.A., 45, 55
Steele, C., 21, 54
Steeves, J.B., 172, 206
Stein, S.E., 42, 49, 54, 55, 98, 148
Steroids, mass spectra of, 121, 257, 258
Stevenson, D.P., 117, 120
Stevenson's rule, 116–117, 126, 186, 231, 232, 240, 245
  examples, 117–119, 298, 331
STIRS, *see* Self-Training Interpretive and Retrieval System
Styrene, 106, 230, 231
Sulfide, *sec*-butylisopropyl, 204, *323*
Sulfides, aliphatic, α-cleavage and, 166, 204, 323
Sulfur
  charge stabilization by, 283, 309, 323, 349
  isotope peak intensities, 77, 78, 84–85, 93–94, 308–309
  isotopic abundances, 58
Sulfur dioxide, **84**, 85

Tabernanthe iboga, 180
Tanaka, K., 10
Tandem mass spectrometry, *see* Mass spectrometry/mass spectrometry
Tchekhovskoi, D.V., 54, 98, 148
Tear gas, 168
Terpenes, ion series, 141, 142
Δ^9-Tetrahydrocannabinol, **39–41**, 61, 63, **218**, 232
  γ-hydrogen rearrangement in, 217–219
  peak cluster intensities, 76, 79, 98, 297
  trimethylsilyl derivative, 63
Δ^9-Tetrahydrocannabivarin, **218**, 219
THC or Δ^9-THC, *see* Δ^9-Tetrahydrocannabinol
Thermodynamic control of reactions, 110–111
1-(2-Thienyl)cyclohexylmorpholine, *see* Phencyclidine, thiophene morpholine analog
1-(2-Thienyl)cyclohexylpiperidine, *see* Phencyclidine, thiophene analog
Thiols, aliphatic, α-cleavage and, 166
Thiophene, 93–94
Threshold for ion detection, 22, 30–31, 41
TIC, *see* Chromatogram, reconstructed total ion current
Tick, Lone Star, 163, 309
Tighe, T., 256
Time-of-flight (TOF) mass spectrometer, 12, 13–15, 26, 29, 54
TNT, *see* Trinitrotoluene
Todd, J.F.J., 54
Toluene, 80–82, 143, **144**
o-Toluylcyclohexylpiperidine, *see* Phencyclidine, *o*-toluyl analog
Toluylmethylecgonine, 273, 343
Total ion chromatogram, *see* Chromatogram, reconstructed total ion current
Transition state, definition, 111–112
Transmission quadrupole, 13, 17–21, 26, 34, 36, 37, 54, 55
  triple (QQQ), 25–26. *See also* Mass spectrometry/mass spectrometry
Tranthim-Fryer, D.J., 126, 149
Triethylamine, **193**, *195*
Trifluoromethyl carbenium ion ($^+CF_3$), 125, 287, 300, 301
Trimethylbenzenes, 166–167, 168, 311
Trimethylsilyl derivatives, 63, 82
Trinitrotoluene, *254*
Triple quadrupole, *see* Quadrupole mass analyzer, triple; Mass spectrometry/mass spectrometry
Tropane, derivatives of, 266, 268. *See also* Cocaine
Tropylium ion, *see* Cycloheptatrienyl ion
Tuning, 33–35
Tureček, F., 53, 68, 98, 106, 109, 120, 121, 141, 148, 235, 237
Tuross, N.C., 98
Tylenol, 196

u (Unified atomic mass unit), 3, 60
Ultraviolet spectrometry (UV), 33
Unsaturations, number of , *see* Rings plus double bonds, formula

Vacuum, *see* High vacuum
Valium, *see* Diazepam
Van der Hart, W.J., 140, 149
Venkataraghavan, R., 54
Villwock, R.D., 55
Vinyl
  carbenium ion, 307
  radical, loss of, 122, 123, 160, 314

Voltages
  accelerating
    magnetic sector analyzer, 15–16
    time-of-flight analyzer, 13–14
  electron multiplier, 32–33, 34
  ion source, 5, 8, 34
  in quadrupole ion trap, 21, 22–24
  in transmission quadrupole, 17–21, 22, 25, 35, 36, 37
Vose, J., 243, 256

Waldbauer, J.R., 98
Wallace, J.R., 145, 149
Water, elimination of, 121, 122, 198–200, 223, 321–322
Watson, J.T., 54, 110, 120
Web sites, 29, 46, 52–53
Weighting factor, in library searches, 42
Wesdemiotis, C., 55
Williamson A.E., 148, 206, 256
Wine, gamma-butyrolactone in, 243, 256
Winkler, H.U., 54
Wolcoff, P., 148

X + 1 peak intensities, *see* Isotope peak intensities, X + 1 peak
X + 2 peak intensities, *see* Isotope peak intensities, X + 2 peak

Yinon, J., 149

Zaikin, V., 54, 98, 148
Zamecnik, J., 286
Zhang, Q.W., 148
Zhu, D., 54, 98, 148

DropBooks